



# Design Concepts for the Robustness Improvement of Self-Compacting Concrete

Effects of admixtures and mixture components on the  
rheology and early hydration at varying temperatures

**Wolfram Schmidt**

/ Department of the Built Environment

**bouwstenen**

**193**

# **Design Concepts for the Robustness Improvement of Self-Compacting Concrete**

—

Effects of admixtures and mixture components on the rheology  
and early hydration at varying temperatures

Design Concepts for the Robustness Improvement of Self-Compacting Concrete –  
Effects of admixtures and mixture components on the rheology and early hydration at varying  
temperatures  
by Wolfram Schmidt, BAM Federal Institute for Materials Research and Testing, Berlin,  
Germany.

PhD Thesis, Eindhoven University of Technology, the Netherlands, 2014

A catalogue record is available from the Eindhoven University of Technology Library.

ISBN: 978-90-386-3598-9

Copyright © 2014 by Wolfram Schmidt

Cover design by Verspaget & Bruinink, Nuenen, the Netherlands

Photograph by BAM

Printed by Universiteitsdrukkerij, Eindhoven University of Technology, the Netherlands

All rights reserved. No part of this publication may be reproduced in any form or by any  
means without permission in writing form from the author.

# Design Concepts for the Robustness Improvement of Self-Compacting Concrete

Effects of admixtures and mixture components on the rheology and early  
hydration at varying temperatures

PROEFSCHRIFT

ter verkrijging van de graad van doctor aan de Technische Universiteit  
Eindhoven, op gezag van de rector magnificus prof.dr.ir. C.J. van Duijn,  
voor een commissie aangewezen door het College voor Promoties, in het  
openbaar te verdedigen op maandag 28 april 2014 om 16:00 uur

door

Wolfram Schmidt

geboren te Keulen, Duitsland

Dit proefschrift is goedgekeurd door de promotoren en de samenstelling van de promotiecommissie is als volgt:

voorzitter:	prof.dr.ir. B. De Vries
1 <sup>e</sup> promotor:	prof.dr.ir. H.J.H. Brouwers
copromotor:	Prof.Dr.rer.nat. B. Meng (BAM Bundesanstalt für Materialforschung und -prüfung)
leden:	prof.dr. A.M. van Herk
	prof.dr.ir. T.A.M. Salet
	prof.dr.ir. G. De Schutter (Universiteit Gent)
	prof.dr.ir. J.C. Walraven (TUD)
	dr. M. Sonebi (Queen's University Belfast)

To my beloved little family, my brave wife Steffi,  
my beautiful daughter Maribel and my wonderful son Merlin.



## Preface

This Thesis about admixtures for concrete and their interactions with cement hydration was started after I had been employed since approximately three years at the BAM Federal Institute for Materials Research and Testing. In parallel I was involved in many other projects related to cementitious systems, from no slump concrete to self-compacting concrete, and from low strength to high strength. The topic of this Thesis was chosen freely based on my experiences and identified research needs.

It is rather common to address the first words of thanks to a mentor, an antecessor, having already pioneered the direction of a thesis. However, this work is not founded on a long lasting tradition at BAM in rheology of construction materials or on admixtures use. Therefore, my mentors, those people, who inspired me can be found in the international scientific community. Hence, I would like to acknowledge those who had the strongest influence on this Thesis for their brilliant scientific publications which became my regular companions during the last couple of years: Prof. Robert Flatt, Dr. Kazuo Yamada, Prof. Johann Plank, Dr. Barbara Lothenbach, Prof. Karen Scrivener, Prof. Ólafur Wallevik, Prof. Nicolas Roussel, Prof. Geert de Schutter, Prof. Kamal Khayat, Dr. Frank Winnefeld. During the work on my Thesis, I had the great honour and pleasure to meet all of these excellent researchers in different places all over the world.

In this context, I would like to thank first of all Prof. and Dir'in Dr. rer. nat. Birgit Meng, who is also co-promoter of this Thesis. As of the beginning of my work at BAM, first as a project co-worker without any ambitions for a doctorate, she supported my international activities and those actions that went far beyond my actual duties. Also after I had started working on my thesis, she continued valuing my many scientific activities beyond this Thesis. I would also acknowledge my further superiors Dr.-Ing. Andreas Rogge, and Dr.-Ing. Hans-Carsten Kühne for giving me the required employment stability and the opportunity to present my entire works on conferences, and not to push too hard a finalisation of this Thesis to the benefit of many other projects. Thanks for letting me independently operate in so many different projects and with the many degrees of freedom. I hope that the wide range of experiences I made is truly reflected in this Thesis.

I would like to thank in particular my promoter prof.dr.ir. Jos Brouwers for all his support. It was such a lucky coincidence that our ways crossed during a fib PhD-symposium in Stuttgart in 2008. I had just started with some conceptual investigations for this Thesis but not yet a supervisor. We had a good talk in which prof.dr.ir. Jos Brouwers also informed me about the peculiarities of Dutch PhD defences. I was very much interested in the topics his group was dealing with and since it was always my intention to write my thesis in English language a Dutch PhD appeared to be very attractive to me. A few days later he sent me a photograph of such a ceremony and asked me if this could be of interest for me. I happily agreed and this was surely the best decision of the past years. Without any doubt, no other person accounts more responsible for the quality of this Thesis than prof.dr.ir. Jos Brouwers. Thank you Jos for your patience. I know that I was not an easy candidate, since my daily business did not always allow a stringent time-line. Thank you Jos for your flexibility and for always being available for me without complaining.

I would like to thank the further members of the Promotion Committee, prof.ir. Elphi Nelissen, prof.dr.ir. Joost Walraven, prof.dr.ir. Geert de Schutter, prof.dr. Alex van Herk, prof.dr.ir. Theo Salet, Dr. Mohamed Sonebi for their thorough reviews and highly valuable contributions and strong support.

For steady supply with information and raw materials, and many interesting discussions, I would like to thank Dr. Christian Hübsch, Alain Phyfferoen, and Dr. Jacob Terpstra.

No scientific work can be conducted on a high level without critical reviewers. Therefore, I would like to thank in particular Dr. Gregor Gluth for thorough reviews of the Chapters 2, 6, 7, 8, and 9 and for highly valuable literature recommendations. Thanks also go to Prof. Aleksandra Radlińska, who thoroughly reviewed two papers, which build the foundation of the Chapters 8 and 9. I would also like to thank Peter Ränge for many wonderful controversial discussions which sometimes helped me reconsidering some thoughts but mostly strengthened my opinions.

I also have to express my words of thank to my wonderful colleagues Maria Barthel, Ksenija Vasilic, Nsesheye Susan Msinjili, and Murat Ünal. First and foremost Maria supported me in the final editing, and all of them supported me indirectly by taking other burdens from my shoulders without complaining. This cannot be rated highly enough. I would also like to thank all my other colleagues, whose expertise and work force can be found somewhere in this Thesis. Thanks in particular go to Götz Hüsken to share your experiences about Dutch promotions with me. Thanks also go to Christian Lehmann for helping me with the XRD analysis and discussion. There is one person who needs special acknowledgement. This is Frank Haamkens, our concrete laboratory engineer at BAM. Thank you Frank for all your support and for being so uncomplicated and understanding during the last years. I know that in the past I came up with a thousand issues, many of which were not well prepared due to lack of time. You never complained (at least not too loudly) and therefore supported this Thesis in a fantastic way. I think, I do not have to tell you that without you, we would all be lost at BAM. My words of thank also address to Ingo Schultz, Jürgen Sichtung, and Dirk Wend who accompanied the investigations presented in this Thesis over a long period of time.

I also have to thank Tobias Schmidt, Andreas Haase, Vera Tschampel, Gaku Mizutani, Alvaro Arrobo, Anne Morgenstern, and David Heinrich, who contributed to this Thesis as interns, working students or by writing an academic Thesis under my supervision, which was directly or indirectly integrated into this Thesis.

I would also not like to forget expressing my great thankfulness to Robert Kremer and Tim Schmedders. Without your influence I would be a structural engineer today.

At last, I definitively have to express my deepest words of acknowledgement to Miruna Florea and Przemek Spiesz who were my connection to the Eindhoven University of Technology and supported me with experience and helpfulness. In particular, I have to thank Miruna for sacrificing such a lot of time. I owe you a lot.

The greatest contributors to this Thesis, however, cannot be found in the scientific community. Certainly my parents had a great share in the entire story of the origin of this Thesis by supporting all of my decisions throughout my life. However, writing a Thesis in parallel to a normal working life and with a family is like an endless daily ordeal. Whatever the focus is put on it gives a permanent feeling of neglecting the duties in the other fields. And for sure the most neglected task over the last couple of years was my family life. Therefore, my deepest gratefulness has to be expressed towards my wife Steffi, who has been so strong over the past years, my wonderful children Maribel and Merlin, who gave me the strength and backbone to take the road and to finish this Thesis eventually.

Wolfram Schmidt

Berlin, February 2014

# Contents

<b>Preface .....</b>	<b>iii</b>
<b>Contents.....</b>	<b>v</b>
<b>1 INTRODUCTION.....</b>	<b>1</b>
<b>1.1 Brief historical overview of SCC .....</b>	<b>1</b>
<b>1.2 Mixture composition approaches .....</b>	<b>2</b>
<b>1.3 SCC definitions all over the world .....</b>	<b>6</b>
<b>1.4 Ready-mixed SCC .....</b>	<b>7</b>
1.4.1 Market share of SCC in practice .....	7
1.4.2 The complexity of different SCC definitions .....	9
1.4.3 Influences of evolving and new constituents.....	10
1.4.4 The view on SCC from different fields of technology .....	12
<b>1.5 Robustness of SCC for the construction site .....</b>	<b>14</b>
1.5.1 Definition of robustness .....	14
1.5.2 Importance of consideration of the ambient temperature .....	14
<b>1.6 Temperature dependent differences between SCC and normal concrete .....</b>	<b>15</b>
1.6.1 Influence of temperature on the workability of normal concrete .....	15
1.6.2 Influence of temperature on the workability of SCC.....	15
<b>1.7 Outline of this Thesis.....</b>	<b>17</b>
<b>1.8 Definitions and abbreviations.....</b>	<b>19</b>
<b>2 THE EARLY HYDRATION OF CEMENTITIOUS MATERIALS.....</b>	<b>21</b>
<b>2.1 The early hydration of ordinary Portland cement.....</b>	<b>21</b>
2.1.1 Introduction .....	21
2.1.2 Early hydration of alite.....	21
2.1.3 The early hydration of aluminat phases.....	25
2.1.4 Hydration of cement.....	27
<b>2.2 Effects during the early hydration of cement.....</b>	<b>28</b>
2.2.1 Loss of workability .....	28
2.2.2 Setting .....	29
2.2.3 Shrinkage .....	29
<b>2.3 Conclusions .....</b>	<b>31</b>

<b>3</b>	<b>EFFECTS OF SUPERPLASTICISERS ON THE RHEOLOGY.....</b>	<b>33</b>
<b>3.1</b>	<b>The rheology of concrete and cementitious systems.....</b>	<b>33</b>
3.1.1	Parameters defining rheological properties .....	33
3.1.2	Mixture composition influences on the rheology .....	36
3.1.3	Grading curve.....	37
3.1.4	Aggregate to powder ratio.....	38
3.1.5	Aggregate and particle shape .....	39
3.1.6	Water-powder ratio .....	40
3.1.7	Stabilising agents .....	40
3.1.8	Plasticisers and superplasticisers.....	40
<b>3.2</b>	<b>Mode of operation of superplasticisers.....</b>	<b>41</b>
3.2.1	Introduction.....	41
3.2.2	Brief history of superplasticisers.....	41
3.2.3	Mode of operation of PCE in comparison to other superplasticisers .....	42
<b>3.3</b>	<b>Cement hydration and PCE performance.....</b>	<b>45</b>
3.3.1	Introduction.....	45
3.3.2	Zeta potential of clinker and hydration phases in pore solution .....	46
3.3.3	Specific surface area .....	47
3.3.4	Counter ions, anions, and competitive adsorption.....	47
3.3.5	Growth of hydration phases .....	48
3.3.6	Intercalations.....	48
3.3.7	Interactions with SCMs.....	49
3.3.8	Cement production factors .....	50
<b>3.4</b>	<b>Influences of PCE modification.....</b>	<b>50</b>
3.4.1	Versatility of the molecular structure of PCEs.....	50
3.4.2	Effects of the graft length of PCE .....	53
3.4.3	Effects of the backbone length of PCE .....	53
3.4.4	Effects of the grafting degree .....	53
3.4.5	Effects of the entire PCE structure.....	53
3.4.6	Effects of the charge density of the PCE on the rheology.....	54
<b>3.5</b>	<b>PCE in practice.....</b>	<b>56</b>
3.5.1	Blends of PCE.....	56
3.5.2	Blends of different superplasticisers .....	56
3.5.3	Blends with different admixture types .....	56
3.5.4	Practical problems to assess the PCE performance.....	56

<b>4</b>	<b>MATERIALS AND METHODS .....</b>	<b>59</b>
<b>4.1</b>	<b>Background of the used concrete mixtures .....</b>	<b>59</b>
4.1.1	Introduction .....	59
4.1.2	Powder properties.....	59
4.1.3	Sand and gravel .....	62
4.1.4	Superplasticisers.....	62
4.1.5	Stabilising agents .....	63
4.1.6	Background of the powder type SCC (POW) .....	65
4.1.7	Required modifications to obtain the SCC mixture “POW” .....	66
4.1.8	Background of the combination type SCC (COM) .....	67
4.1.9	Required modifications to obtain the SCC mixture “COM” .....	68
<b>4.2</b>	<b>Final SCC composition .....</b>	<b>69</b>
4.2.1	Adjustment of mixture compositions to performance criteria .....	69
4.2.2	Composition and properties of the final concrete compositions.....	71
4.2.3	Fresh concrete performance of the adjusted control mixtures .....	74
4.2.4	Calculation of paste from the concrete mixture components .....	76
<b>4.3</b>	<b>Rheometric test specifications .....</b>	<b>77</b>
4.3.1	Paste flow tests.....	77
4.3.2	Slump flow .....	77
4.3.3	V-funnel test.....	78
4.3.4	Sieve segregation resistance test .....	78
4.3.5	The LCPC-box test.....	79
4.3.6	Rotational rheometry .....	80
4.3.7	Concrete rheometry with the ConTec Rheometer-4SCC .....	80
4.3.8	Comparison of the ConTec Rheometer-4SCC method with slump flow testing and LCPC-box method.....	82
4.3.9	Viscosimetry using the basket cell .....	84
<b>4.4</b>	<b>Observations during the setting and hardening.....</b>	<b>86</b>
4.4.1	Vicat penetration test.....	86
4.4.2	Automatic Vicat penetration test .....	87
4.4.3	Isothermal heat flow calorimetry .....	88
4.4.4	X-Ray Diffractometry .....	89
4.4.5	Shrinkage cone .....	90
<b>4.5</b>	<b>Materials selection.....</b>	<b>92</b>
4.5.1	Observations regarding the storage of raw materials for concrete .....	92
4.5.2	Practical problems .....	95
4.5.3	Principle of closed series with identical delivery charges one .....	95

<b>5</b>	<b>A SIMPLE TEST TO ASSESS THE CHARGE DENSITY OF PCE .....</b>	<b>97</b>
<b>5.1</b>	<b>Introduction .....</b>	<b>97</b>
<b>5.2</b>	<b>Basic principle .....</b>	<b>97</b>
5.2.1	Determination of the water demand of a powder mixture - Step 1.....	99
5.2.2	Calculation of mixture composition for each PCE dosage - Step 2.....	101
5.2.3	Mixing - Step 3 .....	102
5.2.4	Spread flow values - Step 4.....	102
5.2.5	Interpretation of the results – Step 5 .....	102
5.2.6	Application of the method with powders and powder blends .....	104
5.2.7	Influence of water .....	107
<b>5.3</b>	<b>Conclusions .....</b>	<b>108</b>
<b>6</b>	<b>FRESH CONCRETE PERFORMANCE OF SCC AT VARYING TEMPERATURES .....</b>	<b>109</b>
<b>6.1</b>	<b>Introduction .....</b>	<b>109</b>
<b>6.2</b>	<b>Temperature dependent behaviour of flowable concrete .....</b>	<b>109</b>
6.2.1	Practical experiences with SCC at different temperatures .....	109
6.2.2	Research on temperature influences – Experiences in paste and mortar .....	110
6.2.3	Research on temperature influences – Experiences in concrete .....	115
6.2.4	Discussion of research experiences .....	122
<b>6.3</b>	<b>Experimental programme .....</b>	<b>127</b>
6.3.1	Matter of investigations .....	127
6.3.2	Investigated concrete mixtures.....	127
6.3.3	Test specifications.....	127
6.3.4	Rheometric measurements and interpretation .....	129
<b>6.4</b>	<b>Results and discussion.....</b>	<b>130</b>
6.4.1	Rheometric results compared to slump flow and V-funnel results.....	130
6.4.2	Influence of the stabilising agent on the interpretation of the results .....	132
6.4.3	Linking rheometric results to visual and haptic observation .....	133
6.4.4	Rheology of POW at varied temperatures.....	133
6.4.5	Rheology of COM at varied temperatures .....	134
6.4.6	Discussion of the results .....	136
<b>6.5</b>	<b>Explanation model for the observed effects based on adsorption of PCE and water/solid ratio.....</b>	<b>140</b>
6.5.1	Differentiation between the SCC types .....	140
6.5.2	Mechanisms behind the sensitivity of POW at high temperatures. ....	140
6.5.3	Mechanisms behind the poor robustness of COM at low temperature.....	142
<b>6.6</b>	<b>Conclusions .....</b>	<b>144</b>

<b>7</b>	<b>INFLUENCE OF STABILISING AGENTS ON THE RHEOLOGY.....</b>	<b>147</b>
<b>7.1</b>	<b>Stabilising agents for concrete.....</b>	<b>147</b>
7.1.1	Necessity of stabilising agent for SCC.....	147
7.1.2	Terminology.....	147
7.1.3	Stabilising agents for concrete .....	147
7.1.4	Stabilising agents in the presence of superplasticisers .....	148
<b>7.2</b>	<b>Starch and diutan gum based stabilising agents.....</b>	<b>149</b>
7.2.1	Starch based stabilising agent.....	149
7.2.2	Diutan gum based stabilising agent.....	151
7.2.3	Differences between starch ether and diutan gum.....	152
7.2.4	Starch ether and diutan gum in the presence of PCE.....	155
7.2.5	Discussion of the recent research .....	157
<b>7.3</b>	<b>Influences of starch ether and diutan gum on dispersion rheology.....</b>	<b>158</b>
<b>7.4</b>	<b>Influence of stabilising agent on rheology of SCC.....</b>	<b>165</b>
7.4.1	Experimental procedure for paste tests.....	165
7.4.2	Experimental procedure for concrete tests .....	166
7.4.3	Influence of temperature on limestone filler paste .....	166
7.4.4	Influence of stabilising agents on combination type SCC.....	167
7.4.5	Influence of stabilising agents on powder type SCC.....	171
7.4.6	Discussion of the observations .....	174
<b>7.5</b>	<b>Conclusions .....</b>	<b>176</b>
<b>8</b>	<b>INFLUENCE OF PCE ON THE EARLY HYDRATION.....</b>	<b>177</b>
<b>8.1</b>	<b>Introduction .....</b>	<b>177</b>
<b>8.2</b>	<b>The early hydration of ready-mixed SCC .....</b>	<b>177</b>
8.2.1	Specific aspects of SCC .....	177
8.2.2	Influence of calcium carbonate on early hydration effects.....	178
8.2.3	Influence of temperature on early hydration .....	179
8.2.4	Influence of superplasticisers on the early hydration .....	183
8.2.5	Influence of water to powder ratio .....	185
<b>8.3</b>	<b>The early hydration from an engineering point of view.....</b>	<b>186</b>
<b>8.4</b>	<b>Experimental setup.....</b>	<b>191</b>
8.4.1	General information .....	191
8.4.2	Setting of pure cement-superplasticiser pastes.....	191
8.4.3	Setting, heat evolution and deformations of the binder paste of COM and POW .....	192
8.4.4	In-situ XRD on pastes of the COM mixture.....	194
8.4.5	Setting of binder paste, mortar, and concrete .....	195

<b>8.5</b>	<b>Results and Discussion .....</b>	<b>195</b>
8.5.1	Effect of PCE on the setting of cement paste .....	195
8.5.2	Effect of PCE type and amount on initial and final set of COM pastes .....	196
8.5.3	Effect of PCE type and amount on heat evolution of COM pastes .....	197
8.5.4	Correlating the heat flow and the final set according to Vicat .....	199
8.5.5	Phase evolution of COM pastes .....	202
8.5.6	Early deformations of COM pastes after the final set .....	206
8.5.7	Influence of the mix design.....	208
8.5.8	Relevance of the paste observations for concrete.....	211
<b>8.6</b>	<b>Conclusions .....</b>	<b>211</b>
<b>9</b>	<b>EFFECTS OF STABILISING AGENTS ON THE EARLY HYDRATION .....</b>	<b>213</b>
<b>9.1</b>	<b>Introduction.....</b>	<b>213</b>
<b>9.2</b>	<b>The early hydration in the presence of stabilising agents .....</b>	<b>213</b>
<b>9.3</b>	<b>Experimental setup .....</b>	<b>218</b>
9.3.1	Materials for the observation of POW and COM pastes .....	218
9.3.2	Materials for the observation of pure cement pastes with and without PCE ..	218
9.3.3	Mixing of pastes.....	219
9.3.4	Setting investigations .....	219
<b>9.4</b>	<b>Experimental results and discussion.....</b>	<b>220</b>
9.4.1	Setting of binder paste from COM pastes .....	220
9.4.2	Setting of binder paste from POW paste .....	224
9.4.3	Setting of cement paste with stabilising agent and PCE .....	224
9.4.4	Discussion of cement paste setting with stabilising agent and PCE.....	227
<b>9.5</b>	<b>Conclusions .....</b>	<b>232</b>
<b>10</b>	<b>RECOMMENDATIONS FOR ROBUST MIXTURE COMPOSITIONS, CONCLUSIONS, AND OUTLOOK.....</b>	<b>233</b>
<b>10.1</b>	<b>Introduction .....</b>	<b>233</b>
<b>10.2</b>	<b>Parameters determining the rheology at different temperatures.....</b>	<b>233</b>
10.2.1	Summary of observed rheological effects .....	233
10.2.2	Critical effects at high temperatures.....	234
10.2.3	Critical effects at low temperatures.....	234
10.2.4	Decision path for the choice of PCE to obtain optimised workability for cold and warm temperatures .....	234

<b>10.3</b>	<b>Improvement of the robustness of SCC for high and low temperature.....</b>	<b>236</b>
10.3.1	The influence of the rheological adjustment on the whole early hydration process.....	236
10.3.2	Decision paths for the optimisation of SCC for high temperatures.....	236
10.3.3	Decision paths for the optimisation of SCC for low temperatures.....	238
<b>10.4</b>	<b>Decision paths for improved temperature robustness of SCC against regularly varying temperatures.....</b>	<b>239</b>
10.4.1	General information.....	239
10.4.2	Choice of PCE.....	239
10.4.3	Choice of stabilising agent.....	239
10.4.4	Choice of additions.....	240
10.4.5	Selection of cement.....	241
10.4.6	Selection of a robust mixture composition.....	241
10.4.7	Decision path for SCC with improved robustness against temperature scatter.....	242
<b>10.5</b>	<b>Conclusions and outlook.....</b>	<b>244</b>
10.5.1	Summary of the intention and the scope of the work.....	244
10.5.2	Major results from the experimental work.....	244
10.5.3	Future research.....	246
10.5.4	Classification into scientific context, exploitation, and outlook.....	247
10.5.5	Concluding remarks.....	248
	<b>Abbreviations and symbols.....</b>	<b>249</b>
	<b>Annex A – Rheometric results of SCC.....</b>	<b>253</b>
	<b>Annex B – Compressive strength of SCC.....</b>	<b>259</b>
	<b>Annex C – Heat flow rates and Vicat setting times.....</b>	<b>261</b>
	<b>Annex D – XRD measurement intervals and patterns.....</b>	<b>265</b>
	<b>Annex E – Vicat setting times of COM and POW pastes.....</b>	<b>271</b>
	<b>References.....</b>	<b>277</b>
	<b>Publications by the author.....</b>	<b>301</b>
	<b>Summary.....</b>	<b>307</b>
	<b>Curriculum Vitae.....</b>	<b>308</b>



# 1 Introduction

## 1.1 Brief historical overview of SCC

Today's self-compacting concretes (SCCs) are sophisticated systems with a wide range of properties. The ancestor SCC was defined as concrete that consolidates only under the forces of the gravitation without segregation upon flow and without blocking at passing obstacles. The basic idea behind the principle of flowable concrete was controlling the flow properties by increasing the paste volume, which can be adjusted to the required properties by adjustment of the volumetric ratio of water and powder, and supplementary superplasticisers (SPs).

The first prototype of such concrete was completed in Japan in 1988 based on the need for compensation of the observed loss of skill of construction workers in Japan [1]. It was originally entitled high performance concrete [2]. As of 1983, it was observed in Japan that with decreasing skill level of the construction workers, the construction quality reduced correlatively [3]. Hence, SCC was the suggested method to ensure durable concrete constructions which was largely independent of the qualification of the casting staff. The invention of SCC in Japan came not by surprise, since traditionally the majority of all concretes recently applied in Japan incorporate some kind of chemical admixtures [4].

When SCC was invented, super flowable concrete was not new in Japan. Flowable consistencies were already achieved using anti-washout admixtures that increase the adhesion and viscosity of the suspension since 1980 based on earlier experiences in Germany [4-6]. Also Colleparidi reports about the application of so called rheoplastic consistencies as of about 1970 in Italy and Hong Kong [7]. In a plenary closing lecture of the Fifth North American Conference on Self-Consolidating Concrete in Chicago, USA, De Schutter gave a historical survey about self-compacting concrete [8], in which he entitled underwater concrete and highly flowable concrete as the "Parents" of SCC. In the same context he referred to the so-called System 'Non Plus' as the "Great great grandfather" of SCC. The system 'Non Plus' was a concreting system first developed in 1906 in Germany and applied in Germany, Netherlands, and Belgium in the 1910's and 1920's. It allowed on-site concrete casting of large housing elements including window and door openings. De Schutter also refers to Thomas Alva Edison, who was granted a patent in 1908 for his idea of a multi storey concrete house cast in a single casting step including concrete bath tubs and shingles [8]. This early precursor of modern SCC was put into practice without significant success in 1917, and some of these houses are still standing.

However, the invention of what is called SCC today is owed to the invention of modern superplasticisers based on polycarboxylates, which were more efficient and more versatile than the products available on the market before. A more detailed overview of the history of superplasticisers will be given later in Section 3.2.

Without doubt, the technology of self-compacting concrete is eternally linked to the name of Okamura, who, took the "stimulating leadership" during the first developments in the early 1990s, as Walraven recently formulated in a keynote paper for the 6th International RILEM Symposium on Self-Compacting Concrete in Montreal [9]. The development was further accompanied by research activities by Ouchi [3, 10], Ozawa [2, 11], and Takada [12, 13]. After some international presentations of the new technology, as of 1994, SCC technology gained interest internationally, and was adopted by researchers from Europe, Northern America, and Asia [1, 5, 9], followed by lively and ongoing research activities at the end of the 20th century, which marks a corner stone for the acceptance of SCC. The pioneering of SCC in Europe is closely linked to Walraven, and Bartos, the introduction to Northern America to Aïtcin and Khayat.

At the same time, the invention of SCC can be linked to the invention of new admixtures, in particular SPs but also stabilising agents (STAs), which allow controlling the rheological properties of a cementitious paste regardless of the water to cement ratio. The plasticising effect of polycarboxylate based SPs was observed for the first time in the 1980s. The first generation of polycarboxylate based SPs for concrete was introduced in 1986. Using a methacrylic backbone instead of an acrylic one made the polymer resistant against the high alkaline conditions, which can be found in cementitious systems [14]. During the following 15 years, significant steps towards improved SPs and particularly the understanding of their modes of operation were made. Until the turn of the millennium, significant research was conducted by Uchikawa, Hanehara, and Yamada [15-18], by Ohta et al. [19], Rivera-Villarreal et al. [20], Jolicoeur et Simard [21], and by Houst et al. [22] in the field of SPs. Comprehensive studies about stabilising admixtures were published before 2000 by Yammamuro et al. [23], Rols et al. [24] and Khayat [25]. In the year 2000, the major mechanisms of polycarboxylic SPs were largely understood and the use of stabilising admixtures was identified as a reasonable option to develop new mixture composition concepts for SCC.

Since then until today, significant research activities have taken place. A first conference on SCC was organised by JSCE in Kochi in 1998. A first international RILEM conference on self-compacting concrete in 1999 in Stockholm was the start of a series of SCC conferences with high international impact. The first technical committee of the Japanese Society of Civil Engineers (JSCE) was already founded in 1994, which published a state of the art report in 1996. On international level, the first RILEM committee on self-compacting concrete (TC 174-SCC) was founded in 1997. Later committees were focusing on the casting (TC 188-CSC), the durability (TC 205-DSC), flow simulation (TC 222-SHC), and the mechanical properties (TC 228-MPS).

In Europe a multi-national research project was initiated entitled “Rational Production and Improved Working Environment through Using Self-Compacting Concrete” [26], followed by another project entitled “Testing SCC”, which helped spreading the benefits of SCC to a wide range of applicators [27]. This project was also the basis of a widely accepted European guideline on Self compacted concrete published by the European industry association bibm, CEMBUREAU, EFCA, EFNARC, ERMCO [28], which again builds the basis of the European standards for the testing of SCC (EN 12350, Parts 8 to 12) as well as for the actual modernisation of the European concrete standard EN 206-1.

## 1.2 Mixture composition approaches

According to the Japanese recommendations for self-compacting concrete, which are based on the works of the subcommittee of the JSCE on self-compacting concrete, the major types of SCC can be distinguished [11], the powder type, the combination type, and the stabilising agent type. Table 1.1 provides some characteristics of these types according to Nagataki [29].

Table 1.1: Powder contents and water to powder ratios for different mixture composition types of SCC according to Nagataki [29].

Classified types	Unit content of powder [kg/m <sup>3</sup> ]	Water powder ratio (%)
Powder type	500-575	30-40
Combination type	500-575	30-40
Viscosity agent-type	400-500	45-55

The powder type can be considered as the ancestor SCC. The mix concept, entitled general purpose approach, goes back to Okamura and Ozawa and the frequently cited publication “Mix design for self-compacting concrete”, which was published in the Concrete Library of the JSCE in June 1995. The idea behind this concept is fixing the volumes of aggregates, sand, and paste, while the paste shall be modified by adjusting the water to powder ratio as well as the SP content to specified flow properties. Relevant boundary parameters suggested by Okamura et al. [1, 3] are a coarse aggregate volume of 50% of the solid volume and a sand volume, which shall be 40% of the mortar volume [2, 3, 12, 13]. The adjustment of the flow properties can be achieved by using the so-called  $\beta_p$ -method, where the relative mortar flow spread area  $\Gamma_m$  is determined at varied volumetric water to powder ratios.  $\Gamma_m$  is the mean spread area divided by the lower spread cone opening area as shown in Figure 1.1 according to:

$$\Gamma_m = \frac{(d_1 \cdot d_2 - d_0^2)}{d_0^2} \quad (1.1)$$

where  $\Gamma_m$  = relative flow spread;  $d_1$  = diameter 1,  $d_2$  = diameter perpendicular to  $d_1$ ,  $d_0$  = diameter of the lower cone opening.

Their values  $\Gamma_{m,i}$  at varied volumetric water to powder ratios are plotted into a graph with the water to powder ratio in the ordinate and the relative slump flow on the abscissa, as shown in Figure 1.2. By determining calculatory the intersection of the correlation line between the measurement spots and the ordinate, a  $\beta_p$ -value can be identified, which marks the water demand or the water content at which no flow occurs [12]. The slope of the curve  $E_p$  is called deformation factor [12] and can be considered as value describing the water retention properties of the paste mix [30]. After identifying the  $\beta_p$ -value the paste can then be modified with SP to achieve flowability. In order to simplify the time intensive determination of  $\beta_p$ , in later publications it was suggested by Okamura that the  $\beta_p$ -value shall be in the range of 0.9 and 1.0, depending on the properties of the powder. Further to the flowability a certain viscosity is required to avoid dynamic segregation of the aggregates in the paste. Therefore, viscosity tests shall be conducted by help of a mortar V-funnel, e.g. as shown in Figure 1.1. According to the general purpose approach by Okamura, the paste at water powder ratio  $\beta_p$  shall be amended by a sand volume, which makes out 40% of the total sand volume. By adding superplasticiser  $\Gamma_m$  shall be close to 5 and  $R_m$  shall be close to 1. Upon reaching this combination of values, the mortar is considered to be able to provide self-compacting properties, when it is amended by coarse aggregate [12, 13]. The rheology of the final SCC mixture composition can then be validated by different test methods as listed in Table 1.2.

It is interesting to know that in Europe the definition of the spread area  $\Gamma_m$  differs slightly from the Japanese Equation (1.1). In Europe most authors and guidelines, e.g. [5, 12, 13, 31, 32], use the following equation:

$$\Gamma_m = \frac{\left(\left(\frac{d_1+d_2}{2}\right)^2 - d_0^2\right)}{d_0^2} = \left(\frac{d_1+d_2}{2d_0}\right)^2 - 1 \quad (1.2)$$

where  $\Gamma_m$  = relative flow spread;  $d_1$  = diameter 1,  $d_2$  = diameter perpendicular to  $d_1$ ,  $d_0$  = diameter of the lower cone opening.

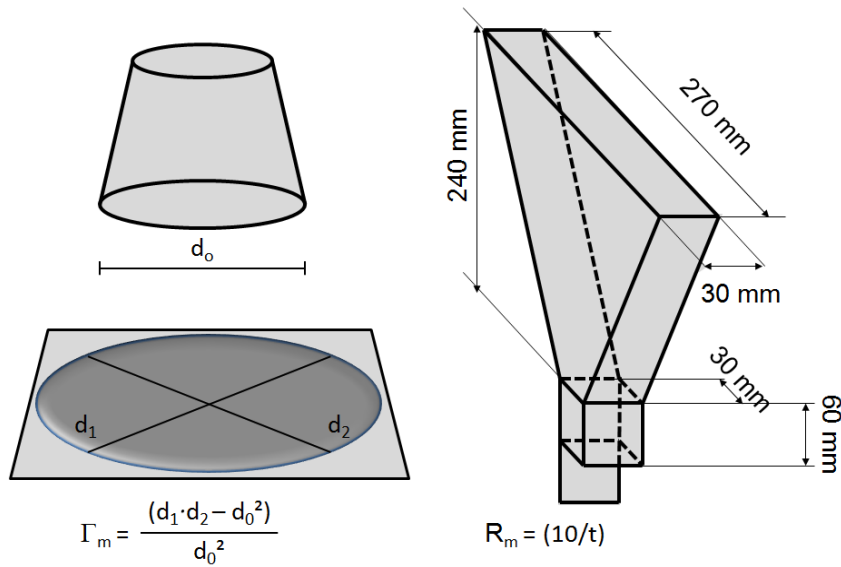


Figure 1.1: Spread flow and efflux test for paste and mortar for the determination of  $\Gamma_m$  and  $R_m$ .

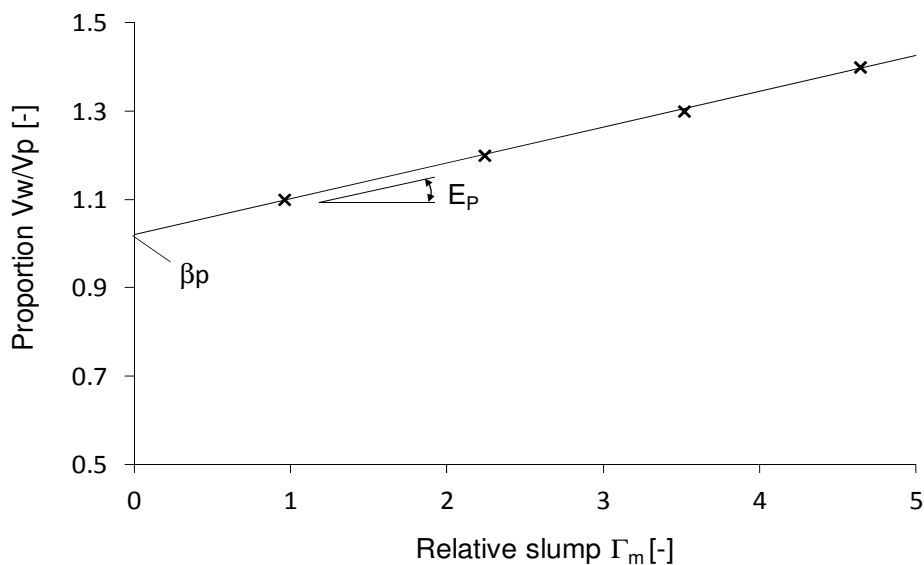


Figure 1.2: Example for the water demand determination according to the Okamura method.

The Equations (1.1) and (1.2) differ in their first term in the denominator, where in Equation (1.1) the final flow shape is calculated as an oval area, while in Equation (1.2) the final flow shape is considered as a circle with the average of the diameters  $d_1$  and  $d_2$ . Hence, in case  $d_1 = d_2$  both equations yield identical results. In case of  $d_1 \neq d_2$  Equation (1.1) generates slightly lower values than Equation (1.2). However, practically this small difference will not be of relevance.

The most common methods to determine the flow properties are the slump flow (SF) using an Abrams cone and the V-funnel efflux time ( $t_v$ ) for concrete, which provide largely unbiased information about yield stress and plastic viscosity, respectively (Figure 1.3). Yield stress can be considered as a value, which determines the flowability and the static segregation resistance, while the plastic viscosity determines the filling speed and the dynamic segregation resistance. Most other methods given in Table 1.2 provide more or less subjective visual or qualitative

results like passing ability or visual filling ability, which cannot be directly linked to rheological properties. A more distinguished discussion about the methods and the rheologic interpretation will be provided in Section 4.3.

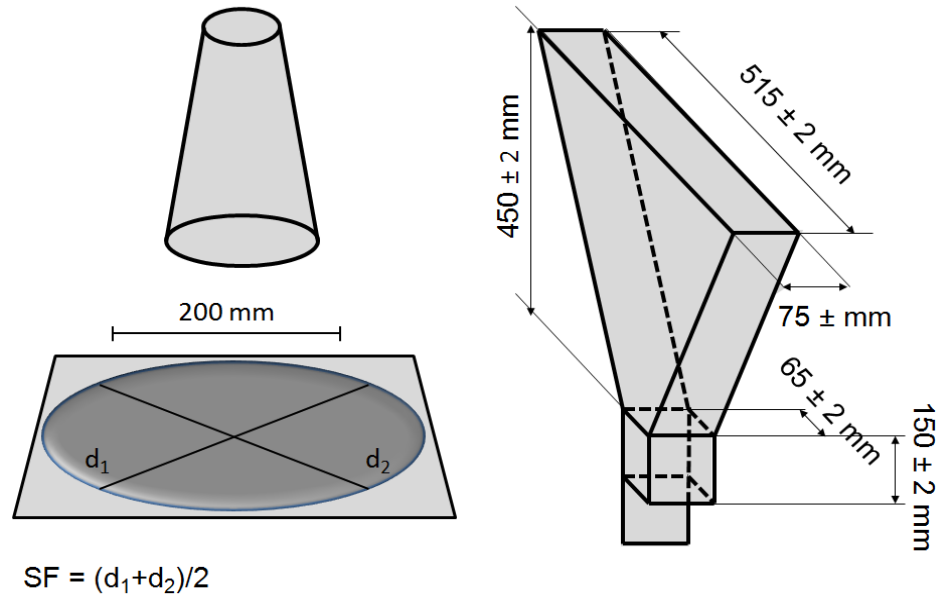


Figure 1.3: Determination of the slump flow (SF) according to EN 12350-8:2010 and geometry of the V-funnel for concrete according to EN 12350-9:2010.

Table 1.2: Different fresh SCC test methods based on [28, 31, 33-38].

Method	Measured value	Rheological property
Slump flow	Spread diameter	Yield stress
$t_{500}$	Flow time for diameter of 500 mm	Viscosity
V-funnel	Efflux time	Viscosity
Efflux cone	Efflux time and flow diameter	Viscosity/yield stress
Marsh cone	Efflux time	Viscosity/Mixed information
LCPC box	Flow distance	Yield stress
Orimet	Efflux time	Viscosity
L-Box	Passing ratio	Mixed information
U-Box	Height difference	Mixed information
J-Ring	Step height, spread diameter	Mixed information
Kajima Box	Visual passing ability	Mixed information
Penetration	Penetration depth	Mixed information
Sieve segregation	Percentage of passing laitance	Mixed information
Settlement column	Segregation ratio	Mixed information

According to the Japanese recommendations, the combination type and the viscosity agent type distinguish only in the presence of viscosity agent, which is added in order to improve the robustness of an SCC against water deflections [11, 29, 39, 40]. However, the use of strong rheology modifying admixtures such as polysaccharides or ultra-fine powders allows higher flexibility in the powders used and economisation by reduced powder contents. The implementation of rheology modifying admixtures, thus, led to the development of mixture approaches with significantly lower powder contents than would be required according to the

general purpose approach, and finally to the establishment of SCCs that can be defined as viscosity agent type. The combination type SCC is therefore often considered as SCC in between a powder type and a viscosity type.

In most countries, the use of fine powders is typically accompanied with higher production costs. Furthermore, systems with high powder contents exhibit high viscosities, which may be a problem for the casting process and they may be prone to higher shrinkage deformations. Therefore, for many applications, efforts were made to reduce the powder content of SCC to a minimum. The increased understanding of influences of the finest particles and admixtures on the rheology of SCC led to mixture concepts that work properly with powder contents that are similarly low as in vibrated concrete. Examples of such mixtures are reported by Collepardi and Valente [41], Su and Miao [42], or Mueller and Wallevik [43].

### 1.3 SCC definitions all over the world

The technical application may suggest different mixture composition approaches. Based on the research of Walraven and co-workers that were also reported in the final report of the “Testing SCC” project, the European guidelines for SCC [28] recommend different suggestions for the slump flow value and the V-funnel efflux time, depending on the constructional element, as shown in Figure 1.4. The European guidelines for SCC can be considered as an outstanding document, since they represent the state of the technology in a wide area all over Europe and thus comprise the whole range of what is considered as SCC all over the world. Luckily the fathers of this document, the participants of the “Testing SCC”-project [27], freed SCC from the narrow frame in which it was bound until the turn of the millennium. They left the doors wide open for a wonderful variety of numerous approaches to SCC that have been developed and established until today (Figure 1.5).

Domone provides an analysis of 68 SCC publications world-wide between 1993 and 2003 and concluded that a majority of all investigated SCCs ranged in their slump flow values between 600 and 750 mm and showed higher strengths than 40 MPa. Limestone was the most common used addition and approximately 50% contained stabilising admixtures and were categorised as combination type SCC [44]. The median powder content was 500 kg/m<sup>3</sup> with water to powder ratios (w/p) of 0.35 by mass.

Though, using the average of all values might generate a well functioning SCC, it is clear that there is an enormously wide range of possibilities to generate SCC. All over the world different mixture composition approaches were established during the last decade, which can vary from the ancestor SCC slightly or significantly. As a result, the definition of what type of concrete can be called self-compacting varies greatly from country to country. For example, an SCC that might be typical for Scandinavian countries would be considered as an F6-concrete in Germany, according to the definition of EN 206 for a very flowable concrete with a spread flow value larger than 630 mm.

An interesting overview of different rheological adjustments established in various countries for SCC all over the world is given in Figure 1.5 by Wallevik and Wallevik [45]. Although the individual situation in each of the countries might be much more diversified today, it provides a good picture of different SCC philosophies, and in which wide ranges SCC can be operated.

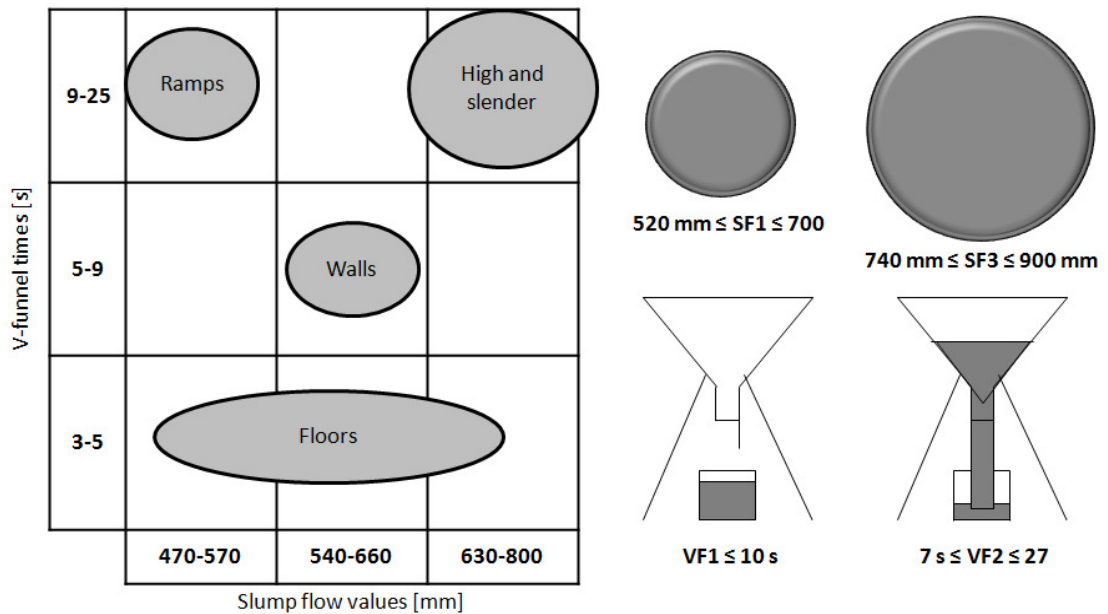


Figure 1.4: Recommendations for slump flow and V-funnel efflux times for different construction elements after Walraven [9] and ranges for these values, covered by the European guidelines for SCC.

## 1.4 Ready-mixed SCC

### 1.4.1 Market share of SCC in practice

Okamura stated in 1990 “When self-compacting concrete becomes so widely used that it will be seen as the “standard concrete” rather than as a “special concrete,” [sic] we will have succeeded in creating durable and reliable concrete structures requiring very little maintenance work.”

Today, more than twenty years later, it can be stated that SCC has become an important, though not yet standard, technology for the pre-cast industry, as it helps accelerating the casting process, allows for worker friendly conditions, and can be well used for fair-face elements. In general, the use of high powder contents had always been practice in most pre-cast applications, and the better defined environment in the plant helps producing on a relatively similar level.

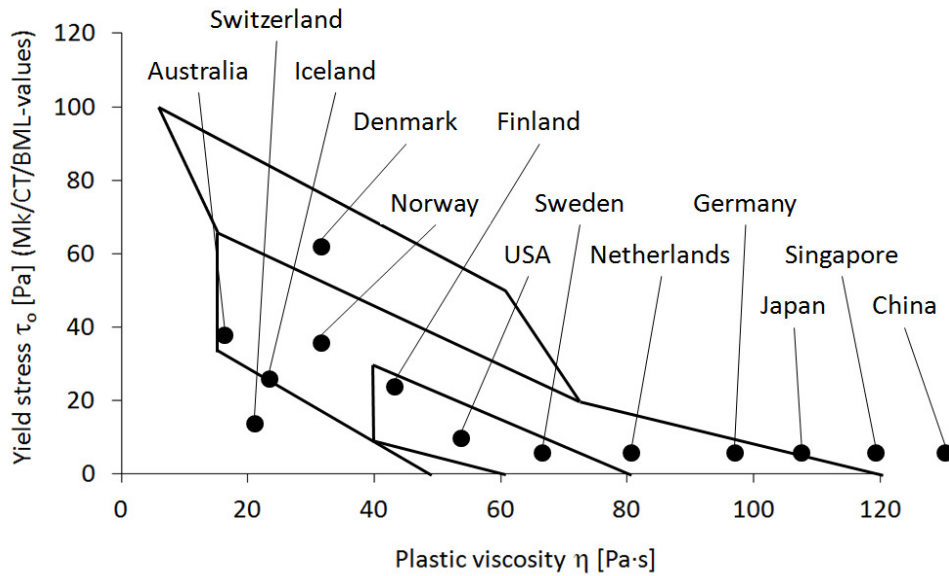


Figure 1.5: Variety of rheological SCC adjustments, which are typical for different countries after Wallevik and Wallevik [45].

With regard to the field of ready-mixed concrete, the idea of Okamura is far away from practice. Figure 1.6 shows the production data of SCC and concrete of the consistency class F6 for different countries in 2010. Denmark, where more than 30% of the total ready-mixed concrete volume is SCC or F6 concrete, emerges most prominently. Significant production data for F6 and SCC are only reported from Sweden, France, and Norway, though much lower than Denmark. Also in other continents, particularly not in Japan, where SCC was invented, noteworthy amounts of SCC are produced in the ready-mixed field.

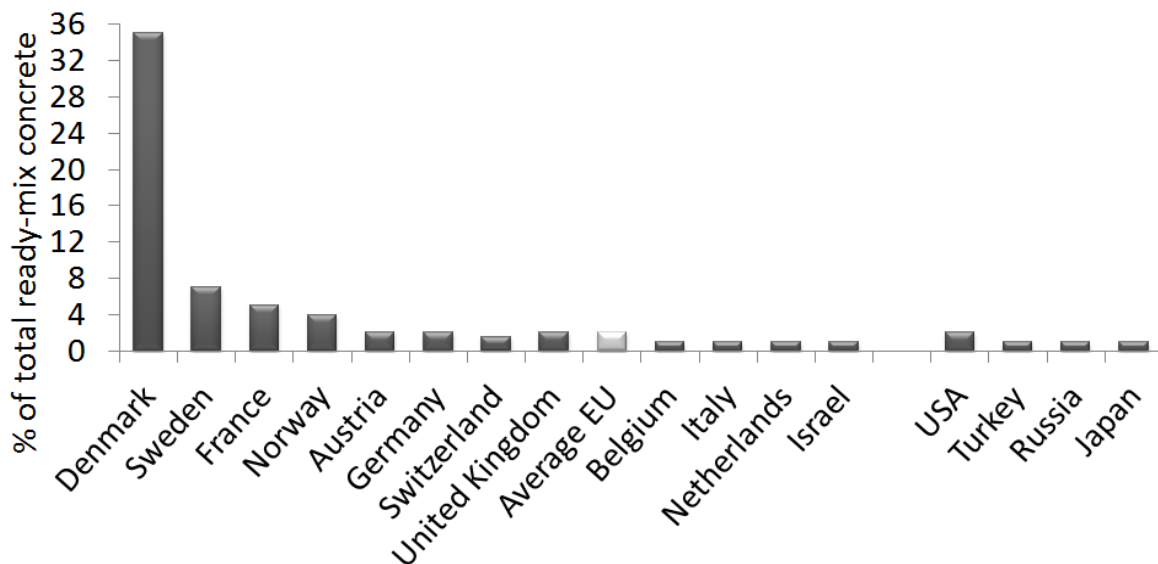


Figure 1.6: Production of ready-mixed SCC related to the total volume of ready-mix concrete for particular countries (selected data from [46]).

The concerns of the ready-mix industry are related to the higher costs of SCC compared to normal concrete as well as to the lack of robustness against the numerous influences that can occur between mixer and scaffold, which are practically hardly controllable.

However, very cost efficient SCC mixture composition were suggested and brought to practice by numerous researchers, e.g. by Collepari and Valente [41], Brouwers and Radix [47], or Mueller and Wallevik [43]. Methods to improve the robustness of SCC were also suggested by numerous authors, e.g. Nunes et al. [48], Vogel [49], or Lowke [50]. It is thus hard to believe that SCC cannot be brought to the construction site on a cost efficient and robust level. The major limiting factor is the high level of expertise that is required and which needs to combine the knowledge of numerous fields of research. In the past ten years, the gap between state of the art and state of applied technology has widened to a crucial extend.

#### 1.4.2 The complexity of different SCC definitions

The different design concepts have been causing confusion during the last decades, since despite different mixture design approaches, research on SCC is typically considered as relevant for all types of SCC. Only slowly the awareness is generated in the scientific community that more emphasis has to be put on the mixture composition approach to better understand SCC, and that in some cases it is necessary to clearly distinguish between the mixture composition approaches. For example in investigation on different mixture composition approaches it was shown by Kühne and Schmidt that the sieve screening test according to EN 12350-11 generates reasonable results for SCC developed as a combination type or stabilising agent type but only gives poor accuracy for highly viscous powder type SCC [51].

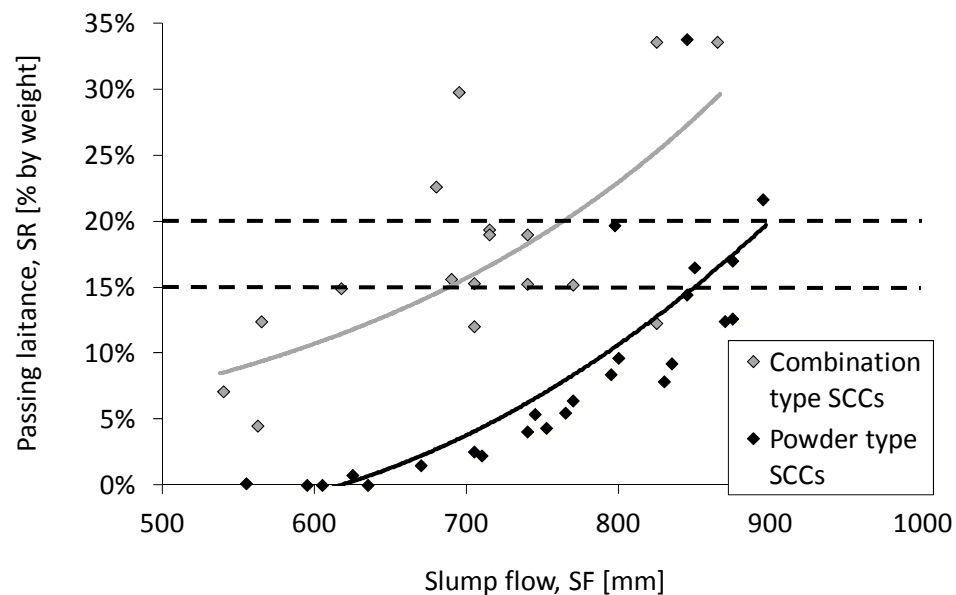


Figure 1.7: Comparison of the sieve segregation resistance vs. slump flow values of various combination type SCCs and powder type SCCs [51].

Figure 1.7 shows that between 600 and 750 mm of slump flow, the sieve screening test cannot provide a good selectivity for the powder type (only 5% range), while the lower viscous combination type shows a range between 10% and 20%. As a result of this, the screening test, according to EN 12350-11, which was invented in France was not well accepted in Germany, where traditionally highly viscous low yield stress SCCs were subject of research. Therefore, researchers in France, who typically apply SCC with lower viscosity for which the method

functions well, could not understand the confusion of their German colleagues. Another example for fields of research, which requires more detailed consideration of the mixture design approach, is the research of the fire behaviour, which is largely determined by the volumetric paste to aggregate ratio. The same is most likely valid for any observation of the transport properties of SCC, which may also be strongly influenced by the paste volume. Figure 1.8 shows a normal concrete compared to different SCC types, which show wide ranges in their constituents' volumes, though all showing good self-compacting properties. Considering these wide ranges, it is getting clear that different SCCs must not be lumped together but have to be observed in a distinguished way.

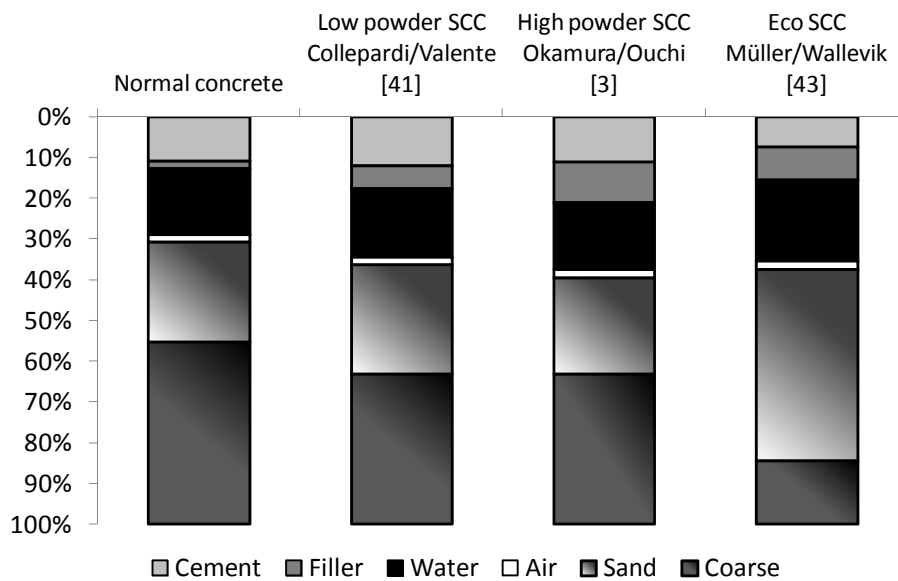


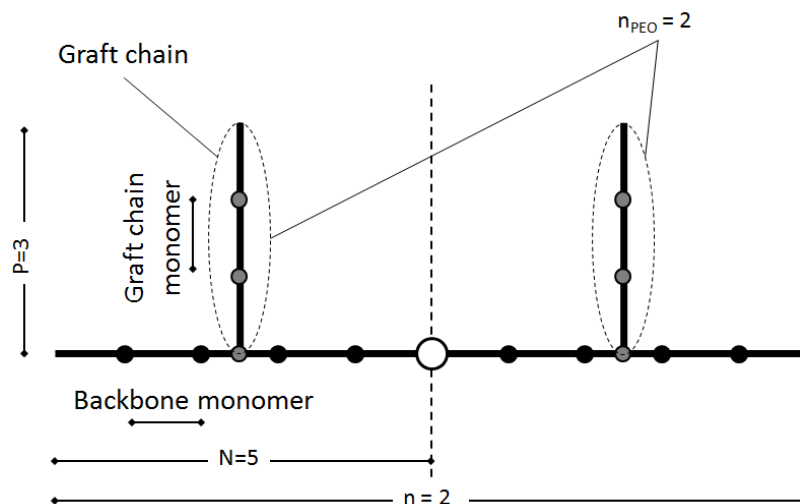
Figure 1.8: Different SCC mixture compositions based on data provided by Colleparidi and Valente, [41], Okamura and Ouchi [3], and Müller and Wallevik [43].

### 1.4.3 Influences of evolving and new constituents

Another important aspect today is that the binder technology is rapidly changing. New fillers are invented, and particularly new cement systems are brought to the market [52]. The traditional ordinary Portland cement is increasingly replaced by binary and ternary systems. This aspect needs to be considered in the interpretation of SCC data.

This applies similarly for the component, which makes SCC work properly, the superplasticiser (SP). It is generally agreed upon that self-compacting concrete shall be best produced with polycarboxylate ether (PCE) superplasticisers. These are recent state of technology, but there is little awareness today, how their peculiarities affect flowable concrete systems. Figure 1.9 shows the parameters that can be varied during the synthesis of these polymers independently. These are the length of the backbone, expressed by the number of repeated segments  $n$  and the number of monomers in the segment  $N$ , and the number of graft chain monomers  $P$  (in literature also often abbreviated by  $n_{PEO}$ ). For the entire polymer often also the number of graft chains per polymer  $n_{PEO}$  is given as characteristic value, which however also derives from  $N$  and  $n$ . Figure 1.10 shows examples of different appearances that result from variations of  $N$ ,  $P$ , and  $n$ . Depending on these parameter variations, the solution and adsorption figures of PCE as well as its adsorption behaviour varies greatly. Nevertheless most of the available literature only refers to PCE as a relatively uniform agent, which does not reflect

reality. The influence of the molecular geometry of PCE and the significant influence of the charge density will be discussed in more detail in Section 3.4.



$n$  = number of repeated backbone segments  
 $N$  = monomers along a backbone segment  $n$   
 $P$  = number of monomers in the graft chain per segment  $n$   
 $n_{PEO}$  = number of grafts per segment  $n$

Figure 1.9: Parameters that can be varied within a PCE macromolecule, the example shows a polymer with  $n=2$ ,  $N=5$ ,  $P=3$ , and  $n_{PEO}=2$ .

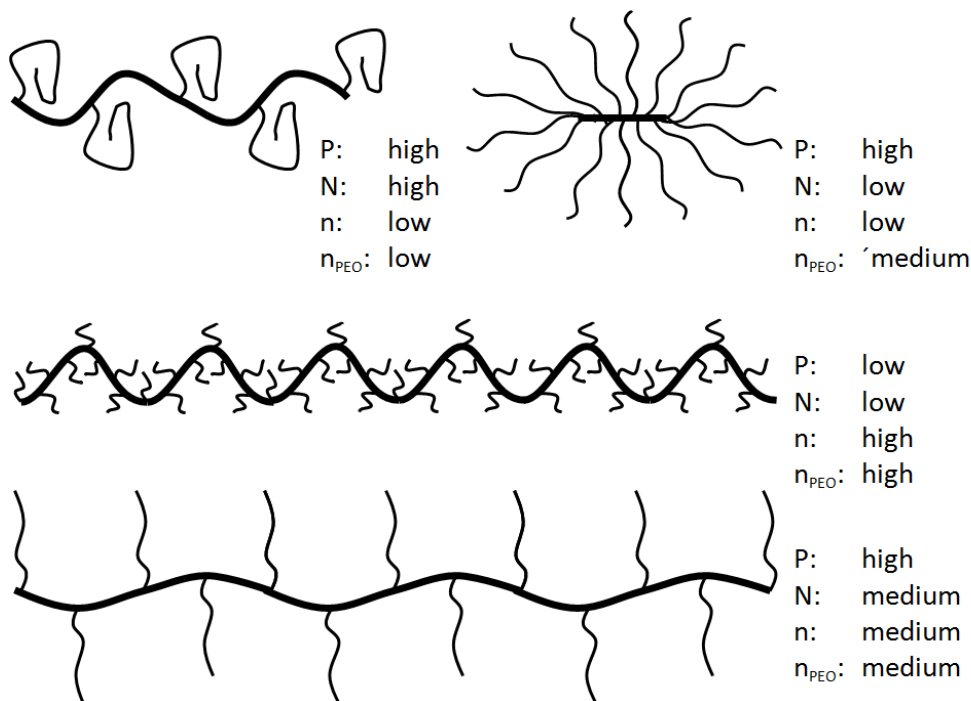


Figure 1.10: Samples of possible PCE modifications, depending on the parameters.

#### 1.4.4 The view on SCC from different fields of technology

Cement chemistry has traditionally been a field of research and many aspects are extremely well understood. One has, however, to be aware that even after more than 150 years of research in cement chemistry and despite sophisticated investigation methods, some aspects are not fully understood today. The invention of more sustainable but in return more sophisticated binder systems does not contribute to reducing the complexity.

Concrete technology is very well established since several decades, and has been steadily updated. Sophisticated mixture design and calculation methods were established, so that today, concrete can be developed according to numerous individual specifications. Nevertheless, it can be observed, that practice is more conservative than research and runs behind the rapid innovations that can be observed during the last two decades. In order to be fair, it also has to be mentioned that it is typically the concrete producing company that has to come up for the risk, in case an innovation fails to function properly.

The construction chemical industry first entered the concrete market in the 1980s with rapidly increasing influence of the technology. After adding significant positive values to the mortar and grout technology, the construction chemistry contributed to many improvements in the field of mass concrete. Technological innovations of the last 20 years, and not at last SCC, were only made possible due to innovations developed by the chemical industry.

There is mutual fertilisation within research from cement and concrete research. Examples of outstanding works that combine the research area of the binder materials with concrete technological aspects for SCC were given by De Larrard and Sedran [53], Toutou and Roussel [54] and Hunger and Brouwers [5, 32], who developed improved SCC by considering the whole particle size range, including finest fillers. Other examples focusing on the specific cement influences can be given by Khayat et al. [55] or Kubens and Wallevik [56, 57].

Significant successes have also been made in the past due to good cooperation between the fields of research in the chemistry of cement and the construction chemistry. Today, the good communication led to significant improvements in the mortar and grout technology. Outstanding works that contributed to the understanding of cement admixture interactions were published by Uchikawa et al. [15, 16], Hanehara and Yamada [17], Mollah [58], Yamada et al. [59, 60], Flatt [61, 62], Plank and Sachsenhauser [63], Lothenbach et al. [64], Winnefeld et al. [65], Schober and Flatt [66, 67].

There is also literature that combines concrete technological aspects with construction chemical aspects. However, publications that show examples of concrete with different PCE modifications, typically do not investigate, why one PCE works well, and another one does not. Most publications, deal with influences of PCEs and the amount, mostly from a concrete technological approach. It is often found that certain additions, cement types or grading optimisations can help saving PCE. It is, however, seldom considered that a simple change of the SP might have caused the same or a similar effect. Unfortunately, the innovations coming from the field of construction chemistry are not very well understood today, and unfortunately, the chemical industry was not willing or did not succeed, communicating their technology to a broad area of technologists. There is also a lack of publications from the field of construction chemistry that deals with concrete instead of cement only. On the other hand, concrete technologists are seldom willing to engage in organic chemistry. As a result, there is hardly good cooperation between these fields, which would significantly improve SCC technology.

Figure 1.11 tries to portray this situation. Good SCC technology would require the expertise from all fields addressed to before. However, there is only little effort to date, trying to bring together all three partners. Based on the literature review conducted by the author of this work, there are only two independent outstanding scientific publications, made by Schober and Flatt [66, 67], and by Yamada [68, 69], who bring together the understanding of all areas of expertise addressed to in Figure 1.11.

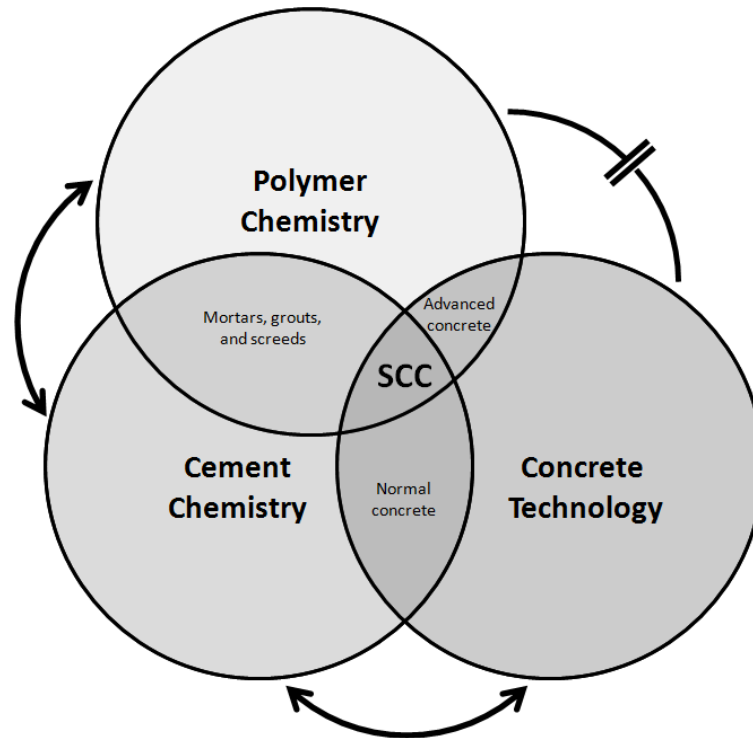


Figure 1.11: Fields of expertise required for SCC technology and communication paths between the relevant industries.

While promising that the remaining part of this work will be more seriously formulated, it must be allowed to change to a more allegoric style to conclude the above passages. In the very first chapter of his PhD Thesis, Hunger entitles SCC as a new type of concrete with “teething troubles” [5]. In the meantime, SCC has become older and can be considered probably as a teenager. In continuation of the picture about teething troubles, and considering that there is a world-wide different understanding of what is SCC, the lack of acceptance might rather be caused by a serious identity crisis of the teenage SCC, whose parents, construction chemistry and concrete technology, avoid self-discovery since they do not communicate appropriately.

## 1.5 Robustness of SCC for the construction site

### 1.5.1 Definition of robustness

In addition to cost, one major obstacle to the extensive usage of self-consolidating concrete (SCC) within the ready-mix industry is the high complexity of its constituents working together. Therefore often SCC is considered to be less robust than vibrated concrete. Hence, in order to use SCC as construction site material, the mixture needs to provide a high robustness against influences from the environmental boundary conditions.

Robustness is typically understood as stability against variations in quality and quantity of the constituents or as the capability to absorb human or process-technological uncertainties [28, 48, 56, 70, 71]. According to the glossary of the state of the art report of the RILEM Technical Committee 228 (Mechanical properties of self-compacting concrete), robustness is defined as “The characteristic of a mixture that encompasses its tolerance to variations in constituent characteristics and quantities, variations during concrete mixing, transport, and placement, as well as environmental conditions”. The latter definition also contains variations of the environmental conditions.

Most problems of SCC can be overcome by a good quality control system and improved logistics and process technologies, since they are related to influences that can be directly controlled by the staff. However, the environmental conditions during the whole concreting process can only be predicted by weather forecast, but moderate to rapid temperature changes at the construction site can cause trouble during SCC casting. During the casting on the construction site, temperatures may vary throughout one day as well as when seasons change. The robustness of ready-mixed concrete with respect to such environmental temperatures can thus be considered as a major key to improving the acceptance of SCC technology for ready-mixed applications.

### 1.5.2 Importance of consideration of the ambient temperature

SCC technology is predominantly applied as pre-cast concrete. As reported by Brameshuber and Übachs [72] already slight changes of the temperature might already cause serious problems for the workability or the durability of SCC. From that point of view temperature dependent performance changes are generally critical for pre-cast, and ready-mixed or construction site concreting. However, the range of temperatures that are likely to occur during casting is much wider in the field of the ready-mixed concrete.

Table 1.3: Overview about temperature ranges in different geographical areas.

Country	City	Annual temperature range [ °C]	Specification
Czech Republic	Prague	approx. -3 to 25	Deduced from Kossobokov et al. [73]
Italy	Bologna	approx. -1 to 30	Deduced from Kossobokov et al. [73]
Belgium	Uccle	approx. -1 to 23	Deduced from Kossobokov, et al. [73]
Canada	Montreal	approx. -25 to 40	Deduced from Khayat et al. [74]
USA	Coopers town	approx. -12 to 25	Deduced from Robinson et al. [75]
Argentina	n/a	10.05 to 22.51	Winter and summer, Seo [76]
China	Laoshan	-16 to 21	According to Saigusa et al. [77]
Japan	Kiryu Exp.	2 to 29	According to Saigusa et al. [77]

Table 1.3 provides examples of different annual temperature ranges collected from literature. The annual temperature differences are of importance in case of casting the same concrete mixture composition at different periods of the year. However, temperatures can also strongly vary throughout a single day, which is even more critically for concreting. For example, the compendium “Digitaler Umweltatlas Berlin, 2001” [78] provides data from July 8, 1991, where daily temperatures measured at a height of 2 m above the ground varied between 10.2 °C and 17.5 °C within 24 hours, depending upon the location. Khayat et al. report about SCC that was cast in Montreal during a day, when ambient temperatures varied between 10 °C in the night and 30 °C during the day [74].

The annual as well as the daily temperature changes are a serious threat to SCC, since the handling of performance loss is much more delicate than it is for normal concrete. While for vibrated concrete stiff consistencies can be partly compensated by higher or longer vibration than usually applied, vibrating SCC can cause segregation, which would likely deteriorate the structure even more than inadequate filling.

## 1.6 Temperature dependent differences between SCC and normal concrete

### 1.6.1 Influence of temperature on the workability of normal concrete

As reported by several authors [79-83], upon addition of water, metal ions, calcium ions ( $\text{Ca}^{2+}$ ), sulphate ions ( $\text{SO}_4^{2-}$ ) hydroxide ions ( $\text{OH}^-$ ) and smaller amounts of aluminates and silicates are precipitated into the solution. Within short time, a gel like layer, which is rich of alumina and silica, forms around the surfaces of the cement grain and within approximately 10 minutes ettringite (AFt) forms stubby rods on the surfaces of the grain and in the solution. The latter are generated from sulphate and aluminate reaction. Depending upon the sulphate and aluminate contents, besides AFt also monosulphate or gypsum can occur. After this initial reaction, an induction period occurs for several hours at which no significant amounts of new reaction products are building. The induction period is often also entitled “dormant period”, which may lead to misinterpretation, since indeed reactions yielding morphological changes on the surfaces take place. According to Locher [80], the AFt phase undergoes re-crystallisation during the induction period although no new reaction products are built or chemical reactions take place, which is brought in context with loss of workability. According to Yamada et al. [18] the specific surface area (SSA) of cement paste increases steadily throughout the first 120 minutes after water addition. The latter changes took place quicker at high temperature and slower at low temperature. SSA is the surface related to the mass and a higher value thus indicates more hydration reactions. Hence, temperature acts as accelerator or retarder of reactions, typically generating a quick loss of workability at high temperature and extended workability time at lower temperatures.

### 1.6.2 Influence of temperature on the workability of SCC

The formerly mentioned effects of temperature on the workability basically taking place in the binder paste are generally valid for SCC and normal concrete. The major difference between SCC and normal concrete is the high amount of SP that is used in SCC. As reported by many authors, SPs adsorb on the surfaces of cement and mineral particles [22, 61, 66, 84-86]. As all common types of SPs provide a negatively charged backbone as adsorbing unit, they are typically attracted by positively charged surfaces or upon flow by areas providing a positively charged zeta potential ( $\zeta$ ). According to Plank and Hirsch [87], adsorption of SPs mainly takes place on the surfaces of the clinker phases tricalcium aluminate ( $\text{C}_3\text{A}$ ) and tetracalcium alumina ferrite ( $\text{C}_4\text{AF}$ ) (see Table 2.1) as well as on the hydration reaction phases monosulphate and AFt (see Table 2.2), of which AFt provides the highest  $\zeta$ . If in case of SCC, high amounts of SP are

added to the mixture, certain amounts of PCE might not adsorb immediately but with time shift upon formation of ettringite. This means that the AFt phase, which reduces the workability of a cementitious system without SP, virtually provides flowability in a system including SP.

Finally two opposing effects act in parallel in SCC, which are determined by the temperature. While increasing temperature negatively affects the workability by accelerating the hydration, the accelerated growth of ettringite quickly provides large adsorption sites for SPs, which again positively affects the flowability. Decreasing temperatures positively affect the workability retention but as a result of slow hydration might not generate sufficient adsorption sites for SPs, so that they remain ineffectively in the solution.

Hence, as presented in Figure 1.12, the temperature dependent behaviour of concrete without or with only small amounts of SP is always controlled by effects of the temperature on the hydration velocity. For concrete containing high amounts of SP varying concrete temperatures affect the hydration velocity and supplementary also the adsorption of SP, while both effects oppose each other.

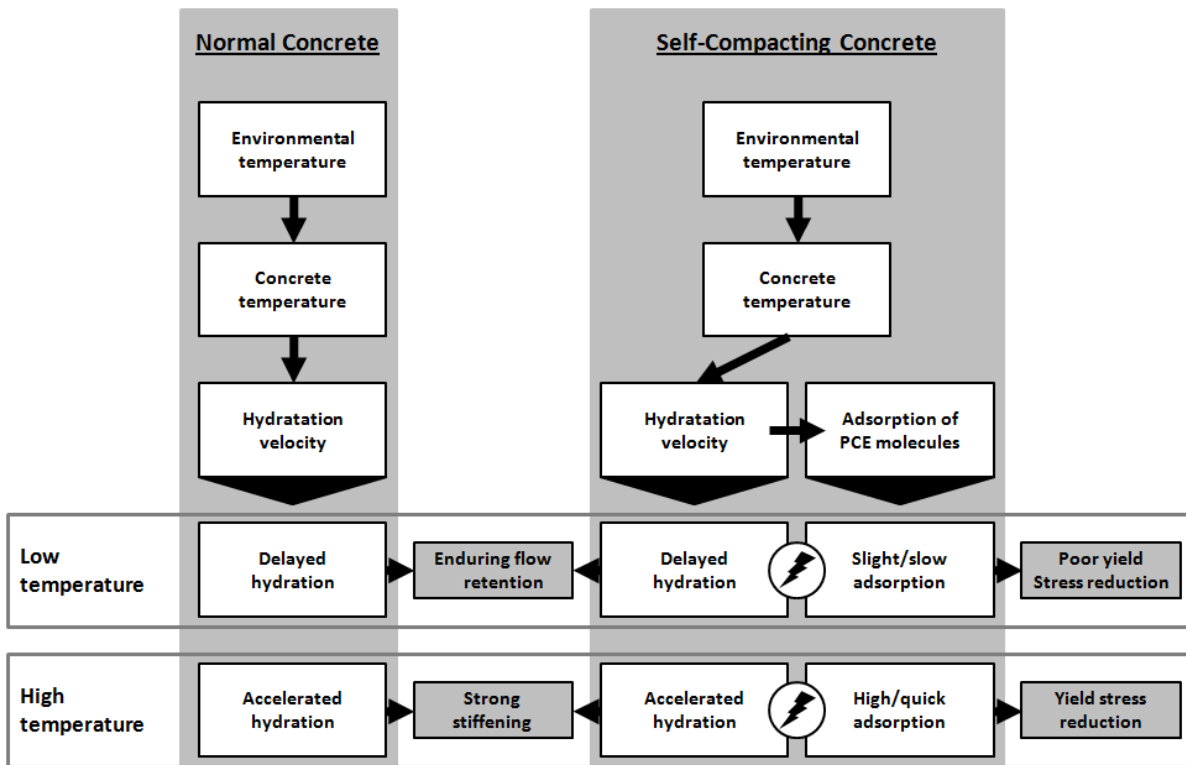


Figure 1.12: Difference between normal concrete and SCC at exposure to varying temperature.

## 1.7 Outline of this Thesis

On international level, SCC today covers an incredible variety of different types of flowable concrete. It is therefore the aim of this work to observe largely free from any normative boundary conditions, and to interpret largely free from any performance limits.

It was concluded that the major factors limiting the use of SCC as ready-mixed concrete are lack of knowledge that helps improving the robustness. A major problem field for SCC in practice are scattering environmental temperatures. The aim of this work is the understanding the influences that affect the performance of SCC at varied temperature. It was further introduced that there is a major lack of knowledge that approaches SCC from all relevant fields of research, the construction chemistry, the cement chemistry, and the concrete technology. This work therefore tries to combine the knowledge existing in all these fields in order to develop a concept that helps improving the robustness of SCC as ready-mixed concrete against influences resulting from the environmental temperature.

This requires detailed understanding of the influencing factors. It was shown in the passage before that the major factor that distinguishes SCC from normal concrete with regard to the temperature performance is the interaction between the high amount of PCE and the cement hydration. It is thus unavoidable to provide deeper understanding of the cement hydration processes in general and the interactions between PCE and cement hydration. Therefore, following this introducing Chapter 1, the Chapter 2 provides a brief overview about the processes during the early hydration up to the decelerating period. Based on this chapter, in conjunction with a fundamental rheology background the functioning of SPs and particular PCEs is introduced in Chapter 3. While the Chapters 2 and 3 provide the relevant theoretical background, prior to the experimental part Chapter 4 explains in detail the background of the applied test methods and the setup of the parameter variations that are necessary for the experimental Chapters 5 to 9.

Based on Chapter 3, a simple experimental setup is developed in Chapters 5, which helps qualitatively estimating the performance of different PCEs for the application in different fields. This experiment will be of importance for the recommendations given in Chapter 10.

Chapters 6 and 7 focus on temperature related effects on the rheology of SCC. Chapter 6 first gives a critical review of the research on the temperature behaviour to date and concludes that PCE influences were neglected so far. The experimental part therefore focuses on influences resulting from the major influencing factor for the temperature related performance, the PCE modification.

However, it will be shown that the temperature related performance cannot be freed from the mixture composition, particularly the water to powder ratio. This finally yields the conclusion that combined effects from the mixture composition and the PCE modification need to be taken into account. Chapter 7 focuses on influences of differently modified stabilising agents (STAs) on the rheology at varied temperatures. It first gives a brief theoretical background of polysaccharides, which is amended by some practical paste tests with and without SPs. Based on these observations the effects of STAs in combination with differently modified PCEs are discussed on rheological experiments on concrete scale.

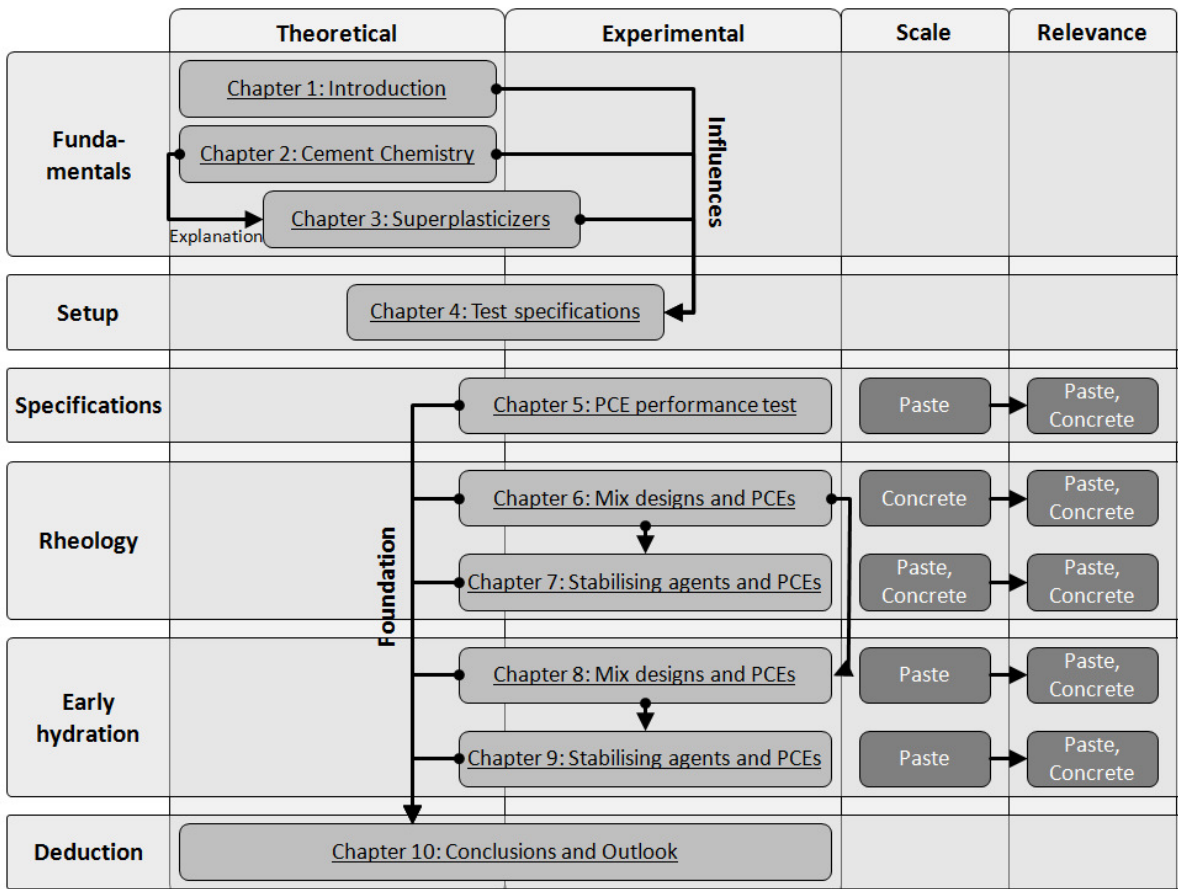


Figure 1.13: Flow chart of the structure of this Thesis.

Chapters 8 and 9 put the focus on observations during the early hydration period. This is an important matter since SPs and STAs are typically added to mixtures in order to modify the rheology. Upon addition they cannot be taken out of the mixture again as soon as the concrete is placed. Hence, rheological optimisations are always accompanied by effects on the early hydration, such as effects on setting, heat evolution, and early deformations. Chapter 7 focuses on the influence of the charge density of a PCE and their particular influence on effects during the early hydration. In Chapter 8, the interactions of STAs with cement hydration are observed under consideration of interactions with differently modified PCEs. The major observations of both chapters are made on paste scale, but conclusions supported by experimental methods transfer the findings of the paste level to the concrete level.

Chapter 10 incorporates the results of the Chapters 6 to 9 and amends them with the rapid PCE performance test suggested in Chapter 5, in order to develop concepts for SCCs for particular climatic conditions or for high robustness against temperature variations. Chapter 10 finally concludes the work by discussion about the range of the findings and suggesting future research focal areas that further help improving the understanding of SCC at variable temperatures and admixture types and dosages.

## 1.8 Definitions and abbreviations

Before issues of SCC are discussed in more technical detail, a brief overview of the most important definitions and abbreviations shall be given. The definitions listed in Table 1.4 largely follow the glossary that is being used in the RILEM Technical Committee 228-Mechanical properties of Self-Compacting Concrete.

Table 1.4: Definitions and abbreviations used in this Thesis.

	Abbr.	Description
Admixtures		Chemical admixtures that modify fresh or hardened concrete properties
Alite	C <sub>3</sub> S	Tricalcium silicate
Belite	C <sub>2</sub> S	Dicalcium silicate
Aluminate	C <sub>3</sub> A	Tricalcium aluminate
Ferrite	C <sub>4</sub> AF	Tetracalcium alumina ferrite
Ordinary Portland cement	OPC	Cement consisting of ordinary Portland cement clinker
Cement	c	Ordinary Portland cement and blended cement
Supplementary cementitious materials	SCM	Inert and reactive materials for the blending of ordinary Portland cement
Fillers		Inert materials finer than 125 µm
Cementitious materials	cm	Reactive materials finer than 125 µm including cement
Additions		Fillers and cementitious materials
Powders	p	Cement, additions, and if specified sand and aggregate components < 0.125 µm
Limestone filler	LSF	Filler consisting mainly of calcium carbonate
Fly ash	FA	Mostly pozzolanic residue of the coal firing
Ground granulated blast furnace slag	GGBS	Glassy, granular, largely latent hydraulic by-product from steel production
Quartz filler	QF	Mostly quartzitic filler
Sand		Fractions between 0.125 µm and 4 µm, if not differently specified
Coarse aggregates		Fractions between 4 mm and 16 mm, if not differently specified
Aggregates		Sand and coarse aggregates
Binder	b	Water, cementitious materials, air content, and admixtures
Paste	p	Water, powders, air content, and admixtures
Mortar		Paste and sand
Concrete		Mortar and aggregate
Self-compacting concrete	SCC	Concrete that levels without need for significant vibration or agitation
Powder type SCC	POW	SCC with high powder content
Combination type SCC	COM	SCC with moderate and low powder content that contains stabilising admixtures



## 2 The early hydration of cementitious materials

### 2.1 The early hydration of ordinary Portland cement

#### 2.1.1 Introduction

Ordinary Portland cement is an inorganic finely ground material, which reacts with water to form a solid structure. The major component is the cement clinker, which is typically produced by in a rotational kiln at about 1450 °C during which the solid impure tricalcium silicate phases and the impure dicalcium silicate phases are sintered into the interstitial aluminate and ferrite phases. The clinker together with gypsum, which acts as set retarder, is later ground to give a particle range between few and about 100 µm. Table 2.1 provides an overview of the four major reactive phases of ordinary Portland cement and different gypsum conformation, which are added or yielded during the grinding process.

Table 2.1: Clinker phases and OPC constituents and abbreviations.

Component	Cement terminology	Chemical formula	Cement notation	Typical ranges [88]
Tricalcium silicate	Alite	$3\text{CaO} \cdot \text{SiO}_2$	$\text{C}_3\text{S}$	45-80%
Dicalcium silicate	Belite	$2\text{CaO} \cdot \text{SiO}_2$	$\text{C}_2\text{S}$	0-32%
Tricalcium aluminate	Aluminate	$3\text{CaO} \cdot \text{Al}_2\text{O}_3$	$\text{C}_3\text{A}$	4-14%
Tetracalcium aluminoferrite	Ferrite	$2\text{CaO} \cdot (\text{Al}_2\text{O}_3, \text{Fe}_2\text{O}_3)$	$\text{C}_4\text{AF}$	7-15%
Gypsum	Calcium sulphates	$\text{CaSO}_4 \cdot 2\text{H}_2\text{O}$	$\bar{\text{S}}$	1-5%
Calcium sulphate hemihydrate		$2\text{CaSO}_4 \cdot \text{H}_2\text{O}$		
Anhydrite		$\text{CaSO}_4$		

Upon addition of water cement immediately starts reacting. The hydration of cement is a complex subject, since several clinker components strongly interact. An overview of some relevant reaction phases, the respective reaction partners and the reaction are given in Table 2.2. During the first hours of hydration, the main reacting clinker phases are  $\text{C}_3\text{A}$  and  $\text{C}_3\text{S}$  as well as calcium sulphates from the set retarder and alkali sulphates, which quickly dissolve from the clinker upon water addition. The major reaction products occurring during the early hydration are  $\text{Ca}(\text{OH})_2$ , C-S-H, AFm and AFt phases.

This chapter focuses on the effect of SPs in different modifications on early effects such as setting and deformations, which can be strongly related to the early hydration of cement. In order to better understand these influences the critical steps in the early hydration are discussed. The major reacting phases, responsible for the early hydration effects are  $\text{C}_3\text{A}$  and  $\text{C}_3\text{S}$ , hence, their hydration characteristics are discussed separately at first before the cement hydration and interactions with SPs are introduced.

#### 2.1.2 Early hydration of alite

Today, the reaction pattern of the alite hydration is well investigated, though investigations of pure  $\text{C}_3\text{S}$  and alite may exhibit differences due to their different degrees of purity. Typically, the hydration process is illustrated by heat flow curves, as shown in Figure 2.1. According to Scrivener and Nonat [89], the hydration can be separated into five phases.

Table 2.2: Reaction phases and abbreviations.

Reaction product	Abbreviation	Reacting phases	Chemical formula	Cement notation	Reaction
Calcium hydroxide (Portlandite)	CH	Alite, belite	$\text{Ca(OH)}_2$	CH	$2\text{C}_3\text{S} + 10.6\text{H} \rightarrow \text{C}_{3,4}\text{S}_2\text{H}_8 + 2.6\text{CH};$ $2\text{C}_2\text{S} + 8.6\text{H} \rightarrow \text{C}_{3,4}\text{S}_2\text{H}_8 + 0.6\text{CH}$
Calcium silicate hydrate	C-S-H		$2\text{CaO} \cdot \text{SiO}_2 \cdot 3\text{H}_2\text{O}$	$\text{C}_{3,4}\text{S}_2\text{H}_8^*$	
Calcium aluminate hydrate	C-A-H	Aluminate	$3\text{CaO} \cdot \text{Al}_2\text{O}_3 \cdot 6\text{H}_2\text{O}$	$\text{C}_3\text{AH}_6$	$\text{C}_3\text{A} + 6\text{H} \rightarrow \text{C}_3\text{AH}_6$
$\text{Al}_2\text{O}_3$ - $\text{Fe}_2\text{O}_3$ -tri	AFt	Aluminate (ferrite), gypsum	$3\text{CaO} \cdot \text{Al}_2\text{O}_3 \cdot 3\text{CaSO}_4 \cdot (30-32)\text{H}_2\text{O}$	$\text{C}_6\text{A}\bar{\text{S}}_3\text{H}_{32}$	$\text{C}_3\text{A} + 3\text{C}\bar{\text{S}}\text{H}_2 + 26\text{H} \rightarrow \text{C}_6\text{A}\bar{\text{S}}_3\text{H}_{32}$
$\text{Al}_2\text{O}_3$ - $\text{Fe}_2\text{O}_3$ -mono	AFm**	Aluminate (ferrite), gypsum	$\text{C}_3\text{A} \cdot \text{CaSO}_4 \cdot 12 \text{H}_2\text{O}$	$\text{C}_4\text{A}\bar{\text{S}}\text{H}_{12}$	$2\text{C}_3\text{A} + \text{C}_6\text{A}\bar{\text{S}}_3\text{H}_{32} + 4\text{H} \rightarrow 3\text{C}_4\text{A}\bar{\text{S}}\text{H}_{12}$ (ettringite conversion); $\text{C}_3\text{A} + \text{C}\bar{\text{S}}\text{H}_2 + 10\text{H} \rightarrow \text{C}_4\text{A}\bar{\text{S}}\text{H}_{12}$
*Example. exact stoichiometry may vary					
**also used to denote sulphate free AFm phases, e.g. $\text{C}_4\text{AH}_{13}$					

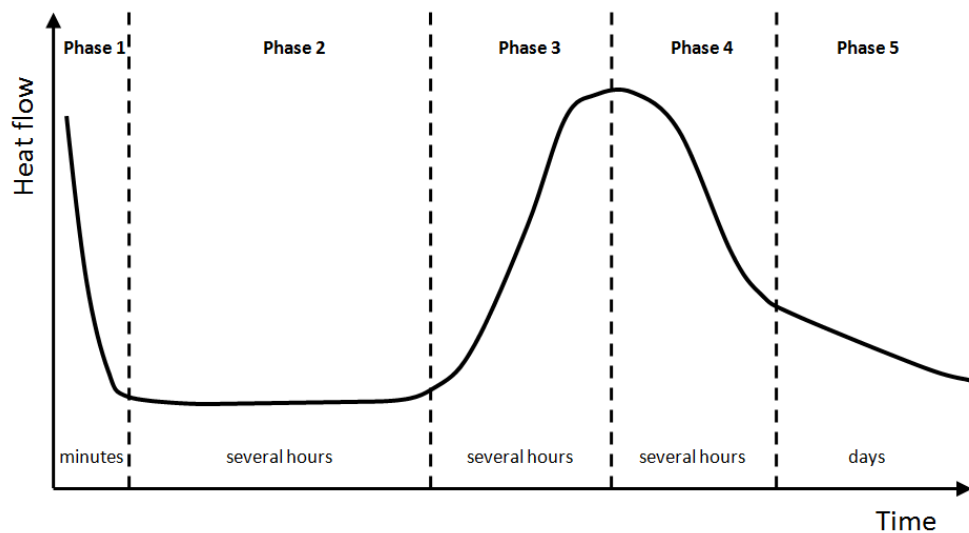


Figure 2.1: Heat evolution rate during the hydration of alite separated into five stages after Scrivener and Nonat [89].

In phase 1, which typically lasts for only a couple of minutes, rapid reactions can be observed between water and  $C_3S$ , yielding a high exothermic signal in the heat flow curves. Phase 2 is characterised by a sudden slow down of the reaction. This period, which can last for about an hour [90] in case no chemical admixtures retard the hydration, is typically called induction period or dormant period. Phase 3 is the acceleration period in which a rapid formation of C-S-H can be observed, which after reaching a maximum slows down in phase 4. Scrivener and Nonat furthermore separately observe the hydration beyond 24 h, here phase 5, where the hydration continues to go on slowly [89]. The latter phase is often not distinguished separately or not paid attention for in research studies or the first three phases are combined to a single phase [79, 80].

To date, it is controversially discussed, which mechanisms lead to the induction period and the onset of the  $C_3S$  hydration. According to a recent review by Bullard et al. [91], the existing theories can be distinguished between a “metastable barrier theory” and a “slow dissolution step hypothesis”. The eldest and widely accepted theory is the first mentioned, based on the assumption that a protective layer consisting of an intermediate reaction phase forms around the grain surfaces, thus hindering the further reaction process by either restricting the access of water or limiting the diffusion of ions or only certain ions away from the surfaces [80, 82, 92-97]. More recently, a new explanation model based on pure dissolution and precipitation driven hydration has been developed that is based on the research of Garrault and Nonat [98]. They state that the level of undersaturation determines the dissolution, so that hydration occurs quickly at high levels of undersaturation but largely comes to a rest above a certain threshold level. The mechanism is explained comprehensively in a review by Scrivener and Nonat [89]. Anhydrous particles dissolve to produce hydrated particles in the solution. The undersaturation caused by the precipitation of one phase gives drive to another phase to dissolve. The dissolution takes place in the order of solubility of the phase in a particular composition of the pore solution. While the dissolving particle decreases, the hydrating particle increases in size.

This theory has been recently linked to the formation of pits related to dissolution processes by Juilland et al. [99]. With increasing level of undersaturation, the opening mechanisms vary from step retreat, etch pit opening from dislocations, or impurity defects or vacancy islands from nucleation, respectively. In the same order, the dissolution rate increases. The morphological

studies were conducted with water to cement ratios in the range of 1000. In experiments with alite, they have shown that a high number of etch pits could be observed in case de-ionised water was used, while this was not the case in a lime saturated solution. This theory has been subject of intensive discussion. Gartner criticises that the solubility of alite assumed for Juilland's research was not based on actual data [100]. According to Juilland's response [101], the assumption of a solubility of moderately soluble salts would not yield different results. Further criticism by Gartner is related to the high water cement ratio that was used in Juilland's investigations and the large number of assumptions required for the calculation of the results. The high water to cement ratio was also criticised by Makar et al. [102]. They refer to own results and report that etch pits do typically not appear before the onset of the main hydration reactions in realistic water to cement ratios [103]. Etch pits only appear earlier in the exceptional case of extremely high reactive surfaces or excessive water, as used in Juilland's study. Juilland responds that the water to cement ratio mainly affects the size of the pits [104].

Scrivener and Nonat provide an overview of the mechanisms driving the early hydration of cement based on the dissolution theory including the occurrence of etch pits upon water addition [89]. They doubt the existence of a protective layer for the two reasons: despite sophisticated observation techniques that are available today a protective layer has not yet been observed directly, and the atomic structure of C-S-H would make it unlikely to build an impermeable layer. According to their review, which combines the approach of Garrault and Nonat [98], and Juilland et al. [99], the hydration is driven by the extra energy provided by over- and undersaturated states of the pore solution. Upon water addition, the undersaturation is high, yielding dissolution and providing extra energy for etch pits on surfaces. After a certain threshold level, the dissolution rate slows down, and further dissolution can only take place through step retreat from existing defects.

Bellmann et al. give new evidence again to the existence of a passivation layer by showing that the free unconstrained dissolution of  $C_3S$  is much higher than the calculated dissolved fraction, obtained from calorimetric investigations. This difference can only occur, if the free dissolution is disturbed. A hydrate layer directly on the surface of dissolved particles would explain this difference [95, 96].

Despite the fact, that discussions about the hydration of C-S-H continue on a high scientific level, two opinions about the induction period still exist, which do not fully harmonise. The dissolution-precipitation model, which explains the hydration initiation by the geochemical approach of differently shaped pitting etches that allow dissolution depending on the saturation level in the solution, is strong. It is supported by considerable names in the scientific community, such as Bullard, Jennings et al. [91] or Scrivener and Nonat [89] and the basic mechanisms are generally agreed upon; e.g. Bellmann [96] does not doubt the basic mechanism, but he points out that the dissolution precipitation process cannot be the only effect.

Bullard and Flatt [90] discuss existing theories and perform simulations under varied boundary conditions. They separate existing research data into two groups, according to either a passivation layer hypothesis or a site de-activation hypothesis, similar to the review of Bullard et al. [91]. They conclude that both hypotheses yield reasonable results in the presence of Portlandite ( $Ca(OH)_2$ ). A hypothetical investigation in which  $Ca(OH)_2$  was not allowed to precipitate, yielded different results depending upon the hypothesis. This hypothetical case is yet not practicably imitable in experiments, since no additive is known that would adsorb on  $Ca(OH)_2$  without affecting  $C_3S$  or C-S-H.

The focus of the Bullard and Flatt's study is not placed on the induction period but on the onset of the accelerated hydration, the transition from phase 2 to 3. This particular step in time is also not yet fully understood. In this phase, two mechanisms take place in parallel,  $Ca(OH)_2$  precipitates, while in parallel C-S-H grows rapidly. According to Scrivener and Nonat [89], the

reason for the onset of the acceleration period follows the same principle responsible for the induction period, a dissolution-precipitation process. Portlandite precipitates, causing reduced  $\text{Ca}(\text{OH})_2$  concentration in the pore solution. This undersaturates the solution with respect to  $\text{C}_3\text{S}$ , which dissolves until supersaturation with respect to C-S-H, which then precipitates.

### 2.1.3 The early hydration of aluminate phases

During the very first stage, rapidly ettringite and AFm are built. Chatterji and Jeffery [105] could not find significant amounts of ettringite during the first hours of hydration with different cement types observed, while Schwiete [106] concludes that ettringite is the main initial reaction product. Schwiete assigns Chatterji and Jeffery's observation to the fact that laboratory cements were used. According to the comprehensive works by Locher [80, 107-109], the formation of ettringite or monosulphate, depends upon the solubility of the  $\text{C}_3\text{A}$ , the set retarder as well as numerous factors related to the cement production and clinker composition. According to Taylor [82] the first reaction products to occur are AFt rods. In recent experiments with synchrotron XRD by Schlegel et al. [110, 111], it was shown that besides monosulphate significant amounts of ettringite are formed immediately upon the addition of water and that after approximately six minutes the reaction levels off (Figure 2.2). In these experiments, cement particles were levitated in an ultrasound trap and water was sprayed onto the particle in parallel to the measurement. By this setup, the very first seconds could be monitored.

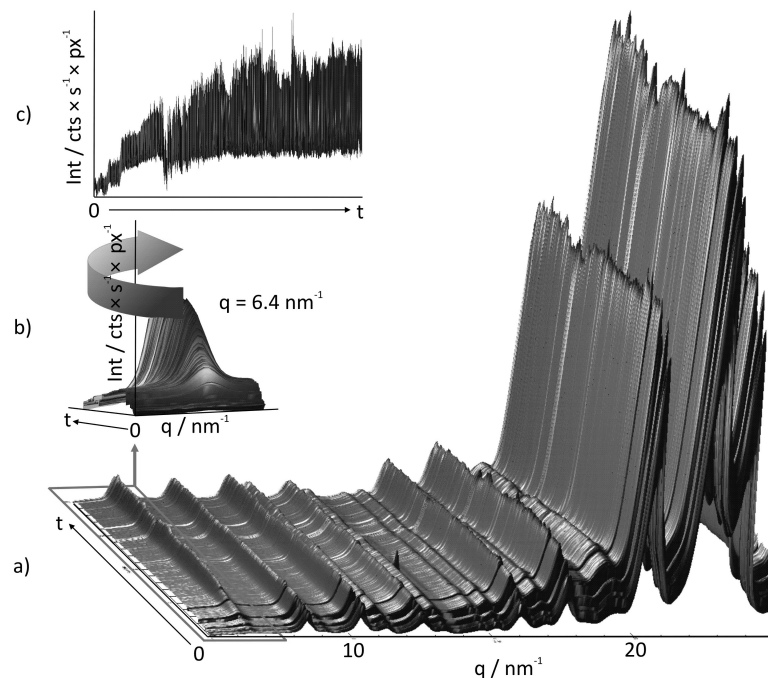


Figure 2.2: Very early ettringite formation ( $t = 0-6$  min) [110].

All these observations, though related to the  $\text{C}_3\text{A}$  hydration, were made with cements. There is not much literature available, which focuses on the hydration of  $\text{C}_3\text{A}$  only. Minard et al. [112] found ettringite on the surfaces of  $\text{C}_3\text{A}$  grains as well as AFm phases after 3 minutes, the latter predominating, for  $\text{C}_3\text{A}$  only. They divide the  $\text{C}_3\text{A}$  hydration into two periods, of which the first can be subdivided again into three stages, as marked with (a), (b), and (c) in Figure 2.3.

During the first period, the consumption of sulphates and calcium is higher than the dissolution rate of gypsum, which can be caused by the formation of AFm and AFt as well as adsorption on  $\text{C}_3\text{A}$ . From experiments with lime saturated solution with and without gypsum

excess, which yield identical heat flow values for  $C_3A$  during the first 30 seconds and varying curves after 45 seconds, Minard et al. [112] conclude that during the first 30 s  $C_3A$  dissolution and instantaneous AFm precipitation occur independently of the presence of gypsum. In the further progress, the hydration slows down significantly. According to Minard et al., calcium and sulphate ions consumed by ettringite formation are replaced by gypsum dissolution. The peak observed in the centre of period (b), is allocated to accelerated ettringite formation, and in the last period (c), sulphate ions are only consumed from the solution, which gives evidence that the gypsum had been already consumed in period (b).

Period 2 is characterised by a sharp exothermic signal followed by a smaller one. Based on the research of Lerch [113], this peak is typically attributed to the depletion of sulphates [114, 115]. According to the research of Minard et al., at this particular point in time, there is an undersaturation of monosulphoaluminate calcium and hence, they conclude that this peak cannot be attributed to the rapid transformation of ettringite to monosulphoaluminate, to which, according to Taylor (without mentioning references) [82], it has often been erroneously linked to. It is in line with the observations of Pratt and Ghose, who ascribe this peak rather to a formation than a decomposition of ettringite [116]. Minard et al. explain this peak by dissolution of  $C_3A$ , which yields supersaturation of AFm, which then precipitates. The second exothermal peak observed in period 2 in Figure 2.3 is then attributed to the slow dissolution of ettringite and the precipitation of more stable AFm.

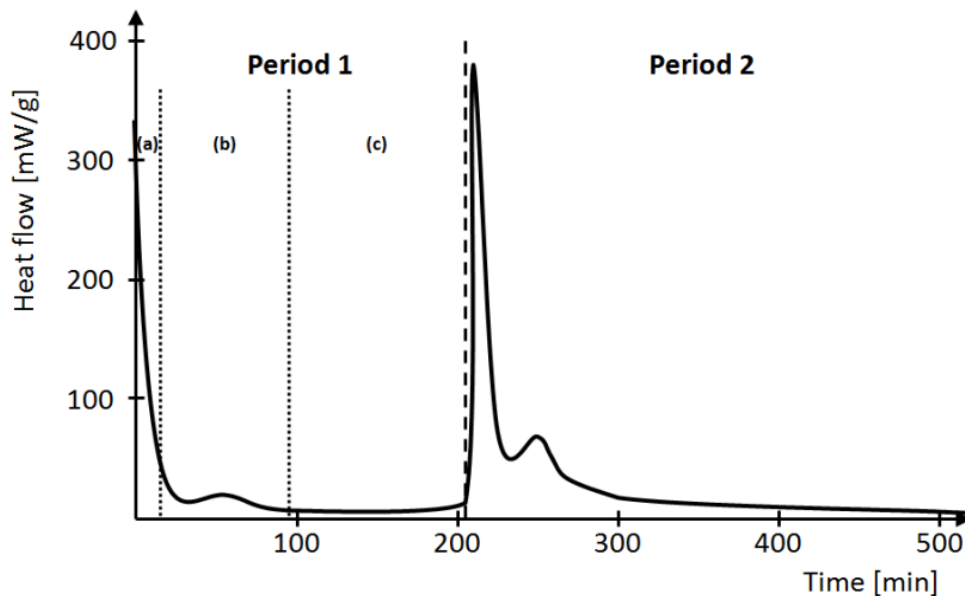


Figure 2.3: Heat flow of  $C_3A$  and gypsum in portlandite saturated solution after Minard et al. [112].

Despite controversial observations in details, the hydration reaction of  $C_3A$  with gypsum shows similar characteristics as the  $C_3S$  reaction, as stated by Scrivener and Nonat [89]. A rapid initial reaction takes place, an induction period, in which the reaction is significantly slowed down can be observed before the reaction accelerates again. As in the discussion about the  $C_3S$  reaction, the reasons for the induction period are discussed controversially. As concluded in a review by Skalny and Tadros [117], in the past, it was assumed that a more or less impermeable ettringite layer forms around the surfaces, which blocks the hydration. The authors, however, conclude that ettringite may not be the primary reason for retardation but rather the reduction of active dissolution sites due to  $Ca^{2+}$  adsorption. Also Scrivener and Nonat doubt the existence of

an impermeable ettringite layer. They state that the stick-like morphology of ettringite crystals makes it absurd to assume these can generate a water-tight layer. As with the hydration of  $C_3S$ , the authors support a dissolution-precipitation driven approach as also proposed by Minard et al. [112].

#### 2.1.4 Hydration of cement

In cementitious systems, the aforementioned hydration characteristics of the alite and aluminate hydration overlap. It is discussed, whether the hydration of  $C_3A$  or  $C_3S$  is quicker. According to Pratt and Ghose the induction period of the alite hydration ends earlier than of the  $C_3A$  hydration [116]. The authors characterise the cement hydration by four characteristic peaks as shown in Figure 2.4. According to Taylor [82], who adopted this graph, the first peak is induced by exothermic wetting and early reactions, yielding a gel coat and AFt phases. The second peak, which is the main peak, is determined by the hydration of  $C_3S$  to C-S-H and  $Ca(OH)_2$ . Taylor conforms to Pratt and Ghose that the third peak is due to renewed hydration of  $C_3A$ , forming rods of ettringite. Peak 4 is either associated with the hydration of the ferrite phase as stated by Pratt and Ghose or with the conversion of AFt to AFm, as formulated by Scrivener [79] and Minard et al. [112].

A time resolved overview of the evolution of the hydration phases can be seen in Figure 2.5, which exhibits the experimental works of Locher et al. from 1976 [80] compared to thermodynamic calculation by Lothenbach and Winnefeld from 2006 [118]. In the latter case the prediction yielded monocarbonate as AFm phase, however, according to the discussion of the authors other AFm phases are likely to precipitate. A further assumption made was the absence of carbonate. This assumption excludes the disappearance of ettringite.

Both figures show results of cement pastes with a w/c of 0.5 and are qualitatively very similar. They only show differences in the behaviour of ettringite and AFm phases. Differing to Locher et al., today, it is generally assumed that ettringite does not fully disappear, as e.g. shown by Minard et al. [112] and Lothenbach et al. [119]. According to Lothenbach [118], ettringite would only disappear in absence of carbonate.

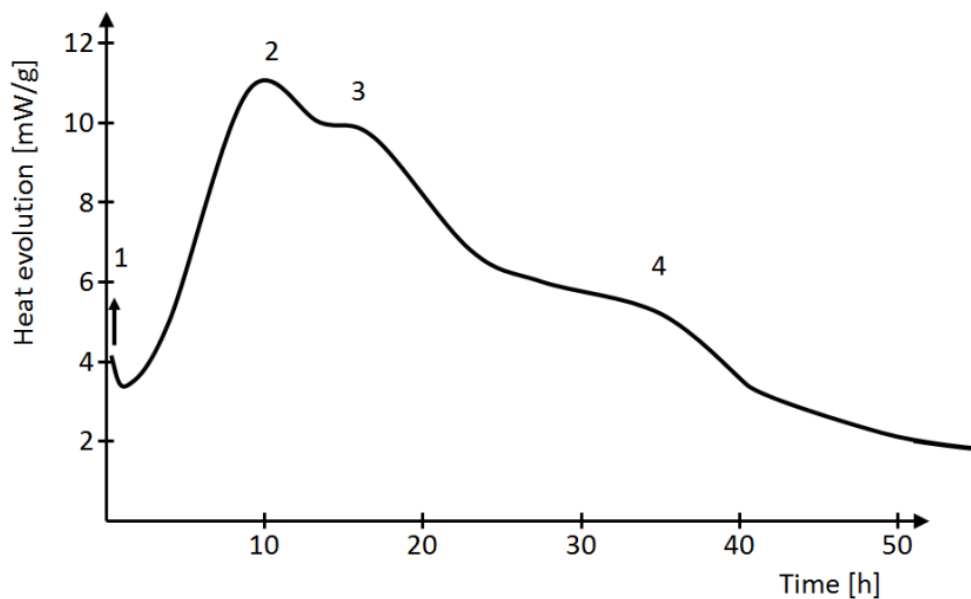


Figure 2.4: Cement hydration after Pratt and Ghose [116]. Peak 1: Wetting and early reactions; Peak 2: Hydration of  $C_3S$ ; Peak 3: Renewed hydration of  $C_3A$ ; Peak 4: Hydration of ferrite and/or conversion of AFt to AFm.

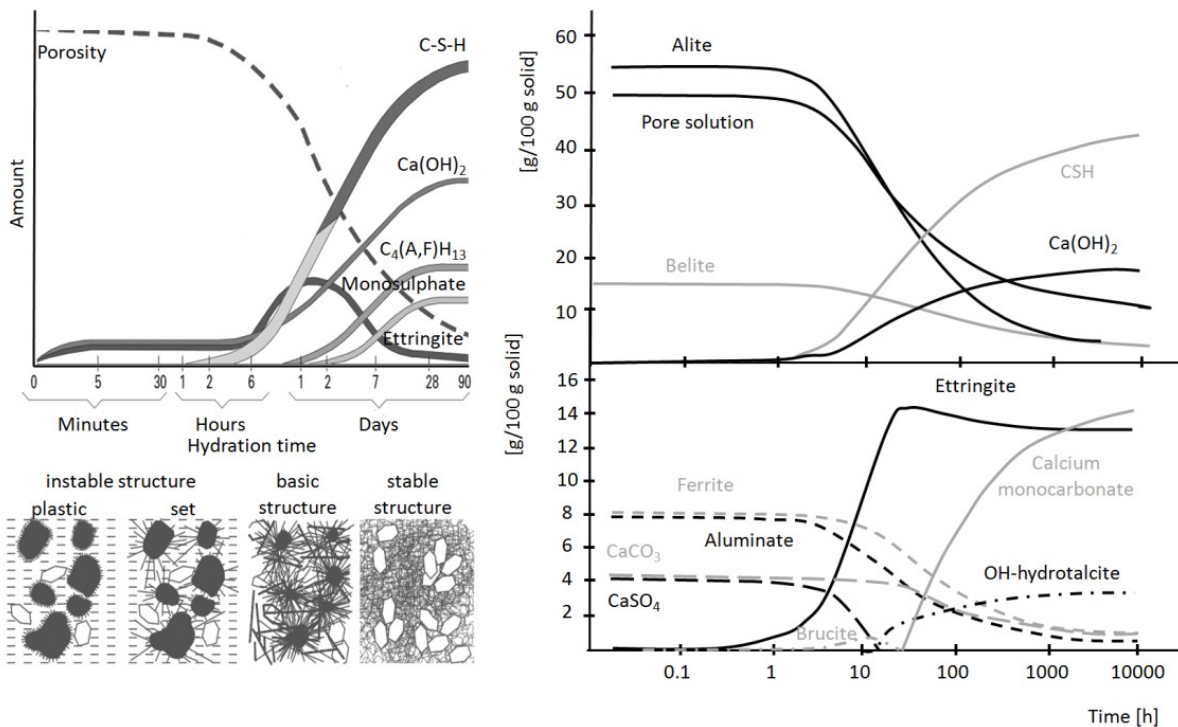


Figure 2.5: Time dependent overview of the hydration phase evolution after Locher [80], left, and Lothenbach [118], right.

As for the hydration of alite and  $C_3A$ , the cement hydration curve shows the typical five stages, as described before. C-S-H continues to grow during the acceleration period around alite grains until a maximum peak is reached, after which the reactions are slowed down. The mechanisms inducing the decelerated period can be either caused by hindered diffusion by the hydrate layer around the alite grain or by reduction of the reactive surface due to impingement of the precipitates. According to Scrivener and Nonat [89], the diffusion controlled slow down cannot hold. If the decelerated period would be controlled by hindered diffusion, the hydrates' thicknesses would be similar regardless of the hydrating particles' sizes, which does not hold true according to Costoya Fernandez [120], who observed greater thicknesses around smaller grains than around larger grains. Furthermore, the diffusion control would fill the so called Hadley grains, which is a layer of lower density between grain and hydrates, much quicker.

## 2.2 Effects during the early hydration of cement

### 2.2.1 Loss of workability

Caused by formation of hydrates, the morphology of the particles changes and precipitates densify the structure. This leads to a loss of workability. Many authors consider the induction period as the period at which the concrete can be placed and compacted, e.g. [30, 81, 121]. From a practical point of view and with regard to concrete application, this can be doubted, since normally, the workability period ends at a distinct point in time earlier than the end of the induction period, as also stated by several authors [80, 88, 122].

After water addition aluminates, calcium and sulphates interact to form ettringite and AFm phases, mainly monosulphate. According to Locher [80, 107], these form a layer around the cement particles, which reduces their mobility. Initially, particles remain mobile against each other but with increasing hydration the workability is reduced. According to Locher, this

mechanism yields setting still during the induction period. Today the setting is rather attributed to the formation of C-S-H [82, 88]. However, with regard to the workability loss, the bridging effect of ettringite, described by Locher may be the major driving force. This is particularly valid, when high amounts of SP are present [123, 124], since they are mainly adsorbed and consumed by the aluminate phase as described in more detail in Chapters 3 and 6.

### 2.2.2 Setting

The setting of a cementitious system is the build up of a solid structure. As mentioned before, the setting today is rather attributed to the formation of C-S-H. This is mainly due to the fact that setting differing from Locher's observations takes place during the acceleration period which corresponds to a rapid formation of C-S-H and  $\text{Ca}(\text{OH})_2$  [82]. Ettringite does not significantly change its morphology at this point in time, and can thus not be the driving force for the setting [82, 88].

The classical test method is the Vicat needle penetration tests. The initial setting ( $t_{\text{ini}}$ ) is defined as the time at which a defined needle does no longer drop to the bottom of a specimen, which means, the viscosity of the system has exceeded a certain threshold so that the needle is stopped by friction. The system at this moment in time is still in a plastic state. The final set time is the point in time, at which a specimen does no longer allow the needle to intrude significantly, which is equal to the point in time, where the specimen has merged from a plastic state into a solid, elastic state. Due to its importance for this Thesis, the method will be discussed in more detail in Subsection 4.4.1.

According to Wadsö [115],  $t_{\text{ini}}$  can be estimated to occur close to the onset of the accelerated period, while the final set takes place in the first half of the upward curve [115]. According to Winnefeld et al. [65], the onset of the accelerated period corresponds to the  $t_{\text{ini}}$  according to Vicat. Chen associates the whole acceleration period with the final set [125].

For normal concrete, the setting is assumed to take place approximately during the first 3 to 6 hours (e.g. [30, 79, 81, 82, 88, 126]). The setting is significantly affected by the water to cement ratio, by SPs as well as by the environmental temperature. Higher water contents slow down the setting [127], increasing temperatures accelerate the setting [128-130], and increasing SP contents retard the setting [131], although it has been reported that at low dosages, the improved dispersion generated by SPs can also yield set acceleration [21].

### 2.2.3 Shrinkage

According to Powers, shrinkage is “manifestly a complex function of the change in relative humidity in the pores of the paste” [132]. It can thus be defined as the material inherent deformation of a cementitious system by changes of the water supply and without application of an external load. Typically, different types of shrinkage are distinguished according to their origin. Shrinkage can be distinguished between chemical shrinkage, plastic shrinkage, drying shrinkage, and carbonation shrinkage [133].

Chemical shrinkage, according to the definition of Lura comprises all volume changes associated with the hydration reactions in a cementitious material [134]. These volume changes can occur due to a size reduction of the hydrate phases compared to the clinker and water as well as due to self-desiccation caused by the incorporation of water into hydration products. Plastic and drying shrinkage refer to deformations that are caused by evaporation of water from the surface in either a fresh, still plastic state or after setting, in the hardened state. Carbonation shrinkage takes place due to the carbonation of the concrete surfaces.

The different shrinkage mechanisms overlap. Hence, it is difficult to distinguish between the different types of shrinkage in detail. According to Sant et al. [135], the strain caused by

chemical and autogenous shrinkage are similar and diverge at a so called time-zero ( $t_0$ ), which denotes the moment at which the system starts to behave like a solid. This time-zero is very close to the final set according to the Vicat test (Figure 2.6).

Typically, autogenous deformations are rather a phenomenon of very dense structures, such as high performance concrete due to their low w/c. In return, due to their dense structure, they do not show significant drying shrinkage. Concrete with higher w/c typically does not suffer strongly from autogenous shrinkage, however, shows larger drying shrinkage deformations due to the more porous structure [133, 136, 137].

The relevant shrinkage mechanisms during the very early hydration period are chemical shrinkage and plastic shrinkage. The chemical shrinkage exhibits similar characteristics as the heat flow during the early hydration as shown by Sant et al. [138] (Figure 2.7), and it correlates well with the hydration degree, as shown by Geiker [139] and more recently on basis of oil well cement by Zhang et al. [140].

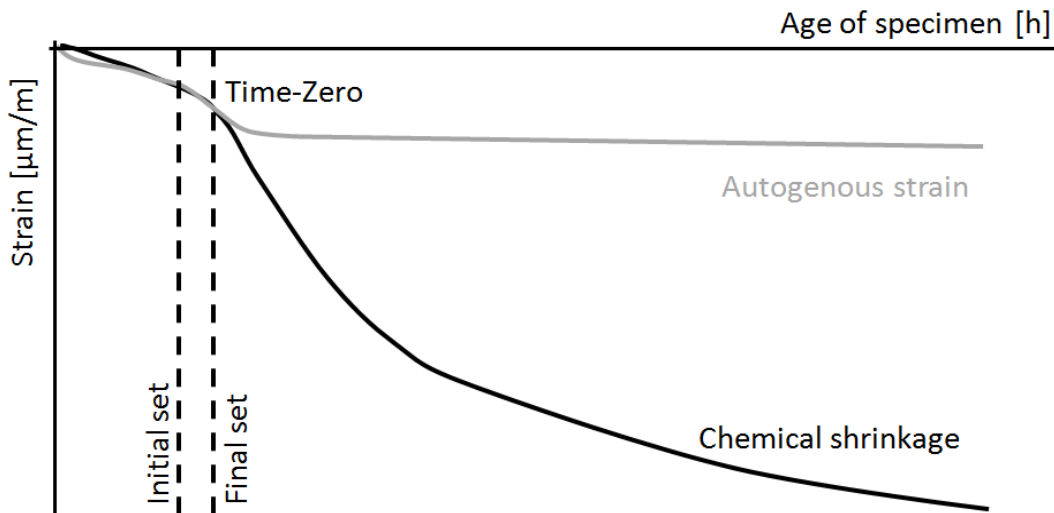


Figure 2.6: Chemical shrinkage and autogenous strain evolution compared to the setting according to Vicat, after Sant et al. [135].

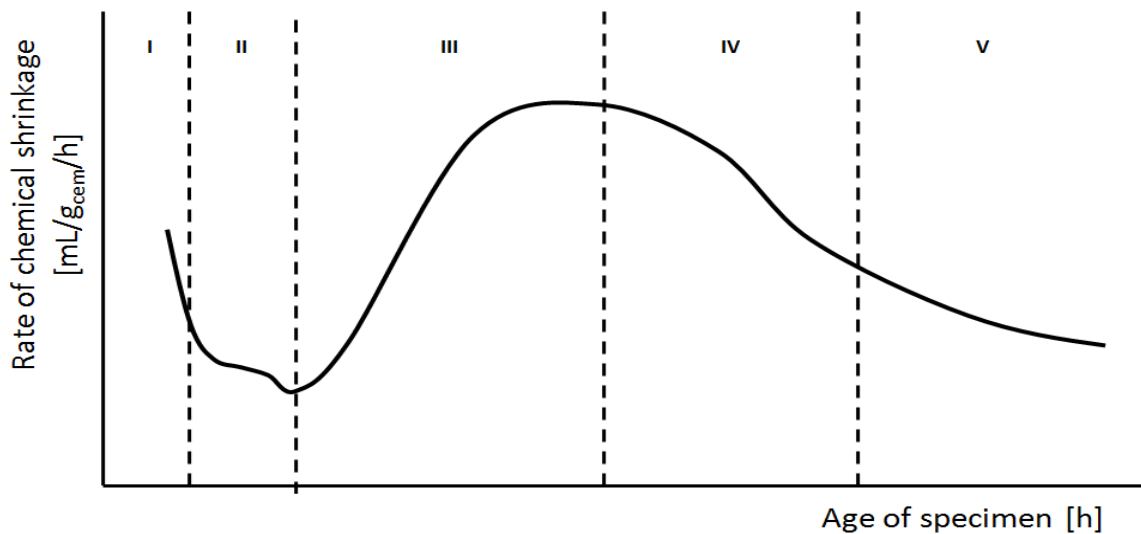


Figure 2.7: Rate of chemical shrinkage related to the hydration periods, qualitatively after Sant et al. [138].

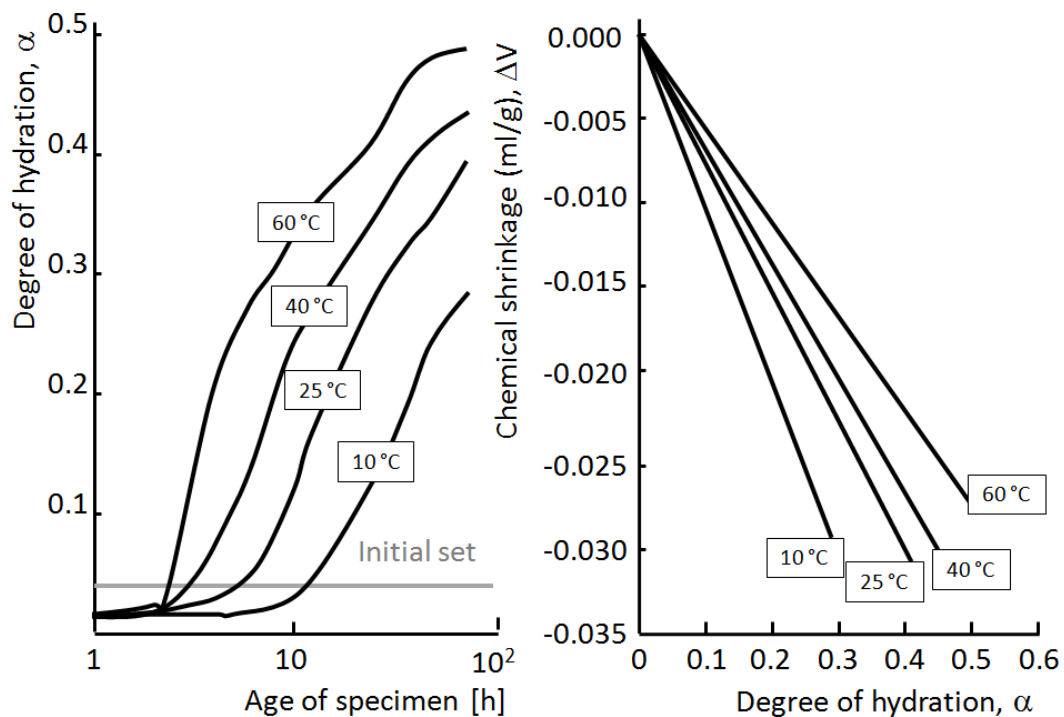


Figure 2.8: Autogenous deformations after the initial set and linear dependency of the chemical shrinkage of the degree of hydration after Zhangg [140].

Shrinkage is mainly a critical phenomenon, when the deformations of the system are restrained, since this generates cracks. Shrinkage typically occurs in the paste, hence, in concrete, the aggregates are a major restraint causing local cracks, further obvious restraints are induced by the structure and by the reinforcement.

As the hydration is strongly affected by the temperature, it can be assumed that temperature shows a similarly strong effect on the shrinkage deformations. Zhang observed the influence of the temperature on the deformations of cementitious systems with  $w/c = 0.35$  and found out that increasing temperatures accelerate  $t_{ini}$  and increase the total deformations [140], as shown in Figure 2.8.

### 2.3 Conclusions

The major early hydration reactions of ordinary Portland cement were given in this chapter. This Thesis focuses on the influence of admixtures in cementitious systems during the early hydration. These admixtures strongly mutually interact with the hydrates that are formed during this period. It is therefore of utmost importance to have a good understanding of the early hydration processes in general, in order to understand how the performance of admixtures can be affected. The most important hydrates during the early hydration are C-S-H, Portlandite, AFm and AFt. Their interactions determine the formation of a microstructure and hence the transition from a fluent towards a plastic and later elastic system, which can be monitored e.g. by setting experiments or shrinkage observations.



### 3 Effects of superplasticisers on the rheology

#### 3.1 The rheology of concrete and cementitious systems

##### 3.1.1 Parameters defining rheological properties

The description of the flow properties of cementitious systems is complicated. In order to better understand the influences of the mixture composition of a cementitious system and particularly how the rheology is affected by superplasticisers (SPs), it is important to keep in mind how different types of fluids behave.

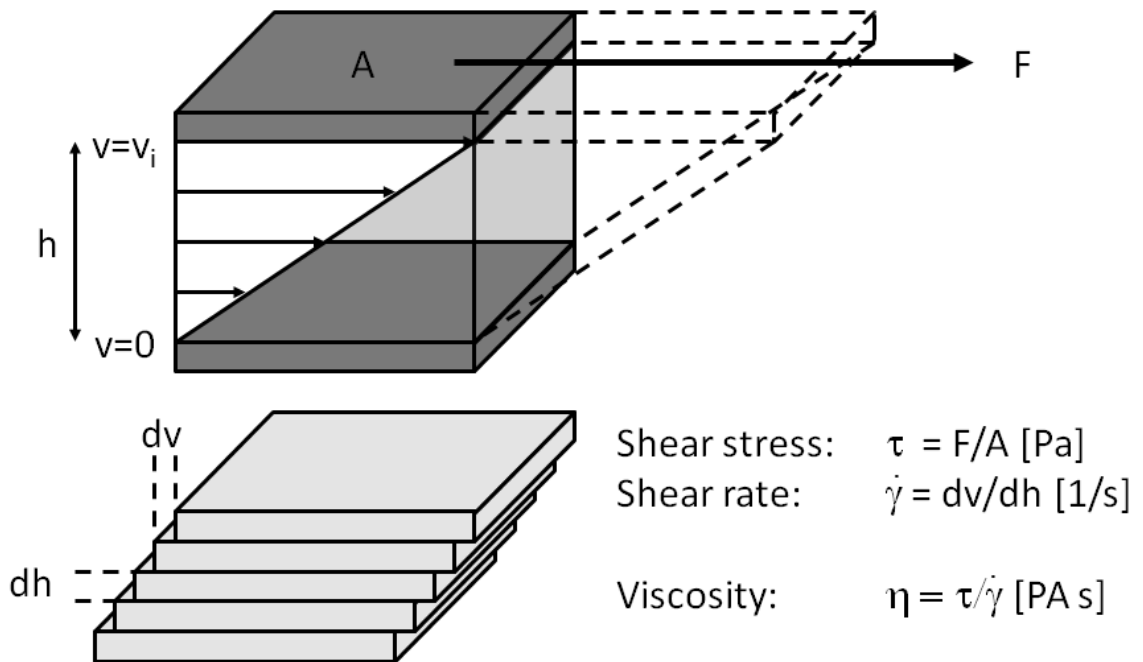


Figure 3.1: Plate model for fluids and laminar deformations

The most common model to describe the flow properties of a fluid is the so called plate model as shown in Figure 3.1, in which laminar flow is assumed and the shear stress between two shear planes is determined according to:

$$\tau = \frac{F}{A} \quad (3.1)$$

where:  $\tau$  = shear stress [Pa];  $F$  = force [N];  $A$  = shear plane area [m<sup>2</sup>].

The force will deform the respective shear plane at a specific velocity relative to the neighbouring shear plane. The derivative of the deformation velocity over the deformation height is the shear rate  $\dot{\gamma}$ , which is defined according to:

$$\dot{\gamma} = \frac{dv}{dh} \quad (3.2)$$

where:  $\dot{\gamma}$  = shear rate [1/s];  $v$  = deformation velocity [m/s];  $h$  = deformation height [m].

Each material has a different resistance against an applied deformation. The material parameter providing information about the fluid's resistance is the viscosity, which is defined by

$$\eta = \frac{\tau}{\dot{\gamma}} \quad (3.3)$$

where:  $\eta$  = viscosity [Pa·s],  $\tau$  = shear stress [Pa];  $\dot{\gamma}$  = shear rate [1/s].

The fluids that can be described in the simplest way are Newtonian fluids. They exhibit a linear relation between the shear stresses and the strain rate, the shear rate  $\dot{\gamma}$ . The viscosity  $\eta$ , which is equal to the slope of the flow curve is a constant value. The flow curve is described by Equation (3.4). Typical examples for Newtonian fluids are water, and many oils and gases. Newtonian fluids immediately start to flow upon application of a load.

$$\tau = \eta \cdot \dot{\gamma} \quad (3.4)$$

where:  $\tau$  = shear stress [Pa];  $\tau_0$  = yield stress [Pa];  $\eta$  = viscosity [Pa·s];  $\dot{\gamma}$  = shear rate [1/s].

Cementitious systems are systems with two phases (solid, fluid) that both exhibit different influences on the rheology. These systems typically do not show Newtonian behaviour. They remain their shape at low shear rates and only after having increased a threshold shear stress, the system starts flowing (see Figure 3.2). The threshold value is called the yield stress  $\tau_0$ . Yield stress is typically a phenomenon, which occurs when particles in a fluid interact with each other in any kind. Yield stress, however, is a most critically discussed value, since the tendency of a fluid or a solid structure to deform strongly depends upon the duration a force is brought up. It is known that even solid like structures creep over long periods of time, giving rise to the idea that according to the formulation of Heraclitus "panta rhei", everything flows. A critical and very comprehensive discussion about the existence of a yield stress is given by Barnes [141]. Nevertheless, the concept of a yield stress has proven to be a useful concept for scientific and engineering applications. This is particular valid for systems that after relatively short period of time with respect to its lifespan change its material properties from fluid towards elastic behaviour, where different material laws (e.g. Hooke's law) are valid, and the resistance against deformations are described by the Young's modulus  $E$ , the Poisson's ratio  $\nu$  and the shear modulus  $G$ .

For many fluids, after exceeding a specific or temporary yield stress, the shear stresses and shear rates are proportional like in Newtonian fluids. Fluids that show this kind of behaviour are called Bingham fluids after E. C. Bingham, who coined the definition of plastic flow behaviour with initial minimum shear force to initiate the flow. This concept clearly distinguished from the popular opinion at that time that plastic flow is equal to incomplete elasticity [142-144]. Examples for Bingham-fluids are cementitious systems or dispersion colours. Bingham behaviour is expressed by:

$$\tau = \tau_0 + \eta \cdot \dot{\gamma} \quad (3.5)$$

where:  $\tau$  = shear stress [Pa];  $\tau_0$  = yield stress [Pa];  $\eta$  = pl. viscosity [Pa·s];  $\dot{\gamma}$  = shear rate [1/s].

However, many fluids do not show constant viscosity. For these fluids the Ostwald-de Waele relation applies [145, 146] according to:

$$\tau = \kappa \cdot \dot{\gamma}^n \quad (3.6)$$

where:  $\tau$  = shear stress [Pa];  $\dot{\gamma}$  = shear rate [1/s];  $\kappa$  = flow consistency index [Pa·s<sup>n</sup>];  $n$  = flow behaviour index [-].

Here a flow consistency factor is introduced as a multiplier to the shear rate and a flow behaviour index in the exponent of the shear rate, which describes, how far the flow behaviour deviates from Newtonian flow.

Fluids with yield stress that do not show constant viscosity are typically described by the Herschel-Bulkley law [147], which is described by

$$\tau = \tau_0 + \kappa \cdot \dot{\gamma}^n \quad (3.7)$$

where:  $\tau$  = shear stress [Pa];  $\tau_0$  = yield stress [Pa];  $\dot{\gamma}$  = shear rate [1/s];  $\kappa$  = flow consistency index [[Pa·s<sup>n</sup>];  $n$  = flow behaviour index [-].

This law is equal to the Ostwald-de Waele relation but supplementary includes the yield stress. Depending upon the characteristic curve, the viscosity can decrease or increase with increasing shear rate. The first behaviour is called shear-thinning or pseudo-plastic behaviour, the latter behaviour is entitled shear-thickening or dilatant. Shear thinning behaviour typically occurs, when components of the fluid, e.g. polymers or air bubbles, align into the flow direction.

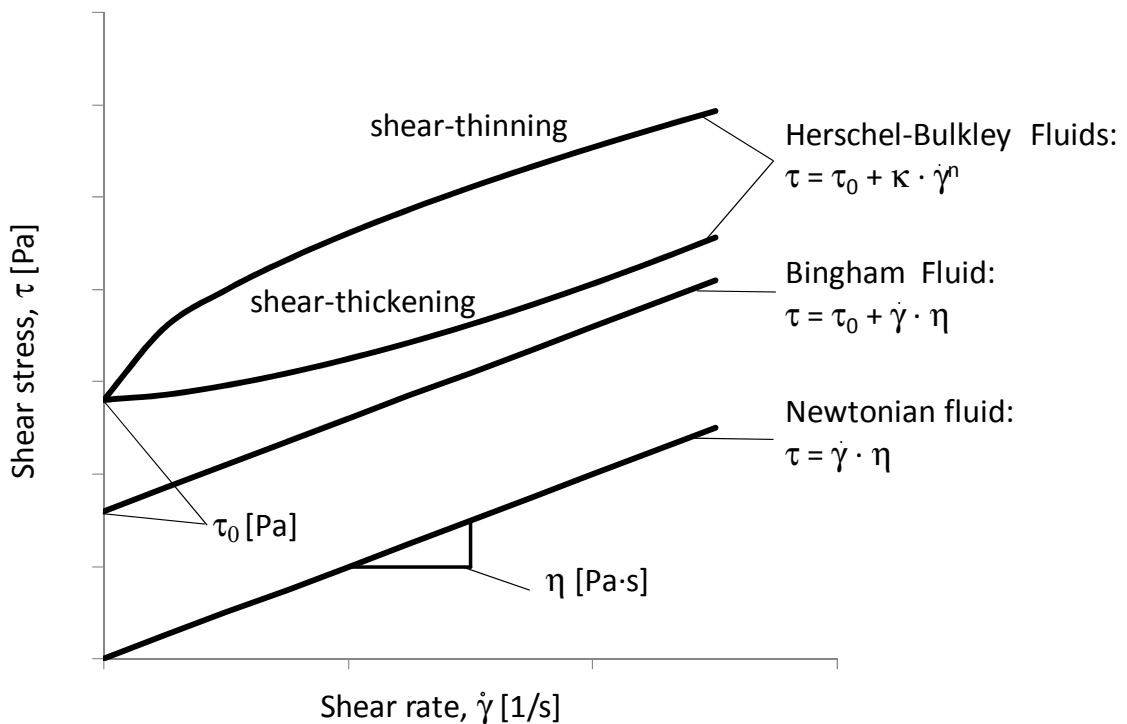


Figure 3.2: Qualitative flow curves following the aforementioned flow laws, see Equations (3.4), (3.5), and (3.7).

Typical examples of shear-thinning fluids are Ketchup or blood. Shear thickening occurs, if one phase, e.g. the solid phase quickly compacts upon load, thus blocking the motion of another phase, which would not be hindered at slower load application. Starch pulp or water filled beach sand show typical shear-thickening behaviour.

The most relevant flow laws are described in the Equations (3.4), (3.5), and (3.6) are illustrated in Figure 3.2. It has to be noted that many fluids may not show uniform flow behaviour if a wide range of shear rates is observed. They may follow different flow laws in different shear rate ranges. For example, gypsum or cement suspensions with admixtures often show shear thinning at low shear rates due to an initial arrangement of some constituents into flow direction, while at higher shear rates rather Bingham behaviour and at very high shear rates shear-thickening can be observed.

### 3.1.2 Mixture composition influences on the rheology

The aforementioned flow laws are only approximations. Despite the rather philosophical discussion about the yield stress as a real threshold for flow initiation versus a point at which flow can be firstly measured [141], in terms of concrete, the yield stress, it is a reasonably good tool to describe the rheological behaviour of fluids. In general, cementitious systems are preferably approximated with the Bingham law, as it is considered to be sufficiently precise to describe the behaviour, and the two major parameters plastic viscosity and yield stress are easily graspable. Unless several influencing factors overlap, normally any influence affecting the yield stress will to a certain degree also affect the plastic viscosity. Nevertheless, measures conducted in order to modify concrete mixtures may have significantly stronger impact on only one of the two relevant parameters. A comprehensive qualitative overview about the effects was provided by Wallevik [148] and is shown in Figure 3.3.

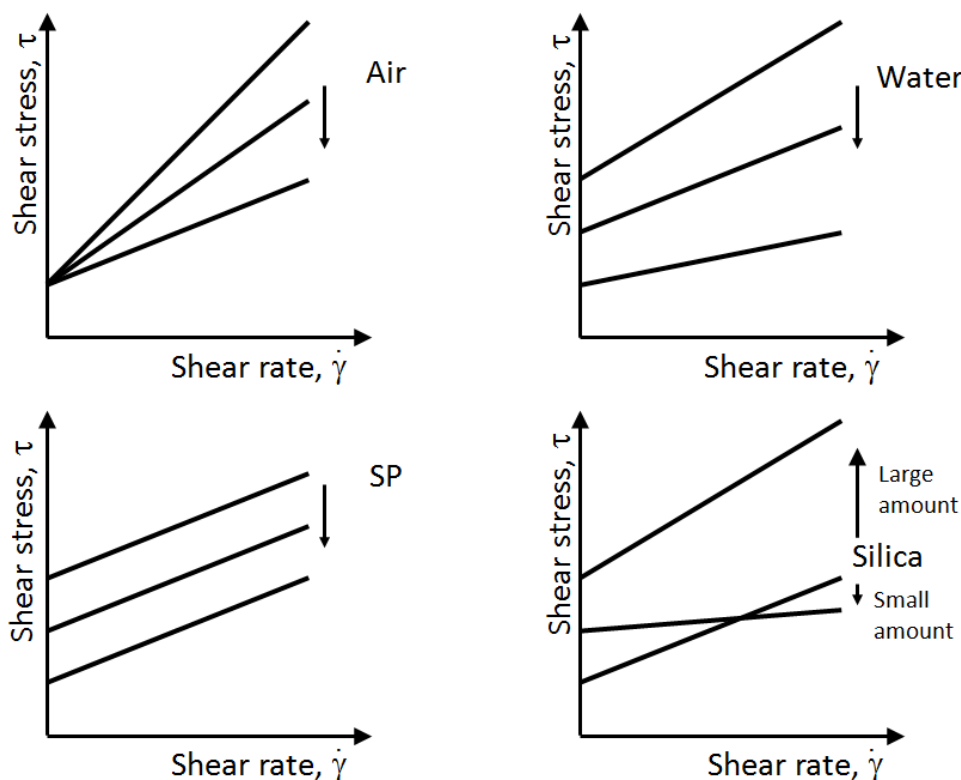


Figure 3.3: Influence of different mixture compositions of the flow properties of cementitious systems after Wallevik [148].

### 3.1.3 Grading curve

Viscosity is mainly driven by interactions between particles upon motion. The more the particles build a lattice between each other, the higher the viscosity, since particles block the motion of other particles. In that context typically sand-rich grading curves often produce higher viscosities and yield stresses caused by the lattice effect [43, 149, 150]. Then again, packing density optimised systems may show higher viscosities and yield stresses. As soon as the particle optimisation continues for the fines, these systems are very densely packed, which hinders internal particle motion. The influence of the particle grading thus is difficult to clearly identify without consideration of further aspects such as the water to powder ratio or the aggregate to paste ratio. Unpublished research on the influence of the aggregate grading curves corresponding to the standardised grading curves according to DIN 1045-2 at identical aggregate to powder volumetric ratios showed particularly very strong influences on both yield stress and viscosity (Figure 3.4). These grading curves approximate a curve following the Equation (3.8). Their detailed specifications are listed in Table 3.1. Steady curves outside these standardised curves are notated by the curves that surround them (AB16 and BC16). The U-curve follows a gap graded curve.

$$P_{(d)} = \frac{100}{1 - \left(\frac{0.125}{d_{\max}}\right)^q} \cdot \left[ \left(\frac{d}{d_{\max}}\right)^q - \left(\frac{0.125}{d_{\max}}\right)^q \right] \quad (3.8)$$

where:  $P_{(d)}$  = cumulative finer fraction [%];  $d$  = particle diameter;  $d_{\max}$  = maximum grain size;  $q$  = distribution parameter.

In Figure 3.4 the grading A16 with the densest particle packing exhibits the highest viscosity at relatively low yield stress, while the oppositional grading, the sand rich C16 shows low viscosity at high yield stress. The curves in between (AB16, B16, BC16) as well as the gap grading U16 do not show a clear trend.

Besides the influence of the grading of the coarse aggregates, another important influencing factor can be related to the grading of the finest particles. The higher the packing density, the less water is required to fill the voids. Rickert found a linear correlation between the water demand determined according to the needle penetration method described in EN 196-3 and the torque measured at not further specified constant rotational speed for differently blended cements (Figure 3.5) [151]. This means that particularly SCCs with high paste volume can be well optimised by sensible adjustment of the grading of the fines.

Table 3.1: Grading curve specifications of standard grading curves according to DIN 1045-2 and classification of the fractions.

	Powder	Sand					Coarse aggregate		
	Mesh size [mm]					Sieve opening (square) [mm]			
	0.125	0.25	0.5	1	2	4	8	16	
A16	Not specified	3	8	12	21	36	60	100	
B16		8	20	32	42	56	76	100	
C16		18	34	49	62	74	88	100	
U16		3	8	12	30	30	30	100	

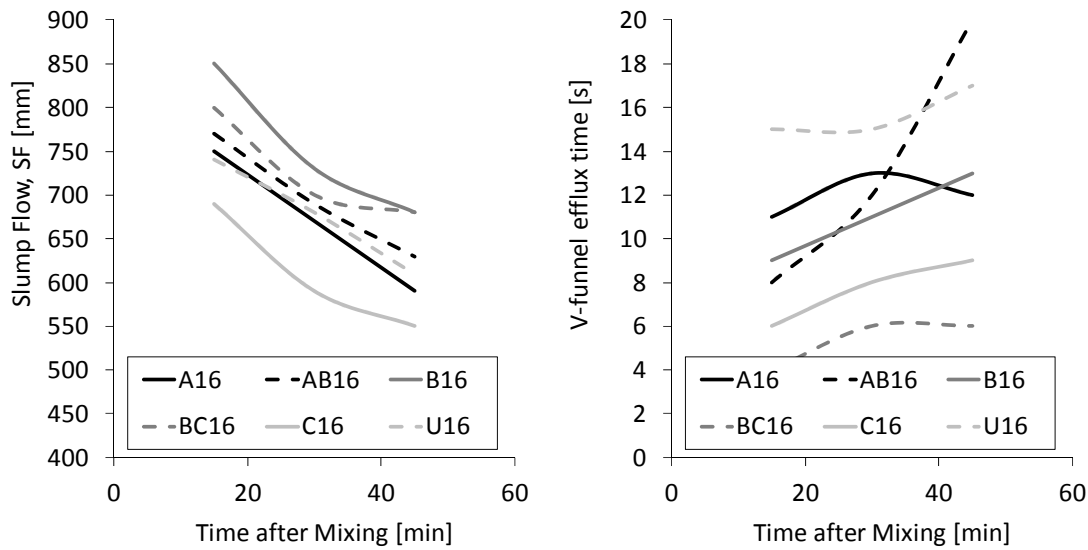


Figure 3.4: Influence of different grading curves at identical paste to aggregate ratios on slump flow and V-funnel efflux time; grading curves according to DIN 1045-2 after [152].

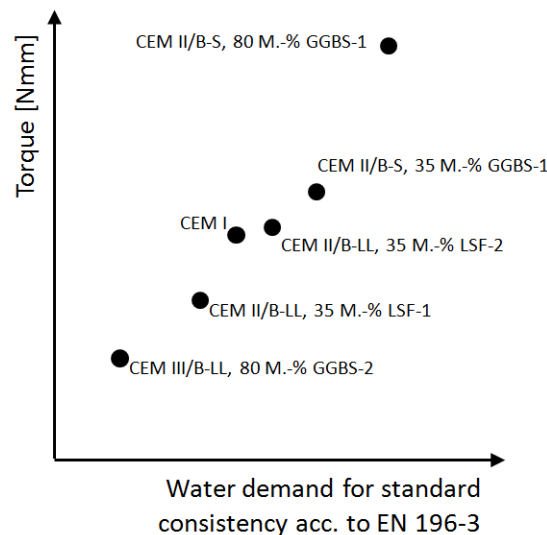


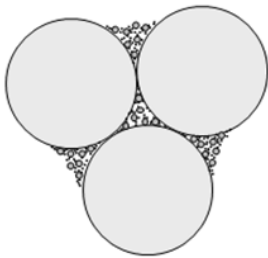
Figure 3.5: Linear correlation between shear resistance and water demand of a cement after Rickert et al. [151].

### 3.1.4 Aggregate to powder ratio

Of course, the degree at which the grading affects the overall flow properties is strongly depending on the paste to aggregate ratio [153]. For flowable systems, Range and Lohaus distinguish between systems, where the coarse aggregates or the fine particles are dominant, or both are co-dominant, as shown in Figure 3.6. It is thus clear that depending on the mixture composition of an SCC as either high- or low-powder concrete different laws apply. High powder content SCC, e.g. according to the approach suggested by Okamura [1, 3] is typically driven by the performance of the paste, which exhibits low yield stress and high viscosity due to the dense powder packing. Low powder content SCC typically exhibits a high yield stress due to the lattice effect and a low viscosity due to typically higher water to powder ratios.

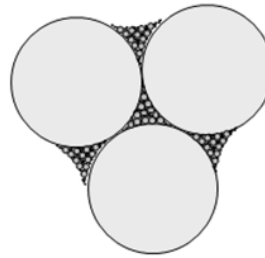
Coarse particles are dominant:

- too many voids, too much water needed
- no proper coherence without additional stabilising agent



Coarse and fine particles are co-dominant:

- lowest possible voids content, lowest water demand
- however, the viscosity is very high



Fine particles are dominant:

- higher water requirement
- low viscosity can be achieved despite a high solid content
- good coherence

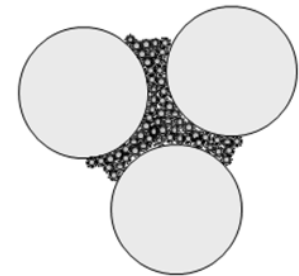


Figure 3.6: Effects induced by different paste to aggregate volumetric ratios after Range [154].

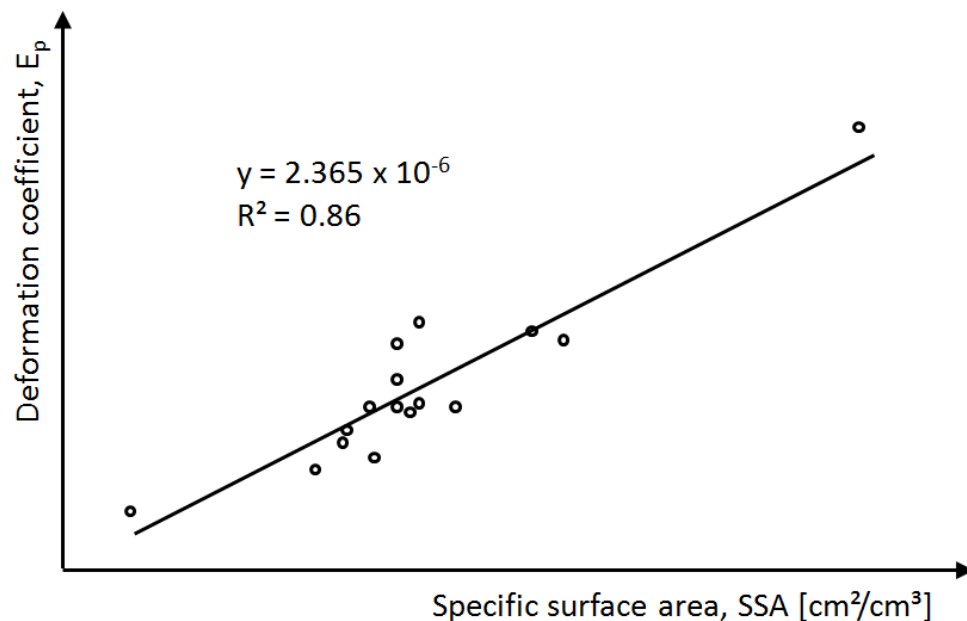


Figure 3.7: Correlation between SSA and EP for two fly ashes [5].

### 3.1.5 Aggregate and particle shape

Another important factor determining the rheology of cementitious systems is the constituents' shapes. Shapes that significantly deviate from regular shapes can adjust into flow direction upon shearing, thus introducing shear thinning effects. Furthermore, the ability of particles to move against each other is strongly determined by the shape. Angular shapes typically reduce the deformability, while in parallel increasing the stability. Furthermore the surface properties of the particles play a major role for the rheology of self-compacting concrete. Their major influence are the packing density and the specific surface area (SSA), which define the water required to

adsorb on particles' surfaces and to fill the voids to achieve good flow properties [32]. Figure 3.7, which is derived from Hunger [5], shows the dependency between deformation coefficient  $E_p$ , which defines the slope of the linear correlation curve of the water demand determination test according to Okamura [1, 3] (see also Figure 1.2). This coefficient, which can be linked to the viscosity increases in a linear way with increasing surface area.

### 3.1.6 Water-powder ratio

The water to powder ratio is a major parameter determining the viscosity of flowable systems. The higher the water volume compared to the fines volume, the better particles can move between other particles as soon as shear force is applied. Hence, as long as a flowable system remains stable from segregation, varying water content affects the viscosity greatly. In case SP is also part of the system, the yield stress is mainly influenced by the performance of SP and not by the water to powder ratio, which allows controlling the paste viscosity within certain limits largely independent of the yield stress by simply changing the water content. This effect can be easily observed, when the slump flow and the V-funnel efflux times of SCC, which can be related to  $\tau_0$  and  $\eta$ , respectively. As long as the superplasticiser addition remains constant, changing water contents will modify the V-funnel times, while the slump flow remains stable.

### 3.1.7 Stabilising agents

Stabilising agents (STAs) can be either mineral components or polymeric admixtures, which are also often entitled viscosity modifying agents (VMA) or viscosity enhancing agents (VEA). Mineral STAs are part of the overall particle size distribution (PSD) and affect the rheology by adding large specific surface areas to fix water and increase the packing density. They can also be considered as additions to the mixture composition of SCC according to the definitions in Table 1.4. Polymeric STAs such as cellulose, microbial gum, or starch are more versatile, and their effect on rheological properties is driven by the type of polymer, the integral mixture composition as well as the amount of agent added since they are large molecules that interact with water but also between particles [25]. They can thus introduce diverse effects into a cementitious flowable system.

### 3.1.8 Plasticisers and superplasticisers

Plasticisers and SPs adsorb on the surfaces of certain cement clinker and hydration phases thus repelling particles by either electrostatic or steric mechanisms, or a combination of both. This stabilisation of particles mainly affects the attraction forces between the particles but does not strongly influence how particles move against each other upon flow. This means, that SPs unless they do not affect the stability of a system do only affect the viscosity generally by increasing the paste's cohesion but the amount of SP has only minor influence on the viscosity, while the yield stress is greatly decreased with increasing SP contents. This effect can also be observed easily upon testing SCC at constant water content. Varying SP contents will have strong influence on the spread flow diameter, which is related to  $\tau_0$ , while the V-funnel, which can be related to  $\eta$  times remain stable. Certainly SPs introduce additional water with certain influence on the viscosity. Unstable systems with high water contents tend to segregate upon increasing SP addition, so that V-funnel times can be affected also by SP additions in certain cases. However, it is evident that PCE addition mainly affects the yield stress of a flowable system.

Superplasticisers are most efficient rheology modifying admixtures. Their specifications strongly affect the flow properties and the temperature related behaviour of SCC as illustrated in Figure 1.12. Understanding the mode of operation of superplasticisers helps improving mixture compositions for SCC. Therefore, the following section will introduce the required background about superplasticisers and in particular those based on polycarboxylates.

## 3.2 Mode of operation of superplasticisers

### 3.2.1 Introduction

Superplasticisers are chemical products that allow the control of the flow properties largely independent of the water demand. These chemical admixtures, which are also entitled high-range water reducing admixture (HRWRA) can be considered as the driving agent for modern concrete technology, since they provide the opportunity either to improve the flow properties at a fixed w/c or to reduce the w/c significantly without losses in the flow properties. These specifications opened the doors for concrete innovations such as self-compacting concrete or ultra-high performance concrete. Spiratos et al. [155] classify SPs into three general groups, which are sulphonated polymers, carboxylated polymers, and synthetic polymers with mixed functionality. The latter group are modified synthetic copolymers, either sulphonated or carboxylated polymers that incorporate supplementary functional groups. Sulphonated polymers only offer a limited range of possibilities to amend functionality, while the range of possibilities for polycarboxylates is wide.

### 3.2.2 Brief history of superplasticisers

The first group of SPs used in concrete were Lignosulphonates (LS). They are the residue of the sulphitation process for cellulose [14]. The effectiveness of lignosulphonates compared to other sulphonates is limited [156, 157]. A significant step forward was made through the invention of synthetic polycondensates in the early 1960s. These were poly-naphthalene sulphonates (PNS) and poly-melamine sulphonates (PMS). These groups were the major chemical admixtures used until approximately the millennium change [155, 158]. In the 1980s linear vinyl copolymers were brought to the market [157]. However, also in the 1980s the first polycarboxylate SPs were introduced [14]. These mark the significant breakthrough in concrete technology and performance development with regards to self-compacting and high-performance concrete. According to the honorific speech given by Prof. Plank for the Hans Khl award, which was awarded during the 1<sup>st</sup> International Conference on the Chemistry of Construction Materials in 2013, the invention of the first polycarboxylate ether superplasticiser with polyethylene side chain goes back to only a single person, the laureate Dr. Tsuyoshi Hirata. Dr. Hirata invented the PCE superplasticiser for concrete right after finishing his Master thesis and received a high number of patents on new PCE technologies since then.

Most polycarboxylic SPs consist of a methacrylic backbone and polyethylene oxide graft chains. The first generation of polycarboxylates exhibited an ester link between the backbone and the graft chains. In order to improve the stability of the polymers, the ester links were replaced by ether links in the late 1990s. Further developments allowed an individual polymer design by individual grafting with Amid- and Imid bonds, or zwitterionic bonds [14]. Recent developments involve the attachment of hydrolysable groups, so called slump loss controlling agents, to the COO<sup>-</sup> groups in the backbone, which release anionic charges over the course of time due to hydrolysis in the highly alkaline pore solution [159, 160]. Such type of SP is particularly useful for cement types with low soluble sulphate content or at high temperature.

Plank provided an overview of the consumption of the SP types without reference to the country or the year of the survey [156]. This data is shown in Table 3.2, pointing out that lignosulphonate is still an important type of admixture used, which according to Plank is mainly related to its cost competitiveness. During the last decade the importance of polycarboxylate ether SP has significantly increased.

These days phosphonate based superplasticisers have become more popular. The latter types are also comb-type polymers, which mainly differ from PCE in the chemical composition of the

backbone, which is phosphonate based instead of methacrylic. As a result, the masses of these polymers are lower, which gives them a lower tendency to adsorb. These superplasticisers show a good cohesiveness, and differing from PCE they reduce the plastic viscosity of cementitious systems [161, 162].

Table 3.2: Annual world's consumption of superplasticisers dated from 2004, after Plank [156].

Superplasticiser type	Category	Annual consumption [t]
Lignosulphonate (LS)	Biopolymer	700,000
Polycondensate resins (PNS, PMS)	Synthetic	550,000
Polycarboxylates (PC)	Synthetic	150,000

### 3.2.3 Mode of operation of PCE in comparison to other superplasticisers

A basic similarity of all aforementioned types of SPs is their anionic backbone, which is considered to adsorb on the surfaces of clinker phases and cement hydration products. This has been reported by numerous authors, some relevant publications of which can be found in the references [15-17, 19, 21, 22, 58, 61, 63, 157, 163, 164]. The adsorption takes place preferably in the interstitial phases between alite and belite and onto early hydration phases such as ettringite and monosulphate [15, 21, 69, 87].

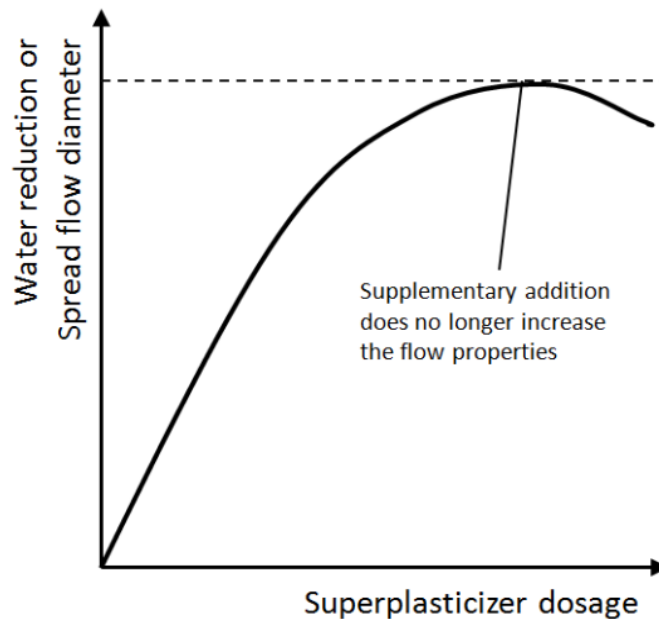


Figure 3.8: Adsorption maximum of SPs.

The adsorption of SPs is considered to largely follow a Langmuir isotherm [165-167]. The characteristics of that isotherm is largely linear at low concentrations and approximates the maximum surface covering in an asymptotic way at higher dosages, which accords to a full monolayer on all available bonds [14]. This means, at a specified time, when the amount of polymers is increased, there will be an adsorption maximum, beyond which any further addition will not further contribute to dispersion. This effect is qualitatively shown in Figure 3.8. The effect can also be derived from Figure 3.9 with absolute values for PCE [68] based on measuring the total organic content of the pore solution (TOC) and by employing size exclusion chromatography (SEC). The distinct qualitative difference can be attributed to intercalations

blurring the results of the TOC measurement. This effect will be given more attention in Subsection 3.3.6.

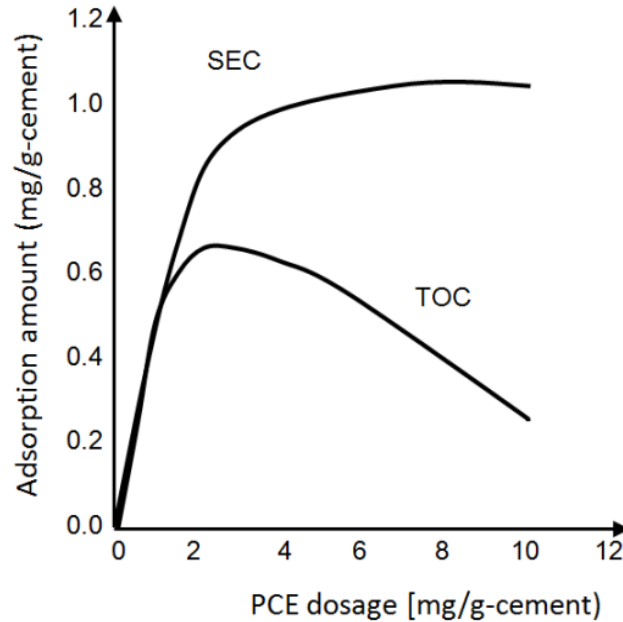


Figure 3.9: PCE adsorption measured with size exclusion chromatograph (SEC) and total organic carbon measurement (TOC) after Yamada et al. [68].

The Langmuir isotherm, however, considers only the adsorption of a single layer [14]. In reality, multi-layer adsorption and the formation of organo-mineral phases can occur [61, 85, 157, 168-170]. These are also responsible for the discrepancy between amount of adsorbed polymers and measurements of the total organic content, which are reported [61, 68] (Figure 3.9). Flatt and Houst therefore suggested to call the difference between added polymers and remaining polymers in solution measured by TOC rather as consumed content than as adsorbed content [61]. Winter suggests using the model by Brunauer, Emmet, and Teller (BET), which allows multi-layer adsorption with decreasing adsorption enthalpy for any further layer [14].

Plank and Sachsenhauser investigated the thermodynamic processes behind the adsorption processes of differently modified SPs on limestone in aqueous suspension [166, 171]. They refer to the Gibbs-Helmholtz equation:

$$\Delta G_r = \Delta H_r - T\Delta S_r \quad (3.9)$$

where:  $T$  = absolute temperature [K];  $\Delta G_r$  = Gibbs free energy [J];  $\Delta H_r$  = reaction enthalpy [J];  $\Delta S_r$  = reaction entropy [J/K].

In case, the Gibbs free energy is negative, the adsorption occurs without energy supply. They found that Gibbs free energy was negative for all three types of PCE, which leads to the conclusion that adsorption is favourable and thus a spontaneous process. Increasing surface loading brought the Gibbs free energy to decrease yielding an adsorption stop at a value of zero. They found also that depending on the molecular architecture of the PCE molecules the contributions of  $\Delta H_r$  and  $\Delta S_r$  varied. The higher the anionic charge density, the higher was the enthalpic contribution to adsorption. Lower charge densities increased the entropic contribution.

Though investigated based on PCE, these observations can be considered as valid for all adsorptive SPs. Due to the higher charge densities of sulphonated SPs, however, their adsorption should be mainly driven by the enthalpic contribution due to the electrostatic attraction forces.

LS, PNS, and PMS provide short chain lengths with high anionic charges [14]. They adsorb on clinker and hydration phases that provide positive charges, thus changing the formerly positively charged surfaces negatively with the effect that each entire particle surface is negatively charged. This keeps particles in distance and provides flowability. Further effects contributing to flowability are a reduction of the surface tension of the water, lubrication of the surfaces, steric repulsion, reduction of the surfaces' reactivity, as well as changes in the morphology of reaction products [164]. The major dispersing mechanism is considered to be the electrostatic effect [16, 17, 172, 173]. This conclusion is based on increasing negative zeta potentials ( $\zeta$ ) that can be observed for cement in the presence of anionic SPs, as shown in Figure 3.10. The role of the  $\zeta$  will be discussed in more detail in Subsection 3.3.2. The exclusive role of electrostatic dispersion forces was first put into question by Banfill [174] in a discussion on two papers published by Daimon and Roy [167, 173]. It was discussed that  $\zeta$  measurements cannot detect effects of the adsorption structure, e.g. in loop or trail formation, which would add a steric effect of the backbone and blur the significance of  $\zeta$  measurements. Steric contribution to the dispersion is also reported by other researchers [69, 164, 174].

Today it is agreed upon that the dominating dispersing mechanism of PCEs is the steric repulsion of particles, though minor electrostatic forces and effects of the reduction of the surface tension of water take place [16, 17, 172]. Steric repulsion takes place, when the Gibbs free energy increases upon approximation of two dispersed particles. Compared to sulphonated SPs, PCEs are relatively lowly charged. The differences between electrostatic and steric repulsion is demonstrated in (Figure 3.11). The graft chains of the polymer are keeping the particles in distance.

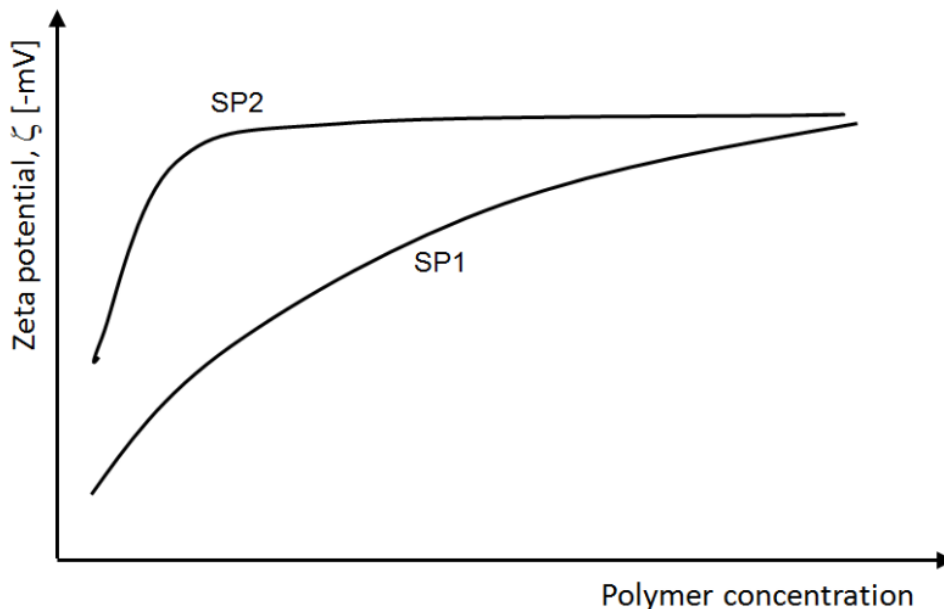


Figure 3.10: Change of  $\zeta$  of cement depending on the admixture concentration for two types of sulphonated formaldehyde condensates, qualitatively after Daimon and Roy [173].

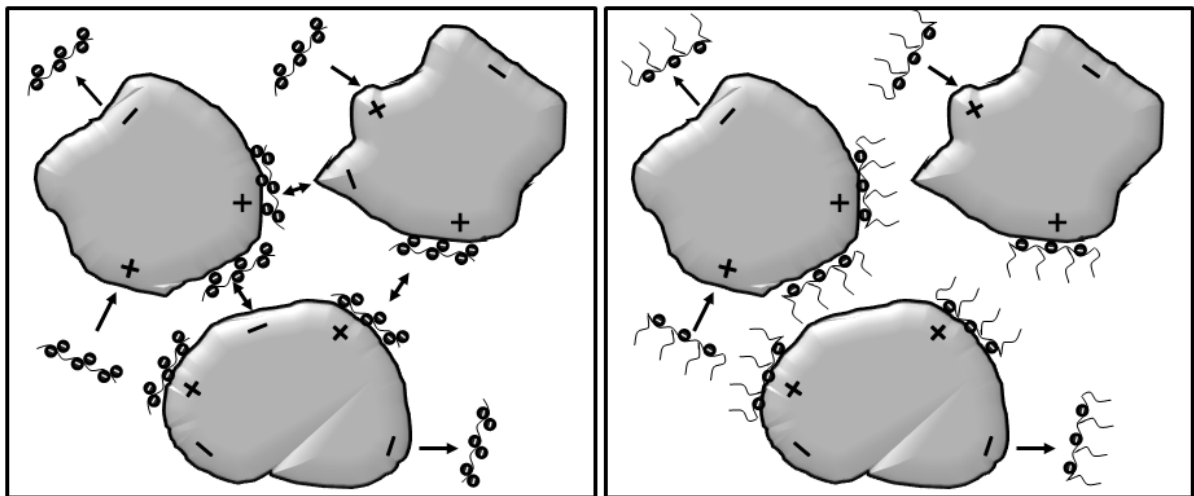


Figure 3.11: Difference between electrostatic repulsion (left) and steric repulsion (right).

### 3.3 Cement hydration and PCE performance

#### 3.3.1 Introduction

Incompatibilities between cement and PCE are reported by several authors [17, 56, 57, 85, 165, 175]. The major effect, inducing these incompatibilities, is brought by scatter in the cement composition, the importance of which were not known from concrete practice without SPs, such as the sulphate and alkali solubility, which strongly affect the adsorption of SPs. Figure 3.12 shows the different ranges of scatter for different production dates of one cement with and without PCE [57]. They used a CONTEC-Rheometer-4SCC, which – based on the electric current at different rotational speed steps - provides the qualitative data G-Yield in [mA] and H-viscosity [mA s], which can be linked to  $\tau_0$  and  $\eta$ , respectively. Since this device was also used for investigations in this Thesis, a more detailed description will be given later in Subsection 4.3.7.

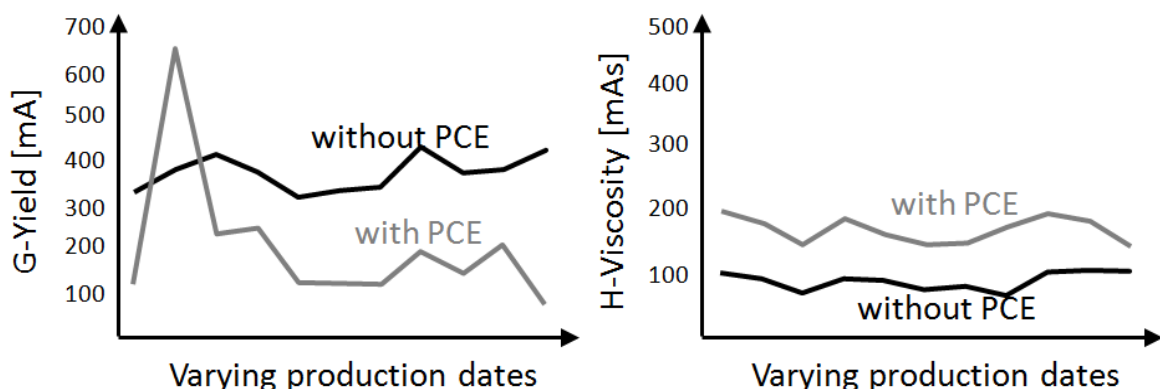


Figure 3.12: Scatter of G-Yield and H-viscosity for identical mixtures tested with different delivery charges of the same cement with and without SP, after Kubens [57]. G-Yield and H-Viscosity changes qualitatively correspond to changes in  $\tau_0$  and  $\eta_{pl}$ , respectively.

The G-yield of the mixture without PCE ranges between 300 mA and approximately 400 mA, which can be controlled during casting. The mixture incorporating PCE varies between 100 and 650 mA, which in practice would cause delicate problems with both, stagnation and segregation. The scatter in H-viscosity and particularly the difference between mixtures with and without PCE is significantly smaller, which indicates that indeed an interaction between cement and SP is the relevant factor for the performance changes. While traditional SPs typically exhibit higher charge densities than PCE, which means, they adsorb quicker and directly onto the cement surfaces, problems with scattering cement production are of less importance than for PCE. However, with PCE, significant effects can occur.

### 3.3.2 Zeta potential of clinker and hydration phases in pore solution

The zeta potential ( $\zeta$ ) describes the potential difference in the transition zone between two phases. Due to the anionic nature of the backbone, it is clear that PCE polymers adsorb on areas that show positive surface charges or positive  $\zeta$ s in suspension. Cement clinker is characterised by alite and belite phases sintered into aluminates and ferrite phases. Hence, the surfaces of clinker grains consist of mosaic-like structures of different clinker phases. Therefore, the entire  $\zeta$  of the particle is not important for the adsorption of PCEs but the  $\zeta$  of the surface exposed clinker phases. Uchikawa opined that adsorptive polymers preferably adsorb on the interstitial areas between alite and belite [15]. This is confirmed by studies of Yoshioka et al. [176]. Nachbaur et al. show that the  $\zeta$  of C-S-H and  $C_3S$  is negative at low CaO concentration but can be positive at higher CaO concentrations [177]. The latter observations are confirmed for C-S-H by Viallis et al. [178]. It is therefore unlikely that high adsorption of PCE takes place on these phases. Plank investigated the  $\zeta$ s of ettringite, monosulphate, syngenite, portlandite and gypsum. While portlandite showed a high negative  $\zeta$ , gypsum showed a negative value close to zero and syngenite exhibited only a negligible positive value. The only phases exhibiting significant positive  $\zeta$  were monosulphate and ettringite of which ettringite provides the highest positive  $\zeta$  [87]. This leads to the conclusion that PCEs initially adsorb only locally on the aluminates and ferrite phases, later on AFm and AFt, as shown in Figure 3.13. At a later stage of hydration, they can also be coupled with  $Ca^{2+}$  on the surfaces of C-S-H [179].

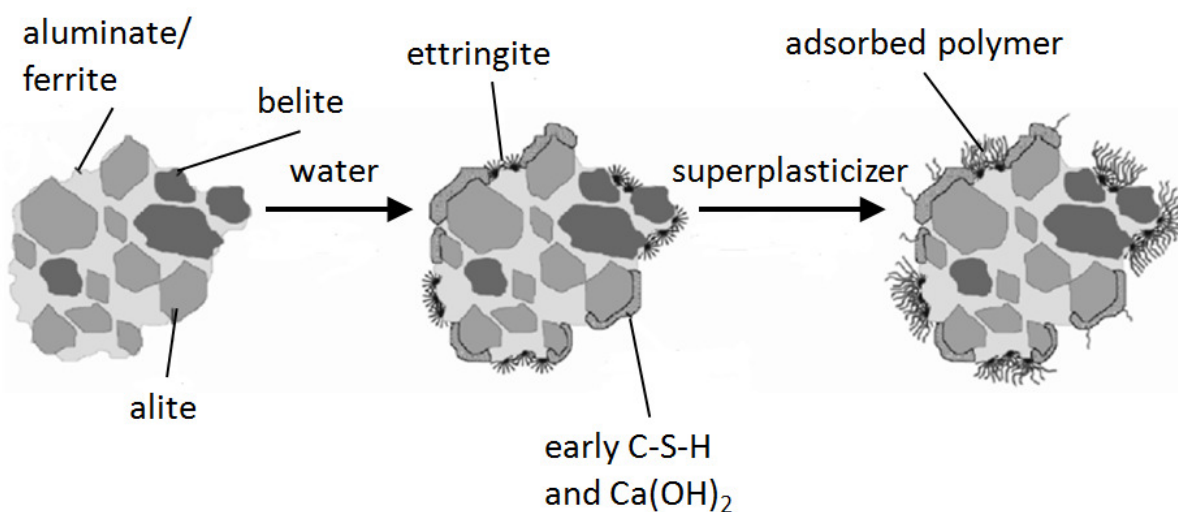


Figure 3.13: Local adsorption of PCE on AFm and AFt phases on the cement grain surface after Plank and Hirsch [87].

### 3.3.3 Specific surface area

Even though the induction period marks a period at which the hydration takes place at low level, continuous hydration can be observed. The particles' surface growth can be considered as a major effect influencing the time dependent flow properties. Yamada reports that the specific surface area and its growth have strong influence on the amount of required PCE to maintain the flow properties [18, 68]. This is supported by Sakai et al. [179]. Considering the different  $\zeta_s$  of the clinker phases, the specific surface growth solely cannot give information about the demand of SPs, since the surface growth can be linked to C-S-H, AFm and AFt formation, of which a major contribution to adsorption can be allocated to the hydration of the aluminate and ferrite phases and not inevitably to the growth of all hydrating phases. Since, however, C-S-H and aluminate phases grow in parallel, it is very reasonable to assume that there is an excellent correlation between the specific surface area of one type of cement and the PCE demand.

### 3.3.4 Counter ions, anions, and competitive adsorption

Due to their anionic backbone, PCEs attract counter ions. They build complexes with cations, such as  $\text{Ca}^{2+}$ . This reduces or neutralises their anionic charge [58, 166], having a strong influence on their adsorption characteristics. The presence and the amount of cations that can be found in the pore solution therefore can be assumed to have a very strong influence on the adsorption of PCE. An increasing amount of cations in the pore solution would therefore block negative charges resulting in reduced adsorption or adsorption velocity.

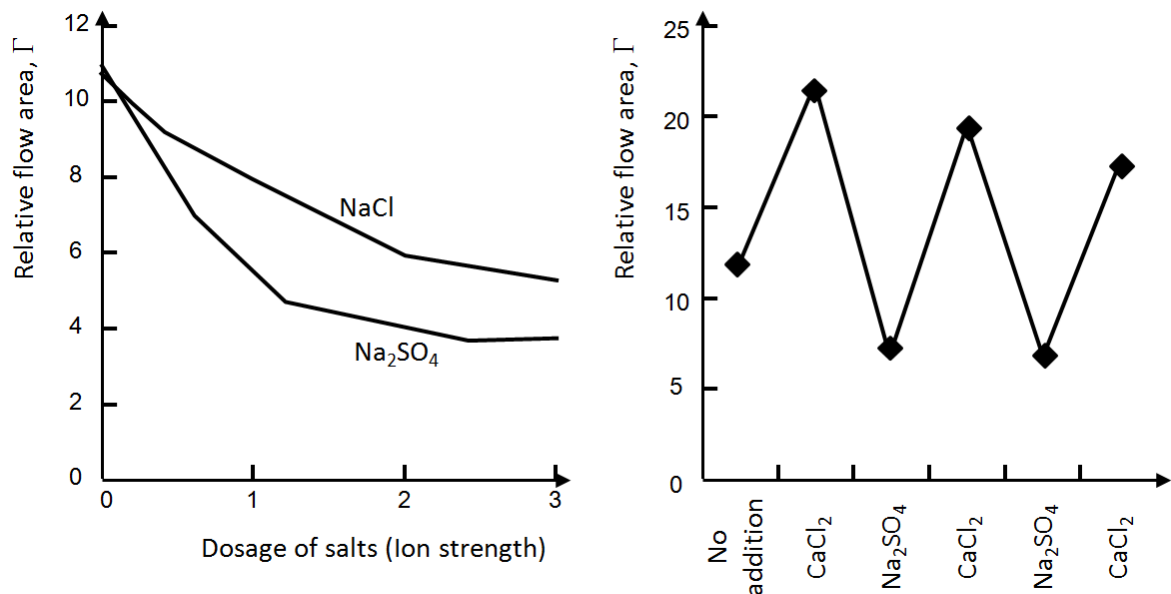


Figure 3.14: Influence of the content of NaCl and  $\text{Na}_2\text{SO}_4$  on the flow of a superplasticised system, and demonstration of the effect of repeated  $\text{Na}_2\text{SO}_4$  neutralisation with  $\text{CaCl}_2$  [60].

PCEs adsorbing on surfaces compete with anions in the pore solution [60, 165, 180]. Increasing contents of anions in the pore solution reduce the adsorption of PCEs, which causes a loss of flowability. Yamada et al. [60] showed that the addition of NaCl and  $\text{Na}_2\text{SO}_4$  to a PCE containing flowable system caused reduced flowability, which can be linked to desorption of PCE in favour of the chloride and sulphate ions (Figure 3.14, left). This process is reversible. By repeated and alternating addition of  $\text{Na}_2\text{SO}_4$  and  $\text{CaCl}_2$ , which is considered to neutralise the gypsum, the flow properties varied depending on the content of sulphate ions in the solution

(Figure 3.14, right). Due to the quick solubility and the high contents added to cement as set retarder, the content of soluble sulphates plays a major role.

### 3.3.5 Growth of hydration phases

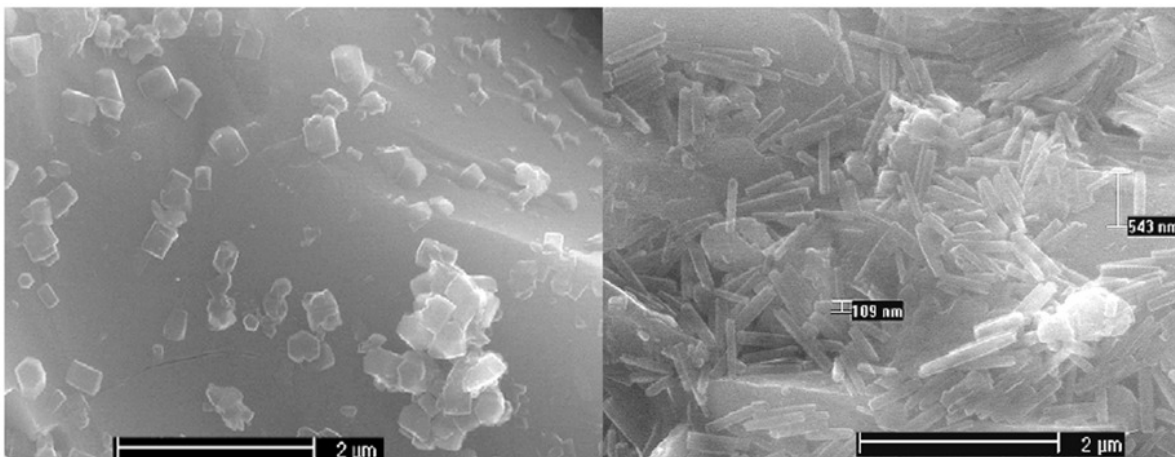
It is assumed that PCEs can modify the modification of the crystal growth. Roessler reports that mainly the  $C_3A$  and the bassanite (hemi-hydrate) hydration are affected [181, 182]. With regard to the AFm phase, Roessler and Sowoidnich [182] showed that at high  $C_3A$  contents AFm foils possess a spheroid shape. Ettringite is formed in long prismatic shapes, when PCE is present. This was not the case without SP or in the presence of PNS [183]. The different crystal modifications can be seen in Figure 3.15.

Roessler et al. also report about changes in the crystal modification of C-S-H [184]. Without superplasticiser and in the presence of PNS, the voids between particles in cement pastes were largely filled with the long acerous C-S-H (Outer product), while the presence of PCE superplasticiser caused bridges with densely grown inner C-S-H (Inner product).

### 3.3.6 Intercalations

It is reported in numerous studies that superplasticisers can form organo-mineral phases with the aluminate phase [61, 157, 168-170, 185]. These are considered as very stable phases [168, 186].

These were reported from PNS superplasticisers as an interaction with the AFm phase, while it is considered to be unlikely that AFt can bind polymers into its structure [61]. Due to intercalation of SPs into organo-mineral phases, the measurement of the TOC in the solution after SP addition is considered as not suitable for the determination of the amount of adsorbed polymers. An example was already given in Figure 3.9.



Short prismatic ettringite,  
CEM I,  
anhydrite/gypsum = 2.6/1.9,  
without PCE

Long prismatic ettringite,  
Laboratory cement,  
bassanite/anhydrite = 2/1,  
with PCE

Figure 3.15: ESEM-FEG wet mode image of ettringite on the left side without PCE and on the right side with PCE [181].

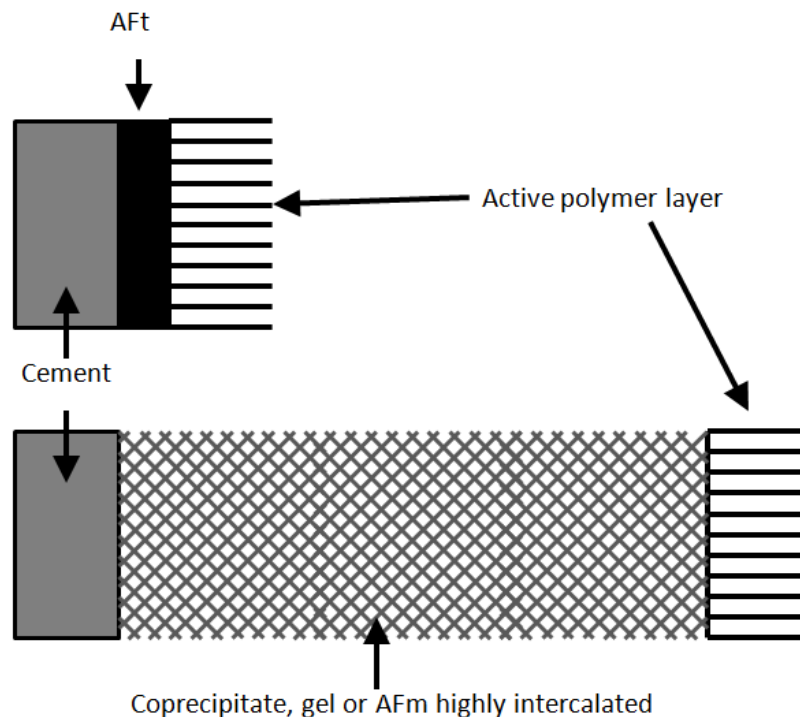


Figure 3.16: Influence of the “chemical sink” effect induced by different times of addition of SPs, after Flatt [61].

Flatt and Houst figuratively define the layer of organo mineral phases as chemical sink [61], which is fostered by circumstances that preferably form AFm instead of AFt. The formation of organo-mineral phases is responsible for the different effectiveness of SPs at immediate and delayed addition (Figure 3.16)

PCE superplasticisers are assumed to avoid intercalations due to the steric effect of the graft chains. Plank et al. have shown that in C-A-H phases obtained from  $C_3A$  hydration in absence of sulphate, intercalations can occur up to side chain lengths  $n_{PEO}$  of 45 Polyethylene units (see Figure 1.9), which makes it theoretically thinkable that intercalates can occur in the presence of sulphate as well. In more recent it was shown by Plank et al. that theoretically intercalations can also occur with Portland cement in case of an undersulphated system and for PCE with low charge density [185]. Ng and Plank presented that the formation of organo-mineral phases takes place also with PCEs [170].

### 3.3.7 Interactions with SCMs

Today’s cements are often containing supplementary cementitious materials (SCMs) such as limestone filler (LSF), ground granulated blast furnace slag (GGBS), fly ash (FA) or other components. Herrmann and Rickert investigated the influence of LSF and GGBS on the  $\zeta$  of cement blended with different amounts of limestone and GGBS, showing a shift of the initially negative value towards positive values at higher dosage with one LSF and two types of GGBS, while another LSF further brought the values into negative direction (Figure 3.17).

Plank et al. report that the influence of SCMs is strongly related to the ionic composition of the pore solution [187, 188]. As shown in Figure 3.17, the content of  $Ca^{2+}$  ions in the solution strongly affects the  $\zeta$  of GGBS due to adsorption on the surfaces of GGBS. Hence SCMs can also interact with SPs, since they modify the ionic composition of the pore solution and offer supplementary adsorption sites, which can attract PCE in competition with cement.

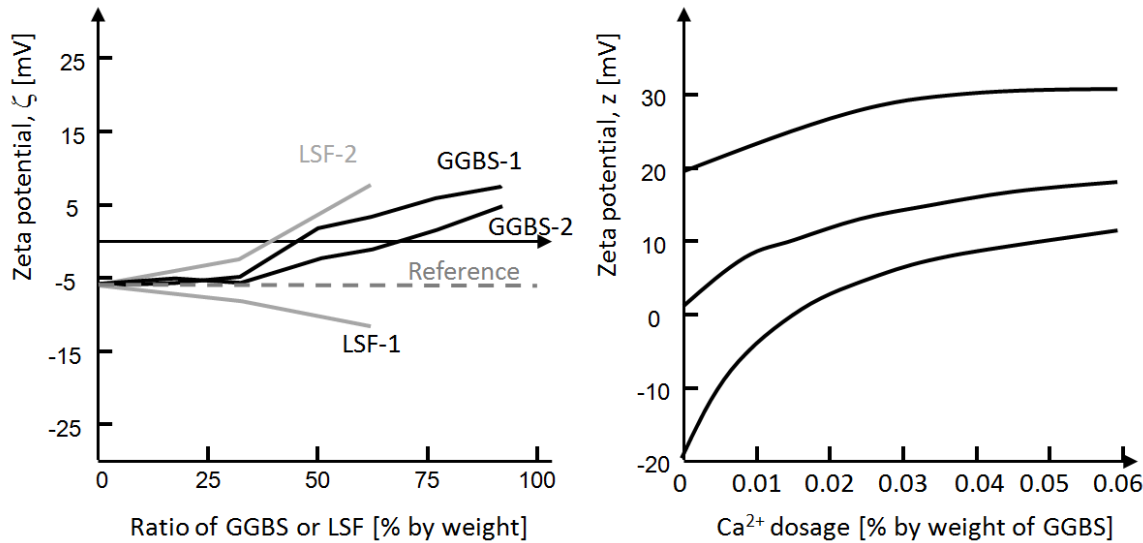


Figure 3.17: Changes of the  $\zeta$  depending on type and amount of different LSFs and ground granulated blast furnace slags [189], and influence of the  $\text{Ca}^{2+}$  content on the changes of the  $\zeta$  depending on the water to GGBS ratio [188].

### 3.3.8 Cement production factors

Flatt and Houst report about commonly used grinding aids based on triethanol amine acetate [61], which enhance the dissolution of  $\text{C}_4\text{AF}$ . This increase of aluminates may foster the formation of organo-mineral phases, thus yielding to a reduced performance of SPs. The milling conditions may also influence the performance of PCE. Yamada emphasises the importance of the milling temperature as well the milling process to avoid excessive hemi-hydrate or reactive anhydrite [68], which would interfere with the PCE performance. The author further emphasizes that solely the processing after milling, during the transportation or storage, can have strong influence on the flow properties in the presence of PCE. Strong effects resulting from the storage conditions of cement on the flow properties of systems incorporating PCE were also reported by Schmidt et al. [123]. These are further discussed in Subsection 4.5.1.

## 3.4 Influences of PCE modification

### 3.4.1 Versatility of the molecular structure of PCEs

Today, the chemical industry is capable to generate individual polymeric structures of PCEs. This means, the length of the backbone, the grafting degree, as well as the graft length can be individually modified. Also polymers with mixed graft chain lengths are possible, which offers a high number of possibilities to develop individual polymers for individual applications. However, the modifications affect the physico-chemical properties of the polymers, since solution structures, adsorbed conformations and anionic charge densities are affected.

Due to their versatility, PCEs cannot be easily described. In order to get a grip on the appearance of polymers in solution, often the Stokes radius, or hydrodynamic radius  $R_H$  as well as the radius of gyration are used. The hydrodynamic radius describes the radius of a hypothetical sphere with identical diffusion properties in a fluid. It is defined by the Stokes-Einstein Equation:

$$R_H = \frac{k_b \cdot T}{6\pi \cdot \eta \cdot D} \quad (3.10)$$

where:  $R_H$  = hydrodynamic radius [m];  $k_b$  = Boltzmann constant [J/K];  $T$  = temperature [K],  $\eta$  = viscosity [Pa·s];  $D$  = diffusion coefficient [m<sup>2</sup>/s].

The radius of gyration, is a measure of the spatial dimensions of a macromolecule, which is defined by the sum of the distances of elements, e.g. monomers, from the mass centre:

$$R_G^2 = \frac{\sum_{i=1}^N (r_i - r_{\text{mean}})^2}{N} \quad (3.11)$$

where:  $R_G$  = radius of gyration [m];  $N$  = number of similar elements (e.g. monomers);  $(r_i - r_{\text{mean}})$  = distance between elements and mass centre of the macromolecule [m].

Both values express different properties, and particularly for polymers, their interrelation may vary in certain range. Kok and Rudin [190] reviewed the relation factors between  $R_H$  and  $R_G$  according to:

$$X = \frac{R_H}{R_G} \quad (3.12)$$

where:  $R_H$  = hydrodynamic radius [m];  $R_G$  = radius of gyration [m].

This factor according to the authors shall be independent of the molar mass or the solvent. For different polymer types they found values in the range of 0.425 to 0.891. Weiner states that values  $X$  close to 1.3 suggest spheres, while values close to 0.65 suggest random coil polymers [191]. None of the given values, hence, can provide a clear figure of the polymeric geometry in solution. This is particularly valid for complex polymers like PCE. They can have very different structures (see. Figure 1.10) with differing ratios of  $R_H$  and  $R_G$ . Hence, the meaning of these values should not be over-interpreted in terms of the assessment of how they interact with surfaces of particles and hydrates in cementitious systems. Nevertheless, it is important to recognise that for PCE both values occur in the order of magnitude of nano metres. Hence, the polymers are typically several hundred or thousand times smaller than the particles they affect.

According to Winter [14], who refers to a paper presented by Uchikawa [192], their hydrodynamic radii range between 30 and 150 nm (this information was not found explicitly in the respective paper). Giraudeau et al. report about radii of gyration of  $5 \pm 2$  for some investigated PCEs with short side chains [157]. The PCE molecules observed by the authors showed  $R_H$  and  $R_G$  in similar order of magnitude. Winter [14] interprets the data provided for different PCEs by Yamada et al. [60] and concludes that the range of unified atomic masses of PCEs vary between 10,000 and 200,000 Da. The latter unit, Dalton (Da, also u) is the unit for the unified atomic mass. It is the twelfth part of the mass of the carbon isotope <sup>12</sup>C. Therefore it is numerically identical to the molar mass in g/mol. The complex interrelations between graft chain lengths, main chain length, number of ethylene oxide units on the backbone, and hydrodynamic radius is shown in Figure 3.18. The figure, taken from a publication by Keller and Plank [193], shows that an arbitrary number of PCEs is thinkable with likewise arbitrary effects on the solution structure and possible effects on rheology.

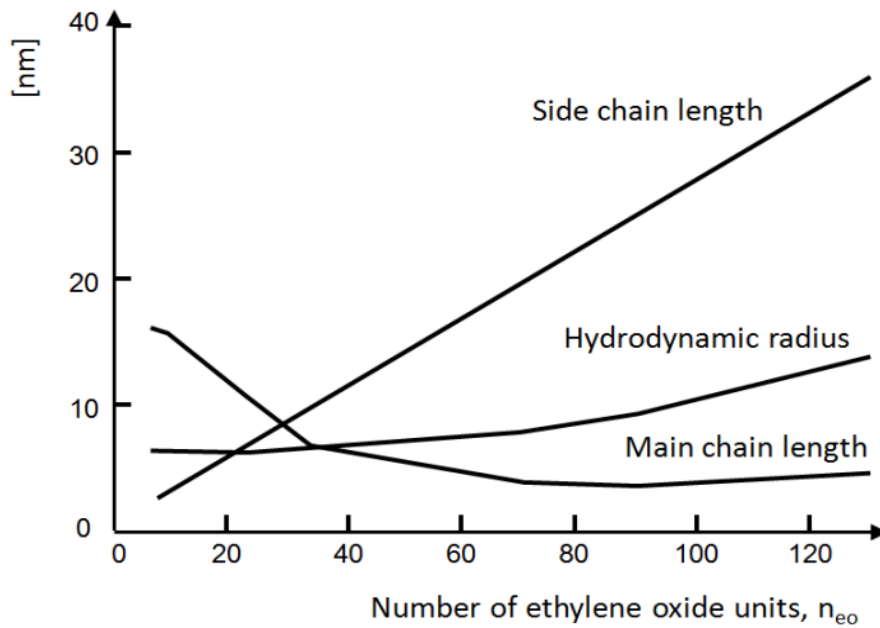


Figure 3.18: Correlation between main chain length, graft length, and hydrodynamic radius depending upon the  $n_{EO}$  on the backbone after Keller and Plank [193].

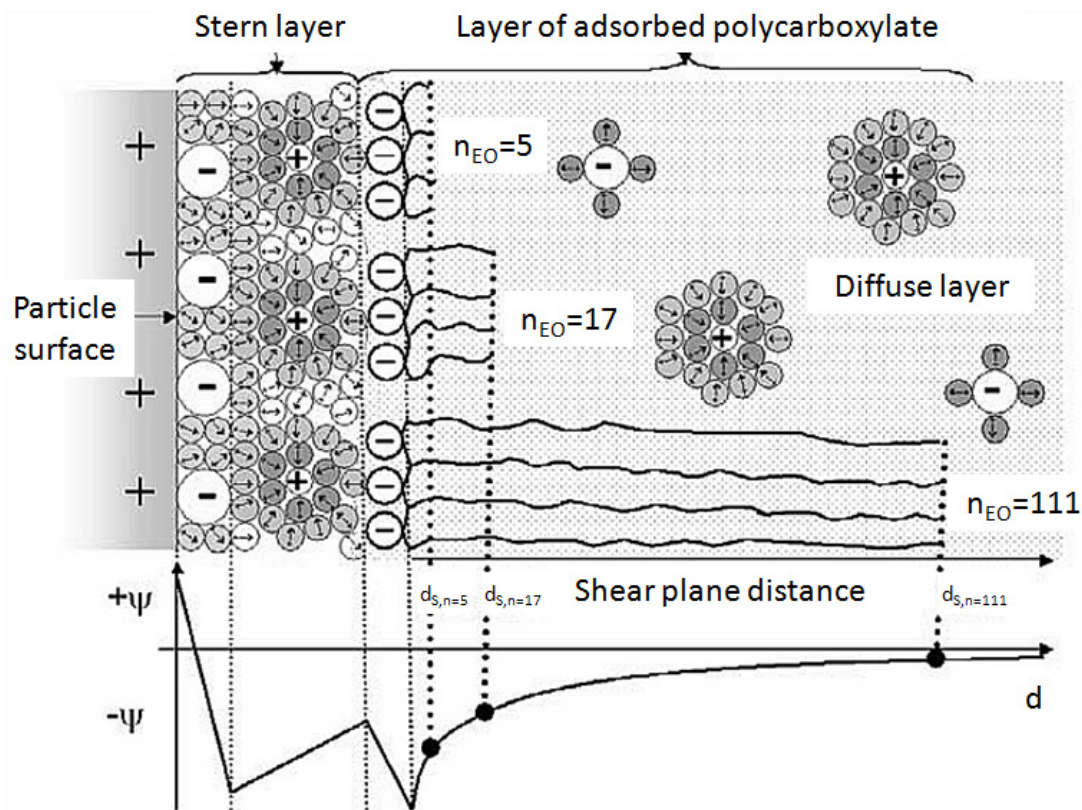


Figure 3.19: Shearing layer distances induced by adsorption of PCEs with different graft chain lengths (expressed in  $n_{EO}$ ) after Keller and Plank [14].

### 3.4.2 Effects of the graft length of PCE

The graft length affects the overall charge of the polymer, the longer the graft chain, the lower the overall charge of the polymer. Another effect introduced by the graft chain length is a modification of the  $\zeta$ . This, according to Winter [14], can be explained by a shift of the shearing layer distance by longer side chains, as shown in Figure 3.19. Increasing graft chain lengths are assumed to improve the dispersion and increase the performance retention [19, 179].

### 3.4.3 Effects of the backbone length of PCE

The backbone length, which is determined by the number of repeated segments and monomers (Figures 1.9 and 1.10) affects the number of anionic charges and thus the entire polymer charge. Depending upon the number of anionic charges within a backbone that can adsorb, the conformation may vary between train, loop, and tail structure [85], as presented in Figure 3.20.

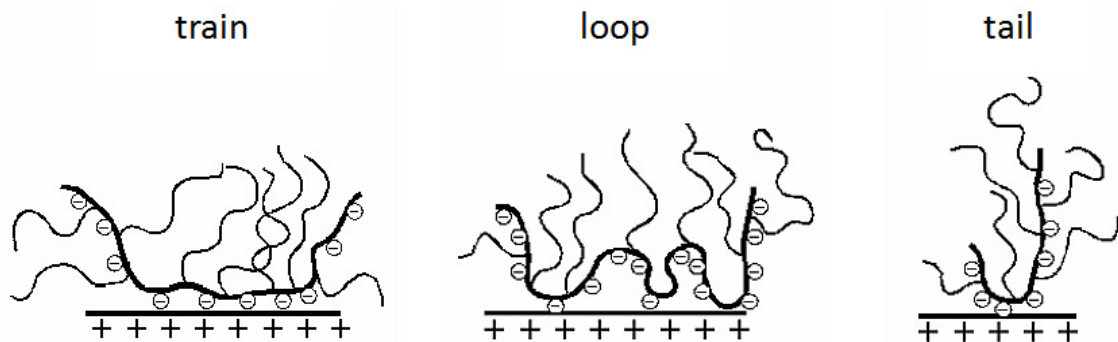


Figure 3.20: Different adsorption conformations. The conformation as train, loop, or tail depends on the number of adsorbed anionic charges [85].

Besides that, the backbone length can affect the length of the dispersing ability. According to Sakai et al. [179], a longer trunk reduces the retention duration. However, for normal cementitious systems, the effect of the backbone length can be considered as of less significance. For ultra-high performance concrete, which typically incorporates very fine and nano-sized particles, short backbone lengths are considered to be necessary in order to avoid particle-particle interactions.

### 3.4.4 Effects of the grafting degree

The grafting degree affects the entire polymer anionic charge but also the anionic charge density of the backbone, since each bond reduces the number of anionic charge carriers. The grafting degree is a major modification parameter for PCEs. For identical backbones, a high grafting degree yields low charge densities and vice versa.

### 3.4.5 Effects of the entire PCE structure

PCEs can be adjusted individually by the chemical industry. The length of the backbone, the length of the graft chain as well as the grafting degree can be individually modified. The factors determining the charge density of the polymer are the graft length and the grafting degree. The longer the grafts or the higher the number of graft chains the lower is the charge density of the polymers. The charge density of the PCE is one driving factor for the adsorption of PCEs.

Due to the possibility to individually adjust PCE superplasticisers with regard to the length of the backbone, the length of the graft chains as well as the grafting degree, numerous polymeric modifications are available on the market.

Gay distinguishes between different characteristic formations as shown in Figure 3.21, depending on the number  $P$  of monomers in the side chain and the number  $N$  of monomers in the backbone as well as the number  $n$  of repeated segments (see also Figure 1.9). The different geometries are entitled decorated chain (DC), flexible backbone worm (FBW), stretched backbone worm (SBW), stretched backbone star (SBS), and flexible backbone star (FBS). Depending on the structure, the adsorption behaviour may vary greatly, thus affecting the  $\zeta$ .

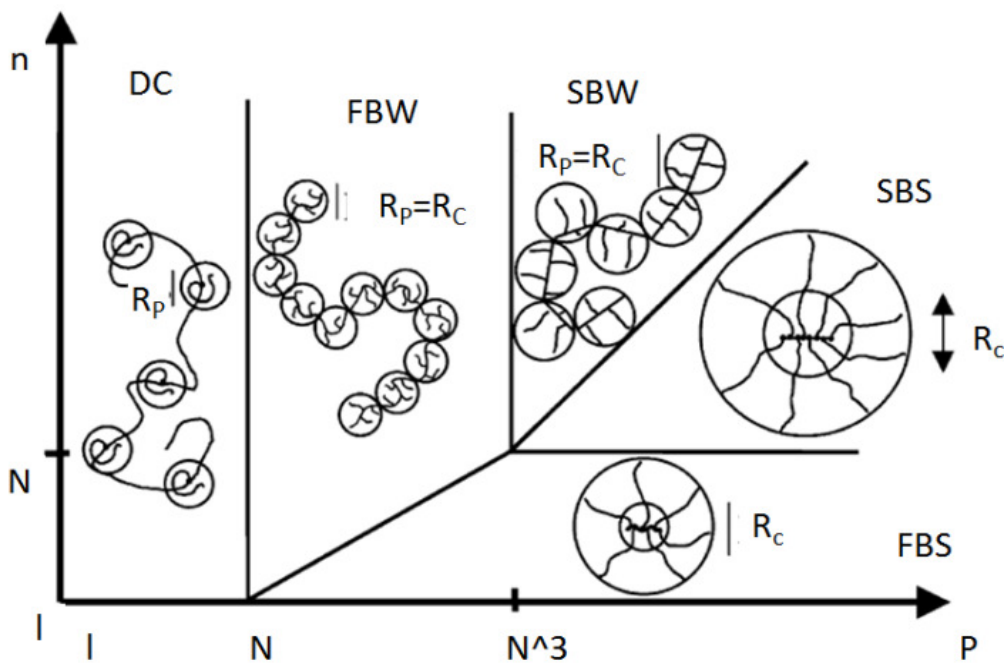


Figure 3.21: Different PCE structures depending on backbone length and grafting degree according to Gay [194].

### 3.4.6 Effects of the charge density of the PCE on the rheology

Houst et al. [22] and Hanehara and Yamada [17] have shown good linear correlations between the number of adsorbed PCEs and the reduction of the yield stress for individual PCE types. Schober and Flatt varied a seven differently modified PCEs and found the influence of PCE on the flow properties is to the major part independent of the molecular structure, but to the largest part only depending on the amount of adsorbed polymers [66, 67] (Figure 3.22).

This observation can be considered as a breakthrough in understanding the performance of PCE superplasticisers, since it reduces the number of possible effects as described in the previous Subsections 3.4.2 to 3.4.5 to a single parameter: the charge density.

This does not mean that effects of the polymeric geometry are negligible, but it means that the influences of the polymeric structure can be largely reduced to the way they affect the anionic strength of the PCE. The lower the grafting degree or the shorter the side chains' length, the higher is the anionic charge of the molecule. These interrelations are comprehensively provided in Figure 3.23.

Understanding this context, it is easy to qualitatively assess the performance of two differently modified PCEs regardless of the effects that may be individually contributed by the cement type or the mixture composition.

The higher the charge density, the better the adsorption, the lower the amount required to achieve a specified flow performance, and the earlier the PCE consumption. Therefore, high charge density polymers are used for pre-cast applications, where quick and strong reduction of the yield stress is required, but a long lasting retention is not required.

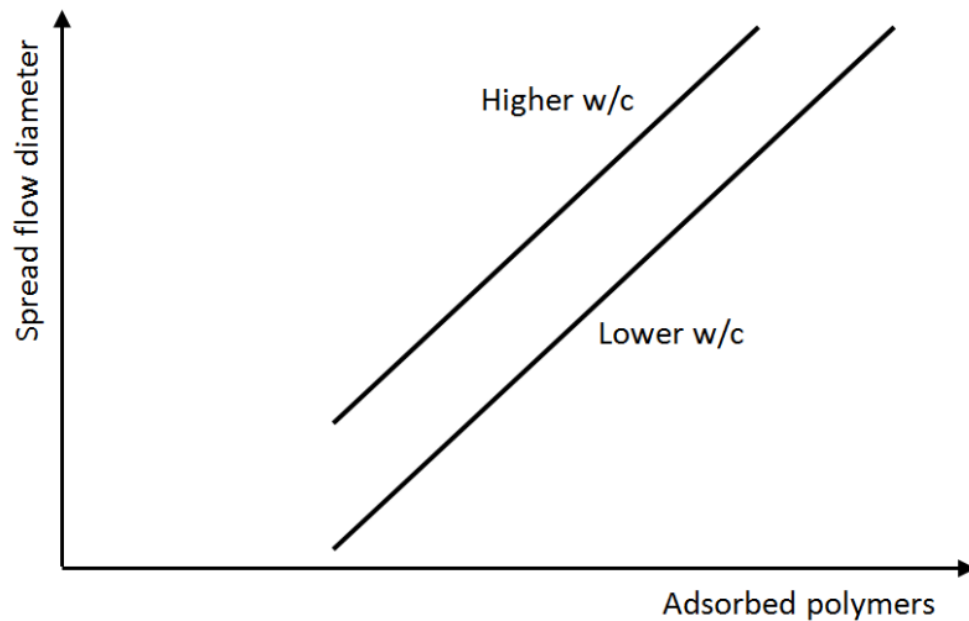


Figure 3.22: Linear correlation between flow properties and amount of adsorbed polymers for different PCE modifications, qualitatively after Schober and Flatt [67].

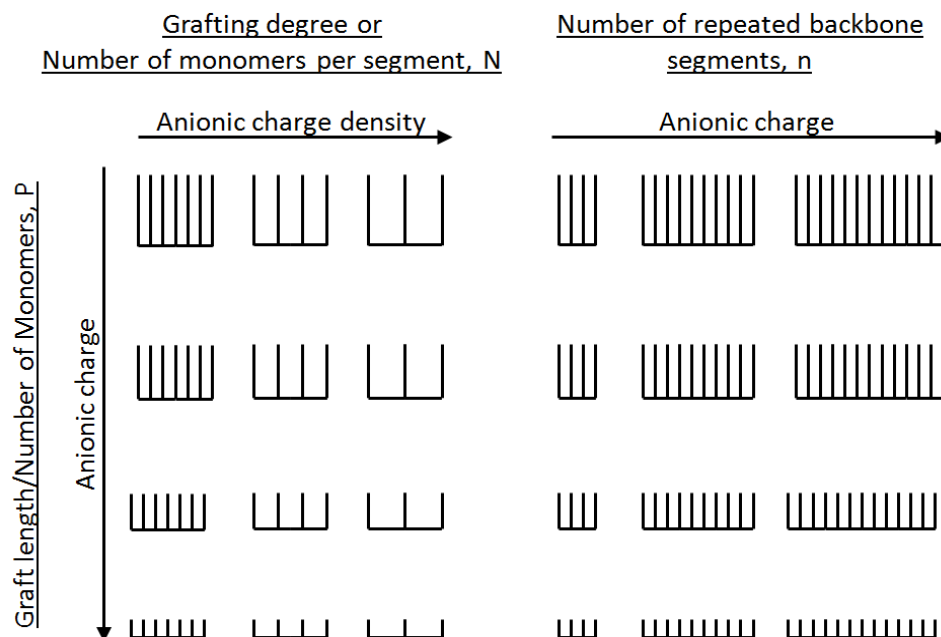


Figure 3.23: Influence of the PCE geometry on the charge density.

The lower the charge density, the slower the adsorption, the higher the amount of required polymers, and the more adsorption takes place at later moments in time. Hence, low charge density polymers are used for ready-mixed applications, where particularly the flow retention can be a crucial aspect.

Due to the competitive adsorption between PCE and sulphate ions, the charge density of PCEs is also the main influencing factor for incompatibilities between cement hydration and SPs [85]. Low charge polymers can be desorbed by sulphate ions or they do not adsorb directly. Delayed adsorption may generate uncontrollable time delayed increase of the flowability, which might cause segregation problems. High charge density polymers can be adsorbed rapidly upon addition but they are consumed quickly by emerging hydration products, thus the retention of the flow properties is poor.

### **3.5 PCE in practice**

#### **3.5.1 Blends of PCE**

The SP market world-wide consists of producers and blenders, of which the blenders dominate most markets, at least regarding their number. Companies that blend admixtures typically make use of the possibility to mix different PCE molecular structures for individual performance adjustment. E.g. it is reasonable to blend a high charge density PCE with a low charge density PCE in order to achieve high initial flowability and good retention. Many companies that blend admixtures can develop individual compounds for their customers.

#### **3.5.2 Blends of different superplasticisers**

It has become practice not only to mix different polycarboxylic SPs, but also to make use of blends between different types of SPs. For example, it is reasonable to make use of the good initial flow improvement by using lignosulphonate instead of a high charge density PCE, which also helps to reduce the market price (or at least the production costs), and to retain the performance with a low charge density PCE.

#### **3.5.3 Blends with different admixture types**

Furthermore, it has also become practice to blend SPs with different functional admixtures, e.g. the market provides many shrinkage reducing SPs or SPs that help increasing the viscosity in order to avoid segregation. These properties are often achieved by simply adding certain amounts of viscosity modifying agents or shrinkage reducing agents. It is not unrealistic to assume that many superplasticising products based on PCE contain up to 15 different components, some of which might only be pigmentation.

#### **3.5.4 Practical problems to assess the PCE performance**

The aforementioned possibilities to develop individual products can be a great support particularly for the pre-cast industry, where often problems occur, which can be linked to individual production boundary conditions. An individual blend can help to increase the robustness of the production process, however, if the boundary conditions change, exactly the opposite can be the case. The number of different influencing factors is high. It is impossible to link effects which may occur due to varied temperatures, varied raw materials or any other change, to responsible admixture components.

For ready-mixed concrete the boundary conditions vary greatly throughout a daily production and throughout a long term production. It can therefore be considered to be impossible to use an individual blend which was developed for defined boundary conditions.

The best way to adjust the right composition of admixtures should be given into the hands of the concrete mixing company, since they can individually adjust the blend to a very particular boundary condition.

Unfortunately, users of admixtures often do not know at all about the ingredients of the applied admixture. The chemical industry avoids giving more information to the user necessary. According to the experiences of the author, also the customer service of construction chemical companies is typically not equipped with all relevant information about the products. Furthermore the producers of concrete exhibit a significant lack of understanding of the complex interactions between cement hydration and admixtures. A tool that helps users to easily distinguish their admixtures qualitatively would support a better and more reasonable use of PCEs in practice. Following the subsequent chapter, which introduces the experimental examinations, such a tool – a simple test method to qualitatively distinguish between PCEs - will be presented in Chapter 5.



## 4 Materials and Methods

### 4.1 Background of the used concrete mixtures

#### 4.1.1 Introduction

As already referred to in Subsection 1.3, all over the world, the understanding of what is SCC varies greatly. One of the major objectives of this Thesis is to develop knowledge about interactions of admixtures and cementitious materials with relevance for SCC in general, without limited relevance for a certain area of standards and philosophies. If such a general relevance is difficult to achieve, the aim is to understand which mixture composition parameters define different behaviours. Therefore, different mixture compositions were subject of the observations. A powder type SCC “POW” and a combination type SCC “COM” were designed, which consist of the same raw materials basis. Both mixture compositions have been applied since that time by various researchers at the BAM Federal Institute for Materials Research and Testing for different research focus areas [123, 195-197]. At first the raw materials’ properties will be given and the historical background of the employed mixture compositions will be explained, before the final mixtures COM and POW will be introduced.

#### 4.1.2 Powder properties

The cement used for the tests was an ordinary Portland cement according to EN 196 from the CEMEX cement plant in Rüdersdorf, Germany. The specification is CEM I 42.5 R. The bulk density of the material was determined by He-pycnometry as 3123 kg/m<sup>3</sup>. The Blaine value was determined according to EN 196-6:1990 as 4110 cm<sup>2</sup>/g. The water demand to meet the standard stiffness was determined according to EN 196-3:1995. A summary of the materials properties is given in Tables 4.1 to 4.3. The chemical composition of the cement was determined according to EN 196-2:2005 and is given in Table 4.1. The resulting clinker composition calculation according to Bogue, e.g. [82], and the modified Bogue calculation according to Taylor [198] is given in Table 4.2. The physical properties are given in Table 4.3. Furthermore, Figure 4.1 shows a SEM micrograph to provide information about the surface geometry of the used CEM I 42.5 R in comparison to the used LSF.

Table 4.1: Oxide composition of the used CEM I 42.5 R.

CaO:	62.80%	Na <sub>2</sub> O:	0.28%
SiO <sub>2</sub> :	20.56%	K <sub>2</sub> O:	0.95%
Al <sub>2</sub> O <sub>3</sub> :	4.36%	TiO <sub>2</sub> :	0.20%
Fe <sub>2</sub> O <sub>3</sub> :	2.27%	P <sub>2</sub> O <sub>5</sub> :	0.00%
MgO:	2.14%	SO <sub>3</sub> :	3.45%
Mn <sub>2</sub> O <sub>3</sub> :	0.03%	Insoluble residue	0.56%
Loss on ignition	2.40%		
Of which CO <sub>2</sub>	1.96%		
SUM:	99.44%		
Na <sub>2</sub> O-eq:	0.91%		

The LSF is from a quarry in Medenbach, Germany. The bulk density of the LSF was 1735 kg/m<sup>3</sup> (He-pycnometry), the Blaine value was 5130 cm<sup>2</sup>/g (EN 196-6:1990). The chemical composition of the LSF was measured by X-ray fluorescence method ( $\mu$ -XRF) as given in Table 4.4. The particle size distributions of the cement and the LSF, measured by laser granulometry are given in Figure 4.2.

Table 4.2: Clinker phase composition according to Bogue calculation, e.g. [82], and modified Bogue calculation according to Taylor [198].

Clinker phase	Standard Bogue calculation	Modified Bogue calculation
C <sub>3</sub> S	49.7%	61.8%
C <sub>2</sub> S	28.4%	20.5%
C <sub>3</sub> A	8.6%	6.2%
C <sub>4</sub> AF	7.7%	7.7%
SUM:	94.5%	96.1%

Table 4.3: Physical properties and strength of the CEM I 42.5 used for the tests according to the producer.

Fineness (Blaine)	[cm <sup>2</sup> /g]	4110
Density	[kg/m <sup>3</sup> ]	3123
Water demand	[%]	28.5
Compressive strength, 1 day	[MPa]	23
Compressive strength, 2 days	[MPa]	37
Compressive strength, 7 days	[MPa]	50
Compressive strength, 28 days	[MPa]	61

Table 4.4: Total oxide composition of the limestone filler from XRF measurement.

Oxide	Percentage by mass
Na <sub>2</sub> O	3.27%
MgO	0.61%
Al <sub>2</sub> O <sub>3</sub>	0.46%
SiO <sub>2</sub>	1.47%
P <sub>2</sub> O <sub>5</sub>	2.19%
SO <sub>3</sub>	0.34%
K <sub>2</sub> O	0.54%
CaO	90.68%
TiO <sub>2</sub>	0.05%
Fe <sub>2</sub> O <sub>3</sub>	0.4%

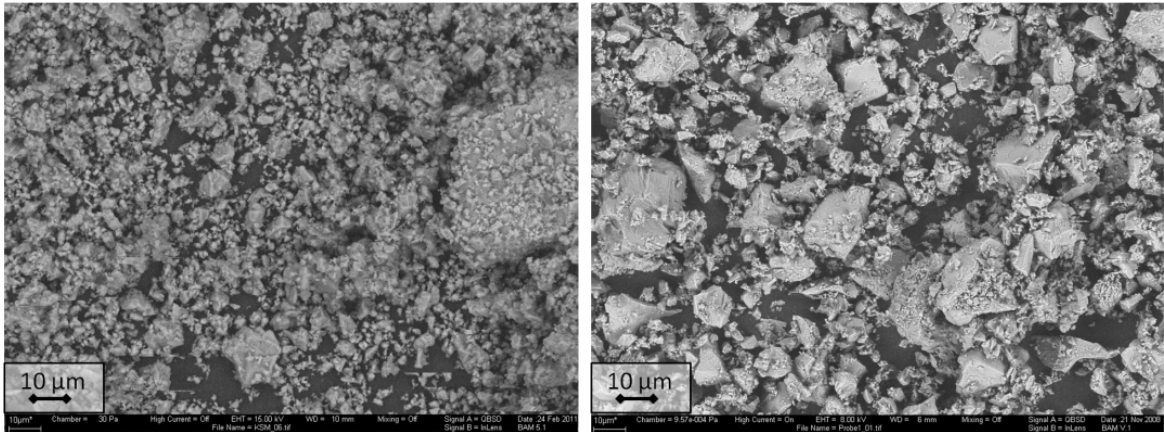


Figure 4.1: SEM micrographs of the LSF (left) and the cement (right) that were used for all tests.

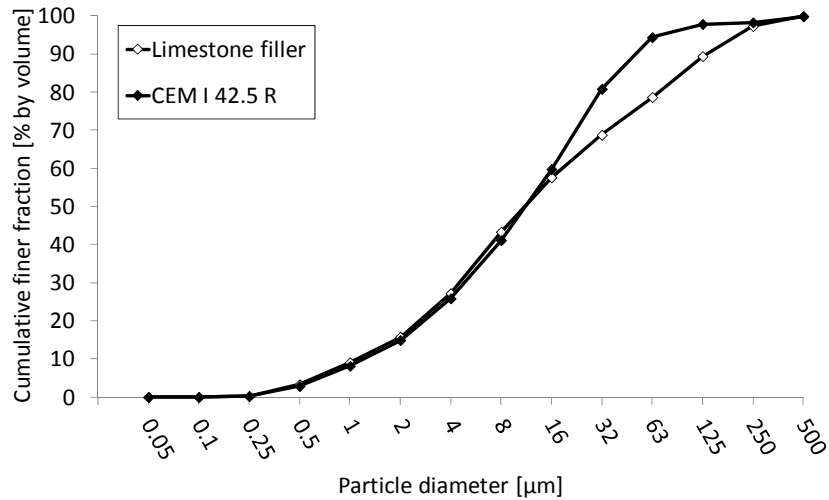


Figure 4.2: Grading curve of CEM I 42.5 R and LSF used for the investigations in this Thesis.

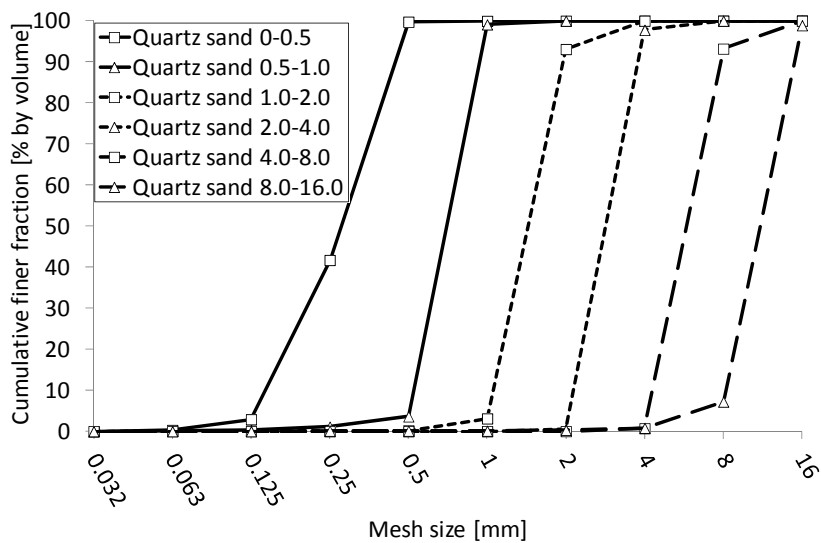


Figure 4.3: Grading curves of the sand and aggregate fractions.

Table 4.5: Specifications of the polycarboxylic superplasticisers.

Abbreviation	LC	MC	HC
Backbone	Polycarboxylate ether (PCE), identical for all modifications		
Graft chains	Polyethylene oxide (PEO)		
Trade name	Glenium Sky 591	Glenium Sky 593	Glenium Sky 595
Specific application	Use for cements with low alkali/alkali sulphate content	High robustness	Use for cements with high alkali/alkali sulphate content
Recommended dosage	0.2 - 3.0% by mass of cement (bmoc)		
Min. dosage	not specified		0.8% bwoc
Max. dosage	not specified		
Density at 20 °C	1.07 ± 0.02 g/cm <sup>2</sup>	1.05 ± 0.02 g/cm <sup>2</sup>	1.05 ± 0.02 g/cm <sup>2</sup>
Solid content	30%	23%	20%
pH at 20 °C	6.5 ± 1.0	6.5 ± 1.0	6.5 ± 1.5
Max. chloride content	0.10% by mass		
Max. alkali content	1.5 M.-% (Na <sub>2</sub> O-eq.)	1.2 M.-% (Na <sub>2</sub> O-eq.)	1.3 M.-% (Na <sub>2</sub> O-eq.)
Graft chain length (Figure 3.23)	medium + low	medium + low	medium
Grafting degree (Figure 3.23)	high	medium	low
Backbone charge density (Figure 3.23)	low	medium	high

### 4.1.3 Sand and gravel

The sand and gravel components used for the tests origin from a quarry in Ottendorf-Okrilla, Germany. Sand and aggregates are delivered fractionated and washed. At delivery they are fully dried and they are always stored indoors. As a result of the washing the powder contents of the sand and aggregates are negligibly small. The grading curves of the single fractions are given in Figure 4.3.

The material is regularly used and re-charged at the BAM. For each charge, the bulk densities are measured according to EN 1097-6. They only vary slightly between 2600 kg/m<sup>3</sup> ± 50 kg/m<sup>3</sup>. For all mixture calculations, hence, the value of 2600 kg/m<sup>3</sup> was used.

### 4.1.4 Superplasticisers

Since one of the major influencing factors for the performance of SPs is the charge density of the polymer [66, 67], the polymer variations were aimed to vary as little as possible but to clearly distinguish by different charge densities. Since the polymers are commercially available products, details about the chemical composition of the modifications were not provided by the producer, but qualitative information was made available about the geometry defining parameters as shown in Figure 1.9.

All polymers contain identical polycarboxylic backbones in chemistry and length. The graft chains consist of polyethylene oxide, which may vary in length between the polymers. Blends of different graft chain lengths are possible, which have minor influence on the polymers' charge densities. The major effect determining the charge density, however, is the number of grafts in the backbone (Figure 3.23). The grafting degree is high for the low charge density polymer and low for the high charge density polymer. The medium charge polymer has a grafting degree in between. Details about the PCEs are given in Table 4.5. As introduced in Section 3.4, high

charge polymers are adsorbed quicker and thus are assumed to reduce yield stress more effectively than polymers with lower charges.

#### 4.1.5 Stabilising agents

The STAs that are used in this Thesis differ in origin and performance. Both are commercially available polysaccharides. Stabilising agent ST1 is based on modified starch. The commercial name of this product is Foxcrete produced by the company Avebe and has been subject of research in the field of SCC in the past years [70, 199, 200]. According to information of the producer, the STAs should be added in typical amounts ranging between 250 and 400 g/m<sup>3</sup>. The second stabilising agent used for the investigations, abbreviated ST2, is a polysaccharide called diutan gum. It is produced by CP Kelco and has also been subject of research in the field of cement and concrete technology [140, 201-203]. The commercial name is Kelcocrete DG-F. According to the product data sheet of the producer, it should be added in amounts between 0.01 and 0.15% by mass of the water.

ST1 does not generate a significant yield stress in water, only when added to water-solid systems. ST2 increases yield stress and viscosity of a fluid system [131, 204]. Thus, particle immobilisation (ST1) and fluid-phase stabilisation (ST2) can be distinguished. It is therefore a reasonable approach to relate the dosage of the starch ether to the powder and the dosage of the diutan gum to the water. In order to avoid confusion, however, and since the water to powder or water to cement ratios were not varied in the observed mixtures, in this work, the STA will always be related to the cement content.

The major difference between the different stabilising mechanisms is how each STA affects fluids and dispersions. The Figures 4.4 and 4.5 shows results of rheological measurement with a cylinder cell. Water was mixed with different amounts of both STAs and a dispersion of a volumetric w/c of 2.0 mixed with different amounts of STA. Since both stabilising admixtures affected the yield stress in significantly different magnitude, a related observation was required to generate rheograms for different STA amounts.

At an addition of 20 g/l of ST1 and 1.0 g/l of ST2 on water, the viscosities of the water STA mixtures were identically 8.02 mPa·s and 8.04 mPa·s, respectively, based on the Bingham Equation (3.5). Figure 4.4 shows the respective yield stress in the fluid system with water only ( $\tau_{0, \text{Water}} = 0$ ;  $\eta_{\text{Water}} = 1.002$  at 20 °C) and yield stress and viscosity at identical STA amounts in the dispersion. It can be observed that at identical influence on viscosity, yield stresses are affected in different ways. While ST1 increases yield stress in a negligible way, ST2 generates a pronounced yield stress. For the operator of the test, the mixture with ST1 looks and like foggy water, while the mixture with ST2 rather looks like glue. If these mixtures are amended by cement, it can be observed that viscosities increase but at the same time significant yield stresses can be observed for both mixtures, pointing out that the effect of ST1 on yield stress is mainly generated by the presence of solid particles.

For the evaluation in rheograms (Figure 4.5), the identical viscosities and the respective yield stresses were defined as reference values  $\eta_{\text{ref}}$  and  $\tau_{0, \text{ref}}$ . Yield stress and viscosity of any other STA addition were then divided by these reference values. It can be observed that with water only, ST1 only affects the viscosity, while yield stress is not affected. The measurements of the yield stress yielded results that scattered closely around zero. Yield stress was thus for the graphic evaluation set as zero. In case of ST2, it can be observed that mainly the viscosity is affected by increasing STA additions. At higher dosages, the yield stress is affected stronger, while viscosity increases less pronounced.

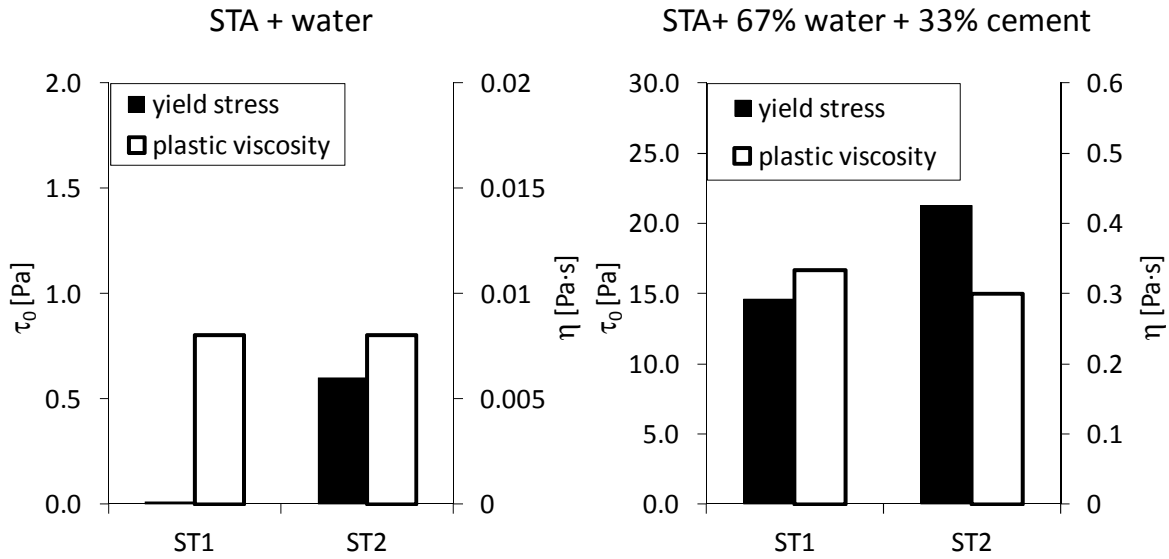


Figure 4.4: The influence of ST1 and ST2 on  $\tau_0$  and  $\eta_{pl}$  when mixed with water (left) and when mixed with a water-powder suspension (right).

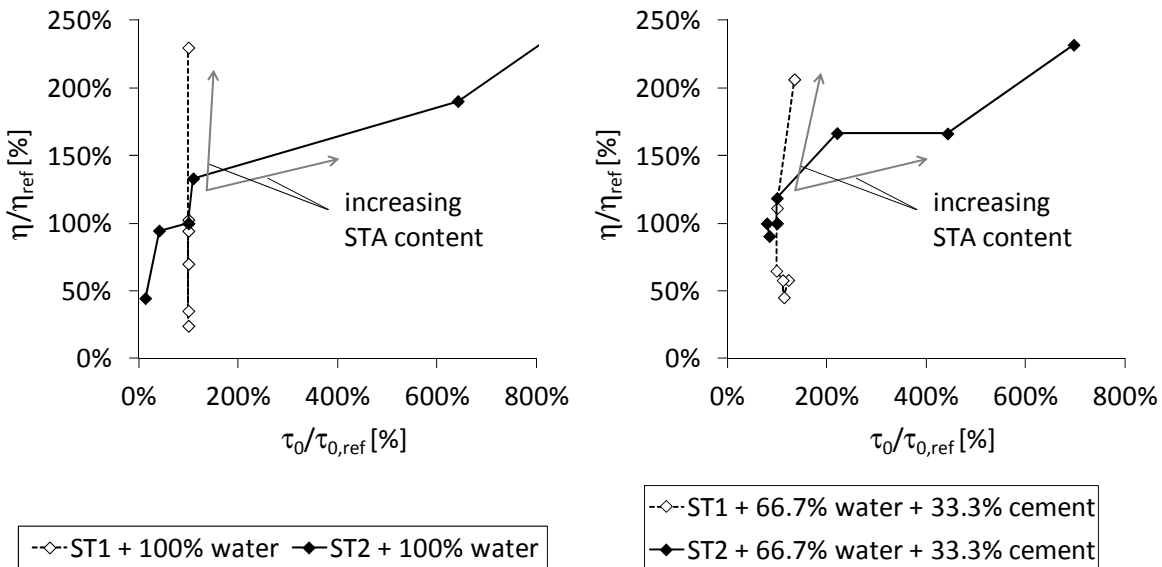


Figure 4.5: Changes of  $\tau_0$  and  $\eta_{pl}$  due to varied dosage of ST1 and ST2 in water and water-cement suspension.

In case of the dispersion, similar viscosities were measured at an addition of 12.4 g/l of ST1 and 2.0 g/l of ST2. Similar characteristics as for the fluid system can be observed for the dispersion with the only difference that in the system containing solid particles, ST1 generates increasing yield stresses with increasing dosages. However, the curve still appears quite steep, hence, it can be concluded that also in the dispersed system ST1 mainly affects viscosity much more than yield stress, while ST2 affects viscosity stronger than yield stress at low dosages and behaves vice versa at higher dosages.

The observations in the Figures 4.4 and 4.5 were made with a maximum volumetric part of cement of 33%. At this solid to fluid ratio, it appears as if ST1 mainly affects viscosity.

However, much more than with ST2, the performance depends on the powder content in the dispersion. A detailed discussion about the strong influence of the solid content, which plays a major role for the performance of starch ethers in comparison to diutan gum, will be discussed later in detail in Subsection 7.2.3.

#### 4.1.6 Background of the powder type SCC (POW)

The powder type mixture (POW) used in the investigations is a modification of an SCC, originally developed strictly according to the approach of Okamura [205]. The prototype of this mixture composition was generated with a CEM I 42.5 and a LSF to amend the powder content (Table 4.6). The LSF used in the original SCC was identical to the LSF used for the experimental part of this Thesis, and it was introduced in Subsection 4.1.2. There are several authors stating that the water demand determined according to the approach of Okamura is too high and that for practical reasons optimisation is required, which can be achieved by reducing the water volume to 70% to 90% of the  $\beta_p$ -value [30, 40, 206, 207] (see Figure 1.2). In a former study about the robustness of the used SCC mixture composition and numerous differing compositions, proposed and supervised by the author, the effect of the reduction of the  $\beta_p$ -value was observed [208]. The water volume yielding from the intercept of the ordinate was reduced between 75%, 80%, and 85%, and the workability properties were observed with different SP contents. The mixture with 80% of the  $\beta_p$ -value appeared to work most robustly. Figure 4.6 shows the resulting average slump flow values for water additions of 75%, 80%, and 85% of the  $\beta_p$ -value at different SP contents. Slump flow (SF) values between 550 mm and 800 mm were considered as reasonably stable mixtures. At 85% of  $\beta_p$  the SP additions that generated good flow properties ranged between 0.75% and 0.90% of the cement content, at 75% of  $\beta_p$  the additions ranged between approximately 0.90% and 1.05%. The widest range of SP additions was possible at a reduction of the water content to 80% of  $\beta_p$ . Here the range of SP additions was 0.30% between 0.80% and 1.10% of the cement content. The mixture at this water content was thus chosen as the development basis for the final mixture that was used for the conducted investigations. The mixture composition of this original powder type SCC is given in Table 4.6 compared to the final mixture composition according to the modifications in Subsection 4.1.7.

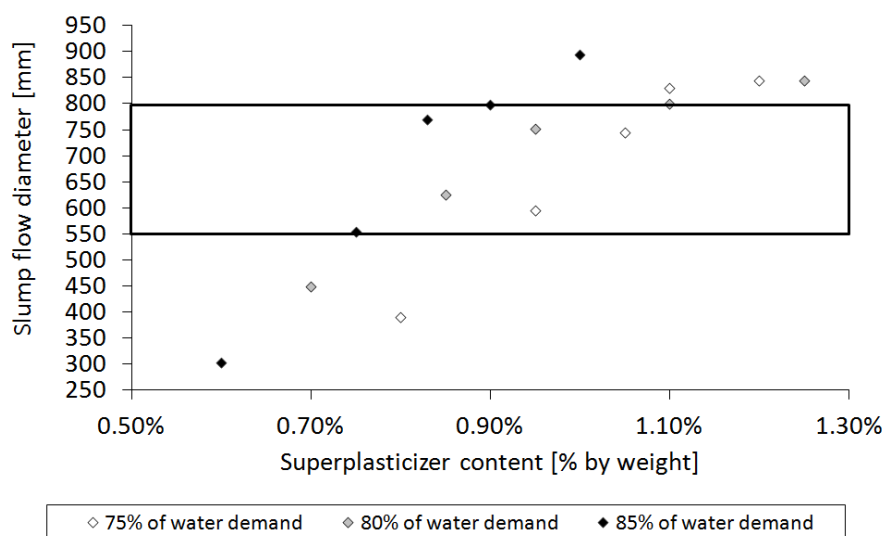


Figure 4.6: Slump flow vs. V-funnel efflux times of SCCs with varying water volumes and PCE contents.

Table 4.6: Mixture proportioning of the original mixture of the powder type SCC compared to the modified mixture proportioning (POW).

Constituents	Original Mixture			POW			
	Bulk density	Mass proportioning	Volume fraction	Mass proportioning	Volume fraction		
	[kg/m <sup>3</sup> ]	[kg/m <sup>3</sup> ]	[l]	[kg/m <sup>3</sup> ]	[l]		
CEM I 42.5 R	3123	296	95	310	99		385
Limestone filler, Medenbach, Table 4.4	2735	296	108	250	91		
Water	1000	168	167	175	175		
Air	-		20		20		
Superplasticiser	-	Glenium 51	-	-	Glenium Sky 591/593/595	-	-
Stabilising agent	-	-	-	-	Foxcrete/ Kelkocrete	-	-
Sand 0.0/0.5	2600	317	122	610	320	123	615
Sand 0.5/1.0	2600	182	70		184	71	
Sand 1.0/2.0	2600	182	70		184	71	
Sand 2.0/4.0	2600	119	46		120	46	
Sand 4.0/8.0	2600	119	46		120	46	
Sand 8.0/16.0	2600	666	256		671	258	
		2344	1000		2334	1000	

#### 4.1.7 Required modifications to obtain the SCC mixture “POW”

One of the objectives of this Thesis was to better understand the effect of the environmental temperature on the performance of admixtures in SCC. In general, a powder type SCC that is developed according to the general purpose approach developed by Okamura and Ozawa [205] works properly without stabilising agents (STAs). With the aim to obtain higher robustness against production process scatter, in practical applications, often STAs are added in addition. Therefore it is of importance to find out how the ambient temperature affects stabilising admixtures also in SCC mixtures with high powder contents. In order to better identify potential effects of temperature dependence caused by STAs, the powder content of the original mixture from Subsection 4.1.6 was reduced from 296 kg/m<sup>3</sup> to 250 kg/m<sup>3</sup>. The missing filler was compensated by STA. By this modification, yielding a water-powder ratio of 0.31 and a total powder content of still 560 kg/m<sup>3</sup>, the basic characteristics of a powder type SCC remain largely untouched, while the role of STA for the functioning of the SCC is increased.

As the total paste volume (Table 1.4) should remain similar to the original mixture, the cement content and the water content were increased, while the volumetric ratio of water and cement remained untouched. In order to fully achieve an identical powder volume at identical volumetric water to cement ratio, content of the cement needs to be increased to 314 kg/m<sup>3</sup>, while the water content needs to be increased to 178 kg/m<sup>3</sup>. The final mixture that was used yielded a water content that is identical to the water content of the COM mixture, which will be introduced in the subsequent Subsections (see Table 4.7). As a result the binder to aggregate ration differs slightly from the original mixture but the difference is minor, so that the characteristics remain similar.

The final mixture shows a higher powder content than specified for a powder type SCC according to Table 1.1 and furthermore STA was added. Since the amount of STA is negligibly

small and the major mechanism of providing the required flow properties, the mixture is henceforth considered as powder type SCC and therefore abbreviated POW.

#### 4.1.8 Background of the combination type SCC (COM)

Also the combination type SCC that was used for the present investigations is based on an SCC mixture composition that had already been established for several years. The mixture is the result of a comprehensive study about the influence of micro-fillers on the performance of various cementitious applications among which one was an SCC [150, 209]. Within the study of SCC an optimised mixture composition was developed by incorporation of small amounts of micronized LSF ( $d_{50}$ : 1.7  $\mu\text{m}$ ; density: 2710  $\text{kg/m}^3$ ; Blaine: 17200  $\text{cm}^2/\text{g}$ ), a FA ( $d_{50}$ : 5.0  $\mu\text{m}$ ; density: 2530  $\text{kg/m}^3$ ; Blaine: 6200  $\text{cm}^2/\text{g}$ ). The main powder components were sulphate resistant cement ( $d_{50}$ : 10.0  $\mu\text{m}$ ; density: 3200  $\text{kg/m}^3$ ; Blaine: 4050  $\text{cm}^2/\text{g}$ ), and coarse LSF ( $d_{50}$ : 30  $\mu\text{m}$ ; density: 2850  $\text{kg/m}^3$ ; Blaine: 3300  $\text{cm}^2/\text{g}$ ). The mixture composition can be found in Table 4.7. All binder components of the original combination type SCC are different materials than those of the POW concrete. Their properties can be taken from the analysis report edited by Kuosa et al. [210]. The FA was used to replace cement in different mass fractions and the fresh and hardened concrete properties were observed. Besides a control mixture without FA, mixtures with 30  $\text{kg/m}^3$ , 40  $\text{kg/m}^3$ , and 50  $\text{kg/m}^3$  cement replacement by mass were generated. Since due to the FA replacement, the total binder volumes varied only between 306 l for the control mix and 310 l for the mix with 50  $\text{kg/m}^3$  FA, the replacement by mass instead of volume can be considered to have no influence on the mixture components.

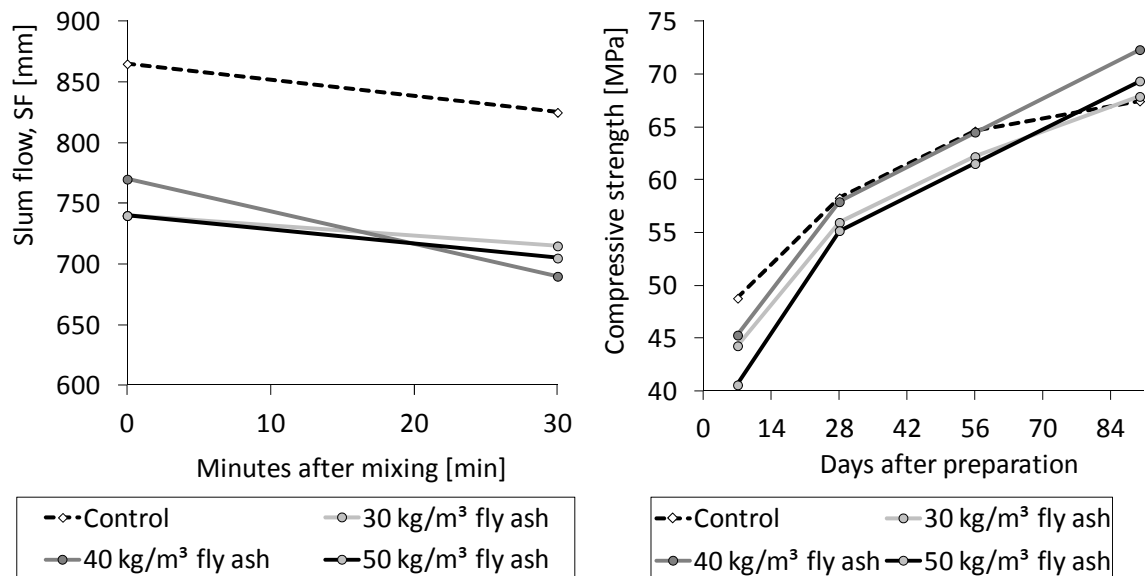


Figure 4.7: Influence of the amount of jet milled FA on slump flow and compressive strength development of SCC [209].

The influence of the general cement replacement on the fresh concrete properties was very pronounced, since the slump flow values at otherwise identical conditions reduced significantly, while the performance retention during the first 30 minutes after casting remained similarly as the control mixture (Figure 4.7). In general, the stability and segregation resistance were improved due to the cement replacement. Figure 4.7 also shows that the strength development was slower with FA. However, all mixtures containing FA had comparably high strengths after 28 days as the control mix and overmatched the control mix after 91 days. The highest strength

values were achieved at a replacement of 40 kg/m<sup>3</sup> cement by FA. Due to that reason, this mixture was selected for a newly developed pre-mixed dry binder compound that can be used with a wide range of aggregate types and particle size distributions to perform robustly as SCC. The possible aggregate grading curves ranged between the curves given in Figure 4.8. This figure furthermore contains the grading curve that was determined to yield optimum performance in terms of rheology and hardened concrete properties. The applicability was proven for the whole range of aggregate grading curves given in Figure 4.8 and the compound was also used on a construction project in Campione D'Italia [150]. However, taking into account economic considerations, the mixture with a replacement of only 30 kg/m<sup>3</sup> pointed out to be most reasonable. Therefore, this mixture was selected as the original concrete mixture for the final combination type SCC used for the investigations in this Thesis.

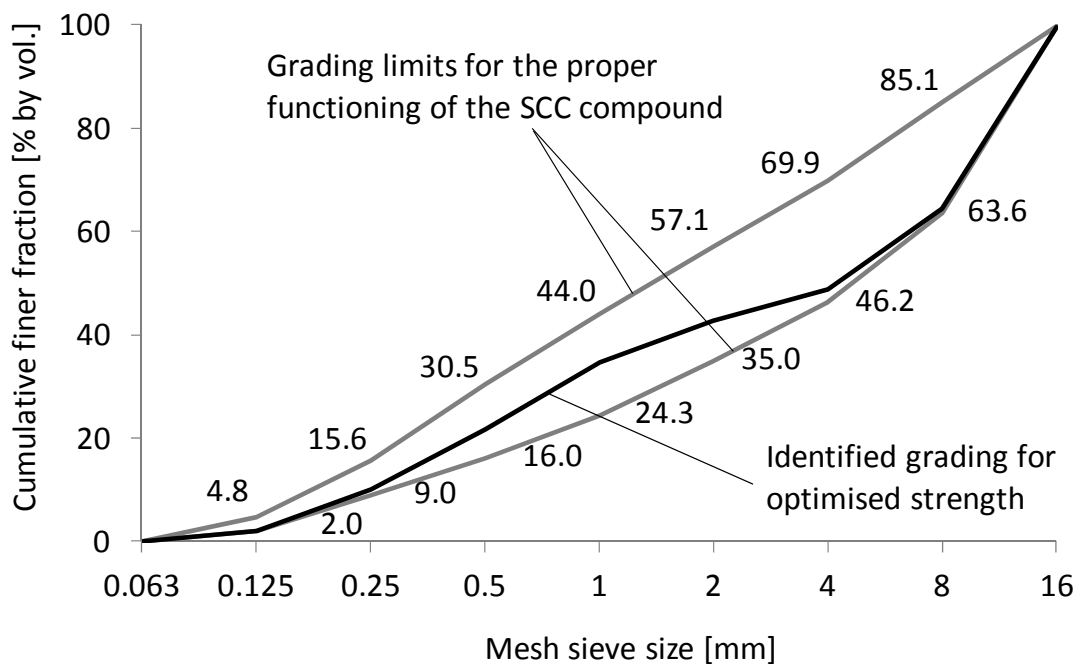


Figure 4.8: Grading thresholds for the functioning of the SCC pre-mix compound and grading for optimum performance.

#### 4.1.9 Required modifications to obtain the SCC mixture “COM”

The original mixture that was used to draft the combination type mixture was quite sophisticated, as it contained two differently graded LSF types and a jet milled FA (see Subsection 4.1.8 and Table 4.7). The use of this mixture for the observation of the influence of the environmental temperature on the performance of SCC would generate too many influencing parameters, thus weakening the interpretability of observations. Furthermore, the original mixture was developed with another cement and limestone filler as used for the POW mixture. In order to reduce the influencing factors to a minimum, the mineral constituents of both mixtures, POW and COM should be identical and the binder composition should be as simple as possible.

As a result, the cement used in the original mixture was replaced by the cement that was also used for the POW mixture and likewise the LSF for the POW mixture was used to replace the original coarse LSF as well as the FA (see Tables 4.6 and 4.7). The micronized LSF was completely eliminated from the mixture composition, while in parallel the water content was slightly increased by 5 l/m<sup>3</sup> in order to give more importance to the STAs.

Table 4.7: Mixture proportioning of the original mixture of the combination type SCC compared to the modified combination type mixture proportioning (COM).

Constituents	Original Mixture			COM		
	Bulk density	Mass proportioning	Volume fraction	Mass proportioning	Volume fraction	
	[kg/m <sup>3</sup> ]	[kg/m <sup>3</sup> ]	[l]	[kg/m <sup>3</sup> ]	[l]	
CEM I 42.5 R	3123	-	-	350	112	
CEM I 42.5 N ferrico	3206	350	109	-	-	
Limestone filler, Medenbach, Table 4.4	2735	-	-	130	48	
Limestone filler, d <sub>50</sub> = 30 μm, [210]	2705	100	35	-	-	355
Fly ash, d <sub>50</sub> = 5.0 μm, [210]	2533	30	12	-	-	
Micronized LSF, d <sub>50</sub> = 1.7 μm, [210]	2863	5	2	-	-	
Water	1000	170	170	175	175	
Air	-	-	20	-	20	
Superplasticiser	-	Tecnos 100 Azur	-	-	Glenium Sky 591/593/595	-
Stabilising agent	-	Cellulose ether	-	-	Foxcrete/ Kelkocrete	-
Quartz fines	2650	54	20	-	-	
Sand 0.0/0.5	2600	306	118	336	129	
Sand 0.5/1.0	2600	226	87	193	74	
Sand 1.0/2.0	2600	152	58	193	74	645
Sand 2.0/4.0	2600	87	33	126	48	
Sand 4.0/8.0	2600	245	94	126	48	
Sand 8.0/16.0	2600	633	244	705	271	
		2358	1000	2334	1000	

This mixture, entitled COM, is a combined approach between powder and admixture stabilisation. The powder content is higher than in ordinary concrete but significantly smaller than in the POW mixture. Due to the missing powder, high contents of STA are required to achieve segregation stability and self-compacting flow properties. According to Table 1.1, the final mixture composition is neither a combination type since the total powder content is lower than 500 kg/m<sup>3</sup>, nor a Viscosity agent type SCC, since the w/p is lower than 0.45. However, as the powder content with 480 kg/m<sup>3</sup> is close to the specified 500 kg/m<sup>3</sup> and the w/p fits in with the specification and furthermore a significant amount of STA was added, the mixture will further on be considered as combination type SCC with the abbreviation COM.

## 4.2 Final SCC composition

### 4.2.1 Adjustment of mixture compositions to performance criteria

The modified mixture compositions in Tables 4.6 and 4.7, discussed in Subsections 4.1.7 and 4.1.9, respectively, needed to be adjusted to obtain similar flow properties by the admixture

adjustment. Three types of SPs and two types of STA were varied, yielding six different admixture combinations for each concrete type. Hence, each mixture composition type needed to be adjusted with each admixture setup generated from a combination of SP and STA according to specified performance criteria. None of the used admixtures was used before with these mixtures, therefore, the amount of required PCE needed to be found out completely from the start. Therefore, a mixing routine was developed as formulated in Table 4.8 that allowed an early estimation whether the PCE addition that was chosen in step 4 was able to provide good flowability. In step 7, a first mix control was conducted by slump flow measurement. In case the flowability appeared too poor, supplementary PCE was added.

Table 4.8: Final concrete mixing procedure.

Step	Time span	Duration	Operation
1	0 – 0.5 min	30 s	Dry mixing
2	0.5 – 1.0 min	30 s	Addition of 2/3 of the total water
3	1.0 – 1.5 min	30 s	Mixing
4	1.5 – 2.0 min	30 s	Addition of remaining part of water + PCE
5	2.0 – 4.0 min	120 s	Mixing
6	4.0 – 8.0 min	480 s	Resting phase
7	In parallel		Mix control by slump flow measurement
8	8.0 – 10.0 min	120 s	Mixing
9	10.0 – 18.0 min	960 s	Resting phase
10	18.0 – 20.0 min	120 s	Mixing

In order to generate appropriate mixture compositions for ready-mixed applications, where effects of the ambient conditions are significantly more critical than in the field of pre-cast concrete the relevant point in time, at which all mixture compositions and admixture setups should have similar performance was set at 30 minutes after mixing. Powder type SCC is typically characterised by low yield stress combined with a high viscosity. SCC with low powder content, in turn, typically shows higher yield stress with lower viscosity. Hence, the definition of a uniform performance criterion is delicate. Therefore, a slump flow (SF) value between 650 and 700 mm was fixed as performance adjustment after 30 minutes. The STA contents for the COM concrete were fixed according to practical experiences with PCE LC and not varied with the different PCE modifications as specified in Table 4.5. For the POW mixtures, reasonable STA additions were detected experimentally. In a first step the slump flow value of the POW mixture was determined without any STA and then again with different STA amounts. Below a threshold addition, the slump flow values were identical to the values without STA. The amounts at the threshold were fixed. These STA amounts also remained unchanged, when the PCEs were varied.

Then slump flow tests were conducted with varying PCEs (Table 4.5) in increasing amounts until a slump flow value between 650 and 700 mm was reached in each particular admixture combination. No specific consideration was made regarding the V-funnel time, since the focus is laid on PCE performance, and PCE mainly affects yield stress. Consequently, the slump flow performance was fixed and the resulting efflux times, which are affected by the water content rather than by the PCE content, taken accepted. For the adjustment tests, a high number of slump flow measurements needed to be conducted within short time. Therefore no V-funnel testing was performed. The adjustment tests took place between 20 and 40 minutes after the end of mixing. In general, it was not possible to achieve the target value immediately. After 40 minutes, the test was interrupted and a repetition was made with modified start value until a

slump flow between 650 and 700 mm was reached. It was, however, not always possible, to achieve the specified slump flow values without segregation at earlier times. The PCEs LC and MC show similar adsorption behaviour (This will be confirmed later in this Thesis in Subsection 5.2.5, Figure 5.4). At a PCE addition of PCE MC that would generate a slump flow of 650 mm after 30 minutes, the higher charge density of PCE MC compared to PCE LC caused a better dispersion at early stages. This caused segregation tendencies of the SCC with PCE MC, while this could not be observed with PCE LC at similar performance after 30 minutes. Segregation stability throughout the whole observation time was considered as another important criterion that outweighs the specification to achieve a minimum slump flow after 30 minutes. Due to the obvious contradictoriness between early segregation stability and flow performance after 30 minutes in case of the use of PCE MC, the specified minimum slump flow after 30 minutes was reduced to 600 mm. This trial and error approach is not further documented, since a final performance test with the identified admixture setup variation was conducted, which is described in the next Subsection.

#### 4.2.2 Composition and properties of the final concrete compositions

Regardless whether the mixture composition was POW or COM, the grading of the aggregates, which is shown in Figure 4.9 was kept identical according to the specifications as suggested in the recommendations for self-compacting concrete published by the German Committee for Reinforced Concrete [31]. This curve is characterised by adapting to the standard grading curves of DIN 1045-2:2008 as formulated in Equation 3.8. The coarse aggregates' grading followed the A 16 curve and the grading of the sand fractions followed the B 16 curve (see Table 3.1). The curve is relatively close to the optimised grading of the ancestor COM mixture as shown in Figure 4.8.

The integral grading curves of POW and COM, including the powder components are given in Figure 4.10. Despite the unsteadiness in the coarse aggregate grading (Figure 4.9), this entire curve can be approximated by a steady function. The packing fraction  $P(d)$  for each particle diameter for the POW and COM mixture can be calculated by to the so-called modified Andreasen and Andersen curve according to Funk and Dinger [211]:

$$P(d) = \frac{d^q - d_{\min}^q}{d_{\max}^q - d_{\min}^q} \quad (4.1)$$

where:  $P(d)$  = cumulative finer fraction [%];  $q$  = distribution parameter [-];  $d$  = particle diameter [ $\mu\text{m}$ ];  $d_{\min}$  = minimum particle diameter [ $\mu\text{m}$ ];  $d_{\max}$  = maximum particle diameter [ $\mu\text{m}$ ].

This steady function is a modification of a curve recommended by Andreasen and Andersen [212], which is similar to Equation (4.1) but does not contain the substrahend  $d_{\min}$  in the numerator and denominator. According to Funk and Dinger, the densest packing of spheres can be achieved by using a distribution parameter  $q$  of 0.37. This function has been employed and discussed by numerous researchers recently [5, 32, 47, 213, 214]. For mixtures without requirement for higher powder volumes to provide good flowability,  $q = 0.44$  would compare to an optimised grading curve yielded by a linear packing density model without taking into account particle interactions, as was shown by Fennis [213]. Hüsken [214] found that optimised packing density for no-slump concrete can be achieved with  $q = 0.35$ . According to Brouwers and Radix [47], Hunger [5], and Hunger and Brouwers [32] distribution parameters  $q$  between 0.22 and 0.25 yield good flow properties and dense particle packing for powder type SCC.

Here the best curve fit for the POW mixture was achieved with  $q = 0.26$ , which is in the order of magnitude of the distribution parameters in the formerly cited studies. The best fit for

the COM mixture, which contains significantly lower powder volumes, was achieved with  $q = 0.29$ . The distribution parameter of the COM mix is significantly lower than the values by Hüsken [214] and Fennis [213], but also significantly lower than the optimum distribution parameter for SCC as recommended in [5, 32, 47]. This difference underlines the strong differences between the POW and the COM mixture.

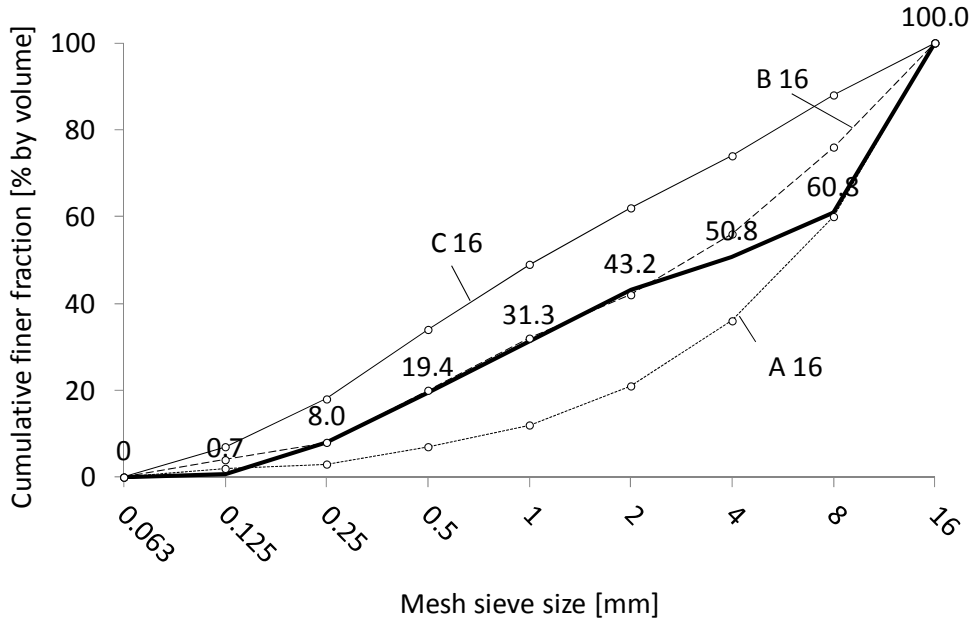


Figure 4.9: Aggregate grading curve of COM and POW in comparison to the grading curves A 16, B 16, and C 16 provided by DIN 1045-2:2008 (see also Table 3.1).

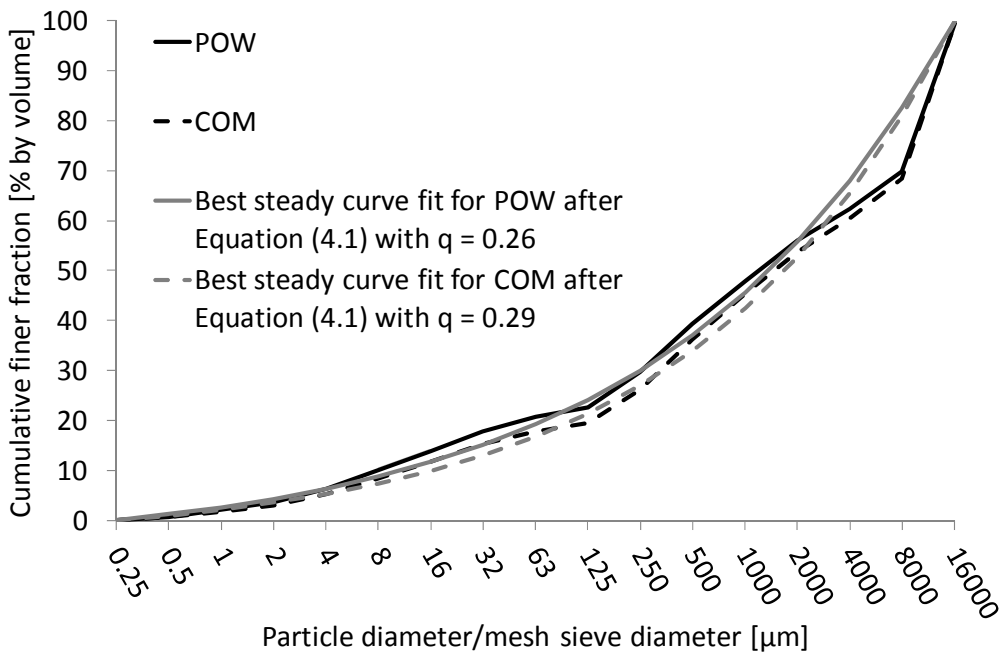


Figure 4.10: Integral grading curves of the COM and POW mixtures in comparison to the steady modified Andreasen and Andersen functions after Funk and Dinger [211] with  $q = 0.26$  for the POW approximation and  $q = 0.29$  for the COM approximation.

In conjunction with the modifications defined in Subsections 4.1.8 and 4.1.9, the final mixtures that provide the specified grading curves can be calculated. The final mineral compositions that were used as basis for all conducted tests can be seen in Table 4.9. The respective admixture setup yielding the specified slump flow values according to Subsection 4.2.1 are listed in Table 4.10. A representative air content of 20 l/m<sup>3</sup> was chosen for the mixture compositions. Based on relation between the measured fresh concrete density and a theoretical density calculated by the volumetric composition of all SCC ingredients without any air content, the air content can be estimated. These results, which are presented in Table 4.11, indicate that the air contents scatter between 0.8% and 3.7% with a mean value of 1.59%. This confirms that 20 l air volume is a good estimation. A closer look at the air contents also shows that at each temperature, the POW mixture seems to contain slightly higher air volumes and that obviously all SCCs showed a trend to increasing air volumes with decreasing temperatures.

Table 4.9: Final mixture compositions of the mineral components.

	POW			COM	
	Density	Mass per m <sup>3</sup>	Volume per m <sup>3</sup>	Mass per m <sup>3</sup>	Volume per m <sup>3</sup>
	[kg/m <sup>3</sup> ]	[kg/m <sup>3</sup> ]	[l/m <sup>3</sup> ]	[kg/m <sup>3</sup> ]	[l/m <sup>3</sup> ]
Ordinary Portland Cement CEM I 42.5 R	3125	310	99	350	112
Limestone Filler	2735	250	91	130	47
Water	1000	175	175	175	175
Estimated air	-		20		20
Sand (0.1-0.5 mm)	2600	320	123	336	129
Sand (0.5-1.0 mm)	2600	184	71	193	74
Sand (1.0-2.0 mm)	2600	184	71	193	74
Sand (2.0-4.0 mm)	2600	120	46	126	48
Aggregate (4.0-8.0 mm)	2600	120	46	126	48
Aggregate (8.0-16.0 mm)	2600	671	258	705	271
Fresh concrete density		2334		2334	

Table 4.10: Final mixture composition of the admixtures to achieve specified fresh performance properties.

Stabi- lising agent	Super- plasti- ciser	Ionic backbone strength	POW			COM		
			PCE bulk	PCE solids	STA	PCE bulk	PCE solids	STA
			% by mass of cement		% by mass of cement	% by mass of cement		% by mass of cement
ST1 (Starch ether)	PCE LC	low	2.05	0.62	0.018	2.25	0.68	0.120
	PCE MC	medium	2.40	0.55	0.018	2.64	0.61	0.120
	PCE HC	high	1.90	0.38	0.018	2.20	0.44	0.120
ST2 (diutan Gum)	PCE LC	low	1.90	0.57	0.001	2.20	0.66	0.010
	PCE MC	medium	2.40	0.55	0.001	2.64	0.61	0.010
	PCE HC	high	1.80	0.36	0.001	2.10	0.42	0.010

Table 4.11: Calculated air contents of the investigated SCC mixture compositions based on the measured fresh concrete densities (average of three values).

		5 °C		20 °C		30 °C	
		COM	POW	COM	POW	COM	POW
PCE LC	ST1	2.90%	1.80%	-	0.80%	1.50%	1.20%
	ST2	2.90%	3.70%	0.80%	2.70%	1.40%	1.90%
PCE MC	ST1	2.10%	1.80%	1.00%	2.10%	1.20%	1.10%
	ST2	2.40%	2.90%	1.70%	1.50%	1.10%	1.00%
PCE HC	ST1	1.40%	1.80%	1.30%	1.60%	0.90%	2.30%
	ST2	2.00%	1.50%	1.40%	2.40%	1.10%	2.00%
Mean value	per mixture composition and temperature	2.28%	2.25%	1.24%	1.85%	1.20%	1.58%
Standard deviation		0.58%	0.86%	0.35%	0.69%	0.22%	0.55%
Mean value	per temperature	2.27%		1.57%		1.39%	
Standard deviation		0.70%		0.62%		0.45%	
Mean value	entirely	1.59%					
Standard deviation		0.70%					

### 4.2.3 Fresh concrete performance of the adjusted control mixtures

The fresh concrete adjustment tests yielded mixtures according Tables 4.9 and 4.10. In order to specify the properties of each of these setups, performance tests were conducted under identical laboratory conditions at 20 °C using the mixing routine of Table 4.8. The results are presented for the POW mixtures in Figure 4.11 and for the COM mixtures in Figure 4.12. All SCCs fulfil the specifications to provide a slump flow value higher than 600 mm after 30 minutes according to the modifications described in Subsection 4.2.1.

Both mixtures including PCE HC and ST1 show higher slump flow values than 700 mm. In the final performance test that are shown in Figures 4.11 and 4.12 the total amount of PCE was added to the mixes during the mixing process. In the trial and error adjustment tests, described in Subsection 4.2.1, the PCE amount was step by step until a certain slump flow diameter was reached. The different ways of adding the admixture, however, can have strong influence on the flow performance, particularly in case of PCE with high charge density. High charge PCE will quickly adsorb on particles. In case of direct addition of the total amount, the system will quickly be well dispersed, generating a very low yield stress, as can be seen for example in Figure 4.11 for POW-HC-ST1. In case of stepwise addition, the system will not disperse well in the beginning. Particles will agglomerate, causing a higher yield stress. At a later additional dosing, the new PCE molecules will maintain the flow performance by adsorbing on existing surfaces but not additionally disperse the system to increase the flow value significantly. Hence, it is expectable that PCE HC yields higher flow value when added directly than after stepwise addition. Since, however within the next 40 minutes, the slump flow diameters of the concerned mixtures reduced to values close to the specified 700 mm, no further adjustment was conducted. The final thresholds of the measured slump flow values over the time for all mixtures in given in Figure 4.13.

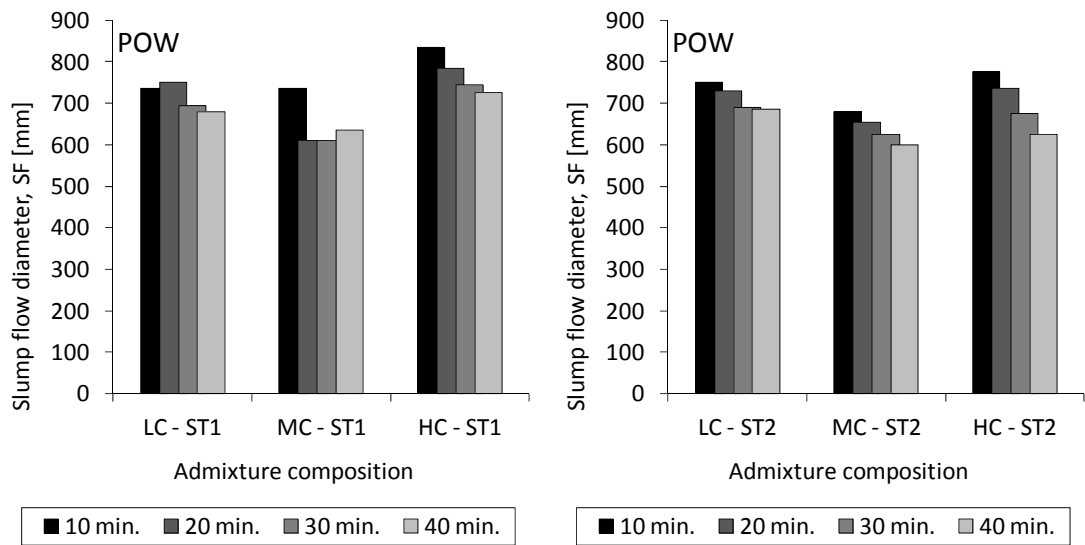


Figure 4.11: Fresh concrete performance of the POW mixtures with varied charge density of the PCE and different STAs.

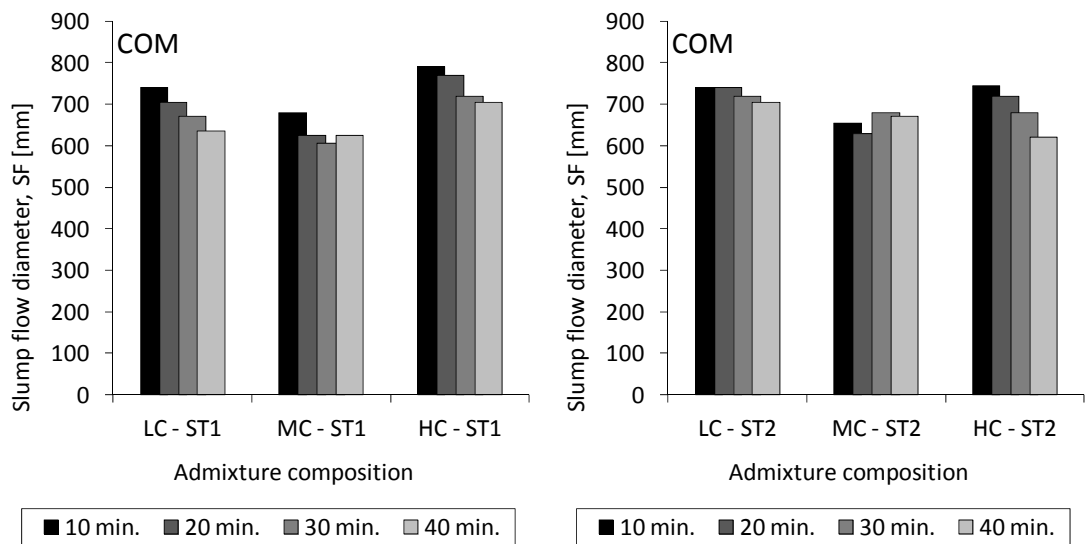


Figure 4.12: Fresh concrete performance of the COM mixtures with varied charge density of the PCE and different STAs.

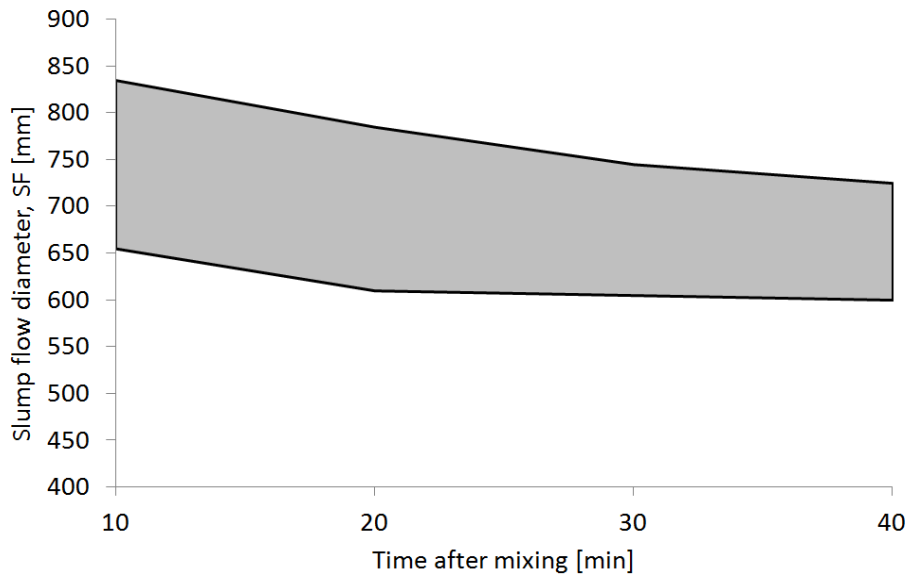


Figure 4.13: Range of measured slump flow values for all mixtures versus time.

#### 4.2.4 Calculation of paste from the concrete mixture components

For the testing that relate to the early hydration, several tests were conducted on paste basis. For these tests, the concrete mixtures were modified by removing the volumetric fractions of sand and aggregates from the compositions given in Table 4.9 and recalculating the mixtures. Since dense aggregates were used, the air content of the concrete was allocated to the paste volume and hence relatively increased accordingly.

The powder content of the sand and the water absorption by sand and aggregates were not taken into account, since the withdrawal of water would yield differing water to powder ratios in the paste and the concrete. Furthermore, due to different paste to aggregate volumes in the POW and the COM mixture, the factor would vary for both mixture compositions. Therefore the volumetric ratios of all binder components of concrete and paste were left identically. This is considered as legitimate, since dried and washed, rounded river sand was used for the concrete. As can be seen in Figure 4.3, the smallest sand only had a negligible content of components smaller than 0.125 mm. None of the sands contained powder components. The specific surfaces of the sands and aggregates were small. A calculation with consideration of the water absorption of sand and aggregate yielded mixture compositions that did not differ distinctively from the mixtures as seen in Table 4.12.

Table 4.12: Final mixture composition of the pastes.

	POW		COM		
	Density	Mass per m <sup>3</sup>	Volume per m <sup>3</sup>	Mass per m <sup>3</sup>	Volume per m <sup>3</sup>
	[kg/m <sup>3</sup> ]	[kg/m <sup>3</sup> ]	[l/m <sup>3</sup> ]	[kg/m <sup>3</sup> ]	[l/m <sup>3</sup> ]
Normal Portland Cement CEM I 42.5 R	3125	804	257	987	316
Limestone Filler	2735	649	237	367	134
Water	1000	454	454	494	494
Air	-		52		56
Total fresh paste		1907	1000	1848	1000

### 4.3 Rheometric test specifications

#### 4.3.1 Paste flow tests

Paste flow tests were performed by using a Haegermann cone with a height of 60 mm, and upper diameter of 70 mm and a lower diameter of 100 mm, the wider diameter pointing down (Figure 4.14). The geometry conforms to EN 13395-1:2002 and EN 1015-3:2007. The cone was placed and fixed by hand on a plastic plate, which was moist but not wet, and filled with paste. Paste without flowable consistency, was compacted by soft tamping. Then the cone was lifted and the paste was left to flow without agitation until it stopped. The largest diameter ( $d_1$ ) was measured as well as the perpendicular diameter ( $d_2$ ). The average value  $d_{SF}$  was defined as the flow spread diameter that calculates according to:

$$d_{SF} = \frac{d_1 + d_2}{2} \quad (4.2)$$

where:  $d_{SF}$  = slump flow value [mm];  $d_1$  = largest flow spread diameter [mm];  $d_2$  = flow spread at 90° to  $d_1$  [mm], see also Figure 1.1.

#### 4.3.2 Slump flow

The concrete slump flow test was conducted according to EN 12350-8:2010. In this test, a cone with a height of 300 mm, an upper diameter of 100 mm and a lower diameter of 200 mm (Abrams cone), which is placed on a moist but not wet plate, is filled with concrete, the wider diameter pointing down (Figure 1.3). In order to avoid uncontrolled lifting of the cone due to the fresh concrete pressure, a collar was placed around the cone, as to be seen in Figure 4.15. Upon lifting the cone, the concrete is allowed to flow freely until rest. The largest diameter ( $d_1$ ) and the perpendicular diameter ( $d_2$ ) are measured. The slump flow diameter SF is calculated according to:

$$SF = \frac{d_1 + d_2}{2} \quad (4.3)$$

where: SF = slump flow value [mm];  $d_1$  = largest flow spread diameter [mm];  $d_2$  = flow spread at 90° to  $d_1$  [mm], see also Figure 1.3.

The slump flow test is an easy method to obtain qualitative information about the yield stress of a concrete. Increasing diameters correlate with reduced yield stresses. The test is relatively independent of the viscosity of the tested SCC. Roussel et al. developed an easy equation that allows the transformation of the slump flow values into fundamental units [215]. As this approach is based on the evaluation of the final shape geometry this approach is only valid for flowable concrete: The yield stress can be calculated according to:

$$\tau_0 = \frac{225 \cdot \rho \cdot g \cdot V^2}{128 \cdot \pi^2 \cdot R^2} \quad (4.4)$$

where:  $\rho$  = fresh concrete density [kg/m<sup>3</sup>];  $g$  = apparent gravity [m/s<sup>2</sup>];  $V$  = cone volume [m<sup>3</sup>];  $R$  = slump flow radius [m].

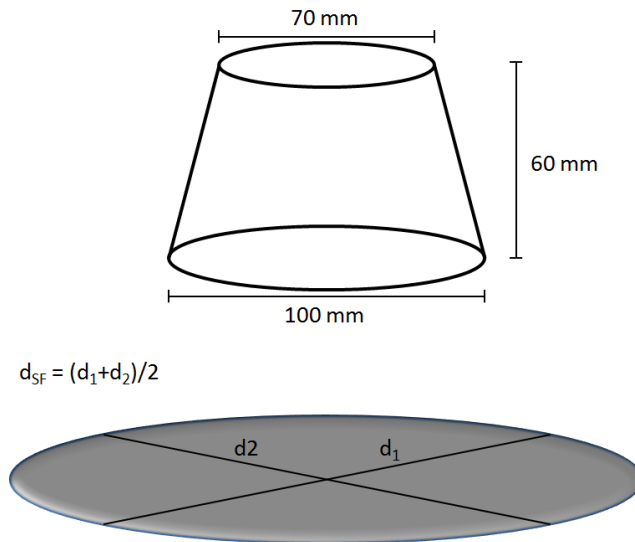


Figure 4.14: Determination of the spread flow diameter  $d_{SF}$ .



Figure 4.15: Slump flow test, V-funnel test and sieve segregation resistance test.

### 4.3.3 V-funnel test

The V-funnel test is a simple method to obtain information about the viscosity of a self-compacting concrete by measuring the time a specified concrete volume needs to pass a specified nozzle. The test was conducted according to EN 12350-9:2010. After a short time of approximately 10 seconds after filling, the trapdoor is opened and instantly the time is measured until one can see vertically through the funnel (Figure 4.15). The efflux time is abbreviated  $t_V$ . The funnel geometry details are given in Figure 1.3.

### 4.3.4 Sieve segregation resistance test

The sieve segregation resistance SR was determined according to EN 12350-11:2010. The test is not based on empirical data and is based on the assumption that the segregation resistance of an SCC can be assessed by the volume of paste that passes through a 5 mm square aperture sieve, when concrete is placed upon it (Figure 4.15). The segregation resistance is calculated as the

ratio of paste mass that passes the sieve divided by the initial concrete mass. For the test, initially, a concrete sample of  $10 \pm 0.5$  l is left to rest in a bucket for  $15 \pm 0.5$  minutes. After the resting period,  $4.8 \pm 0.2$  kg of concrete is poured onto the sieve. After a waiting time of  $120 \pm 5$  seconds, the sieve is removed and the passage is recorded. The sieve segregation resistance is calculated according to:

$$SR = \frac{(m_{ps} - m_p) \cdot 100}{m_c} \quad (4.5)$$

where: SR = sieve segregation resistance [-];  $m_{ps}$  = mass of sieve receiver plus passed material [g];  $m_p$  = mass of the sieve receiver [g];  $m_c$  = initial mass of concrete placed onto the sieve [g].

According to intensive research by Kühne and Schmidt, the test has pointed out to provide good results for lower viscous SCC but it does not inevitably allow a good segregation resistance assessment for highly viscous SCCs [51] (see also Figure 1.7).

#### 4.3.5 The LCPC-box test

Based on considerations about the shape at rest after flow of a fixed volume, Roussel and co-workers developed a method to determine the yield stress of flowable concrete [35, 216] based on the shape factors of the concrete at rest. The relation between yield stress and the flow length is defined according to the equation:

$$\tau_0 = \frac{\rho \cdot g \cdot l_0}{2 \cdot L} \cdot \left( h_0 + \frac{l_0}{2} \cdot \ln \left( \frac{l_0}{l_0 + 2h_0} \right) \right) \quad (4.6)$$

where: L = flow length;  $h_0$  = height of the concrete at the beginning of the box [m];  $l_0$  = box width [m];  $\tau_0$  = yield stress [Pa];  $\rho$  = mass density of the fresh concrete [ $\text{kg}/\text{m}^3$ ];  $g$  = gravitational acceleration [ $\text{m}/\text{s}^2$ ].

For the test 6 l of concrete need to be poured into a flow box of a height of 150 mm, a width of 200 mm, and a length of 1200 mm. The pouring shall take 30 s in order to avoid any effects of inertia. Since the formula, which depends on the varying shapes of the concrete at rest, the calculation of  $\tau_0$  is time intensive without support of a calculation software, the authors offer an easy to handle graphical evaluation method according to Figure 4.16, where only the flow length needs to be marked in order to read the yield stress related to the specific gravity  $\rho_{\text{spec}}$  [35].

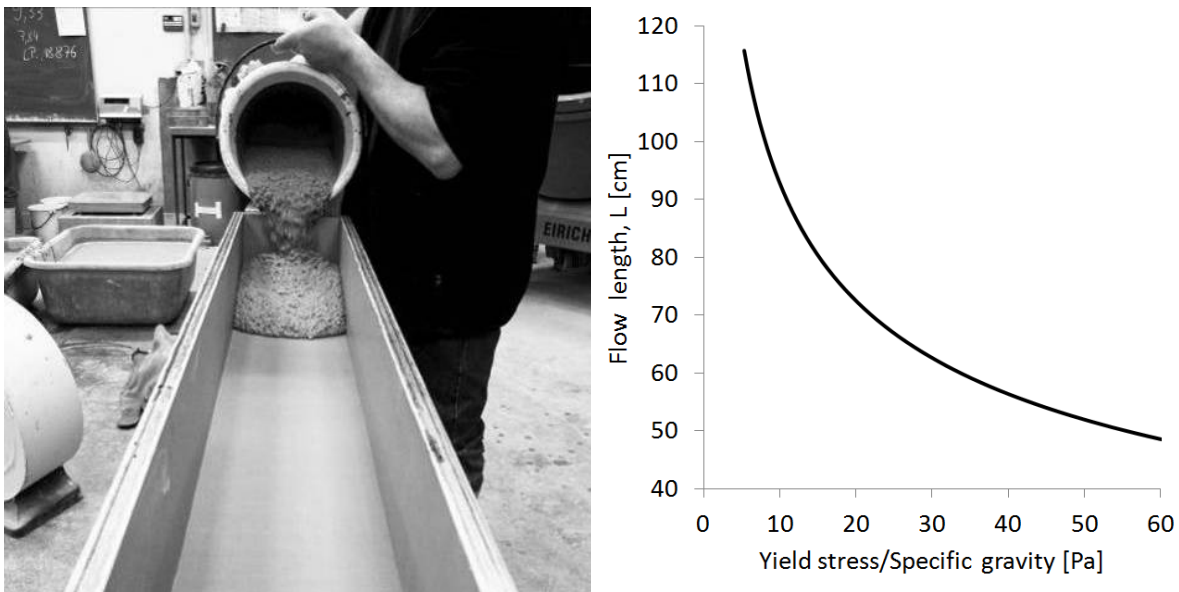


Figure 4.16: LCPC-Box test (left) and correlation between flow length in the LCPC-box and the yield stress to specific gravity ratio (right) according to Roussel et al. [35].

#### 4.3.6 Rotational rheometry

Rheometric devices support the identification of the rheological properties of flowable systems. From a point of view of the range of constituent sizes, from nm to cm, concrete can be considered as a highly complex fluid.

For coarsely dispersed systems such as mortar or concrete, the boundary conditions, physically well-defined rheological methods are based on, can no longer be met. The cell geometry and the necessary equipment would be unreasonably large, since the gap width that is required for the measurement is depending upon the maximum particle size. In addition, the fluid properties vary continuously in cement-based systems due to varying electrostatic charges, the ionic composition of pore solution, morphological changes of the particle surfaces, variations in particle size and the hydration process. The need for suitable methods for measuring rheological characteristics of mortar and concrete is increasing as workability properties are playing an increasing role for modern concrete technology [217]. Therefore, devices that are based on rotational rheometry, which do not fully operate in a physically clearly defined framework but which provide useful parameters are gaining popularity. A number of available rheometric tools are presented in a summary given by Koehler and Fowler [218]. Approximate models support the significance of the results and can help to translate the qualitative results into quantitative values. Typically they are based on the measurement of the torque of an agitator of variable geometry. Due to the maximum grain size no clearly defined shear field can be determined. Furthermore, the transformation of the measurements of the torque at varied rotational speeds into shear stresses and shear rates is not a trivial problem, since due to the wide range of constituents' sizes, concrete cannot simply be considered as homogeneous fluid.

#### 4.3.7 Concrete rheometry with the ConTec Rheometer-4SCC

Here, rheological concrete investigations were performed by using a CONTEC Rheometer-4SCC. The system consists of an electric control, a bucket, an impeller, a drive unit, and a control unit and data logger as shown in Figure 4.17. The systems has the advantage that it is transportable, since for investigations of the rheological properties in varying ambient

conditions, the device can be fully placed and operated in a climate chamber. The volume of measured concrete is 7 l, in which the concrete is fully immersed. The rheometer measures the electric current in mA at varied rotational speeds [56, 219].

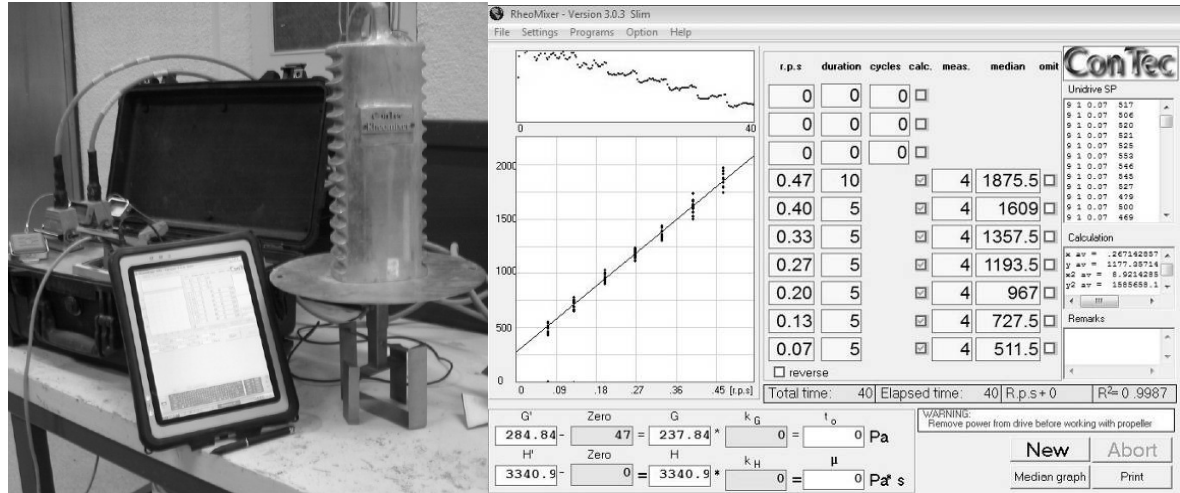


Figure 4.17: Rheometer-4SCC [56] and standard test setup for G-Yield and H-Viscosity.

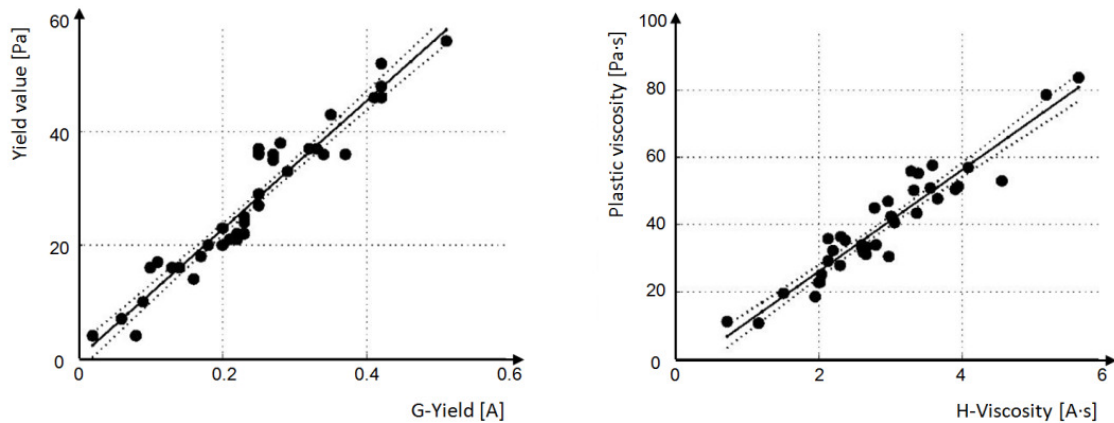


Figure 4.18: Correlation between Rheometer-4SCC and Viscometer 5 [219].

Changes of the rheological properties can be displayed qualitatively, but the results cannot be converted to fundamental rheological units as it would for instance be possible with a coaxial cylinder rheometer. When applying a Bingham curve on the results according to Equation (3.5) with  $\dot{\gamma}$  replaced by the rotational speed and  $\tau$  replaced by the measured current, qualitative information about yield stress (G-Yield) and viscosity (H-Viscosity) of flowable concrete can be obtained, as shown in Figure 4.18. The results can be converted into fundamental units by applying a conversion factor. According to the operation manual [219], tests were conducted, where the results of the Rheometer-4SCC were correlated with the results of the Viscometer 5 for identical materials. Viscometer 5 is a coaxial cylinder system with a concrete volume of 17 litres. The geometric boundary conditions for the transformation of the results into fundamental units are therefore fulfilled to a large extent. The results of the comparison are given in Figure 4.18. There is a very good correlation between the results of both devices. The correlation coefficients for yield stress and viscosity are 0.93 and 0.90, respectively.

The transformation into fundamental values, however, is failure prone, since the results measured with the Rheometer-4SCC can be affected by numerous parameters from the mixture composition.

A standard test routine with default rotational speeds and time intervals, as well as a software tool for the evaluation based on a Bingham model is part of the system. However, rotational speeds and time intervals for each speed step can be adjusted individually and the data can be extracted and interpreted individually. The standard seven steps setup with rotational speeds between 0.07 and 0.47 rps, with 5 s each step and pre-shearing is given in Figure 4.17. For the evaluation as a Bingham fluid, only the last four seconds of each step are taken into account. The Bingham curve is generated from the median value of each step as shown in the left graph of Figure 4.19. A manual extraction of the recorded data allows further interpretation. The centre graph of Figure 4.19 shows the respective flow curve when the mean value is used instead of the median value, the right graph shows the curve when all valid values are taken into account to calculate the Bingham curve. The figure shows that the basic characteristics of the curve and hence, G-Yield and H-Viscosity do not distinguish significantly. However, the correlation coefficient is strongly affected by the way the data is interpreted. The correlation coefficient, however, is considered to be a relevant value to decide whether the Bingham approach can be applied or not. Due to the limited possibilities of the standard software evaluation, in this Thesis a modified programme as well as an alternative data interpretation was chosen, which is described in more detail in Subsection 6.3.4.

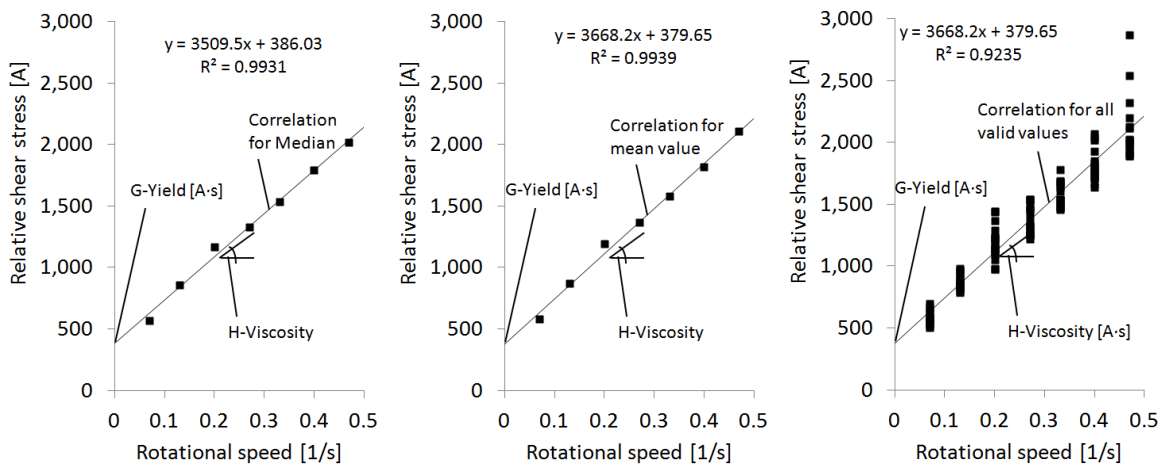


Figure 4.19: Calculation of the G-Yield and H-Viscosity according to the standard method of the ConTec Rheometer-4SCC based on Median values (left) in comparison with alternative calculations based on the mean value (centre) and all valid values (right).

#### 4.3.8 Comparison of the ConTec Rheometer-4SCC method with slump flow testing and LCPC-box method

In order to better evaluate the interpretation of the results, the Original Mixture SCC given in Table 4.6 was modified with different amounts of STA in order to generate varying yield stresses and plastic viscosities. In parallel the slump flow values as well as the V-funnel time of each mixture setup was measured, furthermore the LCPC-box test and a measurement with the Rheometer-4SCC were conducted. Yield stresses were calculated according to Equation (4.4) from the slump flow test and Equation (4.6) from the LCPC-box test.

Figure 4.20 shows the results of the tests. It can be seen that there is very good agreement between the calculation of the yield stress from the rheometer according to the correlation curve

presented in Figure 4.18 and the values calculated from the slump flow results. The rheometer curve and the slump flow correlation curve run in parallel with only a slight shift. The accord with the LCPC-box, however, is less significant.

The larger disagreement with the yield stresses according to the LCPC-box test can be a result of fewer measurements with this method as well as the fact that the slopes of the curve in Figure 4.16 at very high and very low yield stresses become close to horizontal and vertical, respectively. At high yield stresses, small changes in the flow length have strong effect on the interpretation of the yield stress. For example the difference between 46 mm and 48 mm flow length generates a calculative yield stress difference of 20 Pa. Hence, the results determined according to the formula for the slump flow are considered as more precise for the whole range of yield stresses. This formula has furthermore been used by several other authors (e.g. [220, 221]) and can thus be considered as largely validated.

The parallelism of the rheometer curve and the slump flow curve point out that the G-yield values well represent slump flow values and changes in G-yield hence can be expected to occur qualitatively likewise in the slump flow diameter. The close location of both curves furthermore gives evidence that a transformation of the G-Yield value into fundamental units can be made with satisfactory precision.

Applicable calculative methods to determine the viscosity of SCC from standard tests have not been developed to date. Methods to determine the viscosity based on the Marsh cone (Table 1.2) were discussed by Roussel and co-workers [36-38], but they are not applicable for all viscosities and limited to paste tests. Frunz et al. [221] used the V-funnel also for the calculation of viscosities, however, the applied equation has only validity in case of Newtonian or nearly Newtonian fluids. Despite these shortfalls, the V-funnel efflux time is typically considered as a reasonable method to gain qualitative information about the viscosity of SCC. Although only a low number of V-funnel measurements were conducted, Figure 4.20 gives evidence that there is a good coherence between V-funnel efflux times and H-viscosity.

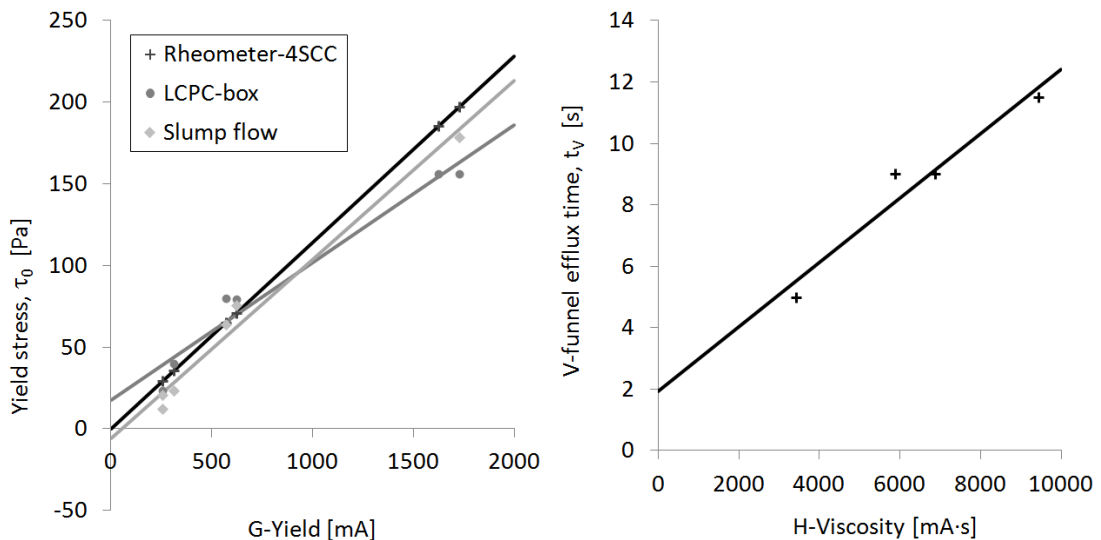


Figure 4.20: Correlation between G-Yield and  $\tau_0$  according to different methods and H-Viscosity and V-funnel efflux time.

### 4.3.9 Viscosimetry using the basket cell

Rheometric investigations on suspensions, pastes, and mortars were conducted with a Schleibinger Viskomat NT. The device is a Couette type viscosimeter, which means, the cup rotates at controllable speed. The bob is fixed into a load cell that measures the responding torque.

The determination of rheological properties of mortars is a challenging task since cylinder or plate cells, which are well defined, are no longer reasonable for grains of millimetre size, since the cell geometry needs to be very large and the engine very strong. Another problem resulting from the two phase characteristics of a mortar are wall slip effects that bias the interpretation. Therefore, similar to the Rheometer-4SCC, typically stirrer geometries are chosen that cannot generate a laminar flow over the entire diameter, but which empirically assure a constant flow behaviour. Changes of the measured torque can then be evaluated against varied rotational speeds. The result qualitatively correlates to the flow curve, but a transformation of the rotational speed into a shear rate is not possible due to lack of knowledge of the shear planes. The results are therefore often entitled relative values.

In order to overcome the problem of not being able to determine fundamental rheological values with the standard measurement equipment for the Viskomat NT as soon as the maximum grain size exceeds powder size, a special mortar measurement cell was developed by Vogel [222, 223]. This cell is a double gap cell with a network structured shear body. The shear body induces a flow that is largely based on the cohesion between the fluid layer on the wall and the fluid, thus minimising wall slip (Figure 4.21).

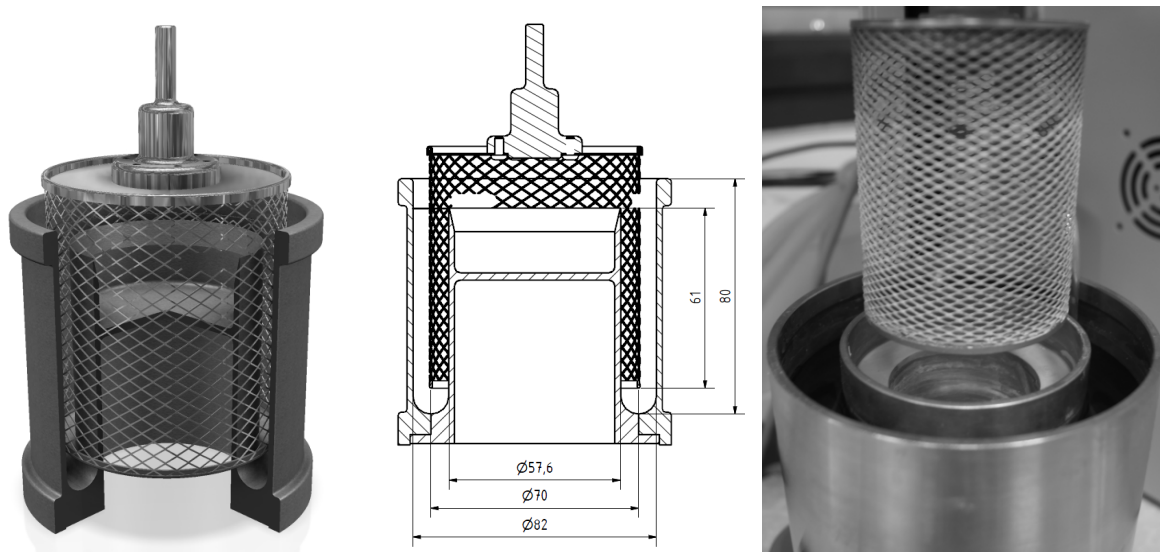


Figure 4.21: Double gap rotational cell (pictures left and centre by courtesy of Schleibinger).

The transformation of rotational speeds and measured torques into shear rates and shear stresses using a wide-gap rheometer remains a challenge, which is called the “Couette inverse problem” [224]. For the solution of the Couette problem in wide-gap rheometers, used for the characterisation of the mortar properties, a direct analysis typical for narrow-gap rheometers (inner radius/outer radius < 0.99) cannot be used, since the basic hypothesis of uniform strain is not valid [225]. Several approaches are known to solve this problems, which are further described by Heirman et al. [226]. The transformation of the used cell was conducted by the producer based on the so called integration method, which is based on experimental data with a well defined fluid [227]. In an attempt to understand the range of results with the used

measurement cell, Vasilic et al. [228] compared the integration method with the so called representative shear rate methods, formulated by Heirman et al. [226, 229], yielding varying results. Figure 4.22 presents the different results obtained by applying both methods. They end in strongly differing values for both yield stress and plastic viscosity, which would generate strongly varying flow performances. The figure compares the flow length in a flow channel after 10 s as well as the times required to reach the first 20 cm mark compared to experimental data. The figure suggests that the integration method at least with regard to viscosity is closer to the experimental data, however, the scatter of the experimental data for further values like the time needed to reach a 40 cm mark or the final shape was too large to validate any of both simulations. Therefore, the way to solve the Couette inverse problem remains a rather philosophical question. The long lasting expertise of the inventor of the cell is considered as a good basis to rely on the given data for the transformation [222, 223, 230]. The cell was calibrated using the cell geometry (Figure 4.21) according to:

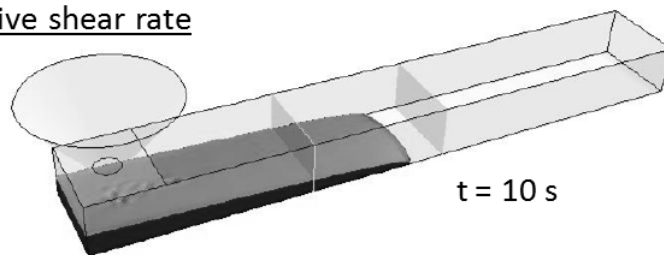
$$\tau = \eta \cdot \dot{\gamma} = \frac{T}{4 \cdot r^2 \cdot \pi \cdot L} \cdot \frac{1}{c_k} \quad (4.7)$$

where:  $\tau$  = shear stress [Pa];  $\eta$  = viscosity [Pa·s];  $\dot{\gamma}$  = shear rate [1/s];  $T$  = torque [mNm];  $r$  = stirrer diameter [mm];  $L$  = depth of immersion of the sensor [mm];  $c_k$  = calibration result by the producer = 0.918 [-].

#### Set 1: Representative shear rate

$$\tau_0 = 11.97 \text{ Pa}$$

$$\eta_{pl} = 3.70 \text{ Pas}$$

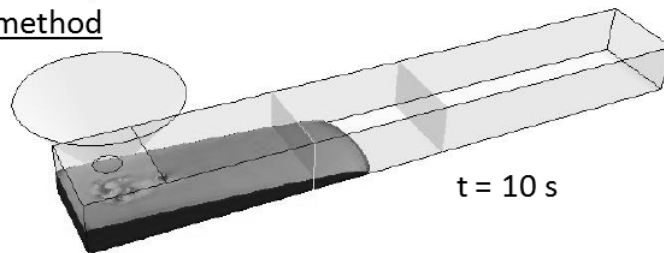


$t = 10 \text{ s}$

#### Set 2: Integration method

$$\tau_0 = 11.97 \text{ Pa}$$

$$\eta_{pl} = 3.70 \text{ Pas}$$



$t = 10 \text{ s}$

$t_{20\text{cm}}$ (time required to flow to a length of 20 cm)		
Experiment	Set 1	Set 2
5.0 s	2.8 s	3.9 s

Figure 4.22: Flow lengths after 10 s from simulations with data based on the method of the representative shear rate and the integration method as well as times required to reach a flow length of 20 cm compared with experimental data after Vasilic et al. [228].

At low shear rates, it has to be investigated whether the fluid is fully sheared. Results below this critical shear rate  $\dot{\gamma}_{\text{crit}}$ , cannot be interpreted. Figure 4.23 gives an example how neglect of

the critical shear rate yields wrong interpretation. Without consideration of the critical shear rate, the Bingham fluid of the example would have to be interpreted as Herschel-Bulkley fluid. The determination of the critical shear rate has to be conducted stepwise according to:

$$\dot{\gamma}_{\text{crit}} = 0.177 \cdot \frac{\tau_0}{\eta_{\text{pl}}} \quad (4.8)$$

where:  $\dot{\gamma}_{\text{crit}}$  = critical shear rates [1/s];  $\tau_0$  = yield stress [Pa];  $\eta_{\text{pl}}$  = plastic viscosity [Pa·s].

Besides the capability to determine fundamental rheological values, the large shear area of the cell allows to measure precise data already at very slow shear rates. This is typically not possible with standard mortar stirrers. Vogel investigated the same flowable grout for comparison on the one hand in the double gap cell and on the other hand with a standard stirrer for mortar [222]. The torques resulting from measurements in the double gap cell were approximately nine times higher than those from the mortar stirrer at significantly lower rotational speed. Furthermore, the torque increase characteristics with time distinguish strongly between both cells. Vogel interprets the different time dependent characteristics by the laminar flow which does not affect the structural build-up, while the stirrer propagates structural breakdown.

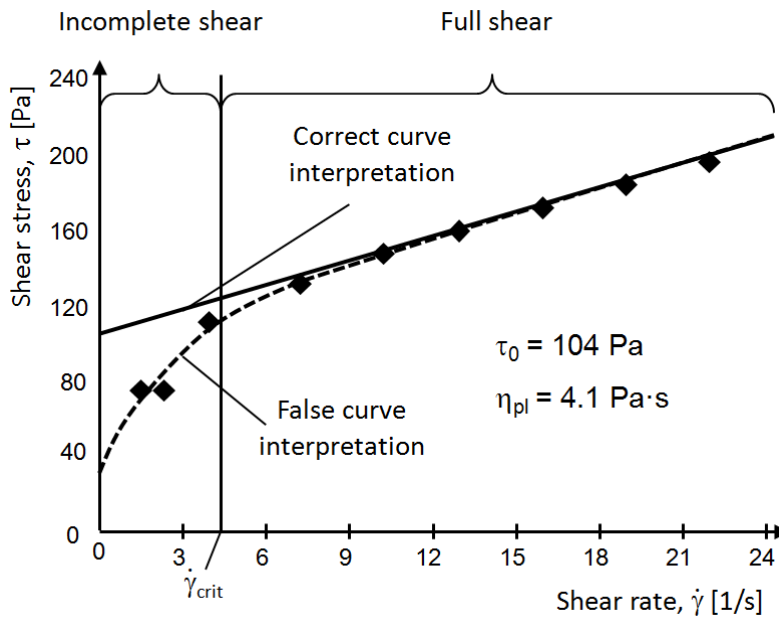


Figure 4.23: Sample of the areas of incomplete and full shear and critical shear rate modified after Vogel [222].

## 4.4 Observations during the setting and hardening

### 4.4.1 Vicat penetration test

In a review about different methods for the determination of the setting since 1912, McKenna [231] defines setting as “[...] the very first stiffening and rapid development of cohesion up to the stage where needle points under moderate pressures do not penetrate the surface, or where small test objects are easily handled without fracture.” The Vicat needle penetration test is a commonly used technique for the determination of the setting of cement. Its principle is based on the measurement of the penetration depth of a needle at defined mass (Figure 4.24).



Figure 4.24: Sketch of the original Vicat device from 1912 taken from McKenna [231] and the employed automatic 11-slot Vicat device for temperature controlled steady measurement.

As long as a cement paste is still fluent, the needle drops to the bottom of the specimen. As soon as a structure starts to form, the paste viscosity and yield stress increase, thus hindering the needle to fully penetrate the specimen, the first instance at which the needle does no longer drop to the bottom is considered as the initiation of the setting. The moment, at which the needle can no longer penetrate the specimen deeper than through the surface skin, is considered as the final set.

The Vicat test is described in EN 196-3:2009 for cement paste and in EN 480-2:2006 for mortars. Both tests are specified to be conducted at water to cement ratios, which have to be determined in advance of the testing based on a standardised consistency. This means, the water content to be used for the test may vary from sample to sample, depending on the water demand of each batch of cement. The basic test setup does not basically differ for cement and mortar. The needle to be used has a diameter of  $1.13 \pm 0.05$  mm, the height of the Vicat ring that holds the paste specimen is fixed to  $40.0 \pm 0.2$  mm. The cement ring provides an upper diameter of  $\geq 65$  mm and  $\leq 85$  mm, the lower diameter is  $75 \pm 10$ . The mortar ring shall have  $70 \pm 5$  mm and  $80 \pm 10$  mm for the upper and lower diameter, respectively. The cement needle has a mass of 300 g; the mortar needle has 1000 g. For the cement test, the specimen has to be stored under water, for the mortar test, the specimen has to be stored in specified climatic conditions. The time of the initial set ( $t_{ini}$ ) is defined for the cement test as the time at which the needle penetrates the specimen less than 37 mm and more than 31 mm. The final set ( $t_{fin}$ ) is defined as the time at which the needle only penetrates 0.5 mm. For the mortar test  $t_{fin}$  is defined as the point in time, at which the needle penetrates the specimen less than 36 mm, the final set is defined as the time at which the specimen reaches a penetration depth of 2.5 mm.

#### 4.4.2 Automatic Vicat penetration test

The setting was measured at samples stored under water using an automatic Vicat device, following EN 196-3:2005 (Toni Technik) with 11 sample spaces (Figure 4.24). A circulation water control system with a cryostatic temperature control regulator was used to keep the ambient temperature around the specimens constant. The device can work with the 300 g and a 1000 g needle. The device allows a manual input of an individual time-zero, e.g. the time at which water was added or any other point in time, which is considered relevant, the

predefinition of the time at which the needle shall penetrate for the very first time, the intervals between penetration steps as well as individually adjustable penetration depth ranges, at which the interval can vary from the standard interval. This allows a steady curve of the penetration depth development with time with refined intervals during the time of the initial and final set.

The device exhibits two parameters which do not fully accord to the standards. According to the standards referred to before, the specimens have to be turned upside down after the initial set. Since the automatic Vicat device requires a fixture of each specimen, this rotation is not possible. Furthermore, for the determination of the final set of cement, a special needle is required, which exhibits a ring of 5 mm diameter around the penetration needle. This ring allows a finer determination of the relevant point in time at which the final set can be expected to occur and avoids a deep immersion of the needle. Since the automatic device has a cleaning unit, which is triggered after each penetration, such a specific needle cannot be installed. However, since this special ring is located behind the top of the penetration needle, the result for the final set can be expected to be identical for both needles.

#### 4.4.3 Isothermal heat flow calorimetry

In order to obtain information about exothermic reactions during the hydration of mineral binders, calorimetric investigations were conducted. These were performed with an 8-channel isothermal heat flow calorimeter (TAM Air). A very detailed description of the device was published by Wadsö [115]. The device maintains the ambient temperature around a specimen constant by a Peltier element. The power, which is required to heat or cool the chamber in order to maintain the temperature when reactions take place, is then measured constantly and thus provides information about the reaction heat  $Q$  evolution over the time. Besides the plotting of the reaction heat vs. the time, it is common to also plot the heat flow curve  $\dot{Q}$  (Figure 4.25) which is calculated according to:

$$\dot{Q} = \frac{\partial Q}{\partial t} \quad (4.9)$$

where:  $\dot{Q}$  = heat flow [J/s];  $Q$  = produced heat [J];  $t$  = time [s].

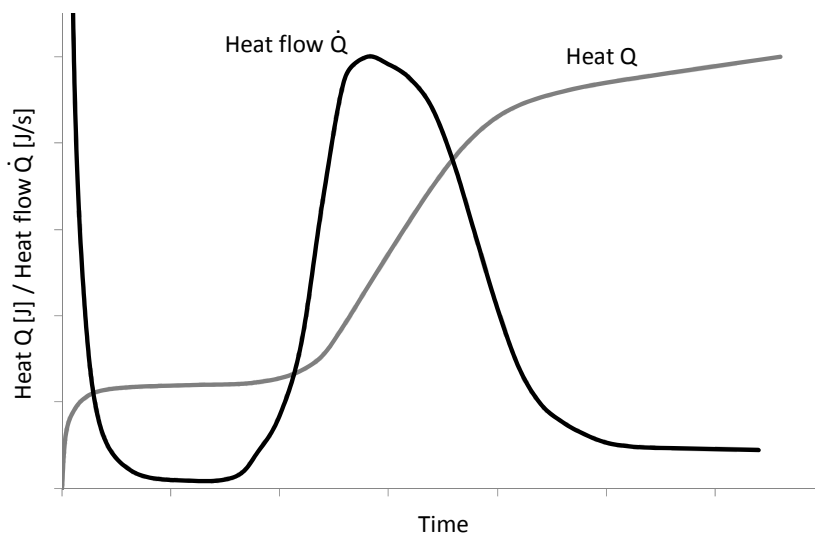


Figure 4.25: Sample of a heat curve vs. time and its derivative the heat flow curve.

The heat flow curve is typically used in order to provide information about the hydration process. The curve exhibits the characteristic items discussed in Section 2.1 (e.g. Figure 2.1, 2.3, and 2.4).

#### 4.4.4 X-Ray Diffractometry

X-ray diffraction in this work was conducted with a Rigaku Ultima IV with a D/teX-Ultra high-speed detector, equipped with a Copper anode ( $\lambda\alpha_1 = 1.5406 \text{ \AA}$ ). The X-ray diffraction method allows conducting in-situ phase analyses. When X-rays hit a crystal, they largely pass the structure. However, a part of the rays is diffracted by the crystal lattice. At certain angles, depending upon the crystal structure, the beam is largely reflected according to Bragg's law:

$$n\lambda = 2d \cdot \theta \quad (4.10)$$

where:  $n$  = integer for the diffraction order;  $\lambda$  = wave length of the incident wave [nm];  $d$  = spacing between the planes in the atomic lattice [nm];  $\theta$  = angle between incident ray and scattering plane.

The diffraction angle is then  $2\theta$ , the wave length of X-rays is known, so that for each angle at which reflection takes place a spacing between the planes of the atomic lattice  $d$  can be determined, which provides information about the crystal structure. Since each crystal structure differs, the conditions for a reflection of the beam vary and show unique patterns over a range of angles.

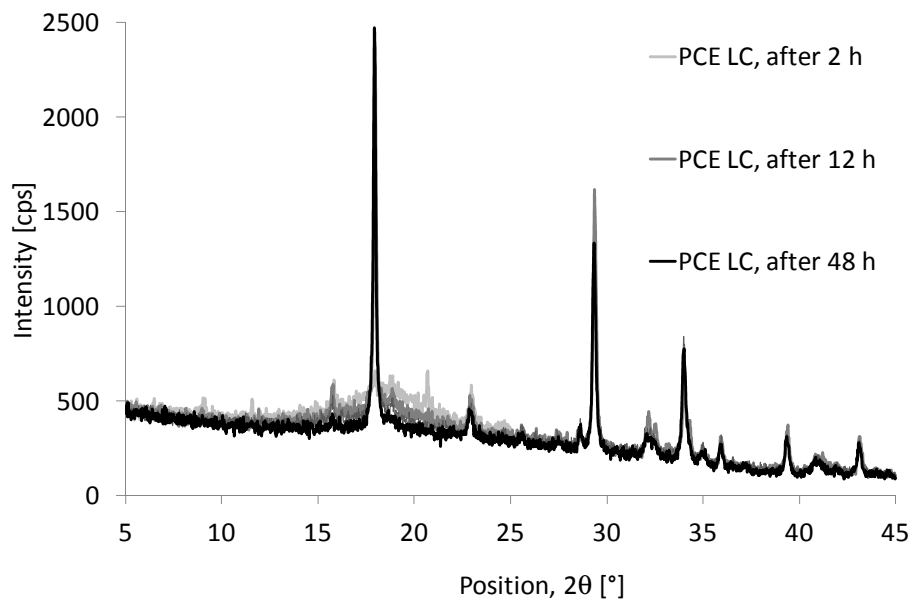


Figure 4.26: XRD pattern of a sample paste measurement.

In the X-ray diffraction method, a sensor is placed behind the specimen, measuring the intensity of the diffracted X-rays. The result is a specific and unique pattern for each specimen at the specific state at which the measurement takes place. Figure 4.26 gives an example of a measurement of a paste according to Table 4.12 with PCE LC (Table 4.5) at different steps in time. A major problem in the phase analysis is that numerous crystals overlap. Furthermore, numerous phases show very similar diffraction patterns. Hence, the occurrence of intensity peaks at certain locations cannot automatically provide conclusions on a certain crystal phase. The identification is only possible when assessing also the other characteristic peaks.

The method only allows identifying crystal phases, the identification of amorphous phases is not possible without further considerations. For the cement hydration analysis this means that the identification of clinker phases and their dissolution can be observed,  $\text{Ca(OH)}_2$ , AFm, and AFt can be measured, but no C-S-H. Since the XRD-patterns of alite and belite are very similar, mostly they cannot be distinguished clearly.

#### 4.4.5 Shrinkage cone

The early deformations were measured in two parallel shrinkage cones (Schleibinger). The device measures the height loss of a specimen with a laser reflector as presented in Figure 4.27. A paste or mortar specimen is poured freshly into the cone. The cone has a  $60^\circ$  apex, which points down. Assuming isotropic shrinkage, the  $60^\circ$  angle makes sure that a change in the radius of the cone takes place in identical magnitude in height.

According to the investigations, conducted by Eppers [133], the results qualitatively compare to autogenous shrinkage measurements according to the well established corrugated tube test method (Figure 4.28). The strain may vary in total, which can be ascribed to the different test methods but the time sensitivity and the qualitative (comparative) results are identical.

Following the recommendations of Eppers, the surfaces of the specimens were sealed with cling film [133, 232], which was placed above the surface, loosely enough to not generate strain upon deformation. A reflector plate was placed in the centre of the specimen. Each specimen was measured in parallel in two cones from one mixing batch (Figure 4.29).

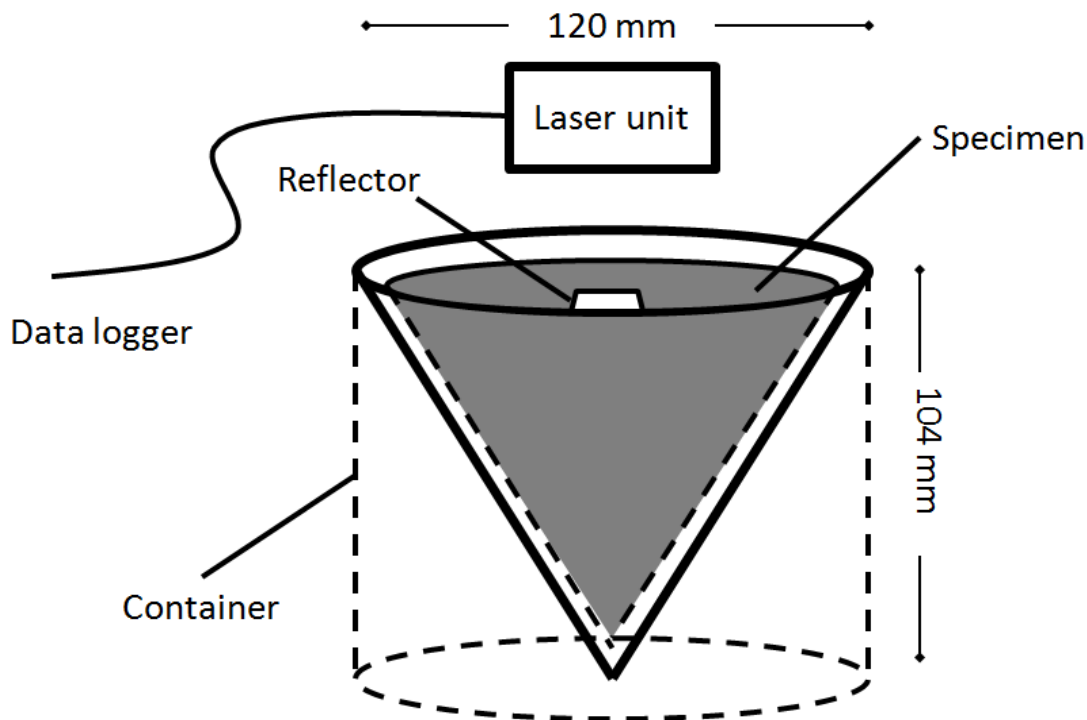


Figure 4.27: System setup of a single unit shrinkage cone.

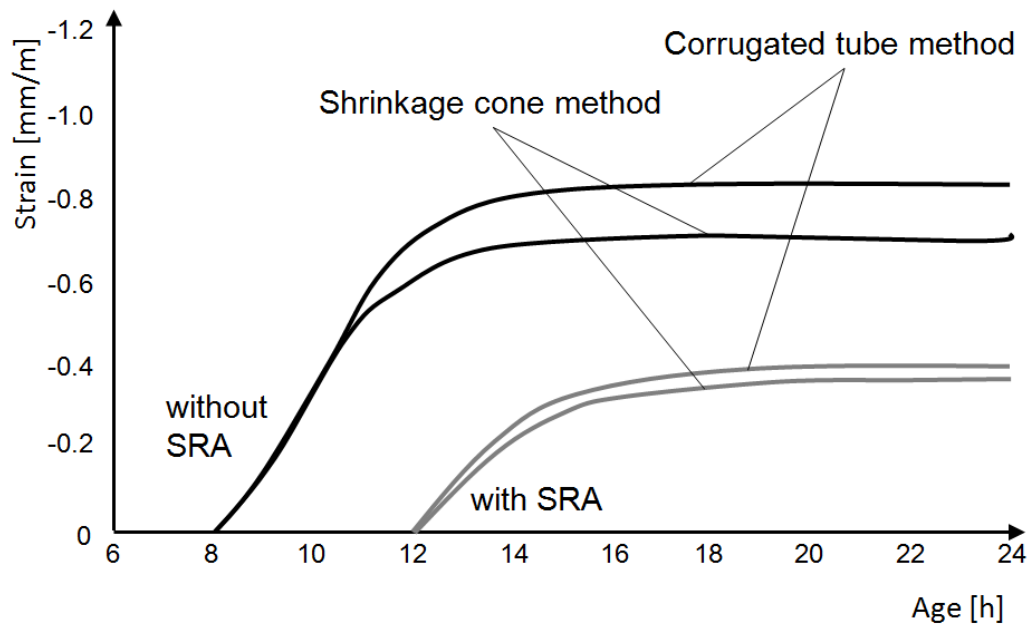


Figure 4.28: Comparison of shrinkage cones and corrugated tube method for two UHPC mixes with and without shrinkage reducing admixture after Eppers [133].

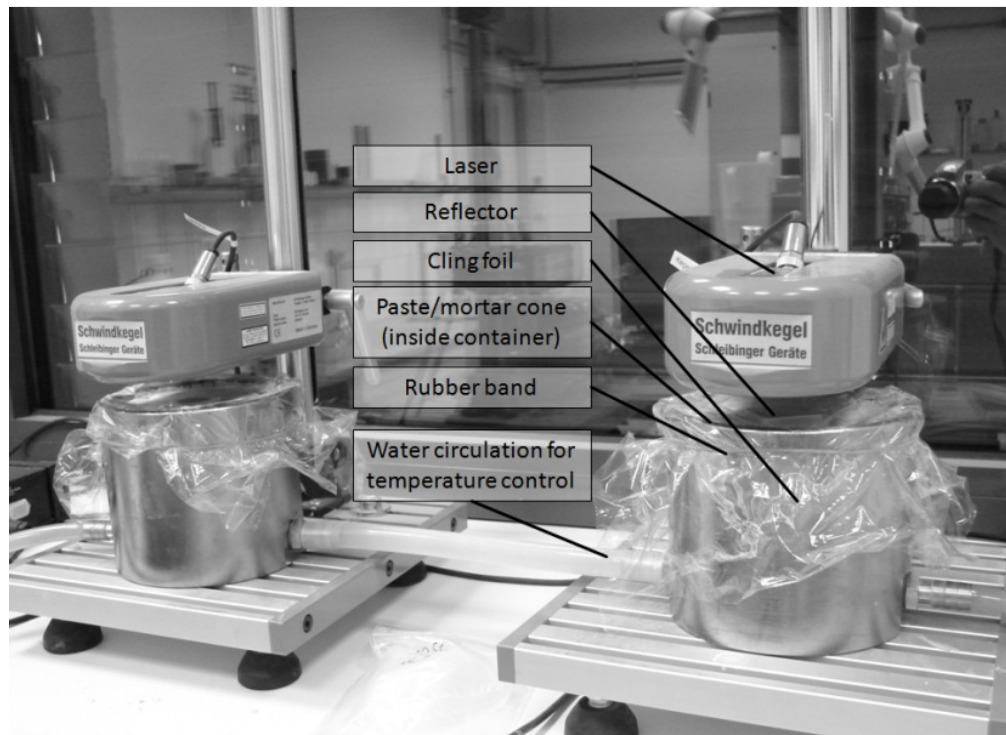


Figure 4.29: Shrinkage cones during measurement.

## 4.5 Materials selection

### 4.5.1 Observations regarding the storage of raw materials for concrete

Investigations about the influence of the climatic conditions during the storage of the unhydrated cement pointed out that cement that is stored over a longer period of time changes its properties. Within the scope of a study that took place in parallel to the research presented in this work, the effect of the storage condition of cement on normal mortar, self-compacting concrete (SCC), polymer cement concrete (PCC) and high performance concrete (HPC) was observed. The self-compacting mortar's constituents and composition were identical to the mortar of the combination type concrete described in Table 4.9 with the high charge density PCE and the starch based stabilising agent ST1.

Different storage conditions and durations did not significantly affect the strength after 28 days (Figure 4.30), however, distinct effects could be observed on the rheology and the setting. Effects that could be observed were limited to those applications containing adsorptive SPs.

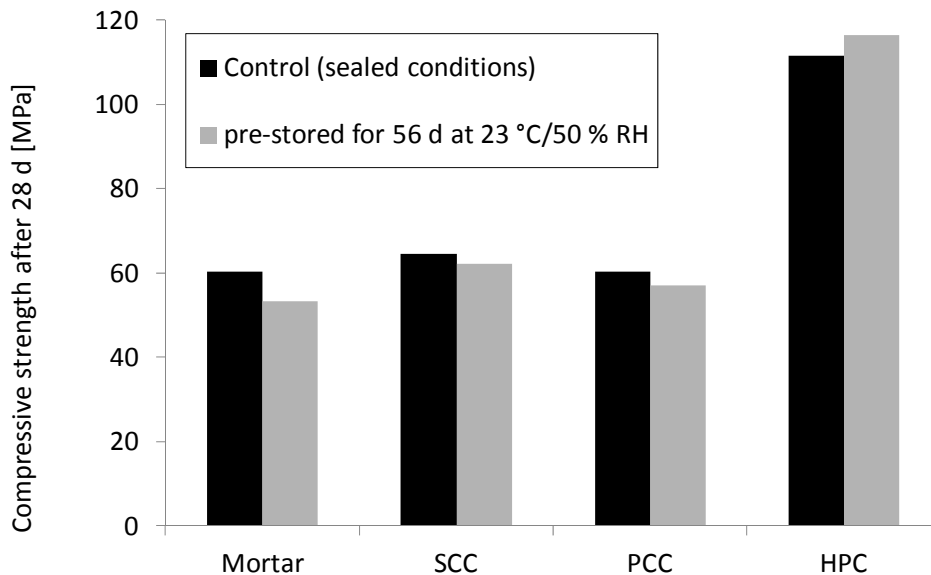


Figure 4.30: Influence of the exposure duration of cement prior to casting on the 28 d compressive strength of different cementitious applications.

Figure 4.31 gives the example of the Haegermann flow table spread test of normal mortar in comparison to the slump flow values of the SCC. No significant effects can be observed for the flow spread values of normal mortar, while the slump flow values of the SCC increase with increasing pre-storage duration of the cement. In parallel longer exposure of the cement correlated with higher viscosity (Figure 4.32). Similar effects as in SCC could be observed for HPC and PCC [123].

Due to the fact that rheological effects could be observed only on those systems that incorporated SP, it was concluded that pre-hydration of the aluminous phases generates supplementary adsorption sites for SPs, which reduce the yield stress. In parallel, the morphological changes on the surfaces might countervail the mobility of particles, thus increasing the viscosity. Indeed, SEM investigations gave evidence that the cement surfaces show pre-hydration products on the surface, which were not specified in detail (Figure 4.33). The pre-hydration products on the surfaces furthermore did not have an effect on the measurement of the Blaine value or the water demand of the powders.

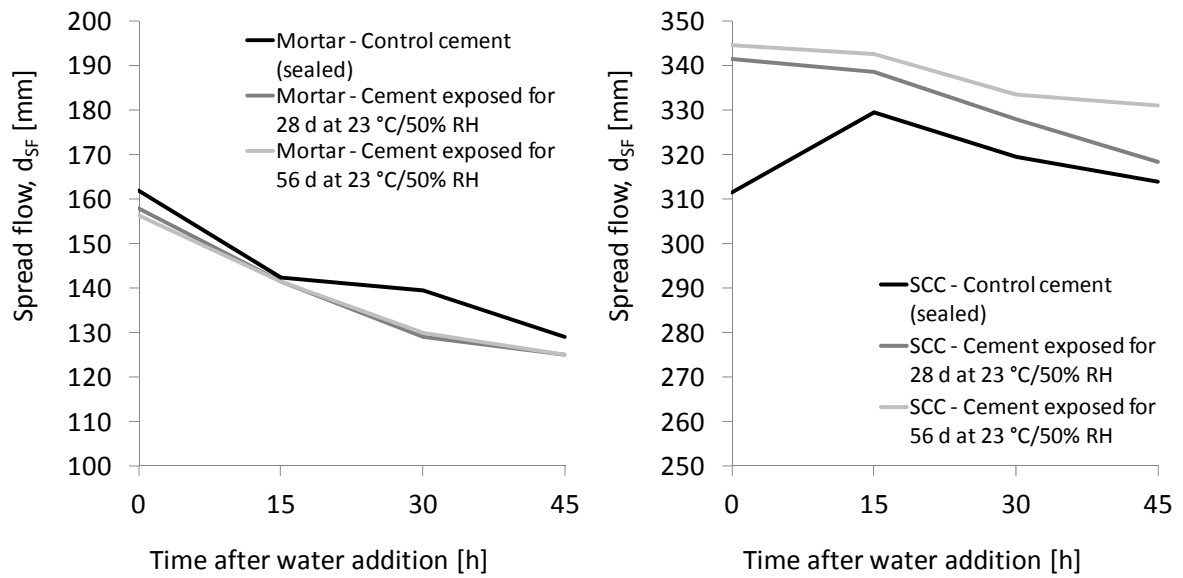


Figure 4.31: Flow values of normal mortar and SCC using CEM I 42.5 R that was exposed to different pre-storage conditions prior to casting after Schmidt et al. [123].

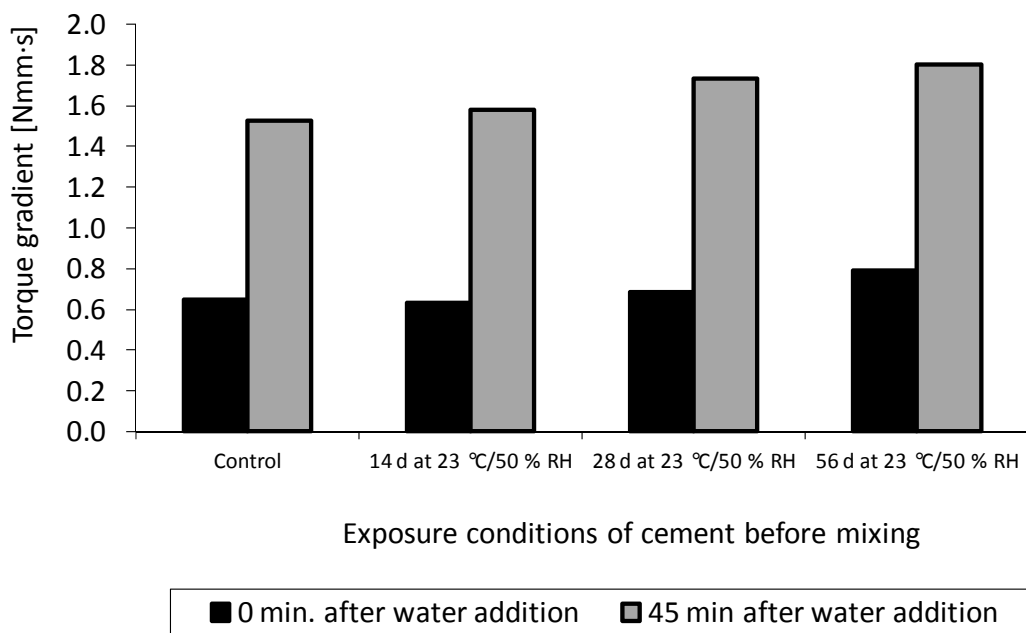


Figure 4.32: Slope of the Bingham curves of SCC for mixes with CEM I 42.5 R that was exposed to different pre-storage conditions prior to casting after Schmidt et al. [123].

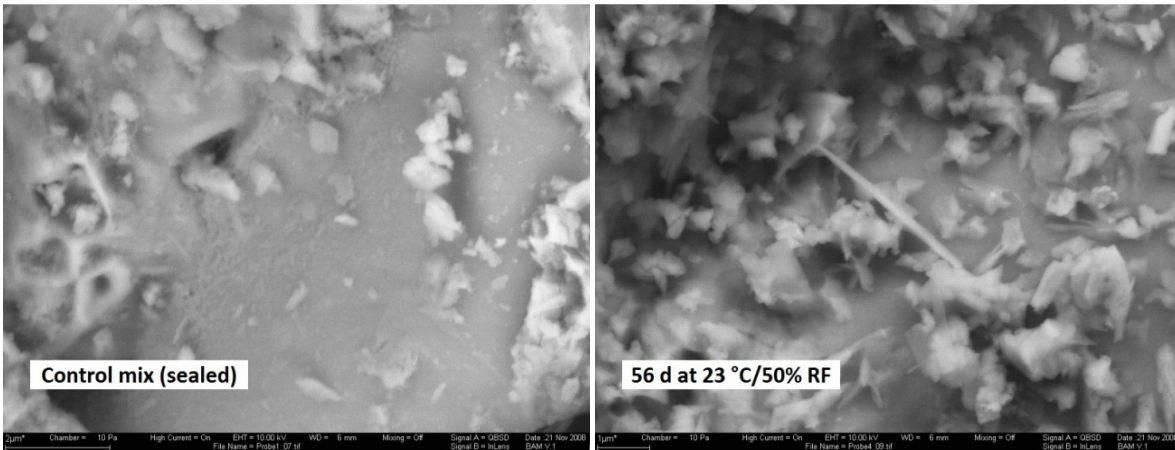


Figure 4.33: SEM micrographs of cement surfaces after sealed storage and after exposure to 23 °C/50% RH for 56 days.

Regardless of the use of SP, increasing exposure duration correlated generally with retarded setting. An exposure of 56 days caused a shift of the final set of a normal mortar by approximately 3 hours and of the SCC by more than 4 hours (Figure 4.34). These shifts can be observed similarly with PCC and HPC [123]. A pre-hydration of C<sub>3</sub>A to C-A-H, which is likely after the conclusions from the rheological investigations, would reduce the aluminium content in the solution, which in combination with a lower solubility of the set retarder due to water incorporation would cause retarded setting.

Finally, the conclusion can be drawn that the storage of cement over a long period of time might result in misleading results in case cementitious systems are investigated with regard to fresh and early properties. This is particularly valid when SPs play a critical role for the performance as in this work. Therefore, in this Thesis special considerations were made in order to avoid misinterpretations of cement superplasticiser effects, which will be described in the next Subsections.

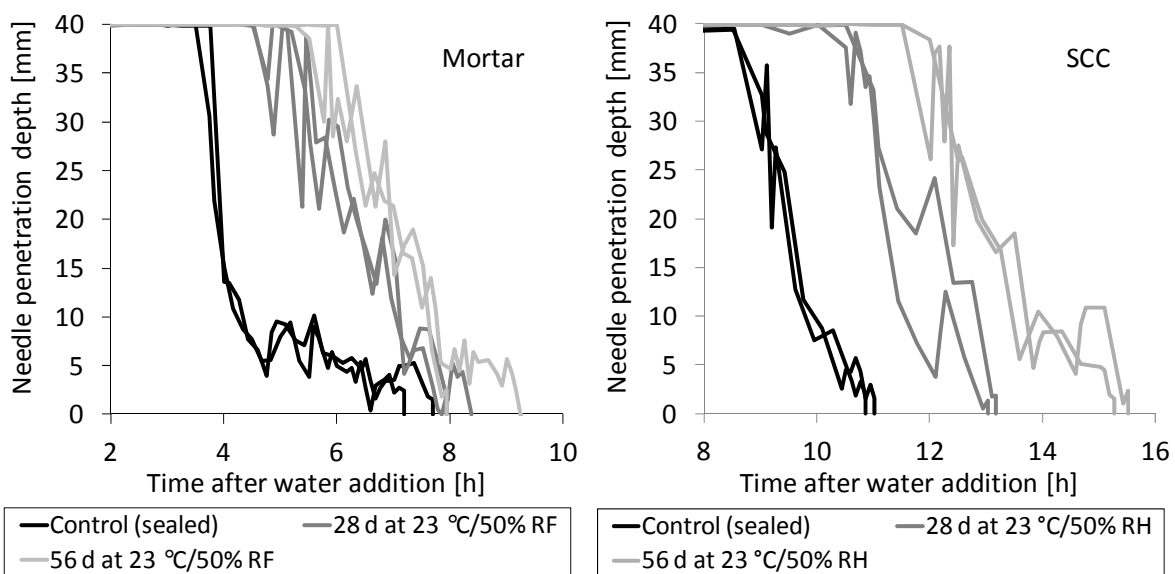


Figure 4.34: Set retardation caused by using CEM I 42.5 after different exposure duration at 23 °C/50% RH.

#### **4.5.2 Practical problems**

The materials that were used for the tests are materials that have been regularly used in the laboratories of the BAM Federal Institute for Materials Research and Testing. They undergo steady quality control and have all shown only little scatter in the basic performances. Particularly the chemistry as well as the particle and surface properties of the cement have not changed during the past years. Cement is re-charged approximately every 2-3 months. Different charges are generally never blended. The investigations in Subsection 4.5.1, however, have shown that the surface modifications are not detected by means of standard investigations according to EN 196. Nevertheless, they had strong influence on the fresh and early properties, particularly in combination with SPs. Since the investigations presented in this work were conducted over a period of several years, the risk of inaccurate precision within the results was high. It was therefore not considered as reasonable option to reserve one charge for all tests.

#### **4.5.3 Principle of closed series with identical delivery charges one**

Due to the findings in Subsection 4.5.1, the separation of raw materials of one and the same delivery charge to be used for all tests throughout the whole period of time in which the tests were conducted was not a reliable option. However, although the used raw materials have not been showing strong scatter, it could not be fully excluded that regular changes in the materials' properties can have effects on the observed properties.

Therefore, all tests were conducted according to the same principle. A closed area of observations, e.g. the influence of the SP modification on the rheology of concrete, or the influence of the STA content on the setting of paste, was always conducted with only one always identical set of raw materials' delivery charges. At the beginning of an investigation, the actually available delivery charges were used and never changed within the same observation series. For another investigation with different focal area, however, different delivery charges might have been used, which, then again, were not varied until the investigation was finished.

As a result, identical mixtures that were investigated at different steps in time (e.g. control mixtures) might show varying performances. In sensitive systems incorporating high amounts of SPs, this effect is hardly avoidable as soon as tests are conducted over a longer period of time. Due to the principle to always use an identical set of delivery charges within a closed area of investigations, it is nevertheless assured that effects caused by concrete constituents can be clearly qualitatively identified.



## 5 A simple test to assess the charge density of PCE

### 5.1 Introduction

In Section 3.4 the importance of the charge density for the effect of PCE superplasticisers was introduced. It was pointed out that the charge density is strongly affecting the adsorption tendency and thus the way how the polymer modifies the yield stress of a cementitious system. Despite the importance to distinguish PCEs based on their charge density, in Section 3.5 it was highlighted that for end-users it is difficult to obtain the required information. In order to better assess the differences in the polymeric structure a simple test setup will be introduced in this chapter, which helps to qualitatively identify the charge density of a PCE. The suggested method allows distinguishing two different PCEs regarding their performance for the initial and the long term flow properties. The test is based on the assumption that PCE adsorption determines the reduction of the yield stress of a flowable system until a maximum adsorption, after which any further addition does no longer contribute to further reduction. By measuring the spread flow diameter with stepwise increased SP contents, a flow initiation dosage and a maximum flow spread can be determined, which helps identifying the influence of the PCE on yield stress. In order to avoid mixing up effects from the water, the test needs to be conducted at a water content at which any contribution to the yield stress reduction can be linked only to the addition of PCE.

### 5.2 Basic principle

It is well known that a minimum threshold of PCEs needs to be adsorbed before effects on flowability of cementitious systems can be observed [66, 67, 179]. This is also the reason why producers often provide data about a minimum dosage for PCE SPs. It can be expected that as soon as all polymers have covered all accessible adsorption sites, a maximum effect of PCE occurs, after which further addition of PCE does no longer contribute to flowability. It has to be emphasised that this only applies for one moment in time and that ongoing hydration will produce further adsorption sites.

Following these considerations, a cementitious system that does not contain any excess water but which is mixed with different amounts of PCE shall exhibit respective slump flow values as shown qualitatively in Figure 5.1. At low additions of PCE, no effect on slump flow can be observed, because only a small part of the adsorption sites is covered by polymers. At a certain threshold dosage, flow is initiated (Point A). Due to the competitive adsorption with sulphate ions, higher charge densities can be adsorbed in higher amounts on adsorption sites, while low charge density PCEs remain partly ineffectively in solution. Therefore, an occurrence of the flow initiation at low dosages is a first indicator for high charge density. At increasing dosage of PCEs, the flow increases until a maximum is reached. Here again, due to the competitive adsorption, PCEs with higher charges adsorb rather than sulphate ions, while PCEs with lower charge remain partly in solution. Therefore, the slopes of the curves for high charge density polymers are expected to be steeper than for low charge density polymers (Point B). Finally, considering that the effect of PCE on yield stress is mainly induced by those polymers that are adsorbed, it can be expected that the higher the charge density is, the higher is the maximum flow spread diameter (Point C) and the lower is the dosage at maximum flow (Point D). As these considerations are based on systems that do not contain excess water, a slight drop of the curve for higher dosages than the maximum dosage can be expected, since it is likely that excess PCEs may mutually reduce their mobility in the solution.

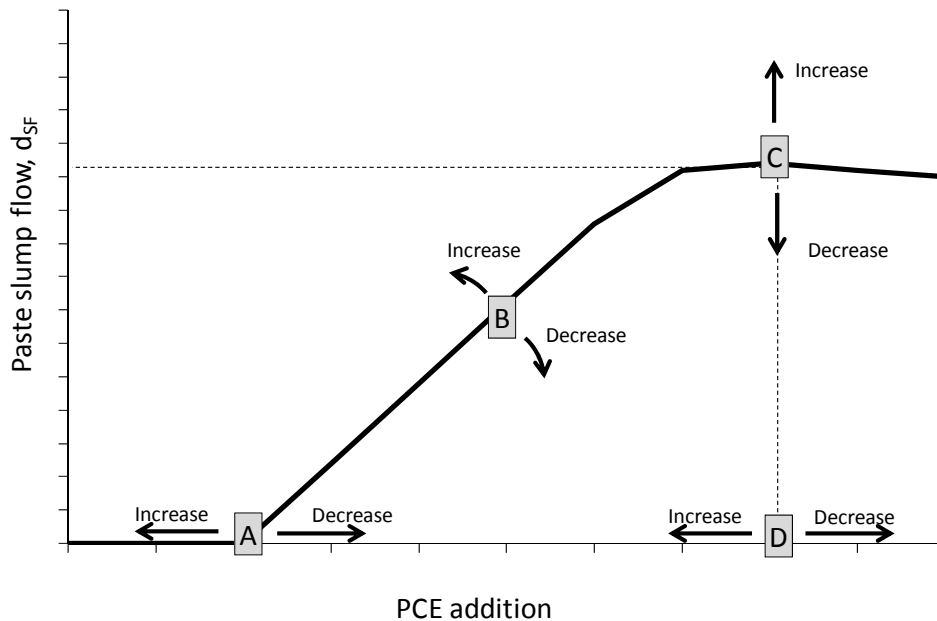


Figure 5.1: Hypothetical characteristics of slump flow vs. PCE content depending on the charge density of the PCE (left). A = Dosage at flow initiation; B = Slope of the Slump flow vs. PCE dosage curve; C = Maximum flow diameter; D = PCE dosage at maximum flow diameter.

Following these considerations, a cementitious system that does not contain any excess water but which is mixed with different amounts of PCE will exhibit respective slump flow values as shown qualitatively in Figure 5.1. At low additions of PCE, no effect on slump flow can be observed, because only a small part of the adsorption sites is covered by polymers. At a certain threshold dosage, flow is initiated (Point A). PCEs with higher charge density have a stronger tendency to be adsorbed on hydrate phases and they are less affected by the competition for adsorption sites with sulphate ions. Therefore, higher charge PCEs can be adsorbed in higher amounts while for PCEs with lower charge density higher amounts remain unadsorbed, thus ineffective, in the solution. Therefore, the occurrence of the flow initiation at low dosages is a first indicator for high charge density. At increasing dosage of PCEs, the flow increases until a maximum is reached. Here again, due to the competitive adsorption, PCEs with higher charges adsorb rather than sulphate ions, while PCEs with lower charge remain partly in solution. Therefore, the slopes of the curves for high charge density polymers are expected to be steeper than for low charge density polymers (Point B). Finally, considering that the effect of PCE on yield stress is mainly induced by those polymers that are adsorbed, it can be expected that the higher the charge density is, the higher is the maximum flow spread diameter (Point C) and the lower is the dosage at maximum flow (Point D). As these considerations are based on systems that do not contain excess water, a slight drop of the curve for higher dosages than the maximum dosage can be expected, since it is likely that excess PCEs may mutually reduce their mobility in the solution.

Ongoing hydration yields the formation of new adsorption sites at which PCE can be adsorbed at high dosages. It is therefore very likely that the value of the maximum and the PCE dosage at which it is reached will change over the course of time. However, for PCE LC and PCE HC it was found that, regardless of the individual effect of the PCEs, the time effect is negligible. Figure 5.2 shows the slump flow values at a PCE dosage of 2% solids of the cement, which for both PCEs is far beyond the adsorption maximum dosage. It can be clearly observed that each PCE differently affects the maximum flow spread diameter, and both curves show time dependent variations of the slump flow. However, the curves never cross and over the course of

time the distance between the curves maintains relatively stable. Hence, a qualitative assessment of the PCE related curves can be made regardless of the observation time.

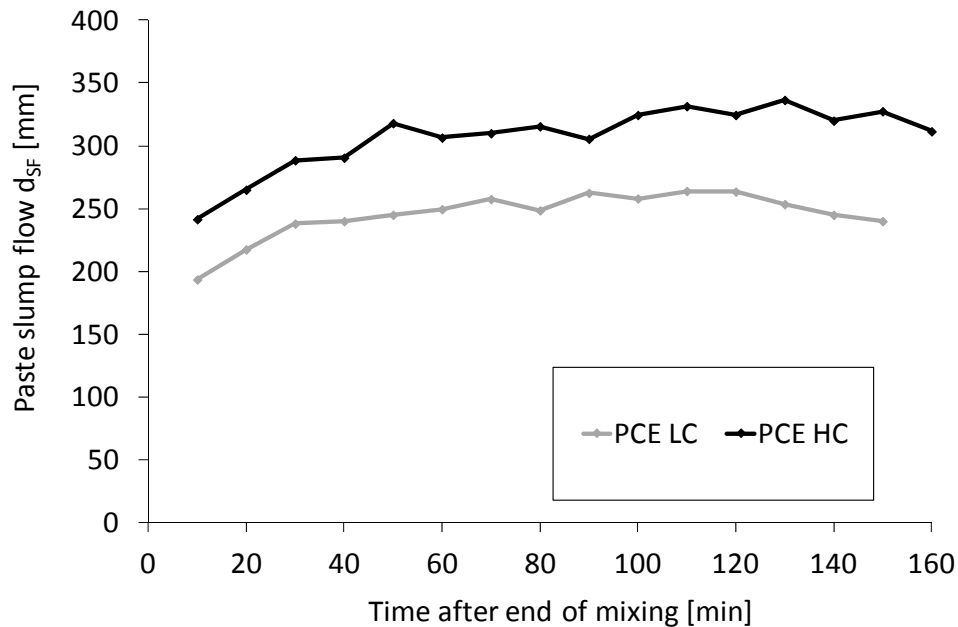


Figure 5.2: Time dependent slump flow values at solid PCE addition of 2% by mass on cement.

### 5.2.1 Determination of the water demand of a powder mixture - Step 1

In a first step, a binder mixture needs to be generated with a water content that just covers the surfaces and fills the voids between particles, but does not generate any flow. There are several methods to find this water content. Hunger provides a comprehensive overview of various different test methods to determine the minimum water demand of powder mixes [5, 32].

The observed methods comprise:

- Puntke test, where water is added stepwise to a granular mix until the surface of the mix starts to smoothen and slightly shimmer [233].
- Modified Marquardt test [234], where the power consumption of the mixing device is measured, and the maximum power is considered as the water demand.
- The Vicat consistency test according to EN 196-3, where water is added to a granular mixture until a specific needle (10 mm diameter) penetrates a specimen of 40 mm height 34 mm deep.
- Spread flow test according to Okamura and Ouchi [3], where the spread flow is determined at varied water to powder ratios. A linear correlation line is put between the values, where the calculated intersection with the ordinate marks the water demand.

According to Hunger's comparison, each method yields different water to powder ratios with the spread flow test generating the highest water volumes. The results from the other alternatives compare much more (Figure 5.3).

For the suggested PCE performance test a precise water demand is not required. However, it should be made sure that it is of highest importance to avoid influences of the water to work with a water content that is low enough to keep the water-particle system stiff without admixtures. This consistency is necessary to make sure that upon addition of SP the flow is only generated by the added polymers and that the mixture is free from any segregation, which would be the case at higher water contents and high SP additions.

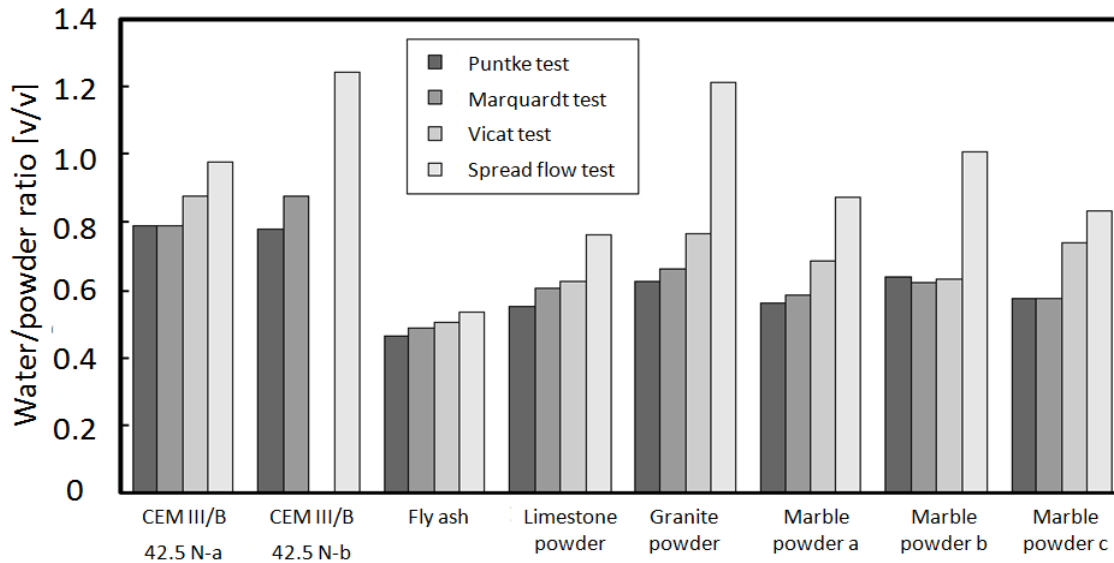


Figure 5.3: Comparison of different test methods to determine the water demand of powder mixtures for different powders [5].

The water demand defined by the Vicat test, where a needle with relatively large diameter penetrates the paste deeply, is not feasible, since the thus determined consistency is typically flowable. Interpreting the data provided in Figure 5.3, it is likely that the test setup according to Okamura and Ouchi will yield even higher contents. The Puntke test or the modified Marquardt test are expected to produce more reliable results, due to the simplicity of the method, for this step the Puntke test is recommended.

For the Puntke test a granular mixture of approximately 50 g is poured into a beaker with flat bottom. Drop by drop, water is added to the powder while the powder is steadily stirred with a stirring tool and the beaker is pushed onto a table from approximately 5 cm height. This procedure is conducted until the powder compacts under the agitation to a point, at which the surface remains slightly rough with a light shimmer but without bleeding on the surface. This consistency is considered as the consistency at the point at which the particles are all wetted and all voids in between filled with water. The test is repeated three times of which the lowest result is chosen to be the relevant water demand  $n_W$ , which is determined according to:

$$n_W = \frac{V_W}{V_W + V_P} = \frac{\frac{m_W}{\rho_W}}{\frac{m_P}{\rho_P} + \frac{m_W}{\rho_W}} \quad (5.1)$$

where:  $n_W$  = water demand [-];  $V_W$  = volume of water [ml];  $V_P$  = volume of powder [ml];  $m_W$  = mass of water [g];  $m_P$  = mass of powder [g];  $\rho_W$  = density of water [g/ml<sup>3</sup>];  $\rho_P$  = density of powder [g/ml<sup>3</sup>]

According to the practical experiences of the author with that test, results that are measured on a vibration table with low amplitude and high frequency do not deviate strongly from results where the beaker is pushed onto a table manually. By this, the test allows a water demand determination of a powder within less than 30 minutes. Practically, it is advisable to first fill into the beaker approximately 50 g of powder ( $m_P$ ), the exact mass is noted. Then the scale is tared to the beaker, the powder, and the stirring tool (spoon, small metal rod) jointly. The reason to

include the stirring tool for the taring is avoiding loss of paste sticking to the tool. In a next step, the water is added until the specified consistency is achieved. Upon weighing the beaker and the stirrer again, the added water amount  $m_W$  can be read on the scale. For cements it is likely that the water demand  $n_W$  will be approximately between 0.39 and 0.46. However, the test functions well also for any other type of powder material, as well as for blends of material. It is therefore also a simple method to optimise the packing density of two powders. The water demands according to the Puntke method for the CEM I and the LSF used in this Thesis as well as for other fillers relevant for this chapter are given in Table 5.1.

Table 5.1: Water demands for the CEM I and LSF used in this Thesis and comparison to the water demand of other fillers.

	CEM I	LSF	Marble LSF	Ultrafine LSF	Dolomitic LSF	Quartz filler	Fly Ash	GGBS
Specification	(Subsection 4.1.2)		$d_{50} = 3.5 \mu\text{m}$	$d_{50} = 1.7 \mu\text{m}$	$d_{50} = 12.8 \mu\text{m}$	$d_{50} = 60 \mu\text{m}$	$d_{50} = 20 \mu\text{m}$	n/a
Spec. gravity [-]	3.12	2.74	2.70	2.71	2.74	2.65	2.26	2.9
$n_W$ [-]	0.44	0.34	0.67	0.35	0.36	0.35	0.35	0.45

### 5.2.2 Calculation of mixture composition for each PCE dosage - Step 2

The determined w/p now is the basis for the mixture composition, which incorporates the PCE under investigation in different amounts. In order to make sure that an influence of surplus water is fully avoided and to make sure that segregation cannot take place, the water content of the bulk SP has to be considered in the mixture composition for every single test with different PCE content.

Taking into account the water coming from the PCE is a complicated calculation, if each mixture composition shall result in the same total paste volume. It is much easier to fix the powder content, e.g. 500 g cement as shown in the sample in Table 5.2. This is uncritical, since each mixture should always contain a higher total volume than required for the spread flow test. As can be seen from Table 5.2, the resulting total volumes do not vary significantly so that influences of variable shear forces within the mixer due to different mixing volumes are fully negligible.

In the next step, the water contribution from the SP needs to be taken into account. Typically the water contents in PCEs vary between 70 and 80% by mass, which needs to be subtracted from the total water content added to the mixture. The total water content for each PCE addition then calculates according to the equation below. A calculation example is given in Table 5.2.

$$m_W = m_{W,Punkte} - m_{W,PCE} = \frac{n_W \cdot c}{1 - n_W} - b_{PCE,bulk} \cdot c \cdot (1 - s_{PCE}) \quad (5.2)$$

where:  $m_W$  = water demand according to Equation (5.1) [g];  $m_{W, Puntke}$  = water dosage after Puntke test [m];  $m_{W, PCE}$  = water content in bulk PCE [m];  $c$  = cement [g];  $b_{PCE, bulk}$  = bulk PCE addition [% by mass];  $s_{PCE}$  = Solid content of the PCE [%].

Table 5.2: Example mixture calculation for the evaluation test with cement pastes.

Component		Unit	Ratios	Density [kg/m <sup>3</sup> ]	Mixtures for test series with modified PCE contents				
PCE	$b_{\text{PCE, bulk}}$	[%]			0%	1%	2%	3%	4%
Cement	c	[g]		3120	1500	1500	1500	1500	1500
PCE <sub>Bulk</sub>		[g]			0	15	30	45	60
PCE <sub>Dry</sub>	-	[g]	$(1-s_{\text{PCE}}) = 30\%$	1070	0	4.5	9	13.5	18
Water <sub>PCE</sub>	$m_{\text{W, PCE}}$	[g]	$s_{\text{PCE}} = 70\%$		0	10.5	21.0	31.5	42.0
Water addition	$m_{\text{W}}$	[g]		1000	378	367	357	346	336
Total water demand	$m_{\text{W, Punkte}}$	[g]	$n_{\text{W}} = 44\% (5.1)$		378	378	378	378	378
Total mix volume		[ml]			859	862	866	869	873
PCE <sub>Solid</sub>	PCE <sub>Solid</sub>	[%]			0.00%	0.30%	0.60%	0.90%	1.20%
		$[m_{\text{PCE}}/V_{\text{Cem}}]$			0.00%	0.94%	1.87%	2.81%	3.74%

### 5.2.3 Mixing - Step 3

A mixing procedure should be chosen that makes sure that a good dispersion of particles can be granted. A time period of 3 to 5 minutes of mixing with all constituents included is suggested. It can be discussed whether it is preferable to add the PCE immediately with the water or with time delay. Significant amounts of SP need to be added to the cementitious system in order to achieve the maximum slump flow, which can account for about 5% of the total water addition. Therefore, the addition of water and SP at the same time shows the advantage that no influences of different water to powder ratios before the addition of SP occur. However, the direct addition of SP fosters the formation of organo-mineral phases, which again negatively affects the test.

### 5.2.4 Spread flow values - Step 4

A Haegermann cone as described in Subsection 4.3.1 has shown to work well to determine the spread flow value. The paste is filled into the cone and the surplus amount is stripped off. Then the cone is lifted and the paste left flowing until an obvious stop can be observed. The mean value calculated from the largest diameter and the orthogonal diameter is taken into account.

Any other geometry will function as well, and will only yield different values depending upon the volume of the paste specimen. It must be emphasised that it is of certain importance to strictly conduct the test, no matter of the stiffness of the paste. From experience, some pastes already show flow, although the haptic sensation would not suggest it.

### 5.2.5 Interpretation of the results – Step 5

A practical example for the interpretation is given for a cement type CEM I and three differently charged SPs. Their details can be found in Subsections 4.1.2 and 4.1.4.

The mixtures were mixed with 450 g of cement in a Kenwood kitchen mixer. After a period of 30 s dry mixing, water and SP were added at the same time. Intensive stirring was conducted for 5 minutes after addition of water and SP. Flow spread tests were conducted directly after mixing, 10 and 20 minutes after the end of mixing. Prior to each test, the mix was shortly agitated in the mixer.

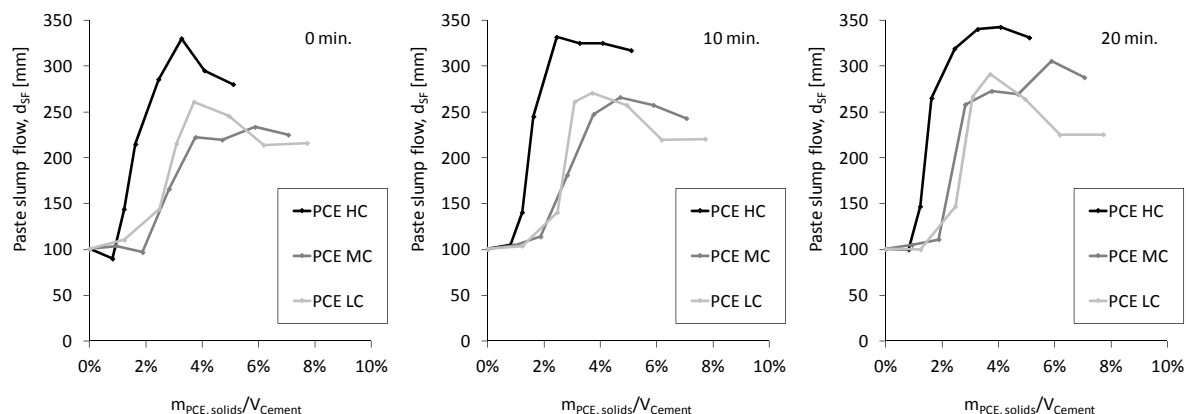


Figure 5.4: The influence the PCE charge density on the slump flow of cement paste with minimum water content according to Puntke at 20 °C at different times after mixing.

Figure 5.4 shows the results at different times for the low charge (LC), the medium charge (MC), and the high charge (HC) superplasticiser as introduced in Subsection 4.1.4. It can be clearly seen that the high charge density polymer starts to induce flow at significantly lower dosage and the maximum values are higher than with the other PCEs. This characteristic can be found at all time steps.

The medium charge and the low charge polymer behave rather similar regarding the maximum value, indicating that their influence on the rheology may be rather similar. A certain time effect can be observed for PCE MC, where the dosage at which the maximum or the transition to significantly smaller slope shifts to smaller PCE dosages in parallel to an increase of the maximum value. It is thinkable that the polymeric geometry of PCE MC may be more complex so that the initial adsorption takes place slower than with PCE LC despite its higher anionic charge. After 20 minutes, the increasing branch of the medium charge polymer runs slightly left of the increasing branch of the low charge density polymer, as it would be expected due to the higher charge density.

The PCE HC, thus can be considered as SP that induces high flowability for short open times, while it can be expected that PCE LC and MC will likely have similar influence on the flow properties. Both SPs can be considered as admixtures for performance retention.

The expected characteristics of the curve could be confirmed by the practical experiments, thus confirming the suitability of the test method to identify the performance of a SP without sophisticated equipment. The method allows distinguishing differently operating SPs that show clear differences in their performances. The selectivity for PCEs that behave very similarly (like in the example PCE LC and PCE MC) is limited.

Figure 5.4 uses the quotient of the mass of added PCE and the volume of cement. For a rapid evaluation of the performance of a PCE with cement, it is reasonable to use the mass percentage of solid PCE for the abscissa. The qualitative interpretation is identical for a single powder, as seen in Figure 5.5.

It can, however, be more reasonable to relate to the volume of powder. This is the case if the test is used with blends of different powders or if powders with different densities are compared (see Subsection 5.2.6). Unfortunately, a simple transformation from % by mass into % by volume is not possible for the solid parts of the PCE, since PCE polymers are dissolved and not dispersed in water. It is thus the only reasonable option without further information about the polymer to refer to the mass of PCE and the volume of powder.

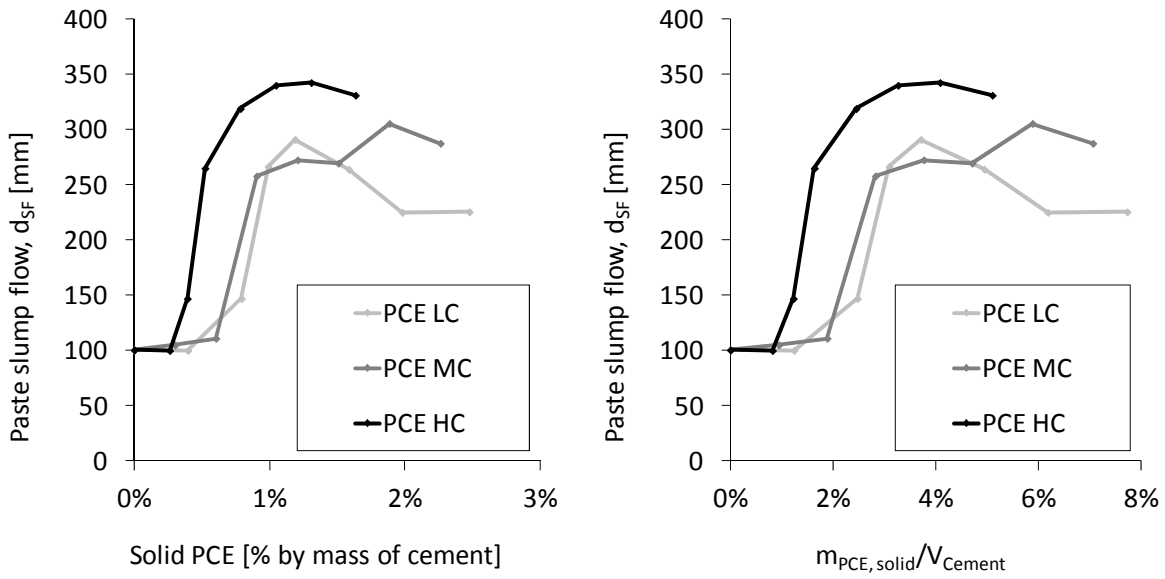


Figure 5.5: Comparison of the resulting curve for one cement for the use of [% by mass] and for [mass of PCE/volume of powder].

### 5.2.6 Application of the method with powders and powder blends

The suggested rapid method to assess the PCE performance is not limited to cement. It can be used with any type of powder. This can be of interest for the composition of a mixture where different fillers are included. The same test as described in Subsection 5.2.5 was repeated with the LSF as specified in Subsection 4.1.2 (Figure 5.6). It can be observed that the flow initiation takes place at significantly lower dosages as with cement and that the final maximum is higher than with cement.

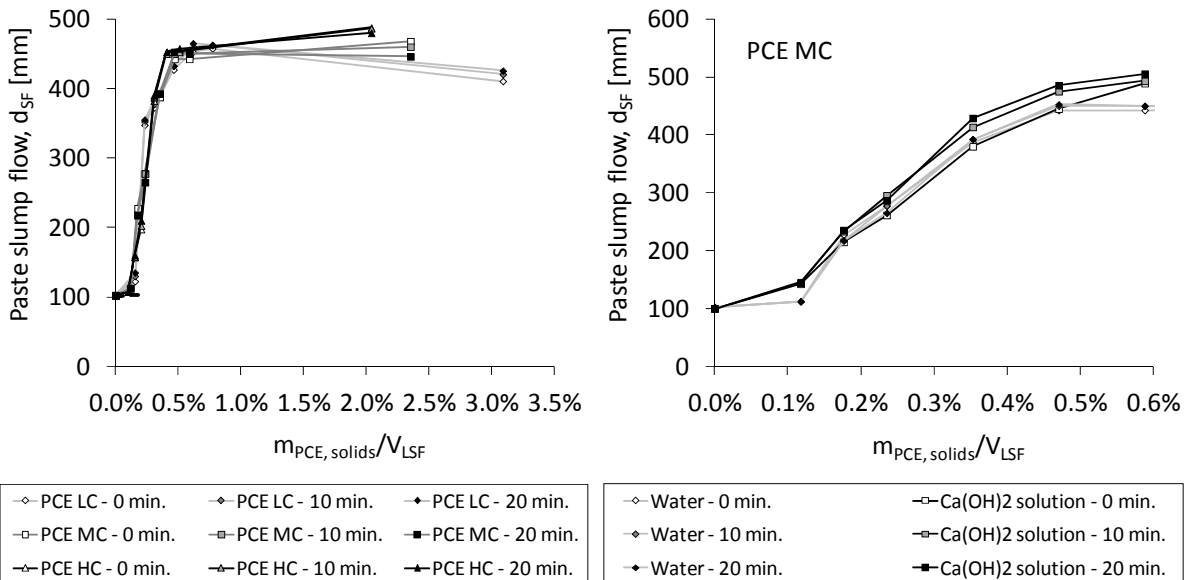


Figure 5.6: Performance of different PCEs with LSF (left) and comparison of PCE MC performance with LSF in water and a saturated  $Ca(OH)_2$  solution.

This yields the conclusion that PCEs also adsorb onto LSF surfaces in the presence of water, which induces the flow. The maximum dosage is much lower than with cement. No significant effect can be observed regarding charge density or time. Since LSF is considered to be largely inert, there are no new hydration products either which would provide new adsorption sites for the SP. Since there are no ions in the system, which would compete with PCEs for adsorption, the influence of the charge density of the PCE is negligible. If the same test is repeated with saturated  $\text{Ca}(\text{OH})_2$ -solution the results do not differ significantly. Differences are that the flow is initiated at lower dosages than with water and there is a time effect causing increasing maximum spread flow values with time (Figure 5.6, right).

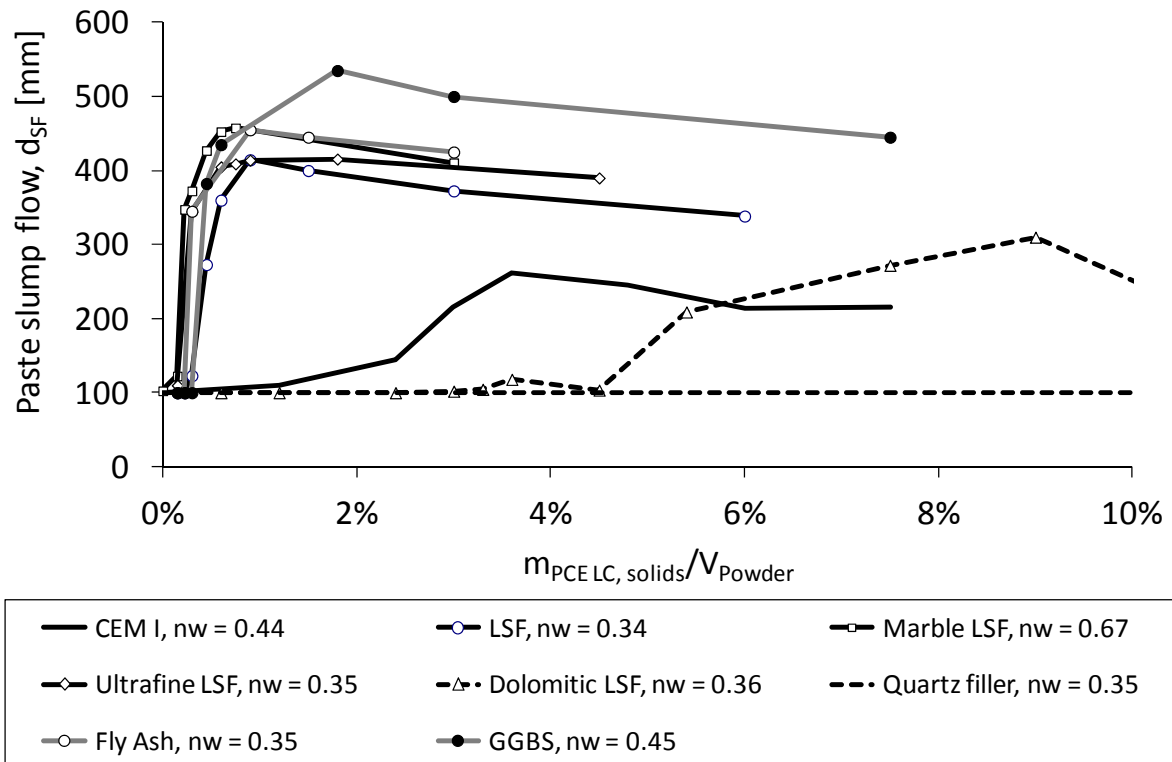


Figure 5.7: PCE effect on the slump flow value of various powders.

The suggested method can also be used to evaluate the adsorption of PCEs on varying powders. In order to compare the PCE influence, the powder properties other than the density are not of importance as long as the powders are kept identical. In order to better evaluate powders with different densities, it is recommended to use the quotient of the mass of PCE and the volume of powder. Figure 5.7 shows curves for different powders (The cement and the LSF specified in Subsection 4.1.2, a marble LSF, an ultra finely ground LSF, a dolomitic LSF, a quartz filler (QF), a fly ash (FA), and a ground granulated blast furnace slag (GGBS)). Their water demands as well as their specific gravities can be found in Table 5.1. It can be observed that with the exception of the dolomitic LSF all other LSFs, the FA, and the GGBS are liquefied by the PCE. For all powders apart from the dolomitic LSF and the QF, the flow initiation as well as the maximum  $d_{SF}$  occurs at significantly lower dosages of PCE than in case of cement, indicating that these powder provide lower surface charges or  $\zeta$ s than cement. The dolomitic LSF requires much higher amounts of PCE than cement in order to start flowing. The maximum flow spread compares to the value of cement. This is most likely induced by the magnesium carbonate in the dolomitic powder. The solubility of dolomite in water is by factor 20 higher and the electronegativity is significantly higher than that of calcium carbonate [235]. Despite the

chemical similarity between dolomite and calcium carbonate, it is thus very likely, that the effect of PCE with dolomite is poor. Thinkable mechanisms might be magnesium complexation or the formation of a low or positive  $\zeta$  for dolomite in water. The observations shown in Figure 5.7 give no evidence that PCEs adsorb on these powders in a cementitious pore solution as well, since  $\zeta$  strongly depends upon ion content and pH-value of the solution [187, 188].

The test can further be used in order to evaluate blends from different powders. Here again, it is most important to calculate the ratio of mass of PCE and volume of powder. Figure 5.8 shows the consumption of LSF and cement as well as different blends with a low charge density PCE. These blends represent the powder composition of a powder type mix and a combination type mix. Their constituents and powder ratios are identical to the POW and COM mixtures as specified in Subsection 4.2.4. The water demands according to the Puntke test for POW and COM were determined as 0.37 and 0.42, respectively (Table 5.3). Furthermore, results are presented for mixtures identical to POW and COM, where the LSF volume is replaced by the same volume of quartz filler (QF), which exhibits a similar grading curve as the LSF.

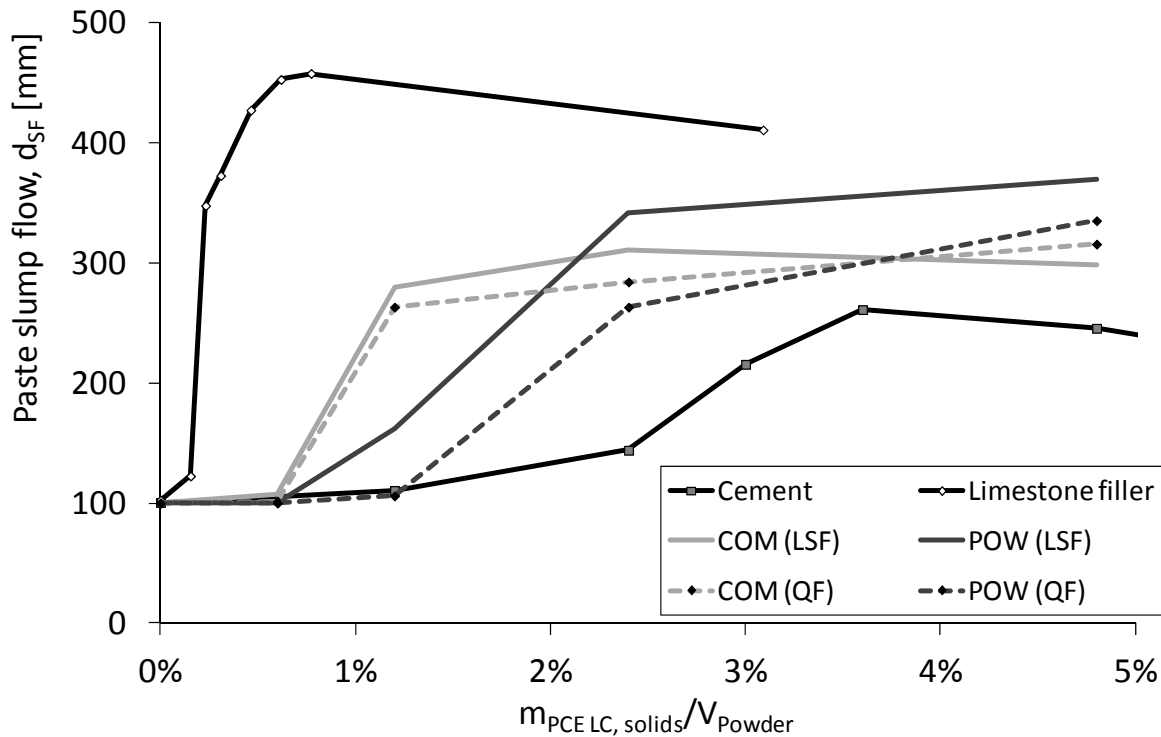


Figure 5.8: Effect of PCE amount on the flow of LSF, cement, and blends of cement and limestone filler (LSF) and cement and quartz filler (QF) in the combination type mixture (COM) and powder type mixture (POW) according to Table 4.12.

It can be observed that the curves of the blends show similar characteristics as those of cement and limestone. They are located between the curves of the single component mixtures. The flow initiation of POW and COM with limestone takes place at approximately the same dosage. Due to the relatively higher content of cement for identical powder volumes, the curve of the COM mixture increases more rapidly due to the higher attraction forces of cement. For the same reason, the point at which the slope of the curve turns approximately horizontal is reached earlier than for the POW mixture. However, due to the higher packing density of POW paste ( $n_w = 0.37$ ), the final slump flow value is higher than that of the COM paste ( $n_w = 0.42$ ).

Table 5.3: Water demands cement, LSF and the powder blends of the COM and POW pastes as well as pastes of COM and POW where LSF is replaced by a similar quartz filler.

	CEM I	LSF	COM (LSF)	POW (LSF)	COM (QF)	POW (QF)
Cement (volumetric fraction)	100		70.2	52.0	70.2	52.0
Filler (volumetric fraction)	-	100	29.8	48.0	29.8	48.0
$n_w$	0.44	0.34	0.42	0.37	0.42	0.37

The comparison of the blends with limestone and those blends that are mixed with QF instead, shows that the final slump flow values with LSF is significantly higher. Figure 5.6 (left) shows that in the presence of water no PCE is adsorbed on the QF. This may indicate that also in the cementitious pore solution LSF adsorbs higher amounts of PCE than QF does, which causes a lower yield stress at the maximum dosage of PCE. This is emphasised by the observation that this difference for the POW mixture, which contains relatively higher LSF on the identical powder content, than for the COM mixture.

### 5.2.7 Influence of water

It is absolutely inevitable to work at this minimum water demand, since any excess water would completely blur the results. This effect can be seen on the example of the COM and POW mixtures prepared with different w/p values (Figure 5.9).

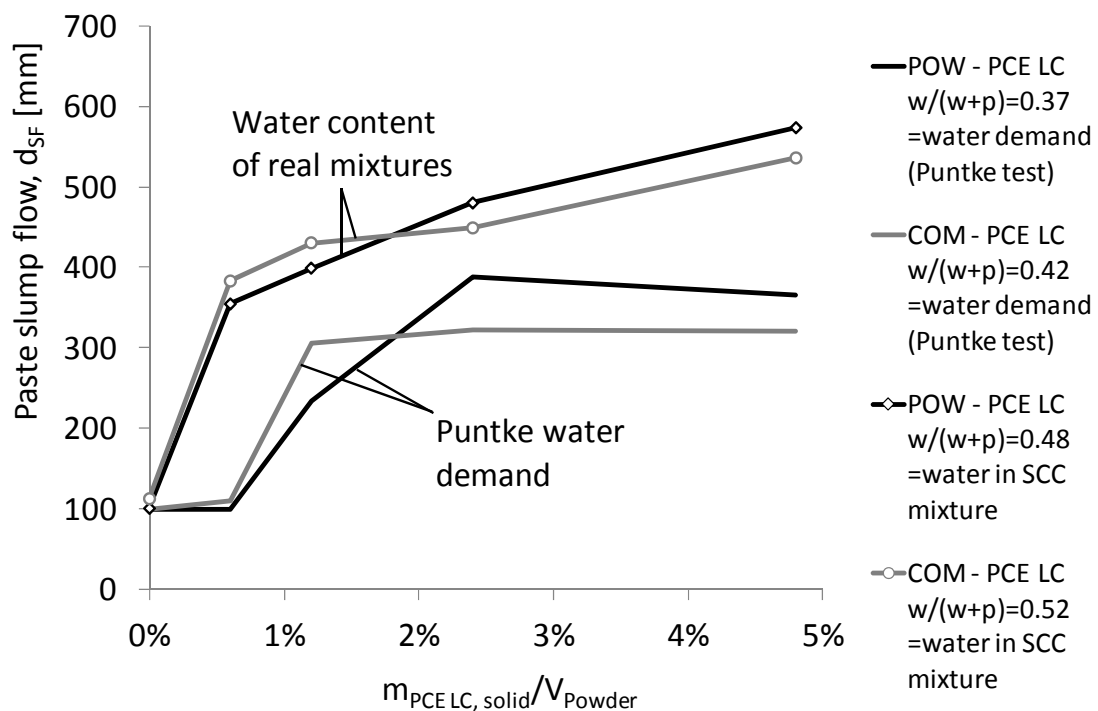


Figure 5.9: Rapid PCE performance test for POW and COM paste compositions at Puntke water demand and real water content according to (Table 4.12).

In case of a test at the minimum water demand according to the Punkte method, a clear distinction can be made between the mixtures. Both mixtures show a prominent amount of PCE that induces the flow as well as a maximum PCE amount. A distinction of different PCEs hence is possible. If the real water contents of the respective mixtures are used, the flow is initiated immediately upon addition of PCE, and a clear maximum cannot be observed. Hence, at higher water content, no clear distinctions between different PCEs is possible any more. Following the procedure described in Subsections 5.2.1 to 5.2.3 is therefore inevitable in order to obtain reliable data about the performances of different PCE modifications.

### 5.3 Conclusions

The interactions between cement hydration and SPs based on polycarboxylate ether are complicated and a high number of effects can take place. Most people who cast concrete with high PCE contents may not be interested in the individual effects that may occur in the pore solution or on the surfaces of particles. Fortunately, this is not necessary if the awareness exists that the number of adsorbed polymers controls the yield stress reduction of a SPs system. As a consequence, the most important factor that determines the adsorption of PCE is the anionic charge density of the polymer. High anionic charges generate rapid, high flowability. Low anionic charges generate lower flowability but long performance retention.

The knowledge about these correlations is a strong tool to individually adjust the performance of concrete to specific requirements. If applied by the caster instead of the supplier of admixtures, quick and effective adjustments can be conducted. In most cases, according to the author's experiences, two PCE types can be enough to adjust a wide range of individual flow properties. A major problem for the users is that they cannot easily identify the charge density of the SP products they are using.

Here a method is suggested that allows an indirect qualitative assessment of the adsorption properties of different SP products. Slump flow values of powder mixtures at a water content that is equal to the water demand of the powder are conducted with varied PCE contents. The resulting curve of slump flow versus PCE content is assessed. In comparison of two different PCE superplasticisers, a higher charge density can be expected,

- the lower the dosage is, at which flow is initiated (Point A in Figure 5.1),
- the lower the slope upon increasing PCE content (Point B in Figure 5.1),
- the higher the maximum flow is (Point C in Figure 5.1), and
- the lower the dosage at the maximum flow is (Point D in Figure 5.1).

The method also allows finding out whether materials adsorb PCEs. Results were provided for different powders in the presence of water. Due to the pH influence of the zeta potential, the same investigations need to be conducted in a representative pore solution, in order to find out whether materials adsorb PCE in a cementitious system. This is a challenging task. However, in order to qualitatively assess interactions between powders and PCE in the presence of cement, also blends of materials can be measured and compared in order to gain information about the adsorption capacities of different powders.

## **6 Fresh concrete performance of SCC at varying temperatures**

### **6.1 Introduction**

The flow properties of SCC are determined by a number of different factors, among which are the quality, quantity, and composition of aggregates, the water to solid ratio of the binder as well as interactions between mineral binder components and polymeric admixtures. While effects of the aggregates are largely invariant for all temperature ranges (a poor grading curve will not turn out to work properly when the temperature changes, and incompactible aggregate shapes will not be perfect for one specific climatic range), the influence of the water to powder ratio and the admixture's performance can vary with varying temperatures. Different mixture composition types have been developed based on different typical water to powder ratios (w/p). Superplasticisers (SPs) based on polycarboxylic acid can be considered as standard components for SCC all over the world. The importance of the influence of SPs has been addressed to in Section 1.6 and Figure 1.12 in particular. This chapter gives a distinguished overview of research to date about temperature effects on SCCs as well as a discussion based on experimental data about influences of the mixture composition and the particular modification of superplasticiser.

### **6.2 Temperature dependent behaviour of flowable concrete**

#### **6.2.1 Practical experiences with SCC at different temperatures**

There is only limited literature available that provides data about the concrete performances in the context of the casting temperature.

Khayat et al. [55, 74] investigated SCC used for the repair of retaining wall elements in Montreal, cast with two types of SP, based on polynaphthalene sulphonate (PNS) and polycarboxylate (PC). The concrete with PNS was cast at ambient temperature of 14 °C, while the fresh concrete temperature was 22.8 °C lowering to 21.0 °C after 60 minutes. The respective slump flow diameters reduced from 640 to 540 mm. The concrete with PC was cast at ambient temperature of 6 °C, while the fresh concrete temperature was 14 °C lowering to 13 °C within the first 60 minutes. The respective slump flow diameters increased within the first hour from 600 mm to 660 mm. These investigations emphasise the hypothesis of Section 1.6 that temperature dependent behaviour of flowable concrete cannot be easily predicted and that the superplasticiser plays a critical role in that.

Heunisch et al. [236] examined various SCC castings for inner shells of tunnels in the time between November 22, 2005 and March 31, 2006. The mixtures incorporated PCE superplasticisers. The ambient temperatures at casting days during this period varied between 0.5 °C and 11 °C. However, the concrete was specified to have temperatures between 8 °C and 25 °C at the mixing plant and between 10 °C and 20 °C on the construction site, which was achieved by good quality management, including a heatable enclosure of aggregates. Concrete temperatures, average slump flow diameters and V-funnel efflux times were recorded on the mixing plant as well as on the construction site. Slump flow values varied between 605 and 740 mm (625 to 725 mm, when maximum and minimum outliers are omitted), and V-funnel times varied between 10.8 and 30.0 seconds (11.0 to 27.0, when maximum outliers are omitted). The authors did not further correlate performance values and temperature values but their data is available in their report and reveals an interesting relation between the fresh performance values and the concrete temperature. Figure 6.1 shows slump flow values and V-funnel efflux times

versus concrete temperatures from the report above. Distinction is made between values taken at the mixing plant and taken at the construction site.

It can be clearly seen that as a result of the transportation, the range of site temperatures is much wider than the range at the mixing plant. Both data sets show a strong and quite linear correlation between concrete temperature and slump flow diameter such that increasing concrete temperatures coincide with smaller slump flow diameters. Regarding the V-funnel efflux times, the scatter is much larger, which might be a result of greater measurement inaccuracies of the methods. However, a trend towards longer efflux times with increasing temperatures is identifiable.

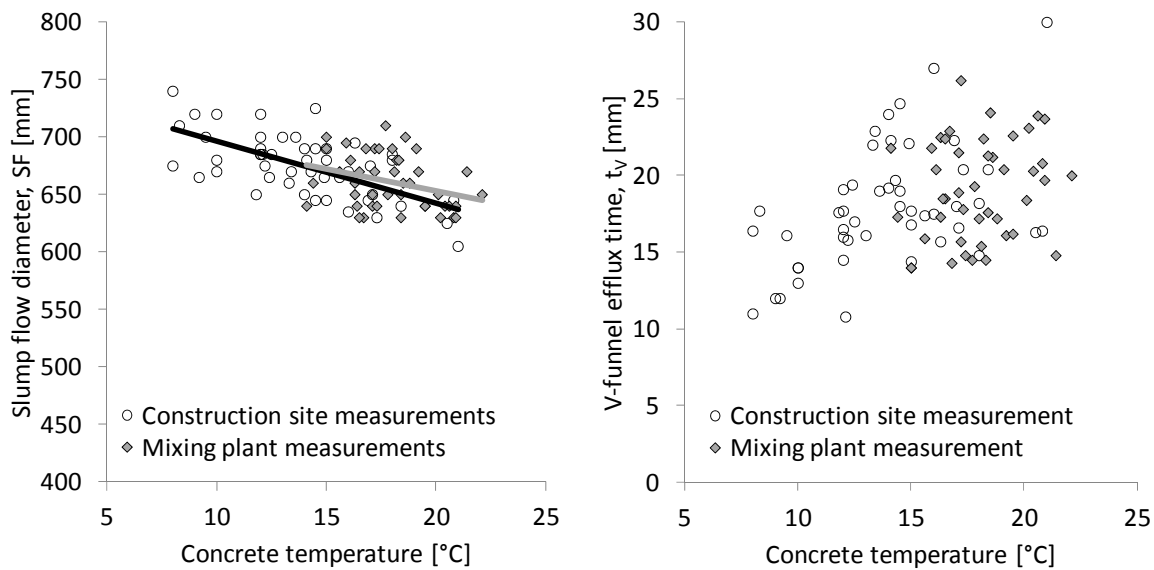


Figure 6.1: Influence of concrete temperature on slump flow diameters and V-funnel efflux times based on data provided by Heunisch et al. [236].

### 6.2.2 Research on temperature influences – Experiences in paste and mortar

Temperature effects on the fresh concrete properties were studied by several researchers with different results. Most of the research is done on paste or mortar.

Based on research of cement pastes blended with and without silica fume (SF), a water to cementitious materials ratio (w/cm) of 0.35, and SP based on PNS, Jolicoeur et al. investigated the effects of temperature and PNS addition on the rheological properties, on the retention of slump area and viscosity as well as on the adsorption of polymers [84]. Temperatures were varied between 0 and 40 °C. Instead of the slump flow diameter, the slump area was used to observe the workability. Regardless of the PNS amount, the influence of the temperature on the initial mini slump area at a particular PNS dosage was low in case of the cement without silica fume, while in case of cement with SF, in the range between 10 and 40 °C, increasing temperatures correlated with reduced areas. Furthermore, the slump loss rate was observed over 50 minutes. Increasing temperatures caused lower slump loss rates, while high rates of slump loss at low temperature were much greater for cement without SF. The investigations of the fluidity (which is defined as the inverse of the viscosity) exhibited that rising temperatures caused a high increase of the initial fluidity in case of cement without SF, while the inverse could be observed for cement with SF, even though the slope was much smaller. The authors conclude that in case of PNS added in excess to the saturation dose (see Subsection 3.2.3) the time dependent rheology is related to the PNS concentration in the solution. However, paste

fluidity is affected by temperature in a sometimes non-linear and unpredictable fashion, which means other effects might enhance or oppose effects of adsorbed SP.

Yamada reports about the influence of the temperature on pastes from OPC with water cement ratio (w/c) of 0.3 and 1.0% PC superplasticiser by mass of cement compared to non-superplasticised paste with w/c = 0.5. Temperatures of 5, 20 and 30 °C were selected. While the flow area decreased without PC at all temperatures between 0 and 120 minutes, at 5 and 20 °C within the same time span, an increase of the flow area could be observed with time, while the flow areas remain stable. The authors show that increasing amounts of PC adsorb with time. The initial adsorption as well as the increase was the smallest at 5 °C, while 20 and 30 °C behave similarly. The authors also show that the specific surface of the cement paste increases with time. The higher the temperature, the more rapidly this effect occurs. Furthermore, it is shown that the flow areas are controlled by the amount of adsorbed PC per surface area. However, as the PC content was kept constant, the increase of the surface would cause a higher loss of performance at high temperature, which was not the case. Hence, it was concluded that this is not the only effect determining the time dependent behaviour. The sulphate ion content was hence observed with time, yielding decreasing contents with and without SP in a similar manner, dropping during the first 30 minutes and levelling afterwards. By varying the sulphate ion concentration in the solution, they showed that PC adsorption is strongly depending on the sulphate ions content in the pore solution. Based on these results, the authors developed a model based on the factors BET surface change and the sulphate ion concentration. While at low temperatures, the high initial sulphate ion content outweighs the relatively small change of the surface, yielding increasing flowability with time, at high temperatures, the effect of the rapidly increasing surface area prevails, causing a time dependent loss of flowability.

Roncero et al. observed the influence of temperature on the flow properties of ordinary cement paste with w/c = 0.33 and two different SPs based on PNS and a copolymer of oxyethylene-oxypropylene [237], the latter of which is typically used as non-ionic detergent. Rheological properties were determined by using the Marsh cone according to ASTM C 939-87 [238]. The observed temperatures varied between 5 °C and 45 °C. It was shown that increasing SP addition reduces the efflux times until a certain saturation point at which the efflux times increase again. The authors qualitatively correlate flow time with yield stress, which is not precise, as Marsh cone and other efflux tests are generally considered to correlate with plastic viscosity rather than with yield stress (see also Subsections 4.3.2 and 4.3.3). High viscosities and yield stress falsify the interpretation of the results [36, 38] (see also Subsection 4.3.8). However, as close to the saturation point, the yield stress can be assumed as low, the results of this research represent qualitative information about the plastic viscosity. The saturation point was at 1.0% solid SP on cement for the PNS and at 0.3% for the copolymer, and it was identical for each SP regardless of the paste temperature. However, the temperature affected the Marsh cone flow time at the saturation level strongly with shorter flow times with increasing temperatures. At initial saturation levels, the retention of the flow time was investigated additionally and did not increase strongly for both SPs below 25 °C and increase more pronounced for higher temperatures. No information is provided about possible changes of the saturation level with time, which would be likely as the ongoing hydration increases the surfaces. The authors conclude that the adsorption of SP polymers is basically depending on the particles' surface area and that upon saturation no further flowability can be provided. As a result of the low amount of hydrates induced by low temperatures, poor flow properties could be observed, and the addition of supplementary SP was not effective anymore to improve the flowability.

Bramshuber and Uebachs investigated the influence of different PCE modifications on mortars from OPC with w/c = 0.55 at 5, 10, 15, 20, and 30 °C [72]. The six different polymers varied in backbone length and side chain length. After adjustment to comparable slump flow

values at 20 °C the mixes were investigated in a rotational rheometer at different temperatures at a constant shear rate of 120 rpm over a period of 90 minutes. The test setup is not very specific as changes in the measured torque at constant shear rate may represent either change in plastic viscosity, in plastic yield stress, or in both. Furthermore, the high shear rate might not be representative for self-levelling cementitious systems and constant shearing might steadily shear off SPs and ions in the pore solution and on the outer particle areas, thus probably affecting the hydration. Nevertheless, significant differences could be observed regarding the initial flow resistance and its incline during the first 10 to 30 minutes, as well as its behaviour over the total time. The results show that the initial shear resistance at low temperatures is higher than at higher temperatures with prominent time delayed liquefaction. Furthermore the polymer modifications showed a wide range of temperature dependent effects, which cannot systematically be linked towards the polymer structure. In another publication the authors also provide data from ramp tests, which provide qualitative data about the development of yield stress and viscosity [239]. The test setup is not very sensitive for yield stress changes, as the utilised stirrer does not generate high torque values at low shear rates but results for viscosity and viscosity changes within time exhibits that depending upon the mortar temperature different rheological models had to be applied. At 20 °C and 30 °C a Bingham approach according to Equation (3.5) can well describe the rheological properties, at 10 °C the mortar showed distinct signs of a Herschel-Bulkley fluid (Equation 3.6) with shear thickening behaviour. The authors mainly attribute effects to the length of the polymers' side chains, which might be the wrong approach, considering the results of Schober and Flatt [66, 67], who show that the flow performance is mainly determined by the adsorbed polymers, while the adsorption depends upon the charge density and the total charge of the backbone. The latter is also confirmed by a study of Plank and Hirsch [87].

Strong effects of the mixture temperature on the rheological properties and their retention are also reported by Svavarsson and Wallevik [240] based on well cement slurries with  $w/c = 0.8$  for slurries without PCE and  $w/c = 0.66$  for slurries with SP at 20, 40, and 60 °C. The two employed cements were produced in Iceland and Norway. The Norwegian cement is classified as G-class well-cement. No further information about the cements is provided. Increasing temperatures came along with higher initial yield stress and more rapid increase with time. The presented effects on the viscosity are not very specific, showing also a trend to higher viscosity with increasing temperature. As it was not the ambition of the authors to observe and discuss temperature effects but rather to compare different mixture composition, no specific conclusions on the effect of temperature and SP were made. However, the authors were the first to formulate that workability is depending on two parameters, which are time and temperature.

This correlation is also emphasised by the research of Petit et al. [241-245] based on rheological analyses of micro mortars with a maximum grain size of 315  $\mu\text{m}$ ,  $w/c = 0.53$  and  $w/c = 0.42$ , and SP based on PNS and PCE. Measurements were conducted using a coaxial cylinder rheometer. The authors observe the change in yield stress over the time for a mixture containing PCE. These curves were then normalised by relating them to the end of the induction period, which was set as unity. The end of the induction period was defined as the moment when the heat flow curve rises after the horizontal curve during the induction period. The authors show that yield stress increases with time in a linear way in case of PNS SP. Initial yield stress and time dependent behaviour are comparable for all temperatures. The authors conclude that temperature basically acts as a catalyst to accelerate or slow down hydration, determining the time depending flow performance. Different observations were made, when PCE was used. Above a specific threshold temperature, yield stresses increases rather linearly with time, while below that temperature, an initial retention or even loss of yield value could be observed until approximately 30% of the induction period had passed (Figure 6.2). Three different mixture compositions containing PCE varying in  $w/cm$  and binder type were observed, showing

individual and widely differing threshold temperatures between 15 and 33 °C. The authors conclude that therefore the threshold temperature, yielding workability retention is thus mixture specific. Influences of mixture temperature occurred significantly more pronounced for PCE than for PNS. It was not further discussed by the authors, which influence predominantly affects the threshold temperature. It is, however, assumable that the major influence is coming from the composition of the binder, as adsorption of SPs is mainly determined by the sulphate ion content and the end of the induction period is strongly influenced by the amount of adsorbed polymers on the surface [85, 165].

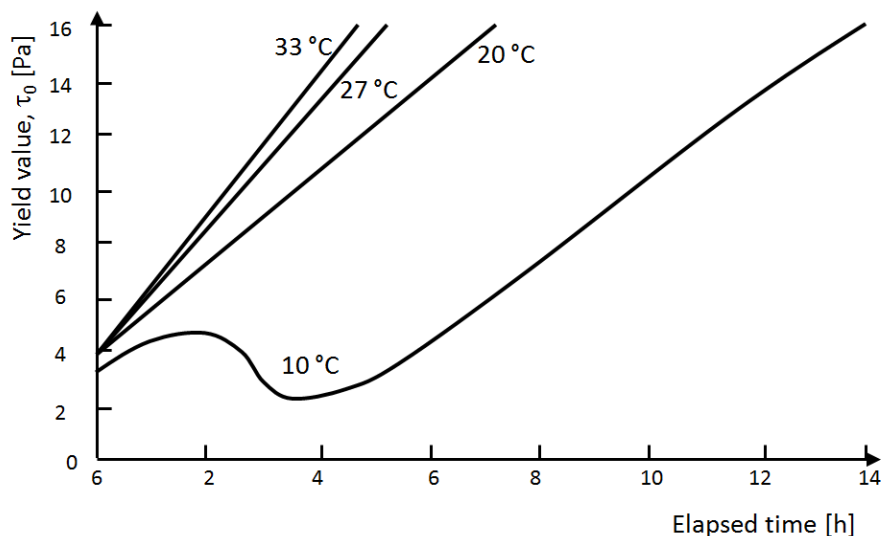


Figure 6.2: Approximation curves for the time dependent development of the yield stress in the presence of PCE at different temperatures qualitatively according to Petit et al. [241].

Based on OPC pastes with  $w/c = 0.33$ , Fernandez-Altale and Casanova [246] observed the influence of SP content, admix time, and temperature on the rheological properties directly after mixing. The study shows that a delayed addition reduces the apparent viscosity at particular shear rate and the shear resistance at a rotational speed of  $1.2 \text{ s}^{-1}$  which the authors defined as yield value. This effect is related to fewer intercalates into early forming mineral layers, which is in line with studies presented by Flatt and Houst [61], and Plank et al. [168]. The difference between early and delayed addition was marked at low PCE additions and diminishing with increasing additions. Furthermore, comparing the shear stresses yielding from an upward and downward shear rate ramp revealed that these effects occur significantly less pronounced for downward ramps. Temperature influences were strong on apparent viscosity in the order that decreasing temperatures coincided with increasing viscosities. No such correlation between temperature and yield stress could be observed. The study only observes a stage directly after mixing. According to Plank et al. [85] PCE can take up to 30 minutes until adsorption equilibrium is reached, the results of this study might be valid only for the presented setup.

Nehdi and Al Martini attempted to develop a prediction model for oscillatory yield stress with mixing time, ambient temperature, and superplasticiser dosage by mass of cement as input parameters [247]. PCE, PMS, and PNS were varied. The  $w/c$  was 0.38. Ordinary Portland cement was used for the experimental part. The empirically developed equations which varied in quality for the different SPs, used As most SPs and particularly PCE cannot be easily classified, it is doubtful that the given equations, which are based on experimental model constants, can be generally valid. Due to the interaction of SPs also with supplementary powders, furthermore the approach to utilise the SP dosage related to the cement content does not allow to use the formula

for general purposes. Nevertheless, within the observed temperature range between 22 and 45 °C and the observed combinations of particular superplasticisers and the particular cement, the predicted results matched the measured values with reasonable accuracy. Individual models had to be chosen, depending on the SP type. In order to obtain temperature parameters for the model, rheological measurements were conducted pointing out that increasing temperatures produce higher yield stresses at particular SP content. The temperature influence was strongest with PMS, followed by PNS and it was lowest for PCE.

The studies by Schmidt et al. [248-250] based on paste and mortar calculated from a SCC mixture composition containing OPC, LSF and FA (the raw materials were equal to those provided for the “Original Mix” in Table 4.7). The mortars with maximum grain size 4 mm had a w/p = 0.35, the pastes only exhibited w/p = 0.28. The w/p ratio of the pastes was reduced in order to achieve stability of the paste, which was prone to segregation due to the lack of sand, which enhanced the stability on the mortar. The influence of temperature and supplementary admixtures to PCE such as a shrinkage reducing agent (SRA) and stabilising agent based on cellulose ether on the flow properties was observed. As the mixture compositions for paste and mortar were based on a stabilising agent type SCC containing STA, the mixtures without STA were not safe from segregation at all temperatures. One of the major outputs of the study is presented in Figure 6.3. Using varied admixture combinations strongly affected the paste. For example STA significantly reduced the Haegermann flow spread diameter  $d_{SF}$ , while supplementary SRA improved the flow properties again. SRA showed positive effects on the flow properties at high temperatures. In contrast, these effects were significantly less prominent in case of mortar tests. With mortar the admixture compounds showed no significant influence at low temperatures, while at 20 °C and at 30 °C each supplementary admixture component contributed to a reduction of the slump flow diameter with higher impact at 30 °C. Comparing the mixes including all admixtures, no marked temperature influence can be observed for the paste, while the diameters at 5 °C are more than 100 mm larger than they are at 30 °C. The authors concluded that although admixtures can strongly affect the flow performance of pastes, this does not inevitably need to have significance for concrete or mortar mixes with large aggregates. The reason for this might be that effects on paste rheology are overcompensated by the rheology of the aggregate granules. It is therefore most important to evaluate observations made on paste level against its relevance for the concrete level.

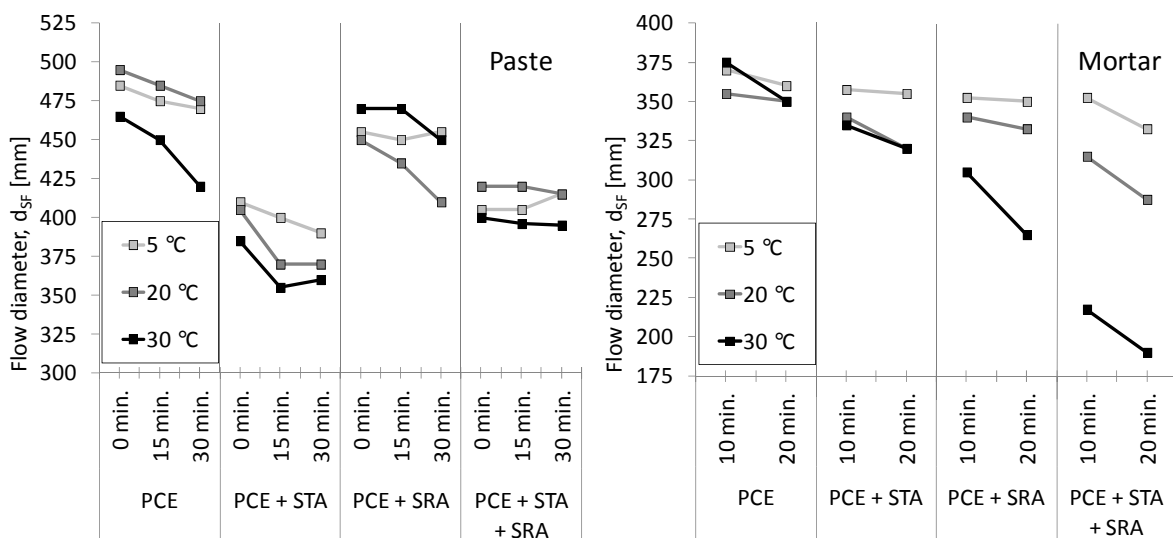


Figure 6.3: Slump flow values  $d_{SF}$  of paste and mortar depending upon time and admixture setup based on the data of Schmidt et al. [250].

### 6.2.3 Research on temperature influences – Experiences in concrete

Höveling and Lohaus present results from J-ring spreading tests of three types of flowable concretes, two of which are SCC with high powder contents and one of which is a flowable concrete with significantly lower powder content. The water to cementitious materials ratios were 0.28, 0.32, and 0.28, respectively [251]. The SCC with the highest powder content incorporating cementitious materials of 600 kg/m<sup>3</sup> showed wide slump flow values (SF) between 750 and 820 mm. At 20 °C the diameter reduced from initially more than 800 mm to approximately 700 mm, and at 30 °C the SCC showed significant loss of performance so that no flowability was provided later than 60 minutes. This correlated with rapidly increasing  $t_{500}$  times (Table 1.2) for the SCC at high temperatures. At 5 °C the initial diameter was significantly lower than at higher temperatures, however, with time the values approximated the values measured at 20 °C. For the SCC with the slightly lower powder content, incorporating cementitious materials of 570 kg/m<sup>2</sup>, no different behaviour could be observed at 20 °C and 30 °C. At both temperatures the initial diameters were approximately 750 mm initially, and they dropped with increasing velocity after 60 minutes to values between approximately 550 and 600 mm. At low temperatures, the initial diameters are only slightly higher than 600 mm but with time, the flowability increases, showing wider diameters than at higher temperatures with time. In general, higher  $t_{500}$  times were measured at 5 °C, which correlates to the paste observation of Fernandez-Altable and Casanova [246].

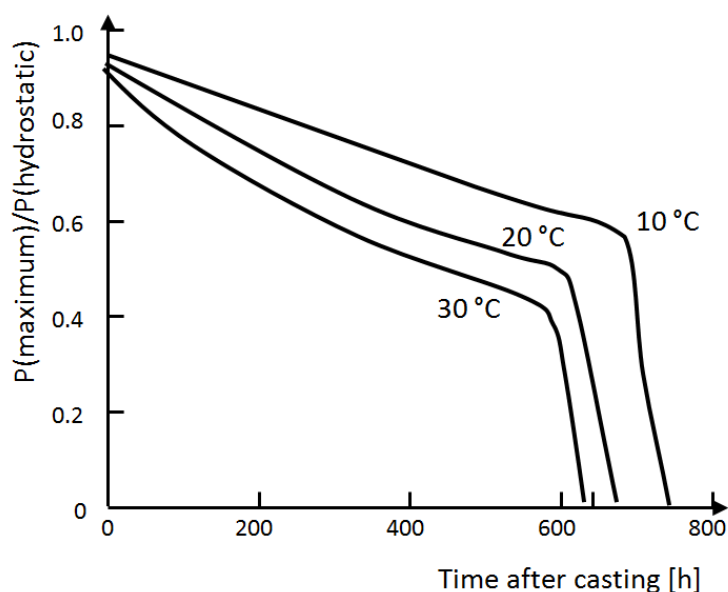


Figure 6.4: Time dependent development of the lateral pressure at varied temperatures qualitatively according to Assaad and Khayat [252].

Assaad and Khayat studied the effect of the casting rate and the concrete temperature on the formwork pressure for SCC [252] with mixes with  $w/c = 0.4$ . The SCCs were observed at 10, 20, and 30 °C, while the PCE content was identical for 10 °C and 20 °C and slightly higher for 30 °C. The mixes also contained STA based on modified cellulose, and an air entraining agent (AEA) at identical amounts for all observed temperatures. The slump flow values after casting were highest at 20 °C with 665 mm but only 10 mm and 20 mm smaller at 10 °C and 30 °C, respectively. As these values are close to each other, no significant temperature effects could be observed. The same is valid for the L-box results according to EN 12350-10 (Table 1.2), which showed comparable passing ability ratios (PL) between 0.81 and 0.85. EN 12350-12 defines PL

as the ratio of height at the end of the flow channel and the height at the beginning of the flow channel, and values above 0.8 are considered as good indicator for good self-compacting ability. A comparative time dependent observation was not presented in the paper. However, the development of the ratio of the maximum lateral pressure to the hydrostatic pressure was presented over the time for the three observed temperatures as shown in Figure 6.4, indicating that increasing temperatures accelerate the decline of the initial formwork pressure, and also lead to earlier moments at which the lateral pressure drops significantly.

Golaszewski and Cygan compared paste and cement generated from two different paste compositions containing LSF at 5 °C, 20 °C and 30 °C [253]. One paste was composted with  $w/p = 0.3$ , the other with 0.4. Regardless of the  $w/p$ , both pastes exhibited the lowest flow spread values at 20 °C. The paste with higher  $w/p$  generated comparable higher spread values, whereas the spread diameter of the paste with lower  $w/p$  at low temperatures was in the same range higher as it was noticed with the other mixture, but at 30 °C the increase was most prominent. In another step, the paste was filled up with aggregates up to 16 mm. The volumetric ratio of paste to aggregate was varied between 1.15 and 1.85 and slump flow values were measured 20 and 60 minutes after water addition. Due to the ratio variation, the powder contents varied between 476 kg/m<sup>3</sup> and 720 kg/m<sup>3</sup>. At all temperatures and for both paste compositions, increasing volumes of aggregates caused wider slump flow diameters. As not all paste to aggregate ratios showed self compacting properties, there is not a single concrete setup, which can be compared for all three observation temperatures. However, at ratios 1.35, 1.40 and 1.45 comparison between 10 °C and 20 °C can be made as well as for 20 °C and 30 °C at ratios of 1.65 and 1.75 in case of the low  $w/c$  mixture (see Figure 6.5). According to this, increasing temperatures reduce the SF and also the time dependent performance loss increases with increasing temperatures.

For the high  $w/p$  SCC, identical mixtures existed at 10 °C and 20 °C for a replacement paste to aggregate paste of 1.35 and for 20 °C and 30 °C at ratios of 1.55 and 1.75. The results are qualitatively the same as they are for the SCC with  $w/p = 0.3$ . The concrete results show identical effects as the paste results at low temperatures. However, at high temperature, the concrete reacted exactly inverted to the pastes. The authors conclude that temperature increase has negative effects on the workability of SCC and that the consideration of paste only might lead to inaccurate conclusions.

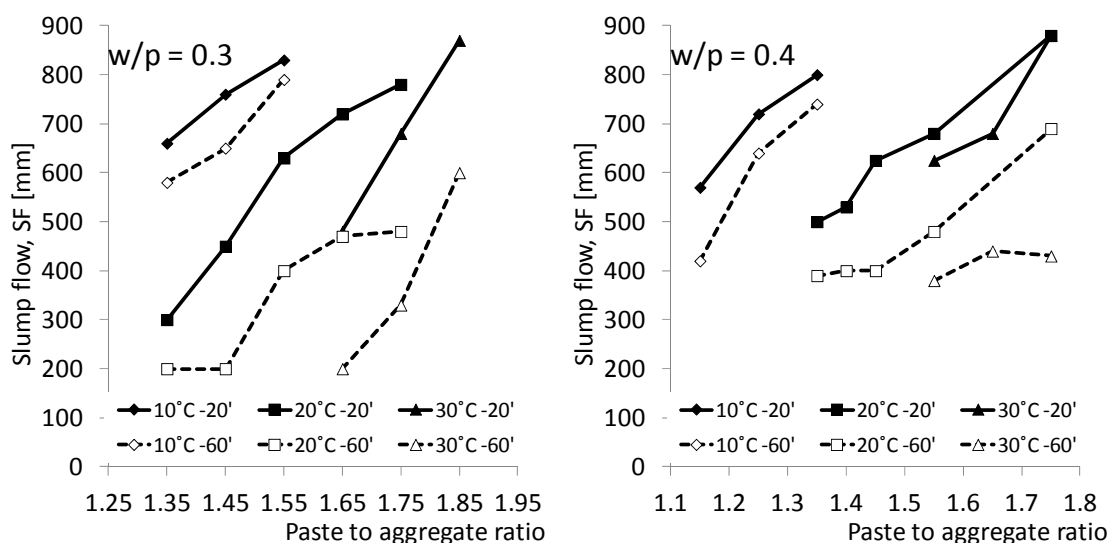


Figure 6.5: Slump flow values of SCCs with  $w/p = 0.3$  and  $w/p = 0.4$  at varied temperature and varied ratios of paste to aggregate based on data provided by Golaszewski and Cygan [253].

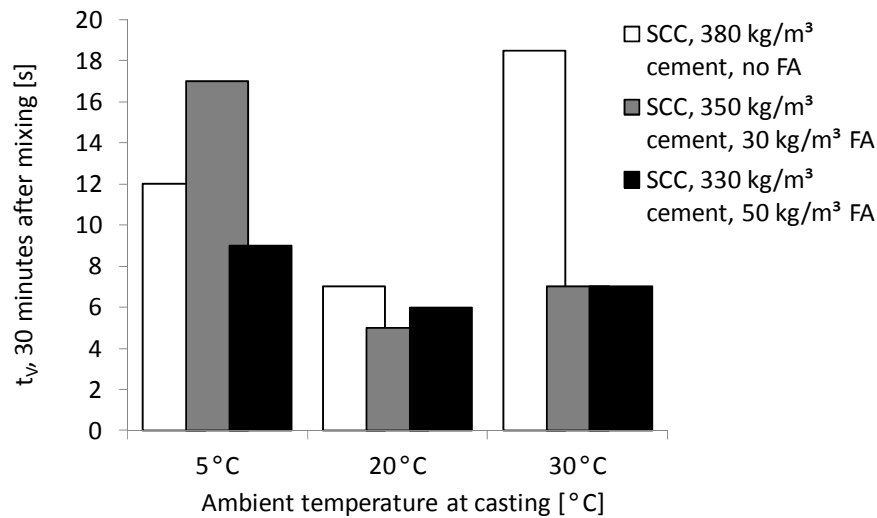


Figure 6.6: V-funnel efflux times after 30 minutes for different SCC mixes containing different FA contents at different temperatures.

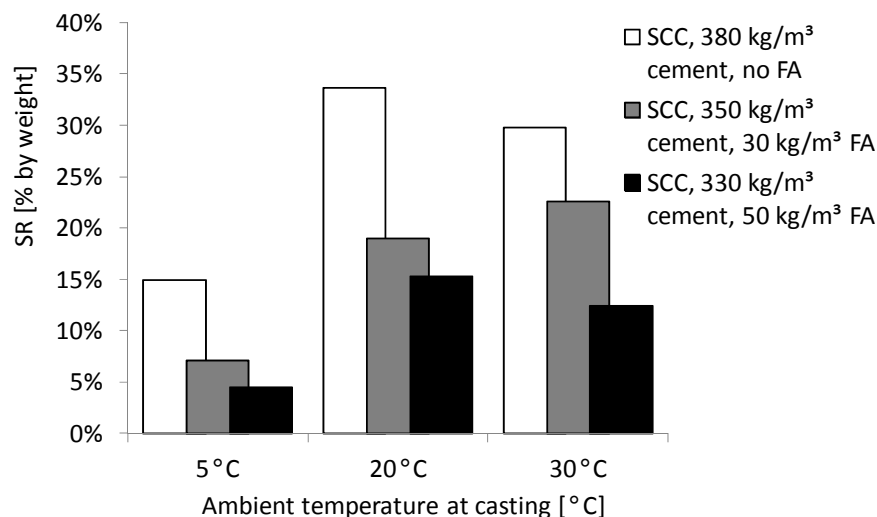


Figure 6.7: Sieve screening test results (test start 5 minutes after mixing) for different SCC mixes containing different FA contents at different temperatures.

Schmidt and Kühne present V-funnel efflux times for three different SCC modifications with  $w/p = 0.35$  containing different FA contents replacing cement. V-funnel efflux times 30 minutes after mixing can vary strongly [250], see Figure 6.6. The lowest efflux times were measured at 20 °C. SCC without FA showed long efflux times at 30 °C due to high viscosity of the concrete. SCC with 30 kg/m<sup>3</sup> cement replaced by FA showed high  $t_v$  times at low temperature, which however was a result of segregated aggregates, blocking the nozzle. In another publication, the authors also presented results of the sieve segregation resistance test (Table 1.2) using the same mixture variations [51]. These are demonstrated in Figure 6.7, showing that in the presented setup, the segregation tendency increases with rising temperature. The results at low temperature are confusing on the first sight, as the high V-funnel time of SCC with 30 kg/m<sup>3</sup> FA in Figure 6.6 was related to the segregation tendency. From observation of this particular mixture, it could be seen, that the segregation tendency caused blocking and thus poor flow properties rapidly

after mixing as seen in Figure 6.8. This figure furthermore shows that for all SCC types at low temperatures, the flow properties are dropping rapidly directly after mixing. For SCC without FA and SCC with 30 kg/m<sup>3</sup> FA the performance as well as the retention are best at 20 °C and deteriorate at 30 °C. For SCC with 50 kg/m<sup>3</sup> FA the initial flow is slightly wider at 30 °C than at 20 °C. However, also a slightly stronger loss of slump can be observed this temperature. As the latter effect is small, it can be concluded that for all SCC mixtures, the best flow properties were measured at 20 °C.

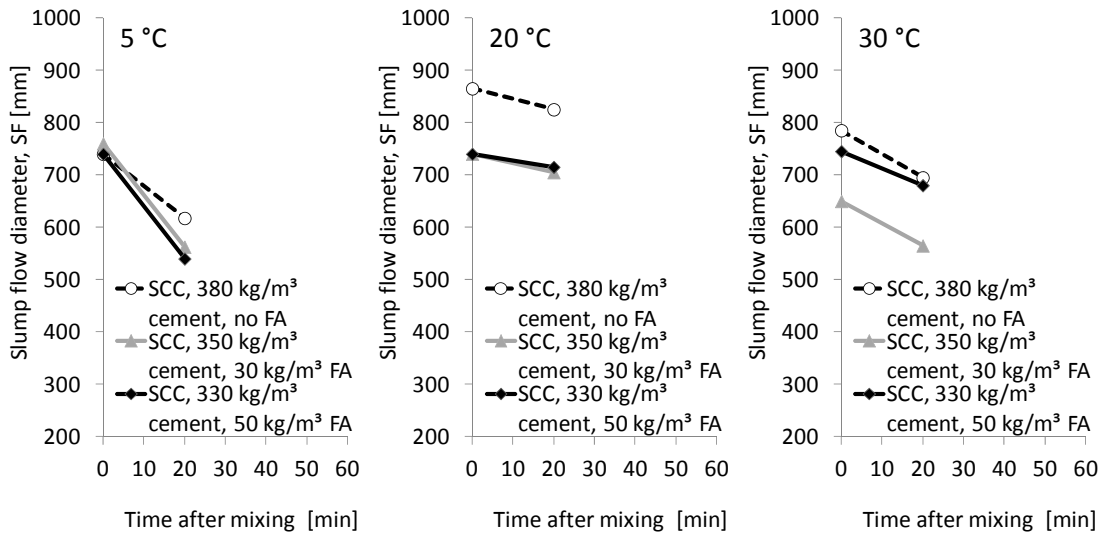


Figure 6.8: Slump flow test results at varied temperature for mixes containing different FA contents.

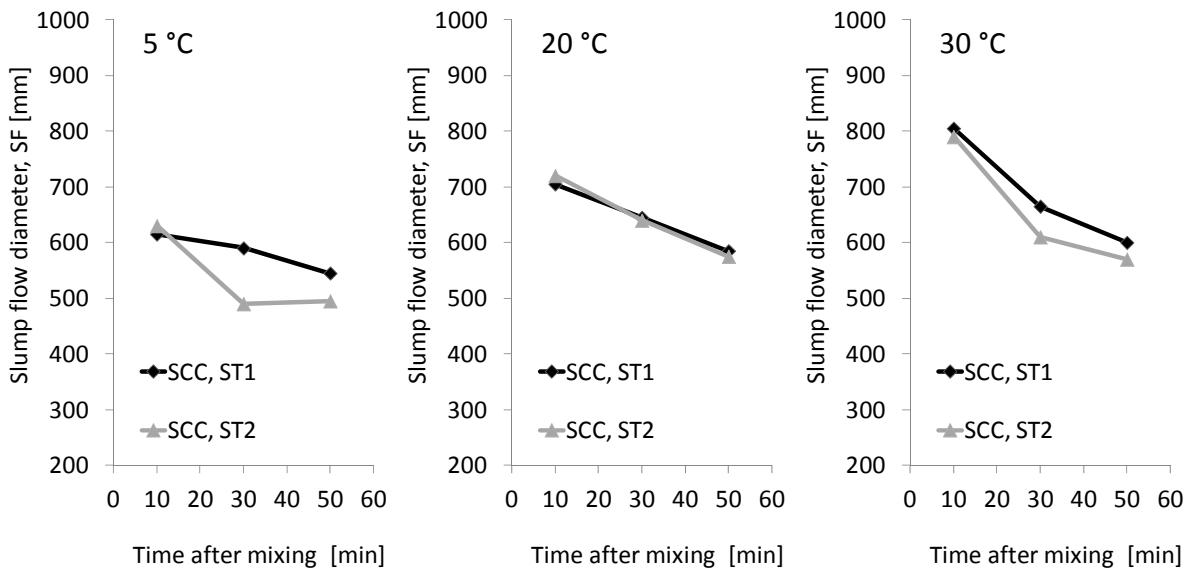


Figure 6.9: Slump flow test results at varied temperature for mixes composed with different STA types and contents.

Results of powder type SCC mixture compositions are presented in another study of the same authors [129], which are shown in Figure 6.9. The presented mixtures exhibit  $w/p = 0.36$  and vary in type and amount of STA. ST1 and ST2 were the same as described in 0. A strong loss of performance initially and with time could be observed at 5 °C. However, at 30 °C both mixtures show significantly wider slump flow diameters than at 20 °C and approximated with time toward similar slump flow values. The increase of the slump flow correlated for the mixture incorporating starch ether STA with an uncritical but noticeable segregation brim during the initial slump flow test, which was not observed in the same manner at 20 °C (Figure 6.10). Measurements were conducted immediately after mixing. At cold temperatures, the authors state that within 15 minutes at cold temperatures a retarded liquefaction took place.

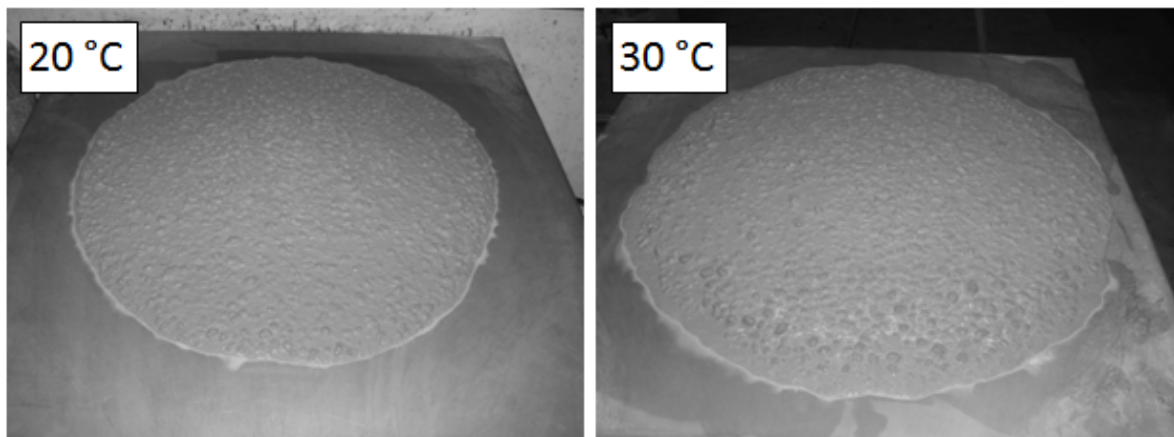


Figure 6.10: Initial slump flow specimens for the SCC with STA1 from Figure 6.9 at 20 °C and 30 °C.

Weisheit et al. investigated the effect of temperature on the rheological properties by observing slump flow values, V-funnel times, and comparing them to results from a rotational concrete rheometer [254]. The rheometer could not generate fundamental units for yield stress and plastic viscosity. The comparison was based on a momentum gradient over the rotational speed for the plastic viscosity and an extrapolation for the determination of torque at rest, which is a qualitative indicator for the yield stress, which is why the authors entitled this value relative yield stress. The SCC contained only cement as powder component and the  $w/c$  was 0.45. The cement used for the investigations was a blast furnace cement (CEM III). Results from slump flow are given in Figure 6.11, showing that increasing temperatures caused wider slump flow diameters and reduced the yield stress. Comparing V-funnel times to the qualitative results for the viscosity indicated that viscosities were lowest at 20 °C. It has to be stated that the used test equipment for the rheological properties is not very precise for comparative viscosity measurements. In a second step the authors adjusted identical slump flow at all temperatures by adding or reducing PCE, finding that highest contents of PCE were required at cold temperatures and lowest at high temperatures. With these mixtures adjusted to particular performance at all temperatures, rheological tests were repeated, showing a significant gain in flow properties within the first 30 minutes at cold temperature and a marked loss at high temperatures (Figure 6.12).

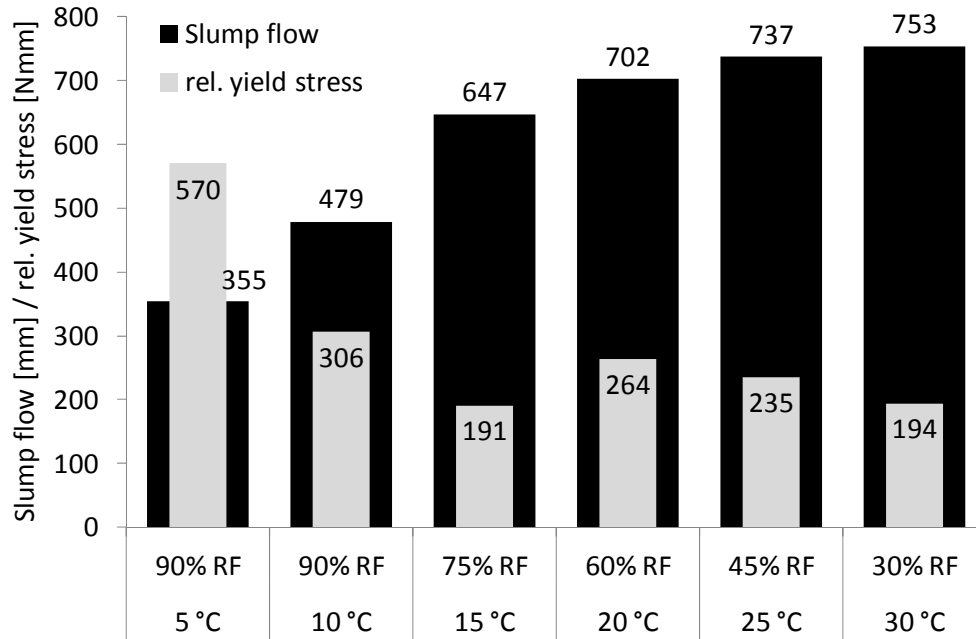


Figure 6.11: Slump flow at different climatic conditions vs. respective yield stress measurements according to Weisheit et al. [254].

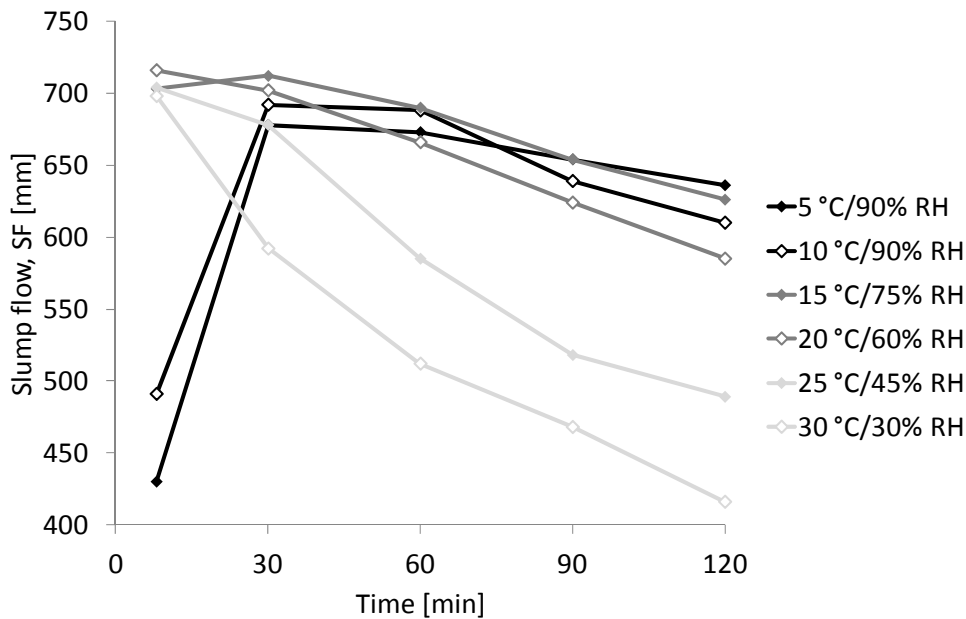


Figure 6.12: Slump flow loss at different climatic conditions after Weisheit et al. [254].

Al Martini and Nehdi present comparative results of the influence of temperatures between 22 °C and 45 °C on the rheological properties of OPC paste and concrete both with  $w/p = 0.38$  [255]. Measurements were made at 20, 50, 80, and 110 minutes after water addition, during which the paste and cement was continuously mixed. The PCE saturation dosage, at which further addition of PCE does not further reduce the yield stress, was more or less identical for cement paste at all temperatures. Below this dosage, the yield stress increased quickly with time, which occurred more pronounced at 35 °C and 45 °C than at 22 °C. For concrete, the saturation

dosage increased with increasing temperature. The authors conclude that PCE should be added at the saturation dosage at high temperatures, in order to make sure that time and accelerated hydration do not negatively affect the rheological properties.

Ghafoori and Diawara observed the influence of temperature on the performance of the same SCC mixture composition modified by three different PCE and STA contents [256]. The slump flow value at 21 °C was defined as reference value and the deviations at other temperatures were defined as slump flow loss or gain. The observed ambient temperatures varied between -0.5 °C and 43 °C. Only the powders and aggregates were tempered prior to testing, while the water temperature was approximately 20 °C at all times, the final mixture temperatures particularly at low temperatures deviated strongly from the ambient temperatures after mixing. Hence, concrete temperatures between approximately 8 °C and 42 °C were created for the slump flow tests. Measurements took place immediately after a mixing sequence of 14 minutes. Figure 6.13 shows the results, which exhibit a level performance of the observed mixtures for ambient temperatures between -0.5 °C and 20 °C. Above this temperature, SF reduces with increasing temperature, whereupon this trend accelerates with rising temperature. Supported by results measured with UV/VIS spectroscopy, the authors conclude that the temperature behaviour was determined by the adsorption per specific surface area of the paste and further by the aggregates' moisture contents, which are influenced by the storage at varied temperature and relative humidity in advance. Partial evaporation of the mixing water at elevated temperatures also contributed to the slump flow loss at higher temperatures. Based on these observations, the authors develop a flow chart explaining temperature effects, which is largely similar to the interpretation of Yamada et al. [18] (see Subsection 6.2.2), showing qualitatively that the adsorption per specific surface determines the flow properties at varying temperature. The model is further amended by influences of the water content and the respective contribution of the aggregates and is used to predict the additional SP amounts in order to achieve the same slump flow levels as the control mixtures at those temperatures, which were higher than the control temperature. This very comprehensive study, however, does not consider time effects but only shows a particular spot in time, which might not be relevant for real applications, as the fresh properties might change rapidly within the first minutes after mixing.

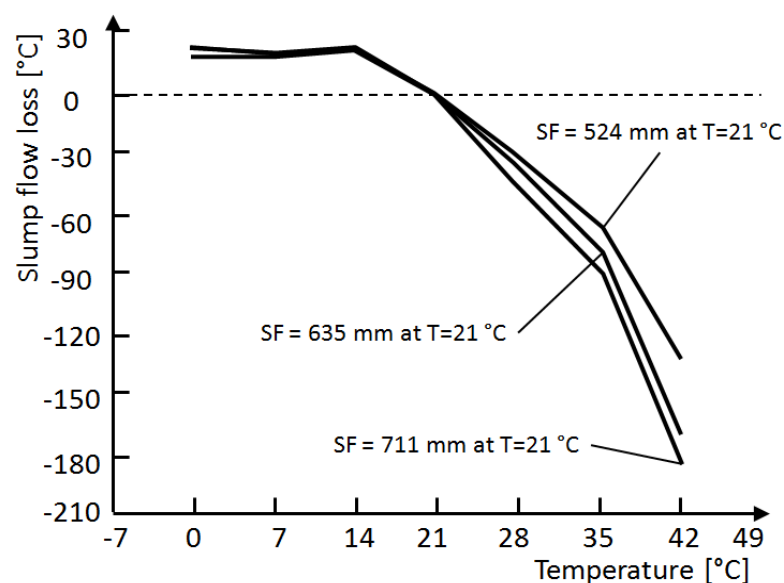


Figure 6.13: Slump flow losses and increases depending on temperature for SCC mixtures with three different SF adjustments at 21 °C after to Ghafoori and Diawara [256].

### 6.2.4 Discussion of research experiences

From the presented research on self-compacting paste, mortar, and concrete a major conclusion that can be drawn is that the observation of the flow properties at a single moment in time is not sufficient to describe the temperature dependent effects. This is also emphasized by Göller et al. [86], who confirm that the retention ratio is the main parameter, which is affected by superplasticiser type, w/c, and ambient temperature. The initial flow might differ strongly from the time dependent performance. So, all authors agree about the temperature effects on the adsorption of SPs on particles. This is influenced by the initial and the time dependent specific surface of the paste, which differs depending upon the particular mixture temperature from slow increase at low temperatures toward quick increase at high temperatures.

However, neither the specific surface of the paste or its growth, nor the adsorption of SP is fully capable to explain the behaviour of SPs. As all types of SP do not completely adsorb on cement particles to become effective, either sterically or electrostatically. Several authors report about intercalation of SPs into lamellar aluminous hydration phases (mainly AFm) yielding so called organo-mineral phases (OMP) [61, 168, 193]). The intercalated PCE can no longer contribute to flowability. The risk of intercalations can be significantly reduced by delayed addition of SPs. As PCE can either adsorb or intercalate reduced measured SP amounts in the solution do not automatically contribute to dispersion of a cementitious system. In order to cope with this conflict, Flatt and Houst [61] suggest to use the term consumption rather than adsorption (see Subsection 3.3.6). This consumption of SP is not automatically linked to improved flowability, as the dispersion is only provided by those polymers being adsorbed at the outer particle areas. A qualitative differentiation between adsorbed and consumed polymers is difficult and repeatable conditions unlikely to be implemented, as intercalation depends upon many factors, such as the point of addition, the sulphate content and its solubility as well as the type of polymer itself. Early addition and low sulphate contents cause higher amounts of intercalates as besides AFt also AFm is formed, which fosters intercalations [61]. The polymer structure determines the layer thickness to certain degree, whereas intercalations are more likely with decreasing side chain length [193] and unlikely when the side chain length exceeds a threshold value [168].

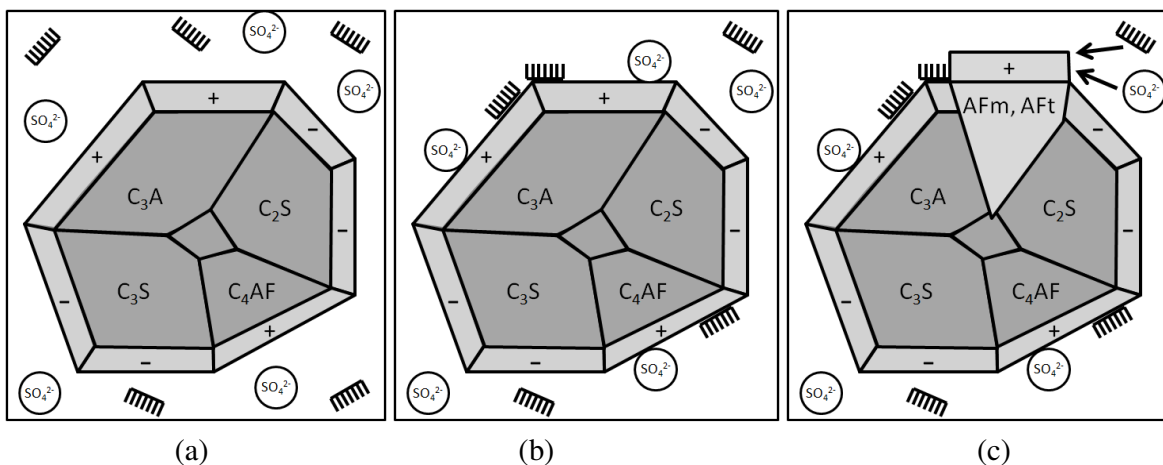


Figure 6.14: Competitive adsorption of PCE and sulphate ions on hydrated cement over the course of time: a) upon contact with water, b) after initial adsorption, c) after formation of ettringite.

As presented by Plank and Hirsch [87], after initial adsorption on  $C_3A$  and  $C_4AF$ , PCE molecules mainly adsorb on surfaces of AFm and AFt, as they provide a positively charged zeta potential ( $\zeta$ ), AFt providing the highest  $\zeta$ . The interactions are illustrated in Figure 6.14. Upon contact of water (a) ions will be adsorbed on the surfaces, yielding different  $\zeta$  around the shear planes of different clinker phases, depending on which sulphate ions and PCE will be attracted or repelled (b). By reaction of water, sulphate, and calcium aluminate, ettringite is formed, which can attract further PCE due to its high positive  $\zeta$ . The adsorption on C-S-H, which can also take place upon high  $Ca^{2+}$  ion concentrations in the solution is negligible, as the amount of adsorbable polymers compared to the high specific surface area of C-S-H is small (approx.  $0.2 \text{ mg/m}^2$  according to Plank and Hirsch [87]). Hence, a high surface area by itself does not automatically promote the adsorption of PCE. However, it is evident that surface growth is to a large part caused by the ongoing hydration of ettringite or its re-crystallisation with time during the so called induction period, at which C-S-H hydration is reduced to a rate close to zero. It is now depending upon the amount of PCE in the system whether AFm and AFt growth contributes to or adversely affects the flowability. At high concentrations of PCE, it is likely that hydration causes stiffening when insufficient PCE is available. This is due to morphological changes of the particle surfaces and hydrates filling up the gaps between particles upon hydration in the solution, which according to Winnefeld et al. is fostered by PCE addition [257]. At excess PCE dosage, time delayed adsorption of PCE causes improved flowability. These effects as already addressed to in Subsection 1.6.2 explain different observations that can be made regarding the temperature dependent behaviour of SCC.

As neither the adsorbed part of the consumed PCE can be precisely determined nor can the influence of the surface growth on the rheological properties be easily predicted, the adsorption of PCE per surface area cannot precisely predict the influence of the temperature on the flow properties of SCC. However, qualitatively the results should correlate well with real observations. Intercalations can be assumed not to play a major role for temperature related influences. They occur less prominently with PCE than with other SPs due to lower charge densities and longer graft chains, and if specific performance properties are adjusted, their negative effect can be ignored as long as the mixing regime remains identical. Finding a general rule for how temperature affects intercalations, is difficult to discuss, as this might be much more dependent on the individual cement chemistry, particularly the  $C_3A$  content and surface, and the set retarder's solubility. Increasing temperatures might either foster growth of ettringite due to quicker precipitation of sulphate ions, which would yield a lower amount of intercalates or it could foster the hydration of monosulphate, thus creating more intercalates, as the reactivity of the aluminates is improved. Also the surface growth definitively affects the workability. It is likely that the C-S-H hydration generally affects the workability negatively. Also ettringite and monosulphate show negative effects on the flowability, depending upon the amount of PCE they only undergo a certain early period at which they can show indefinite behaviour.

Due to the specific role of the ettringite growth, it is thus problematic to observe only a single step in time to evaluate temperature effects, as done by several authors. As seen e.g. in Figures 6.2, 6.9 and 6.12, the flow performance changes significantly with time. A single moment in time can thus only be an arbitrary choice, which is not sufficient to explain phenomena. This is particularly a problem when rheological properties are investigated immediately after mixing. The flow properties directly after mixing can be strongly affected by thixotropy and time shifted influences of the steady high shear force in the mixer, which affects the formation of AFm, AFt and secondary gypsum. As seen e.g. in Figure 6.8, at cold temperatures, the initial performance of the observed SCCs immediately after mixing was good. However, already after a couple of minutes, the flow properties reduced critically. Furthermore effects of mixing time can be assumed to play a significantly higher role for the measurements

immediately after mixing. As seen in Figure 6.15, during the first 20 minutes, the influence of the mixer type plays an important role for the performance of SCC. From these results, SCC with high powder content seems to be more flowable after mixing at high intensity shearing in an intensive mixer (Eirich R09, 150 l mixing capacity) compared to a pan mixer (Teka, 250 l filling capacity). Considering later times, the performance is similar for both mixer types.

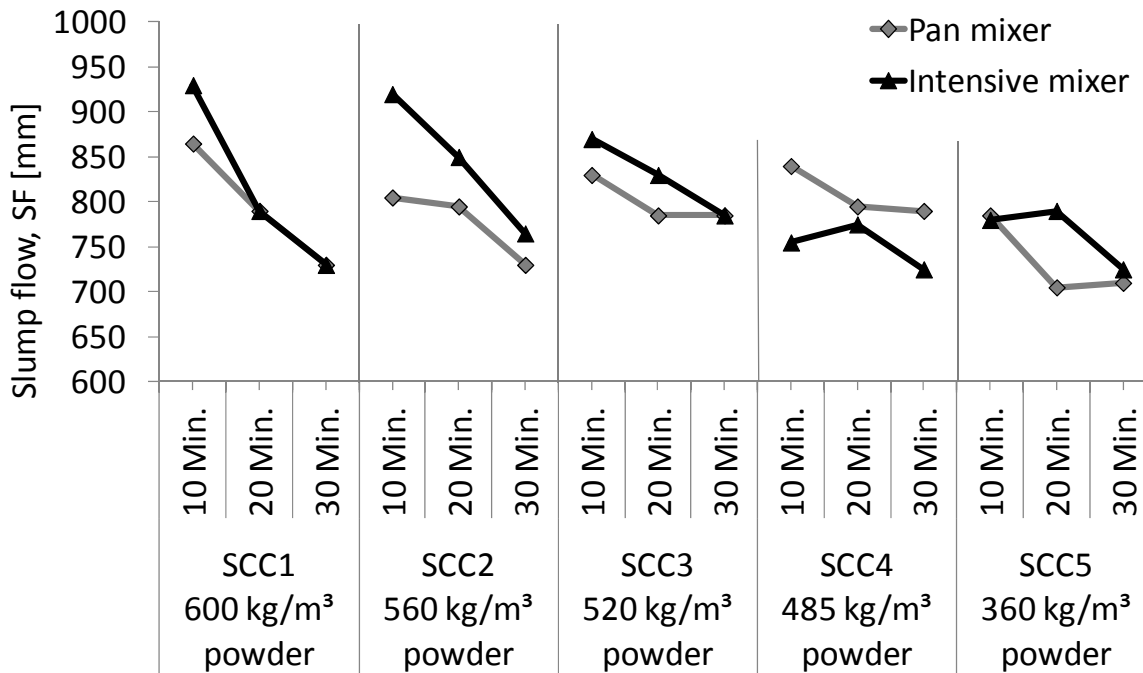


Figure 6.15: Slump flow performance of different mixture compositions over a period of 30 minutes depending on the mixer type.

Hence, a comprehensive observation of temperature effects can only be conducted when time aspects are considered adequately. The latter are diffused by the hydration of mainly ettringite and, with minor importance, monosulphate. Considering the important role of AFm and AFt, most researchers neglected that PCE superplasticisers are significantly more versatile in their configurable appearance than elder generations of SP. Backbone and graft chemistry, and length can be modified largely independent from each other. A good overview about different solution structures of PCE molecules is given by Plank et. al. [85]. Only Brameshuber and Uebachs give attention to the influence of the molecular structure [72], however, the observations do not lead to a simple regularity. The authors can only conclude that the graft chain length might have a certain, not tangible influence on the temperature dependent behaviour of SCC. It is assumable that the authors did not have information about the charge density of the backbone of the investigated polymers, which would probably supplement the research results and yield new findings.

From an engineering point of view, Schober and Flatt published an important study on the influence of the architecture of PCE on the rheological properties of SCC with validity for paste and concrete [66, 67]. This study was emphasized by a case study published by Schober and Mäder [258]. The first result of practical importance is that there is a linear correlation between slump flow diameter and amount of adsorbed polymers (Figure 3.22). The second important result is that upon adsorption, the flow performance is not significantly influenced by the

molecular structure. The adsorption is mainly determined by the anionic charge of the backbone, which means a longer backbone or a higher anionic charge density increase the adsorption of polymers.

Also the time dependent adsorption of PCE is depending on the charge density. As presented by Yamada and Hanehara [165] and by Plank et al. [85], SPs adsorb in competition with sulphate ions. Although the adsorption of PCE is partly determined by entropic effects [166, 171] (see equation 3.9), the adsorption is to a large part driven by electrostatic attraction between the backbone and the opposite charge of the adsorption site. High charge densities of the backbone favour the adsorption of PCE, while PCE with low charge density of the backbone might be pushed back by sulphate ions to remain firstly ineffectively in the solution. These polymers, however, adsorb with time upon hydration of ettringite.

The influence of the delayed adsorption of PCE is illustrated in Figure 6.16. The influence of the charge density is shown considering the aforementioned mechanisms. High charge density causes early and favoured adsorption of PCE with quick consumption by ongoing hydration, low charge density causes delayed adsorption but retarded consumption. As the temperature accelerates or slows down the hydration and thus the occurrence of new adsorption sites, it is becoming evident that the charge density of the polymer can be identified as the driving influencing factor for the performance of SCC at varying temperature. The temperature influence in the Gibbs-Helmholtz Equation (3.9) supplementary gives rise to the importance of the charge density. Increasing temperatures cause a more negative term of the Gibbs energy, which favours spontaneous adsorption of PCE. According to the observation of Plank and Sachsenhauser with lower charge density of the PCE the entropic part of the equation increases and with higher charge the enthalpic part increases [171]. Following this observation, increasing temperatures should particularly increase the adsorption of low charge density PCEs.

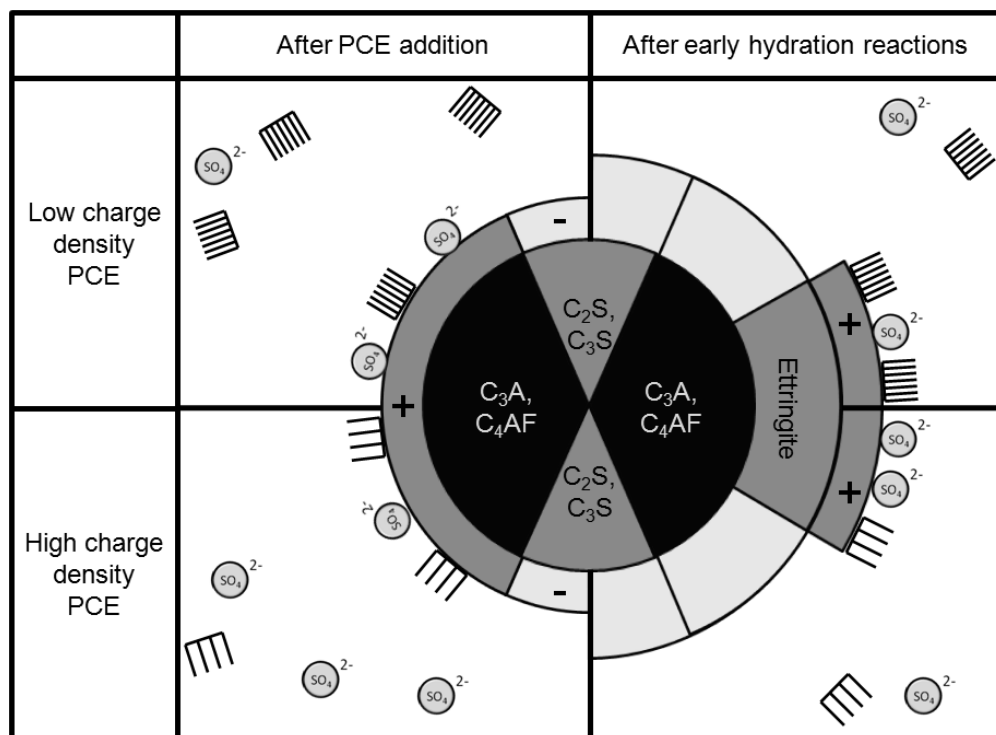


Figure 6.16: Influence of the charge density on the adsorption tendency and the competition with sulphates over the course of time.

Another major aspect determining the flow properties is the mixture composition of the SCC. In general an SCC with high powder content and lower w/p has a low yield stress and a high plastic viscosity, while viscosity modifying agent type SCC typically has a higher yield stress but lower plastic viscosity. Powder-rich SCC and powder-poor SCC differ significantly in how strongly PCE affects rheology. The flow properties of powder type SCC are resulting from an optimised particle packing, while the water has mainly a lubricating role. For this type of concrete, the effectiveness of a dispersing agent is of highest importance. In viscosity agent type SCCs, particles are typically less densely packed. The higher viscous fluid phase contributes much more to the flow properties. As the contribution of PCE to rheological properties might vary depending upon the mixture composition type, it is likely that the before mentioned influence of the PCE charge density also varies depending on the mixture composition type. This would also explain controversial observations that were made in concrete tests [51, 250, 251, 253, 254].

Schmidt and Kühne [129] and Weisheit et al. [254] report about poor flow performance at low temperature and wider flow values with increasing temperature, while Golaszewski and Cygan [253] report about contrary behaviour. Similar behaviour is also reported by Ghafoori and Diawara [256]. However, as the tests took place immediately after mixing, these might be of limited significance. Taking a closer look at the mixtures employed by Golaszewski and Cygan, although changing depending upon the paste to aggregate ratio, all mixtures that can be compared to an identical mixture at different temperatures contain powder contents higher than 535 kg/m<sup>3</sup>, most of which contain powder contents between 600 and 700 kg/m<sup>3</sup>. The mixture compositions from Schmidt and Kühne and Weisheit et al. contain powder contents between 420 kg/m<sup>3</sup> and 480 kg/m<sup>3</sup>. The first results can thus be attributed to SCCs, which represent concrete rich of powder, while the latter rather represent viscosity modifying agent types with lower powder contents. The results give a hint that in considering temperature dependent effects on SCC, the mixture composition type can have a decisive role the way PCE affects the rheology. The results of Lohaus and Höveling [251] supports this hypothesis. Both investigated mixtures with high and medium powder contents exhibited smaller flow diameters at cold temperatures. However, in case of high powder content, the difference to 20 °C was small, while with low powder content it was pronounced. Another aspect, which also contributes to the idea to closer observe mixture composition influences, is the fact that SCCs with high powder contents typically contains high amounts of fillers that contribute to accelerated hydration by acting as hydration seeds. At last, it has to be considered, that depending on the  $\zeta$  that builds up in the individual pore solution, PCE does not only adsorb on cement, but also on fillers [151]. It is hence likely that strong differences between powder type SCC and viscosity modifying agent type SCC should be observed at varying temperature, at least in case the filler contributes to dispersion by attracting superplasticisers.

The influence of the charge density was not yet subject to intensive research in general and no publication is known to the author that distinguishes between different charge densities in the context with temperature dependent workability. The experimental research in this chapter shall illuminate effects resulting from differently modified PCEs, paying special attention to the mixture composition type.

## **6.3 Experimental programme**

### **6.3.1 Matter of investigations**

As seen, two major influences on the temperature related early performance of SCC are the charge density of the PCE polymer and the mixture composition. In order to gain new information on how these affect the rheology, different mixture compositions were analysed with a concrete rheometer over a period of 90 minutes. Each mixture composition was furthermore investigated with the stabilising agents (STA) ST1 and ST2 (Subsection 4.1.5) and the three PCE variations LC, MC, and HC (Subsection 4.1.4).

### **6.3.2 Investigated concrete mixtures**

The studied mixtures were identical to the mixture compositions and admixture adjustments provided in Subsection 4.2.2. The concrete mixture compositions can be found in Table 4.9, the admixture setups are listed in Table 4.10. All tests were conducted with raw materials from identical charges as described in Subsection 4.5.3. Since a time of about 15 months passed between the adjustment of the mixtures and the rheological tests, the fresh concrete performance of the rheological investigations varied from the adjustment tests. All concretes tested during the experiments showed higher yield stresses than the concretes from the adjustment tests (Subsection 4.2.1). The reasons for the different behaviour are manifold and an explanation for it can only be speculative, e.g. it is imaginable that changes in the cement production caused a variation in the solubility of the set retarder, which causes modified adsorption behaviour of the PCE. Also other process modifications are possible, e.g. it is known that grinding aids have a strong influence on the performance of PCE [61, 68, 259, 260]. Furthermore, Yamada recently published studies on the effect of the milling temperature on the specific surface areas, which in turn affects the PCE adsorption behaviour [68]. It is also conceivable that the periods over which the cements were stored during the adjustment tests and the rheometric tests at varied temperature differed significantly.

It is, however, finally not of importance which of the constituents' properties caused the performance difference, since it can be assumed that the SPs' properties can be considered as stable, since all employed modifications were freshly purchased prior to these tests. If any of the above mentioned matters changed the adsorption behaviour of PCE significantly, this change applied for every mixture, since the mixture compositions were neither varied in the contents nor in the relative ratios of each component.

### **6.3.3 Test specifications**

The rheometric investigations were conducted in a large climate chamber at 5, 20 and 30 °C and a constant relative humidity (RH) of 50% for all temperatures. The mixer as well as the rheometric equipment was placed in the chamber and all tests were conducted directly in the chamber at the particular climate conditions.

In advance, it was ensured that the raw materials including water were adjusted to the particular test climate. 30 l of concrete was mixed for the tests in a pan mixer. Since in these investigations no individual adjustment of the admixtures was conducted, the mixing procedure as shown in Table 4.8 was simplified according to Table 6.1. The stirrer speed was adjusted to 70 rounds per minute. Rheometric investigations were investigations 0, 30, 60, and 90 minutes after the mixing with the CONTEC Rheometer-4SCC (see Subsection 4.3.7). Prior to testing the rheological properties at 30 minutes, the concrete was fed back to the mixer and stirred intensively. By this, the transportation to the job-site in a truck mixer should be simulated. For later testing times, the concrete was only gently stirred in the rheometer with a brick trowel in

order to avoid effects of possibly separated aggregates. The mixing was conducted according to the mixing regime shown in Table 6.1.

Furthermore, concrete cubes (15x15x15 cm<sup>3</sup> according to EN 12390-1:2001) were cast directly after the measurement that took place after 30 minutes. The cubes were covered with foil and remained in the climatic chamber until the end of the fresh concrete test. After testing, they were stored in the concrete laboratory at approx. 20 °C until de-moulding after 24 h. After de-moulding they were stored under water at 20 °C according to EN 12390-2:2001 until testing.

It has to be noted that due to mixing, the fresh concrete temperatures were not identical to the adjusted ambient temperatures, and the temperatures were changing over the course of time. The fresh concrete temperatures were not measured regularly but randomly for at least four different mixture modifications per temperature at 0, 30, and 90 minutes after mixing. The average values and standard deviations for each time and temperature are presented in Table 6.2.

The Table 6.2 shows that the ambient temperature does not completely correspond to the fresh concrete temperature and that time dependent adjustment takes place. At all observed ambient conditions, the temperature directly after mixing is higher than the ambient temperature directly after mixing. The temperature increase can be linked to the mixing energy and the high shear forces introduced through mixing. A significant temperature reduction can be observed during the first 30 minutes, while in the further course the temperature drop is only slight. After 30 minutes, the concrete temperature at 5 °C is approximately 4 °C higher than the environmental temperature of 5 °C, at 20 °C approximately 2.5 °C and at 30 °C it is identical. For the interpretation of the results, it can be stated that each ambient temperature yields a characteristic concrete temperature, which does not significantly change after 30 minutes and which clearly distinguishes from the concrete temperatures observed in differing climatic conditions. Hence in all figures the ambient temperature is used to distinguish temperature effects.

Table 6.1: Mixing regime throughout the conducted tests.

Step	Duration [s]	Action
1	60	Dry mixing of all powder components
2	60	Addition of 2/3 of total water
3	30	Wet mixing + addition of STA
4	60	Addition of remaining water mixed with PCE
5	30	Scraping walls of mixing pan
6	120	Mixing
7	120	Resting phase
8	120	Mixing

Table 6.2: Average concrete temperatures at different times compared to the ambient temperatures.

Ambient temperature	Directly after mixing		30 minutes after mixing		90 minutes after mixing	
	Mean value	Standard deviation	Mean value	Standard deviation	Mean value	Standard deviation
5 °C	10.2 °C	0.67	9.3 °C	0.36	8.3 °C	0.22
20 °C	23.9 °C	0.26	22.4 °C	0.16	22.1 °C	0.27
30 °C	32.8 °C	0.26	30.0 °C	0.29	29.2 °C	0.35

### 6.3.4 Rheometric measurements and interpretation

A modification of the standard setup of the Rheometer-4SCC (Subsection 4.3.7) was chosen that has proven to function properly with SCC. The standard test setup consists of seven steps, while the modified programme consists of nine steps, five seconds each. As a result, the total measurement duration was 50 seconds, including five seconds pre-shearing at the maximum velocity of 0.45 rounds per second. The full rheological testing procedure for each measurement is given in Table 6.3. The first step includes 5 seconds of pre-shearing of the SCC before the actual measurement starts in order to avoid effects of the starting torque to assure measuring at steady state. An example of the setup and the output data (POW-LC-ST1 at 20 °C after 90 minutes) is presented in Figure 6.17. In order to avoid unreasonably high deviations due to the change of the rotational speed, only the last 4 seconds of each step were used for the further interpretation based on the assumption that the concrete behaves like a Bingham fluid. The transformation of the data into a flow curve and the formula for the correlation line and the respective correlation coefficient are also presented in Figure 6.17. As discussed in detail in Subsection 4.3.7 the correlation curve and the correlation coefficient were developed based on all valid measuring data. This operation differs from the standard interpretation tool provided by the producer, which uses the median of each rotational speed step only. Hence, the correlation coefficient here is significantly lower than with the standard programme. From practical experience, both methods do not distinguish in a prominent way. However, due to the higher sensitiveness of the calculation with all values it was expected to have an indicator in case certain setups might show behaviour other than Bingham behaviour.

Table 6.3: Rheological test regime for the rheometric temperature investigations.

Step	1	2	3	4	5	6	7	8	9
Rot. speed [1/s]	0.45	0.40	0.35	0.30	0.25	0.20	0.15	0.10	0.05
Duration [s]	10	5	5	5	5	5	5	5	5

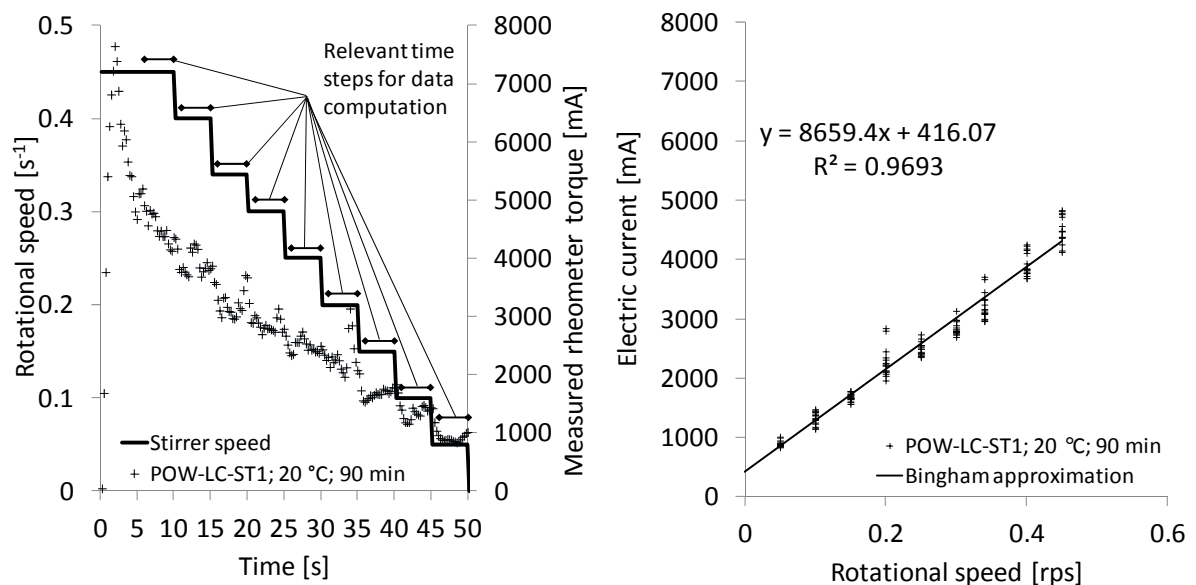


Figure 6.17: Rheometric setup, output data and Bingham approximation exemplary for the SCC POW-LC-ST1 at 20 °C after 90 minutes.

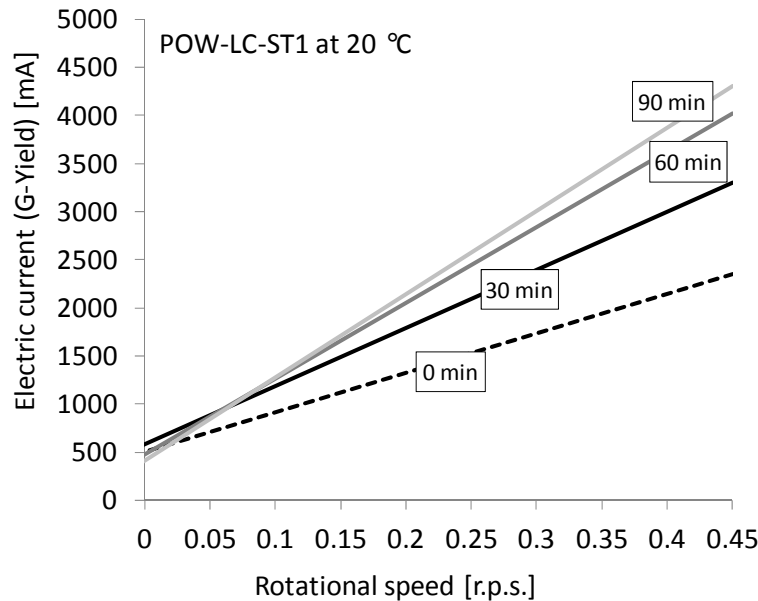


Figure 6.18: Influence of time on the flow curves of POW-LC-ST1 at 20 °C.

The intersection with the ordinate and the slope of the line were calculated and defined as G-yield value and H-viscosity, respectively. These values were determined for each mixture composition, each admixture setup, each temperature and each time step. A sample for POW-LC-ST1 at 20 °C is given in Figure 6.18. It can be observed that the G-yield remains constant over the whole observation period. The viscosity increases with reducing rate over the time.

## 6.4 Results and discussion

### 6.4.1 Rheometric results compared to slump flow and V-funnel results

The observations in this study focus on changes with admixture variation and time. It is therefore of less relevance to derive absolute rheological values from the measurements, since the changes can be displayed dimensionless or with arbitrary values. Subsection 4.3.7 gives information how a transformation into physical properties in fundamental units can be conducted. This transformation, however, is failure prone, particularly with increasing stiffness of the mixes, since the flow test based calculation methods for yield stress loose validity if the consistencies are too stiff. Since observations were made over a long period of time significant stiffening of the consistencies could be expected. Therefore the interpretation based on the electric current of the Rheometer was chosen. The information contents using fundamental units or arbitrary units are identical: the steeper the slope of the flow curve, the higher the viscosity; the higher the intersection point with the ordinate, the higher the yield stresses.

However, in order to provide supplementary information, a COM mixture and a POW mixture were measured in a separate investigation with the Rheometer-4SCC and in parallel slump flow and V-funnel tests were conducted.

The comparison is presented in Figure 6.19 for the slump flow SF and in Figure 6.20 for the V-funnel times  $t_v$ . Apart from the initial values directly after mixing, a good coherence between slump flow and G-yield can be observed for both COM and POW mixture. In general, it can be observed that the yield stresses of the COM mixture is higher, which is also represented by the smaller slump flow diameters (SF). The coherence between V-funnel times ( $t_v$ ) and H-viscosity

is better than for the slump flow comparison. In general, the viscosity of the COM mixture increases more rapidly with time than the viscosity of the POW mixture.

If the values for COM and POW are combined, as presented in Figure 6.21, the relation between SF and G-yield (left) as well as  $t_v$  and H-viscosity (right) become evident. A general linear trend can be identified. However, the large scatter emphasises the assumption that the transformation into fundamental units might be failure prone and that the qualitative comparison based on the electric current is sounder. This however also suggests comparing mixtures only of which the basic characteristics are identical (COM with COM, and POW with POW), and that values among the two mixture types (COM and POW) can only be compared relatively.

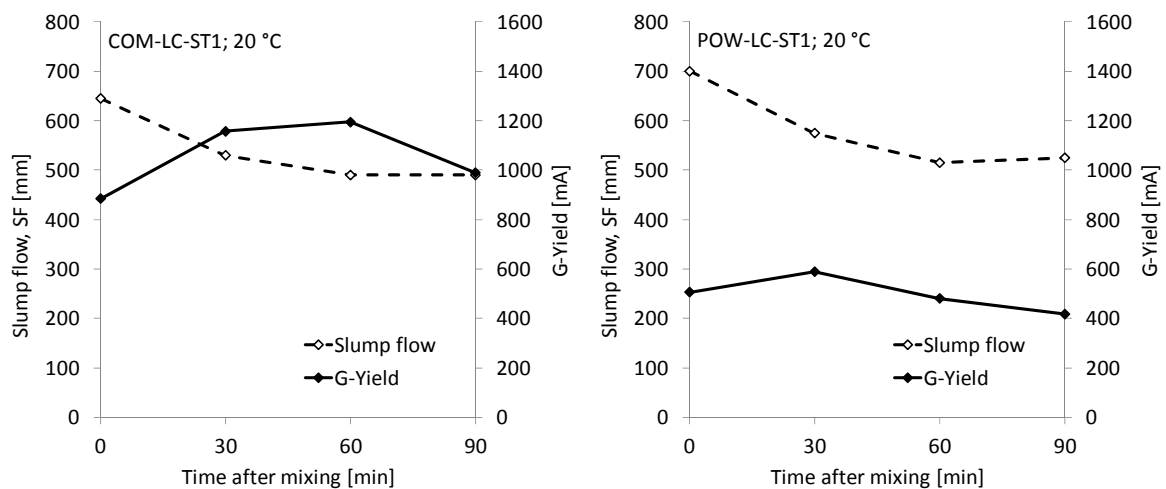


Figure 6.19: Slump flow values compared to G-Yield of COM and POW vs. time.

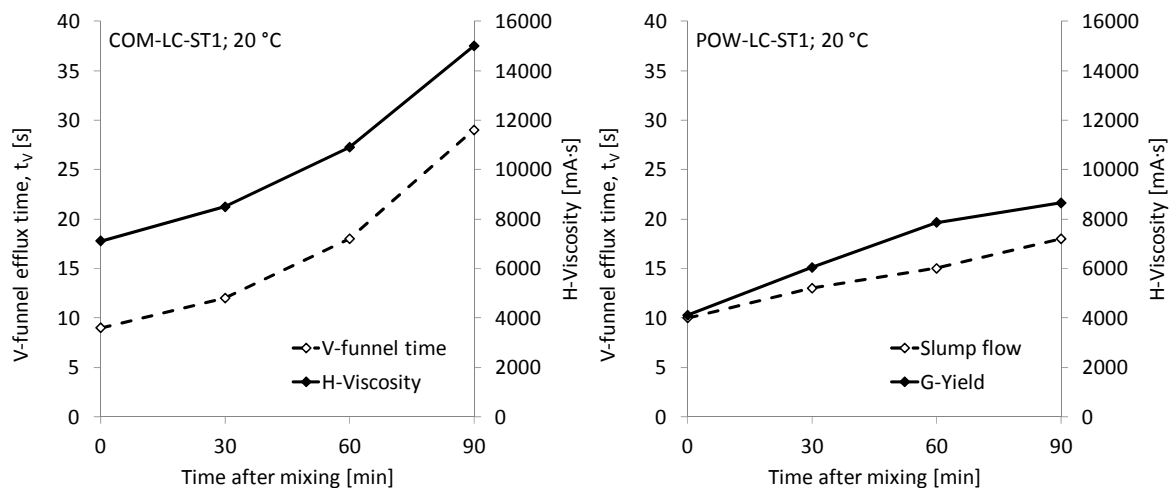


Figure 6.20:  $t_v$  values compared to H-Viscosity of COM and POW vs. time.

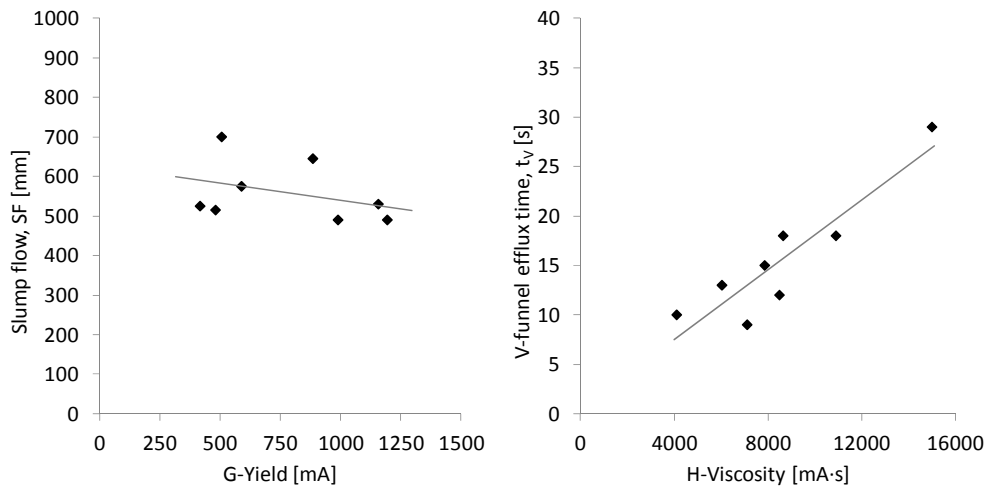


Figure 6.21: Correlation between SF and G-Yield, and  $t_v$  and H-Viscosity (COM and POW).

### 6.4.2 Influence of the stabilising agent on the interpretation of the results

The COM and POW mixture compositions were varied with different PCEs. Each of these variations was again varied with different STAs. The STAs showed strong effect on the performance of the SCCs. These effects were occurring regardless of the effects that could be observed from the PCE modifications. This can best be seen in Figure 6.22, where the effect of different PCEs and STAs at the dosages given in Table 4.10 is shown on yield stress versus time at 5 °C. The low temperature had the strongest influence on the STAs' performances. Each STA yields a time dependent rheology, which differs characteristically from the other STA. The magnitude of the shift of the curves, which is induced by the different PCE modifications, however, remains similar, pointing out that effects of STA and PCE can be observed independently. A detailed discussion of the effect of the STA takes place in Chapter 7 (Section 7.4). In order to avoid repetitive presentation of results, in this chapter, only the results for ST1 are presented. The observations that are discussed were identically made with ST2. All results for both STAs and for all time steps can be found in Annex A.

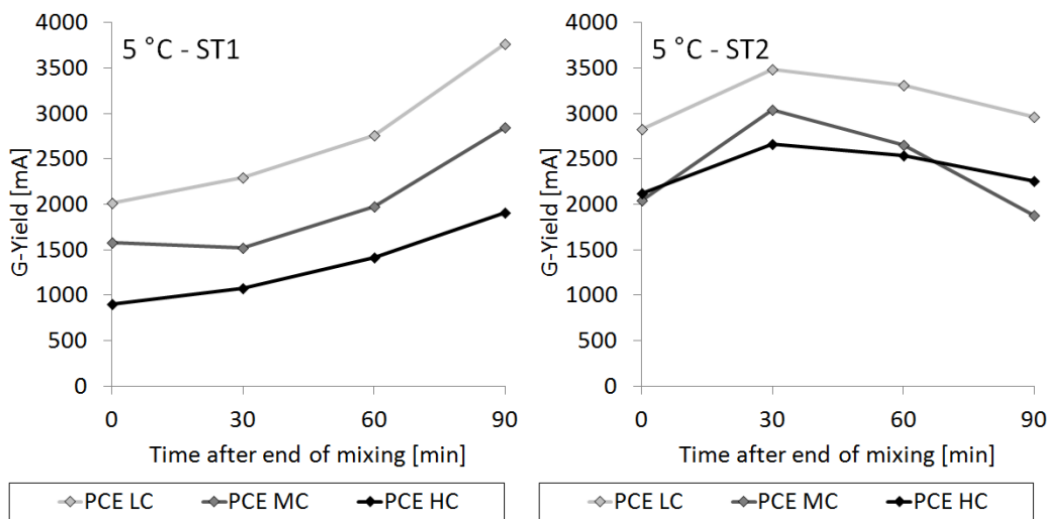


Figure 6.22: Effect of ST1 and ST2 on yield stress of the COM SCC at 5 °C.

### 6.4.3 Linking rheometric results to visual and haptic observation

A major problem for SCC is that measurement results solely cannot cover the full performance of a system. For example, an SCC with a slump flow of 800 mm and a funnel efflux time of 25 s would firstly be interpreted as a highly viscous low yield stress SCC. Such SCC is typically considered to be free from (at least dynamic) segregation. However, an SCC with poor segregation resistance can generate identical values. In the slump flow test, the paste would flow further than the aggregates, yielding a wide diameter. In the V-funnel, the coarse aggregates would block the nozzle causing long efflux times. Inversely, a high yield stress SCC can achieve wide diameters through operational influences, e.g. lifting the cone too rapidly and too high. Therefore, it is important to amend the measurement results with optical and haptic impressions from the tests. This helps to better identify thresholds from the measurement results.

All SCCs that were observed were entirely free from dynamic segregation at 20 °C and 30 °C. The G-yield values were all higher than 500 mA, which gives evidence that the respective yield stress is 50 Pa or higher (see also Figure 4.20). At 5 °C partly segregation could be observed, the reason for which is lack of PCE adsorption. This issue will be discussed later in this chapter in Subsection 6.4.6. For all mixes and temperatures a good workability was observed between 500 mA and 1500 mA G-yield. At G-yield values higher than 1500 mA, the SCCs were still well flowable but the slump flow values were smaller than approximately 500 mm. At G-yield values above 2000 mA, the SCCs were too stiff to work properly

### 6.4.4 Rheology of POW at varied temperatures

A strong influence of the PCE modification on the yield stress can be observed for the powder type mixes, as shown in Figure 6.23. At 5 °C, the initial yield stress is maintained throughout the whole observation time with all PCEs. Only minor variations of yield stresses can be observed between the PCEs directly after mixing. The meaningfulness of these very early results, however, should not be over-interpreted, since directly after mixing thixotropy effects might diffuse the results as well as the fact that no adsorption equilibrium of the PCEs is yet achieved. Over the entire observation period of 90 minutes, no significant changes in the yield stress can be observed due to different PCE modifications.

At higher temperatures, influences of the charge density of the PCE can be identified. The effect of PCE LC does not vary significantly with different temperatures. At all temperatures, the initial flow performance can be maintained with only small variations over the entire observation time.

This differs for the medium charged PCE. In general, the yield stresses are higher than with PCE LC. At 5 °C and 20 °C, the yield stress retention is very good. The initial flow performance can be maintained throughout the observed 90 minutes. At 30 °C, however, an increase of the yield stress from 1000 mA to approx. 1500 mA can be observed, which is maintained until 90 minutes.

The most pronounced effects of the different temperatures can be observed for the high charged PCE. While at 5 °C the initial performance can be held throughout the whole observation time, at 20 °C the yield stress increases in a linear way from 500 mA initially to 2000 mA. This indicates that the concrete is difficult to handle at 90 minutes. The mixture with the high charge density PCE shows a G-yield of approx. 1000 mA initially but rapidly stiffens, so that the G-yield is already higher than 3500 mA after 30 minutes, which means it is not self-compacting anymore after 30 minutes. Any later measurement failed, since the consistency was too stiff for a measurement with the Rheometer-4SCC.

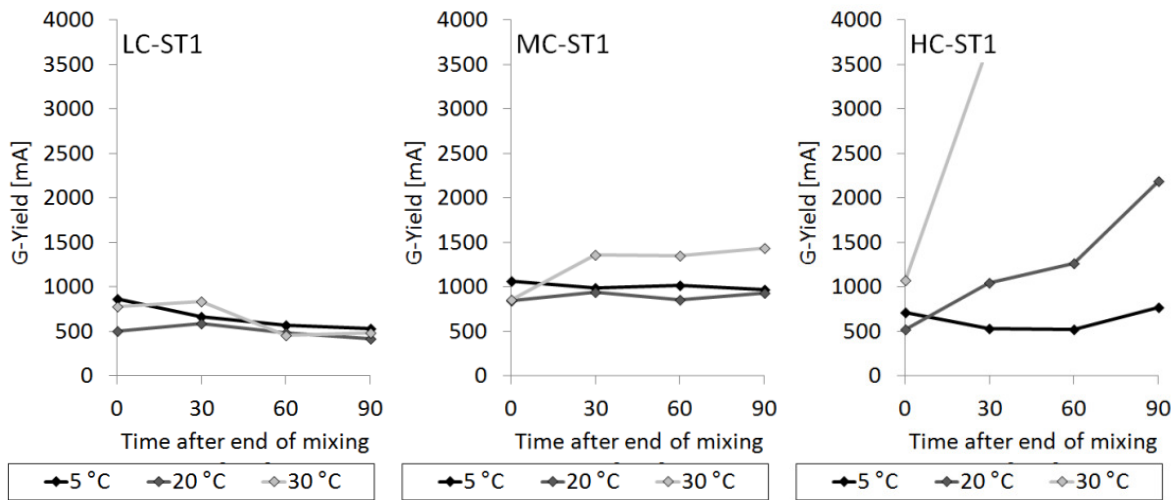


Figure 6.23: G-Yield vs. time of POW mixes with ST1 for PCE LC, PCE MC, and PCE HC.

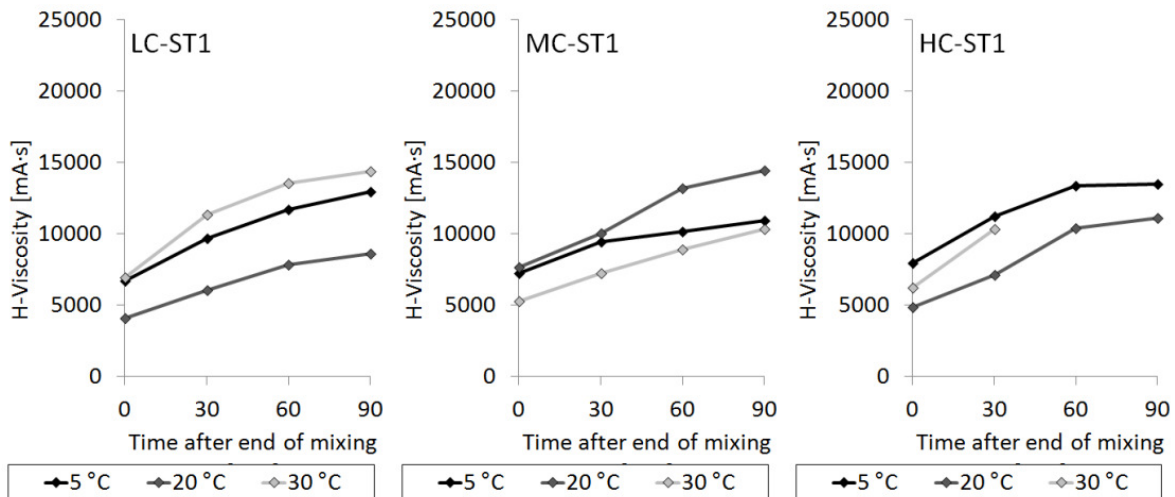


Figure 6.24: H-Viscosity vs. time of POW mixes with ST1 for PCE LC, PCE MC, PCE HC.

Figure 6.24 shows the respective H-Viscosities. As stated already in Subsection 4.3.6, the viscosity data is less precise to interpret quantitatively. Therefore, differences in H-viscosity values at identical time steps will not be interpreted. However within one series changes in the value with time can be identified. For the POW mixtures, no effect of the PCE on the viscosity can be observed depending upon the PCE modifications. All mixtures show initial H-viscosities in the range of approximately 5000 mA·s and 7500 mA·s. H-viscosities increase steadily with decreasing gradient until the values are reached between approximately 9000 mA·s and 15000 mA·s.

#### 6.4.5 Rheology of COM at varied temperatures

Also for the combination type concretes a significant effect of the PCE modification on the temperature dependent behaviour of the SCC can be identified. The results for G-yield for the different PCE modifications are shown in Figure 6.25. SCC with PCE LC shows relatively steady values at 20 °C. The G-yield is initially as well as after 90 minutes approximately 1000 mA, the values in between are slightly higher. At 30 °C the initial value is 1500 mA and decreases with time until 1000 mA after 90 minutes. At 5 °C the initial G-yield value is

approximately 2000 mA, increases steadily with time and reaches a value above 3500 mA after 90 minutes. At this temperature, the workability was poor at all observed times and a thin layer of segregated paste could be observed in the concrete.

In case of the use of the medium charged PCE, at all temperatures, an increase of the G-yield with time can be observed. At 20 °C and 30 °C, the performance is quite similar. The initial values are approximately 1000 mA. They increase steadily with decreasing slope. The values after 90 minutes are 1500 mA at 20 °C and 2000 mA at 30 °C. At 5 °C the initial yield stress with PCE MC is 1500 mA, thus higher than at 20 °C and 30 °C. It is retained over the first 30 minutes and then increases rapidly.

With PCE HC, a similar behaviour can be observed at 5 °C and 20 °C. At 20 °C the initial G-yield is 500 mA and increases in quite linear manner to a value of approximately 1700 mA after 90 minutes. At 5 °C the initial yield value is approximately 1000 mA and increases steadily with time until a value of approximately 2000 mA is reached. At 30 °C the initial G-yield is 500 mA, thus similar to the initial value at 20 °C, but it increases rapidly with time, so that after 60 minutes the G-yield values already lies at approximately 2300 mA. At 90 minutes, the G-yield is approximately 2600 mA.

With regard to the H-viscosity results, which are given in Figure 6.26, it can be observed that the influence of the PCE modification is negligible. Only at 5 °C, a performance, which significantly differs from the other modifications, can be observed for the SCC with the low charge PCE. The decrease of the curve from 60 to 90 minutes, however, is most likely a result of the general stiffness of the concrete, causing that the rheometric measurement results at 90 minutes are no longer reliable. However, also when the 90 minutes value is omitted, the viscosity of SCC with PCE LC increases more rapidly than with the other PCEs. This is another result of the segregation that could be observed. The segregated aggregates accumulate on the lower part of the bucket and density the fluid, yielding high yield stresses and higher viscosities.

All H-viscosity values increase with time. Apart from the above mentioned strongly segregating mixture with PCE LC at 5 °C, at all temperatures the difference between the initial value and the value after 90 minutes is approximately 5000 mA·s. The curves' time dependent characteristics are similar at all temperatures, however, it can also be observed that in general the viscosities reduce with increasing charge densities.

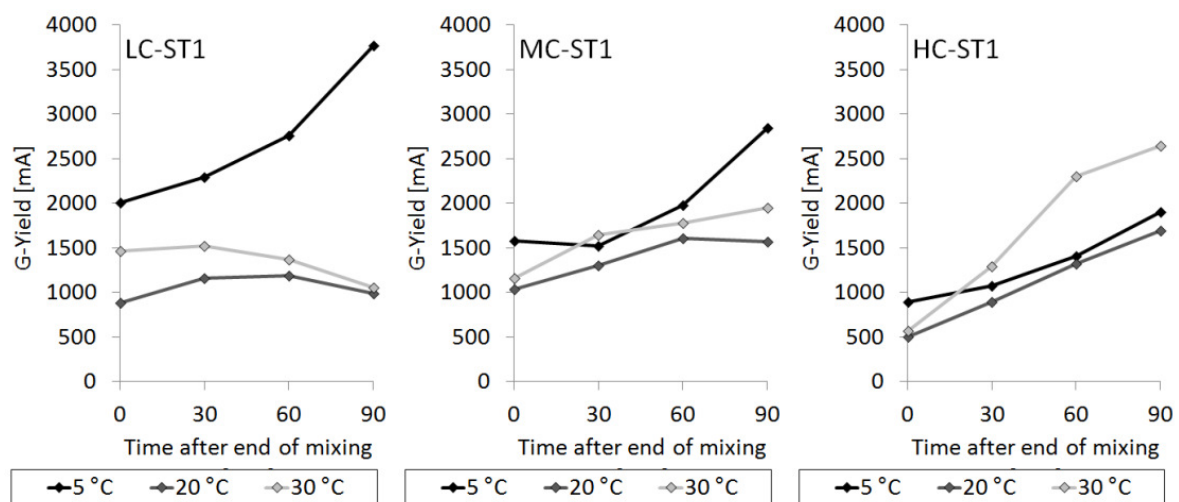


Figure 6.25: G-Yield vs. time of COM mixes with ST1 for for PCE LC, PCE MC, PCE HC.

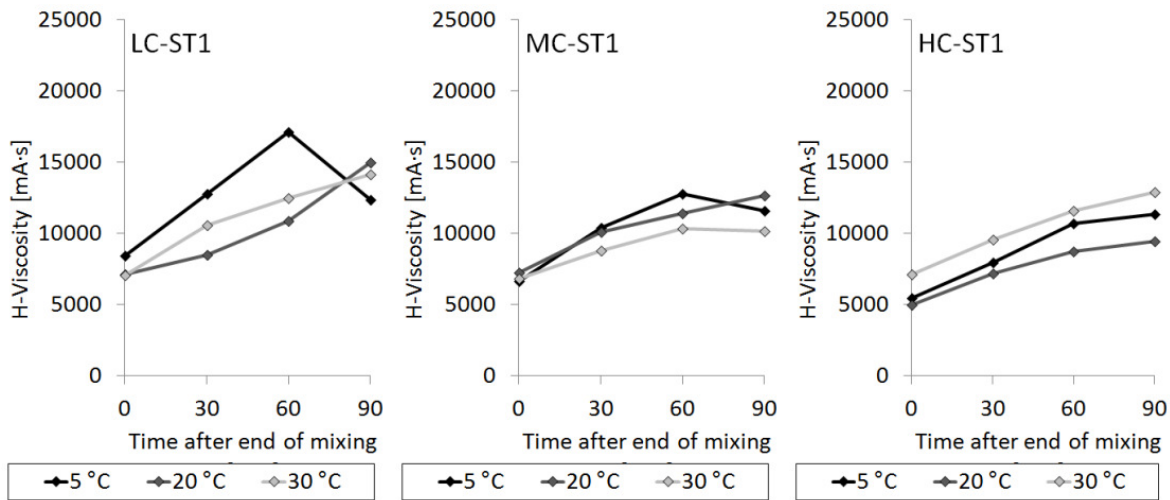


Figure 6.26: H-Viscosity vs. time of COM mixes with ST1 for for PCE LC, PCE MC, PCE HC.

#### 6.4.6 Discussion of the results

The initial hypothesis that neither the performance of PCE nor that of SCC can be described without further consideration of their individual performance can be confirmed. The observed results simultaneously verify and falsify previous research results focusing on concrete, e.g. by Weisheit et al. [254], Golaszewski and Cygan [253], or Nehdi and Al Martini [247]. This means many research results so far show validity for the specific mixture setup observed, in particular for a specific PCE and a specific mixture composition. These results, however, cannot be generalised for mixture compositions and PCE modifications that differ significantly.

Numerous effects induced by either the mixture composition, the temperature, or the PCE modification, can be observed. The POW mixture shows quite similar time dependent yield stresses at 5 °C and 20 °C but significant effects of the PCE at 30 °C. The COM mixture shows quite similar behaviour time dependent yield stresses at 20 °C and 30 °C, but significant effects at 5 °C.

For POW mixtures the influence of the PCE modification on yield stress is negligible, while a certain effect of the polymers can be observed for the COM mixture. This effect is induced by the different stabilising mechanisms of the different mixture compositions. POW mixtures have a higher particle packing density and are stabilised by the low water to powder ratio. Water is only added in a volume that is required to provide flowability. The particle distances upon flow are limited so that the influence of the PCE is small. The influence of PCE on viscosity is generally small, since their adsorption mainly affects the yield stress. Nevertheless, some effects can be observed for the COM mixtures. These have a higher water to powder ratio. Thus the stability of the system depends besides STA also on the dispersion and repulsion of the PCEs. The better adsorption ability caused by higher charge densities causes better particle repulsion, which gives better mobility among the particles.

A basic dependency between the flow properties and the charge density can be observed. Although for many environmental conditions no clear effects of the charge density can be observed as the performance is similar for all charge densities, this is getting clear at the particular cases when clear differences can be observed between the low charge polymer and the high charge polymer. In this case, the medium charged polymer behaves always in between these performances. E.g. as shown in Figure 6.27 for the COM mix at 5 °C, PCE HC generates low yield stress and PCE LC high yield stress and the curve of PCE MC lies in between these performances. The curve characteristics are very similar. In Figure 6.28 it can be identified that at

30 °C the yield stress retention for POW is good with PCE LC, very poor with PCE HC, and in between with PCE MC.

There is no specific influence that can be considered as critical for the performance in general. The majority of all modifications generated good or medium flow performance and the retention was acceptable. Table 6.4 provides an overview of all setups with regard to flowability in general and the retention of the G-yield.

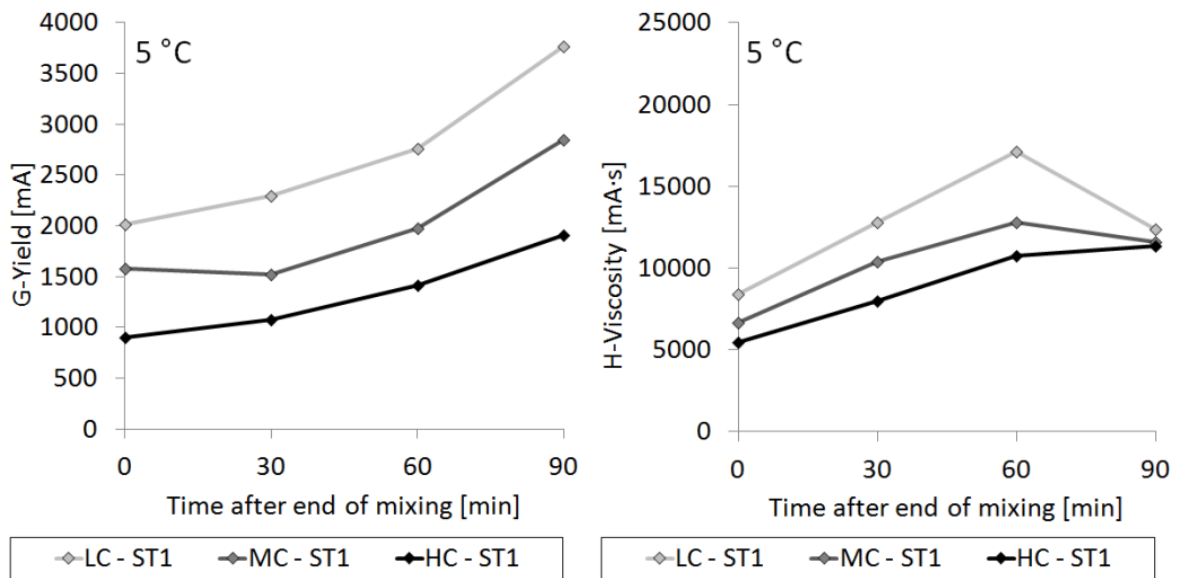


Figure 6.27: G-Yield and H-Viscosity of COM SCCs at 5 °C.

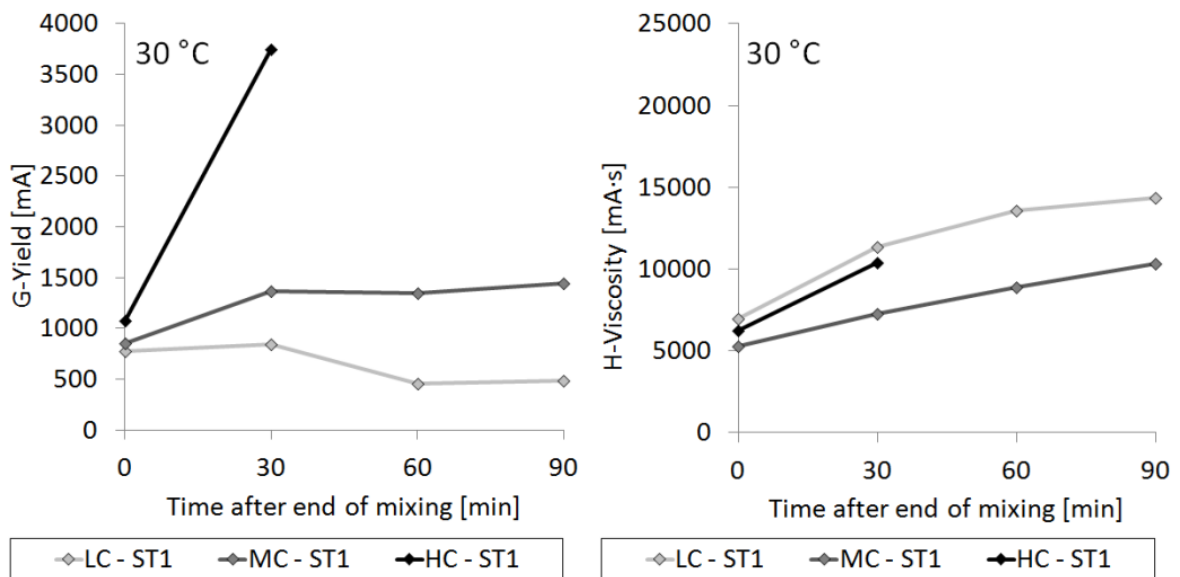


Figure 6.28: G-Yield and H-Viscosity of POW SCC with different PCEs at 5 °C.

Table 6.4: Summary of SCC performances at varied temperatures.

Mixture type	Temperature	Charge density of the PCE			Specific observations
		low	medium	high	
POW	5 °C	Good flowability	Good flowability	Good flowability	Mixture is not strongly affected by the charge density
		Good retention	Good retention	Good retention	
	20 °C	Good flowability	Good flowability	Good flowability	Mixture is not strongly affected by the charge density
		Good retention	Good retention	Medium retention	
	30 °C	Good flowability	Good flowability	Only initial flowability	Mixture is sensitive to PCE charge density
		Good retention	Medium retention	Minimal retention	
COM	5 °C	No flowability at all	Good flowability	Good flowability	Mixture is sensitive to PCE charge density
		Medium retention	Medium to poor retention	Medium retention	
	20 °C	Good flowability	Good flowability	Good flowability	Mixture is not strongly affected by the charge density
		Good retention	Medium retention	Medium retention	
	30 °C	Good flowability	Good flowability	Good flowability	Mixture is not strongly affected by the charge density
		Good retention	Medium retention	Medium to poor retention	

Two specific combinations of admixture setup and temperature ranges behave clearly different from all other mixtures. These are the powder type mixture at 30 °C and the combination type mixture at 5 °C (Table 6.4). At these temperatures a clear influence of the PCE modification can be observed. Apart from these specific cases, all other mixtures show good or medium flow and performance retention properties. In general, it seems that apart from the mentioned special cases, the POW mixture features a better performance retention.

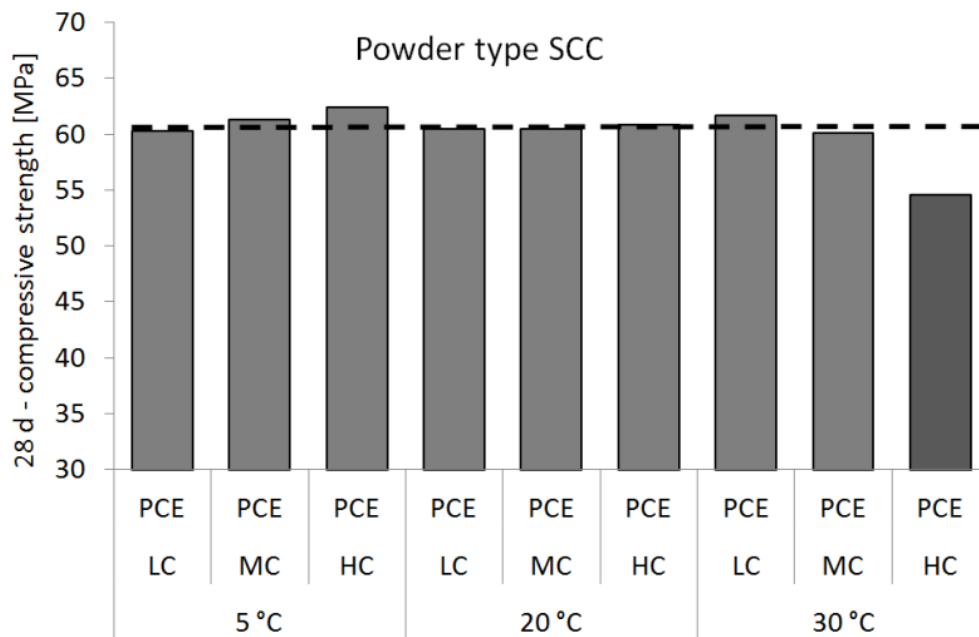


Figure 6.29: Compressive strength results after 28 days for the observed POW SCCs (average of three cubes 150 mm x 150 mm x 150 mm).

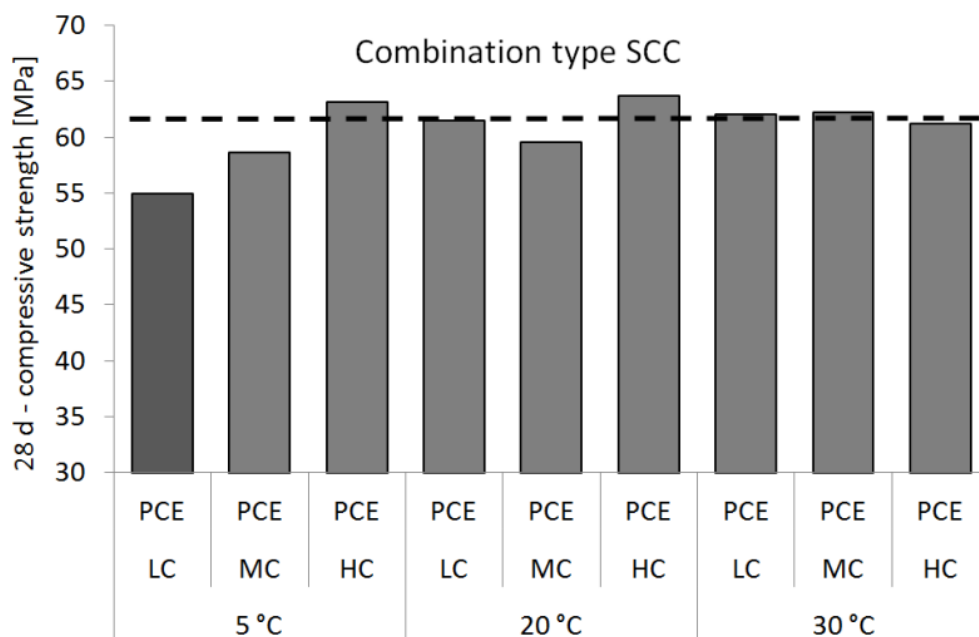


Figure 6.30: Compressive strength results after 28 days for the observed COM SCCs (average of three cubes 150 mm x 150 mm x 150 mm).

However, at 30 °C the powder type shows poor retention of the flow properties, in case the high charge PCE is used. The yield stress values for this particular combination of mixture composition and temperature is shown in Figure 6.28. While the flow performance with the low charge density PCE is very good throughout the entire time, the retention of the yield stress reduces with increasing temperatures. At 30 °C the stiffening takes place so rapidly that already at 30 minutes the consistency is too stiff to provide flowability. The reason for the rapid stiffening with high charge density polymers can be attributed to the rapid consumption of the PCE due to the accelerated hydration, which was discussed in further details in Section 6.2.

At 5 °C the low charge density polymer shows no flowability at all in case the low charge density polymer is used. The G-yield values and the respective H-viscosities are shown in Figure 6.27. The only PCE that generates good flow properties and long performance retention is the high charge density polymer. The medium charged polymer can generate good initial flow but the performance reduces with time. The low charge density polymer cannot generate good flow properties at all.

The reduced flow properties as described do not only negatively affect the workability properties, but they have tangible effect on the mechanical strength of the resulting hardened concretes. The mixtures, with significantly poorer workability properties were compacted less than the other mixes, which finally affects the mechanical properties. The 28d-strength values of the POW mixes were significantly lower at 30 °C with the high charge PCE (Figure 6.29). The same is valid in similar order of magnitude for the COM mixture at low temperature for the low charge density polymer (Figure 6.30). The medium charge density polymer at cold temperatures also shows poorer strength properties, emphasising that at cold temperatures a very high charge density is required for the PCE to generally yield flowability when the SCC exhibits a high water to solid ratio. All results of the compressive strength tests including those with ST2, which qualitatively show the same performance, can be found in Annex B.

## **6.5 Explanation model for the observed effects based on adsorption of PCE and water/solid ratio**

### **6.5.1 Differentiation between the SCC types**

In order to understand why powder type and combination type SCC have different temperatures at which they are sensitive to the PCE modification, and why admixtures with specific charge densities cannot provide sufficient flow properties, it is important to take a closer look at the special features of each mix.

The characteristic difference between the mixture compositions observed in these tests is the water to powder ratio. The POW mixture has the higher powder content. As a result, the particles are arranged densely in the fluid and have limited mobility among each other. The COM mixture is characterised by the lower powder content and a relatively higher w/p. As a result, particles have larger distances and better mobility against each other. Therefore, morphological changes caused by hydration reactions have significantly stronger effects on the mobility of the particles in powder-rich systems as illustrated in Figure 6.31.

### **6.5.2 Mechanisms behind the sensitivity of POW at high temperatures.**

Whereas for the POW mixture no critical effects of the PCE charge density can be observed at 5 °C and 20 °C, a distinct influence can be observed at 30 °C. In systems with low water to solid ratio, the mobility of the particles is restricted strongly by neighbouring particles. Thus the loss of mobility of particles is the stronger the higher the temperature is.

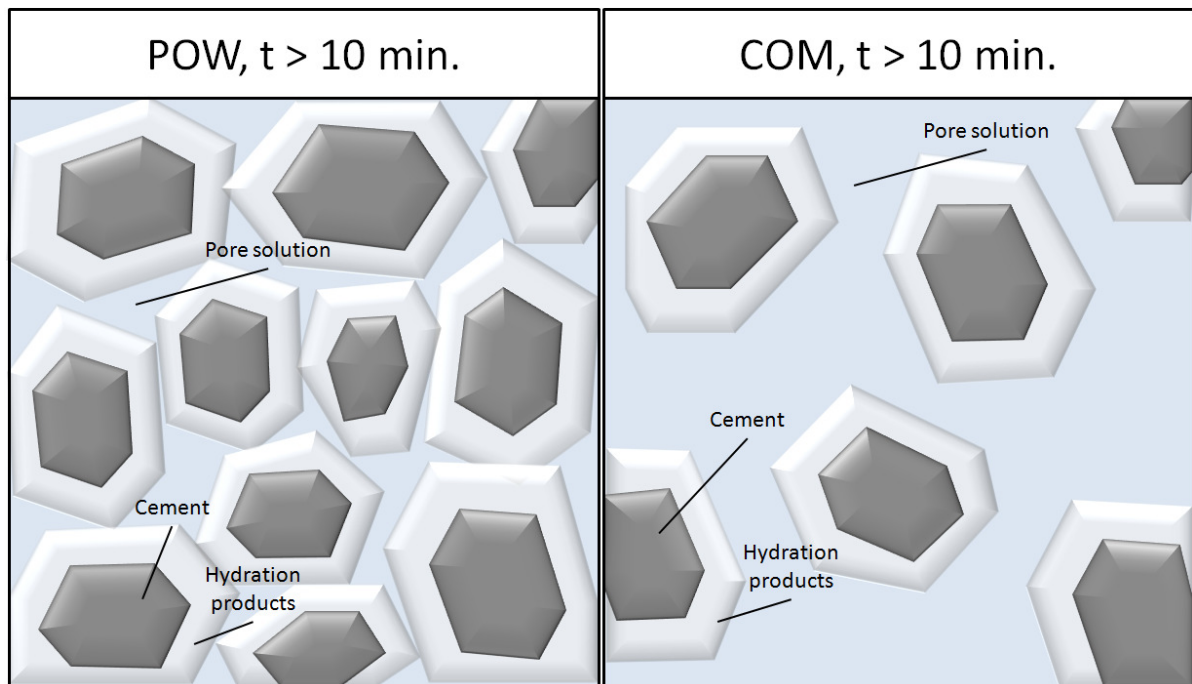


Figure 6.31: Qualitative arrangement of particles in the POW mixture (left) and the COM mixture (right), and particle mobility reduction due to hydration reactions.

With a low charge density (Figure 6.32) PCE adsorbs only in small amounts, while a distinct part of the polymers remains in solution, pushed aside by ions with higher anionic charges, most prominently  $\text{SO}_4^{2-}$  [85, 165]. Furthermore, low charge density polymers typically contain a higher number of graft chains, thus a more complicated geometry, which supplementary fosters the slow early adsorption capacity. These non adsorbed polymers do not have any effect on the flowability. High temperatures accelerate the hydration, quickly generating C-S-H, AFm, and AFt (Table 2.2) that increase the specific surface area of the particles. The crystals growth and crystal modifications change the morphology of the particles, which annihilates the effect of the already adsorbed polymers and furthermore reduces the mobility of the particles. The large number of PCEs that did not find adsorption sites and remained ineffectively initially can now adsorb with time on the newly formed crystals, mainly AFm and AFt (and ettringite and monosulphate in particular), thus maintaining the repulsion of particles, which leads to a sufficiently lasting retention of the flow properties.

A highly charged polymer will adsorb quickly as shown in Figure 6.33. Fewer polymers will remain ineffective in the solution. This causes high flowability directly upon addition, which can even generate strong segregation initially. The quickly adsorbed PCEs are quickly consumed and overgrown due to rapid hydration at high temperature. Morphological changes of the surfaces quickly reduce the mobility of the particles. The small number of PCEs that did not yet adsorb cannot maintain the repulsion of particles and thus, a yield stress, which is lowly enough to provide good flow properties cannot be maintained.

Finally, the major driving force for the performance loss at high temperature is the dense particle packing combined with the accelerated hydration. The only possibility in this case to safely provide good flow properties is choosing a low charge PCE. Since at lower temperatures the influence on the hydration is smaller, the influence of the charge density of the PCE is less pronounced.

### 6.5.3 Mechanisms behind the poor robustness of COM at low temperature.

For COM it could be observed that the influence of the charge density of the PCE was small at 20 °C and 30 °C but at 5 °C significant effects could be observed. The mechanism is different in systems with high water to solid ratio.

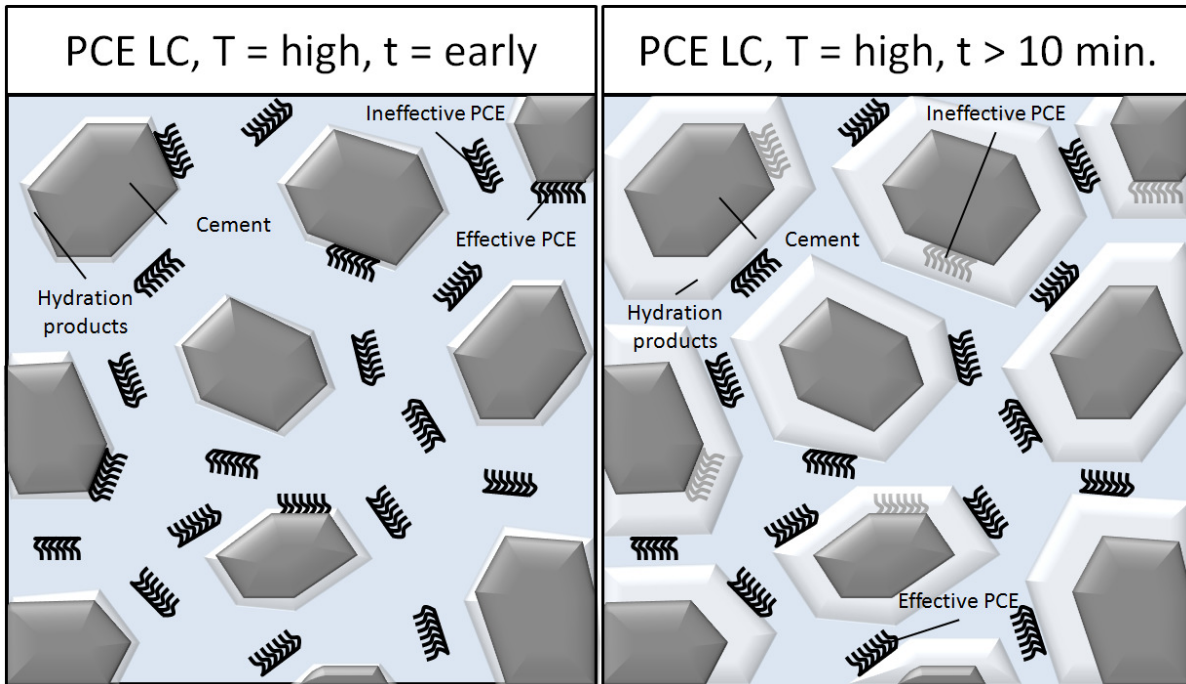


Figure 6.32: Delayed adsorption of low charge PCE in a powder-rich system at high temperature causing good performance retention despite the rapid hydration process.

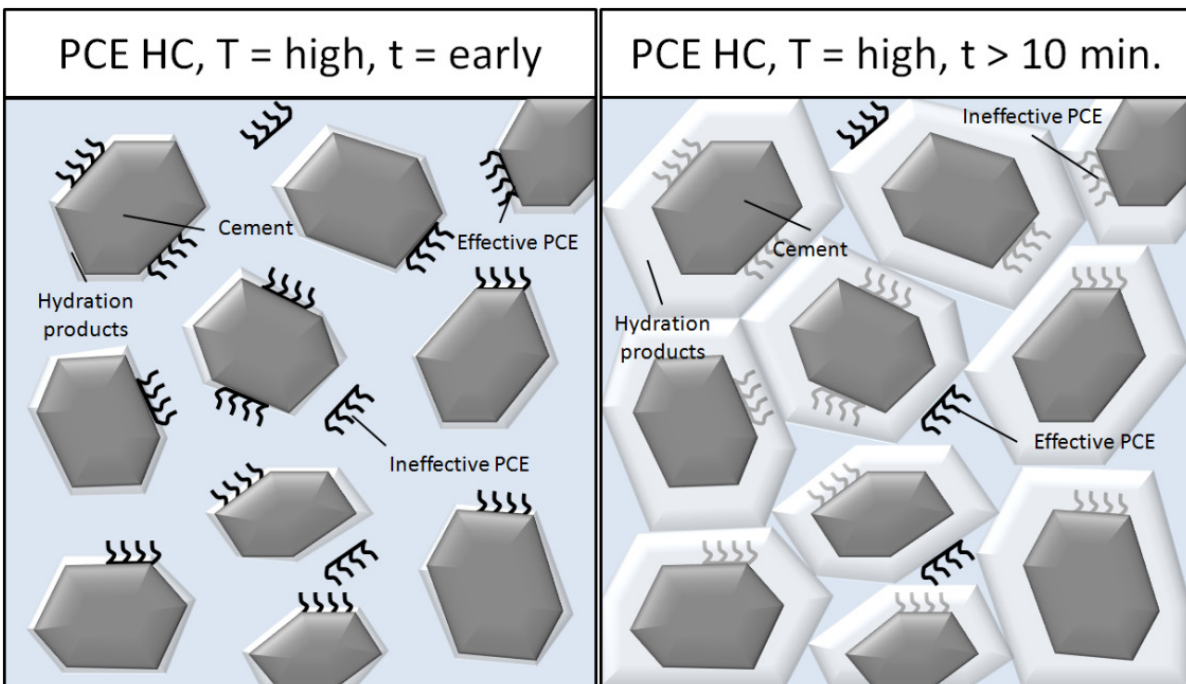


Figure 6.33: Rapid early adsorption of high charge PCE in a powder-rich system at high temperature causing rapid loss of workability.

Differing from the powder-rich systems that exhibit a sensitive performance at high temperatures, the problems occur at low temperatures. Here again, the adsorption of PCE determines the flow properties but the driving force for poor flowability is induced by segregation.

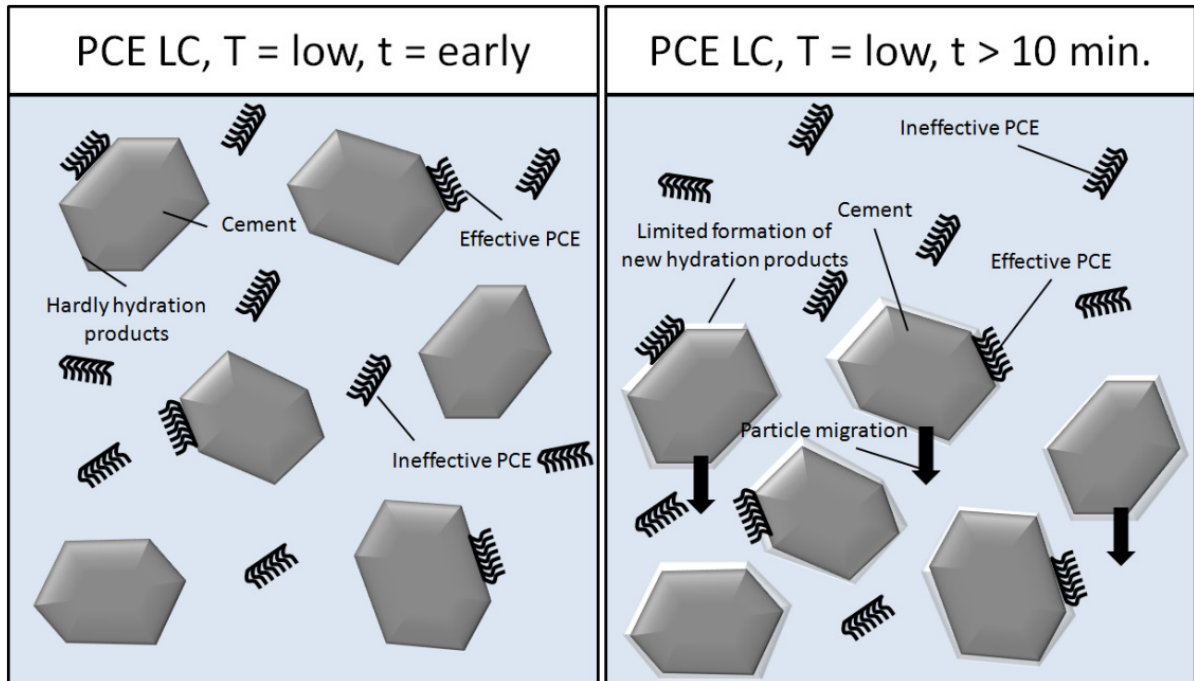


Figure 6.34: Segregation caused by the lack of adsorption of low charge PCE in systems with low w/p at low temperature.

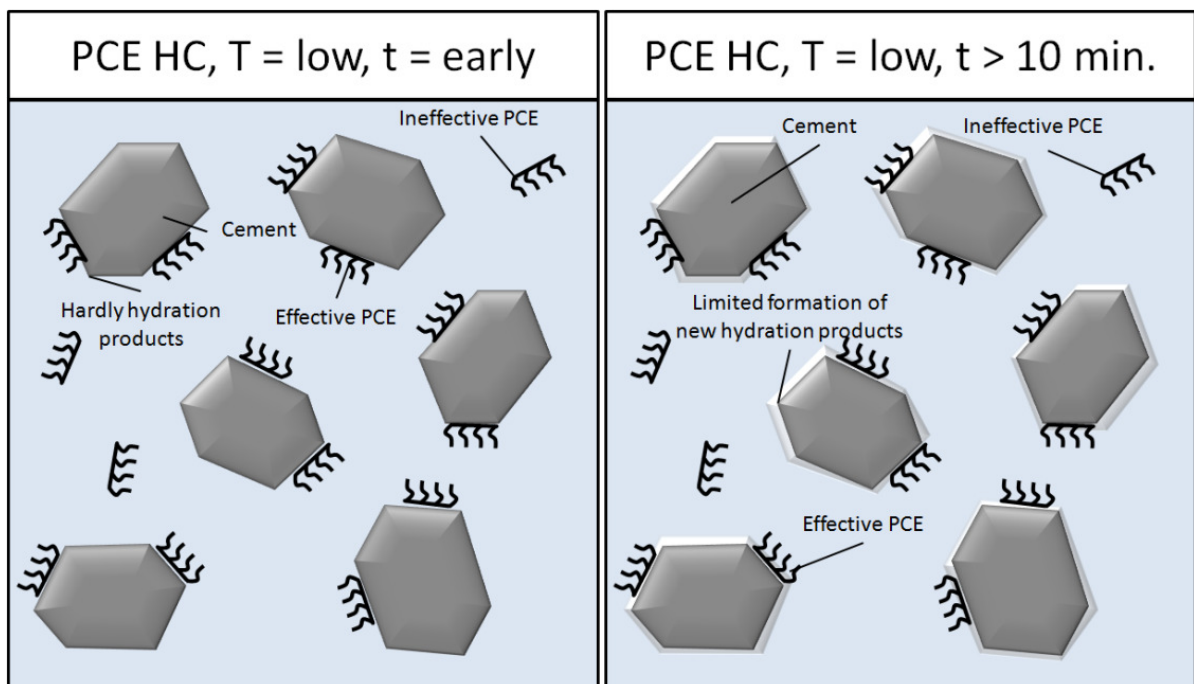


Figure 6.35: Good adsorption properties of high charge density PCE causing good flowability despite slow hydration reactions at low temperatures.

Again low charge density polymer adsorbs only partly while a significant part of the polymers remains ineffective in the pore solution as shown in Figure 6.34. At low temperatures, the hydration is slowed down, which means, C-S-H, AFm, and AFt only grow slowly. As a result, only few new adsorption sites for the not yet adsorbed PCEs can be generated so that the large number of unadsorbed polymers does also not find adsorption sites with time. The steric repulsion of the particles is not sufficient to stabilise them in the fluid. Upon flow, particles cannot be kept in distance and block each other, which reduces the mobility, thus causing poor flow properties, which can be seen in the high yield stress results. In the rheometric results furthermore high viscosity can be observed, since the concrete is not safe from segregation. The densified concrete in the lower part of the bucket causes high viscosity results.

The described problem of poor flowability due to lack of repulsion capacity can be overcome by the use of a high charge density PCE. As illustrated in Figure 6.35, a high charge density PCE will adsorb quickly on the particles and the few early formed hydration phases. It is not depending on the formation of new adsorption sites by the hydration process and can thus provide good flow properties.

At higher temperatures, a sufficient amount of hydrates is formed, which is the reason why these effects cannot be observed at 20 °C and at 30 °C.

## 6.6 Conclusions

The hypothesis that a general prediction of the temperature dependence of SCC is not possible has been confirmed. Temperatures affect mixture compositions with high water to powder ratios differently than mixture compositions with low water to powder ratios. Depending upon the mixture composition, the charge density of a PCE has a different effect.

In the presented investigations, the influence of environmental temperatures on the flow properties of self-compacting concrete was observed by concrete rheometry. Two different mixture compositions that distinguish themselves by their water to powder ratio were varied with SPs of different anionic charge densities. The results presented herein confirm that the fresh properties of normal concrete, for varying temperatures, differ from those of self-compacting concrete. A simple transfer of knowledge of normal concrete to self-compacting concrete is not possible. One major difference between normal concrete and self-compacting concrete is the extensive use of SP in the latter. Differing from normal concrete, SP is an essential component for the functioning of SCC. The admixture performance, however, is strongly affected by the environmental temperature, since the temperature related hydration rate affects the rate of the adsorption as well as the amount of adsorbable polymers. Nevertheless, the adsorption behaviour can be influenced by the polymer modification. Particularly the charge density of a PCE determines the temperature dependent behaviour of SCC.

The influence of the charge density in conjunction with the temperature related performance of SCC was largely neglected to date. Furthermore, it is often not distinguished among different other specific mix parameters. The results of the rheometric investigations at varied admixture adjustments and at different temperatures have shown that for a robust temperature performance of SCC the charge density and the mixture composition have to be taken into account. The major conclusions are:

- In order to assess temperature influences and qualitatively predict the flow properties of SCC, it is important to distinguish between mixture compositions with low and high water to powder ratio.
- At low temperature, a powder rich mixture showed good performance and to be not significantly affected by the PCE's charge density. However, at high temperature, the powder-rich concrete is prone to quickly lose flow properties.

- The situation is exactly inverted for mixtures, which contain low powder contents. They perform significantly more robust and are less affected by the PCE modification than powder rich mixtures at high temperatures. On the other hand, they are prone to failure at low temperature.
- Regardless of the water to powder ratio, low charge density polymers appear to be the best choice at high temperature, since they are consumed slower than high charge polymers.
- In contrast, high charge density polymers adsorb quickly, even, if the formation of new adsorption sites takes place slowly. Hence, regardless of the mixture composition type, highly charged PCEs can be considered as the best choice for low temperatures.
- For each critical combination of temperature and mixture composition, however, the SP's charge density affects the functionality of the SCC.
- For the similar PCEs considered herein, PCEs with a charge density that lies between two charge densities will also perform in between the thresholds given by the higher and lower charge density PCEs in terms of flow and flow retention
- A powder rich concrete fails at a high temperature, when a high charge density polymer is used, while it functions properly when a low charge polymer is used. The reason is the time shifted adsorption of the low charge polymer, yielding good flow properties even when the particles specific surfaces increase rapidly.
- A mixture with low powder content fails at low temperatures when a low charge polymer is used, while it works properly when a high charge polymer is used. The reason is that low temperatures cause a slow hydration process, so that not sufficient new adsorption sites appear for the low charge PCEs to adsorb, while high charge PCE adsorbs directly and does not need supplementary sites to be generated with time to provide flowability.

For the applicator of SCC, these insights imply two ways of improving the robustness, depending on the individual boundary conditions. Often producers do not vary their SPs but they are open to cast various concrete mixtures. Other producers may provide several SP modifications that can be varied according to the required specifications. Then again, it has to be distinguished whether an optimised performance is required at a particular temperature or whether a high robustness is required for a wide range of temperatures.

In case the type of PCE can be varied it is advised to use a low charge PCE for high temperatures in order to provide sufficiently long lasting flowability. For low temperatures, a high charge density PCE is the best choice, in order to ensure that PCE molecules adsorb quickly on particles.

In case, the PCE is a non-variable mixture component, the best option for concrete at high temperatures is a concrete mixture composition with high water to powder ratio. In this case, the influence of the PCE modification, which is most likely unknown to the user, is minimised. At low temperatures, a powder-rich mixture composition should be chosen so that the SCC is not depending on a quick adsorption of PCE. This yields independence of the charge density of the PCE.

The medium charged PCE showed to operate in between the performances that were generated by the higher and the lower charged PCE, respectively. Hence, for general temperature robustness, a medium performance PCE can be considered as the best choice.

The different options to operate accentuate that SCC is delicate to handle when the climatic boundary conditions vary. The most challenging consequence from the demonstrated results is that neither SCC nor PCE can be considered stereotypic. The variety of mixture compositions of an SCC and PCE performance properties has to be taken into account. Experiences from a powder type SCC may not be used blindfold for a powder poor type and vice versa. The same

holds for PCE, maybe even to a greater extent: experiences from a low charge PCE may not be valid for high charge PCE and vice versa.

A high level of knowledge is required in order to assure good performance. Particularly understanding the effect of the charge density of a PCE seems to be the key to develop high robustness and optimised performance of SCC with regard to the casting on the construction site.

## 7 Influence of stabilising agents on the rheology

### 7.1 Stabilising agents for concrete

#### 7.1.1 Necessity of stabilising agent for SCC

During the last 15 to 20 years the variety of approaches to the mixture composition of self-compacting concrete (SCC) has changed worldwide. The original SCC, the so-called powder type SCC, has been replaced in many cases in favour of less powder rich concrete types. These developments were mainly driven by the need to reduce costs for the more expensive powder as well to reduce the shrinkage, which is often considered as a problem for SCC. In order to maintain stable flowability despite a low powder volume, the water to powder ratio needs to be increased. This in turn lowers the viscosity of the paste, causing a problem for stable flowability and static segregation risk. Therefore, SCC mixture compositions with low powder volumes are typically amended by stabilising admixtures that increase the viscosity of the paste. These admixtures are also often called viscosity modifying agents (VMA) or viscosity enhancing agents (VEA). Since these admixtures do not affect solely viscosity but may also have strong impact on yield stress, in this Thesis they are generally referred to as stabilising agents (STAs).

#### 7.1.2 Terminology

For the description of polymer masses, in this Thesis consistently the unified atomic mass unit  $u$  was chosen. The unit  $u$  is equal to the unit Dalton (Da), which is more commonly used in the United States. One  $u$  is defined as  $1/12$  of the mass of an atom of carbon isotope  $^{12}\text{C}$ , which is why the dimensionless unit  $u$  is numerically equal to the molar mass  $M$  [g/mol].

#### 7.1.3 Stabilising agents for concrete

According to Khayat [25], for mortar and concrete applications, commonly polysaccharides are in use as polymeric STAs. The variety of these products is huge. Often cellulose, gums from plants or microbes as well as starches are used as basic components. Cellulose and starch are very versatile and can be supplemented with various functional groups through etherification.

Typically, the mode of operation of STAs is explained by their capability to absorb water. The absorption capacity increases with increasing molecular mass [ $u$ ]. However, there is no linear relation. Figure 7.1 on the left shows the example of cellulose, taken from Pourchez [261], where increasing molecular masses yield higher water retention properties. However, this effect appears lesser pronounced with increasing molecular mass. Water retention was determined according to ASTM C91, by vacuum suction of water from a mortar sample placed on a perforated dish. The water retention  $R$  is then calculated in % of the initial mass according to:

$$R = \frac{m_{W,0} - m_{W,\text{lost}}}{m_{W,0}} \quad (7.1)$$

where:  $R$  = water retention capacity [% by mass];  $m_{W,0}$  = initial mass of water [g],  $m_{W,\text{lost}}$  = mass loss of water after suction [g].

On the right side of Figure 7.1 results based on melamine sulphonate confirm that the mass effect is strong within a certain range of molecular masses and loses importance outside these thresholds. It is shown that increasing molecular masses reduce the mortar flow at unchanged apparent viscosity. Since flow spread is predominantly determined by the yield stress of a

system, this means, that higher molecular masses tend to rather affect the yield stress than the plastic viscosity, which can be explained by flocculation.

It is typically assumed that most polysaccharides may be incompatible with the hydration of cement due to degrading in the high alkaline environment in the cement paste or loss of effectiveness due to shrinkage in the presence of metal ions [201, 261, 262]. Izumi [262] investigated a number of polysaccharides and showed that the majority of STAs exhibit decreasing viscous behaviour in solution with increasing ion concentration. Pourchez found adverse results with regard to the stability of different cellulose derivatives, which showed a high stability in an alkaline environment [263]. In general, the threat of a high ionic solution is well known to the producers of commercial STAs, so that the available products on the market can be considered as sufficiently stable and functioning.

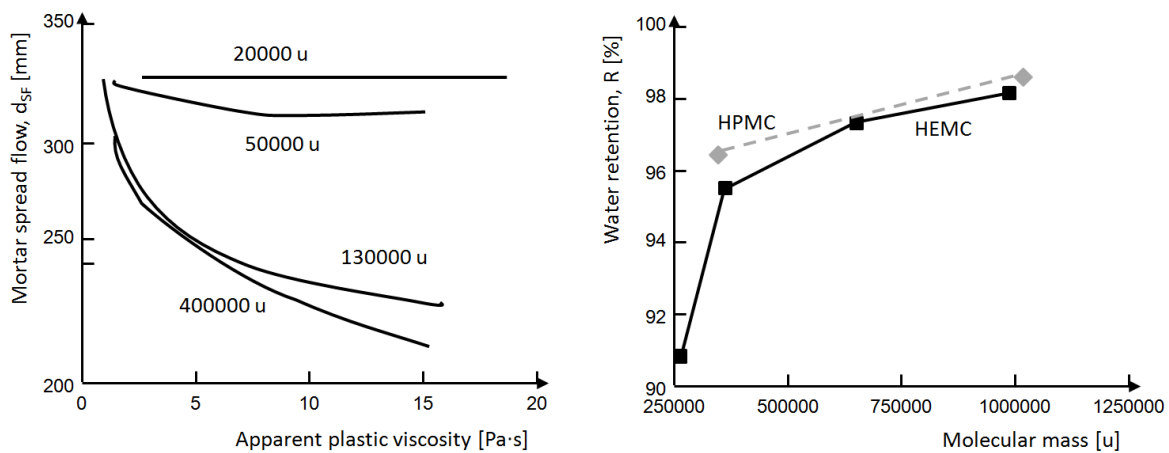


Figure 7.1: Influence of molecular mass of STAs on water retention after Pourchez [261] and on mortar flow after Yammamuro [23].

#### 7.1.4 Stabilising agents in the presence of superplasticisers

As explained in the previous chapters, self-compacting concrete contains high amounts of SPs, typically PCE. STAs and PCEs distinguish strongly from each other. PCEs may have molar masses between 10,000 and 200,000 g/mol and typically radii of gyration (see Subsection 3.4.1 and Equation 3.11) between 5 and 150 nm [14, 85, 87, 157, 264], while for different polysaccharide STAs molar masses between 300,000 and 5,000,000 g/mol and radii of gyration between several tenth and 500 nm are reported [201, 262, 265, 266]. Admixtures such as cellulose, welan and diutan gum are known to adsorb on particles [25, 201, 266-269]. Also adsorption of starch was reported by Palacios et al. [270], however, in comparison to welan gum, the adsorption was low. It is reported that the adsorption of present superplasticisers (SPs) prevents the adsorption of diutan gum on particles [201]. Since adsorption is not the sole stabilising mechanism of diutan gum, this lack of adsorption in presence of PCE does not inhibit a stabilising effect, but it assures no negative influence on the efficiency of PCE. The tendency for STA to adsorb competitively with PCE also strongly depends on the order at which PCE and STA are added. However, there are results that suggest that adsorption takes place to a certain amount in the presence of superplasticisers [203]. A delayed addition of STA was found to cause less STA adsorption, since adsorption sites were already blocked by PCE [270]. The anionic charges of diutan and welan gum generally make interactions between the polymers or competitive adsorption between both types of polymers likely. Due to the strong influence of the temperature on the hydration rate as well as the solution chemistry, it is further likely that temperature effects may be strong on interactions between both types of admixture.

Due to the enormous variety of products of SPs and STAs, it is surely difficult to detect generally valid laws regarding possible interactions between these admixtures. However, a better understanding is required since producers of flowable and self-compacting concretes often use both types, without being aware of the fact that their SP product contains stabilising components as well. A high number of SP products are blended products containing several polycarboxylic polymers but also additional functional components such as STA, colouring, or shrinkage reducing agents. In the latter case, the ratio of SP to STA is fixed. Then, it is particularly important to know possible interactions that may be induced or modified by effects of the ambient temperatures, since any modification of the dosage in order to adjust the performance directly affects the SP and the STA contents.

Since interactions between STAs and PCEs are possible that may result from the anionic characteristics of both polymers, it is important to observe possible influences of the charge density of the SP, and if this parameter may have influence on interactions. Based on the findings of Chapter 6 regarding the influence of the charge density of the PCE, investigations of STA in presence of PCE are undertaken with one largely non-adsorptive STA based on potato starch and another adsorptive STA based on diutan gum.

## 7.2 Starch and diutan gum based stabilising agents

### 7.2.1 Starch based stabilising agent

Starch is a polysaccharide, which typically consists of two types of macromolecules composed of differently linked glucose monomers (Figure 7.2). Though, chemically identical to cellulose, the starch chains as well as the macromolecular structure differ in a pronounced way. The glucose units of cellulose are arranged in alternating order, while they are arranged identically for starch. Furthermore, cellulose strands are linear, while starch consists of two types of macromolecules, amylose and amylopectin. Figure 7.2 shows the chemical composition of the glucose monomer of a starch as well as the six locations for additional bonds.

Amylose is a polymer with regular 1,4-bonds. As a result, the polymer is linear and the solution structure is assumed to build a helix structure. Seldom, singular branches can occur with branch points constituting 0.3-0.5% of all linkages [271]. Different values are given for the average molecular masses of amylose, ranging between 50,000 u and 1,000,000 u [271, 272]. According to Swinkels [265], the average degree of polymerisation (DP) of potato and tapioca amylose is 3000, which accords to a molecular mass of 486000 u, with DPs ranging from 1000 to 6000 [272]. Different amyloses investigated by Burchard [273] provided radii of gyration in the range of 19.4 nm and 60.1 nm. The investigated amylose of potato starch exhibited 31.8 nm.

Amylopectin is a more complex macromolecule with 1,4-bonds and 1,6-bonds. While the majority is constituted by 1,4-bonds, 1,6-bonds are reported to occur every 12 to 17 glucose units [274] or every 15-30 glucose units [275]. As a result, a tree like structure forms in solution. The molecular mass of amylopectin is estimated to be between 10,000,000 u and 100,000,000 u [271, 275]. Also significantly higher values are reported by Swinkels [265], who specifies values about 400,000,000 u at an average DP of 2,000,000 [265]. The radii of gyration of amylopectin are in the range of 50 to 500 nm.

The structures of amylose and amylopectin in comparison are given in Figure 7.3. The ratio between amylose and amylopectin depends upon the type of starch. Typical values found in literature are listed in Table 7.1. amylopectin is much more stable than amylose, which tends to retrogradation [265]. In context with starch, the term retrogradation is used for the discharge of water and crystallisation to granules

The starch granules are basically insoluble in cold water and need tempering between 50 °C and 70 °C to gelate [274]. For construction materials starches need to be modified to be cold-water soluble. This is typically conducted by heating starch-water slurries to let it gelatinize. Then, films of the dried material are milled to cold water soluble powder [271]. Furthermore, for construction materials application, starches need to be stabilised by ether or ester bonds in the hydroxyl groups (2, 3, and 6 in Figure 7.2). Typical modifications are attachments of groups of methylene, ethylene, propylene, and acetate. The stabilisation is typically made for the reason to reduce the tendency for retrogradation and to minimise intermolecular interactions [271].

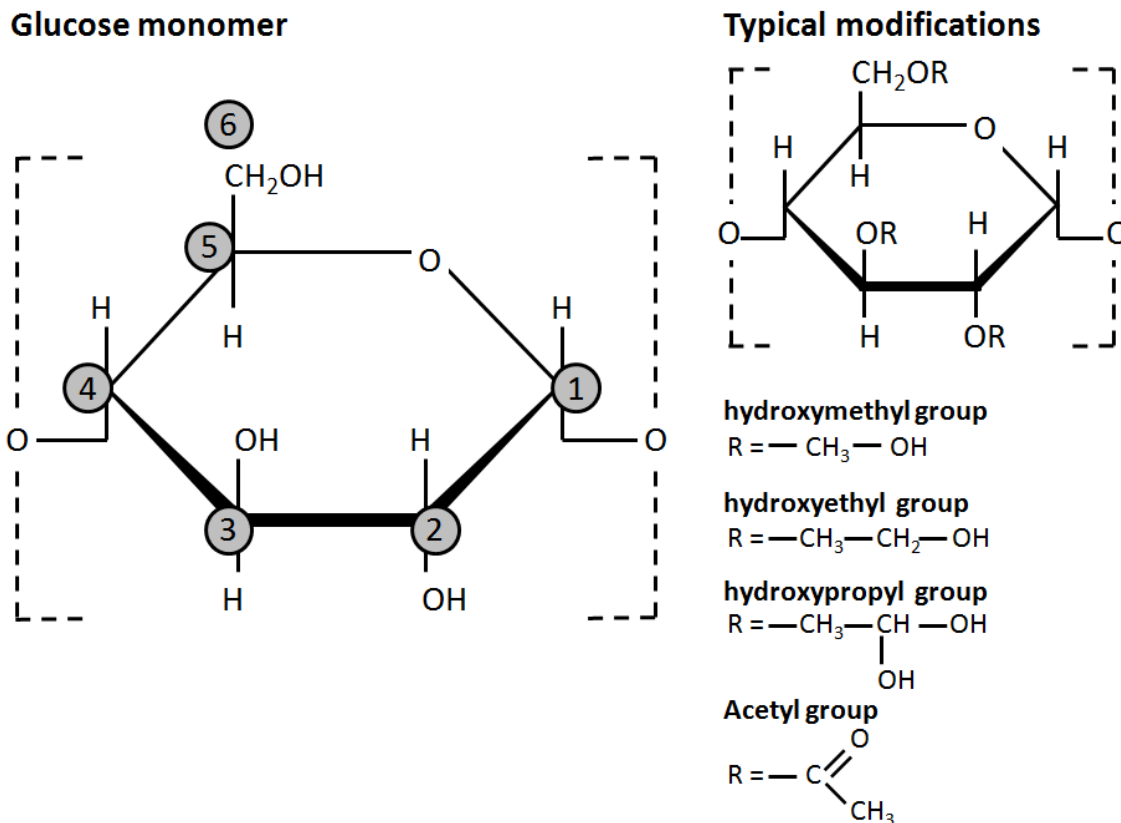


Figure 7.2: Single glucose unit as regularly repeated with 1,4-linkages in cellulose and starch. Functional groups (R) can be found in 2, 3, and 6. Typical modifications are hydroxymethylation, hydroxyethylation, hydroxypropylation, and acetylation.

Table 7.1: Contents and ratios of amylose and amylopectin depending on the starch origin after [265].

Source	Amylose		Amylopectin		Starch	
	Content	Degree of polymerisation (DP)	Content	Av. number of glucose units	Ratio Amylose/Amylopectin	Av. degree of polymerisation
Potato	21%	1,000-6,000 (Average 3,000)	79%	2,000,000	200	14,000
Cassava	17%		83%	2,000,000	150	18,000
Maize	28%	200-1,200 (Average 800)	72%	2,000,000	1,000	3,000
Wheat	26%		74%	2,000,000	1,000	3,000
Waxy Maize	0	-	100%	2,000,000	-	2,000,000

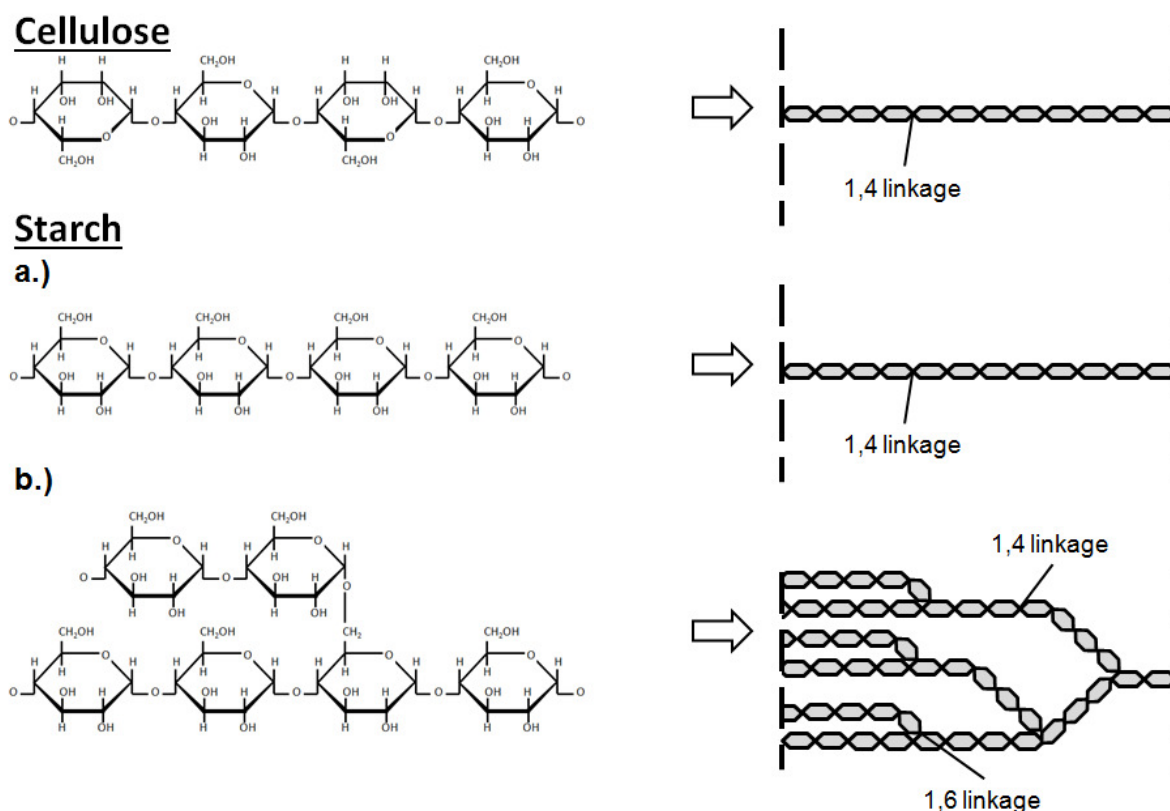


Figure 7.3: Chemical structures and macromolecules of celluloses and starches. Starch consists of two types of macromolecules: a.) amylose and b.) amylopectin.

### 7.2.2 Diutan gum based stabilising agent

Significantly less information can be obtained for diutan gum. It is a microbial polysaccharide of the group of the sphingans. The name of the group refers to the bacteria of the genus *Sphingomonas* [276], which is the origin of these polysaccharides. They are produced by aerobic fermentation at a temperature between 20 and 38 °C for about 35 to 60 hours at pH around 7 [201, 277, 278]. Other sphingans beside diutan are gellan, welan, rhamsan. The backbone structure of all sphingans contains the regular configuration of rhamnose, glucose, glucuronic acid, glucose units [276].

Their side chains vary in chemistry and geometry. Only welan and diutan are considered to be compatible with cement hydration. They differ in their main chain length and side chain geometry. Diutan is up to three times longer than welan [279]. While welan has either one rhamnose or mannose side chain, diutan has a two sugar rhamnose side chain [201]. The rhamnose side chains are attached to each second glucose unit [201, 276]. A carboxylate group attached to the glucuronate gives anionic charges to the backbone [201]. These are considered to sterically shield the carboxylic acids, thus avoiding cross-linking by calcium ions. According to Phyfferoen et al., the average molecular mass of commercial diutan lies between  $2.88 \times 10^6$  u and  $5.18 \times 10^6$  u [201]; Coleman states that the molecular mass can be up to several million u [276]. The structure of the polymer is shown in Figure 7.4.

Table 7.2: Molecular masses and radii of gyration for potato starch and diutan gum based on data provided by [201, 265, 271, 273, 275, 276].

	Potato starch		Diutan gum
	Amylose	Amylopectin	-
Content	Approx 20%	Approx 80%	100%
Molecular mass [u]	50,000 to 500,000	10,000,000 to 100,000,000	2,900,000 to 5,200,000
Radius of gyration [nm]	Approx. 30	50 to 500	N/A

## Diutan Gum

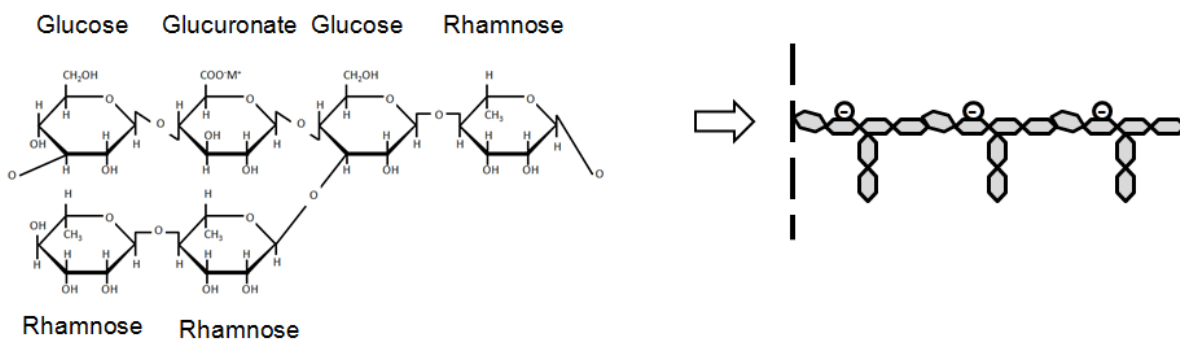


Figure 7.4: Chemical structure after Phyfferoen et al. [201] and macromolecule of diutan gum.

### 7.2.3 Differences between starch ether and diutan gum

The Figures 7.3 and 7.4 show that starch based and diutan gum based stabilising agents generally distinguish in their structure. The average molecular mass of diutan is approximately  $3 \times 10^6$  to  $5 \times 10^6$  u, which is in the range of starch with approximately  $2 \times 10^6$  to  $2.5 \times 10^6$  u. The latter values can be calculated by multiplying the molecular mass of the repeated linked glucose unit (162.14 u). According to Swinkels, therefore the molecular mass of starch is similar to  $162 \text{ u} \times \text{DP}$ , regardless of the molecular formation [265]. Table 7.2 shows an overview of the molecular masses and the radii of gyration.

Nevertheless, it has to be considered that the high molecular mass results from the amylopectin molecules with a DP of 2,000,000. However, there is only one amylopectin on 200 amylose molecules, which means that in starch there is a huge range of molecular masses. Amylopectin has an approximately 100 times higher molecular mass, while the molecular mass of amylose is approximately 10 times smaller.

The polymeric structures are completely different. Diutan gum has a linear main chain with regular side chains. Starch has two types of molecules, of which the amylose is relatively small and occurs in high number and the amylopectin is huge but occurs in low number. Diutan incorporates anionic charges, while starch can be considered as non-ionic (unless it is no carboxymethyl-starch). Though, Palacios et al. have shown that small amounts of starch molecules can be found adsorbed [270], the adsorption was relatively low. Hence, it can be assumed that the modes of operation of the STAs differ greatly.

Khayat attributes effects of welan gum to the binding of water, which in turn increases the viscosity of the cementitious system [25]. Though these results are related to welan gum, they can be considered to qualitatively occur likewise with diutan gum, since these basically show

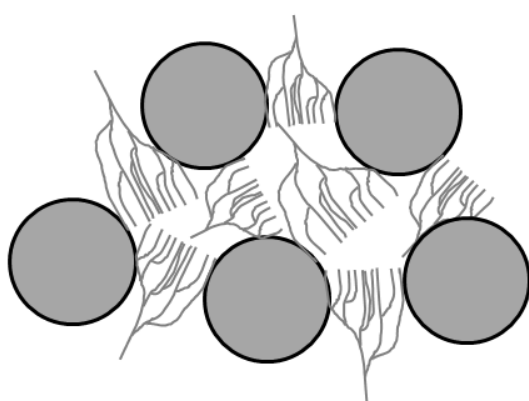
similar behaviour. For welan and cellulose, Khayat distinguishes between three modes of operation, which occur depending upon the concentration [280]:

- Adsorption: Polymers adhere to and immobilise water
- Association: Molecules form a network, causing gellation, which blocks the water motion
- Intertwining: At low shear rates, polymer chains intertwine and entangle. This effect is basically found at high addition amounts.

Sonebi observed marked shear thinning behaviour in mixes incorporating SP and welan or diutan gum [202, 203]. Shear-thinning was stronger with diutan gum. This effect is attributed to the higher molecular mass of diutan gum compared to welan gum. A higher molecular mass indicates higher water retention ability, based on the results found by Pourchez for cellulose [261]. The study reports about the strong effect of diutan gum on the apparent viscosity at low shear rates. It is assumed that the long chains of diutan lead to great degree of entanglement and intertwining. At higher shear rates, the polymers will direct into the flow direction, thus lowering the viscosity.

Rajayogan [281] and Terpstra [70] published studies that show the effectiveness of starch ether as a STAs. According to Simonides and Terpstra [200], the stabilising mechanism of starch ethers differs greatly from diutan gum. As shown in Figure 7.5, the mode of operation is basically attributed to the effect of the amylopectin which spreads out in solution into its tree-like structure, thus keeping particles at distance, thus avoiding segregation. The effect therefore mainly affects the static yield stress and does not show a strong influence on the viscosity. This observation is confirmed for low solid content systems by the results shown in Subsection 4.1.5, particularly Figures 4.4 and 4.5. Based on this, it can be assumed, that differing from cellulose or diutan gum, the water absorption capacity and thus the molecular mass may play a minor role for the stabilising effect and that the ratio between amylose and amylopectin may be of significantly higher importance.

### Particle stabilisation mechanism



### Depletion flocculation mechanism

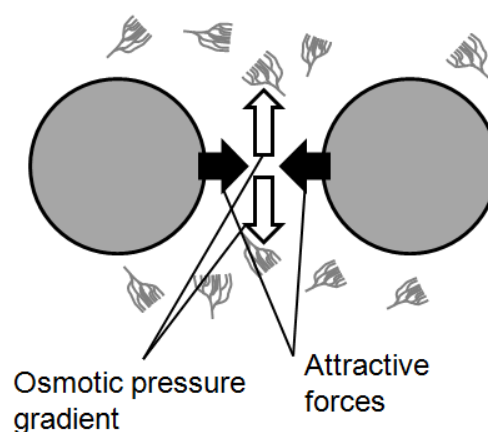


Figure 7.5: Suggested stabilising mechanisms of starch ether according to Simonides and Terpstra [200] and according to Palacios et al. [270]. On the left side, particles are stabilised by a buffering effect due to the huge amylopectin molecules. On the right side the stabilisation takes place due to an osmotic pressure difference between areas which are and which are not accessible for polymers.

Table 7.3: Relative costs of different rheology modifying agents related to tartaric acid after Plank [156].

Admixture	Product category	Source	Function	Relative cost (%)
L(+)-Tartaric acid	Natural product	Wine	Set retarder	100
Starch (ether)	Nat. and deriv. product	Corn, potato	Viscosifier	20–50
Cellulose (ether)	Derivation product	Cotton, wood	Water retention	200
Guar gum (ether)	Nat. and deriv. product	Guar plant	Viscosifier	15–120
Xanthan gum	Biotechnological product	Bacterium	Viscosifier	200
Welan gum	Biotechnological product	Bacterium	Viscosifier	600
Scleroglucan	Biotechnological product	Fungus	Viscosifier	350
Succinoglycan	Biotechnological product	Bacterium	Viscosifier	500
Curdlan	Biotechnological product	Bacterium	Viscosifier	350
Rhamsan	Biotechnological product	Bacterium	Viscosifier	550
Chitosan	Biodegradable product	Insect chitin	Viscosifier	350

The same observation regarding the yield stress increase of starch was observed by Palacios et al. [270]. The authors, however, discuss depletion forces to be responsible for this effect. Depletion forces occur, when particles pass closer to one another than the size of the dissolved molecules. As a result an osmotic pressure gradient occurs between areas of different polymer concentrations. The fluid tends to drain from the lower concentrated area into the higher concentrated area, thus attracting the particles. However, according to Israelachvili [282] depletion forces become the more effective, the higher the concentration is and the smaller the radius of gyration is and the lower the molecular mass is. STA is typically added in a relatively low amount and the molecular mass of the amylopectin is extremely high. It is therefore unlikely that depletion forces solely can explain the strong effect of starch on the yield stress.

Concluding from the above experiences with starch and diutan, it can be concluded that both admixtures work on different modes of operations. diutan gum mainly affects both, viscosity and yield stress through binding high amounts of water. The thus increased viscosity of the fluent phase finally affects the rheology of the overall system. In contrast to that, starch mainly affects the yield stress and much lesser the viscosity. It does not bind high amounts of water but spreads out between particles, thus keeping them on their location at rest. The working of STAs can thus be distinguished between:

- Stabilising through space filling between the particles (starch)
- Stabilising of the fluent phase (diutan gum)

Despite the chemical similarity with starches, cellulose ethers typically show behaviour like diutan gum, which means, they tend to significantly increase the yield stress of a watery system without influence of the particles. The results presented for diutan gum are thus valid for cellulose ethers as well. These different modes of operation have influence on the effectiveness.

Rajayogan et al. compared hydroxypropyl starch to welan gum in SCC mixtures and found that starch is required in significantly higher amounts in order to obtain similar effects as welan gum. Depending upon the water to powder ratio, related to cement starch needed to be dosed 8 to 15 times higher. Finally the overall performance regarding stability and early hydration were similar with the only difference that the starch increased the viscosity. The latter effect, which is in contradiction to Simonides and Terpstra [200] is discussed in more detail in Section 7.2.5. The factor between the dosages of welan gum and starch of approximately 10-15 as reported by Rajayogan are in line with experiences of the author as well as with the data sheets of the

producers. This ratio can also be confirmed by the adjusted mixtures shown in Table 4.10, where the ratio between diutan gum and starch at similar rheology is 1:18 and 1:12 for POW and COM mixtures, respectively. Plank reports that welan is added between 0.002% and 0.1% by mass related to the total formulation, while cellulose (which might be most comparable to starch due to its chemical analogy) is added between 0.2 and 0.7% by mass [156]. According to Plank, the costs for the admixtures are mainly related to the effort that needs to be spent for the derivation process. Biopolymers produced by fermentation are hence the most expensive agents. The costs of different rheology modifying agents are shown in Table 7.3. It can be seen that welan is 12 to 30 times more expensive than starch ether, which levels the higher efficiency of welan.

#### 7.2.4 Starch ether and diutan gum in the presence of PCE

Most STAs are used to stabilise flowable systems and to reduce bleeding. They are thus mostly combined with plasticisers or SPs, and it is likely that both admixtures may interact.

Figure 7.6 taken from Khayat [25] shows that small changes of the PNS based SP dosage showed large effects on the apparent viscosity. With increasing content of welan gum, the robustness against variations in the SP dosage could be significantly increased. In return, higher amounts of SP were required to achieve similar reduction of the apparent viscosity.

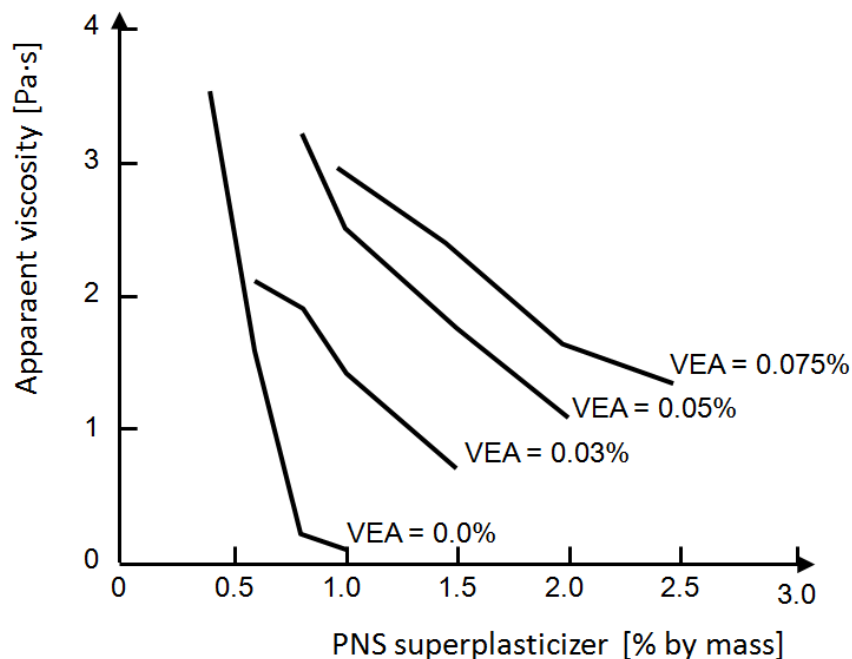


Figure 7.6: Influence of SP and welan gum amounts on apparent viscosity after Khayat [25].

Yammamuro et al. investigated the interactions of SPs with adsorptive and non adsorptive STAs [23]. Polyethylene glycol was used as non-adsorptive agent, which was compared with an adsorptive cellulose derivative. As can be seen in Figure 7.7, the non-adsorptive STA did not affect the adsorption of SP at all, while increasing amounts of STA reduced the adsorption of SP significantly, while in parallel the STA adsorbed. The SP used here was not specified by the authors. The authors conclude that competitive adsorption takes place between SPs and adsorptive STAs. As a result, in case of non-adsorptive STAs, yield stress and viscosity can be adjusted largely independently. The latter, however, needs to take into account at the adjustment of the SP. Figure 7.8 shows that there is a strong relation between the number of adsorbed polymers and the fluidity of mortar. The non-adsorptive STA did not affect the adsorption of

melamine sulphonate SP but affected strongly the adsorption of naphthalene sulphonate. The authors concluded that polyethylene glycol forms complexes with naphthalene sulphonate, thus hindering the SP adsorption.

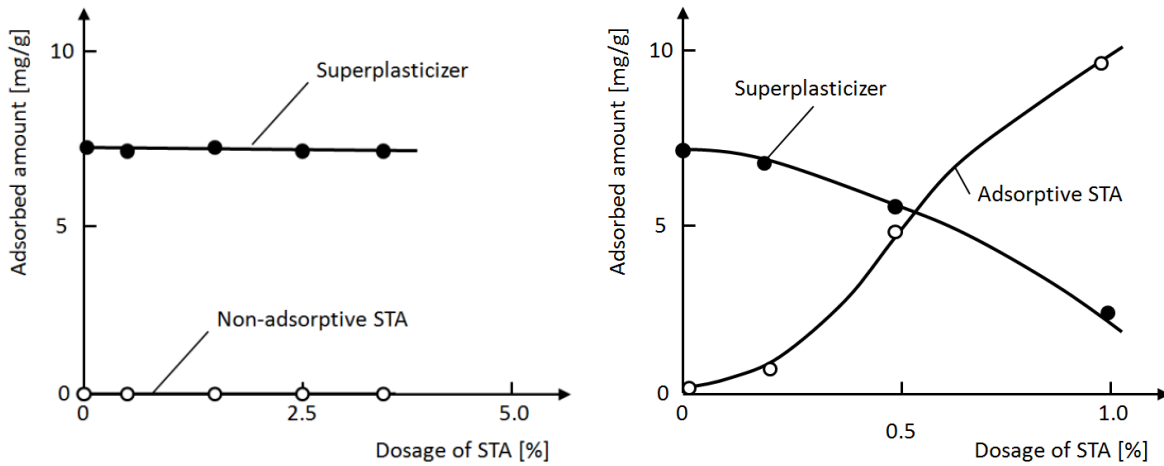


Figure 7.7: Influence of the adsorption properties of STA on the adsorption of SP after Yammamuro et al. [23]. On the left side, the non-adsorptive STA has no influence on the adsorption of SP. On the right side, the amount of adsorbed SP decreases with increasing amount of adsorptive STA.

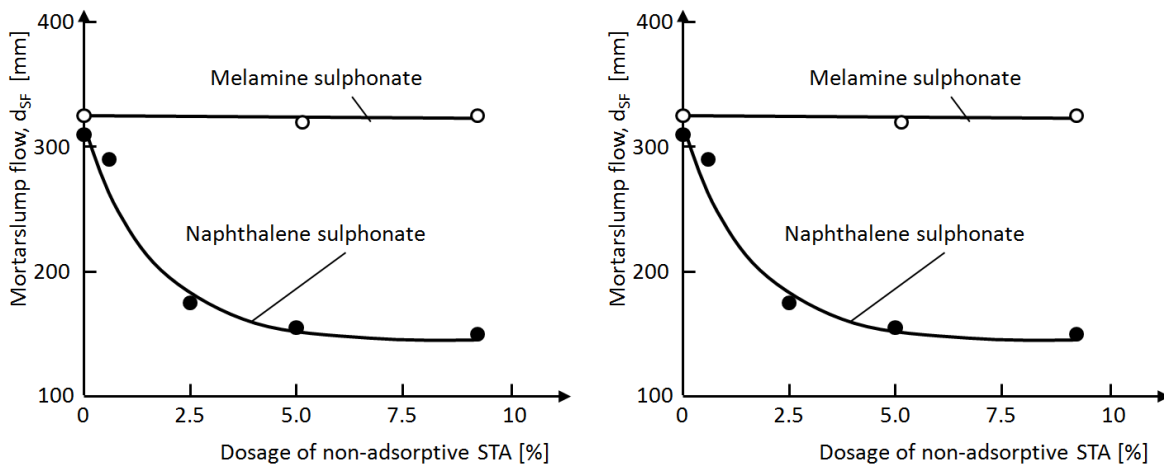


Figure 7.8: Influence of the SP type on the effect of non-adsorptive STA [23]. The figures show a good relation between adsorbed SP and mortar slump flow. Obviously with increasing dosages the non-adsorptive STA negatively affected the adsorption of PNS negatively while the PMS was not affected.

Diutan gum STA has an anionic backbone. Hence, Phyfferoen et al. opine that it shows a tendency to adsorb on cement particles. This effect, however, is supposed to be eliminated in the presence of SPs [201, 283]. Interactions are assumed to be hindered by steric shielding of the anionic charge by the double rhamnase side chain.

Both views can be challenged. Plank has shown that the adsorption of polymers in cementitious systems is not only driven by electrostatic forces but also by an enthalpy term [171]. This is likely to be valid as well for diutan gum. Hence, even if PCE provides higher anionic charge densities in solution, the adsorption of diutan gum on surfaces cannot be fully

excluded. Furthermore it can be assumed that at PCE dosage below the adsorption equilibrium anionic polymers will also adsorb. Finally, even during the induction period, the hydration of C-S-H, AFm and AFt continues, which may lead to time delayed adsorption of diutan, when PCE is already consumed. Calcium bonds between PCE and diutan gum cannot be excluded either.

### 7.2.5 Discussion of the recent research

In Subsection 7.2.3 the stabilising mechanisms are distinguished based on the phases they affect. In this context stabilising of the particles and stabilising of the fluent phase were distinguished.

Khayat distinguished between adsorption, association, and intertwining as the major mechanisms for the stabilisation of the fluid phase with regard to welan gum and cellulose use. Their performance is similar to diutan gum. The polymer dosage is thus the driving force that determines, which of these mechanisms occurs to which extent. Considering the huge size radius of gyration of STA polymers, it can be furthermore assumed that not only the polymer dosage but also the water to powder ratio and the overall packing density of a cementitious system may affect which of these effects predominates. Polymers that would preferably interact with the surrounding water molecules under free conditions in a fluid are likely to intertwine or entangle when they are forced to compress in narrow passages, e.g. at high powder particle density. It is furthermore conceivable that not only interactions take place within a molecule or between two molecules but that molecules might even intertwine with the surrounding particles. It is thus very likely that not only the polymer dosage but also the powder composition and hence the mixture composition has a strong effect on how diutan gum affects the flow properties of an SCC.

The latter is valid for starch STA as well. Considering the structure of amylopectin, which despite its lower number of molecules accounts for approximately 80% of the mass of starch, the proposed stabilising mechanism of the particles by Simonides and Terpstra [200] seems to be reasonable (Figure 7.5). In this case, according to the authors, the yield stress would be affected much more by starch than the plastic viscosity. This, however, contradicts clearly to the observations of Rajayogan et al., who observed a large increase of the plastic viscosity when starch STAs were used [281]. It is therefore necessary to take a closer look onto the testing conditions that were prevailing. A major difference between the mixtures that were observed in these studies were the amounts of starch in the mixture compositions, the water to powder ratios as well as the binder to aggregate ratios. Simonides and Terpstra [200] were using SCC with a powder content of 400 kg/m<sup>3</sup> and a w/p of 0.47. The starch dosage was 0.06% of the powder. Rajayogan et al. were using much higher powder contents, between 550 and 650 kg/m<sup>3</sup> and with a w/p ranging from 0.34 to 0.4 [281]. The starch dosages ranged between 0.11% and 0.23% of the powder (due to a variation of the FA dosages, this corresponds to dosages varied between 0.2% and 0.375% when only related to cement). Hence, the systems observed by Rajayogan et al. had significantly higher particle packing and higher starch contents. It can be assumed that the effect demonstrated in Figure 7.5 is the major effect of stabilisation in relatively fluid systems as observed by Simonides and Terpstra. At higher powder densities and lower water volumes and higher starch contents, the space filling effect of starch might be outweighed by intertwining and association of polymers and entanglement of finer particles, which would in return cause significant increase of the viscosity.

### 7.3 Influences of starch ether and diutan gum on dispersion rheology

In Subsection 4.1.5 the different performances of the starch based ST1 and the diutan gum based ST2 were presented without cement and with 33.3% by volume of cement were discussed,, pointing out that starch does not strongly affect the yield stress, while it affects mainly the viscosity. The diutan gum based STA affected both rheological properties depending on the amount of added admixture. The observed systems, however, were very fluid, which does not represent the situation that is typically available for cementitious applications. As discussed before, an effect of the water to powder ratio is likely to occur.

In another test, therefore, the effect of the powder content on the rheological properties of powder systems was observed. Investigations were conducted on water-limestone systems and water-cement systems with different water to solid ratios. The powders' particle size distributions and oxide compositions can be found in Figure 4.2, and Tables 4.1 and 4.4, respectively. Figure 5.8 shows results of slump flow tests of the used cement and limestone when supplemented by water at their respective water demand according to the Puntke method [233] at increasing PCE solid additions. The flow induction of LSF happens at significantly lower dosage and the maximum spread flow diameter occurs at lower dosage and is wider than with cement, which indicates that significantly higher amounts of PCE can be adsorbed on cement. It also indicated that the dispersing forces of PCE are lower in cementitious systems than in LSF-systems. Nevertheless, the basic mechanism of dispersion can be observed for both powders, so that depending on the observation type, limestone filler systems can possibly replace cementitious systems without the negative effect of the rapid change of rheology due to the ongoing cement hydration.

The STAs were observed in water only, and in water to powder systems at medium and high powder content. For all investigations, STA was first dissolved in water. Due to the different water demands of LSF and cement, their volumes were varied between 0%, 33.3% and 50%, and 0%, 25% and 40%, respectively. Furthermore the combined influence of PCE and STA was studied for each powder at the highest observed powder concentration. In these investigations, the PCE solid contents were varied for LSF between 0.06% and 0.30%, which approximately are the dosages required to induce flow and to achieve maximum spread flow according to Figure 5.8. For cement, the same dosages were chosen and supplemented by a dosage of 1.20%. Here the first dosage represents a very low PCE dosage, and the latter dosages represent the onset and the maximum. In the LSF investigations, the STA content was fixed at 0.5% of the water. However, due to the significantly higher efficiency of ST2, for the cement tests more diverse dosages were chosen. ST1 was varied between 0.5% and 5%, ST2 was varied between 0.05% and 0.5%, each percentage related to the water content. In flowable cementitious systems 0.5% for ST1 and 0.05% for ST2 represent typical dosages for use as stabilising agent, while significantly higher dosages would only be used for special applications. The mixture proportioning for the LSF tests and the cement tests is given in Tables 7.4 and 7.5, respectively.

The Couette type viscosimeter Viskomat NT was used with a double gap cell as described in Subsection 4.3.9. The established ramp profile is given in Figure 7.9 in conjunction with example measurement data resulting from the mixtures with a volumetric ratio of water and solids of 1:1 when the stabilising agents are varied. After a rapid increase, the rotational speed was kept at 120 rpm until 60 s. After that, the shear rate was steadily reduced until it reached zero at 240 s. Only the values at decreasing shear rates were used to calculate yield stress ( $\tau_0$ ) and plastic viscosity ( $\eta_{pl}$ ) based on the assumption that the fluids largely exhibit Bingham behaviour. Therefore, for the interpretation of the flow curves only the values above the critical shear rate  $\dot{\gamma}$  were considered. The critical shear rate for Bingham behaviour was calculated according to the manufacturer's specifications for this cell after Equation (4.17).

A Bingham interpretation does not fully represent the performance of STAs, particularly at low shear rates and in the pure water-STA systems without limestone or cement particles. However, the strength of the Bingham model is the clear differentiation of the yield stresses, and the effect on yield stress is assumed to be one of the major distinctive features between ST1 and ST2. Furthermore, the Bingham approach is the most commonly used model in cement and concrete technology and the observed systems exhibited Bingham behaviour over a wide range of shear rates.

Table 7.4: Conducted tests with STAs and LSF at varied powder contents.

Water [% by volume] + ST*	100	66.7	50.0	50.0	50.0
Limestone filler [% by volume]	-	33.3	50.0	50.0	50.0
PCE LC [% by mass of powder]				0.06	0.30
* ST1: 0.5% by mass of water ST2: 0.5% by mass of water					

Table 7.5: Conducted tests with STAs and cement at varied powder contents and varied STA dosages.

Water [% by volume] + ST*	100	75.0	60.0	60.0	60.00	60.00
Cement [% by volume]	-	25.0	40.0	40.0	40.0	40.0
PCE solids [% bwo cement]	-	-	-	0.06	0.30	1.20
* ST1: 0.5% by mass of water ST1: 5.0% by mass of water ST2: 0.05% by mass of water ST2: 0.5% by mass of water						

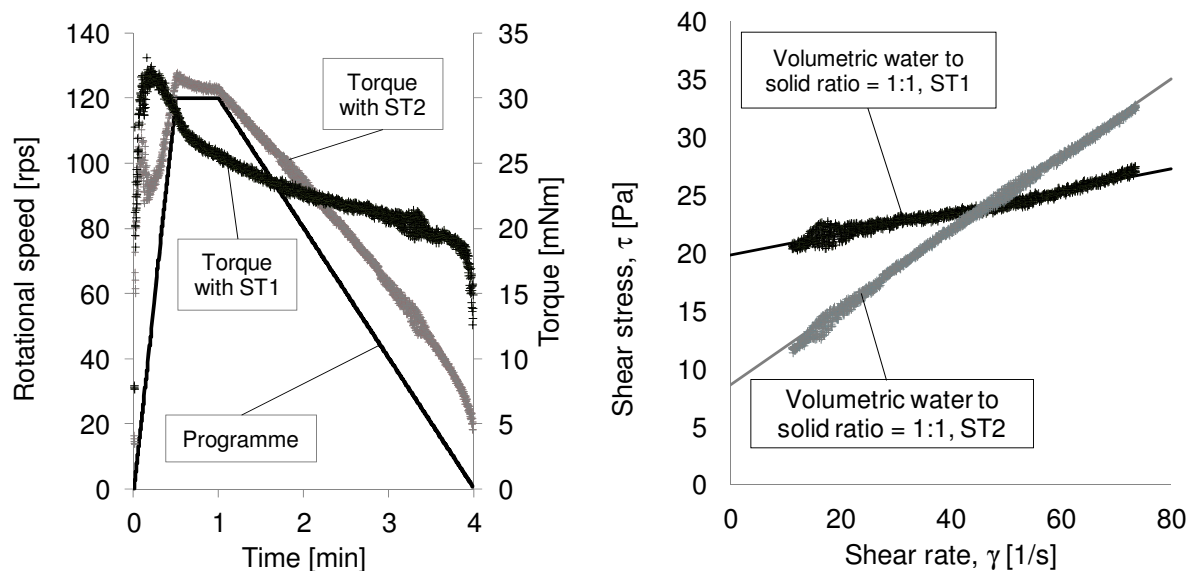


Figure 7.9: Measurement for the observation of the influence of solid limestone particles with sample measurement results (left) and sample flow curves and Bingham approximations (right). The STA dosages were 0.5% of the limestone filler for ST1 and ST2.

Since shear forces strongly affect the cement hydration and the adsorption of polymers, for cementitious systems it is of utmost importance to keep the measurement time as short as possible. The applied profile is considered to be a reasonable compromise between precision and compactness. Due to the initial formation of ettringite and monosulphate, the performance of PCE in cementitious systems can change rapidly during the first 3-5 minutes. In order to make sure that the cementitious systems were stable, the measurements were conducted not earlier than 10 minutes after water addition.

Figure 7.10 shows yield stresses and plastic viscosities for ST1 and ST2 for different water to solid ratios compared to identical reference water-limestone suspensions without any STA. It can be clearly observed that ST1 does not strongly affect  $\tau_0$  compared to a mixture without STA when added to water only and to a mixture with only 33.3% solids. At the same time, with ST2 in water only, a clear yield stress can be observed which increases only slightly at low solid content. These observations are in line with Figures 4.4 and 4.5. In mixtures with a high solid content ST1 increases  $\tau_0$  strongly, while the effect of higher powder contents is only small for ST2. Despite the strong effect of ST1 on  $\tau_0$  upon addition of high solid contents  $\eta_{pl}$  is only slightly affected. A pronounced increase of  $\eta_{pl}$  can be observed at high solid contents with ST2 although at the same time the increase of  $\tau_0$  is small.

Regarding the yield stress, at 0% solids, the starch system does not distinguish itself from the control system with water, and starch only increases  $\eta_{pl}$  slightly. At 50% of solids,  $\tau_0$  increases prominently, while the increase of  $\eta_{pl}$  is relatively low. This clearly indicates that for ST1 a threshold for the solid particle amount exists, which triggers the rapid increase of  $\tau_0$ . This cannot solely be explained by the higher particle volume, since then  $\eta_{pl}$  would exhibit at least a similarly strong increase. This is clearly not the case in Figure 7.10. Since the polymer concentration in water is maintained for all tests, intertwining of polymers does not seem to be the driving force for the significant yield stress increase. It seems the effect of depletion forces as described by Palacios et al. [270], induced by non-adsorbed starch molecules, cannot be neglected in the discussion. However, due to the large molecule size of the amylopectin, depletion forces may be mainly only induced by the amylose, which is an order of magnitude smaller than amylopectin. In terms of mass amylose only represents 20% of the starch so that a dominating depletion force controlled mechanism seems to be unlikely. Another mechanism that can explain the observed effect would be a particle-amylopectin-particle lattice effect, which is activated by the closer particle distance of LSF when added above a threshold dosage. The cause is similar to that of depletion: large particles cannot access a zone in between two particles. However, the forces are lesser induced by osmotic pressure than by the pure size of the molecule. This means the huge amylopectin molecules act like springs – or rather like deformable particles between the finest solids, as shown in Figure 7.5. In this context it may be negligible whether the amylopectin can be found adsorbed or non-adsorbed on particles. Adsorption of starch on cement is reported in literature [270]. As starch can be attracted on surfaces with positive zeta potentials  $\zeta$  [284] it can be assumed that it can be adsorbed on limestone fillers as well. The adsorption of small molecules such as amylopectin would add a steric repulsive component. This contradicts to the observation, though such effect cannot be excluded. In case amylopectin adsorbs, this would add a bridging component to the mechanism. However, considering the tree-like structure of amylopectin as well as its enormous size in the order of magnitude of finest solid particles, the number of adsorbed branches would be small compared to the non-adsorbed branches, which would make bridges relatively flexible. Furthermore, similar behaviour was observed for a high number of differently modified starches regardless of the presence of different charges [285], which also indicates that the effect of starch on rheology is not only induced by adsorption mechanisms. For the described stabilising mechanism, due to the flexibility of the starch filler, upon shear the interparticular mobility

remains good so that low viscosity can be maintained despite high yield stresses. Nevertheless, the rapid increase of  $\tau_0$  at high solid content also indicates that starch polymers might entangle at dense particle packing. The latter would explain why Rajayogan et al. [281] found - differing from the results presented here - high viscosity induced by starch at low w/p.

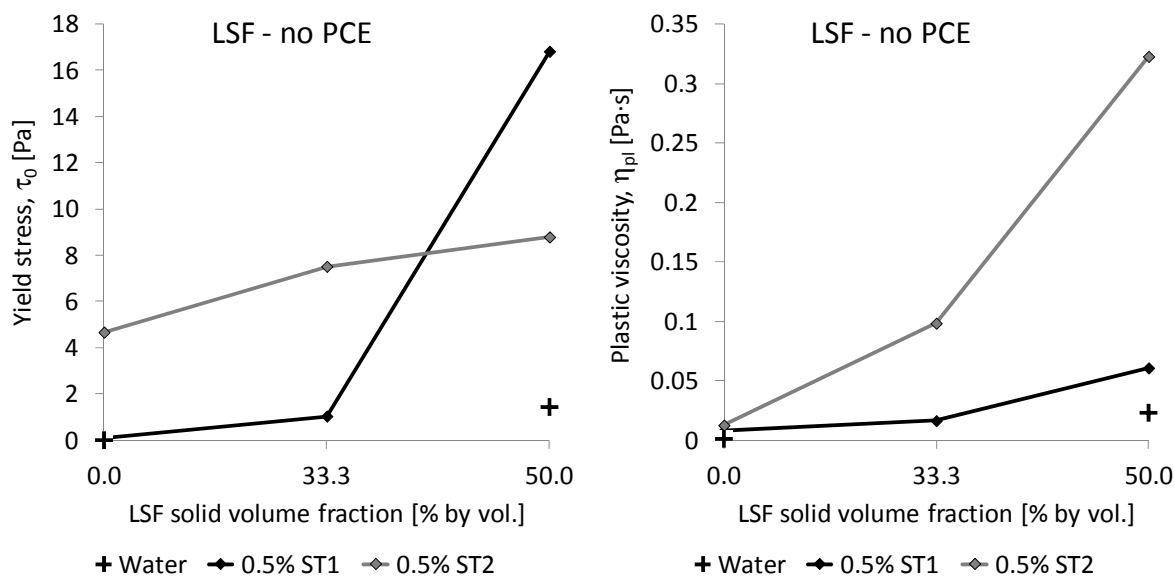


Figure 7.10: The influence of the solid volume fraction on yield stress and plastic viscosity of LSF-water systems without and in the presence of ST1 and ST2).

The diutan gum based ST2 strongly immobilises water and forms a network. Thus, it strongly stiffens the fluid even at no or low solid contents. At higher particle dosages, the network maintains stable so that additional solids do not significantly increase the yield stress. Nevertheless, the strong increase of viscosity at high solid contents points out that also entanglement of the polymers or between polymers and particles takes place, which reduces the mobility of particles.

In the cementitious systems (Figure 7.11), ST1 shows similar behaviour as in the limestone system. At low cement volume, no significant effect on  $\tau_0$  can be observed. For the low dosage of ST1,  $\tau_0$  is even lower than in the reference system without STA. Also  $\eta_{pl}$  is slightly lower than in a system without STA, however, at higher dosage of ST1,  $\eta_{pl}$  is strongly increased due to higher particle volumes.

While in absence of PCE the effect of ST1 is similar in LSF and cement systems, the behaviour of ST2 with different solid types needs further discussion. The influence of the particle solid content on  $\eta_{pl}$  is similar to the LSF system. In case of 0% and 25% cement and 0.5% ST2, also in terms of  $\tau_0$  a similar behaviour can be observed as in the LSF system. At lower dosage of ST2, no significant effect on  $\tau_0$  can be observed. However, at both dosages at 50% particle content,  $\tau_0$  is increased significantly towards values above the yield stress induced by ST1. This is a clear distinction between the LSF system and the cement system. The reason for this might be explained by the stronger attraction forces of the cement (and monosulphate and ettringite in particular) causing higher adsorption of ST2 polymers and stronger bonds, which form bridges between the particles.

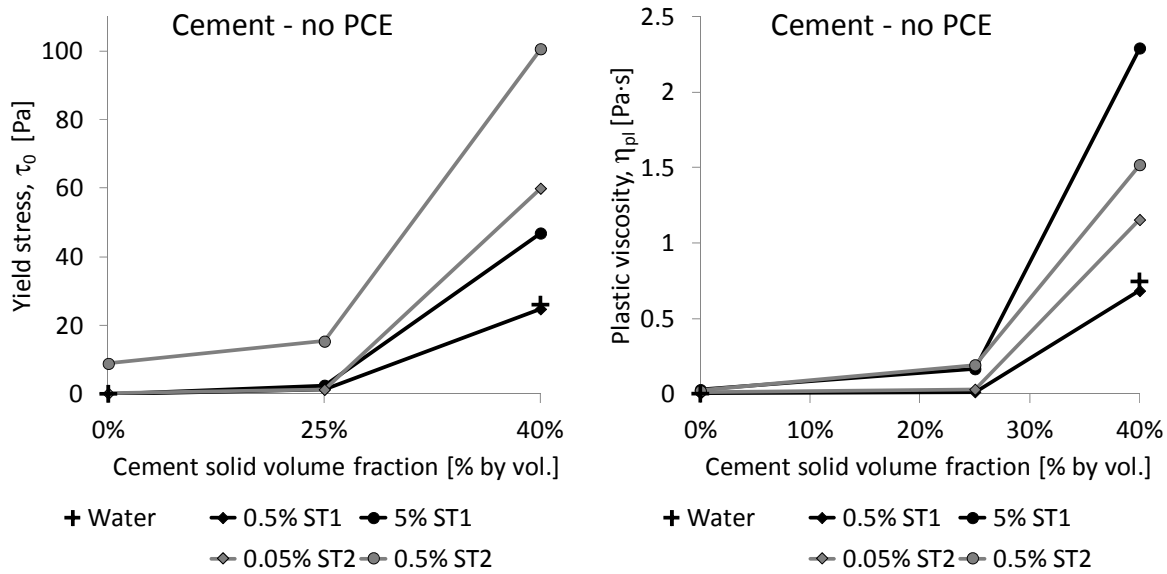


Figure 7.11: The influence of the solid content on yield stress and plastic viscosity of cement-water systems without and in the presence of ST1 and ST2).

It can thus be concluded that the stabilising mechanism of ST1 may be more complex than that of ST2, since the enormous size and the special tree-like structure of the amylopectin supplement the stabilising mechanism by an additional particle-polymer interaction, which is triggered by a threshold particle density. ST2 mainly interacts with the fluid phase of a dispersed system, however, with a major effect on  $\eta_{pl}$  at increasing solid concentrations. In cementitious systems at higher solid concentration, the anionic character of the polymer may cause a strong tendency to adsorb and increase  $\tau_0$  by bridging flocculation by adsorption on more than one particle.

In the presence of PCE the behaviour of both STAs differs (Figures 7.12 and 7.13). Small amounts of PCE already significantly reduce  $\tau_0$  of the pastes regardless of the STA type. Already at the low dosage of 0.06% of PCE in LSF and cement systems, the yield stresses are approximately bisected. It is noteworthy that differing from the LSF system in the cementitious system 0.5% of ST1 exhibits the same yield stresses as cementitious systems without any STA. With further addition of PCE the yield stress values approximate the values of systems without PCE. Above a PCE dosage of 0.3% in the cementitious system, only the system with 5% ST2 can maintain a significantly higher yield stress than the water system without STA.

In the LSF system, the addition of PCE causes an increase of  $\eta_{pl}$  at 0.06% PCE, while a significant drop of  $\eta_{pl}$  can be observed for ST2. The latter effect may be induced by the competitive adsorption of PCEs. Further addition of PCE does not significantly modify  $\eta_{pl}$  values for both STAs in LSF.

In comparison to the LSF systems, the addition of PCE causes a significant drop of  $\eta_{pl}$  in the starch systems. It can be assumed that in the LSF system only little or no adsorption of ST1 takes place, while in the cementitious system more ST1 can be found adsorbed without PCE. Therefore, effects of competitive adsorption occur more pronounced in the cement system. For the systems with ST2 the influence of the PCE is similar in LSF and cement systems with the difference that the slope for the loss of  $\eta_{pl}$  is smaller at low dosages than in the LSF system, which underlines the observation that cement gives a stronger tendency for the ST2 to adsorb.

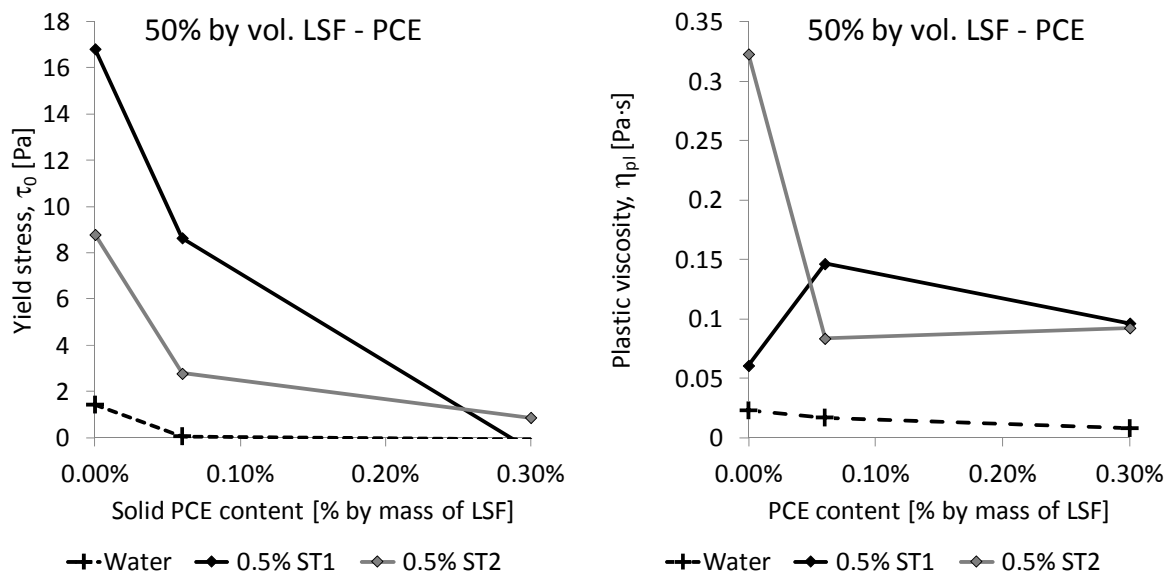


Figure 7.12: The influence of the PCE dosage on yield stress and plastic viscosity without and in the presence of ST1 and ST2 (at a LSF solid volume fraction of 50%).

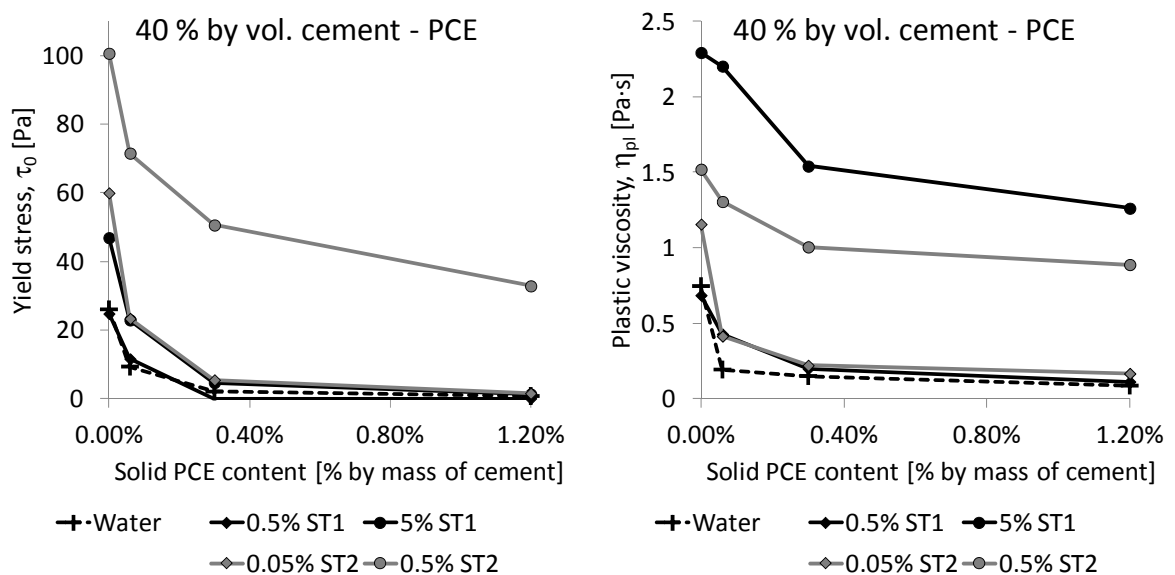


Figure 7.13: The influence of the PCE dosage on yield stress and plastic viscosity without and in the presence of ST1 and ST2 (at a cement solid volume fraction of 40%).

For all mixes with STA,  $\eta_{pl}$  remains higher than in the reference system without water. At the same time with the exception of ST2 at 0.5% dosage at high PCE dosages the effect of the STAs on  $\tau_0$  is small. Different dosages of ST1 only show little effect on  $\tau_0$ , while the increase of  $\eta_{pl}$  at higher dosages is very pronounced. Higher dosages of ST2 affect both  $\tau_0$  and  $\eta_{pl}$  towards significantly higher values.

At dosages of 0.5% for ST1 and 0.05% for ST2, which can be considered as typical values for the stabilisation of cementitious systems, the behaviour of both STAs in presence of PCE is very similar. However, deviating behaviour could be observed for systems without PCE.

The rheometric investigations can only indicate effects, and due to the systems' complexity, it may be impossible to clearly separately observe single parameters that control the effect of stabilising agents. The latter is particularly valid for the starch stabilising agents due to the extremely differing characteristics of amylose and amylopectin. Based on the present results the following main mechanisms are suggested to account for the observed rheological effects.

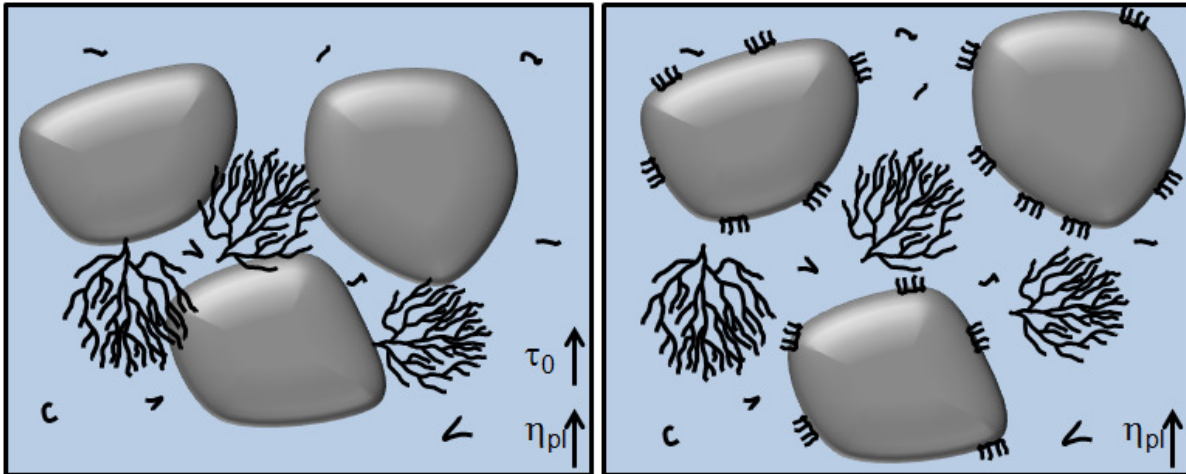


Figure 7.14: Suggested stabilising mechanism of amylopectin without and with PCE. Without presence of PCE (left), the large amylopectin molecules act as buffers between the particles. In presence of PCE(right) the attractive forces between particles and amylopectin are reduced with a strong effect on the yield stress reduction and only a small effect on the plastic viscosity.

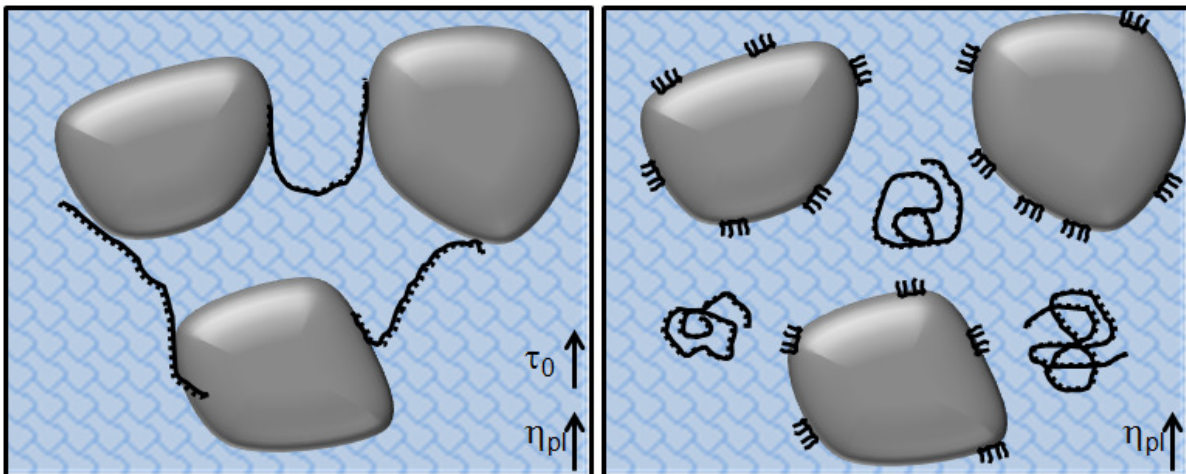


Figure 7.15: Suggested stabilising mechanism of diutan gum without and with PCE. Without PCE addition (left), the diutan gum increases the plastic viscosity and the yield stress of the fluid phase. Bridging flocculation due to adsorbed polymers supplementary contributes to yield stress increase. In the presence of PCE (right) polymers and particles are dispersed. Effects of the increased yield stress of the fluid phase are negligible, while the higher plastic viscosity maintains. The stabilising mechanism is comparable to the mechanism in Figure 7.14, right.

For ST1 it can be concluded that the amylopectin is the main driving parameter for the stabilisation (although supplementary mechanisms may overlap). The stabilising mechanism is considered to be similar to a filler effect with the difference that the filling medium amylopectin remains deformable under shear forces (Figure 7.14). This mechanism requires a sufficient

volume of particles in order to become active. The PCE causes better dispersion of the solids, thus reducing  $\tau_0$  significantly. Since the amylopectin molecules remain in the solution they continue hindering motion between particles, which causes that  $\eta_{pl}$  is largely unaffected by PCE addition in LSF-water systems and that  $\eta_{pl}$  is affected significantly less than the yield stress by PCE addition in cement-water systems (Figure 7.14).

It can be assumed that the major effect of ST2 on yield stress is caused predominantly by water immobilisation, which is the reason why ST2 increases  $\tau_0$  and  $\eta_{pl}$  significantly without solids or only with low solid particle volumes only. At a higher particle volume a rapid increase of  $\tau_0$  can be observed for cementitious systems, which is assumed to be caused by bridging effects due to adsorption (Figure 7.15). Upon addition of SP the adsorption of ST2 seems to be reduced as suggested by Phyfferoen et al. [201]. Therefore, the stabilising mechanism in presence of PCE is very similar to that of ST1 (Figure 7.15). The yield stress is reduced significantly and the viscosity remains higher than in a system without STA. These results underline that in coarsely dispersed systems particle interactions significantly contribute to the stabilising mechanism of starch, while diutan functions by immobilising the fluent phase between the particles and by bridging. Upon addition of high amounts of PCE, however, the effects induced by both STAs are similar.

Compared to diutan gum, starch ether is more complex for the use in cementitious systems, since its performance depends on factors such as the particle size distribution and the water to solid ratio. However, since its influence seems to be more independent from the adsorption of particles, it might less interfere with PCE adsorption. It is therefore obvious that the effects of STA on the rheology cannot be comprehensively understood without observing the entire system.

## 7.4 Influence of stabilising agent on rheology of SCC

### 7.4.1 Experimental procedure for paste tests

In order to examine temperature effects on pastes incorporating STAs, paste tests were conducted with LSF as powder component. LSF was chosen in order to avoid effects of temperature related influences on the hydration rate (see Subsection 7.3). Limestone-water pastes are considered to be largely inert.

1.0% of STA was mixed with water, and the water-STA system was measured with a basket cell as described in Subsection 4.3.9. Furthermore, mixtures containing 33.3% by volume of LSF and 66.7% by volume of water were measured likewise. The programme can be seen in Figure 7.16. The basket cell is not specifically constructed to measure low viscous liquids. The measuring principle of the basket cell is based on the assumption that the interface between sensor and fluid is characterised by the cohesion of the fluid [223]. In case of very low viscous systems such as water but also the water-STA fluids, the basic boundary conditions for the measurement are not fulfilled. Hence, the measurement results for the water-STA systems cannot compare to real rheological data of water.

The graph in Figure 7.16 on the right side shows flow curves from measurements with the basket cell of pure water at varied temperature compared to flow curves with viscosity values taken from a textbook [286], namely 1.52 mPa·s at 5 °C; 1.00 mPa·s at 20 °C; 0.80 mPa·s at 30 °C. It can be seen that the intersection with the ordinate does not occur at a value of zero as it should for a Newtonian fluid like water. Also the curve slopes representing the viscosity (see Subsection 3.1.1) are much steeper than in case the literature values for water are used. Nevertheless, the qualitative differences between the literature values and those measured with the basket cell are very similar. Since for the limestone-water suspensions the basic conditions

for a fluid in fluid shearing can be fulfilled, it can be assumed that these results can be considered as fundamental values.

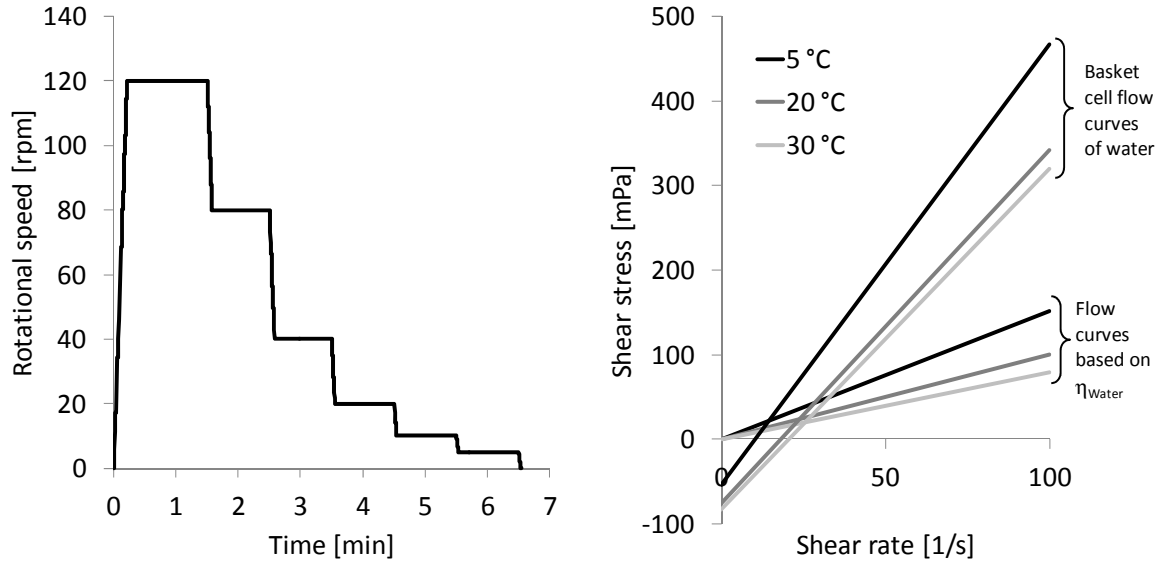


Figure 7.16: Measurement setup for paste measurements with basket cell and comparison of results for pure water.

#### 7.4.2 Experimental procedure for concrete tests

The rheometric tests focusing on the STA in concrete were conducted exactly similar to Section 6.3.

#### 7.4.3 Influence of temperature on limestone filler paste

Figure 7.17 shows the results of the limestone paste measurements for systems with water and STA as well as for systems with water (67% by volume), LSF (33% by volume), and STAs. All systems were investigated without PCE. The dosage of the starch based ST1 was 1% by mass of water. The dosage of the diutan gum based ST2 was 0.05% by mass of water. The ratio of ST1:ST2 was 1:20 based on the approximately 20 times higher efficiency to increase the viscosity of ST2 in the paste (Subsection 4.1.5). Differing from the investigations in Subsection 4.1.5, for the temperature tests, the dosages were brought to realistic values in terms of concrete mixtures. In a comparable manner as already shown in Subsection 4.1.5 and Figure 4.4, ST1 does not generate a significant yield stress in water, while ST2 does. The addition of solids increases the yield stress of the system with ST1 prominently, while the yield stress of the limestone pastes with ST2 increases only slightly. This emphasizes the different modes of stabilisation as discussed in Section 7.3. There is no clear effect of the temperature that would put this mechanism into question.

Nevertheless, temperature effects can be seen, which can be observed for ST1 and ST2. For both, a higher viscosity can be observed at 5 °C in the watery system as well as in the suspension, while there is no significant effect observable between 20 °C and 30 °C. The yield stress of the LSF suspensions behaves adversely to the viscosity. It is lower at 5 °C while higher values can be observed at 20 °C and 30 °C, where yield stress shows similar values with both STs. This might be explained that a slightly higher viscosity of the fluid phase may keep particles at distance, thus slightly reducing the yield stress. Since these effects occur qualitatively similarly for both STs it is likely that these effects can be mainly attributed to the

behaviour of water. The viscosity of water at 5 °C is 1.52 mPa·s, at 20 °C it is 1.0 mPa·s, and at 30 °C it is 0.80 mPa·s. This means that the viscosity change between 20 °C and 30 °C is small, while at 5 °C water is significantly higher viscous than at 20 °C. The rheometric tools do not allow distinguishing between the values at 20 °C and 30 °C but the higher viscosity of the water at 5 °C can be clearly identified.

In general, the differences in yield stress and viscosity that can be observed due to temperatures in inert systems can be considered as minor. It is therefore assumable that there is no effect of temperatures in the range between 5 °C and 30 °C that affects the polysaccharides' performance in a critical way.

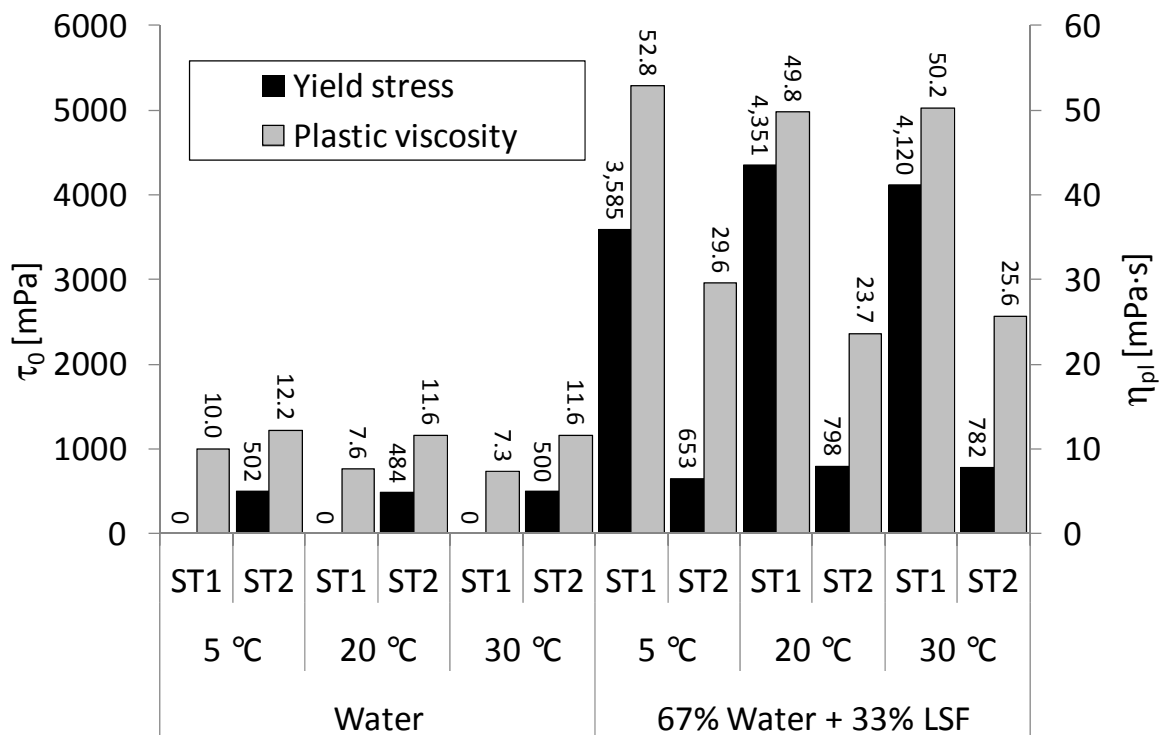


Figure 7.17: Effect of temperature on ST1 and ST2 with water and with water-LSF suspensions. In order to assess the viscosity increasing effect of the stabilising agents: the viscosities of pure water at 5 °C, 20 °C, and 30 °C are 1.52 mPa·s, 1.00 mPa·s, and 0.80 mPa·s, respectively.

#### 7.4.4 Influence of stabilising agents on combination type SCC

In a full scale concrete system, incorporating cement and coarse aggregates the effect of the STAs have different quality than in the pure LSF suspensions. Besides temperature effects on the STAs, temperature effects determining the performance of the differently charged PCEs need to be taken into account.

Figure 7.18 shows the effects on the combination type SCC COM (Tables 4.9 and 4.10) that can be observed at 5 °C based on the G-yield and H-viscosity values (see Subsection 4.3.7). G-yield and H-viscosity qualitatively correspond to the yield stress  $\tau_0$  and the plastic viscosity  $\eta_{pl}$ .

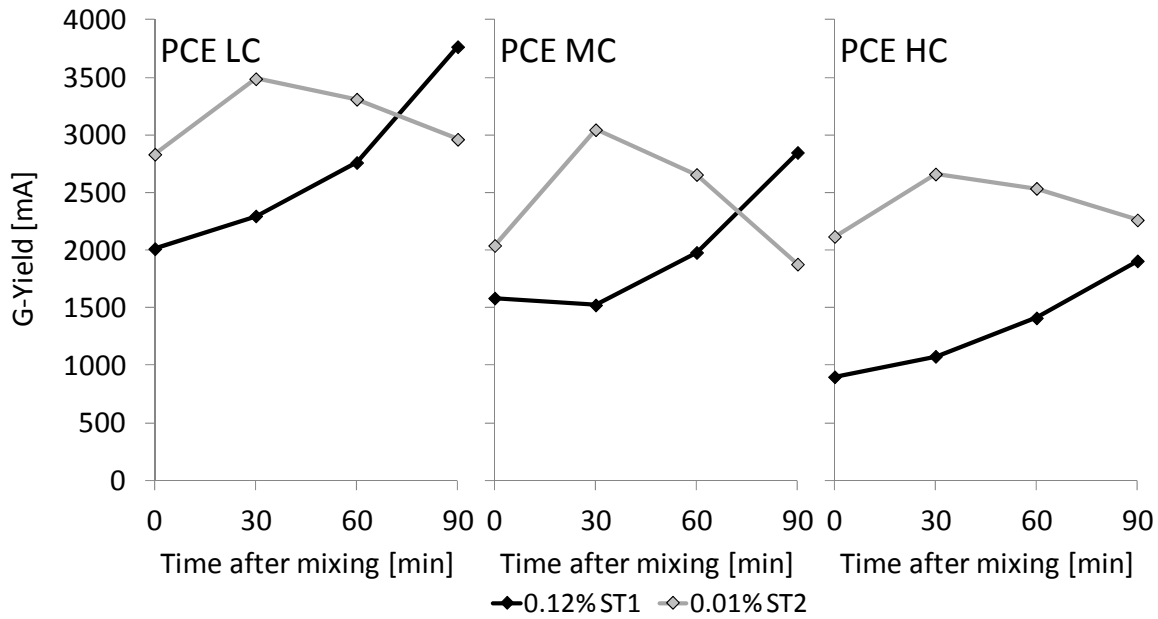


Figure 7.18: G-Yield over the course of time of COM SCC at 5 °C with ST1 and ST2.

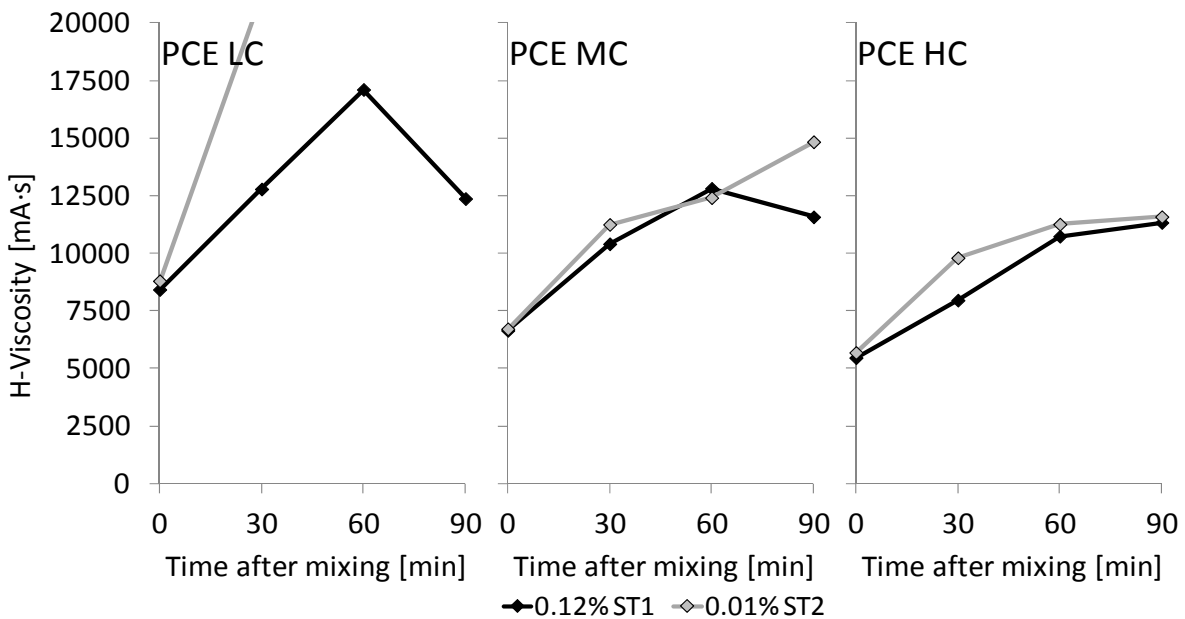


Figure 7.19: H-Viscosity over the course of time of COM SCC at 5 °C with ST1 and ST2.

Therefore, increasing G-yield values correspond to reduced slump flow values and increasing H-viscosity values correspond to longer flow times and vice versa. An effect that is directly obvious is the reduction of the yield stress due to increasing charge density of the PCE. This effect was already discussed in Chapter 6. The smaller the charge density, the smaller the amount of adsorbed PCE on aluminate and ferrite phase on the clinker grains. At low temperatures, the hydration is drastically slowed down, hence, the major adsorption sites for PCE occur in significantly reduced amounts, so that only few PCEs adsorb with time. Therefore higher charged PCEs reduce yield stress more effectively. This observation can be made regardless of the STA type.

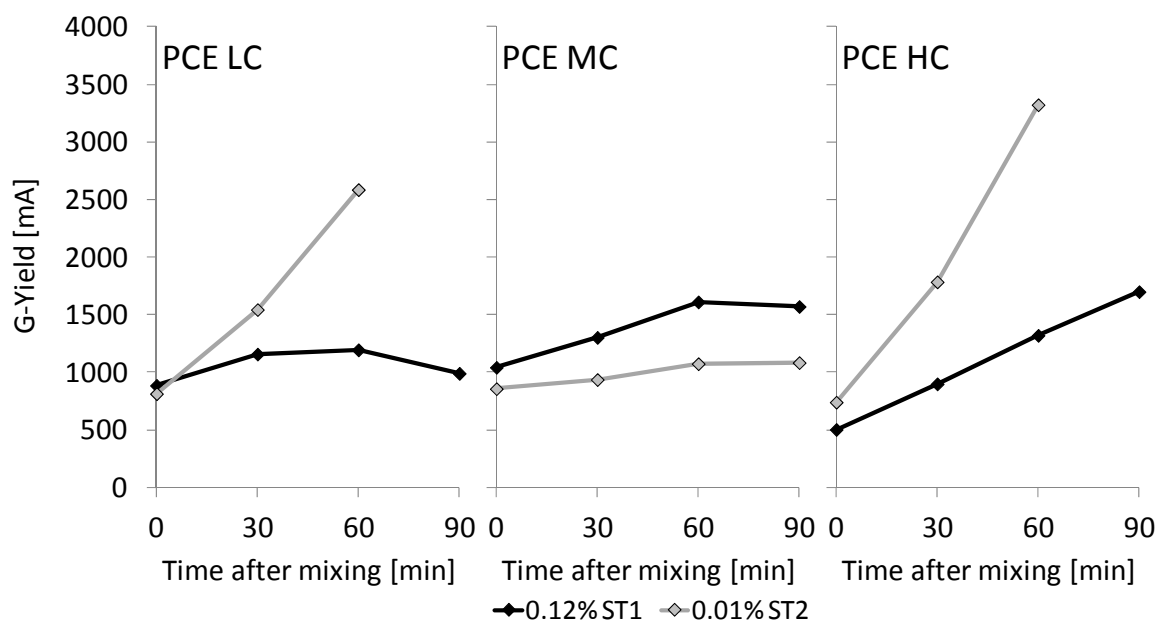


Figure 7.20: G-Yield over the course of time of COM SCC at 20 °C with ST1 and ST2.

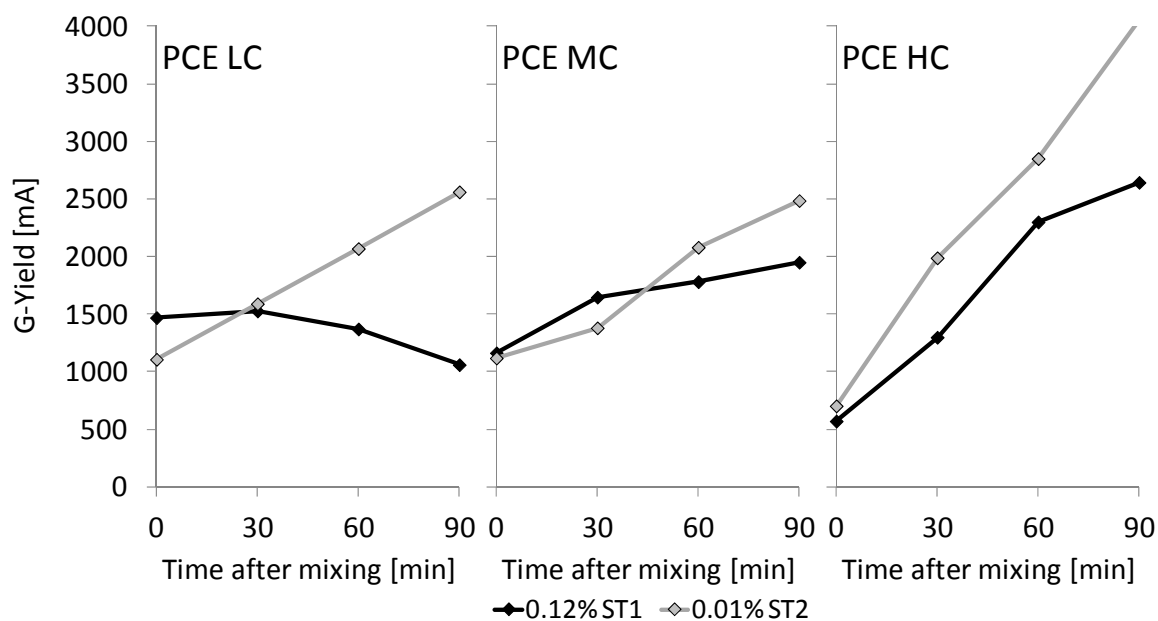


Figure 7.21: G-Yield over the course of time of COM SCC at 30 °C with ST1 and ST2.

Each STA shows characteristic behaviour with time. The yield stress with ST1 increases steadily with time, while the yield stress with ST2 increases between 0 and 30 minutes and then reduces steadily until at 90 minutes values close to the initial values can be measured. After 90 minutes, the values of the mixes with ST2 are lower than with ST1 in case of PCE LC and PCE MC. With PCE HC both values are similar at that time.

Since the time dependent behaviour of each STA is very similar while there is only a parallel shift induced by the charge density of the PCE, it can be concluded that at 5 °C the effects of PCE and STA largely overlap. The performance is mainly driven by the PCE's performance. As discussed in Chapter 6.5.3, a low charge density PCE does not adsorb in sufficient amounts to

keep particles of a combination type mixture stable. The amount of STA that is required to provide good flow performance at 20 °C cannot effectively stabilise the system at 5 °C. Segregation can thus be observed at 5 °C with the low charge PCE for both STAs. As a result of the segregation, the measured viscosities of these mixtures are high (Figure 7.19). With the medium and the low charge density PCE, the SCCs are sufficiently stable as already shown in Chapter 6.4.5. In this case, the influence of the STA type on the concretes' viscosities is low. Viscosities increase sharply until 60 minutes and then stabilise. The lowest viscosities can be observed with the highest charge density PCE but the behaviour does not differ strongly from the behaviour of the SCC with PCE MC. The characteristics of the time dependent behaviour of PCE MC and PCE HC are identical.

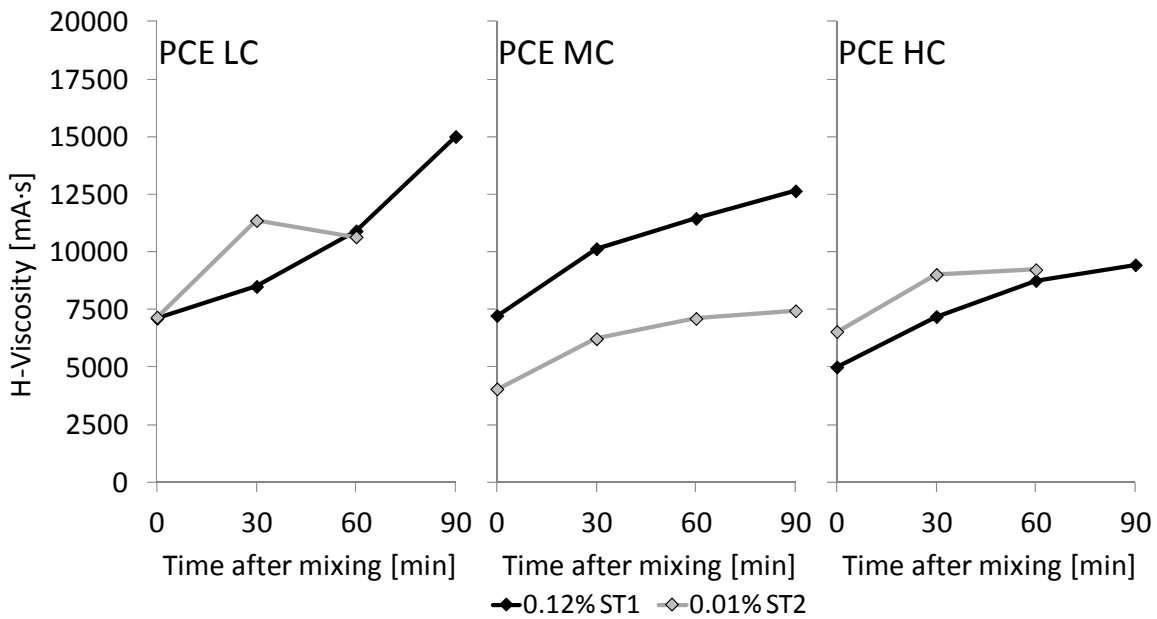


Figure 7.22: H-Viscosity over the course of time of COM SCC at 20 °C with ST1 and ST2.

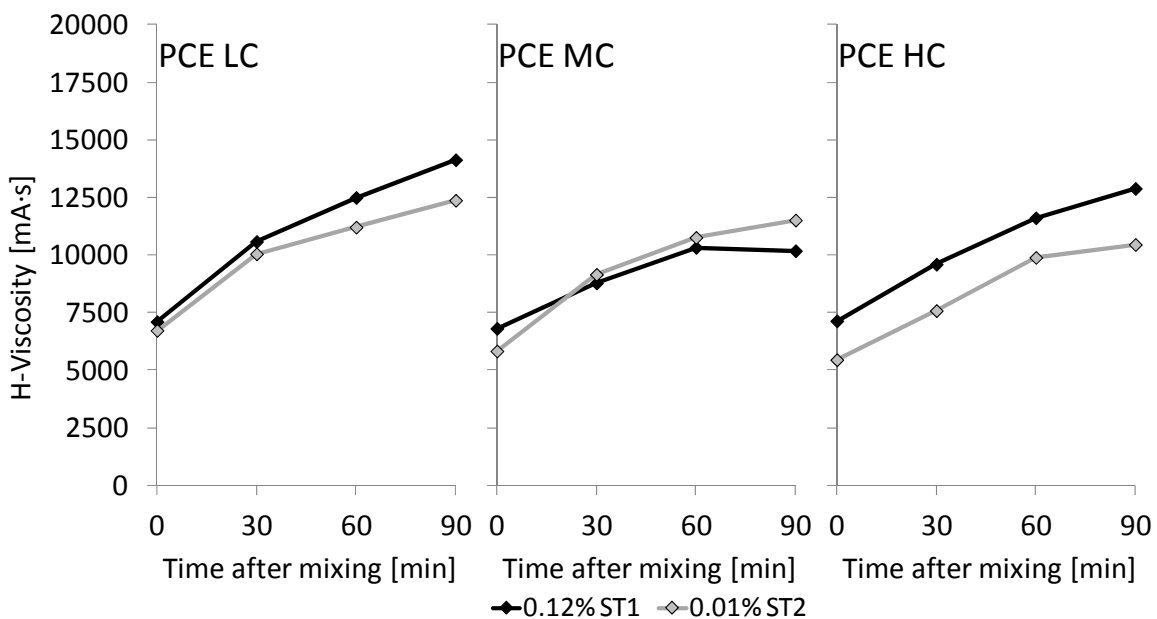


Figure 7.23: H-Viscosity over the course of time of COM SCC at 30 °C with ST1 and ST2.

The Figures 7.20 and 7.22 show the influence of different STAs on SCC with varied PCEs at 20 °C and 30 °C, respectively. The observations at both temperatures are very similar. Different charge density affect the time dependent yield stress differently, however, the influences compare at both temperatures with the only distinction that the yield stress increases slightly quicker with time at the higher temperature.

With the only exception of the mixture with PCE MC at 20 °C, in all cases the yield stress increases significantly more pronounced with time when ST2 is used. This can be observed although there is no crucial influence in these mixtures of the PCE type or the STA on the viscosity, as can be seen in Figures 7.22 and 7.23 for 20 °C and 30 °C, respectively. The SCC with PCE MC and ST2 at 20 °C behaves unusual (Figure 7.20, centre), since the yield stress maintains stable and therefore lower than with ST1 throughout the whole observation time. This observation can be a result of the specific effect taking place between the two different polymers at this particular admixture setup. However, considering that the same effect cannot be observed at higher temperature and for all other admixture setups the differences between 20 °C and 30 °C are low, this appears unlikely. Taking a look at the respective viscosity (Figure 7.22, centre), which is also significantly lower for the setup with PCE MC and ST2 at 20 °C, while the influence of STAs apart from that is always very low, it is becoming more likely that this mixture may have been faulty during the test. Apart from the mentioned SCC with PCE MC and ST2 at 20 °C, the time dependent characteristics of the plastic viscosity is similar regardless of the charge density of the PCE, the STA type, or the temperature (Figures 7.22 and 7.23).

#### 7.4.5 Influence of stabilising agents on powder type SCC

Powder type SCC is typically not very sensitive to segregation. Nevertheless, the use of small dosages of STA has become practice in order to increase the robustness against external effects. For the POW mixtures (Table 4.9) the influence of the STA depending on the temperature and the charge density of the PCE was largely negligible for the powder type mixtures. At 5 °C, the performance of all SCC mixtures is similar throughout the whole time (Figures 7.24 and 7.25). As shown in Chapter 6, the powder rich SCC mixture performs very stable at 5 °C, regardless of the charge density of the PCE. STA is only used in very small amounts here (Table 4.10) so that its influence can be neglected.

As could be observed for the combination type SCC, the performance of SCC at 20 °C and 30 °C is comparable, with the only exception that yield stress increases slightly quicker at the warmer temperature (Figures 7.26 and 7.27). The influence of the STA again, is negligible. The major driving force for higher or lower yield stress, and better or worse retention of the yield stress is the charge density of the PCE. With high charge density, the retention time is diminishing, as already discussed in Chapter 6.

The viscosity results (Figures 7.28 and 7.29) are less systematic. The scatter in the results is generally much larger. It has to be considered that the precision regarding the viscosity results yielded by measurement from Rheometer-4SCC is lower than for the yield stress (see also Subsection 4.3.7 and Figure 4.18). It seems that effects of the PCE modification are of more importance in mixtures with a dense particle packing, since the PCE is the major driving force for the liquefaction. Therefore, the STAs might show different effects on the viscosity depending upon the charge density of the PCE. There is, however, no systematic influence depending on temperature, time, or charge density of the PCE identifiable.

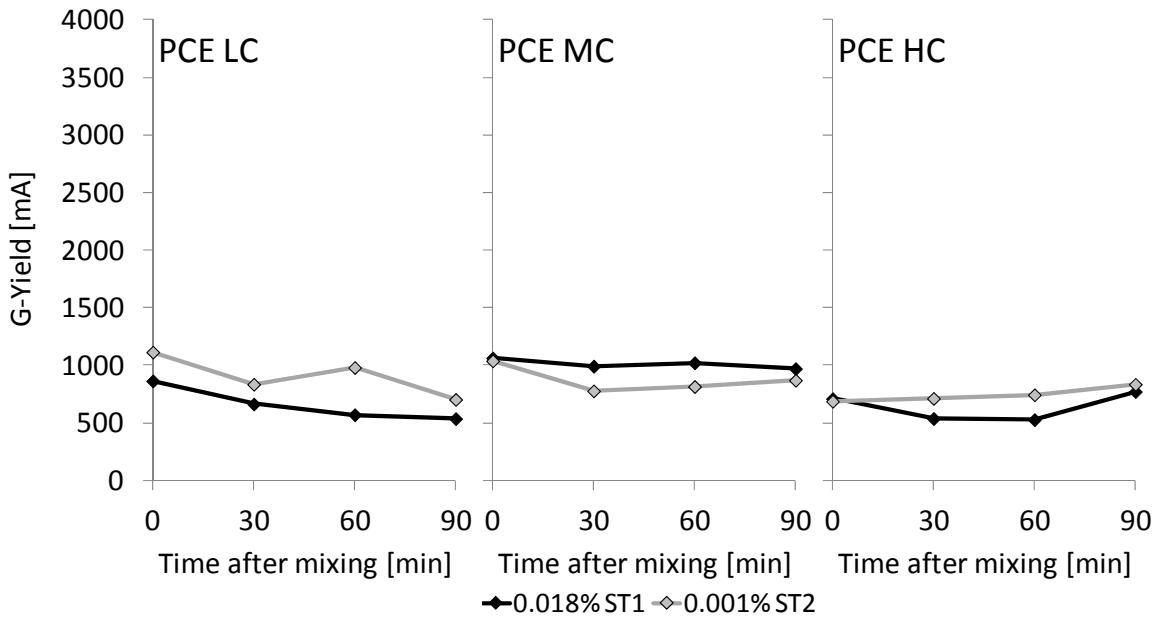


Figure 7.24: G-Yield over the course of time of POW SCC at 5 °C with ST1 and ST2.

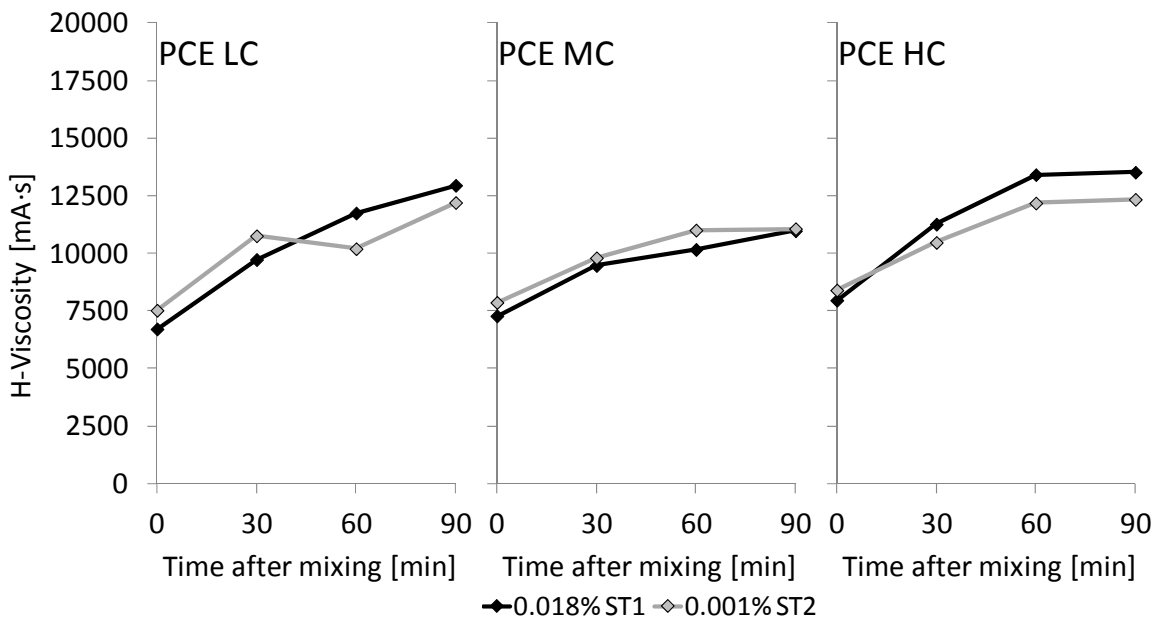


Figure 7.25: H-Viscosity over the course of time of POW SCC at 5 °C with ST1 and ST2.

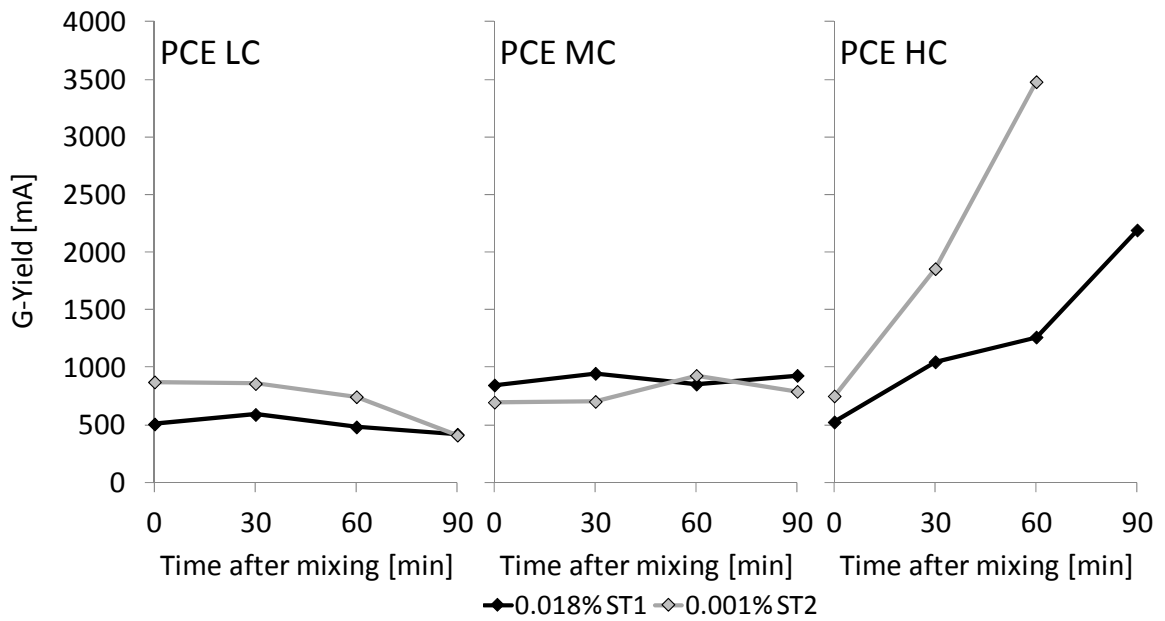


Figure 7.26: G-Yield over the course of time of POW SCC at 20 °C with ST1 and ST2.

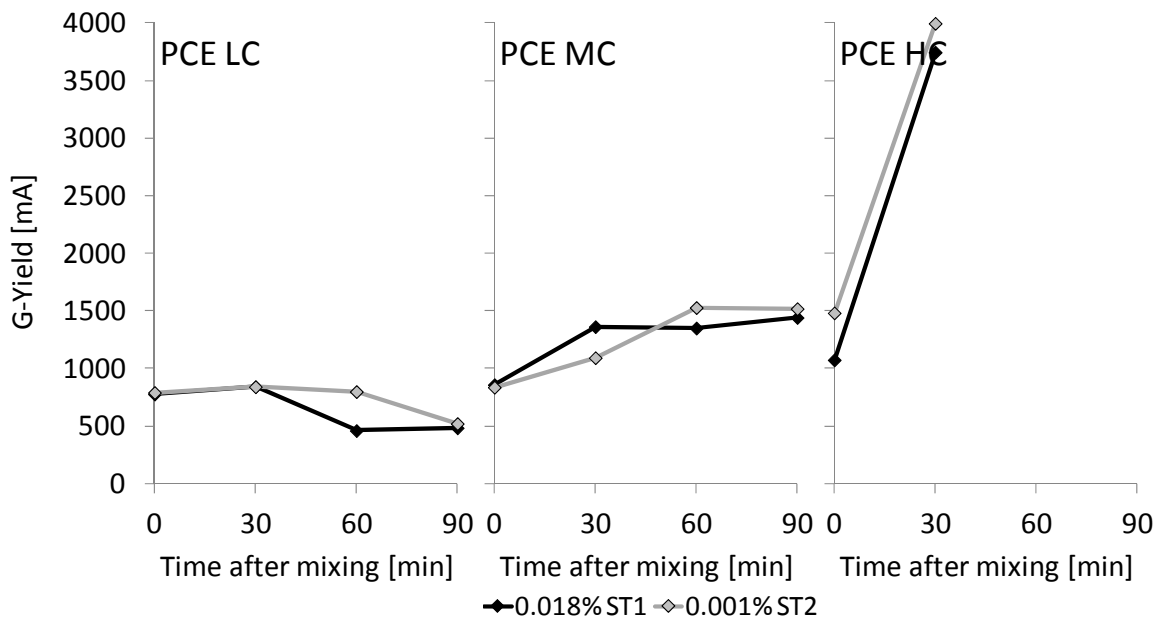


Figure 7.27: G-Yield over the course of time of POW SCC at 30 °C with ST1 and ST2.

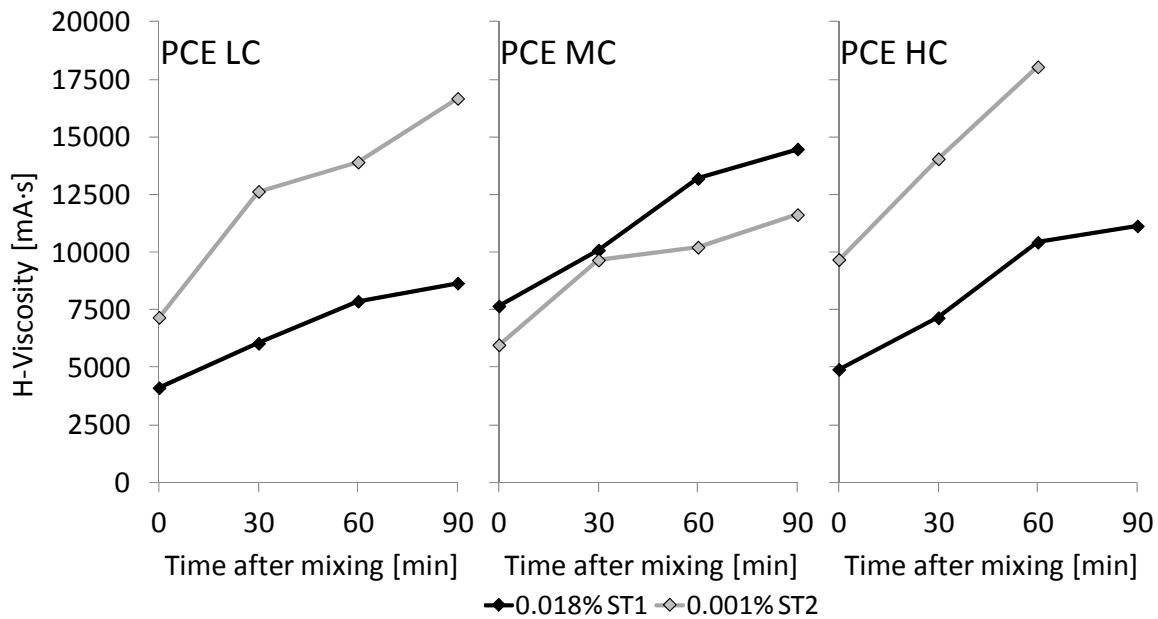


Figure 7.28: H-Viscosity over the course of time of POW SCC at 20 °C with ST1 and ST2.

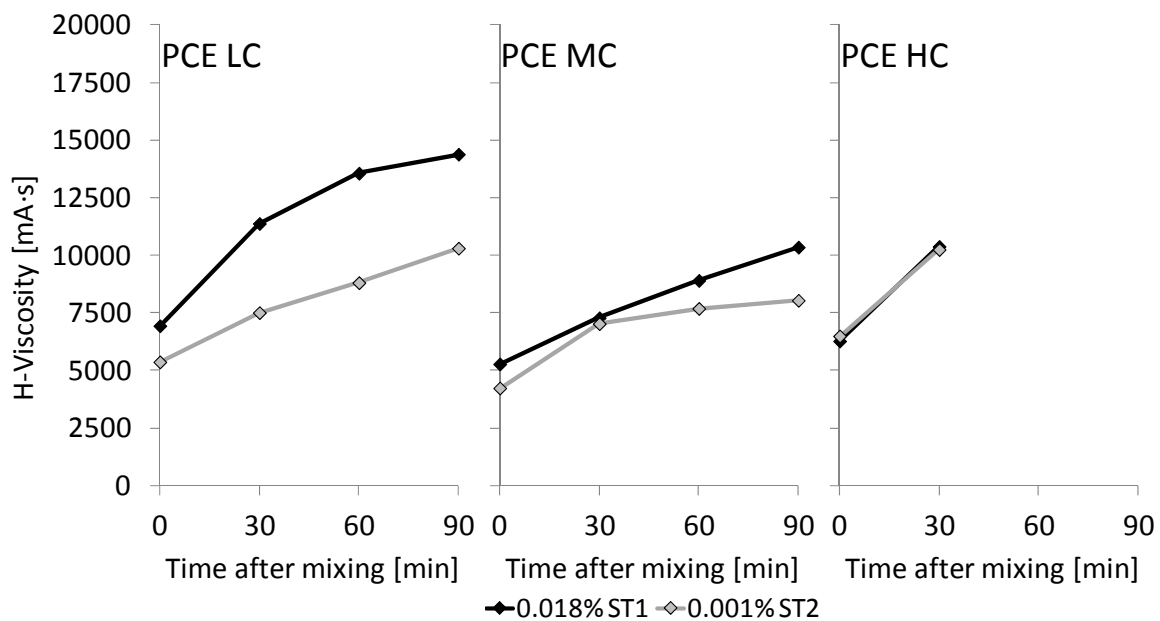


Figure 7.29: H-Viscosity over the course of time of POW SCC at 30 °C with ST1 and ST2.

#### 7.4.6 Discussion of the observations

For the powder type SCCs a systematic temperature effect cannot be identified, but a clear distinction can be made between cold (5 °C) and high (20 °C and 30 °C) temperatures. The only effect that can be observed between 20 °C and 30 °C is quicker stiffening due to accelerated hydration processes. At 5 °C, effects of PCE and STA occur clearly distinctive and supplementary (Figure 7.18). The time dependent characteristic behaviour of the yield stress is similar with all PCE modifications, while the PCE charge density determines the initial yield value. With ST1, a steady increase of the yield stress with time can be observed, which indicates that PCE and ST1 do not mutually interfere. This seems to be different in case of mixtures with

ST2, which shows a maximum yields stress at 30 minutes and a subsequent prominent reduction of the yield stress, regardless of the PCE type. A time dependent reduction of yield stress signifies that time-shifted adsorption of PCE takes place. It seems that at cold temperatures the hydration is very slow so that the quick increase of yield stress during the first 30 minutes cannot be explained by a full consumption of PCE molecules. The latter would also be unlikely, since this effect takes place regardless of the PCE type and amount. The fact that increasing PCE charge densities cause lower initial yield stresses suggests that adsorption takes place, which is driven by electrostatic forces. The initial yield stress using ST2 is always significantly lower than with ST1 regardless of the PCE charge density. This indicates that in the presence of ST2 a smaller amount of PCE is adsorbed. The mechanism behind the latter observation can be a link between the anionic ends of PCE and ST2 through positively charged ions such as  $\text{Ca}^{2+}$ . The occurrence of cohesion between different anionic polymers in high metal salt concentrations as in the pore solution of cementitious systems was also shown by Izumi [262]. The additional increase of the yield stress during the first 30 minutes may be caused by adsorption of the STA at the expense of PCE. The time-shifted reduction of yield stress can then be caused by new adsorption sites generated by the ongoing hydration or changes in the solution chemistry with time, which loosens existing links between the polymers.

Apart from a slightly quicker hydration reaction and thus the shorter performance retention, the observations at 20 °C and 30 °C for the combination type SCC are similar. Mixtures with ST2 show poorer yield stress retention than with ST1 although the viscosity is not affected. This also indicates that there is a certain effect of the anionic charges of these polymers. A reasonable explanation for such an effect would be the delayed adsorption of the anionic ST2 on particles, which reduces the effectiveness of SPs. This would increase the yield stress, while the effect on viscosity caused by the large size molecules would remain similar to the effect induced by ST1.

In general, it can be observed, that both STAs show little effect on the viscosity of combination type SCC in case the system is largely stable (which confirms the use of the terminology STA used in this Thesis rather than viscosity modifying agent). The major determining factor for the yield stress remains the charge density of the SP in case of both STAs but the anionic charges of ST2 furthermore seem to interact with PCE molecules, having negative effect on the performance retention. This observation applies likewise for the powder type SCC.

Also the temperature shows little effect on the viscosity of the combination type SCC, but substantially affects the yield stress. Higher initial values but also better retention can be observed at low temperatures, and the opposite effect at higher temperatures with increasing magnitude with increasing temperatures. This, however, is driven by charge density effects of the PCE as discussed in Chapter 6.

In case of powder type mixtures no direct effects of the STAs on yield stress or viscosity can be observed. These mixtures contain only a negligible content of STA so that any interaction between STA and PCE can be considered as negligible compared to the predominating effect of the PCE modification.

The domination of the PCE with regard to the temperature related performance also accounts for the fact that the SCC observations do not reflect the results from the rheometric paste tests. The paste tests showed low yield stress and higher viscosity at cold temperatures for both STAs. This occurred exactly inverted in concrete. It is clear that the yield stress is mainly driven by the charge density of the PCE, so that any possible effect of the STA disappears. In concrete systems, the whole system determines the viscosity. So, the small amount of STA cannot modify the system to an extent that is measurable. This clearly indicates that observations about STAs made in rather liquid systems do not inevitably have to be viable in denser systems.

## 7.5 Conclusions

Investigations were conducted to demonstrate the difference in the stabilising mechanism of the two selected STAs, based on potato starch ST1 and diutan gum ST2. It was shown that it is very important to distinguish between flowable systems with and without PCE.

In systems without PCE, each STA shows a characteristic influence on yield stress and plastic viscosity. Upon addition of PCE, the influence of the STAs on the yield stress of suspensions minimise, while effects on viscosity are partly maintained. While PCE does not strongly affect the viscosity in the presence of ST1, a significant drop of viscosity could be observed with ST2 in the presence of already small amounts of PCE. The latter effect can be explained by ST2 that entangles the particles by adsorbing on their surfaces when no PCE is present, while this entanglement is largely avoided in the presence of PCE.

In rheometric investigations with water and LSF suspensions, minor effects of the two observed STAs with temperatures could be observed. While no distinct difference between 20 °C and 30 °C could be observed for yield stress and viscosity, at 5 °C the yield stresses were lower and viscosities higher, regardless of the stabilising agent type.

The paste observations, however, could not be found in the concrete tests. It is likely that other effects, which originate from the integral mixture composition, control the viscosity, while effects of the PCE are outperforming any other effect on the yield stress performance.

All observable effects induced by STAs were related to yield stress effects. No significant effects could be observed for the viscosity characteristics with time. This applies for the STA type as well as the charge density, and the temperature.

Due to the negligible additions in the powder type SCCs, effects of the STA were negligible at all temperatures. The only observable temperature effects were caused by the charge density of the SP.

No specific influence of the non adsorbing STA could be found with regard to temperature effects. The adsorbing ST2 showed influences that vary at 5 °C from those that could be observed at 20 °C and 30 °C.

At 5 °C, SCC with ST2 showed higher initial yield stresses than with ST1. The yield stress increased to a maximum at 30 minutes and subsequently dropped again. The observations suggested that interactions between the anionic backbones of both polymers take place, which determine the time dependent behaviour.

The behaviour at 20 °C and 30 °C only differed in the time dependent flow characteristics. The yield stress happened quicker at higher temperature due to the hydration acceleration. In both cases ST2 caused quicker loss of yield stress than ST1. This effect can be explained by the adsorption of the STA with time, which quicker reduces the effectiveness of the SP.

Concluding, the effects resulting from different temperatures on STAs are significantly less important than those induced by the charge density of the PCE. The non-adsorbing ST1, based on potato starch, can better maintain a low yield stress than the anionic ST2, based on diutan gum. It is likely that this effect is mainly attributed to interactions with PCE.

## 8 Influence of PCE on the early hydration

### 8.1 Introduction

The adsorption of superplasticisers (SPs) based on polycarboxylate ether (PCE) on mineral phases and on hydration products of cement has a strong influence on the yield stress of cementitious systems. This was described in detail in Chapters 3 and 6. The driving force for the reduction of the yield stress is the amount of adsorbed SP molecules [66]. The adsorption process is influenced by the charge density of the polymers [63, 87]. The main factor determining the backbone charge is the molecular structure of the PCE molecules, particularly the grafting degree and the graft length. Charged adsorption sites rather attract a higher number of lowly charged than highly charged polymers. Hence, when a specific flow value needs to be achieved for a cementitious system, a low charge PCE requires a higher amount of solid polymers than a high charge PCE. Typically, high charge density polymers provide maximum flowability quickly upon addition, but the performance retention is poor, as they are also quickly consumed by the continuing hydration process. Low charge density polymers on the other hand, typically do not provide ultimate flowability and their effect on yield stress is limited, but they can maintain flow performances for a longer period of time, since they adsorb with retardation [131, 287].

The influence of PCE on the early hydration is not limited to the period in which the workability properties are of importance. It is known that an increasing amount of PCE prolongs the induction period and retards setting [115, 264, 288]. The reason for the prolonged induction period due to SP addition remains controversial. Effects that are reported in literature are hindrance of  $C_3S$  dissolution, possible calcium ion complexation, prevented C-S-H precipitation, and changed growth of hydrates [64, 289, 290].

The setting behaviour can vary dependent on the PCE type [131, 264]. It was observed that at identical amounts of PCE, cement mixes with low charge density polymers exhibit earlier setting than mixes with high charge density polymers [131]. As such, it is becoming clear that both amount and type of PCE greatly determine the early hydration characteristics and related effects, such as heat evolution and setting. The knowledge about the influence of the PCE molecular structure on early deformations, however, is limited. This chapter highlights effects of the polymer structure of the PCE on early properties of cementitious systems. Results from calorimetry, X-ray diffraction (XRD), Vicat needle penetration test, as well as from observations of the autogenous deformations during the first 48 hours are presented and discussed with relevance for the concrete scale.

### 8.2 The early hydration of ready-mixed SCC

#### 8.2.1 Specific aspects of SCC

As described in Section 2.1, there is still controversy concerning the early hydration of cement. Major matters of discussion are whether the induction period is purely controlled by dissolution and precipitation processes or if a metastable barrier is formed as interim phase (Subsection 2.1.2) and which processes are responsible for the onset of the accelerated period (transition from phase 2 to 3 in Figure 2.1). Fundamental research can only be conducted in pure systems. Already two different ordinary Portland cement pastes may yield completely different results, depending among others upon the alkali content, the clinker phase composition, the modification and solubility of the gypsum, the particles' fineness, and the water to binder ratio. Hence, observations on the early hydration period of pastes can only partly reflect the behaviour of even

much more complicated systems. Concrete systems supplement the complexity of cement paste systems by influences of the water absorption, the shape and size distribution of the aggregate, influences of fillers, and a variety of water to cement ratios. Nevertheless, observations in the paste system should at least qualitatively yield representative results. This means if a specific parameter accelerates or slows down the hydration in a cement paste this is likely to occur in concrete systems at least qualitatively as well, as long as no other critical parameters change.

Self-compacting concrete is even more complicated than normal concrete, as high volumes of constituents that can affect the hydration are used, such as additions and admixtures. Furthermore, the total binder content, which mainly determines early hydration processes, is typically higher than in ordinary concrete. Hence, effects can be expected to occur at a higher magnitude in SCC. If furthermore SCC is considered from a construction site application point of view, attention needs to be paid to the influences of the environmental conditions of which the temperature can be considered as the most crucial one.

### 8.2.2 Influence of calcium carbonate on early hydration effects

SCC is typically designed with a higher powder volume than ordinary concrete. The powder content above the necessary cement content is typically amended by a variety of inert or reactive fillers. Several authors have put emphasis on the early hydration of cements blended with ground granulated blast furnace slag, (e.g. [125, 291, 292]), fly ash (e.g. [293, 294]), silica fume (e.g. [295-297]), or even more complicated systems with combined additions (e.g. [298-300]). The mixture compositions observed in this work contain LSF as supplementary powder component.

Both mixtures as formulated in Subsection 4.2.2 contain high amounts of limestone filler (LSF), hence a significant amount of calcium carbonate is added to the system, which needs to be taken into account. Though often considered as inert filler, limestone is reported to strongly modify the hydration of cementitious systems. Ramachandran investigated the effect of limestone additions on  $C_3S$  and  $C_3A$  plus gypsum and observed accelerated hydration of  $C_3S$  as well as an accelerated formation of ettringite [301]. Stark and Gathemann [302] as well as Pera et al. [303] present calorimetry curves that give evidence about the accelerated hydration process. According to Lothenbach et al. [119] this is caused by the additional surface that is provided for the nucleation and growth of hydrates. Ye et al. investigated the microstructure of different cementitious systems including two types of SCC pastes and observed the heat of hydration by calorimetry, the phase evolution by TGA and the structural changes by backscatter scanning electron microscopy [304]. They found that the LSF did not participate in the chemical reactions of the cement hydration but acted as accelerator during the early hydration. Craeye et al. investigated the autogenous shrinkage of cementitious systems with LSF and concluded that LSF accelerated the hydration and caused an earlier “time zero”, which they defined as the time at which the formation of a solid structure was assumed from ultrasonic transmission testing [294]. The phenomenon of building a solid structure at the thus defined “time-zero” is similar to what happens at the time of the final setting  $t_{fin}$  (see Subsection 4.4.1).

The faster hydration can also be observed indirectly by accelerated early strength development, e.g. as shown by Voglis et al. [305]. According to the research of Vuk et al., the effect of limestone also depends on its fineness [306]. While coarse limestone mainly accelerated the early strength development, more finely ground LSF had further effect on the setting as well as the final strength.

By thermodynamic calculations Lothenbach et al. [119] show that the addition of LSF in a cementitious system yields predominantly monocarbonate ( $C_4A\bar{C}H_{11}$ ), instead of monosulphate ( $C_4A\bar{S}H_{12}$ ), which in return stabilises ettringite ( $C_6A\bar{S}H_{32-36}$ ), at the expense of monosulphate [119]. According to Lothenbach et al. [119] and Damidot et al. [299], upon addition of  $CaCO_3$ ,

first hemicarbonate ( $C_4A\bar{C}_{0.5}H_{12}$ ) will be found, and with an increasing content of  $CaCO_3$  monocarbonate occurs in increasing amounts until a maximum threshold level is reached. A major part of the presented results focuses on the time until the maximum peak of the heat flow curve occurs, hence, the formation of monocarbonate may be of minor interest in this chapter, since the formation of monocarbonate does not start before the second day of hydration ([119], Figure 8.1).

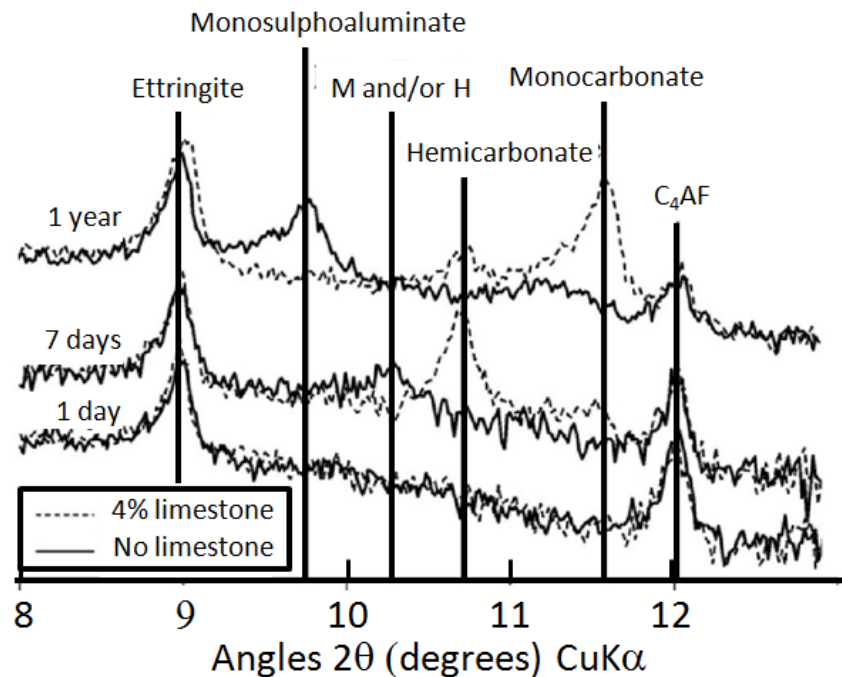


Figure 8.1: XRD patterns of mixes with and without  $CaCO_3$  at different stages of hydration after Lothenbach et al. [119].

### 8.2.3 Influence of temperature on early hydration

Temperature effects have been discussed in Chapter 6 with regard to the workability properties. In general, the temperature accelerates or slows down the hydration, as for instance formulated by Petit et al. [242, 244]. These observations are confirmed by Hesse et al. [307], who used XRD measurements at varied temperatures to study their effects on the hydration.

Mounanga et al. [308] have shown that decreasing temperatures slow down the hydration. The temperature did not affect the relation between  $Ca(OH)_2$  and the degree of hydration, and for all mixtures a threshold for the degree of hydration at 7% could be identified at which  $Ca(OH)_3$  precipitated. This threshold, however, occurred the later, the lower the temperature was. Further to this, characteristic time steps describing the hydration progress like  $t_{ini}$  and  $t_{fin}$ , as well as the knee point of the autogenous deformations occurred time shifted with decreasing temperatures (Figure 8.2). Geiker has found a linear correlation between temperature and the chemical shrinkage at infinite time [139] (Figure 8.3). Furthermore the author observed that temperatures may shift the chemical shrinkage from a linear process to a parabolic process. The decrease of the final shrinkage value with increasing temperature was attributed to changes in the volume of non-evaporable and adsorbed water, though also processes during the first half hour after mixing that could not be detected in this work were suggested to also play a certain role.

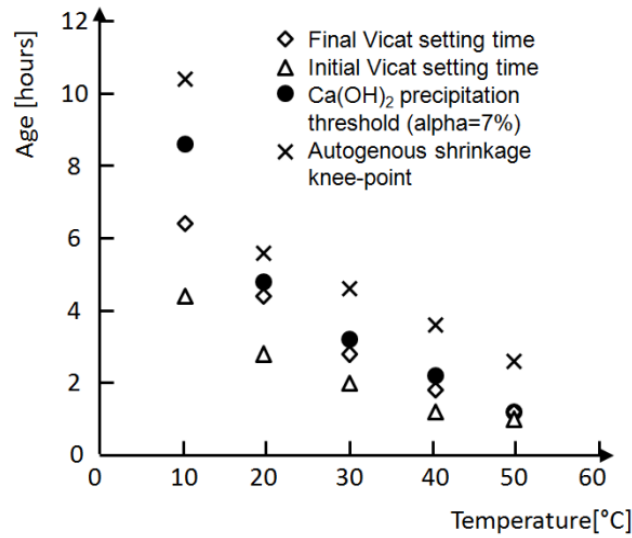


Figure 8.2: Influence of the temperature on characteristic points in time during the early hydration [308].

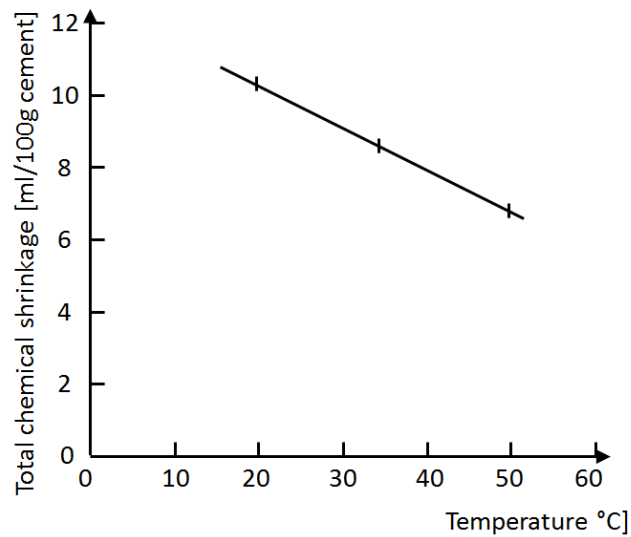


Figure 8.3: Linear correlation between temperature and chemical at infinite time [139].

Heikal et al. observed the effect of temperature on the electric conductivity of systems, which typically correlates qualitatively with the setting, as well as on the initial and final set [309]. The conductivity results point out that at 55 °C the initial conductivity of cement paste is higher than at lower temperatures. However, it also drops much quicker to very low values, regardless if SP is used or not, or if it is blended with silica fume or not. At 20 °C and at 35 °C similar conductivity characteristics could be observed. The conductivity results were not in very good accordance with the setting results, which exhibit sparsely systematic results. At increased temperatures an accelerated initial set of OPC systems could be observed. This observation was made in presence of SP and without SP. The blend with 10% silica fume caused significantly accelerated setting at 35 and 55 °C compared to 20 °C, however, the setting took longer at 55 °C than at 35 °C. If SP was added, 35 °C caused a set which was retarded compared to 20 °C, while 55 °C markedly accelerated the setting [309]. The respective histogram is presented in Figure 8.4.

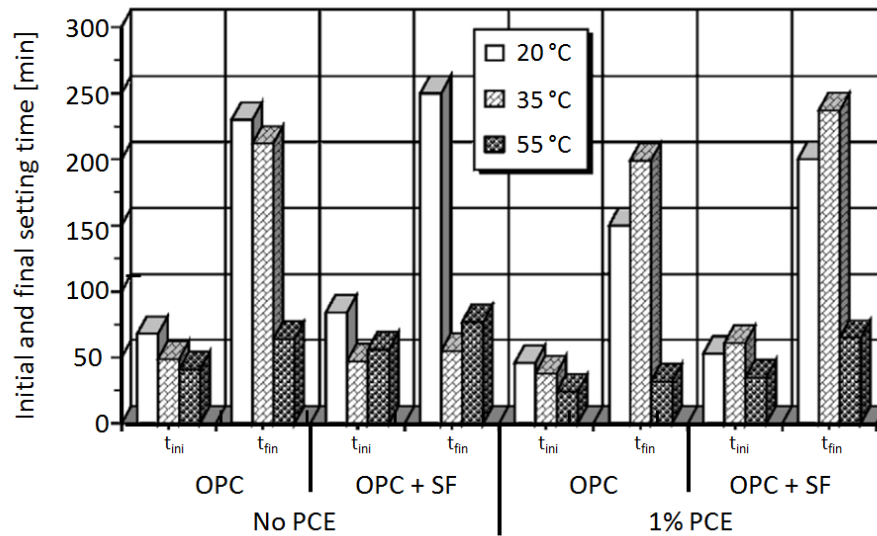


Figure 8.4: Influence of high temperatures on OPC paste and silica fume blended cement paste with and without SP [309].

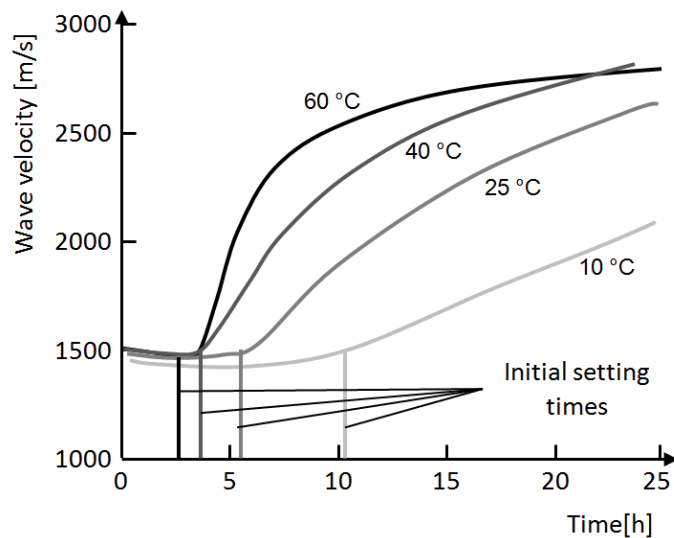


Figure 8.5: Influence of the temperature on ultrasonic wave velocity and initial set after Zhang et al. [140].

Zhang et al. present results, where Vicat  $t_{ini}$  corresponds well with ultrasonic wave velocity measurements, both methods showing that increasing temperatures caused accelerated hydration [140]. These results are shown in Figure 8.5. With regard to the temperature behaviour, they state that due to the fact that setting is caused by percolation, the temperature affects the time at which setting occurs but not the degree of hydration at the moment of setting.

Sohn and Johnson [310] observed the evolution of the hardness of cement pastes at temperatures above room temperature by using a penetration device that measures the force required to drive a penetrator into a specimen. The hardness was defined as the quotient of the force and the frontal area size of the penetrator. The authors show a significant acceleration of the hardness with increasing temperatures.

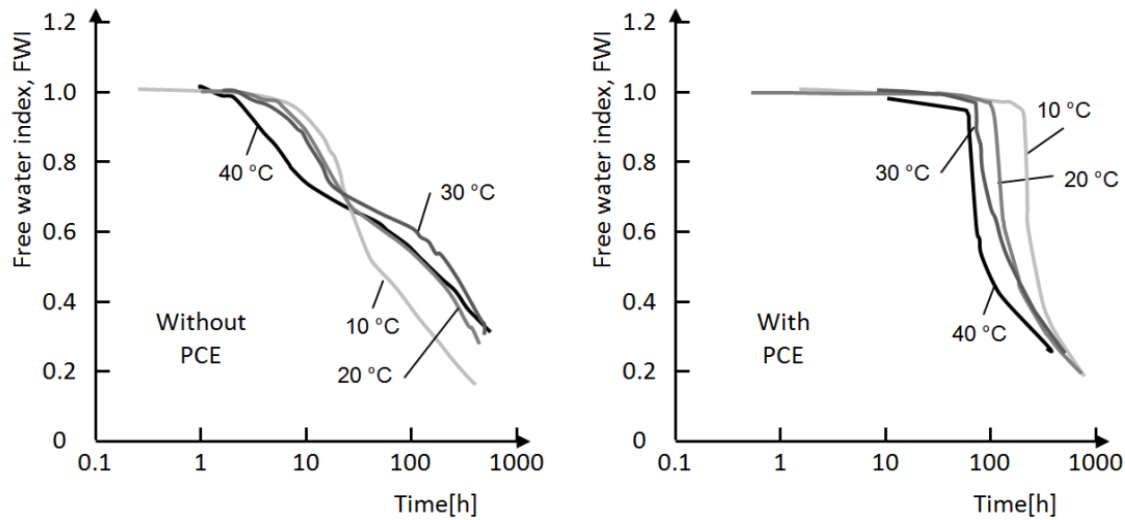


Figure 8.6: Influence of the temperature free water with time without and with PCE superplasticiser after Ridi et al. [311].

Ridi et al. link the hydration retardation to the time dependent evolution of the free water in the system [311]. Therefore, they calculate a free water index FWI based on the equation below, which was validated against experiments based on neutron scattering results by Fratini et al. [312].:

$$FWI = \frac{\Delta H_{\text{exp}}}{x_{\text{H}_2\text{O}} \cdot \Delta H_{\text{init}}} \quad (8.1)$$

where: FWI = free water index [-];  $\Delta H_{\text{exp}}$  = enthalpy change of the water melting determined by differential scanning calorimetry [J/g];  $x_{\text{H}_2\text{O}}$  = the average weight fraction of the water in the pastes [-];  $\Delta H_{\text{init}}$  = theoretical value of fusion enthalpy of water at 0 °C in  $\text{C}_3\text{S}$ -water pastes [J/g]

Ridi et al. calculated the FWI based on differential scanning calorimetry (DSC) according to (8.1) without superplasticiser and in the presence of superplasticiser. They varied between a PNS a polyacrylate, and a polycarboxylate based PCE. Qualitatively the results of all mixtures with SP showed similar curves as shown in Figure 8.6 for the example of the PCE. The authors relate the horizontal part of the free water index curve to the induction period. The change of slope is connected to the beginning of the diffusion regime (Figure 8.6). With increasing temperature the induction period is reduced with and without SP.

Ke-feng and Nichols confirm the acceleration of hydration due to elevated temperatures [313]. They investigated the influence of the temperature on a series of differently proportioned concretes made of the constituents cement, silica fume, fly ash, slag, sand, gravel. Supplementary, a no further specified superplasticiser was added in the not quantified amount required “to get a workable concrete”. For mortars with different The authors show that the 3-days compressive strength values at 65 °C were higher than those of reference mixes at 20 °C, regardless of the w/c. However, they furthermore show a negative effect of this early hydration acceleration by presenting results that reveal 28- and 56-days strength values of specimens cured at elevated temperatures that were significantly lower than the strengths of the reference mixes. The latter effect occurred more pronounced for higher w/c.

#### 8.2.4 Influence of superplasticisers on the early hydration

SPs have a strong influence on the whole period of the early hydration. As discussed in Chapter 6, they strongly interact with the aluminate phase hydration, influencing the workability. Roessler et al. [181] have shown that SPs interact with the calcium sulphates from the set retarder and  $C_3A$ , yielding less ettringite formation. In their study they varied different combinations of anhydrite, gypsum, and hemi hydrate (see Table 2.1.). Furthermore, due to the SP, ettringite forms rather in a long prismatic shape, which might affect the setting [181]. Roessler and Sowoidnich have shown that besides the effect on the workability, SPs can further foster the dissolution of  $C_3A$ , particularly, in case the system contains disproportionally high amounts of  $C_3A$  compared to the available set retarder [182]. This fosters the formation of high amounts of AFm phases, which in turn increases the risk of delayed AFt formation, thus reducing the durability. Another effect during the early hydration of aluminate phases is that the precipitation in the presence of SPs is rather shifted into the solution instead of the surfaces of  $C_3A$  [257, 314]. Furthermore, SPs might intercalate into AFm phases forming so called organo-mineral phases which differ strongly in their behaviour from the hydrate phases produced by cement hydration [61, 168, 170, 185, 186, 193, 315]. However, for PCE superplasticisers, intercalations typically do not play a role, though they were observed for highly charged PCE as well under specific conditions [170] as their ionic strength is lower and their side-chains are longer than for PNS, for which intercalations have been reported to occur.

Beyond the aluminate hydration a major effect of SPs is the retardation of the alite hydration. Particularly a prolongation of the induction period reported by numerous authors, e.g. [65, 115, 131, 136]. According to the observations of Pourchet et al. [316], the retardation can be approximated linearly depending on the amount of carboxylic charges that interact with the  $C_3S$  surface. However, which mechanism accounts responsible for the retardation is not fully clarified yet.

According to a review of possible interactions between all common types of SPs, Mollah et al. conclude that three mechanisms might account for the retarding effect. The first option is a barrier that is generated by the SPs that hinders the diffusion of water and calcium ions. The second option is calcium complexation, which in return would prevent nucleation and precipitation of C-S-H. The third option is a change in the kinetics and morphology of hydrate phases induced by the dispersive action of the SPs [58].

Rieger et al. studied the precipitation of  $CaCO_3$  with and without presence of PCE by X-ray microscopy [317]. In the presence of PCE, the added  $CaCO_3$  nano-particles remained stable upon full coverage with PCE. They dissolved only when the amount of PCE was insufficient for a full coverage. Although this study has evidence only for  $CaCO_3$  nano particles, it indicates that PCE indeed can hinder the dissolution of phases upon surface adsorption.

Ridi et al. observed the activation energies for the acceleration period without and in the presence of different SPs based on PNS and PCE. The authors conclude that in the presence of SPs significantly higher activation energies are required for the accelerated period [311]. This provides evidence that in the presence of SP the hydration mechanism changes. SEM micrographs shown by the authors suggest that it is reasonable to assume that the morphology of the hydration products change in the presences of SPs.

Based on observations of the composition of the liquid phase and investigations of the solid phases, Lothenbach et al. conclude that SPs mainly retards the dissolution of alite, which in conclusion delays the formation of portlandite and C-S-H. No significant retardation of the ettringite formation could be observed. Since the pore solution was not strongly affected by the presence of SPs, the authors conclude that the retarding effect cannot be caused by calcium

complexation or other interactions with dissolved ions, and that it should rather be caused by sorption on solid phases [64].

Pourchet et al. investigated the influence of different PCE superplasticisers on the hydration of  $C_3S$  [289]. They conclude that carboxylic additives strongly decrease the dissolution rate of  $C_3S$ . This is shown in Figure 8.7, where the fraction of dissolved  $C_3S$  in a 11 mmol/l lime solution over the first 25 minutes of hydration in presence of carboxylated latex was significantly lower than without admixture. The dosage of carboxylated latex was 0.4 g on 1.5 mg  $C_3S$  on 200 ml of the solution. From comparative conductivity tests, with a lime saturated solution and soda solution at the same pH without calcium ions, which exhibited different results, they conclude that the SPs build calcium complexes. The authors did not further evaluate the effect of calcium complexation, but a retardation of the C-S-H hydration would be a possible consequence of de-activated calcium ions. Referring to former studies, they state that SPs preferentially adsorb on C-S-H than on  $C_3S$  due to the difference in specific surface.

The authors defined the hydration delay to the period at which the observed system undergoes a period of low conductivity and the increase of the conductivity was linked to the end of the induction period (Phase 2 in Figure 2.1). They found that the hydration delay was linearly related to the functional  $COO^-$  groups per g of  $C_3S$  incorporated into the system by the superplasticiser (Figure 8.8).

Winnefeld et al. opine that the major driving force for the retardation is the hindered dissolution of alite, while no evidence for retarded dissolution of aluminate phases could be experimentally observed [65, 318]. The authors furthermore investigate the effect of the molecular structure of PCEs on the hydration reaction and find out that polymers with higher charge density adsorb to larger extent than polymers with lower charge density. They did not find an influence of the molar mass on the setting. However, a strong influence of the charge density of PCE could be observed. With increasing charge density the induction period was prolonged, when identical amounts of polymers were added to the system. It has to be amended that the charge density was varied through side chain length and not through grafting degree.

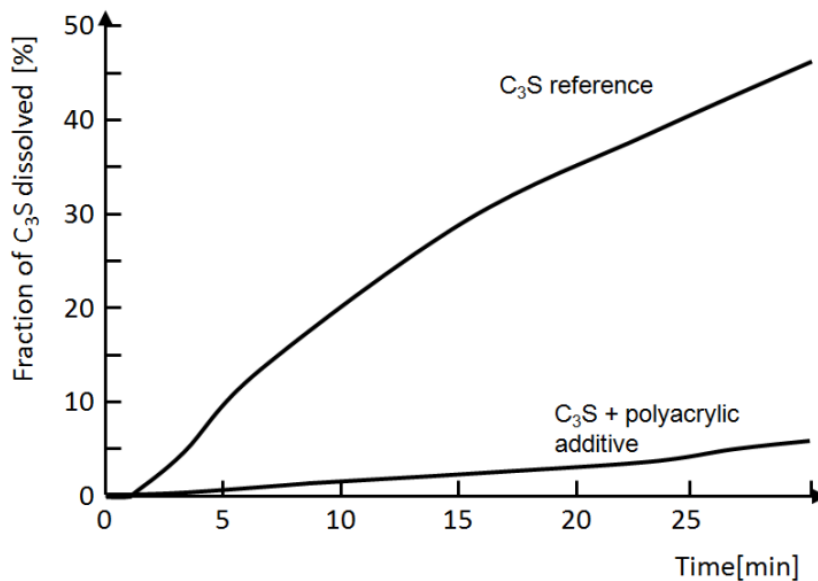


Figure 8.7: Time-resolved alite dissolution with and without polyacrylic additive after Pourchet et al.[289]. 1.5 mg  $C_3S$  was given into 200 ml of a 11 mmol/l lime solution. The mixture incorporating PCE had a dosage of 0.4 g.

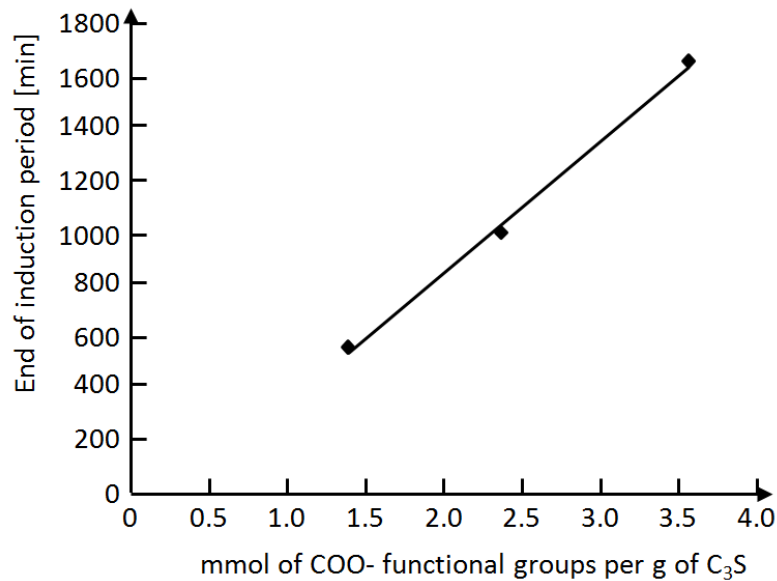


Figure 8.8: Effect of adsorbed amount of SP on the end of the induction period of the C<sub>3</sub>S hydration determined by conductivity measurement after Pourchet et al. [289].

Sowoidnich and Roessler could not find evidence for reduced dissolution of C<sub>3</sub>S in the presence of PCE [319]. In their experiments, the calcium and silicate ion concentrations in their solutions were rather increased in the presence of the different used PCEs. However, by electric conductivity tests, they could show that precipitation of C-S-H as well as of portlandite were hindered by the SPs. They conclude that the retarding effect of SPs might be induced by hindrance of C-S-H growth due to unadsorbed SPs.

### 8.2.5 Influence of water to powder ratio

Already in 1867, when cement as we know it today was still in its infancy, Michaëlis [320] reports about conducted investigations with cement at varied water to cement ratio, in which higher w/c values delayed the setting of powders ground from a piece of Portland cement clinker (“aus einem Brande ein Stück Cement”). The setting of the less finely ground powder was retarded from 7 to 10 minutes and the setting of the more finely ground powder was retarded 3 to 4 minutes. Furthermore, the temperature increase reduced from 6.2 °C to 5.0 °C and from 11.5 °C to 9.0 °C, respectively.

These observations are confirmed by studies with more modern materials. The higher the water to cement ratio, the slower the heat development and the later the setting occurs. Hesse et al. [307] show heat flow experiments where the maximum heat flow reduces and shifts to a later point in time with increasing w/c. Sohn and Johnson show that the rate of hardening increases the lower the w/c is [310]. Increasing w/c furthermore increase the chemical shrinkage. In observations after 20 h of hydration, Geiker found that the rate of chemical shrinkage increases with increasing w/c in cement pastes and that there is a strong linear correlation between the chemical shrinkage at infinite time and the w/c [139] (Figure 8.9).

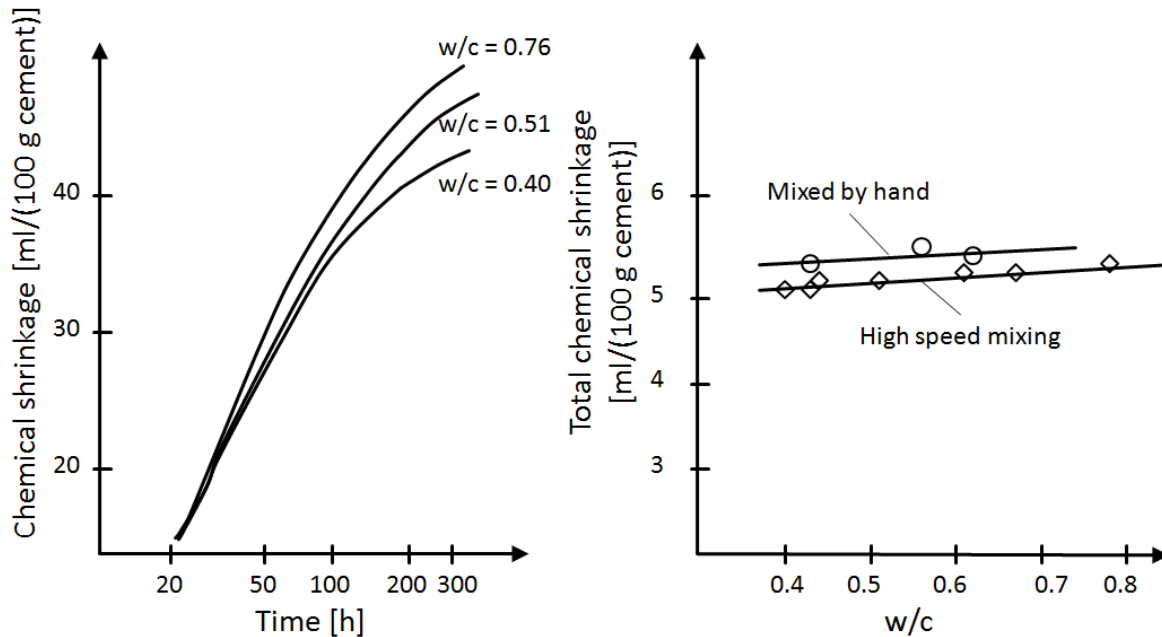


Figure 8.9: Relation between w/c and chemical shrinkage evolution (left) and linear relation between chemical shrinkage at infinite time and w/c after Geiker [139].

### 8.3 The early hydration from an engineering point of view

Many sophisticated studies have been conducted with regard to the early hydration. Despite a high number of still not yet completely understood aspects, many details about what happens during the first day of hydrating cement's life can be considered as largely known. It is, however, also of importance to link the abundant knowledge about cement chemistry to practical applications.

If the early age of concrete is considered from an engineering point of view, many matters of discussion might sound absurd. If a person is involved in the edification of a concrete bridge, this person might rather be interested in controlling the effect than in understanding the physico-chemical cause for it. The constructor is hence mainly interested in concrete that is delivered to the construction site in the demanded consistency, whether he can maintain the schedule for demoulding, and that the concrete remains without serious cracks. From that point of view, there might be other specific points in time that are of major interest than those characterising the early hydration. These are for example the period during which the concrete is cast, the early strength development and the time during which the concrete is prone to cracks.

As shown in Chapter 6, in case of SCC the workability period is determined in a critical extent by the amount and the charge density of the PCE. The influence on the yield stress reduction is predominantly determined by the amount of adsorbed polymers [66, 67, 258]. At a specific time polymers with a higher charge will have a stronger tendency to be adsorbed [65], which can be explained by the competition with the sulphate ions [85] (see Subsection 3.3.4). This means when a high charged polymer is chosen to achieve a specified slump flow, less polymers will be in the system than in case of a low charged polymer. This is emphasized by the admixture compositions with varied PCE charges at similar flow properties, presented in Table 4.10, where the PCE with the highest charge density is always added in the lowest amount, and decreasing charge densities always yield higher required additions (Figure 8.10). If different PCEs are available, they would not be added in identical amounts, but rather individually in the

amount that is required in order to achieve a specified flow property (e.g. Figure 8.10). From that point of view, the influence of the molecular geometry of PCE at identical addition, as e.g. discussed by Winnefeld et al. [65] might be without importance for engineering applications. So the polymeric structure of a PCE only plays an indirect role as it determines whether a higher or a lower amount of polymers has to be added in order to achieve specified flow properties. It is therefore likely that the influence of the amount of total PCE outweighs any influence of the polymer geometry.

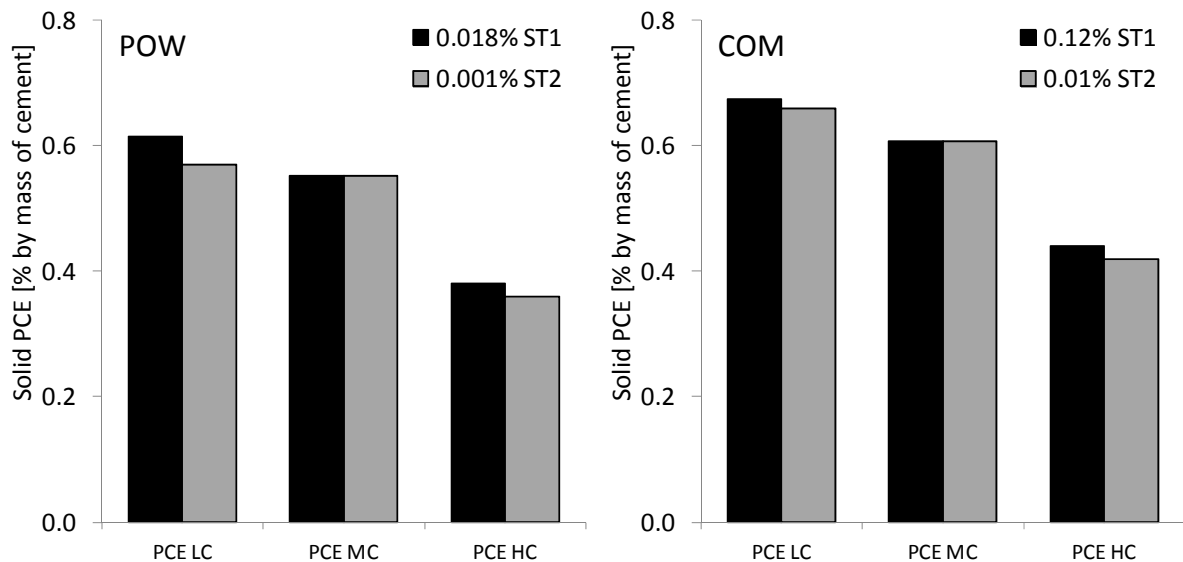


Figure 8.10: Required additions to achieve similar flow properties after 30 minutes for differently charged PCEs.

Although setting cannot predict what happens during a later stage of hydration, particularly not when components are added to the binder supplementary to cement, it is a good indicator for the early strength development. If the concrete system remains unchanged, it is unlikely that effects that shift the setting time into a certain direction will have adverse effects on the early strength. Therefore the setting can be considered as a very relevant point in time.

If typical early deformation curves are evaluated, it can be observed that deformations occur at a high rate during the induction period and change to lower rates around the time of the setting. This transition is not directly linked to the time of the setting, as it can be observed e.g. in Figure 8.2, where the knee point of the autogenous shrinkage curve is observed later than the final setting time, with increasing effect with reduced temperatures. Hence, there is a quite undefined period in time, which starts around the initial set and ends at a time, when the concrete has achieved sufficient resistance against cracks due to strength evolution. During this period, the concrete is prone to cracks.

These mentioned critical periods are shown in Figure 8.11. It is obvious that these identified points are not linked to characteristic points of the hydration evolution curve, marked with numbers 1 to 4 after Pratt and Ghose [116] similar to Figure 2.4. According to Nachbaur et al. [321], the Vicat setting time is not considered as a specific point in time and does not correspond to a significant structural evolution. This is true when looked only from a hydration point of view. If the angle of observation is turned, however, the maximum rate of hydration is meaningless and not relevant for any construction site purposes. For a more distinguished evaluation it is thus necessary to integrate the characteristic points of time for practical applications into the hydration curve.

This fact is particularly important if SCC is taken into account. SCC always contains SP, causing a prolonged induction period and a broadened hydration peak. Thus there are distinct time differences between the characteristic points of the hydration as well as those identified as relevant from an engineering point of view.

For normal concrete, the setting is assumed to take place approximately during the first 3-6 hours (e.g. [30, 79, 81, 82, 88, 126]). This is close to the onset of the acceleration period. However, also the accelerated hydration does not take long. Hence, the initial or the final set somehow both can be linked to the beginning and the end of the acceleration period. However, in case of mixtures containing high amounts of SP, the onset of the accelerated hydration can be significantly retarded [123, 124]. The same is valid for the time difference between onset and end of the acceleration period. Initial and final set take place somewhere in between. However, between all these characteristic points several hours can pass.

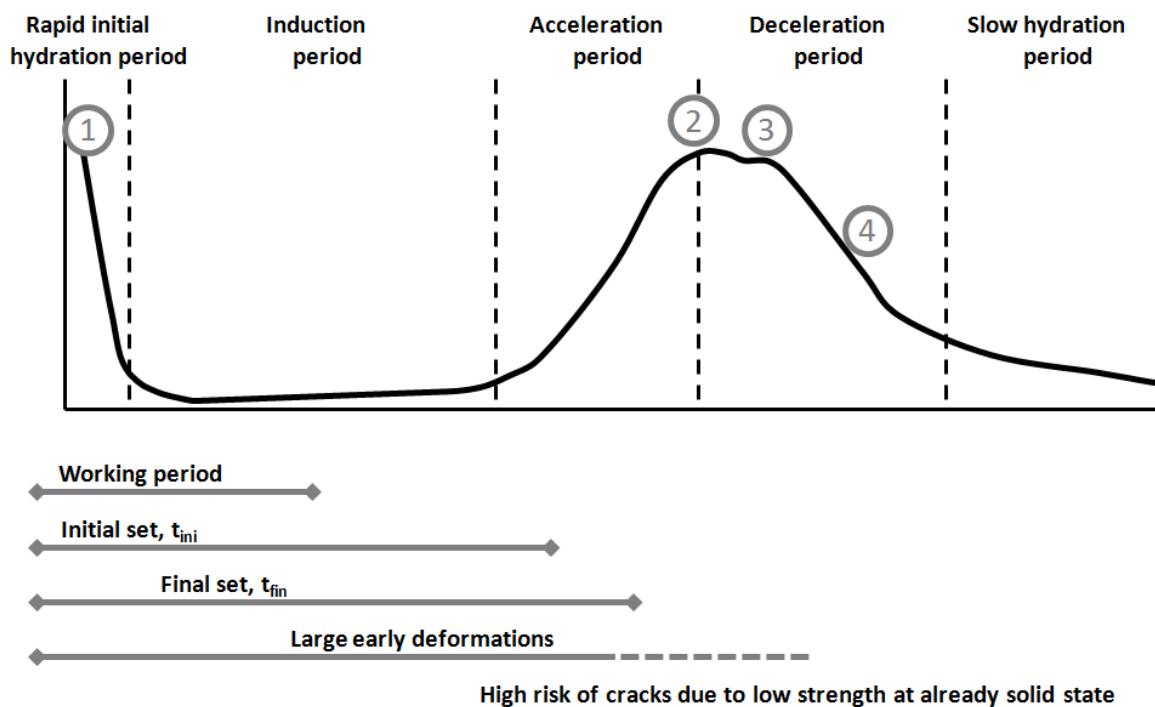


Figure 8.11: Characteristic periods of the early hydration from an engineering point of view compared to the characteristic points from a cement hydration point of view. Peak 1: Wetting and early reactions; Peak 2: Hydration of  $C_3S$ ; Peak 3: Renewed hydration of  $C_3A$ ; Peak 4: Hydration of ferrite and/or conversion of  $AFt$  to  $AFm$ .

It is now evident that the time of the setting can be considered as a relevant value and has to be given special attention, particularly when SCC is discussed. Setting gives information about the strength development and furthermore represents the transition from a plastic state into a solid state.

For cementitious systems without SP it is not necessarily important to distinguish between initial and final set since the time in between might range from 20 to maximum 60 minutes. As mentioned before, in superplasticised systems the time in between can last drastically longer.

Nachbaur et al. [321] opine that any different test setup (e.g. another needle) would yield different results. This can be doubted for the final set, but it is surely true for the initial set. Sleiman et al. calculated the yield stress from the Vicat measurement and compared it with

results from rheometric investigations by using a vane cell [322]. Their results point out that the initial set represents a significant marker in the yield stress curve, after which the rate drastically increases (Figure 8.12). However, this is only a rheological phenomenon and does not provide any evidence about a structural formation in cement or concrete. For example, if modelling clay is taken into account, the needle would drop and stop somewhere in between the top and the ground plate but the clay would not behave as a true solid.

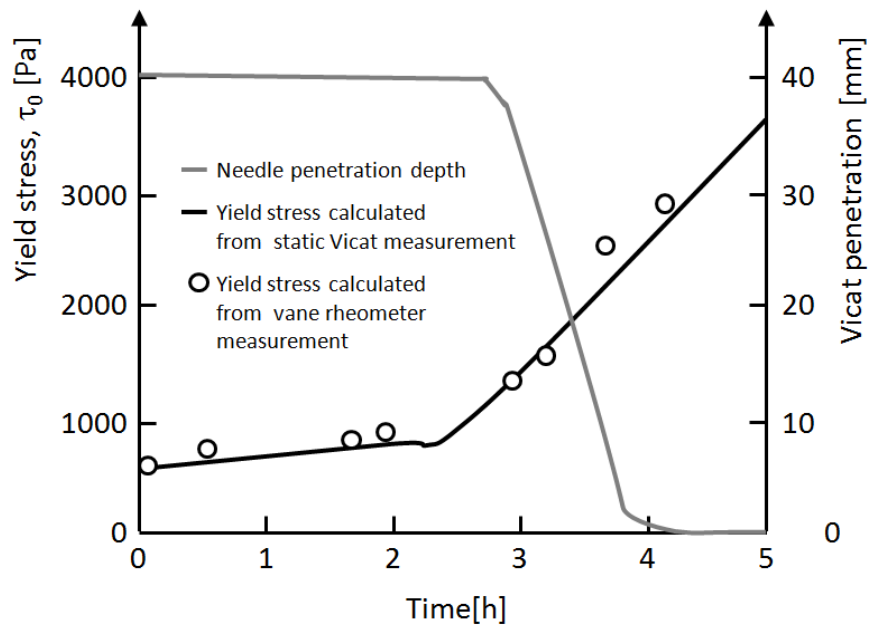


Figure 8.12: Yield stresses computed from Vicat test and rheometer using a vane geometry cell compared to the corresponding Vicat needle penetration depth according to [322].



Figure 8.13: Consistency of a cement paste at the very moment of the initial set.

Figure 8.13 gives an example of a cement paste exactly at the moment of the  $t_{ini}$  according to Vicat (the specimen itself is from a rheological measurement with a ball system). The photograph shows a consistency very similar to modelling clay. The very thin skin on the top of the specimen is only a surface phenomenon and can be intruded easily by a dropping needle. The point in time when the needle does no longer drop to the bottom of the Vicat device is depending upon the plastic viscosity and the yield stress of the system at that time. These can be assumed to depend on the particle packing density, the water to solid ratio and the SP content. Hence, there is no direct link to the formation of a solid structure.

In this context it has to be considered that the definition of the initial set may vary strongly. According to EN 196-3:1995, the initial set is defined as the point in time at which the needle drops to a specimen height of  $4 \text{ mm} \pm 1 \text{ mm}$ . According to Sant et al. [138], who refer to ASTM C 191 the initial set is defined as the point in time at which the needle penetrates less than  $25 \text{ mm} \pm 0.5 \text{ mm}$ . Hence, according to the European standard, which serves as reference for this work, the consistency differences at initial and final set are more pronounced than according to the American standard.

It is now evident that the initial setting time does not provide significant information about the transition from a plastic state. This, however, is not valid for the final set. If a specimen is just observed haptically and optically at the time of the final set, the difference between a specimen which is not yet set and which is just set can be sensed easily. McKenna defines the final set as “firm resistance to any penetration or deformation” [231]. Following this definition from 1912 already, it is quite self-explanatory that at the moment the Vicat needle can no longer penetrate a specimen deeply, any other needle would behave likewise unless it is not pushed into the specimen by strong force. Indeed, a standardised final set, which does only relate to a specified needle penetration depth (e.g. 0.5 mm according to EN 196-6:2005 and ASTM C191) does not inevitably have to correspond to this transformation from a plastic body to a rigid body. E.g. the surface of a specimen may show bleeding and can interact with the surroundings, causing that the point in time at which the needle reaches the specified penetration depth can be significantly retarded. If, however, the transition of the penetration depth curve towards a horizontal line is considered as the final set, the final set can be considered as a very significant point in time during the early hydration process. Figure 2.6 gives further evidence, showing that at the time of the final set, the chemical shrinkage and the autogenous strain start to diverge.

Concluding, it can be stated that for a comprehensive overview of the effect of SPs on the early properties of self-compacting cementitious systems, it is necessary to take a closer look onto the final set and the early deformations, particular at the very time when the system is prone to cracks induced by restraints in the construction.

## 8.4 Experimental setup

### 8.4.1 General information

Three types of investigations were conducted on different pastes, mortars and concretes in three different series. Each investigation was conducted with cement from different delivery charges. However, according to the principles formulated in Subsection 4.5.3, within one closed observation series the used materials' qualities were not varied.

- The first investigation provides information about the influence of the charge density and the amount of PCE on the setting of pure cementitious systems (Subsection 8.4.2).
- The second investigation uses the pastes of the COM and POW mixtures in order to observe individual adjustment parameters affecting the early hydration reactions and deformations. This major investigation series is described in Subsection 8.4.3.
- In a third investigation the relevance of the former paste observations for the concrete scale was observed. These results will be presented in Subsection 8.4.5.

### 8.4.2 Setting of pure cement-superplasticiser pastes

In the first investigation, the influence of the temperature and the PCE charge density and amount on the setting was observed. Therefore, pastes from cement and water were mixed and the amount of dosed PCE was varied. Cement and superplasticiser specifications can be found in the Subsections 4.1.2 and 4.1.4, respectively. In order to reduce the influence of the water content and to avoid any segregation at high SP dosages, the water content was adjusted to the water content according to the Puntke test [32, 233], which is also described in Subsection 5.2.1. The respective mass related w/c was 0.25. This corresponds to a Puntke-water-demand of 44.1% by volume. Bulk PCE (water + solids) was added to the paste in 4% steps referring to the volume of cement. Above 20%, the steps were increased to 5% steps. The resulting water content of the PCE was taken into account and deducted from the mixing water. Since each PCE modification has different solid to water ratios, the solid contents corresponding to the bulk PCE dosages vary.

Table 8.1: Mixing regime for paste investigations.

Step	Duration [s]	Mixing velocity	Action
1	60	1 (slow speed)	Dry mixing of cement and limestone filler
2	60	1 (slow speed)	Addition of 1/2 of total water
3	30	1 (slow speed)	Addition of PCE
4	30	1 (slow speed)	Addition of 1/2 of total water
5	60	3 (medium speed)	Mixing
6	30	-	Manual scraping off residue
7	60	3 (medium speed)	Mixing

Three differently charged PCEs were used that are described in Subsection 4.1.4. The observations were conducted at 5, 20, and 30 °C. All mixture ingredients were stored prior to testing in the particular observation climate. The mixing was conducted in a mortar lab at 21 °C to 23 °C. The mixing regime as used for the paste tests can be seen in Table 8.1.

In case a mixture did not contain PCE, the addition was skipped. However, the mixing time was maintained. Mixing took place in a kitchen mixer Kenwood Chef Classic Platin KM 416. This mixer allows better homogenisation at low mixing volumes than a mixer according to

EN 196-1:2005. Directly after mixing, the specimens were poured into the Vicat rings and placed in the automatic Vicat device as described in Subsection 4.4.2. The zero-time was set as the time of the first water addition. For each specimen only one test was conducted, which was considered as sufficiently precise since due to the systematic increase of the PCE, a scattered result would become obvious immediately.

### 8.4.3 Setting, heat evolution and deformations of the binder paste of COM and POW

In the second series the influence of different amounts and modifications as well as the temperature on the early hydration were observed using the COM and POW pastes (Table 4.12). Since all these factors have a strong influence on the consistency, the standardised method for the determination of the setting according to Vicat at defined stiffness of a paste or mortar system were not reasonable to be applied. This would namely always demand for a re-adjustment of the w/p ratio so that influencing factors would diffuse. The tests were thus conducted at identical mixture compositions and at the consistency that resulted from each mixture and admixture adjustment.

The studied mixtures are the paste mixtures from Table 4.12. In order to distinguish between the influence of the polymers at identical polymer content and at polymer amounts required for comparable rheology, two series were observed. These can be found in Table 8.2.

Series 1 concerned mixtures with PCE contents according to Table 4.10. For the stabilisation of the paste ST2 was chosen since it was considered to be more stable at cold temperatures than ST1. ST2 was added to the mixture at the end of step 2 shown Table 8.1. Segregation had to be avoided since this would critically affect the measurement of the deformations and the setting. While the POW paste was not modified, the STA content of the COM mixture needed to be modified in order to avoid segregation. The STA content given in Table 4.10 was multiplied by a factor of 2. By this, the general characteristics of the pastes, such as the ratio of powder to water and solid PCE remained unaffected. Since the STA content was kept constant for all paste tests, this allowed observing the effect of different PCE types.

Series 2 dealt with the influence of the differently charged PCE at identical solid contents. In this series only the COM pastes were observed. The high charge density polymer was added in the smallest solid amount. Therefore, its solid content was fixed and taken as a reference dosage for the PCEs LC and MC. By this it was avoided that overdose of PCE takes place, which would cause segregation of the paste. The PCE solid contents for Series 1 and 2 are shown in Table 8.2.

The tests were conducted at 5, 20, and 30 °C. All mixture ingredients were stored prior to testing in the particular observation climate. The mixing, however, was conducted in a mortar lab at 21 °C to 23 °C. Specimens were homogenised according to Table 8.1. The mixer used for the mixes was a mortar mixer in compliance with EN 196-1:2005.

The ambient temperatures in the calorimeter were calibrated prior to each specified observation temperature. This made it necessary to store the whole device in a climate chamber for the measurements at 5 °C in order to avoid condensation. The tests were conducted according to Subsection 4.4.3. The sensitivity was adjusted to  $\pm 20 \mu\text{W}$ . A weight of approximately 15 g of paste was used for each investigation. The specimens were filled in plastic vessels. Each specimen was measured twice from one batch. Inert reference samples filled with quartzitic sand and water to sand ratio of 0.5 were set up in order to reduce effects of the so called “cross-talk” which implies that vessels mutually interact.

The shrinkage cones were placed in a climate chamber adjusted to the temperature under investigation. The measurements were conducted according to Subsection 4.4.5.

Table 8.2: Qualitative PCE properties and additions for identical flow properties in the COM pastes and identical polymer contents in the COM pastes.

Series	Paste mixes	PCE HC	PCE MC	PCE LC
1	POW	Different PCE content, adjusted to similar rheology		
		Abbreviation		
		HC-0.36%	MC-0.55%	LC-0.57%
		PCE solids		
		0.36% of cement	0.55% of cement	0.57% of cement
	COM	Different PCE content, adjusted to similar rheology		
		Abbreviation		
		HC-0.42%	MC-0.61%	LC-0.66%
		PCE solids		
		0.42% of cement	0.61% of cement	0.66% of cement
2	Adjusted to similar PCE content, different rheology			
	Abbreviation			
	HC-0.42%	MC-0.42%	LC-0.42%	
	PCE solids			
	0.42% of cement	0.42% of cement	0.42% of cement	

The Vicat samples were stored under water at controlled temperature, which was adjusted to each observation temperature. The tests were conducted according to Subsection 4.4.2.

The practical application required two operators. The first operator immediately filled the Vicat rings after the end of the mixing. In order to avoid that during the handling part of the filling gets lost, the specimens were at first only filled up the  $\frac{3}{4}$  of the height. In a next step, the water in the specimen chamber was emptied until the water level was slightly lower than the brims of the Vicat rings. This was necessary to avoid that at fluent consistency the paste mixes up with the water. When the specimen was filled and at rest, the water level was carefully raised again until all specimens were fully covered with water. In parallel, another operator filled the shrinkage cones directly after mixing and placed them into the frame with a cover on top of the paste. After this the vessels for the calorimetry were filled. After placing the samples into the calorimeter, the shrinkage cone was covered with foil, the reflector plate was placed in the centre and the laser was adjusted.

All devices were located in close range so that by this operation, it was assured that all specimens were placed in individual climate and left untouched after 5-10 minutes. The quick operation was considered necessary since interactions with temperature that deviate from the observation temperature should be avoided. Since all test devices allow a backward calculation

from the measurement start to the zero-time, the starting of the measurement could then be conducted more calmly upon placement of all samples.

For the tests  $t_{ini}$  was specified according to EN 196-3 at a penetration depth of  $34.0 \pm 3.0$  mm. For  $t_{fin}$ , a penetration depth of 2.5 mm was defined as in the mortar standard. This was necessary since particularly at cold temperatures the full hardening of the paste zone between specimen and water surface took a long time. The knee-point of the curve, after which the needle penetration depth levels, occurred before the penetration of 0.5 mm could be reached (Figure 8.14). For this test setup, where high w/p mixes and high amounts of SPs were used, the knee-point is considered as the relevant value for the setting. Since paste was observed, the needle was adjusted as in EN 196-3 with 300 g.

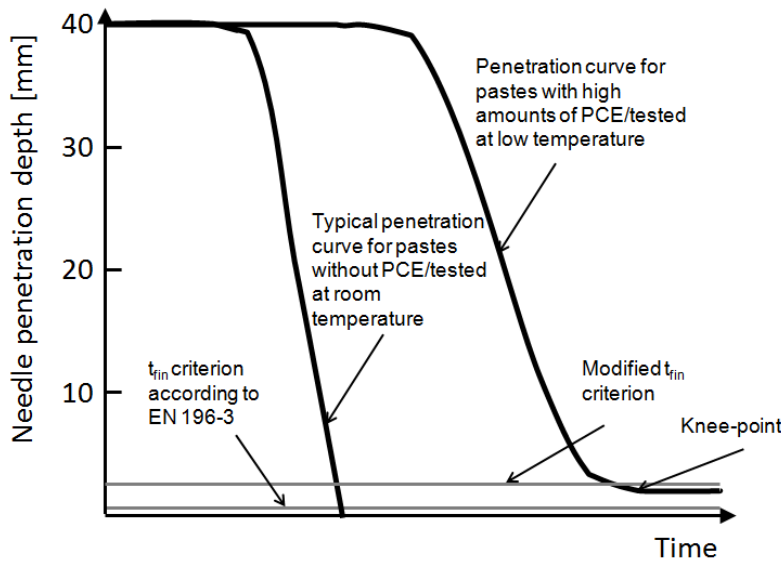


Figure 8.14: Sample of a typical needle penetration curve in comparison to a curve resulting from high PCE dosages or low temperatures and respective modifications of the  $t_{fin}$ .

#### 8.4.4 In-situ XRD on pastes of the COM mixture

The XRD measurements were conducted with a Rigaku Ultima IV device with a D/tex-Ultra high speed detector, equipped with a copper anode as described in Subsection 4.4.4.

For these investigations the COM pastes were observed (Table 4.12) with PCE LC and PCE HC since the former observations pointed out that the medium charge polymer behaves very similar to the low charge polymer, these two PCEs were considered as representative for a typical low and high charge PCE. The dosages were chosen according to Table 8.2 for the same rheological properties as well as for an identical solid content for PCE LC and PCE HC.

Table 8.3: Schedule for XRD measurements of fresh pastes.

Time after measuring start	0 to 2 h	2 to 12 h	12 to 24 h	24 to 48 h
Diffraction angles $2\theta$	5°-25°	5°-45°	5°-45°	5°-45°
Scanning interval	10 min	1 h	2 h	4 h
Number of measurements	12	10	6	6
Sample numbering	1-12	13-22	23-28	29-34

All fresh paste samples were poured into round sample holders with a diameter of 20 mm and a height of 2 mm. Samples were covered with X-ray transmitting Kapton-foil to prevent evaporation and air-tightly connected to the sample holder with putty. All measurements were conducted at a scanning speed of 5°/min. Measurements during the first 2 hours were made every 10 minutes at diffraction angles  $2\theta$  from 5° to 25°. The small range of angles was adjusted to have shorter observation intervals and since at these early times no significant changes in the alite peaks were expected. After that, the diffraction angles  $2\theta$  were switched from 5° to 45° in a scanning frequency of one scan per hour for the next ten measurements. At identical diffraction angles, the following six measurements were conducted at a frequency of one per two hours followed by another six measurements every four hours. This adjustment is given in Table 8.3. All consecutive measurements and a table of the individual times of each measurement after water addition can be found in Annex D.

#### 8.4.5 Setting of binder paste, mortar, and concrete

In a third investigation, the results are evaluated on mortar and concrete scale. Vicat tests were conducted for the admixture variations with paste, mortar, and concrete. In order to avoid a rupture of the needle upon impact with a coarse grain, instead of the standard needle, a more stable needle with a diameter of 2 mm was used. The mass of the penetrating needle was 1000 g.

First, the aggregates, required for a mortar and paste sample of 400 ml were separately homogenised before and put aside into buckets. Then a litre of paste was mixed according to Table 8.1. In a last step, the required amount of paste for the 400 ml mortar and concrete samples were weighed of the already homogenised paste and the whole mix was stirred for 30 s each at low rotational speed. After that the Vicat rings were quickly filled and the test was started.

### 8.5 Results and Discussion

#### 8.5.1 Effect of PCE on the setting of cement paste

In general, a strong effect of the temperature could be observed on the setting with varied PCE contents. The slope of the setting curves increased significantly with decreasing temperatures. This means, the colder the temperature is, the more pronounced is the retarding effect of the SP. Furthermore, the gap between  $t_{ini}$  and  $t_{fin}$  widens with decreasing temperature (Figure 8.15).

At all temperatures, there was a strong influence of the PCE content on the setting. All curves show a systematic behaviour, which occurs more pronounced with regard to  $t_{fin}$ . Below a threshold dosage depending on PCE type and temperature the setting times increase in a linear way with increasing PCE dosages at a slight slope. Above this threshold dosage, the slope becomes significantly steeper. This effect occurs very pronounced at 5 °C and less pronounced at 30 °C. At dosages between zero and this characteristic point, the influence of the PCE charge density is small at all temperatures. As soon as the slope increases the effect of the charge density increases. The PCE with the high charge density PCE HC shows earlier  $t_{ini}$  and  $t_{fin}$  at all temperatures compared to the low and medium charge density PCEs PCE LC and PCE MC. This confirms the observations of Winnefeld et al. that the induction period is extended with increased charge density [65]. On the other hand, the dosages of PCE HC to adjust the required fresh concrete performance were smaller than those of PCE LC and MC. This compensates the negative effect on setting by the molecule structure of the PCE to a certain extend. Furthermore, a significant effect of the charge density of the PCEs LC and MC can only be observed at cold temperatures. At 20 °C and 30 °C, PCE LC and MC behave similarly and there is no systematic effect of the charge density. It has to be noted that the distinction of the charge densities between

low, medium and high does not give any evidence about the quantity. Already from the adsorption tests of the PCEs (see Subsection 4.1.4) it became obvious that the performance difference between PCE LC and MC is significantly smaller than the difference between these two PCEs and PCE HC.

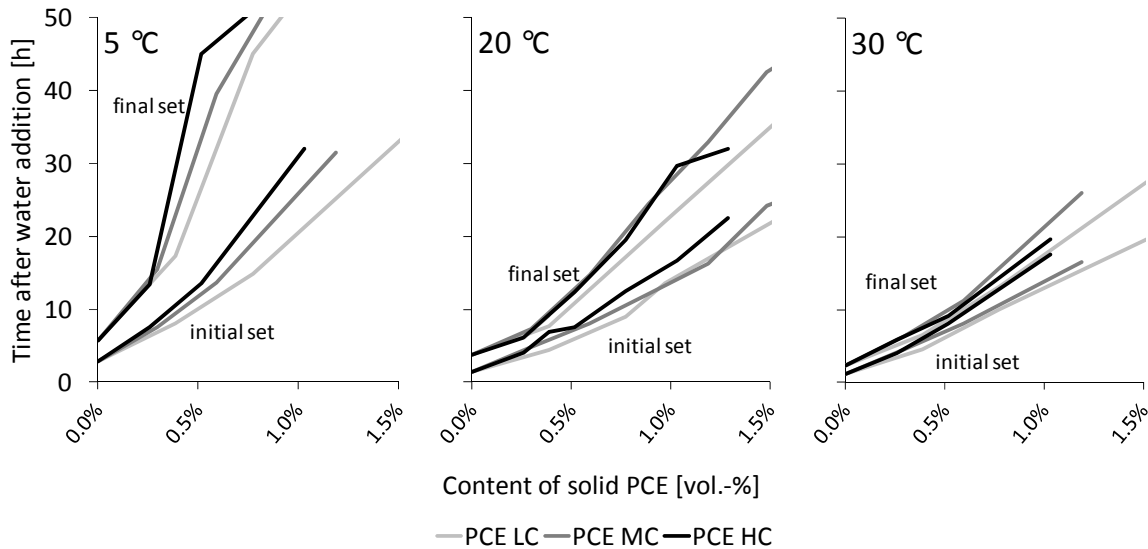


Figure 8.15:  $t_{fin}$  and  $t_{ini}$  of cement pastes with varied PCE contents and PCE charge densities at temperatures of 5 °C, 20 °C, and 30 °C.

### 8.5.2 Effect of PCE type and amount on initial and final set of COM pastes

As could be seen from the former results on cement paste, the charge density of PCE induces two opposing effects. On the one hand, higher charge densities slow down the hydration, on the other hand, they need to be added in smaller amounts. The hypothesis of Section 8.3 is that the effect of the dosage is likely to outweigh effects of the molecular architecture or the respective charge density (Figure 3.23). In order to find out which effect predominates, pastes of the COM mixture were investigated with varied PCEs at dosages that are required to achieve similar flow properties as well as at identical dosage of solids. These are given in Figure 8.16. At identical flow properties (left) mixes with the high charge polymer set significantly earlier than mixes with the medium and the low charge density polymers. This behaviour can be observed at all temperatures but it occurs significantly more pronounced the lower the temperature is. The low charge density polymer only sets slightly earlier than the medium charge polymer. There is no clear relation between the polymer content and the time of setting. However, it is important to notice that the high charge PCE was only added at a dosage of 0.42%, while the similarly behaving low and medium charge PCEs (0.66% and 0.61%, respectively) were added in similar and significantly higher amounts than the high charge polymer. As stated before, it seems in general PCE LC and PCE MC behave very similarly, not only with regard to the flow properties, so that the effect, induced by the charge density is not as pronounced as between them and the PCE HC. At this similar addition of polymer solids the effect of the molecular architecture again is of increasing importance, so that the PCE LC sets earlier than PCE MC despite the slightly higher solid content. This is confirmed by the results of the final setting times at identical solid polymer contents (Figure 8.16, right). At identical polymer contents, the times of the  $t_{fin}$  are much closer to each other, regardless of the observation temperature. A clear correlation between charge density and setting time cannot be observed. Since no pronounced effect of PCE charge densities at identical solid contents can be observed, and on the other side a very

pronounced effect can be observed with regard to the total amount of polymers, the hypothesis of Section 8.3, can be confirmed. The amount of total polymers, regardless of their charge density, is the decisive factor determining the set retardation.

Even if an effect of the charge density would exist, e.g. as described by Winnefeld et al. and Zingg et al. al. [264, 318, 323], who observed an increasing retardation with increasing charge densities at identical polymer concentrations, these effects would be outweighed by effects resulting from higher polymer contents. PCE is typically added according to rheological specifications. In order to achieve these specifications, a high charge density PCE has to be added at lower dosages due to its higher efficiency and a low charge density PCE has to be added at higher dosages. As a result it can be stated that from a point of view of the applicator of cementitious materials, high charge density PCE retards the setting less than low charge density PCE, due to the lower required addition rate.

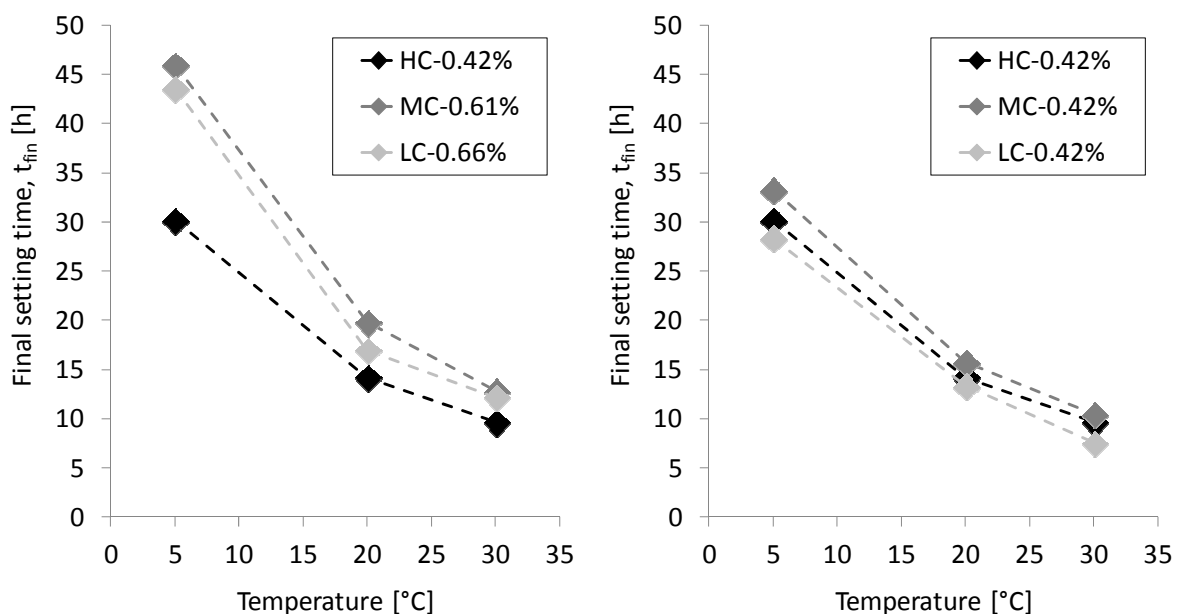


Figure 8.16:  $t_{fin}$  at PCE dosage for identical flow (left) and identical polymer content (right).

### 8.5.3 Effect of PCE type and amount on heat evolution of COM pastes

The results of the setting measurements are in good agreement with the results of the heat flow analyses. Figure 8.17 shows the effect of the temperature on the curves of the heat flow  $\dot{Q}$  (Subsection 4.4.3). The peak maxima reduce with decreasing temperature and occur at later times, while the period of hydration significantly broadens. Figure 8.17 only shows the effect of the temperature. A more specific observation for 5 °C, 20 °C and 30 °C is presented in Figures 8.18 to 8.20, respectively. The left figure always shows the curves at identical flow performance and the right figure shows the curves at identical solid dosages, regardless of the flow properties. Vertical lines of the same grey level as the heat flow curves represent the respective final Vicat setting times.

At all temperatures, the curves qualitatively look alike and they confirm the results from the Vicat tests shown in Figure 8.16. PCE modifications and amounts that caused earlier final setting are accompanied by earlier accelerated heat evolution. It can also be observed here that the curves for mixes with different PCE charge densities show much more similar behaviour when the PCEs are added at identical solid contents, while the curves diverge much more when the PCEs are added in an amount that yields similar flow properties. In the latter case, always

the high charge PCE causes prominently earlier hydration due to its small required addition amount.

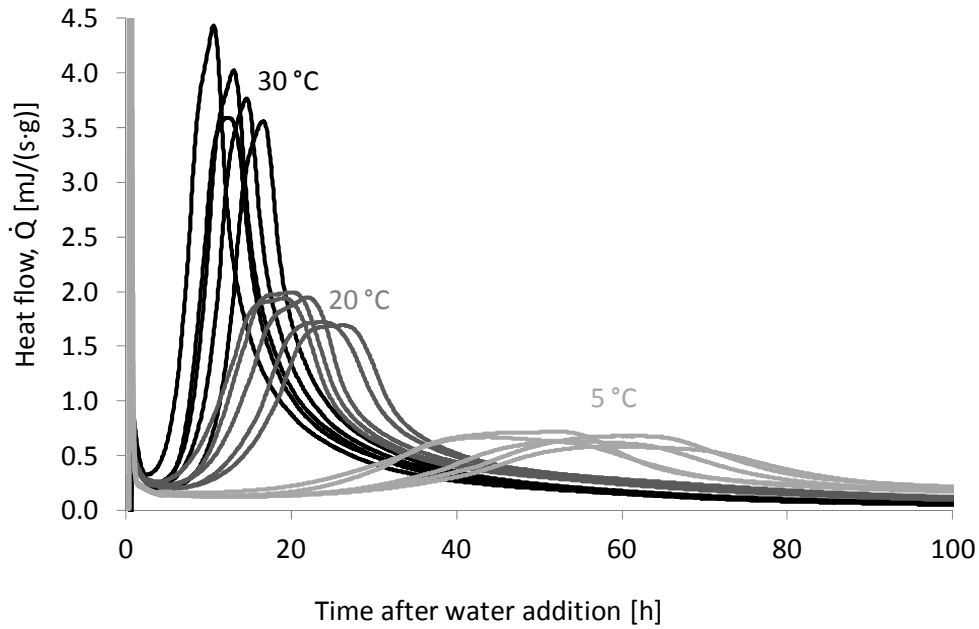


Figure 8.17: Heat flow of all COM pastes at varied PCE types and amount (Table 8.2) at 5, 20, and 30 °C.

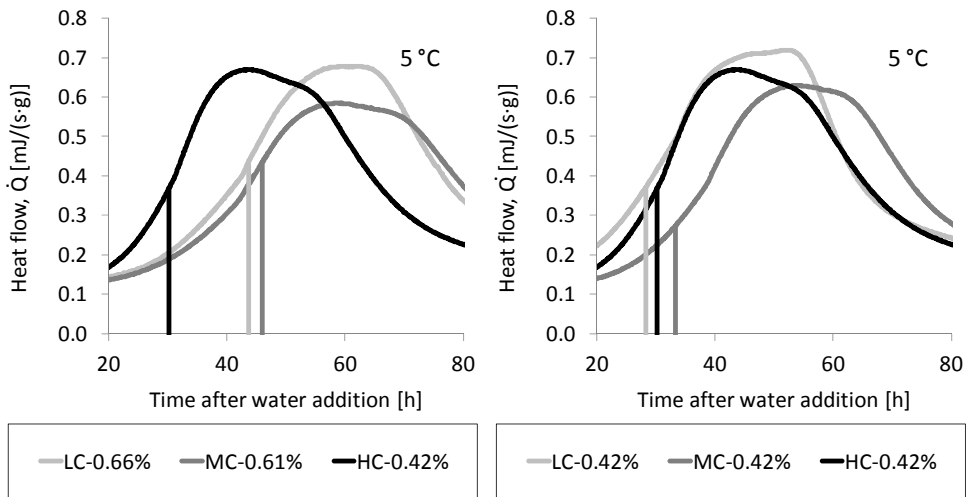


Figure 8.18: Heat flow at 5 °C for the COM pastes. Vertical lines indicate  $t_{fin}$ .

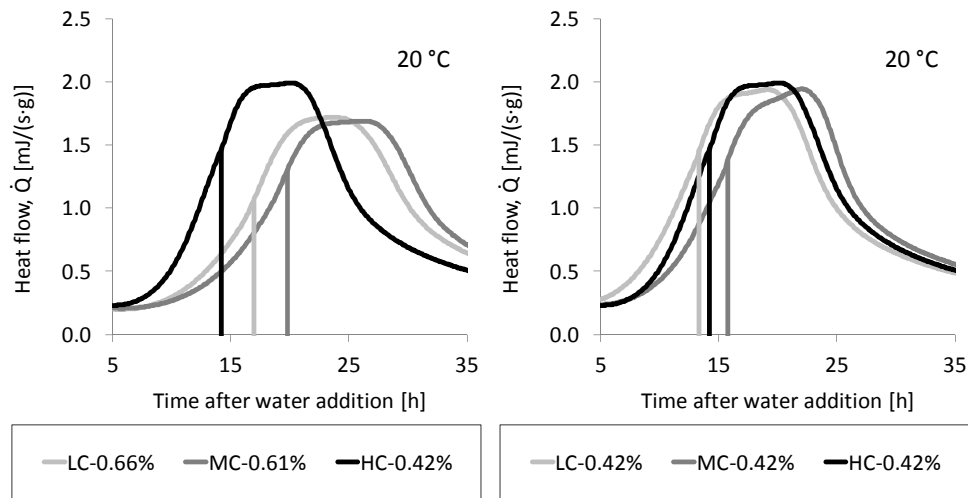


Figure 8.19: Heat flow at 20 °C for the COM pastes. Vertical lines indicate  $t_{fin}$ .

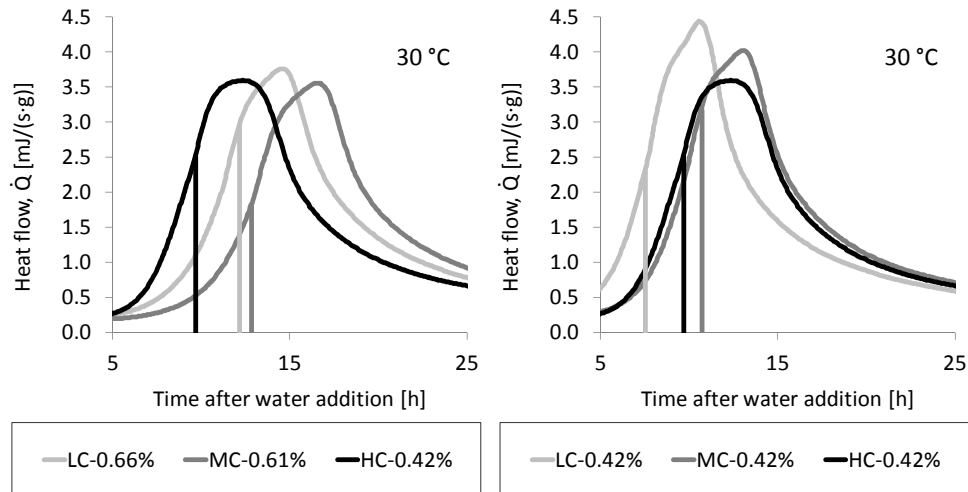


Figure 8.20: Heat flow at 30 °C for the COM pastes. Vertical lines indicate  $t_{fin}$ .

#### 8.5.4 Correlating the heat flow and the final set according to Vicat

It has become evident that the setting and the heat evolution are in good agreement. Final set retardation coincides with retarded hydration heat evolution. However, if the times of the occurrence of the final Vicat setting are observed and compared to the different curve characteristics, it is difficult to allocate a certain time related position to the occurrence of  $t_{fin}$ . It can only be concluded that  $t_{fin}$  occurred somewhere after the first third of the acceleration period and prior to its end. Figure 8.21 shows the two threshold examples, where the  $t_{fin}$  occurred closest to the onset of the accelerated hydration and on the other side closest to the maximum heat flow. It is only a coincidence that both thresholds occurred with the mix incorporating PCE MC-0.42%. No systematic effect of the temperature or of the PCE charge density could be observed.

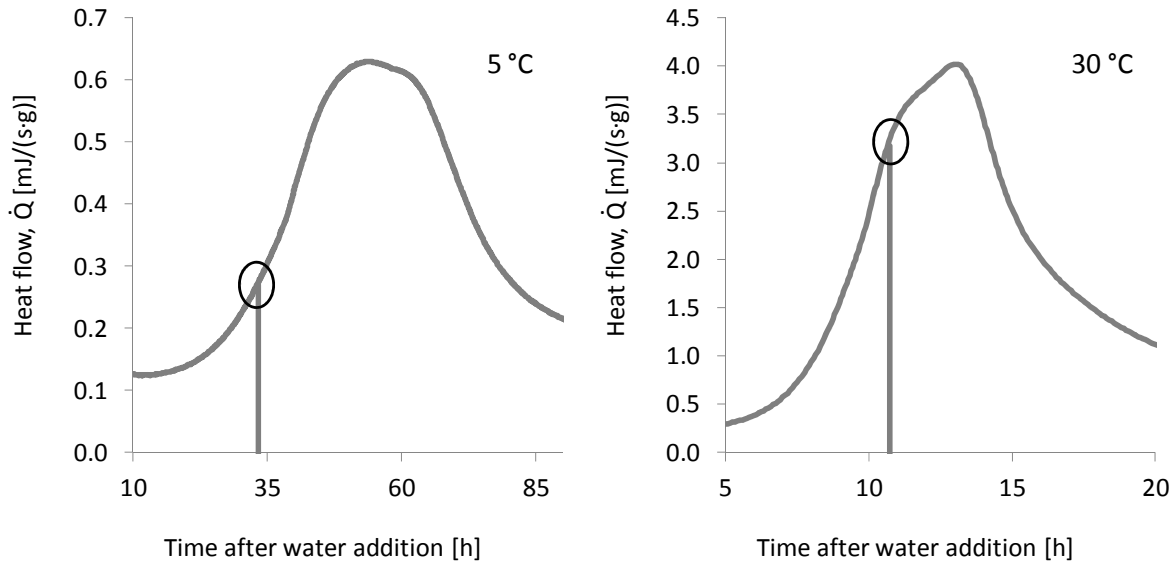


Figure 8.21: Occurrence of final set during the accelerated period for MC-42% at 5 °C and at 30 °C. Vertical lines indicate  $t_{fin}$ .

In an attempt to analyse the exact time of  $t_{fin}$  in the context with the ongoing hydration, the first derivative  $\ddot{Q}$  of the heat flow curve was calculated.  $\ddot{Q}$  can be calculated according to:

$$\ddot{Q} = \frac{\partial \dot{Q}}{\partial t} \quad (8.2)$$

where:  $\ddot{Q}$  = heat flow rate [ $J/s^2$ ];  $\dot{Q}$  = Heat flow [ $J/s$ ];  $t$  = time [ $s$ ].

From a physical point of view its unit  $J/s^2$  may appear meaningless at first sight. However, as it is the second derivative of the energy with respect to time, it can be interpreted as the energy acceleration curve. Regardless of its exact physical meaning, its characteristic helps to identify distinctive points of the heat flow curve more clearly. These curves in combination with the respective final setting times are shown in Figure 8.22 at an exemplary temperature of 20 °C. A clear relation between occurrence of  $t_{fin}$  and the heat evolution can be identified.  $t_{fin}$  according to Vicat takes place very close to the maximum of the heat flow rate, which is equal to the inflection point of the curve of the heat flow  $\dot{Q}$ . This observation also holds true when  $t_{fin}$  deflects distinctively from the half distance between onset and maximum of the heat flow curve.

The good correlation between  $t_{fin}$  and inflection point of the heat flow curve can be observed throughout all tested temperatures, as shown in Figure 8.23. The figures for all temperatures are provided in Annex C. Such a relation was already described indirectly by Taylor for pastes without PCE [82]. He linked this inflexion point to the point in time where the C-S-H shells around the particles start coalescing with neighbouring shells and hence defines this point as the cohesion point, which “coincides with the maximum rate of heat evolution and corresponds approximately to the completion of setting”.

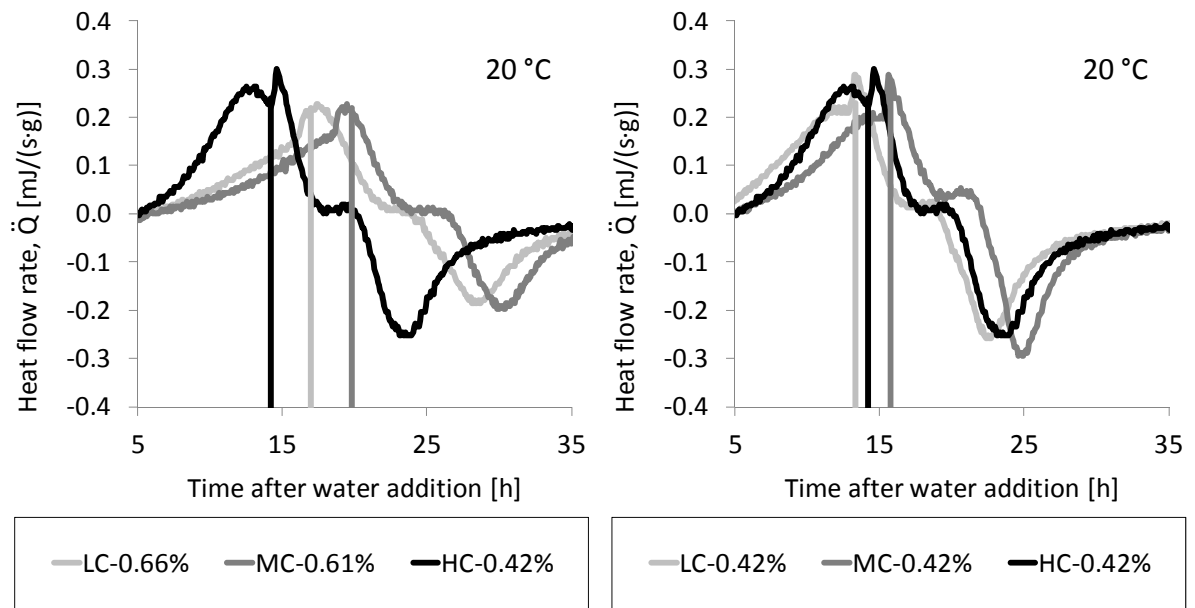


Figure 8.22: Heat flow rates  $\dot{Q}$  at 20 °C for the COM pastes. The vertical lines indicate  $t_{fin}$ .

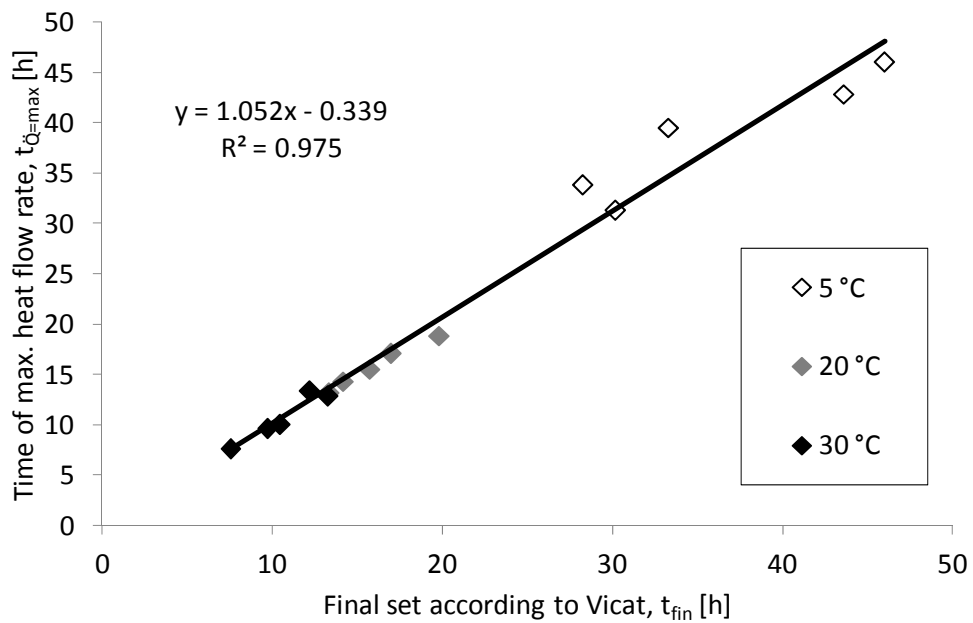


Figure 8.23:  $t_{fin}$  vs.  $t_{\dot{Q}=\max}$  for the COM pastes with different PCEs and dosages (Table 9.1) at 5 °C, 20 °C, and 30 °.

Table 8.4: Correlation coefficient for different characteristic time steps, which are correlated to the final set according to Vicat.

Characteristic step in time correlated to final set	Maximum heat flow rate	Onset of accelerated period	Maximum heat flow	Half time interval between onset maximum heat flow
$R^2$	0.975	0.957	0.947	0.957

According to Scrivener and Nonat [89], the maximum of the hydration curve defines the transition from solution-controlled to rate-controlled hydration (see Subsection 2.1.4). However, in a cementitious system it can be assumed that locally condensed areas can be found at which a rate controlled hydration takes place, while in other areas still solution control dominates the hydration. Upon coalescing of the C-S-H shells it is likely that in the interfering zones the reactive site surfaces reduce. It is hence worth considering that the cohesion point might be the trigger to start a slow process where locally rate-controlled hydration starts, so that the period from this point until the maximum heat flow can be considered as a phase during which the hydration slowly evolves from solution-controlled to rate-controlled hydration. As such,  $t_{\text{fin}}$  can be considered as a significant point during the hydration.

The occurrence of  $t_{\text{fin}}$  very close to the inflexion point of the heat flow shows that the formation of a solid macrostructure coincides with decelerated hydration. The correlation coefficient was 0.9752. Compared to the correlation coefficients that were determined for other characteristic points such as the onset of the setting, the maximum of the setting or the centre between onset and maximum, this was the best value, as shown in Table 8.4. Since the hydration curve from heat flow calorimetry corresponds in large parts to the hydration curve of  $C_3S$ , the good correlation between heat flow curve inflexion point and  $t_{\text{fin}}$  gives rise to the assumption that indeed the setting is more related to the  $C_3S$  hydration than to the hydration of  $C_3A$ , as suggested e.g. by Locher [80].

With regard to  $t_{\text{ini}}$  there were no such clear systematic similarities to the heat flow curve. This supports the hypothesis that  $t_{\text{ini}}$  does not provide important information about the hydration. As it typically occurs not too far from  $t_{\text{fin}}$ , it surely hints to the point in time at which the final set occurs, but there is no causal connection to any phenomena of the hydration. This is gaining importance with lower temperature and the presence of SP, since these extend the period in between  $t_{\text{ini}}$  and  $t_{\text{fin}}$ .

### 8.5.5 Phase evolution of COM pastes

For a better understanding of setting and heat evolution, in-situ XRD measurements were conducted with PCE HC and PCE LC on the pastes of the COM mixture. PCE LC was added at a content that yields an identical flow as PCE HC and also at the identical polymer content as PCE HC. In addition a reference COM paste mix without any admixtures was measured. Here only the points in time are discussed that were considered as most prominent. The XRD patterns for all mix variations at all observed steps in time during the first 48 h of hydration are given in Annex D. Figure 8.24 compares the patterns at approximately 3 and 24 hours in the range between  $2\theta = 15^\circ$  and  $2\theta = 45^\circ$ . The peak heights and their changes with time allow an approximate evaluation of the mineral composition, especially with regard to relative alterations in amount during hydration, occurring as clinker minerals decrease and hydrate phases increase.

The peaks close to  $2\theta = 18^\circ$  and  $2\theta = 32.5^\circ$  are considered as being representative for portlandite formation and alite dissolution, respectively. The alite peak needs further discussion since it does not distinguish characteristically from a peak that would occur because of belite. According to Scrivener and Nonat, belite is always less soluble than alite and hence, alite will dissolve earlier [89]. It is thus assumable that at this early stage the peak changes concern alite. Since the boundary conditions of all mixtures were identical the peak heights allows a qualitative assessment of the amounts.

The patterns of all mixtures with PCE show similarities. During the first 24 hours a high amount of portlandite is formed. Here it seems that the higher the PCE content, the more portlandite is formed. Furthermore, the graphs give evidence that PCE with lower charge fosters the formation of portlandite. Furthermore, alite dissolves between 3 and 24 hours. Here, it seems

there is no effect of the PCE solid amount, but at a higher dosage, more alite dissolves. Other characteristic peaks behave similarly regardless of the type and amount of PCE.

The mixture without PCE differs significantly in its characteristics. Considering the peaks at  $2\theta = 18^\circ$ ,  $23^\circ$ ,  $32.5^\circ$ ,  $34^\circ$ , and  $42^\circ$ , major differences can be observed compared to the mixtures with PCE. Significantly less portlandite is formed. The amount of dissolved alite ( $2\theta = 32.5^\circ$ ) between 3 and 24 h is much smaller, and also at 3 h, the total amount of alite is much higher than in case of mixtures with PCE.

Though differences induced by the amount and type of PCE could be observed regarding portlandite formation and alite dissolution, in general it can be seen that with PCE high amounts of portlandite are formed between 3 and 24 h and a high amount of alite is dissolved at the same time. Both observations cannot be made with the mix without PCE. It thus seems that the hydration is generally affected rather by the presence of high amounts PCE than by its amount or modification.

However, according to the former observations, a strong relation between polymer type and respective content on both the heat evolution and the setting exists, which should be identifiable in the phase development as well. Figure 8.25 shows the XRD patterns approximately at the specific times of the final set according to Vicat and the maximum of the heat flow curves.

As before, the differences of those mixtures containing PCE can be mainly observed at  $2\theta = 18^\circ$  (portlandite) and  $2\theta = 32.5^\circ$  (alite). The mixture without PCE shows the highest alite peak and the lowest portlandite peak compared to the other mixtures. The mixture LC-0.66% with the highest PCE content shows the highest portlandite peak and the lowest alite peak. The mixtures LC-0.42% and HC-0.42%, which both contain identical polymer contents, behave very similar. In general, it can be observed that all mixtures containing PCE exhibit higher contents of portlandite and a quantitatively larger decrease of the peak that can be assigned to alite. In comparison with Figure 8.24, it can be observed that between 3 h and the final set alite has dissolved, which supports the findings by Sowoidnich and Rößler that the retardation due to PCE cannot be attributed to a hindered dissolution of alite [319].

Considerable differences between the mixes with and without PCE can be observed here as well in those peaks close to  $2\theta = 34^\circ$  (framed by a circle), the left of which is significant for portlandite, the right of which for alite. No changes can be observed for these peaks for all mixes with PCE. The mix without PCE, however, shows a prominent increase of portlandite during this period, while the alite content is reduced. No significant changes can be observed for any mix including PCE. This again emphasises that the hydration of mixes with and without PCE varies significantly such that for cementitious systems without PCE, significant reactions can be observed after  $t_{\text{fin}}$ , while for mixes with PCE,  $t_{\text{fin}}$  rather marks the point in time at which much of the hydration reactions are already conducted.

Although the dissolution of the alite phase as well as the portlandite formation occurred at increasing magnitude with increasing PCE content, the times of these processes were shifted towards later points in time, depending on the PCE amount. Figures 8.26 and 8.27 contain time-resolved qualitative diagrams of the evolution of the portlandite and the alite peak height, respectively. The vertical lines represent the respective Vicat final setting times. After a certain induction period, for all mixes the portlandite content increases significantly, then reaches a maximum plateau after which it slightly drops before it levels off.

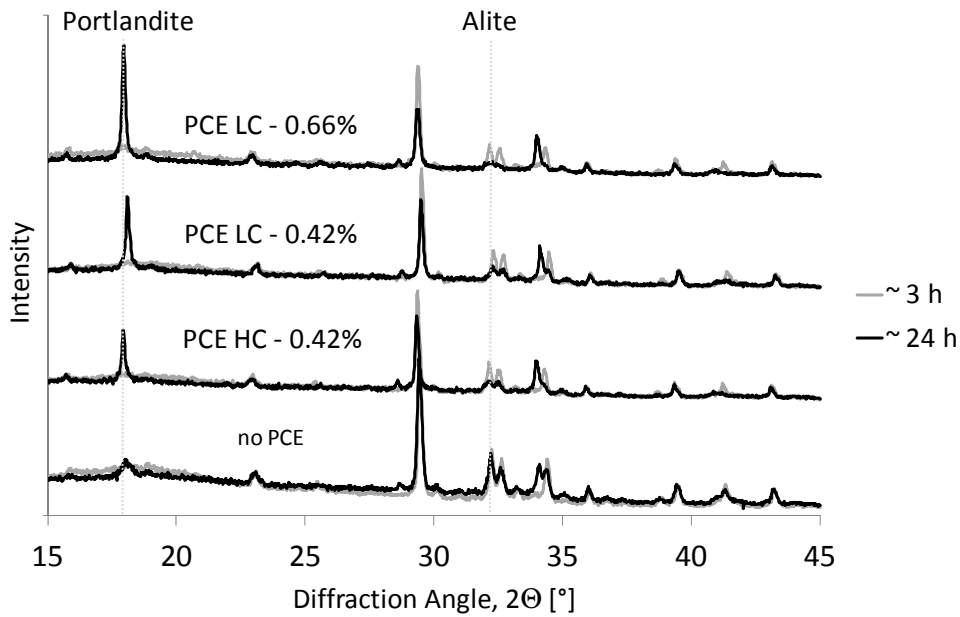


Figure 8.24: XRD patterns for mixes with varying admixture setups at 3 and 24 h.

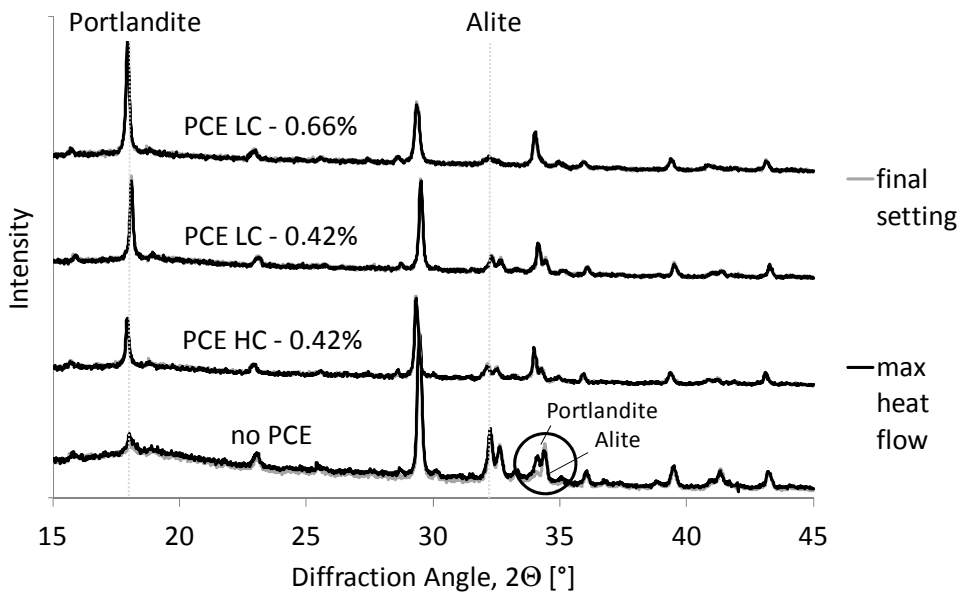


Figure 8.25: XRD patterns for mixes at final set and maximum heat flow.

This observation is highlighted when the evolution of the portlandite and alite peak is made dimensionless (related to the maximum) in time. For all mixes with PCE the transition towards a horizontal line of both, portlandite and alite, takes place very close to  $t_{\text{fin}}$  according to Vicat. This effect cannot be observed for the mixture without PCE, where  $t_{\text{fin}}$  occurs rather at the onset of the portlandite increase and the beginning of the alite depletion. The explicitness of this observation underlines the importance of distinguishing between systems with and without PCE, while it seems of secondary importance how much or what kind of PCE is present.

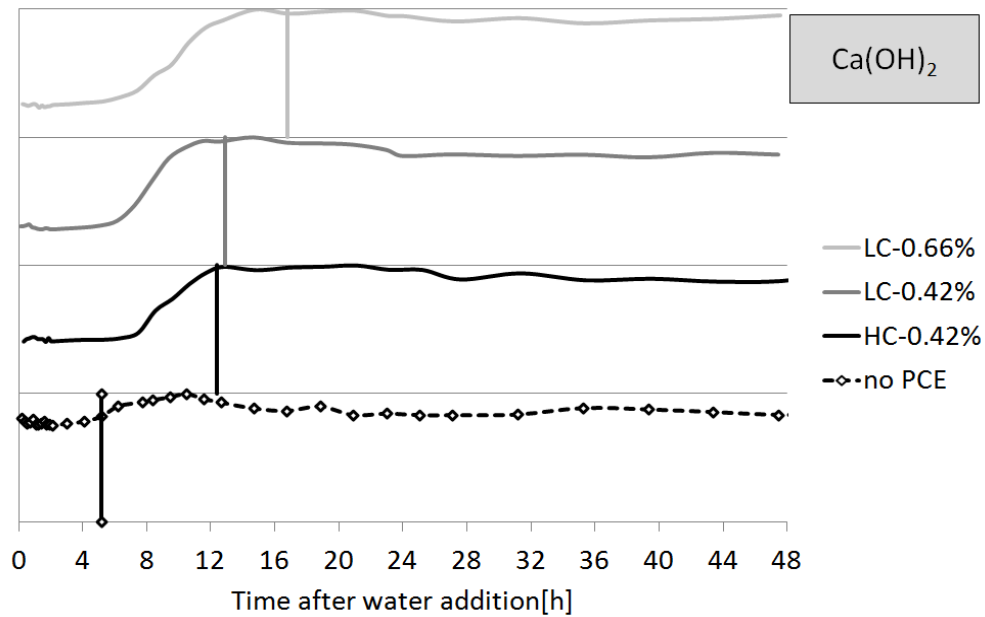
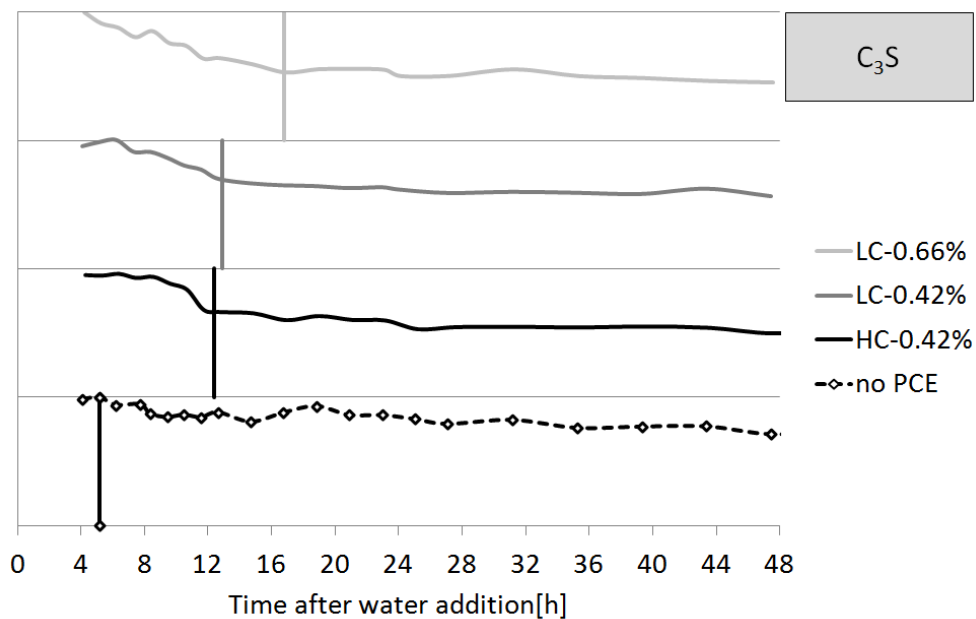


Figure 8.26: Evolution of main portlandite peak with time.

Figure 8.27: Evolution of alite and belite peak at  $2\theta = 32.5^\circ$ .

The results show that systems with and without PCE generally distinguish in their characteristics during the hydration, regardless of the type and the amount of PCE. However, furthermore, specific effects of systems with PCE can be identified depending on type and amount. The alite peak develops with inverse characteristics for all mixes but with similar time dependent evolution. After an induction period, the content decreases and levels off. The rapid increase of the portlandite peak correlates well with the reduction of the alite peak and the maximum of the portlandite peak occurs at the transition of the alite peak towards a horizontal plateau. Increasing PCE contents shift the onset and the end of the portlandite evolutions and the

alite decline towards later points in time. The curves of the mixes with identical polymer content, but that only differ in the PCE modification, behave very similar. This underlines the observation from calorimetry and Vicat testing that effects on the hydration due to PCE are predominantly caused by the amount of polymers in the system and less by their modification.

### 8.5.6 Early deformations of COM pastes after the final set

In parallel to the observations of hydration and setting, the early deformations were studied on the pastes used before in a shrinkage cone as described in Subsection 4.4.5. The test setup cannot distinguish between the sources of these deformations, which are basically caused by settlement, and chemical and autogenous shrinkage. The total shrinkage for all COM mixes at 5, 20, and 30 °C after the measurement start is shown in Figure 8.28. Since the results are not fully comparable to linear measurement methods and the influence of the varying diameters over the cone height cannot be quantified, the deformations are expressed as  $\Delta h/h$  [ $\mu\text{m}/\text{mm}$ ]. The total deformation, however, can only be measured after the start. Between paste filling and first measurement several minutes pass unavoidably. The figure shows that particularly during the first hours large deformations are measured and that within minutes large deformations can occur. This period, during which no information can be gathered, thus manifests that the total shrinkage values cannot be compared without referring to a particular time-zero. Nevertheless the curves can be compared in their time dependent evolution. Typically the curves show a first interim peak after several hours of rapid deformations, for a short period the shrinkage reduces, before it rapidly increases again until a certain steady state is reached. At this state, the deformations take place at distinctively slower rate and resemble horizontal lines.

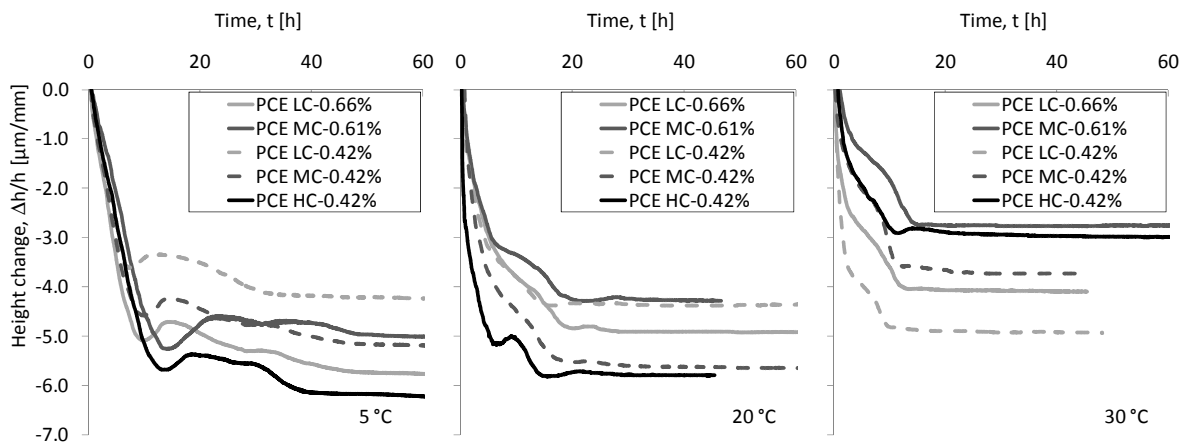


Figure 8.28: Paste deformations after the water addition.

The curve characteristics vary with PCE type, PCE amount, and temperature in the peculiarities of the characteristic peaks, but this hardly occurs in a systematic way. In general at low temperatures, the transition towards slow rate shrinkage occurs latest, while it occurs earliest at high temperature. However, regardless of the temperature, PCE type, or PCE amount, this transition happens at similar times. This is an indicator that the early deformations might be much more affected by the cement type and the w/p, which were all identically in these observations. Although time differences can be observed due to the PCE adjustment, which are most prominent at 5 °C, these are of significantly lower magnitude than the time differences that were induced by the PCE amount with regard to the setting (Figure 8.16). Figure 8.29 shows an example in which the amount of PCE causes a large shift of the final set times, while the deformation curves behave similarly. Both deformation curves show increasing shrinkage

between 30 h and 40 h, which level off afterwards. The mixture with PCE HC sets at approximately 30 h, which causes that these strong deformations already take place at solid state. PCE LC sets at approximately 42 h, causing that these strong deformations between 30 h and 40 h still take place in a plastic state. The large deformations of the mix with PCE HC can be considered as most critical since at this stage concrete is already in a solid state but the strength is still negligible. This makes the system prone to cracking at constrained conditions.

The deformations for all mixes and admixture variations after the final Vicat setting time  $t_{fin}$  are shown for the PCE amounts yielding similar flow properties in Figure 8.30 and for identical PCE amounts in Figure 8.31. The curves show complicated behaviour and a discussion is delicate. Therefore, only those observations shall be discussed here which can be considered as most obvious. Regardless the PCE type and amount, it seems that the lowest deformations can be observed generally at 20 °C, while higher deformation occur at lower as well as at higher temperatures. Here, at each temperature, two different mechanisms determine the deformations after the setting. At high temperatures, the deformations are fostered due to the quicker consumption of water caused by accelerated hydration. At low temperatures, the hydration is slowed down significantly. Even after the setting, the structural build up takes a long time and the resistance against deformations increases only slowly.

The deformations after  $t_{fin}$  at higher PCE dosage (Figure 8.30) are always smaller than the deformations at lower dosage (Figure 8.31). This effect occurs since the amount of PCE did not significantly affect the deformation characteristics but they shifted  $t_{fin}$  strongly in time. This leads to the conclusion that high amounts of PCE generally reduce the risk of early cracks due to the shifting of the time of  $t_{fin}$  to a later stage. Reversely, lower dosages increase the cracking risk, as a significant part of the early deformations take place in an already solid state.

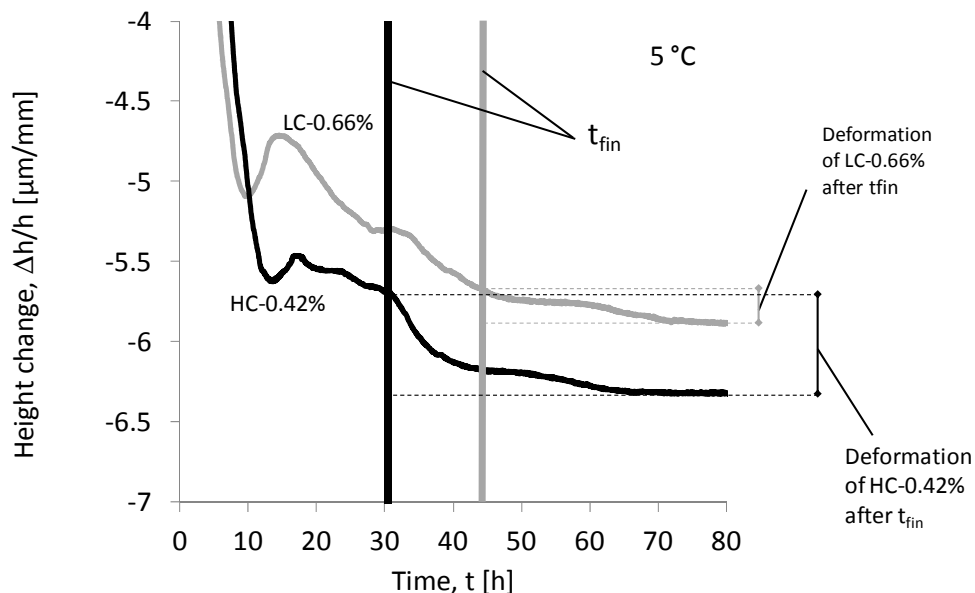


Figure 8.29: Paste deformations during the first 80 h after mixing at 5 °C. Vertical lines mark the respective Vicat final setting times  $t_{fin}$ .

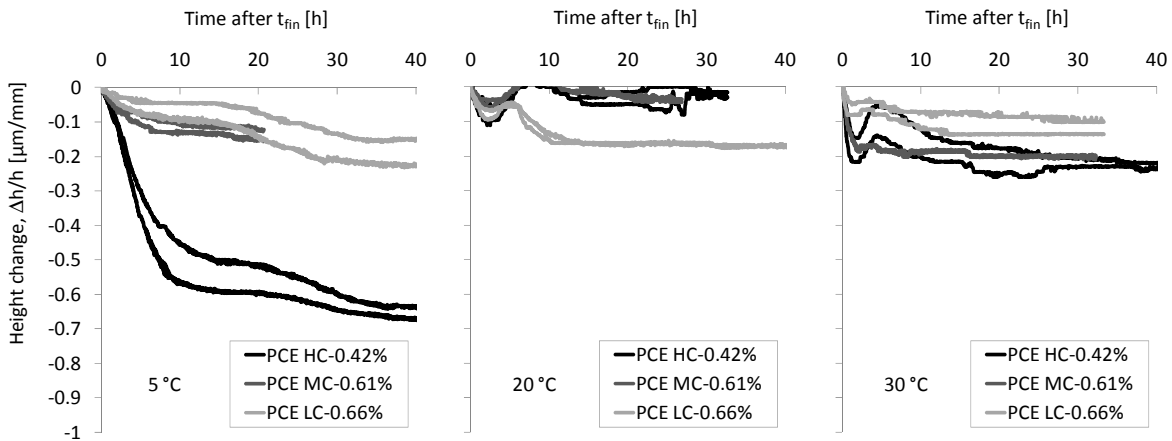


Figure 8.30: Paste deformations after the final set ( $t_0 = t_{fin}$ ) at different temperatures for mixes with PCE HC, MC, and LC at dosages to achieve similar flow properties.

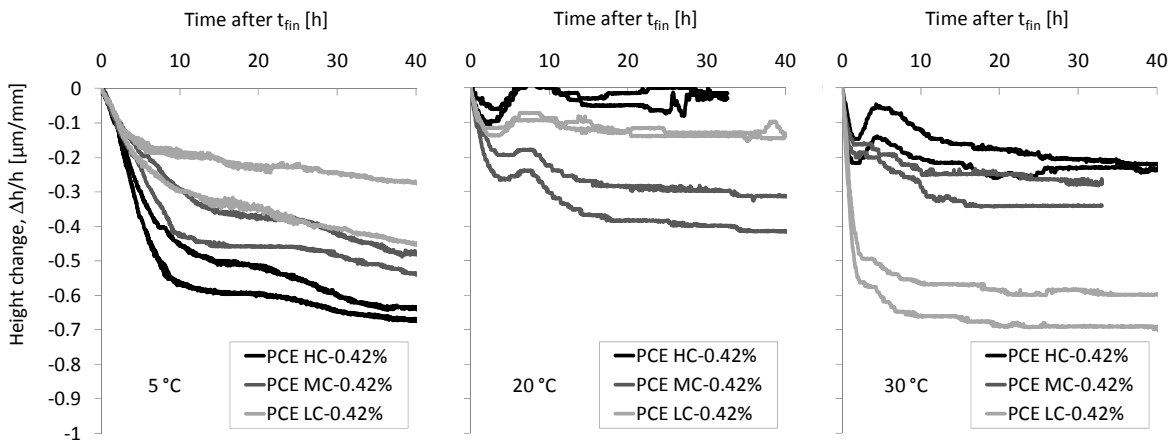


Figure 8.31: Paste deformations after the final set ( $t_0 = t_{fin}$ ) at different temperatures for mixes with PCE HC, MC, and LC at identical solid amounts.

### 8.5.7 Influence of the mix design

The results presented in the former Subsections 8.5.2 to 8.5.6 were performed on mixes based on the SCC of the combination type. Due to the high complexity of the formerly described tests, these could not be conducted to the same extent with all POW pastes. Nevertheless, in order to assess the influence of the mixture composition type, setting and shrinkage were also measured for a POW mixture with the high charge density PCE. The results for the setting are shown in Figure 8.32 and compared with the COM mixture containing PCE HC.

In general, the setting of the POW mixtures occurs significantly earlier. This earlier setting is induced by three major driving factors. For identical rheological properties, the POW mixture required less PCE solids. Furthermore, the w/p of the POW mixture is lower, both effects cause less retardation in setting. Finally, the POW mixture contains a higher amount of LSF, which accelerates hydration due to supplying the hydrating system with hydration nuclei. The formation of monocarbonate is unlikely to play a role. In Subsection 8.2.2 it was presented that calcium carbonate has two different effects on the hydration. The first effect is hydration acceleration by providing hydration nuclei; the second is a formation of monocarbonate rather than monosulphate. In this chapter the focus is placed on the period during the setting. This

takes place at normal and elevated temperatures during the first day. As can be seen from XRD measurements presented by Lothenbach et al. [119] (Figure 8.1), the hydration products after and one day of hydration between a mixture with and without calcium carbonate are very similar, and effects from the modified hydration can be observed at a later point in time.

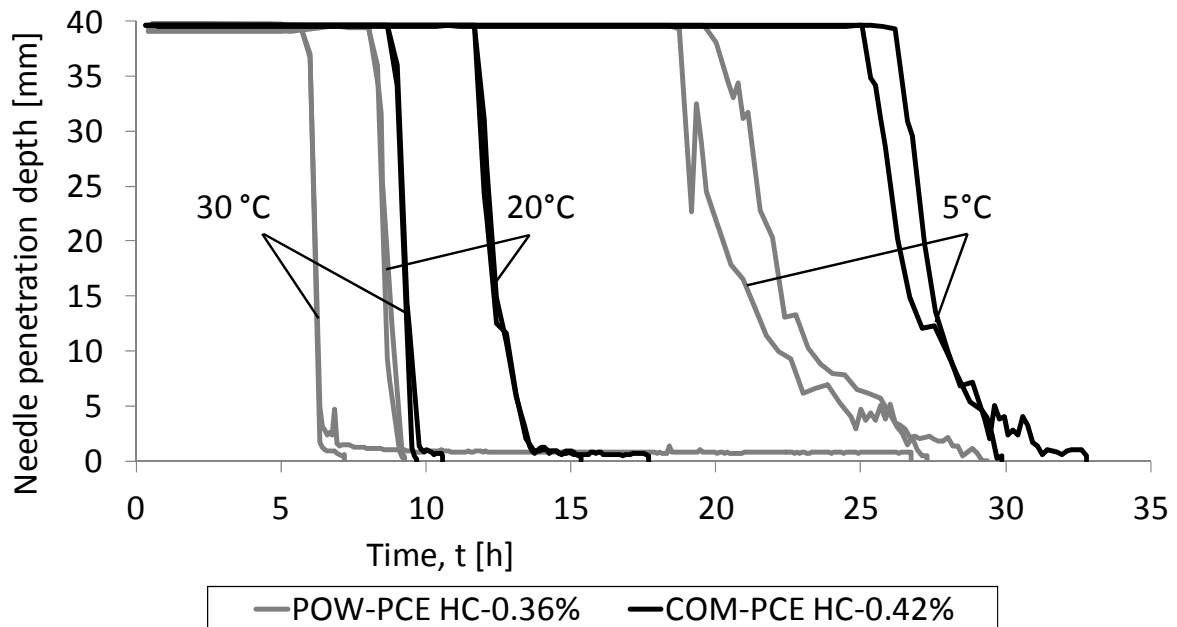


Figure 8.32: Setting of COM and POW paste mixtures with PCE HC at varied temperature.

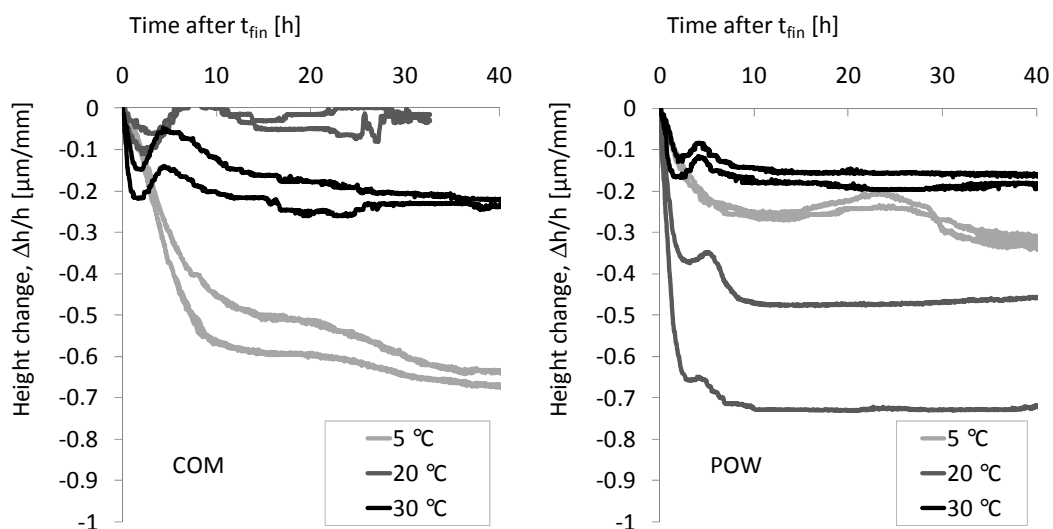


Figure 8.33: Deformations after final set ( $t_0 = t_{\text{fin}}$ ) of COM and POW pastes with PCE HC.

At 20 °C, the POW mixture shows larger deformations than the COM mixture after  $t_{\text{fin}}$ . At 5 °C, the situation is reversed. At 30 °C, the deformations after  $t_{\text{fin}}$  are similar (Figure 8.33). At low temperatures, the POW mixture develops its strength much quicker than the COM mixture, due to its lower w/p and the higher amount of LSF in the mixture. Hence, after setting the resistance of the POW mixture against deformations increases rapidly, and therefore the crack risk is lower. With increasing temperature, the quicker hydration reactions of the POW mixtures may foster shrinkage again, while the deformation resistance after  $t_{\text{fin}}$  might be similar for POW

and COM. Hence, POW mixes shows larger deformations than COM mixes. At 30 °C both mixtures may be similarly affected by the hydration reaction and the deformation resistance development by structural build-up, so that at this temperature the influence of the mixture composition can be considered as negligible.

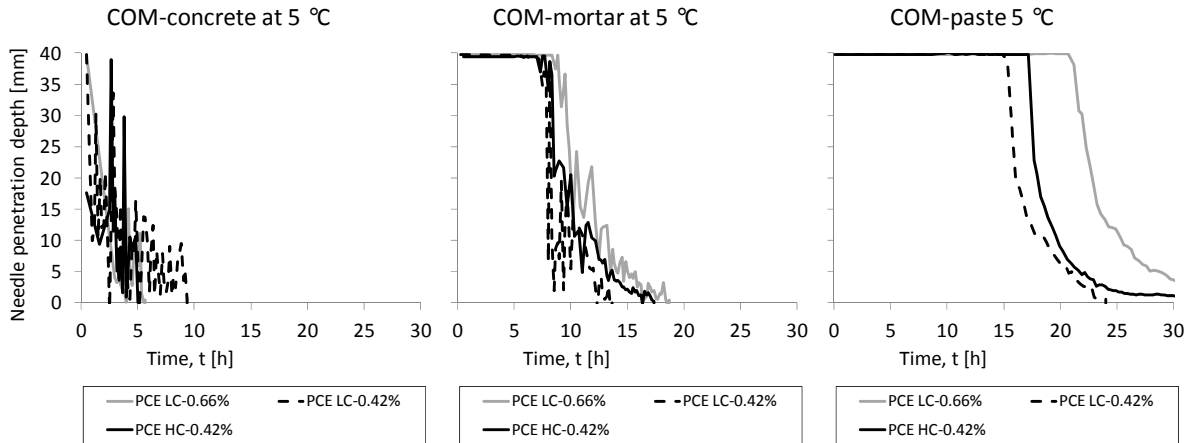


Figure 8.34: Setting of COM concrete, mortar, and paste at 5 °C.

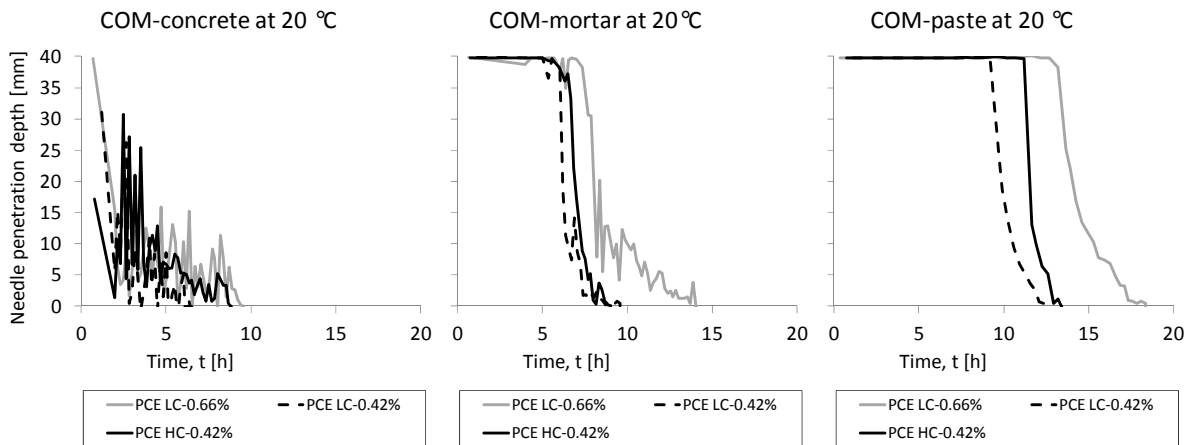


Figure 8.35: Setting of COM concrete, mortar, and paste at 20 °C.

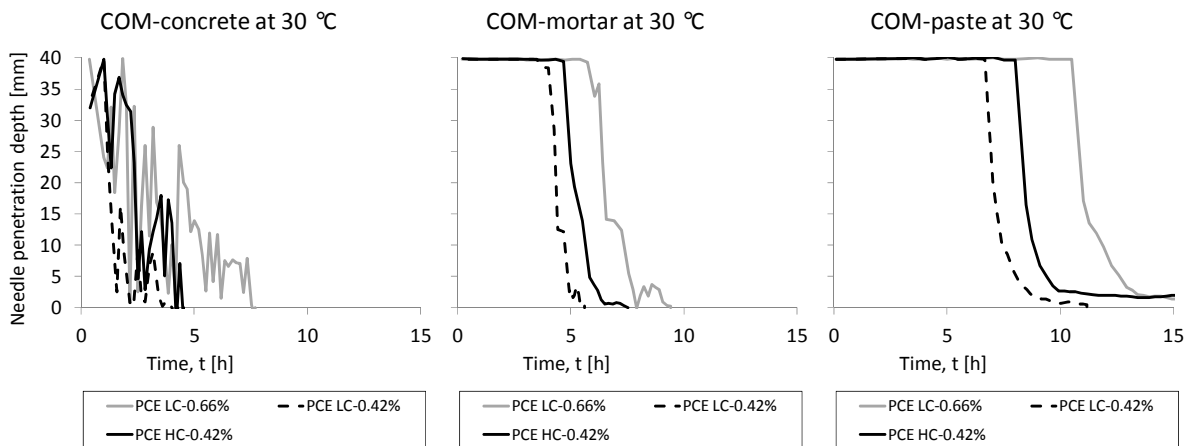


Figure 8.36: Setting of COM concrete, mortar, and paste at 30 °C.

### 8.5.8 Relevance of the paste observations for concrete

In order to assess whether the findings of this chapter have relevance for the application of concrete, modified Vicat tests were conducted with paste, mortar and concrete samples (see Subsection 8.4.5). The results for the concrete samples, which are shown in Figures 8.34 to 8.36 cannot identify the initial set since due to the aggregates the needle cannot drop to the bottom of the Vicat ring. Furthermore, the curves scatter strongly, since depending on the arrangement of aggregates inside the sample, the needle penetrates more or less deep. Nevertheless,  $t_{\text{fin}}$  can be estimated, as at the point in time when the needle can no longer penetrate the sample, the effect of the aggregate becomes negligible.

The general observation about the setting to be rather affected by the amount of PCE than by the PCE modification can be confirmed by these observations. The final set of PCE LC-0.42% and PCE HC-0.42% occurs always at similar points in time, while  $t_{\text{fin}}$  occurs later, when PCE LC-0.66% is used. However, the lower the paste content of the overall mix, the less pronounced, this effect occurs. While still significant at mortar level,  $t_{\text{fin}}$  is similar for all admixture modifications, when concrete is investigated.

Furthermore, it can be observed that the setting occurs the earlier the lower the paste content is. Also the strong effect of the temperature on the setting becomes less. While the difference between 5 and 30 °C caused a set retardation of approximately 15 h for pastes, on mortar scale this difference is only 7-8 h, and on concrete scale even only 3-5 h.

## 8.6 Conclusions

Investigations of setting, heat evolution, phase evolution and early deformations were conducted on identical paste mixtures, modified with differently charged PCE types.

There was no systematic influence of the PCE charge density on the occurrence of the final set according to Vicat. At identical dosages the final setting occurred in the order PCE LC, PCE HC, PCE MC. Compared to the influence of the content of PCE on setting, any influence of the molecular structure on setting was negligible. For practical reasons, PCE is added according to flow specifications and not according to a defined content. It can thus be concluded that low charge density PCEs yield higher retardation of the setting than high charge PCEs, since in general the latter typically demands less solids for identical flow properties.

The influences of the PCE type on the setting were confirmed by the heat flow curves. A good correlation between final set and the inflexion point of the heat flow curve was demonstrated.

Time-resolved XRD measurements and discussions of alite dissolution and portlandite evolution over the course of time confirmed the former observation that the influence of the total PCE content on the phase development outweighs influences from the polymer structure. Regardless of the charge density, the observed PCEs showed similar XRD patterns when added at identical polymer amounts. However, the amount of formed portlandite seems to increase with lower charge density of the PCE and with increasing PCE content. The  $C_3A$  dissolution was not too strongly affected by the PCE modification.

In general, all mixtures including PCE showed different phase characteristics at specific points of the hydration that the control mixture without PCE.

While the final setting for mixes without PCE occurred close to the onset of an accelerated formation of portlandite and the beginning of a stronger dissolution of clinker, the setting of the mixes with PCE occurred at the end of the portlandite evolution and end of the accelerated alite dissolution. This observation was valid for all mixes with PCE, regardless of charge density or

amount. This points out that a modification of the hydration kinetics and the mechanisms for setting are mainly affected by the PCE presence itself.

The strong influence of the PCE amount on setting and hydration was not observed for the early deformations. As a result, higher contents of PCE shifted large parts of deformations to a still plastic state and generated smaller deformations at elastic state, due to set retardation. It can hence be concluded that higher amounts of PCE reduce the risk of early cracks due to their retarding effect.

The observations regarding the setting were valid for powder type and combination type mixtures. In general, the powder type mixtures showed significantly earlier setting due to the high amount of calcium carbonate, the lower w/cm as well as the lower PCE content that was required to adjust the specified flow performance.

Regarding the shrinkage it was observed that at cold temperatures, the POW mixture seems to be less prone to cracks, since the deformations after the final set were smaller. This effect was allocated to the accelerated hydration. At 20 °C the situation reversed, since the accelerated hydration reaction at warmer temperature fosters shrinkage deformations. At 30 °C no significant difference between the mixture compositions could be observed.

The setting observations were also conducted with mortar and concrete. In general, the conclusions that are drawn above are applicable for mortar and concrete as well. Nevertheless, it can be seen that the magnitude of the effects reduced the lower the paste content is in the total system. Effects that occurred prominently either due to PCE or temperature, occurred significantly less pronounced in mortar and even less in concrete.

## 9 Effects of stabilising agents on the early hydration

### 9.1 Introduction

The variety of polysaccharide stabilising agents (STAs) is wide (Subsection 7.1). Their effects on the early hydration of cement are not well understood and contradicting information can be found in literature. [25, 261, 263, 266, 268-270, 324-326]. SCC often combines stabilising admixtures with SP to provide segregation resistance and high viscosity in a low yield stress system. This increases the probability of interactions between the admixtures, not only with regard to rheology, but also during the early hydration. Only few published studies discuss the combination of both admixture types, e.g. [25, 124, 131, 203, 204, 279, 327]. This chapter presents effects of different STAs on cementitious binder pastes exposed to varied climatic conditions during casting and early hydration. It is demonstrated that due to interactions, the typically observed retarding effect of stabilising agents on the setting of cementitious systems does not necessarily occur when SPs based on polycarboxylate ether are present.

### 9.2 The early hydration in the presence of stabilising agents

Rheological modifications are generated on purpose, but the adjustment towards specific rheological properties by help of admixtures can be accompanied by significant effects with regard to the early hydration. As seen in Chapter 5, the charge density of a PCE determines the amount needed to achieve the specified flow behaviour, while the total amount of PCE is the main influencing factor on the hydration. If stabilising agents (STAs) are used for concrete these are typically added in significantly lower amounts. Hence, it can be assumed that their effect is smaller than that of SPs. Nevertheless a number of researchers report about effects on the setting induced by the addition of STAs [25, 261, 263, 288, 324, 326].

Khayat published a very comprehensive state of the art report in 1998 [25]. In this report he links the influence on the setting to the type and concentration of STAs, as well as to the type and the dosage of SPs. He furthermore states that the cement type and the w/c can have an effect on how STAs affect the setting. He opines that the set retardation is caused by the adsorption of STAs onto cement grains, which may interfere with the precipitation of ions into solution. According to the author, cellulose may cause delay, while acrylic-type stabilising agents do not show a retarding effect. The author further reports that the set retardation induced by hydroxypropylmethyl cellulose (HPMC) in combination with polymelamine sulphonate superplasticiser (PMS) could be observed regardless of the w/c. The same was valid for welan gum in the presence of naphthalene based SP (PNS). Both systems only showed minor effect of the STAs when no SPs were present simultaneously.

Peschard et al. observed effects of different polysaccharides, viz. cellulose ether, starch ether, native starch, white dextrin, yellow dextrin [324]. Dextrins are hydrolysis based degradation products of starch which occur in white colour if based on potato and in yellowish colour if based on maize [328]. At the observed mass related dosage of 0.5% of the cement the different polysaccharides all retarded the hydration in different order of magnitude. A qualitative evaluation of the retarding effects is given in Figure 9.1.

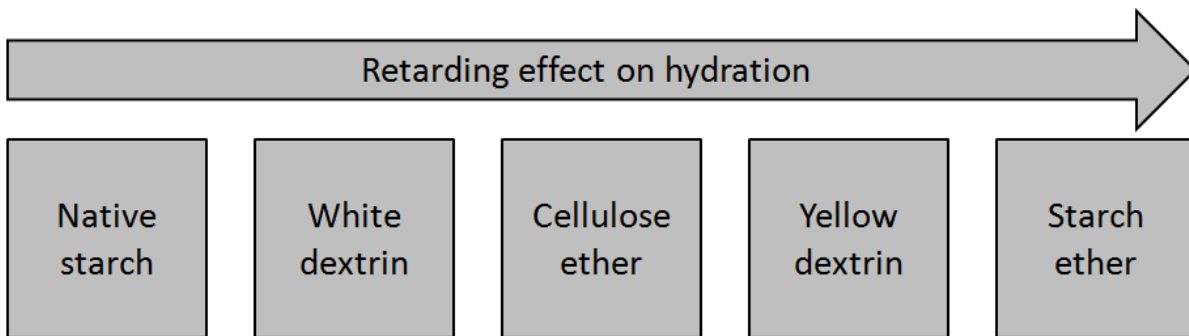


Figure 9.1: Qualitative evaluation of the retarding effect of different polysaccharide at equal dosage according to the observation of Peschard et al. [324].

Peschard et al. [324] observed that ettringite was stabilised by all these polysaccharides, which delayed the conversion of ettringite to AFm (Figure 2.4 and Subsection 2.1.4). They conclude that polysaccharides affect rather the growth of hydrates than their nucleation, which again would yield the hypothesis that the retarding effect is mainly induced by the adsorption of the STAs and a less permeable coating. Although they observe retardation of C-S-H formation caused by polysaccharides, they conclude that the  $C_3A$  content in the system is the key parameter for the retardation. The lower the  $C_3A$  content, the higher the retardation.

Schmidt and Kühne report about retarded hydration and setting caused by the addition of STAs (Figure 9.2 and Figure 9.3, respectively). In this study pastes were modified with PCE, STA based on cellulose ether, and a shrinkage reducing agent (SRA). The agents' effects were investigated separately and in combination. Retardation occurred most pronounced when blends of PCE and cellulose ether STA were used. Shrinkage reducing agents added supplementary partly compensated the retarding effect of the STA. [130]

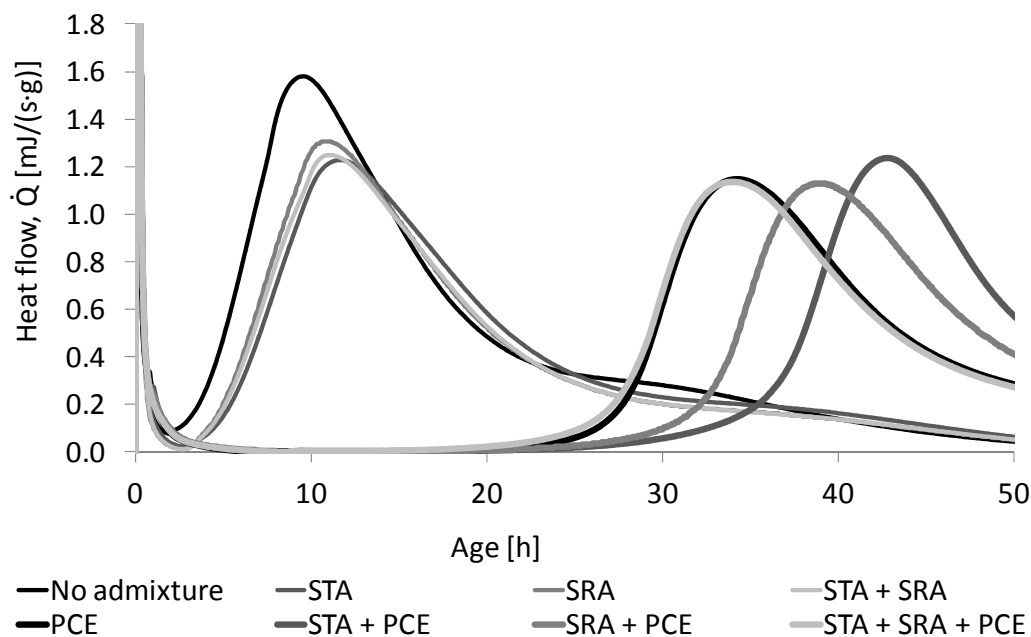


Figure 9.2: Influence of different admixtures on the heat flow evolution at 20 °C [130]. PCE = Polycarboxylate ether superplasticiser, STA = Cellulose based stabilising agent, SRA = Shrinkage reducing agent.

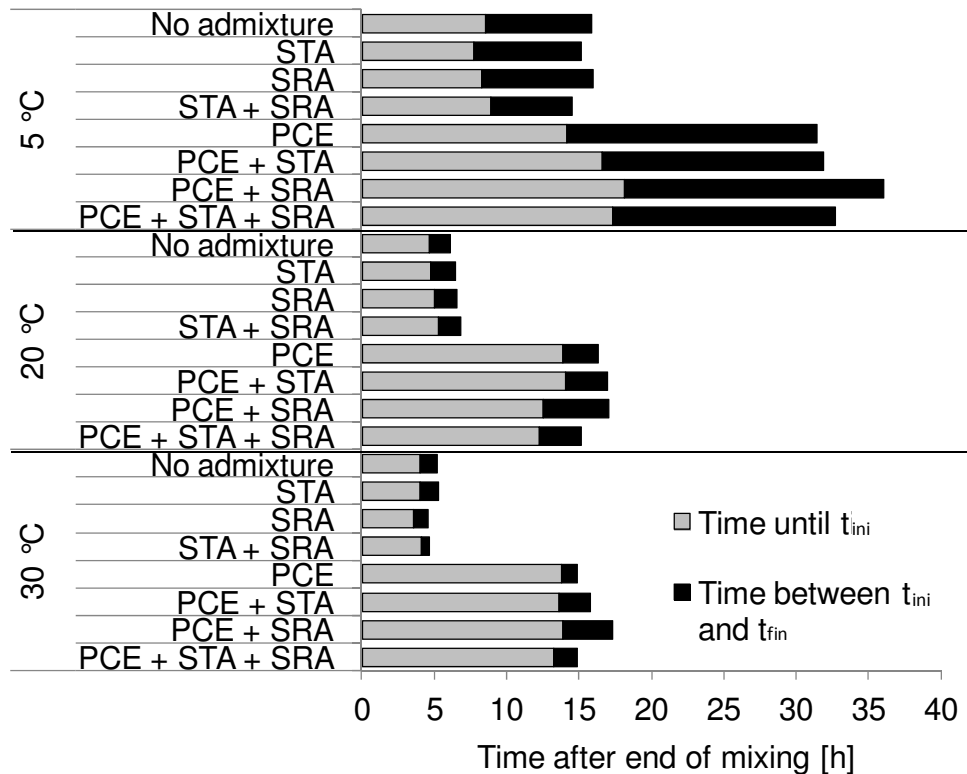


Figure 9.3: Influence of different admixtures on the setting [130]. PCE = Polycarboxylate ether superplasticiser, STA = Cellulose based stabilising agent, SRA = Shrinkage reducing agent.

Leemann and Winnefeld investigated the effect of different STAs on the rheology of mortar and concrete, among which ethylene oxide (EO), natural polysaccharide (PS), and modified starch (ST) were observed as well as mineral STAs [326]. The natural polysaccharide and the starch derivative were added in amounts of 0.4% by mass of cement, the ethylene oxide agent in 1.0%. Supplementary 1% PCE was added to the mixtures. All organic admixtures showed no significant influence on the early hydration. The results indicated that only the one day strength was slightly slower in the presence of STA. Figure 9.4 shows the effect of the agents on the heat flow, also indicating that there is no considerable effect on the hydration curve. However, it seems that the starch derivative slightly accelerated the early accelerated period, while the natural polysaccharide slightly slowed the process. Ethylene oxide also caused a slight acceleration.

Pourchez et al. studied the retarding effect of different cellulose modification, varying in the number of methoxyl, hydroxypropyl, and hydroxyethyl groups (Figure 7.2) among others by measuring the electric conductivity of the pastes [261]. All observed mixture modifications with cellulose derivatives affected the hydration to different degrees, but all admixtures showed a retarding effect. The authors conclude that a higher number of methoxyl groups or hydroxypropyl groups correlates with retarded time of the portlandite precipitation, which yields a hydration slow down (Figure 9.5). Based on this, the authors assume that the retardation is either caused by adsorption of polymers on cement or that degradation products such as carboxylate might retards the setting.

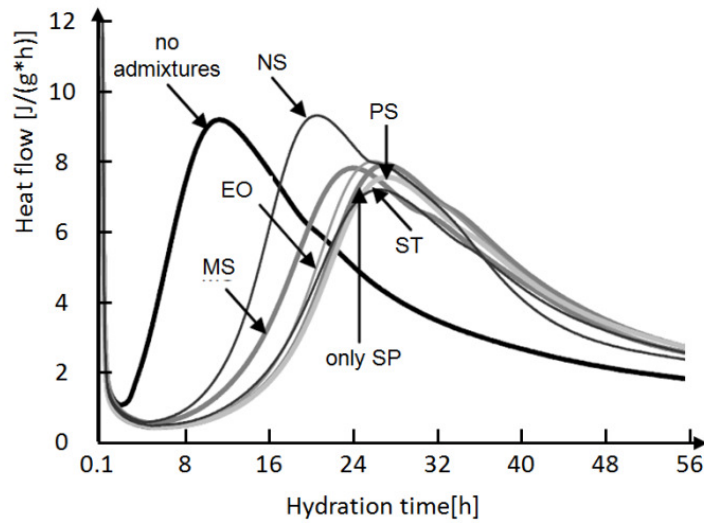


Figure 9.4: Influence of different admixtures on the hydration heat flow evolution modified after Leemann and Winnefeld [326]. NS: nano silica; PS: natural polysaccharide; EO: ethylene oxide derivate; ST: modified starch; MS: microsilica.

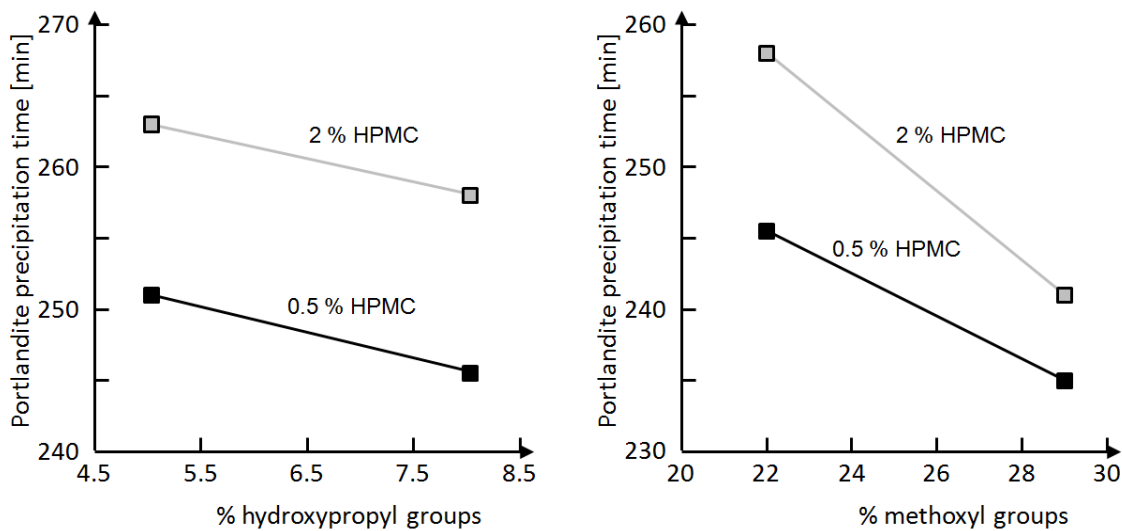


Figure 9.5: Influence of the percentage of hydroxypropyl groups and methoxyl groups on the calcium hydroxide precipitation time after Pourchez [261].

In a further study Pourchez et al. [263] investigated the alkaline stability of cellulose ethers. They state that polysaccharides tend to yield hydroxyl carboxylic acids in alkaline media. Therefore they investigated the performance of differently modified celluloses and their possible degradation products. They identified lactic acid and glycolic acid as the major degradation products from cellulose ethers. The study focused on two major driving forces that are assumed to retard the hydration, which are the calcium complexation as well as effects induced by the sugars that form as degradation products. Both effects turned out not to be responsible for the hydration retardation of cement. Only minor calcium binding capacity could be observed for the cellulose ethers and the stability of the observed celluloses was high so that the influence of the degradation products was negligible.

Phyfferoen et al. opine that also for diutan gum, calcium complexation can be considered as negligible, since the double rhamnose side chains sterically shield the anionic carboxylate backbone [201]. Zhang et al. [140] report about retarding effects of maltodextrin, hydroxyethylcellulose (HEC), and diutan gum.

Rajayogan et al. observed the setting of SCC mixtures with different dosages of welan gum and hydroxypropyl starch by using a penetrometer test [281]. There was no systematic influence of the amount of added STA, and the results point out that there is only a negligible retardation induced by the hydroxypropyl starch. The strength developed slower with increasing amount of both STAs and also the final strength reduced with increasing amount of admixture.

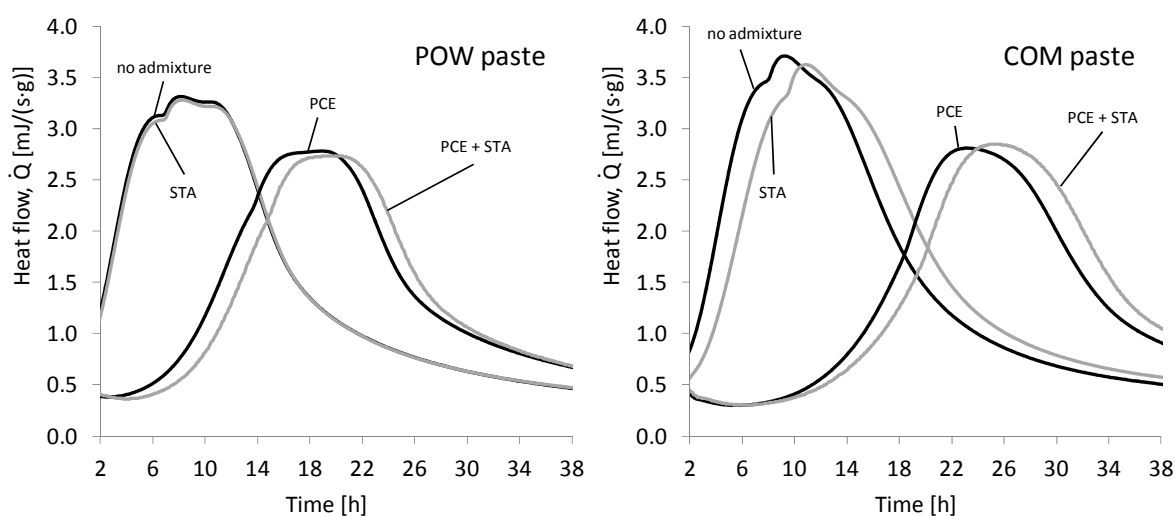


Figure 9.6: Hydration retardation caused by STA on powder type and combination type SCC paste [288].

Schmidt presents results of isothermal heat flow experiments with paste from combination type and powder type SCC mixtures and different admixture variations [288] (Figure 9.6). A starch based STA was used in these tests. For the combination type paste incorporation of high amounts of STA yields a strong retardation, with and without SP. For the powder type mixture, which only contains low STA contents, retardation could only be observed in the presence of SP.

Despite singular observations on accelerated hydration in some cases [324], in general it is reported that STAs induce set retardation. Variations in the behaviour between systems with and without supplementary SPs are also reported ([25, 288, 326]). These effects are not comprehensively understood yet. As presented in Chapters 6 and 7 stabilising admixtures, the charge density and the dosage of SP strongly affect the rheology of a system. In Chapter 8 it was shown that the influence of SPs is not limited to rheology but continues during the whole early hydration period. This is also likely to occur with STAs as well. Particularly, interactions with the SP cannot be excluded.

According to the presented studies, the STAs have an effect on the setting, but they are not well understood to date. Furthermore, the current knowledge is based on investigation at constant climate. This chapter focuses on the effect of varied temperatures on potato starch based and diutan gum STA in the presence of differently modified SPs on the early hydration of cementitious systems.

### 9.3 Experimental setup

#### 9.3.1 Materials for the observation of POW and COM pastes

In a first series effects of the temperature on the early hydration of POW and COM pastes under variation of the STA type and the PCE modification were observed. These mixtures can be found in Table 4.12. The pastes of both, COM and POW were investigated without admixture, with STA only, with PCE, and with PCE and STA. The paste compositions can be found in Table 4.12. The STAs were varied between the potato starch based ST1 and the diutan gum based ST2 (Subsection 4.1.5). PCE LC, MC, and HC were used (Table 4.5) at dosages adjusted to the amounts yielding similar flow properties (Table 4.10).

#### 9.3.2 Materials for the observation of pure cement pastes with and without PCE

In a second series, the influence of the amount of STA was tested at varied STA and varied PCE modification. For these tests, only cement pastes with and without admixtures were prepared. The cement used in this second series was an OPC CEM I 32.5 instead of the CEM I 42.5 (Table 4.1) which was used for all other tests in this Thesis. However, the cement was from the same clinker. The reason for the change in the cement was due to the principle not to use different cement charges within on series of observations (Subsection 4.5.3). It was not sure that the whole observation series could be conducted with the available CEM I 42.5. The author wished to avoid blending of different cement delivery charges. Hence, the most reliable solution was using the lower fineness cement from the same clinker as the standard cement. Since these test results were not directly linked to results with the different cement, the observations can be considered as reliable.

In this second series, where only effects on cement pastes were tested, the mixtures without PCE had a w/c of 0.55 and mixes with PCE had a w/c of 0.4. These tests focus on how STAs affect systems with and without PCE. Hence, an adjustment to a specific flow property was not conducted. The bulk addition of PCE (water + polymers) was adjusted to 2% by mass of cement. This dosage, which corresponds to a solid dosage of 0.6% for PCE LC and 0.4% for PCE HC, is clearly high enough for the PCE to become effective but clearly below the saturation dosage as shown in Figure 5.5. In order to identify effects of the STA dosage, the STAs dosages were varied according to Table 9.1. The maximum dosage 0.07% by mass of water is a realistic value for ST1 but in terms of flowable concrete very high for ST2 (although ST2 can be added according to the producer's specifications up to 0.15% by mass of water for other applications). Due to their different efficiencies, different increments were chosen for the dosages of ST1 and ST2 so that the ST1 dosages were closer to the maximum and the dosages for ST2 were generally lower, while still the effects of identical dosages could be observed for a number of tests. By this it was assured that the majority of dosages was within the range of dosages specified by the producers of both STAs (see Subsection 4.1.5) while at the same time overlapping dosages for ST1 and ST2 could be observed (see Figure 9.7).

Table 9.1: Admixture adjustments for SCC and SCC paste tests.

STA type	Dosage [% by mass of water]				
ST1 (potato starch)	0	0.02	0.04	0.05	0.07
ST2 (diutan gum)	0	0.01	0.02	0.04	0.07

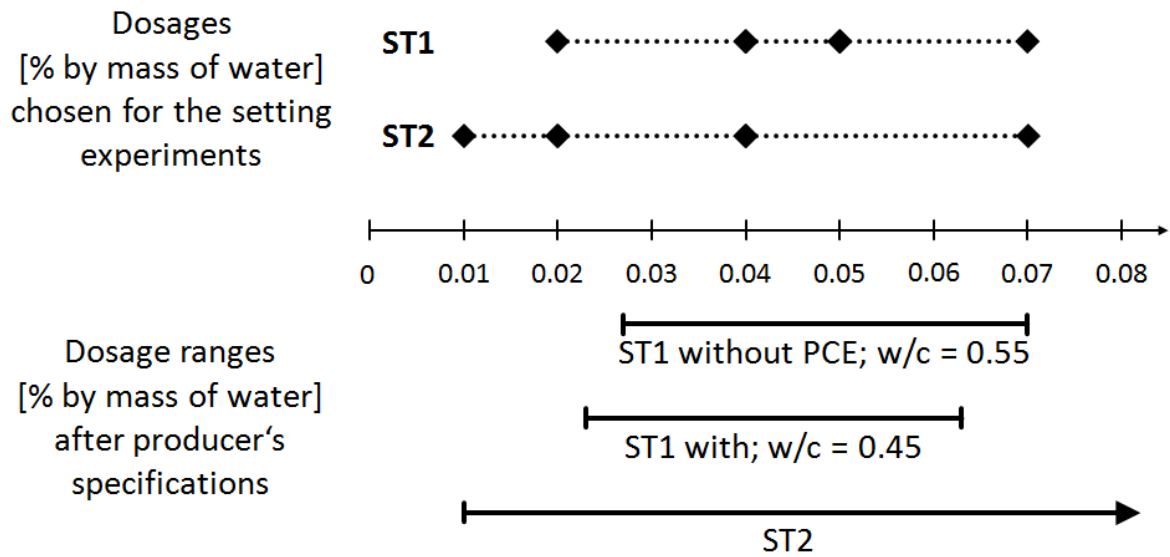


Figure 9.7: Dosages of ST1 and ST2 used for the observation of the setting of cement pastes with and without PCE. Since the dosage recommendation for ST1 is related to the entire mixture, the dosages related to the water content vary depending on  $w/c$ .

### 9.3.3 Mixing of pastes

The mixing of the pastes was conducted in a Kenwood Chef Classic Platin KM 416 mixer, as described in Subsection 8.4.2. The mixing regime was conducted for all investigations according to Table 9.2.

Table 9.2: Mixing regime for paste investigations.

Step	Duration [s]	Mixing velocity	Action
1	60	1 (slow speed)	Dry mixing
2	30	1 (slow speed)	Addition of 1/2 of total water
3	-		Addition of STA at the end of step 2
4	30	1 (slow speed)	Addition of PCE
5	60	1 (slow speed)	Addition of 1/2 of total water
6	180	3 (medium speed)	Mixing
7	60	-	Manual scraping off residue
8	300	3 (medium speed)	Mixing

### 9.3.4 Setting investigations

Setting investigations were conducted in an automatic Vicat device, as described in Subsection 4.4.2, according to EN 196-3:2005 with a 300 g needle. During the test, the specimens were stored under water at 5, 20 and 30 °C. The zero time was taken as the time of the water addition. Specimens were filled immediately after mixing. All results can be found in Annex E.

## 9.4 Experimental results and discussion

### 9.4.1 Setting of binder paste from COM pastes

A major result of Chapter 7 is that the time dependent flow behaviour can be affected by the STA, which is likely to be induced by interactions between STAs and PCEs. It is thus likely that these interactions also modify the setting. As seen in Chapter 5, the retardation of PCE generally correlates well with the amount of PCE in the system. However, it is also important to know in which way STAs may interact or overlap with effects of PCE.

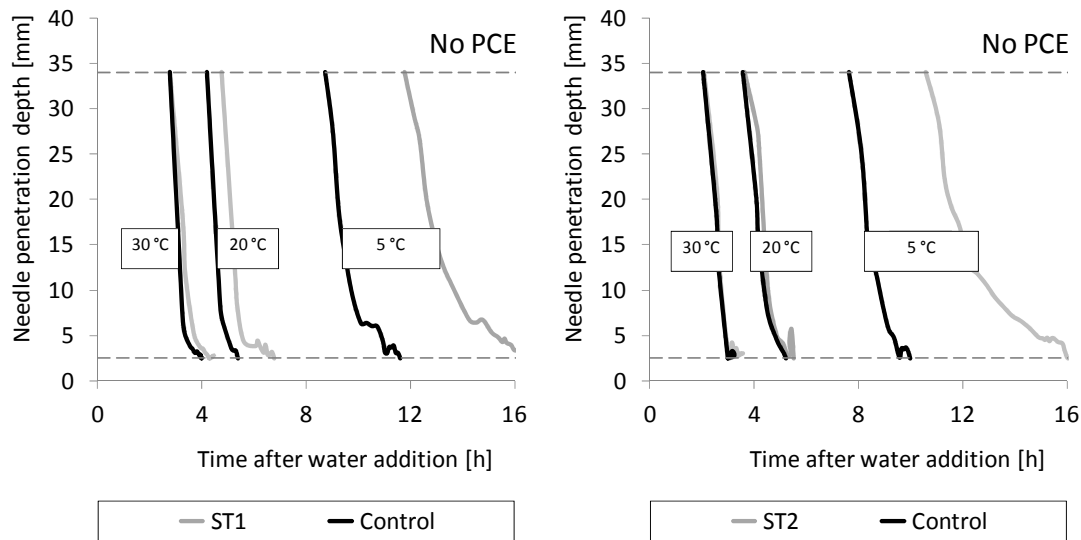


Figure 9.8: Needle penetration depths of COM pastes without PCE and 0.12% ST1 (left) and 0.01% ST2 (right) at different temperatures.

Figure 9.8 shows the effect of the STAs on the setting at varying temperatures. Without PCE it can be observed that both agents have a retarding effect at all temperatures. At 30 °C the retardation is negligible for both STAs. At 20 °C ST1 shows a retardation by approximately 1 h while the retardation is negligible with ST2. At 5 °C for both STAs a prominent shift in the setting of approximately 4 h can be observed. Considering that  $t_{fin}$  takes place at about 12 h and 10 h, this is a retardation by 33% and 40%, respectively, which is a significant effect.

The effect of PCE LC in combination with the two different STAs can be seen in Figure 9.9. At all temperatures ST1 shows a retarding effect, which is negligible at 20 °C and 30 °C but noticeable at 5 °C. The parallel shift of the setting curve with ST1 is approximately 3 hours. The transition towards a horizontal curve of the control mix at 5 °C takes place at about 50 h, so that the retardation is approximately about 6%. No such retardation can be observed in the presence of the diutan gum ST1 at 5 °C. ST1 even causes slightly earlier setting (approximately 2%) than the mixture without. At 20 °C and 30 °C, as with the potato starch ST2, the retarding effect is negligible.

Influences of the STAs combined with PCE MC can be taken from Figure 9.10. Both STAs generate retarded setting at all temperatures. At 20 °C and 30 °C, the effect is negligible; at 5 °C the effects are significant. The potato starch agent causes stronger retardation than the diutan gum agent. The first causes retardation about 10%, the latter about 4%.

Figure 9.11 shows the results for the combination with the high charge density PCE. Qualitatively, the results compare to those with the low charge density PCE. No significant

retardation can be observed at 20 °C and 30 °C regardless of the STA's modification, while a prominent retardation can be observed with ST1 and earlier setting with ST2. The retardation induced by ST1 is about 7%, while the setting takes place earlier by about 2%.

Diutan gum as well as the highly modified starch ether can be considered as stable in alkaline surrounding. ST1 does not contain anionic charges. The carboxylic groups within the ST2 polymer are sterically shielded by the double chain rhamnose [201]. It is hence not to be expected that the possible reasons suggested by Pourchez et al. [261, 263], namely degradation sugars or calcium complexation can support any explanation of the observed effects.

It is obvious from the observations of the COM pastes that both STAs show a stronger relative effect on the setting when no PCE is in the system. This occurs most pronounced at 5 °C but also at 20 °C and 30 °C the observations are similar, apart from the earlier setting at 30 °C, which is induced by the higher temperature. With and without PCE, the retardation at these temperatures was small. However, considering that PCE generally causes significant retardation, the percentage of the retardation is larger when no PCE is present in the system. E.g. in the mix without PCE at 20 °C, ST1 causes a retardation of approximately 0.5 h, which is about 10% extension of  $t_{fin}$  at about 5.5 h. The same mixture with PCE is retarded with ST1 by approximately 1 h, which however, is only 4% retardation referring to  $t_{fin}$  at 23 h. For those mixtures with PCE, the retardation is increasing with decreasing charge density. This effect was discussed already in Chapter 5, and it is mainly caused by the higher required amount of solid polymers when a low charge PCE is used in order to obtain similar flow properties.

In general, the retarding effects that occur only due to STAs at 20 °C and 30 °C are too small to allow sound conclusions. Considering the strong retarding effect of PCE, the minor modifications caused by STAs at these temperatures can be considered as negligible for practical applications.

At 5 °C, when setting is generally retarded, the effects occur significantly more pronounced. While both STAs cause about 40% more retarded setting in all cases without PCE, setting is only retarded between 6% and 10% with ST1 and 4% with ST2 and PCE MC. The setting of the systems with ST2 and PCE LC, and ST2 and PCE HC even occurs by 2% earlier than the comparably system with PCE only. Obviously, the presence of PCE reduces the retarding effect of the STAs, which would occur in systems without any PCE. This observation is valid for both STAs. However, the ST1 generally caused more retardation than ST2. In the presence of PCE LC and PCE HC, ST2 even resulted in a relative set acceleration compared to a mix with only PCE but without STA. This observation is in line with the results of Chapter 6 that indicate that ST2 interferes with PCE. By the interaction, a certain amount of PCE was withdrawn, thus increasing the yield stress. This effect would also become effective during the hydration of C<sub>3</sub>S and would cause a relatively earlier setting.

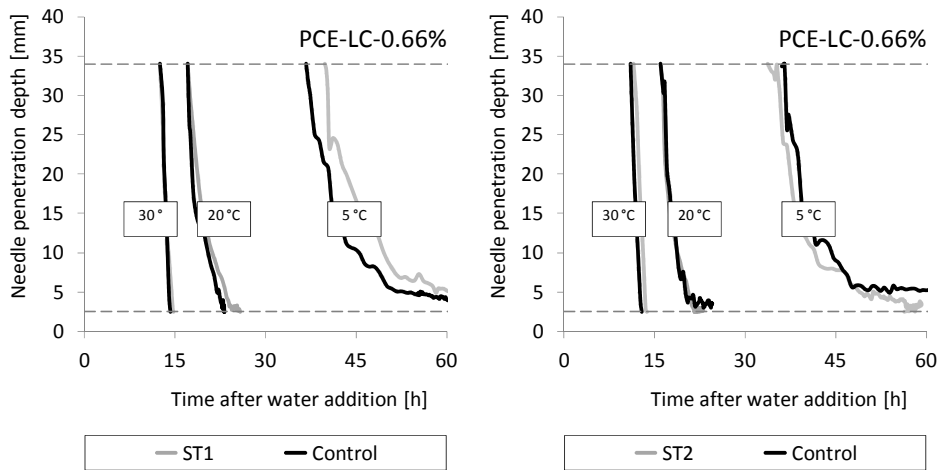


Figure 9.9: Needle penetration depths of COM pastes with PCE LC and 0.12% ST1 (left) and 0.01% ST2 (right) at different temperatures.

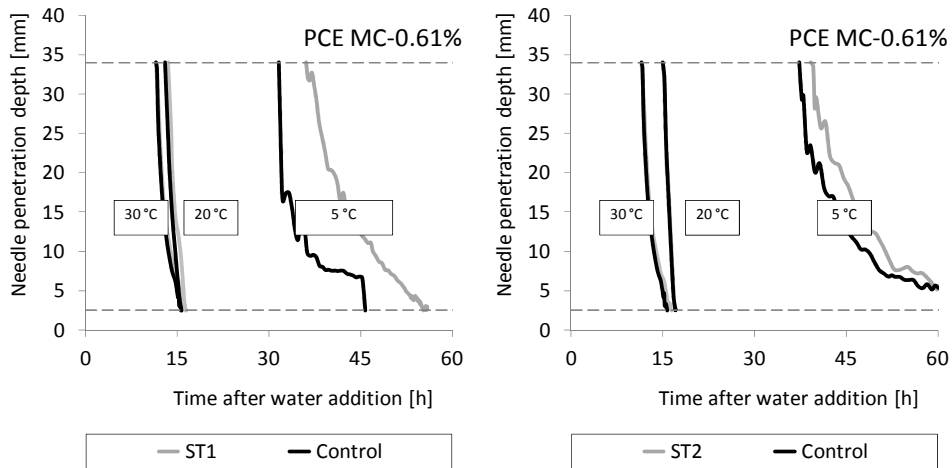


Figure 9.10: Penetration depths of COM pastes with PCE MC and 0.12% ST1 (left) and 0.01% ST2 (right) at different temperatures.

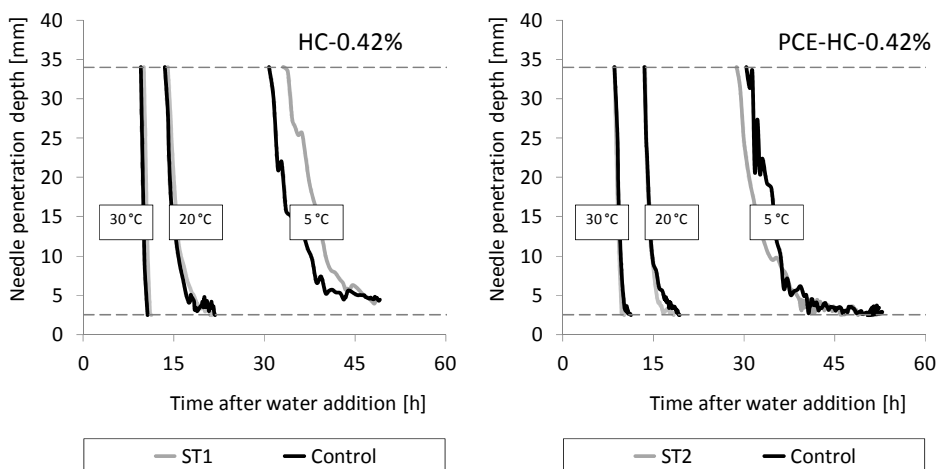


Figure 9.11: Penetration depths of COM pastes with PCE HC and 0.12% ST1 (left) and 0.01% ST2 (right) at different temperatures.

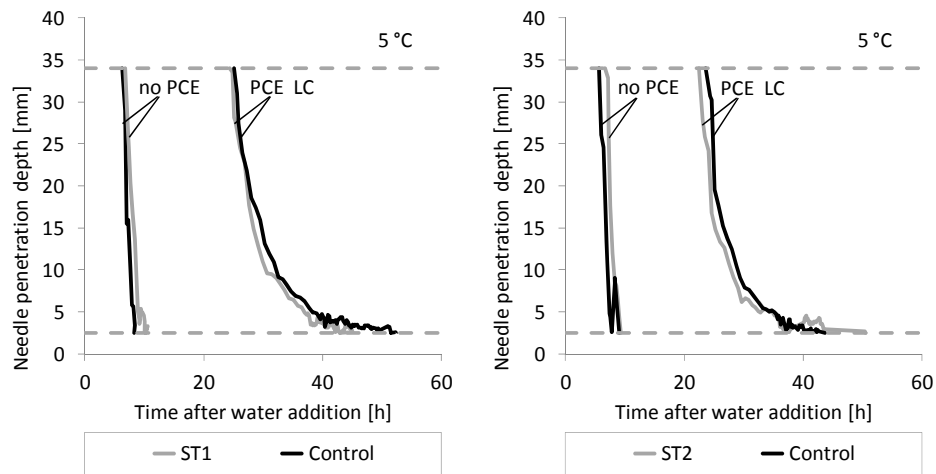


Figure 9.12: Needle penetration depths of POW pastes with PCE LC and 0.018% ST1 (left) and 0.001% ST2 (right) at 5 °C.

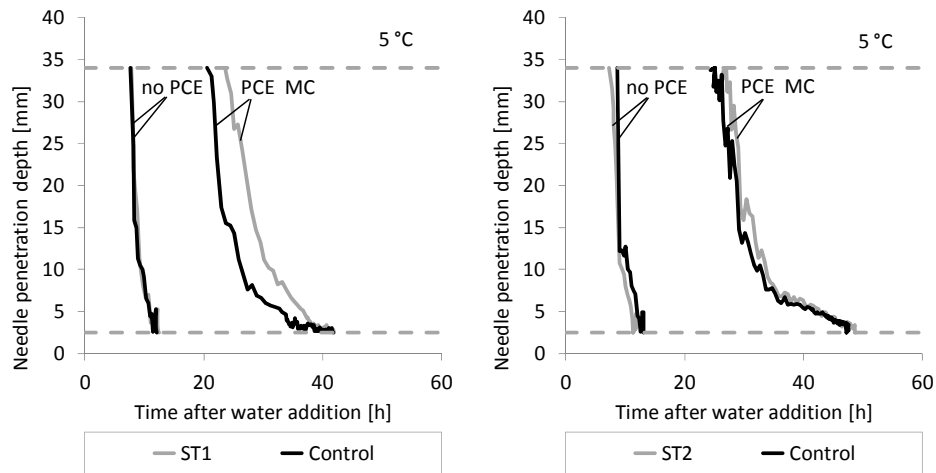


Figure 9.13: Needle penetration depths of POW pastes with PCE MC and 0.018% ST1 (left) and 0.001% ST2 (right) at 5 °C.

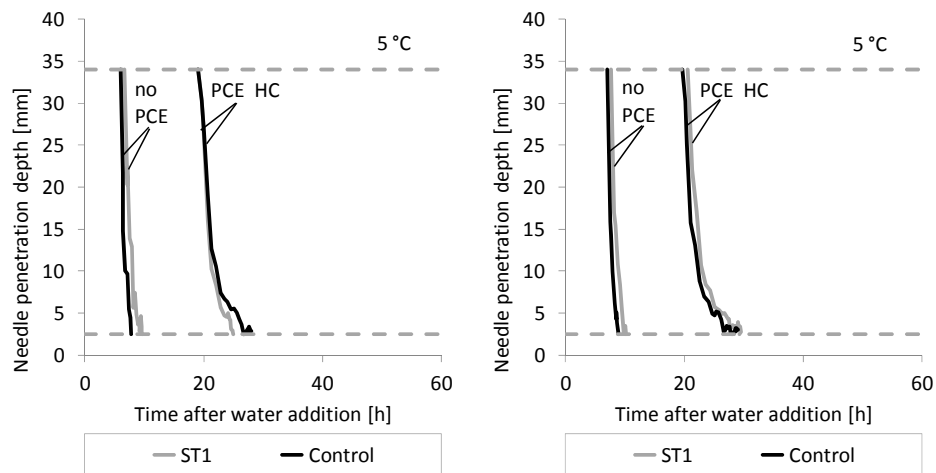


Figure 9.14: Needle penetration depths of POW pastes with PCE HC and 0.018% ST1 (left) and 0.001% ST2 (right) at 5 °C.

### 9.4.2 Setting of binder paste from POW paste

The POW pastes contain significantly less STAs (Table 4.10). Therefore the effect of STA was expected to be small. Indeed, at 20 °C and 30 °C the setting curves with and without STAs are too close for any interpretation. Also at 5 °C the curve characteristics are very similar with and without STAs. They are shown in the Figures 9.12 to 9.14. In case of mixtures without PCE, retardation can be observed, which is negligible, compared with the strong retardation that can be observed for mixtures without PCE at 5 °C for the combination type mixtures (Figure 9.8). For those mixtures containing PCE it can be observed that both STAs cause minor acceleration with PCE LC, retardation with PCE MC and no effect with PCE HC. This is qualitatively similar to the observations from the combination type mixtures, where with PCE MC significant retardation could be observed with PCE and minor acceleration or retardation, depending on the STA type, could be observed with PCE LC and PCE HC. From the magnitude of the effects that occurred influences of STAs might be negligible for powder type mixtures, where STAs are added only supplementary and in insignificant amounts. Nevertheless, a major aspect needs to be emphasized. The COM and POW mixtures distinguish significantly from each other in case no PCE is present. STAs retards setting when added in high amounts as for COM, and do not have a significant influence when added in small amount as for POW. In the presence of PCE, certain effects that were observed with POW could be observed with COM as well. This gives reason to assume that STAs affect the way how PCEs influence the early hydration, which might not be or only partly affected by the amount of STAs.

### 9.4.3 Setting of cement paste with stabilising agent and PCE

The investigations discussed in the Subsections 9.4.1 and 9.4.2 focused on the binder pastes of the COM and POW mixtures including LSF. For a better understanding of how STAs and varying amounts of STAs affect the setting of cement only, in another series only cement pastes were investigated. The individual results for  $t_{fin}$  times for 5 °C, 20 °C, and 30 °C are presented in the Tables 9.3 to 9.5, respectively. A graphic presentation of the final setting times is given in Figure 9.15 to 9.17.

As shown in Figure 8.14 pastes incorporating PCE or consistencies varying from the standard consistency according to EN 196-3 do not always allow a distinct determination of  $t_{fin}$ . As can be seen in Figure 9.9 to 9.11, a clear definition of a final set is difficult. Since the curves scatter and the consistency of the investigated pastes strongly differs from the standard stiffness and segregation and volume reduction is likely to occur, the standard value at 0.5 mm would not reflect reality. This effect occurred most prominently at cold temperatures, when hydration was generally strongly retarded. In some cases the height reduction would never identify  $t_{fin}$  at 0.5 mm. Therefore, the values used for the interpretation of the setting of cement pastes were specified at a needle penetration depth of 30 mm. This modification was necessary, since for the later evaluation in histograms sound values needed to be extracted.

The final set can thus be expected to take place at the time the curve merges towards a horizontal line, but the definition of an inflexion point is delicate. Taking the setting at a penetration depth of 10 mm seemed to be a reasonably good choice, since a penetration of 10 mm is already very close to the inflexion point that marks the transition towards a solid structure, but the curve is still steep enough that a unique value can be extracted. Thus the influence of any height loss during the early period can be minimised and the values are close to the point in time when the still plastic specimen begins to behave like a solid.

Since the general effect of the charge density, which determines the amount of required polymers to achieve specific flow properties has been discussed in the former chapter and can be considered as confirmed, in the present cement paste tests only PCE LC and HC were varied. PCE MC can be assumed to behave within the thresholds defined by PCE LC and HC.

Both PCEs retarded setting at all temperatures. Mixes with PCE HC showed earlier setting than mixes with PCE LC, which was mainly caused by the fact that in these investigations the bulk PCE addition was fixed but PCE LC and PCE HC contain different solid contents. The solid content of PCE HC is at 20%, while it is at 30% for PCE LC. Consequently the mixtures with PCE HC set earlier.

In general the observed effects of STAs were qualitatively and quantitatively similar for both STAs. Furthermore, no systematic effect of the amount of STA could be observed for both types.

Table 9.3: Real times of final set for cement pastes without and with different PCE modifications at varied stabilising agent types and amounts at 5 °C.

5 °C	Time of the final set [h]								
	-	ST1 (potato starch)				ST2 (diutan gum)			
ST Dosage	-	0.02	0.04	0.05	0.07	0.01	0.02	0.04	0.07
Control	24.5	37.0	36.0	37.6	32.5	26.7	25.6	23.7	24.7
PCE LC	42.2	45.6	44.3	46.6	41.4	47.9	45.5	44.9	45.0
PCE HC	31.9	38.1	39.7	42.7	40.2	34.5	35.3	34.1	47.5

Table 9.4: Real times of final set for cement pastes without and with different PCE modifications at varied stabilising agent types and amounts at 20 °C.

20 °C	Time of the final set [h]								
	-	ST1 (potato starch)				ST2 (diutan gum)			
ST Dosage	-	0.02	0.04	0.05	0.07	0.01	0.02	0.04	0.07
Control	10.8	11.7	11.5	11.3	10.8	10.8	11.6	11.5	11.7
PCE LC	31.7	31.8	27.6	27.7	27.2	28.1	26.5	26.2	26.2
PCE HC	24.3	27.6	28.8	27.8	28.4	27.8	27.8	26.3	27.4

Table 9.5: Real times of final set for cement pastes without and with different PCE modifications at varied stabilising agent types and amounts at 30 °C.

30 °C	Time of the final set [h]								
	-	ST1 (potato starch)				ST2 (diutan gum)			
ST Dosage	-	0.02	0.04	0.05	0.07	0.01	0.02	0.04	0.07
Control	7.8	8.1	8.3	7.8	7.9	8.2	8.8	9.4	8.6
PCE LC	21.8	17.5	18.1	17.7	17.8	18.5	18.5	18.5	17.7
PCE HC	18.2	14.6	14.8	14.4	14.5	13.6	13.2	12.5	12.4

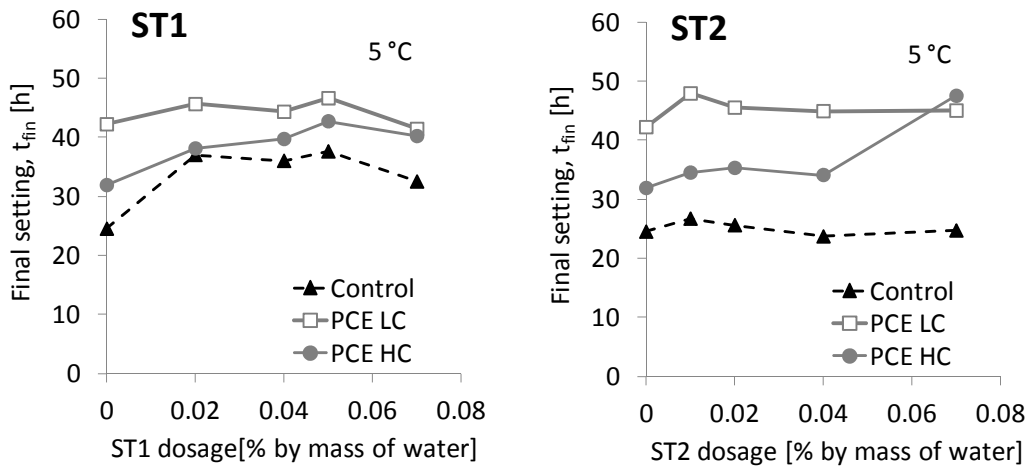


Figure 9.15:  $t_{fin}$  at 5 °C with and without PCE depending on the dosage of ST1 and ST2.

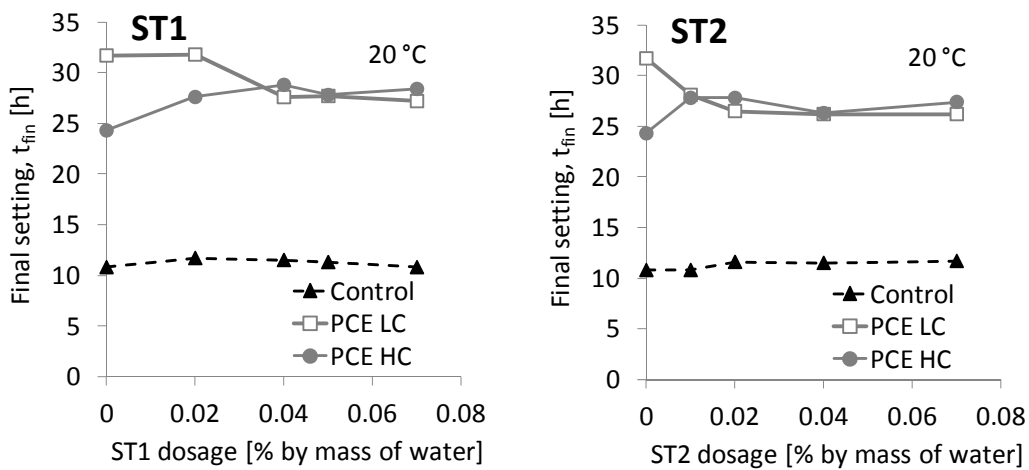


Figure 9.16:  $t_{fin}$  at 20 °C with and without PCE depending on the dosage of ST1 and ST2.

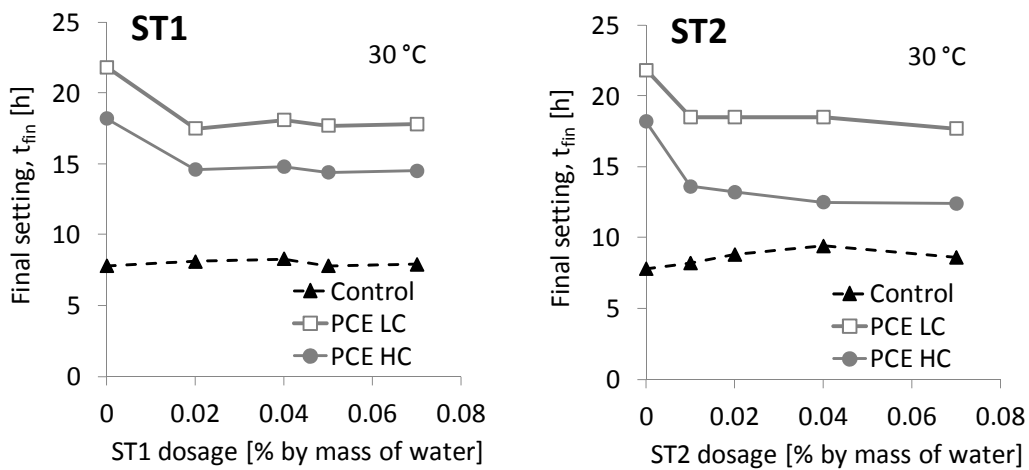


Figure 9.17:  $t_{fin}$  at 30 °C with and without PCE depending on the dosage of ST1 and ST2.

#### 9.4.4 Discussion of cement paste setting with stabilising agent and PCE

The observations of the pure cement pastes confirm the observations from the SCC paste investigations (Subsections 9.4.1 and 9.4.2) that effects introduced by STAs into systems without PCE do not inevitably have to occur likewise in systems containing PCE.

The best overview about this can be given if the set retardation and acceleration is evaluated against a reference without STA. If the setting time at each particular temperature and PCE is set as 100%, the relative acceleration due to different STAs and amounts can be observed. The histograms (Figure 9.18 to 9.20) show the ratio of the time of the final set with STA vs. the time of the final set without STA. Hence, values higher than unity represent a set retardation, values lower than unity represent acceleration. Due to relative observation, these effects can be separated from effects of PCE and can be clearly attributed solely to the STAs.

This evaluation can be seen for the mixture without PCE in Figure 9.18. The line at 1 represents  $t_{\text{fin}}$  at each temperature for a system without STA. It can be clearly seen that ST1 only caused minor retardation at 20 °C and 30 °C but significant retardation at 5 °C. ST2 caused minor retardation at all temperatures with a slightly increasing tendency due to increasing temperatures. For both STAs no significant influence of the amount of STA can be identified.

In case of PCE LC (Figure 9.19) the observations are very different to those of mixtures without PCE shown in Figure 9.18. At cold temperature, both STAs cause mentionable retardation at 5 °C, which is however significantly smaller than in the mix without PCE for ST1 and of the same magnitude for ST2. What is even more remarkable is the acceleration induced by both STAs that can be observed at 20 °C and 30 °C. No distinct differentiation can be made neither between the two types of STA nor regarding the amount of admixture.

The results for PCE HC (Figure 9.20) show different behaviour. Both STAs cause retardation at 5 °C and 20 °C. There is no significant effect of the type and amount of stabilising admixture. At 30 °C, a significant acceleration can be observed for both STAs, which occurs more pronounced for ST2.

In all cases, no effect of the amount of STA could be observed in case PCE is added. It seems, with and without PCE, STA generally affects the hydration regardless of the addition amount. This clearly contradicts to the assumption that STAs might affect the hydration through either calcium complexation or transformation into degradation sugars, which again confirms the observations by Pourchez et al. [263].

These observations do not fully reflect the observations from the SCC paste investigations where the influence of the PCE was small and the effect of the STA strong. This observation occurs reversely in the cement paste tests. A clear distinction between the two different STAs cannot be made, however it seems that there is an effect of the type of the PCE.

It is thus very likely that the differences that can be observed at 20 °C for PCE LC and PCE HC, which cause acceleration and retardation, respectively, is induced by the different PCE polymer contents that yield from the identical bulk addition of SPs. As shown in Chapter 8 that the total amount of PCE polymers strongly affects the setting.

It has to be emphasised that in general both systems vary strongly. The SCC paste systems contain LSF and a more finely ground cement. The w/c as well as the PCE dosages differ from those of the cement paste investigations. The observations thus cannot fully be compared.

Nevertheless, a significant similarity becomes obvious. Regardless of the setup, STAs cause accelerated setting or only slightly retarded setting in systems with PCE compared to systems with PCE only. In systems without PCE generally retardation by STAs can be observed and the retardation occurs more pronounced than in the presence of PCE.

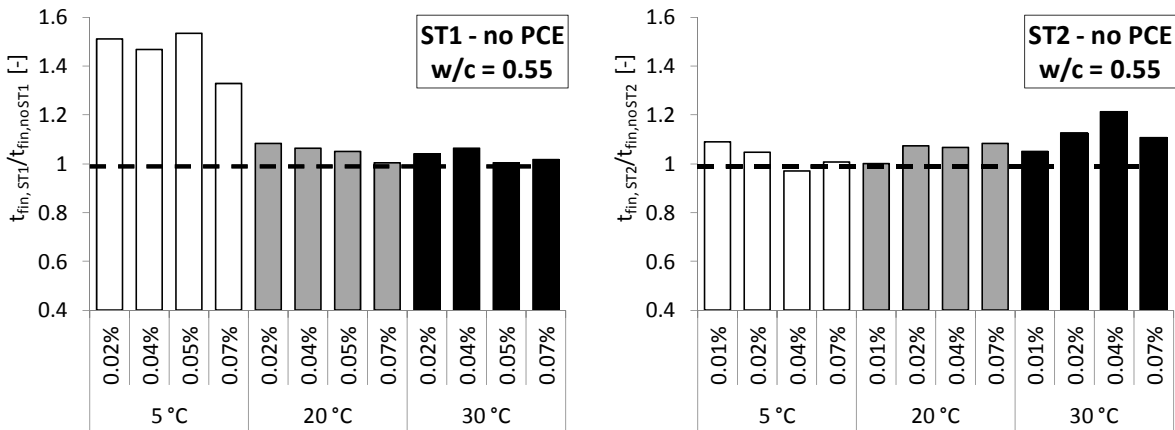


Figure 9.18: Setting of cement pastes without PCE and different amounts of ST1 and ST2 in percent of the setting of analogue cement pastes without STA.

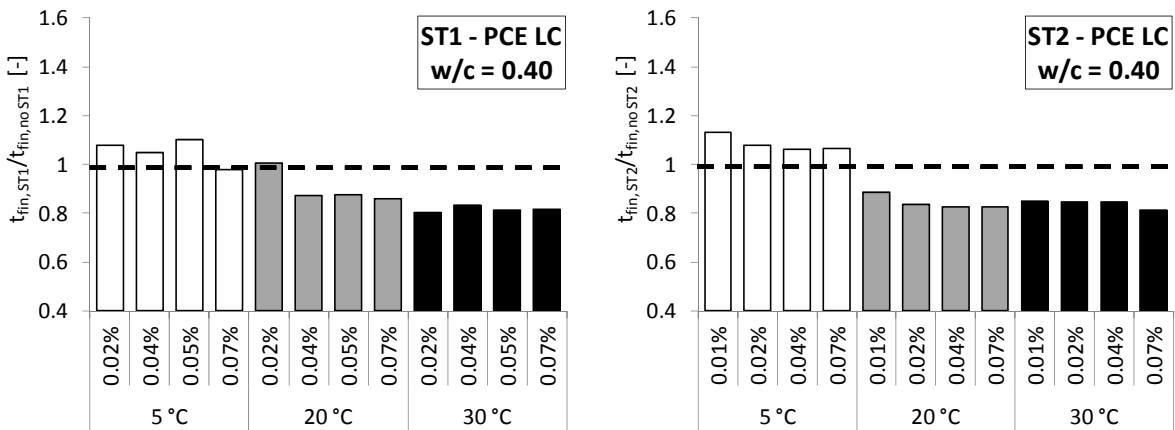


Figure 9.19: Setting of cement pastes with PCE LC and different amounts of ST1 and ST2 in percent of the setting of analogue cement pastes without STA.

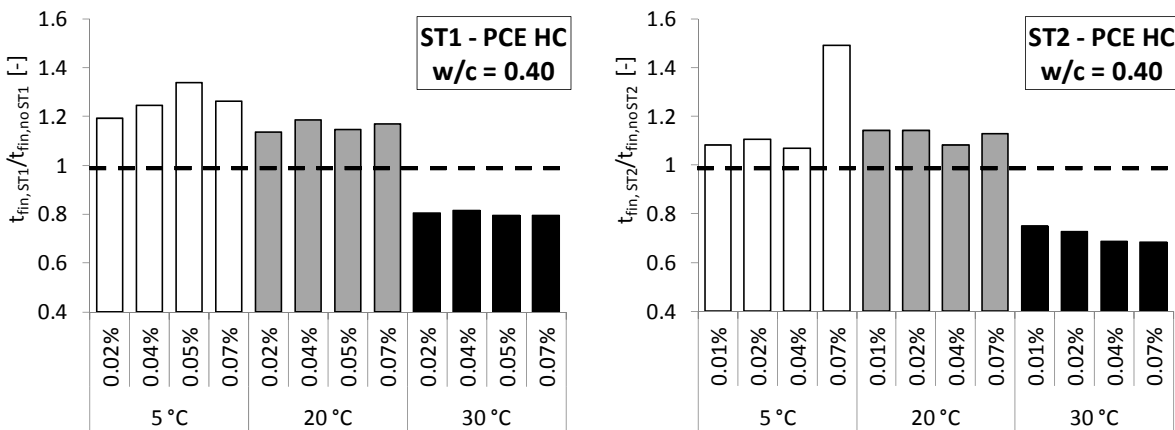


Figure 9.20: Setting of cement pastes with PCE HC and different amounts of ST1 and ST2 in percent of the setting of analogue cement pastes without STA.

Hence, it can be concluded that the retarding effect of combined PCE and STA seems to be less than the sum of their individual retarding effects, regardless of their modifications. In other terms, although both STA and PCE retard the setting when added each exclusively, when added in combination, their interaction causes that the smaller retarding effect of the STA supersedes the stronger retarding effect of PCE. This causes relatively earlier setting, which can even yield an acceleration effect due to the combination of both admixtures when compared to PCE only (Figure 9.21). The discussion of these observations is rather hypothetical but an explanatory theory, a so-called “Ansatz” can be developed.

Regardless of each other, both STAs and PCEs cause set retardation, of which, however, the effect of PCE is significantly stronger. For example the set time shift caused by ST1 at 20 °C is approximately 1 h (Figure 9.8), while the shift caused by PCE LC is approximately 18 h (Figures 9.8 and 9.9). The earlier setting of mixes containing PCE and STA compared to mixes with PCE only is thus most likely an effect of an interaction between both polymers that reduces the retarding effect of PCE.

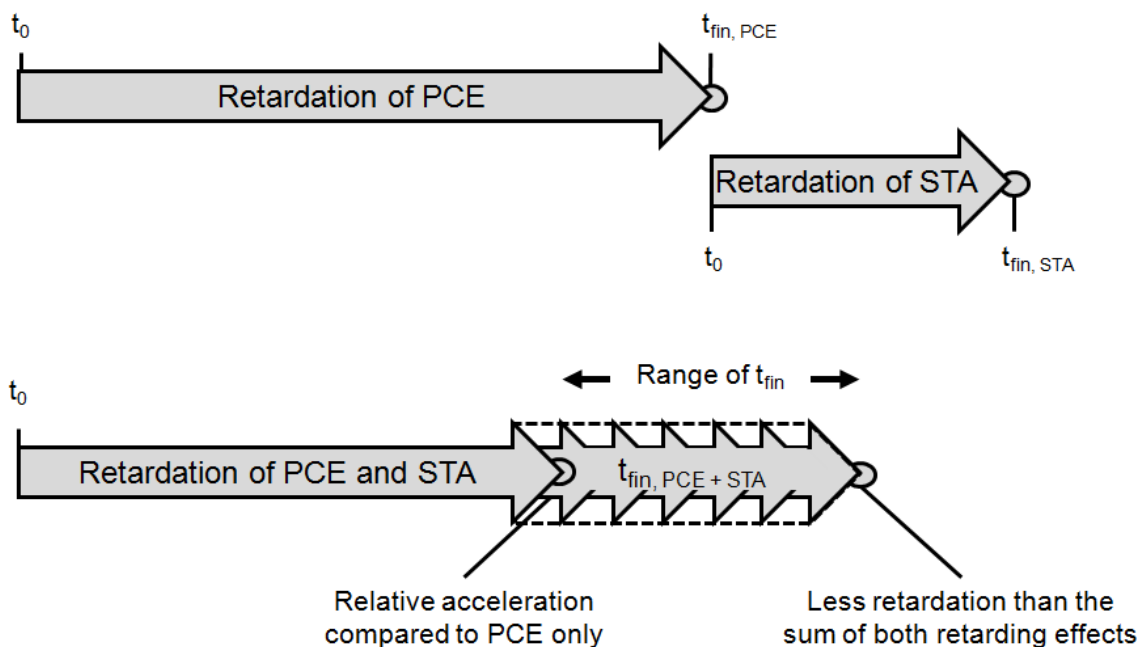


Figure 9.21: Illustration of overlapping effects of PCE and STA.

This effect was already discussed by Schmidt et al. [204, 329] based on the assumption that the setting is basically driven by the hydration of  $C_3A$  and the formation and re-crystallisation of ettringite as described by Locher [80, 107]. It was concluded that the interaction between PCE and STA overcompensates the retarding effect of PCE solely. It was assumed that the STAs might reduce the mobility of PCE in the pore solution, fostering the adsorption of sulphates on aluminates phase, which would generate higher amounts of ettringite that accelerates the setting. The fact that this observation was not made at 5 °C could thus be explained by the fact that at this low temperature, dissolution and precipitation take place much slower, so that even a reduced PCE mobility the adsorption of sulphates would be augmented.

Considering the conclusions of Chapter 8, this hypothesis cannot fully explain the effects taking place. It was shown that there is clear evidence that setting in the presence of PCE is mainly linked to the hydration of C-S-H. This result has to be taken into account for a modified explanation of the effects.

The presented results and also the studies of Pourchez et al. [263] give reasons to believe that neither calcium complexation nor alkaline instability cause retarding effects. Furthermore, they point out that PCE and STAs interact, so that effects that STAs cause in non-superplasticised systems do not occur in the same manner in PCE containing systems. It is known that PCE dosages above the maximum adsorption dosage continue to have a retarding effect on the hydration [131, 319]. Hence, if STAs polymers would adsorb and push away PCE polymers, this would rather cause supplementary retardation, which is not the case according to the results of this chapter. Furthermore, an adsorption to the disadvantage of PCE is a reasonable assumption only for the diutan gum based ST2 since it contains anionic charges. The starch based ST1 does not contain anionic charges. Therefore, it is unlikely that electrostatic forces are the major driving force for the interaction between the STAs and PCEs. If this is taken into account and the hydration retardation is assumed to be induced by a retardation of the C-S-H formation, the reason for the earlier setting of PCE systems in the presence of STA can be explained by a reduction of PCE polymers interfering with the C-S-H reactions.

In this context, it is worth to recall the hypothesis that the reduced mobility of PCEs caused by supplementary STAs may in a first step have an effect on the  $C_3A$  hydration. PCEs mainly adsorb on aluminates and ferrite clinker phase surfaces [176]. However, the major adsorption sites for PCE during the very early hydration are ettringite and monosulphate, of which ettringite can attract significantly higher amounts of PCE [87]. Assuming that the STAs reduce the mobility of PCEs much more than the mobility of interacting ions, since PCE molecules are much larger than ions, it is conceivable that indeed systems with STA and PCE generate higher amounts of ettringite than systems with only PCE, since preferably sulphate ions instead of PCEs adsorb on aluminates phases. The lower mobility of PCEs could either happen through the following effects or their combination:

- increased viscosity of the pore solution,
- a slowed down unfolding of the PCE molecules to their solution structure, due to interactions with STA polymers,
- or through entanglement of the PCE.

Due to the lower mobility of PCEs a favoured adsorption of sulphates would take place due to lack of or less competitive adsorption between PCE and sulphate ions. The available aluminates would preferably interact with the quicker sulphates, fostering a formation of ettringite rather than monosulphate. This assumption is in line with findings of Peschard et al. [324], who found that STAs stabilise ettringite and gypsum. The increased amount of ettringite would attract higher amounts of PCE in the further progress of hydration and these polymers would then no longer interact with the C-S-H hydration. As a result, a system with higher ettringite content would attract more PCEs and in turn leave less PCE molecules to interfere with the later C-S-H hydration, thus contributing to earlier setting. This “Ansatz” is given as flow chart in Figure 9.22. In this context, it is not relevant whether PCE retards setting by formation of a diffusion barrier, by calcium complexation, modified morphology of hydrates, or retardation of the dissolution of alite [64, 289, 290] (Section 8.1).

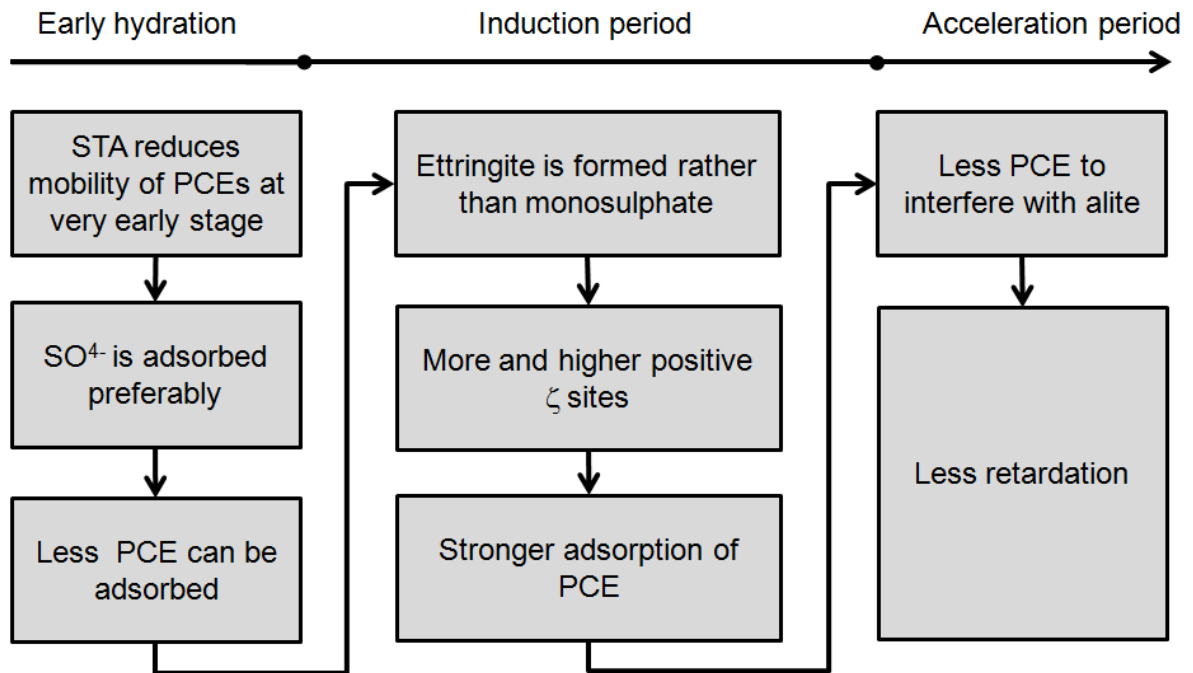


Figure 9.22: Flow chart of the hypothetical mechanism effect on the set retardation caused by STA in combination with PCE.

At 5 °C the dissolution and precipitation processes are generally much slower. The mobility reduction of the PCEs by STAs retreats into the background as a withdrawal of PCE from early reactions would not automatically increase the reactivity of aluminate and sulphate due to the general slowdown of the hydration. Hence, retardation can be observed, regardless of the presence of PCE.

Such consideration would also explain why at 20 °C STAs cause retardation with PCE HC but acceleration with PCE LC, while at 30 °C accelerated setting can be observed with both PCEs. At 20 °C the hydration velocity is slower than at 30 °C, giving the PCE the chance to interact with the aluminate. As high charge density polymers are attracted with higher force and exhibit less complicated solution structures, they might still interfere with sulphate-aluminate reactions, propagating the formation of AFm at 20 °C when the hydration is slower than at 30 °C.

This hypothesis is only an “Ansatz” that needs further investigations. It is based on measurements of macroscopic phenomena and considerations about intrinsic effects. The measurement results do not give conclusive evidence, but they provide a logical consistent approach, which explains the small retarding and partly accelerated effect of STAs in the presence of PCE in comparison to the otherwise strong retarding effect of solely PCE.

## 9.5 Conclusions

Results of investigations about effects of varied ambient temperatures and potato starch and diutan gum based stabilising agents ST1 and ST2 in combination with the different SPs PCE LC, MC; and HC on the setting were presented. The major conclusions are:

- PCE and STAs caused both retardation of the setting, of which the effect of PCE was significantly stronger. In the presence of combined admixtures, the retarding effects did not sum up.
- For all SCC paste mixtures of the POW and the COM pastes, the relative effect of STA was strong when no PCE was in the system and markedly reduced when PCE was in the system
- In the paste of an SCC mixture, both stabilising agents caused retardation without presence of PCE. Decreasing temperatures increased the retardation.
- For all mixes with and without PCE and regardless of the PCE type, effects of the STA on the setting were negligible at 20 °C and 30 °C. At 5 °C distinct effects could be observed.
- In SCC combination type paste (COM) at 5 °C, ST1 caused retardation with all PCEs. ST2 caused minor retardation with PCE MC and acceleration with PCE LC and PCE HC.
- In pure cement paste systems without PCE, both STAs caused retardation at all temperatures. Effects were small at 20 °C and 30 °C but significant at 5 °C.
- In pure cement paste systems with PCE, both STAs caused retardation at 5 °C. At 20 °C acceleration could be observed with low charge PCE and retardation with high charge PCE. At 30 °C both STAs caused acceleration with low and high charge PCE.
- The paste investigations could not raise strong influences of the STA type. Both agents showed similar behaviour, giving evidence that the interaction between PCE and STA cannot be mainly driven by an anionic charge.
- No influence of the dosage of STA could be found within the range of dosages that was investigated, which gives reasons to assume that the retarding effect of STAs cannot be induced by calcium complexation or alkaline instability.

Considering that the influence of stabilising agent on setting is generally not satisfactory understood and results are not always consistent, the presented results on setting raise several questions that cannot be answered without further research. The results point towards a strong general interaction between STAs and PCE, regardless of the PCE and the STA modification and dosage. It can thus be concluded that the influence of STA in the presence of PCE is driven by an interaction which reduces the generally very strong effect of PCE on early hydration. A first hypothesis concerning the acceleration by STAs in cementitious systems with PCE is suggested, based on the idea that STAs might reduce the mobility of PCEs at early stage, which would augment ettringite formation. This in return would foster time delayed adsorption and consumption of PCE. At time of the setting, which is mainly driven by C-S-H hydration, these PCEs would be already consumed and no longer interact with C-S-H formation. In this context, the influence of the charge density of the PCE is of importance and should be subject of future research. The present results cannot conclusively prove this hypothesis. Nevertheless the results show that STAs generally reduce the retarding effect of PCE. Assuming that the general retarding effect of STAs is neither based on calcium complexation nor on alkaline instability, and that adsorption to the disadvantage of PCE is not likely to play a major role, the hypothesis gives a plausible explanation of the observed effects, based on the cement hydration. Further investigations could focus on understanding how the different polymers interact and how this interaction modifies the cement hydration.

# 10 Recommendations for robust mixture compositions, conclusions, and outlook

## 10.1 Introduction

Chapters 6 to 9 contain research about effects of the ambient temperature on SCC. Chapter 5 suggests an easy method to distinguish different PCEs qualitatively. The Chapters 6 and 7 focus on the rheology and the performance retention of SCC at varying temperatures depending on mixture composition, PCE modification, and stabilising agent (STA). Chapters 8 and 9 conclude on how the amount and type of PCE and STA affects the early hydration. The results strongly suggest measures how SCC can be optimised for particular temperatures or how it can be modified to be robust against large scatter of temperatures.

## 10.2 Parameters determining the rheology at different temperatures

### 10.2.1 Summary of observed rheological effects

First and foremost, SPs are added to cementitious systems in order to control the rheology. Also, in conjunction with SCC, the rheological properties are the most prominent features that distinct SCC and conventional vibrated concrete. In many productions the effects induced by a rheological adjustment are not further considered but accepted as side effects of the benefits brought by the self-compacting properties. Therefore, in this Thesis an approach is suggested how SCC can be optimised for particular temperatures, ignoring any accompanying effects, such as retarded setting or large shrinkage deformations.

Temperature effects on the flow properties of SCC are mainly linked to the influence of the temperature on hydration. Due to the dependency of the adsorption of PCE on the hydration process, temperature effects are more complex for SCC than for normal concrete. Hence, observations cannot be interpreted without deeper consideration of the mixture composition and the charge density of the PCE.

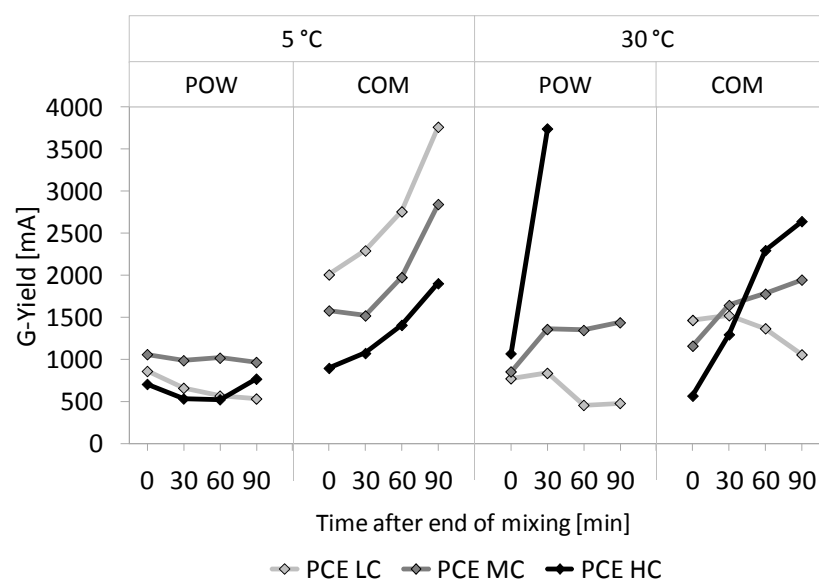


Figure 10.1: Summary of the observed effects of mixture composition and PCE modification at varied temperature.

In general, both mixture composition types, COM and POW showed good self-compacting performance over reasonably long lasting durations at most temperatures. Table 6.4 shows a qualitative overview of all observations. Figure 10.1 shows the condensed results of Chapter 6. The powder type mixture composition points out to function in a robust way at low temperature, regardless of the PCE, while the combination type mixture only functions properly with high charge PCE. At high temperature, the situation is inverted. The powder type mixture is very sensitive against influences of the PCE. The sensitivity against PCE influences is significantly lesser for the combination type SCC.

### **10.2.2 Critical effects at high temperatures**

At high temperatures, the critical effect is the rapid hydration, which can cause rapid loss of workability. The accelerated hydration causes morphological changes of the particles' surfaces which reduce their mobility against each other. Mixture compositions with low w/p therefore promote the rapid loss of workability due to their dense particle packing. High charge density PCEs also cause a rapid workability loss since they adsorb fast on the particles' surfaces and thus are consumed quickly. In turn, high w/p values and low charge density PCEs can help maintaining the workability even at high temperatures when the hydration is accelerated, since the more loosely particle packing fosters their mobility and the low charge density contributes to delayed adsorption of PCE.

### **10.2.3 Critical effects at low temperatures**

At low temperatures, the major reason for a performance loss is the lack of adsorption sites for PCEs due to the slowed down hydration process. As a result, PCE cannot adsorb in sufficient amounts to stabilise the system. A dense system with low w/p is capable to maintain the flow performance, but mixtures with high w/p tend to perform poorly as a result of segregation of the finest particles. In this case, only high charge PCEs can provide good flow properties due to the stronger adsorption tendency onto the cement particles.

### **10.2.4 Decision path for the choice of PCE to obtain optimised workability for cold and warm temperatures**

Most concrete producers are not aware of the delicate interactions that take place between cement and PCE. However, most of them have made experiences with cement-SP-incompatibilities at least once. As a result, many producers are extremely conservative with regard to the implementation of a PCE that differs from the standard PCE in use. Others again would never adjust their mixture composition, but they may consider the PCE modification not as invariable part of it.

The results presented in this work give evidence that the improvement of the performance of SCC can be achieved by either a reasonable mixture composition or the choice of an optimised PCE. For the latter method, the rapid PCE performance test as suggested in Chapter 5 provides a strong tool to better distinguish available PCEs according to their performance in general and to conclude how they can be used at varied temperatures.

A clear distinction between the different SCC classifications as defined in Table 1.1 is hardly possible, since many reported SCC mixture compositions exhibit characteristics of more than one of the listed classes. In this Thesis it is shown that temperature related interactions between PCE and cement hydration can be attributed to the charge density and the w/p. Therefore, the decision trees recommended in the following subsections distinguish between low and high w/p SCC mixture compositions. A clear distinction cannot be made either, but ranges can be provided based on exemplary mixture compositions, which are listed in Table 9.5.

It is not possible either to define generally valid temperature thresholds at which the effects presented in this Thesis occur. However, the temperatures observed in this Thesis clearly exhibited different performances depending upon the individual temperature range. Table 6.2 shows that the internal concrete temperature was about 10°C when the ambient temperature was set at 5 °C. Hence, it can be assumed that the observed effects and counteractions are valid for temperatures below 10 °C. At an ambient temperature of 30 °C the concrete temperature did not show strong deviations from the ambient temperature. Therefore, conservatively the decision trees recommend actions for temperatures above 30 °C only. In practice, it can be assumed that the recommended actions will also become effective at lower temperatures already.

Table 10.1: Thresholds for low and high w/p.

	Low w/p SCC		High w/p SCC	
	Lower threshold	Upper threshold	Lower threshold	Upper threshold
w/p by mass	0.21	0.33		0.48
w/p by volume	0.59	0.93		1.42
Sample SCC binder composition	350 kg/m <sup>3</sup> cement 350 kg/m <sup>3</sup> filler 150 kg/m <sup>3</sup> water	350 kg/m <sup>3</sup> cement 200 kg/m <sup>3</sup> filler 180 kg/m <sup>3</sup> water		350 kg/m <sup>3</sup> cement 70 kg/m <sup>3</sup> filler 200 kg/m <sup>3</sup> water

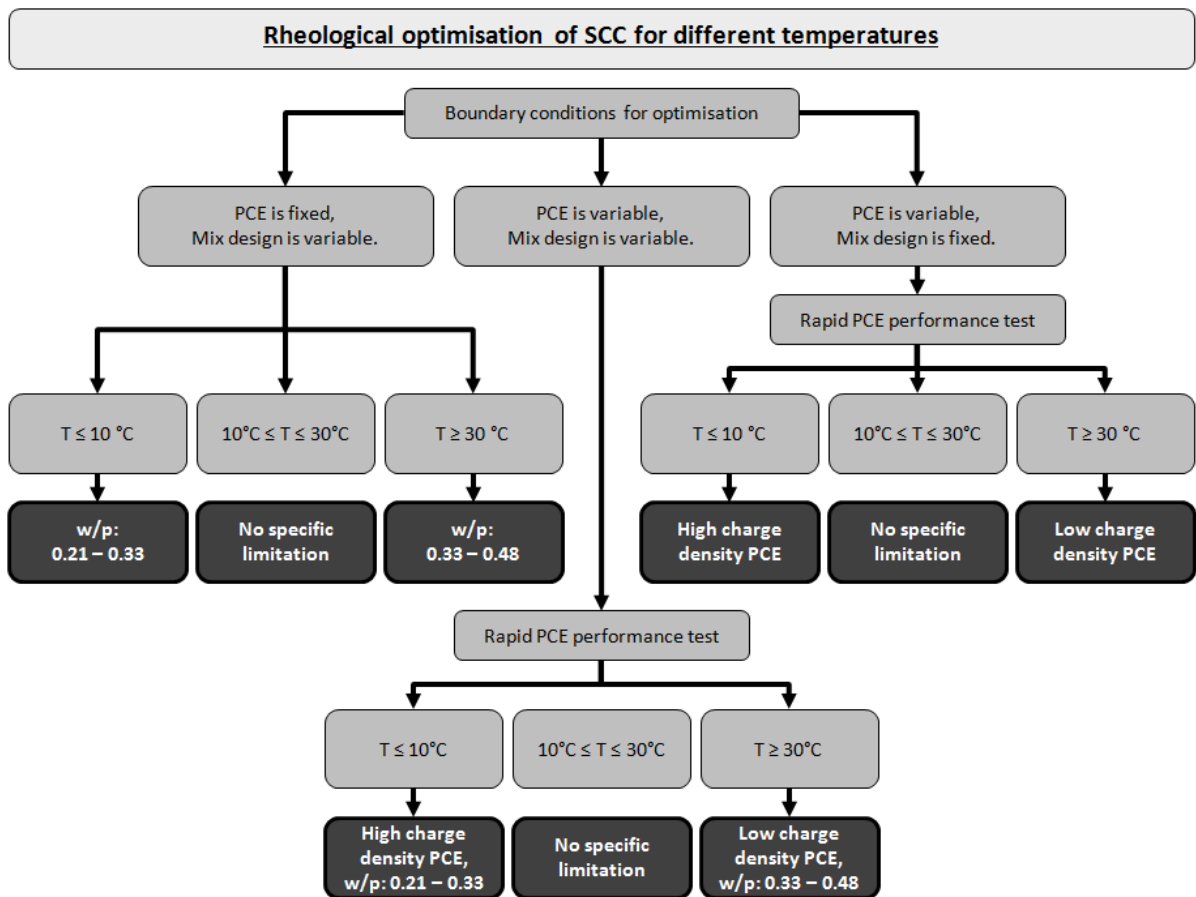


Figure 10.2: Decision tree for the rheological optimisation of SCC for different temperatures depending on the boundary conditions of the production.

A decision tree for the adjustment of SCC mixtures and different boundary conditions is given in Figure 10.2.

In case the PCE cannot be changed, or no information about the performance is available, it is advisable to choose a powder type SCC at low temperatures (e.g. similar to the POW type used in this Thesis) and a high w/p SCC at high temperatures (e.g. similar to the COM type in this Thesis) since they perform well in the particular temperature ranges regardless of the PCE modification.

In case the mixture composition cannot be modified, it is reasonable to use a low charge density PCE at high temperatures to avoid rapid consumption of the molecules, and to use a high charge density PCE at low temperatures, in order to assure that sufficient PCE can be adsorbed.

In case of flexibility in both, mixture composition and PCE, a combined approach might yield an optimum performance.

### **10.3 Improvement of the robustness of SCC for high and low temperature**

#### **10.3.1 The influence of the rheological adjustment on the whole early hydration process**

Upon addition of any type and amount of SP these admixtures are part of the hydrating system, and any further effect comes unavoidably. Considering the large effects that were observed in Chapters 8 and 9 on shrinkage and setting, due to the amount of PCEs, it may be reasonable to abandon ultimate rheological performance and accept moderate flow properties instead, in order to avoid the side effects induced by PCEs, such as retarded setting. Robustness is not inevitably linked to the workability. If concreting needs to be optimised for a particular temperature range, it is therefore necessary to integrate the results of the Chapters 8 and 9 into a decision tree that considers rheological effects as well as possible side effects.

#### **10.3.2 Decision paths for the optimisation of SCC for high temperatures**

Regarding the optimisation of the rheology, the rules described in Subsection 10.2.4 apply. If the mixture composition cannot be varied, it remains reasonable to choose a low charge density PCE, and if the PCE is fixed, it remains reasonable to better choose a mixture composition with a high w/p.

A more distinguished discussion can be made for flexibility in both aspects. In Chapter 6 it is shown that mixtures with high and low w/p can work well at high temperatures. For mixtures with low w/p, however, the choice of a low charge density PCE was required in order to maintain reasonably workability retention. Low charge density PCE can keep up the workability better than PCE with high charge density, but high charge density polymers can be used if a high w/p is chosen. If no further consideration is made regarding setting or shrinkage, the adjustment of mixture composition and PCE type can help optimising the rheological properties with regard to time. A reasonably long but not excessive performance can be achieved when using a mixture with high w/p and high charge density PCE. Extremely long lasting performances can be achieved using a low charge density PCE.

It was shown in Chapter 8 that the set retardation is linked closely to the amount of total PCE in the system, which is only negligibly depending on the type of PCE. In order to adjust a specified flow property, higher amounts of low charge PCE are required than high charge PCE, so that low charge PCE unavoidably causes a higher total PCE content than high charge PCE. If rapid setting is required, it is therefore advisable to use high charge PCE, which, however, turned out to be critical at high temperatures due to the quick consumption, and should therefore only be used at high temperatures in combination with a high w/p.

It was further shown that the influence on the transition of the early autogenous deformations towards a slow deformation rate occurs significantly less dependent on the used PCE than the shift of the setting. Therefore the amount of PCE in a system determines, whether a part of the still large early deformations occurs prior to or after the setting. The latter case is considered as critical with regard to the risk of cracks. In consequence, a high content of PCE generally reduces this risk due to the extreme set retardation. If early cracks have to be avoided it is reasonably to use mixtures incorporating low charge density PCE.

Rapid setting may be favourable for a rapid construction process and a reduced cracking risk contributes to the durability of a structure. According to the aforementioned observations, effects that foster a rapid setting and oppose to effects that reduce the risk of cracks at high temperatures. As a result, if good workability, rapid setting and low crack risk are required in combination, the most reasonable way to optimise an SCC for high temperature applications is choosing a high w/p mixture in conjunction with a medium charged PCE. The graphical summary of these considerations can be found in Figure 10.3.

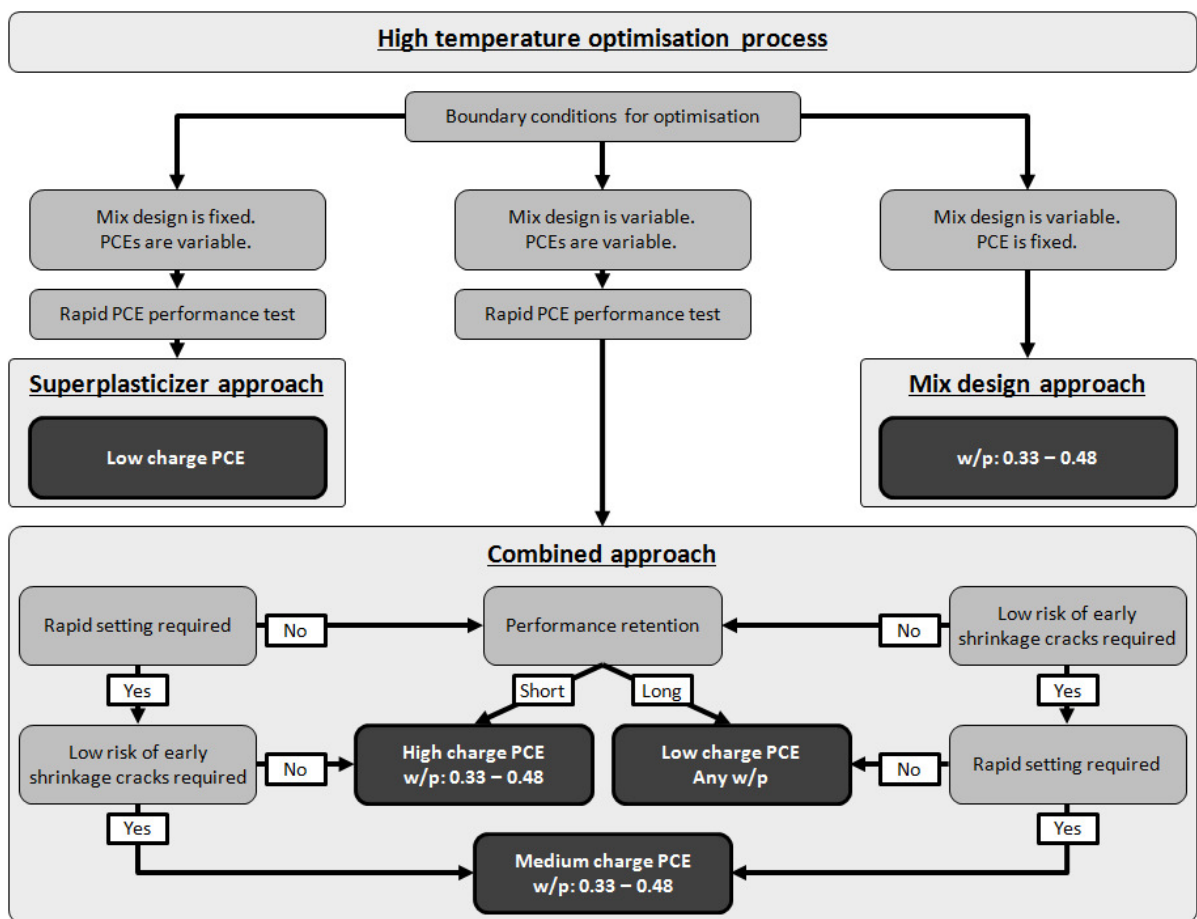


Figure 10.3: Decision tree for the optimisation of SCC for high temperatures depending on the boundary conditions of the production, and considering setting and cracking risk.

### 10.3.3 Decision paths for the optimisation of SCC for low temperatures

The adjustment of SCC to work properly at low temperatures is more critical than to high temperatures. A major difficulty at low temperatures is that poor flowability cannot be improved by supplementary addition of SPs, since the slow hydration velocity, induced by the low temperatures, causes a lack of adsorption sites. It is therefore advisable to generally use PCE with high charge density regardless of the mixture composition to make sure that sufficiently high adsorption of PCE takes place.

The results presented in Chapter 6 show that at use of high charge PCE mixes with both high and low w/p can function, while the low w/p mixture maintains the workability significantly longer than the high w/p mixture. SCCs with low w/p function well at low temperature with any type of PCE. Hence, for reasonably long but not excessive workability, a mixture with high charge density PCE is suggested, while for extended workability generally a low or medium charge density PCE should be chosen. The latter choice functions only in a sound way, if the w/p is low.

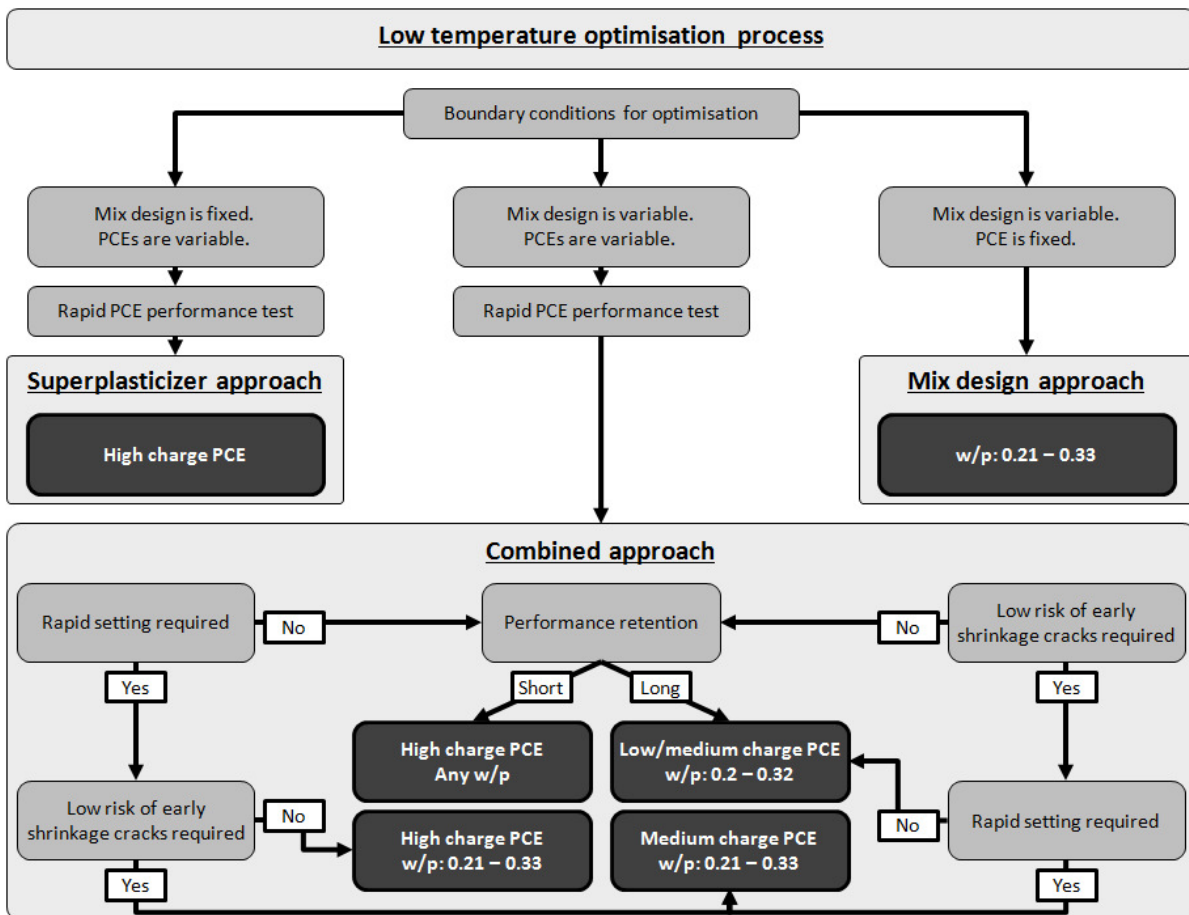


Figure 10.4: Decision tree for the optimisation of SCC for low temperatures depending on the boundary conditions of the production, and considering setting and cracking risk.

In order to generate earliest possible setting, mixtures with a low w/p need to be chosen. A high charge density PCE supplementary accelerates setting since it is required in lower amounts to achieve specified flow properties than low charge density PCE.

Though, a high charge density PCE is considered to be the safest choice at low temperatures to avoid loss of performance, high charge density PCE turns out to bear the risk that large

shrinkage deformations occur at an already rigid state after setting. This is particularly critical at low temperatures, since the resistance against early deformation builds up only slowly due to the retarded hydration. In order to reduce the risk of early cracks, hence, PCE with low or medium charge density need to be chosen. However, these function only well at low temperatures if the mixture composition is based on a low w/p.

A compromise between low cracking risk and early setting at good workability can be put into effect by using a medium charged PCE, which, however, inevitably requires a low w/p. An overview of the decision paths is given in Figure 10.4.

## **10.4 Decision paths for improved temperature robustness of SCC against regularly varying temperatures**

### **10.4.1 General information**

The considerations mentioned before focus on the generation of maximum robustness for a particular temperature range. In practice, it can be necessary to cast SCC at a large range of different temperatures, which are not always predictable and where an individual adjustment just in time cannot be made. In order to determine the right approach towards robust mixture composition for a wide range of temperatures, first the influencing factors need to be discussed.

### **10.4.2 Choice of PCE**

The suggested rapid PCE performance test, based on the observations of mixtures with different SP contents and proportioning according to Equations (5.1) and (5.2), allows the determination of the performance of one PCE in comparison with another PCE. This gives a reasonable tool to adjust the workability time and the flow properties at a relevant time individually. It is shown in Chapter 6 that in general good performance can be achieved at all observed temperatures regardless of the charge density. This, however, strongly depends on the mixture composition. Such an individual adjustment, thus, requires sophisticated knowledge about interactions between PCE type and mixture composition. Without further consideration of the mixture composition, it is shown that the choice of a medium charge density PCE is basically the right decision to achieve robustness over a wide range of temperatures.

### **10.4.3 Choice of stabilising agent**

The results presented in Chapter 7 show that the behaviour of SCC at varying temperatures is dominated by effects resulting from the PCE, but STAs may add supplementary effects. In the presented results, mixtures with adsorbing STAs show a tendency for a rapid workability loss. This was assumed to be in context with interactions with PCEs, such as calcium complexes. This aspect may be a concern at high temperatures, where loss of flowability is the major critical effect.

An unbalanced combination of PCE and STA can thus cause significant performance loss upon temperature change. This is summarised in Figure 10.5, where mixtures at 20 °C and 30 °C function properly during the early period in all combinations, while at 5 °C only a single combination (PCE HC + ST1) can provide sufficient workability at all.

None of the results presented in this work shows that STAs improve the robustness of SCC against varying temperature. This, however, does not mean either that they generally negatively affect the robustness against temperature variation. While ST1 behaves rather neutral, the adsorbing ST2 showed that the performance can be negatively affected, or that negative effects induced by unfavourable combinations of PCE and mixture composition can be amplified. In this context, it is also referred to the observation presented by Schmidt et al. [131] that the

stabilising effect of the non-adsorbing ST1 is lost over the course of time. This can cause problems of slow segregation, particularly at low temperatures since then setting is extremely retarded. In the latter case, workability performance loss might be rather acceptable than static segregation. Finally, this leads to the conclusion that STAs can be used for the improvement of the robustness of SCC against processing variations, with regard to the robustness at varying temperatures. However, only the awareness of their individual effects can avoid undesired effects induced by the ambient temperature.

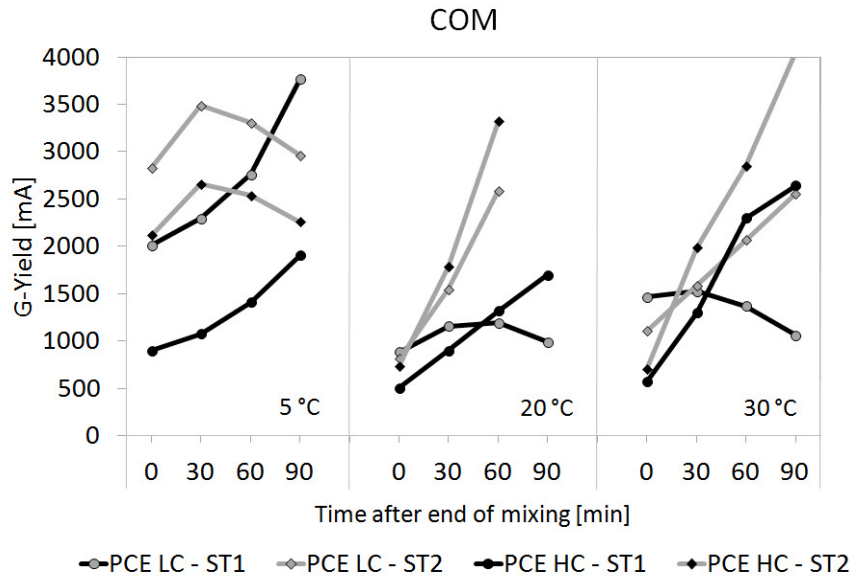


Figure 10.5: Influence of ST1 and ST2 on yield stress of COM SCC at varied temperatures.

#### 10.4.4 Choice of additions

In Subsection 5.2.6 it was shown that LSF interacts with PCE. Unlike cement the interaction with PCE is hardly affected by the charge density of PCE, which can be attributed to the low reactivity of LSF. It is therefore likely that fillers that are less reactive than cement improve the robustness against temperature variations, since they adsorb PCEs independently of any hydration reaction rate change. This effect can be shown on results from the rapid PCE performance test with LSF compared to cement using the water demands provided in Table 5.1 and the mixture composition concept after Subsection 5.2.2. The test results for different temperatures are shown in Figure 10.6. The slump flow curves for LSF are very similar, regardless of the PCE charge density or the temperature, while prominent differences can be observed for the curves of cement.

The lower PCE dosages for flow initiation and maximum with LSF, however, suggest that LSF attracts significantly less PCE than cement. The fact that blend of LSF and cement show flow initiation at higher PCE contents than pure LSF mixtures (Figure 5.8) indicates that PCE is preferably adsorbed by cement, so that an improvement due to LSF only applies when cement is already largely saturated with PCE. The latter observation is confirmed by the comparative curves also shown in Figure 5.8 with blends of quartz fines and cement, that show similar behaviour than LSF cement blends until the maximum dosage of PCE is reached, beyond which only the mixtures with LSF can supplementary yield wider slump flow values. However, at high dosages fillers that interact with PCE can supplementary contribute to the improvement of the flow properties. The rapid PCE performance test can help identifying fillers that positively contribute to the robustness of SCC mixtures against temperature scatter.

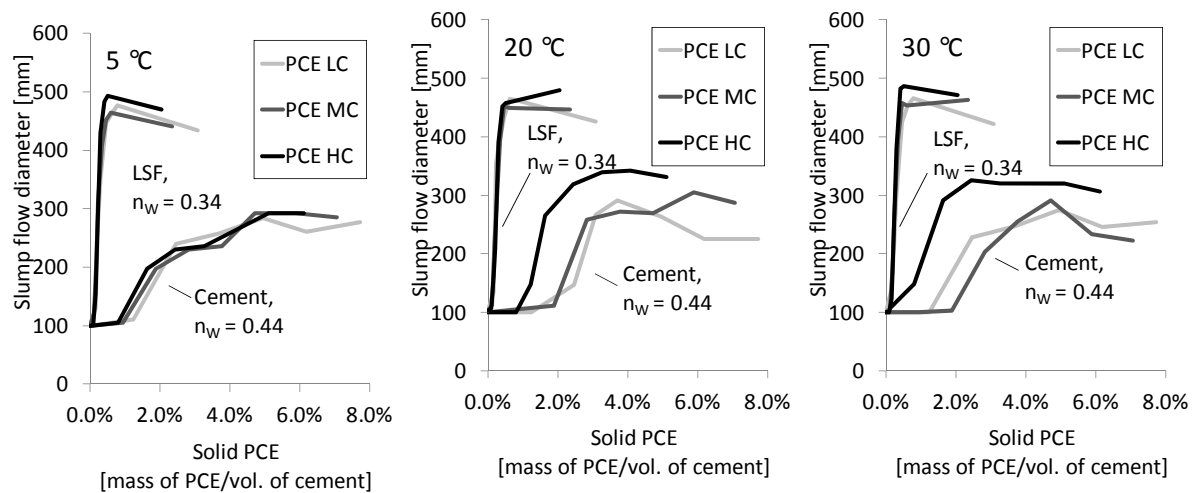


Figure 10.6: Influence of temperature on the performance of PCE with cement and LSF at their individual water demands  $n_w$  according to the Puntke test (Subsection 5.2.1).

#### 10.4.5 Selection of cement

This Thesis does not address the influence of varied cement types. For the completeness of the discussion, however, some consideration about influences of the cement type need to be made.

As the major influence for the flow performance at varying temperatures interactions between PCE, and AFm or AFt were identified. Sulphate resistant cements with low content of  $C_3A$  are thus likely to be more stable at varying temperature since the flow properties are to lesser degree determined by the hydration of  $C_3A$ . This, however, remains hypothetical and cannot be supported by the conducted investigations.

Further indicators for cement types are discussed in Subsection 10.4.4, where the role of fillers is addressed. The positive influence of the LSF suggests that blended cements, where PCEs interact with less reactive powders, may positively affect the temperature sensitivity of SCC.

#### 10.4.6 Selection of a robust mixture composition

Mixtures with higher w/p are generally more robust against influences of the PCE charge density at high temperatures, while mixtures with lower w/p are more robust against these influences at low temperatures (Figure 10.2). The results presented based on the COM and POW mixture composition, however, cannot give any evidence for any of these mixture compositions to be more robust in general against variations in temperature.

The rapid PCE performance test applied on the COM and POW mixture with PCE LC at 5, 20, and 30 °C, shows that neither high nor low temperatures significantly affect the adsorption of PCE (Figure 10.7). The figure shows that at maximum adsorption minor effects on the maximum yield stress can be induced by the temperature, however, they give little evidence that temperature effects may occur differently pronounced depending on the w/p. Hence, temperature effects cannot be directly related to a mixture composition, but only to a combination with the PCE and the mixture composition.

Nevertheless, the latter conclusion may be subject to discussion since these results were conducted at the minimum water demand as explained in detail in Subsection 5.2.1. The conclusions at higher water contents may vary.

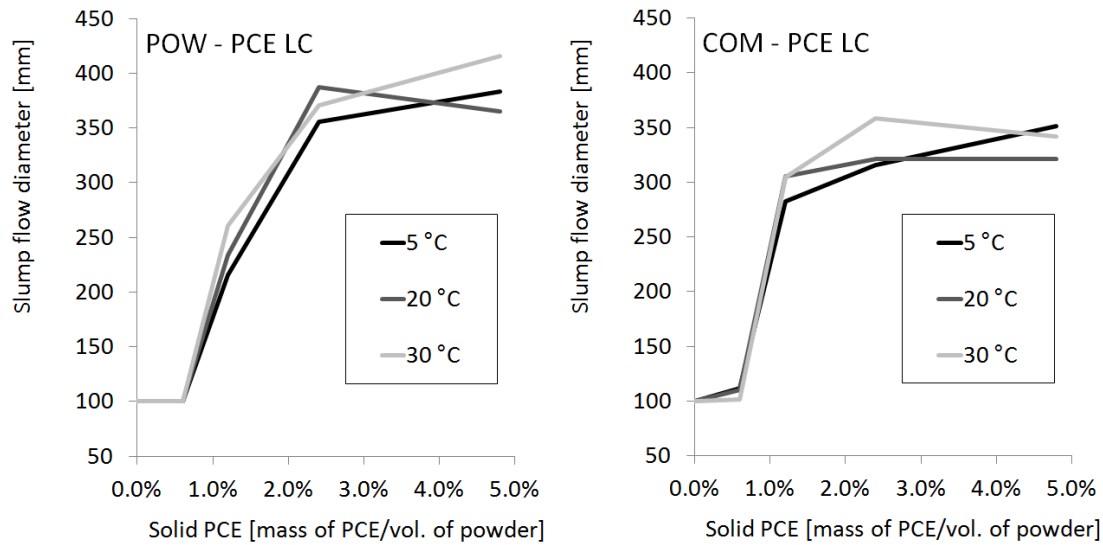


Figure 10.7: Rapid PCE performance test for POW and COM mixture compositions at 5, 20, and 30 °C.

If furthermore influences of the additions and STAs are taken into account, an influence of the mixture composition, which is independent of the PCE, can be identified. A powder rich mixture allows using higher contents of fillers which, if interacting with PCE, were shown to improve the temperature robustness. Furthermore, STAs were identified to be an uncertainty factor at varying temperatures. Flowable concretes with low w/p are typically achieved with high powder contents. High powder content allows using higher amounts of fillers as well as reduced or no STA contents so that concluding, a powder type SCC may be the better choice to improve the robustness against varying temperatures.

#### 10.4.7 Decision path for SCC with improved robustness against temperature scatter

The aforementioned considerations point out that, based on the adjustment of the mineral constituents, numerous options exist to improve the robustness of SCC against varying temperatures. Hence, if a mixture composition is fixed and cannot be optimised, the only remaining solution is using a medium charged PCE, which may not generate ultimate flow properties but in turn stable properties over a wider range of temperatures. If no further investigations are made regarding a STA, it may be advisable to better avoid using STA if the risk is high that uncontrollable temperature scatterings may occur. If STA is unavoidable, it might be better to use a non-adsorbing agent to be on the safe side and to avoid possible interactions with PCE. If the mixture composition can be modified, further improvement options exist. A summary of them is given in Figure 10.8.

If early setting is a relevant criterion, it is reasonable to use as little PCE as possible. In order to assure good flow properties, hence, a high charge density PCE need to be used. High charge density PCEs may be critical at high temperatures, since particle surfaces change rapidly and PCE is consumed too quickly. In order to maintain particles' mobility, the w/p should be high. Mixtures with high w/p turned out to be critical at low temperatures, though high charge density PCE should be able to avoid segregation of the paste, it is suggested to use high cement content within the total powder components. The suggestion to use a mixture with high w/p may be accompanied by the necessity to use STA supplementary to PCE. The results presented in Chapter 9 point out that due to interactions between STAs and PCEs, adsorbing STAs cause

earlier setting than non-adsorbing STAs. Therefore, the use of cellulose or welan or diutan gum may be preferable.

If a low risk of early shrinkage cracks is required, it is necessary to retard the setting as much as possible, which can be achieved by using a low charge density PCE. Low charge density PCEs were found to be a risk at low temperatures, since mixtures with low powder content may not be stabilised sufficiently due to the low adsorption of polymers. Therefore, at low temperatures a higher w/p is recommended to improve the stability of the mixture composition. Since low charge density PCEs demand for higher amounts of polymers than high charge density PCEs for similar flow properties, low charge density PCEs will be available in high amounts. In order to make use of the beneficial effect of fillers for the temperature robustness, the mixture should contain high amounts of fillers within the total powder content, provided that PCEs are adsorbed on filler surfaces. Mixtures with low w/p are normally more stable than mixtures with high w/p. If the temperature performance of STA is unknown, it should be considered to avoid using STA. If STA is required, a non-adsorbing type may improve the retention of the flow properties.

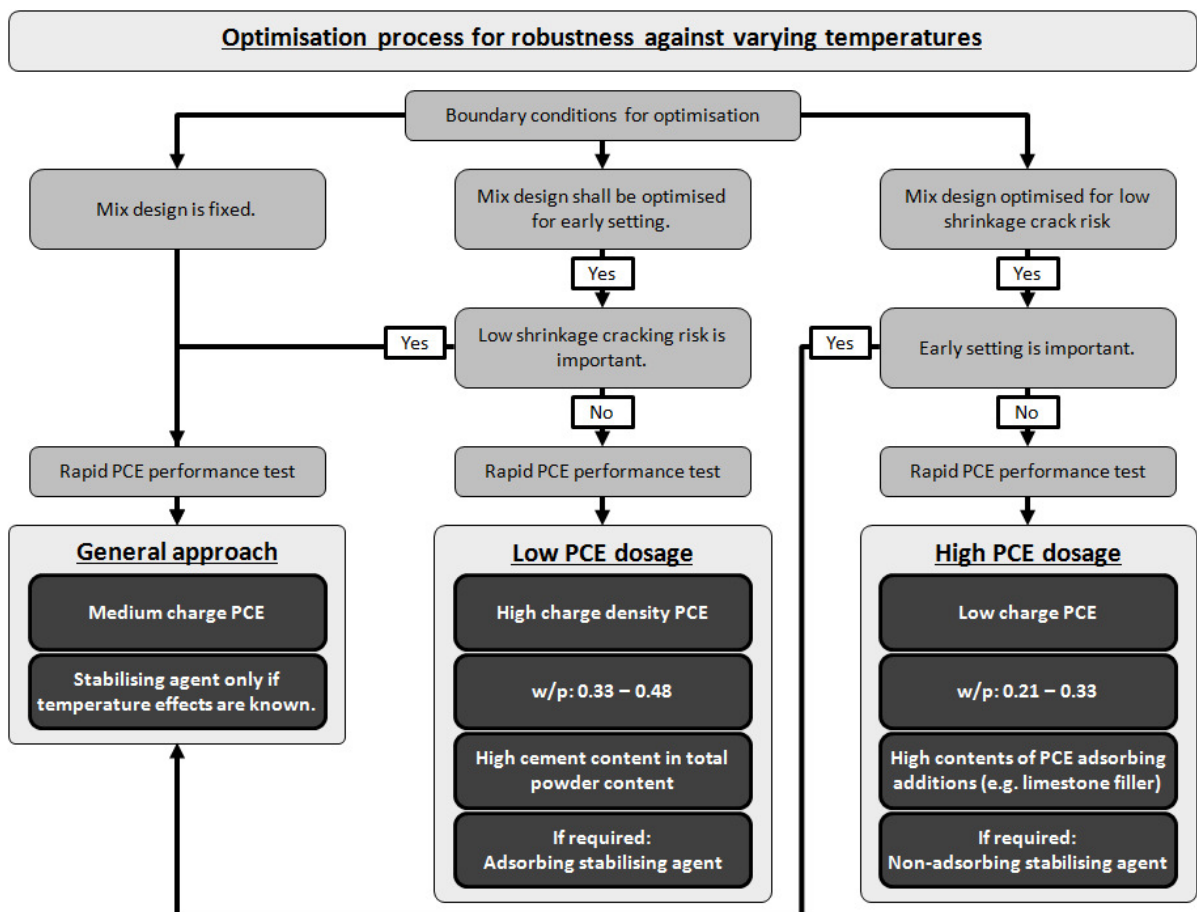


Figure 10.8: Decision tree for the optimisation of SCC for a variety of temperatures.

## 10.5 Conclusions and outlook

### 10.5.1 Summary of the intention and the scope of the work

The application of self-compacting concrete as ready-mix application is negligible world-wide. A major concern of the industry is the lack of robustness and the fear of undesired rheological effects that cannot be controlled. One of the most critical influences on the performance of SCC is the ambient temperature. SCC reacts significantly more sensitive against temperature effects than conventional vibrated concrete. The performance changes for vibrated concrete are conceivable: High temperatures accelerate the hydration causing accelerated loss of workability, low temperatures slow down the hydration, yielding extended setting. Due to the high amounts of PCE SPs, which are required to generate flowable consistency for SCC, the performance at varied temperatures is depending on two effects, the hydration rate and the related adsorption of PCE, the latter strongly depending on the amount and the charge density of the polymer. Upon addition of PCE for the flow modification the admixture is a fixed component in the hydrating cementitious system. Thus measures to optimise the rheological properties are inevitably accompanied by further effects that may be induced by both, type and amount of PCE.

In this work, investigations on SCC are presented that cover the whole early period of hydration until the setting. The observations focus on influences of the mixture composition, the charge density of the PCE and type of stabilising agent STA at 5, 20, and 30 °C. The major observations focus on rheological effects, influences on the heat flow of hydration, the setting, and the early autogenous deformations until the deformation rate slows down.

The aim of the work is to provide solution strategies to optimise the robustness of self-compacting concrete in either a particular high or low temperature range or for a broad range of varying temperatures.

### 10.5.2 Major results from the experimental work

The major conclusions were summarised in Sections 10.2 to 10.4. These will not be repeated here, but the most remarkable results will be summarised in a condensed way.

A practical problem of concrete producers is the lack of knowledge about their admixtures' performances with ongoing cement hydration. The major influence on both, initial yield stress reduction and flowability retention is the charge density of a PCE. A simple distinction between different PCEs can be made if the flow properties are observed versus the amount of added polymers at cement pastes with very low water content. PCEs with higher charge density start to flow at lower dosages and generate wider slump flow values.

The charge density of a PCE is also the most relevant parameter that influences the fresh concrete performance of SCC. However, also the water to powder ratio of the mixture composition determines whether a PCE is suitable or not for a particular temperature.

The temperature affects predominantly the yield stress of SCC. The viscosity is only affected to a negligible degree. Poor performance at a particular mixture setup and temperature range can always be linked to the yield stress of the SCC.

At high temperatures the hydration reaction is accelerated, the trigger for poor performance of an SCC is the rapid growth of the particles surfaces that may lead to a quick immobilisation of particles. This effect can be avoided by either using mixture compositions with high water to powder ratio or PCE with low charge density, which has the capability to adsorb on hydration phases with delay. Performance loss can be compensated by an increased dosage of SP.

At low temperatures, the trigger for performance loss is lack of adsorption sites for PCE polymers due to slow hydration reaction. As a consequence, particles are not stabilised

sufficiently by PCE, thus segregate upon flow. This can be compensated by either using a mixture composition with low w/p, which provides good stability, or the use of a high charge density PCE, which adsorbs immediately. Performance loss at cold temperature cannot be compensated by supplementary addition of PCE.

Considering the last two conclusions, it can be stated that powder type SCC is very robust against any effect induced by PCE at low temperatures, while combination type mixtures with high w/p are more robust than powder type SCCs against influences of the PCE at high temperatures. Low charge density PCEs are generally better suitable to avoid rapid performance loss induced by high temperatures, while high charge density PCEs are safer at low temperatures, since they assure a high polymer adsorption rate.

The stabilising agents starch ether and diutan gum were found to have significantly less influence on the flow properties at varying temperatures than PCEs. However, they showed effects and partly amplified effects induced by the PCE.

In general diutan gum tended to cause quicker loss of workability than starch based STA. This was assumed to be linked to interactions between the anionic backbones of the polymers. As PCEs at varying temperatures, effects induced by STAs mainly occur with regard to the yield stress, while the viscosity remains unaffected.

In order to achieve a certain flow property, or more specifically a certain yield stress reduction or slump flow value, lower solid amounts of high charge density PCE are required than of low charge density PCE. This fact causes significant effects on the early hydration.

The setting, as well as the temporal evolution of the heat flow of flowable cementitious systems, is predominantly driven by the amount of solid PCE. Although high charge density PCEs may cause slightly higher retardation of the hydration than low charge density PCEs, due to the aforementioned relation between charge density and yield stress reduction, low charge density PCEs will retard hydration significantly more than high charge density PCEs, since they need to be added in higher amounts.

The moment of the final set and the maximum of the first derivative of the heat flow curve were found to be closely linked. The occurrence of this particular step in time depends largely only on the total amount of solid PCE, while the charge density is negligible.

XRD measurements revealed that processes at  $t_{fin}$  vary greatly for cementitious systems with and without PCE, regardless of the PCE modification. While in systems without PCE the final set marks the onset of a significant alite dissolution and  $\text{Ca}(\text{OH})_2$  precipitation, in systems with PCE it marks the end of a significant alite dissolution and  $\text{Ca}(\text{OH})_2$  precipitation.

The amount of formed  $\text{Ca}(\text{OH})_2$  at this time was the higher the lower the charge density of the PCE was, while no significant influence of the charge density on the alite dissolution amount could be found.

The early autogenous deformations at all temperatures follow a specific pattern that shows high deformation rates first, followed by a small plateau after which again a higher rate can be observed, which finally changes to a slow deformation rate, which is close to a horizontal line (Figure 8.28). The transition towards this slow deformation rate appeared to be strongly affected by the temperature, and it occurred at a time close to  $t_{fin}$  (Figure 8.28). Neither a strong, nor a systematic influence of the charge density or the amount of PCE on the time of the transition could be found.

Since no prominent influence of the charge density or the amount of PCE could be found on the transition towards a slow deformation rate, but significant influences were found on  $t_{fin}$ , it can be concluded that low charge density PCE, which causes strong set retardation, allows to shift  $t_{fin}$ , which marks the transition towards an elastic structure to a slow deformation rate, thus

minimising the risk of early cracks. At the same time, high charge PCEs cause early setting, which occurs at a point in time where still high early deformations can be observed, which may cause early cracks.

The latter aspect was found to be less important at normal and high temperatures where the ongoing hydration causes that the aforementioned critical steps in time occur largely at the same time. Hence a rapid internal resistance against cracks is build up due to the associated strength development. At low temperatures, where the hydration is taking place at a lower velocity, the strength development takes place slowly and the time shift between  $t_{fin}$  and transition towards a slow deformation rate can take several hours.

Influences of the STA on early hydration effects were found to be small. In general, it was found that diutan gum and starch induced a set retardation without and with PCE. This was negligible at moderate and high temperatures, while more pronounced at low temperatures. Generally, starch led to stronger retardation than diutan gum.

It was found that at moderate and high temperatures, the retarding effect of both STAs could be turned into an accelerating effect, depending on the charge density of the PCE. Acceleration was observed at 20 °C and 30 °C for the combination of STA with low charge density PCE and at 30 °C for the combination of STA with high charge density PCE.

The latter observation was assumed to be linked to a reduced mobility of PCEs due to the presence of STAs. The reduced mobility of PCEs fosters the adsorption of sulphate ions, the latter less pronounced in case of high charge density PCE. The higher adsorption of sulphate ions again fosters the formation of ettringite, which in a next step attracts higher amounts of PCE than monosulphate, which would occur in higher amounts, if PCE would adsorb competitively with sulphate ions.

### 10.5.3 Future research

The use of varying characteristic mixture compositions, varying characteristic PCEs, and two differently operating STAs, is an attempt to bring the findings of this work into a general context, which is freed from any regional boundary condition. The findings are assumed to be applicable for flowable and self-levelling concrete and a wide variety of mixture compositions. Nevertheless, as with any research, the findings cannot be all-embracing.

First of all, only two mixture compositions were observed. They were distinguished mainly in their w/p ratio. The w/p of the POW mixture was 0.31 and the w/p of the COM mixture was 0.36. In order to better evaluate the influence of the w/p or to find threshold values for certain effects, a more systematic comparison between higher numbers of mixture composition variations can definitively contribute to a better understanding of temperature effects.

The investigations in this work were conducted with an ordinary Portland cement. The observations and conclusions can be considered to basically maintain their relevance also in blended cement systems, since the mechanisms behind the varying performances are depending on adsorption of superplasticisers and the solid volume fraction of particles in a dispersion. Cement extenders will incorporate different surface properties such as charges and surfaces. This can have a strong influence on the adsorption of polymers and the water demand of a system, but the basic physical principles that determine the adsorption of polymers and the dispersion of particles maintain their validity. Nevertheless, future research should validate this point of view and cement extenders and fillers need to be identified which affect the temperature related performance of SCC positively.

Three types of commercial PCEs were varied. Their performance data was based on qualitative information provided by the producer. This limits the prediction options. Systematic variations of the graft chains and deeper information on the polymer geometry would

significantly help identifying optimised admixtures and better understanding and probably even modelling interactions induced by temperatures.

ST1 based on potato starch and ST2 based on diutan gum were chosen thoughtfully, as they were considered to represent different groups of STA. Though it may be the most commonly used stabilising agent for cementitious systems, cellulose was not investigated in this Thesis. Based on experiences of the author, the behaviour of cellulose compares to the behaviour of diutan gum, but generalising the diutan gum results to cellulose remains hypothetical. Furthermore, cellulose and starch STAs are very versatile, and both offer a high number of supplementary ways to steer the polymer performance, such as adding functional groups or modifying the polymer size. Therefore future investigations will also include differently modified cellulose derivatives.

Some hypotheses about interactions between the anionic groups of diutan gum and PCE were made. These hypotheses were suggested by considerations about the early hydration of cement in the presence of polymers in conjunction with observations of the rheology and the setting. More sophisticated investigation methods are required to verify the hypotheses.

Effects of the charge density of the PCEs on the early hydration and particularly the precipitation of calcium hydroxide and the dissolution of alite were presented. These observations suggest a number of further investigations to better understand the effect of PCE, which is still in discussion. To better evaluate the influences on the hydration phases, ESEM investigations, and to find possible hydration modifications at the very early stage synchrotron XRD, are considered to support further progress.

Finally, conclusions were drawn on the cracking risk depending upon the occurrence of the final set and the transition towards slow deformation rates. It was assumed that large restrained deformations cause a significant crack risk for systems that have just turned from a plastic state into a solid structure and the strength is still very low. In order to verify this hypothesis, investigations on larger scale are required.

#### **10.5.4 Classification into scientific context, exploitation, and outlook**

In the introduction chapter it was discussed that world-wide a large gap exists between the fields of research that focus on admixtures and on concrete technology. The rapid development in concrete technology requires that the two shores are connected. It is unavoidable that concrete technologists consider the optimisation of the admixtures as equally important as the optimisation of the grading, the particle shape, the binder system, or the volumetric mineral mixture composition. In turn, it is unavoidable for chemists to understand that the casting of concrete is depending on an ungraspable number of uncertainty factors, which can never be simulated by models or laboratory trials, in best case with separated phases in controlled environment.

This work attempts to combine both fields. One focus is placed on the mode of operation and the important parameters in context with concrete applications. At the same time more sophisticated considerations are made on the cement admixture interaction scale, without neglecting the discussion of the relevance for the concrete level. Thus, the work aims to contribute to better understand influences of admixtures and mixture composition on fresh concrete and paste, early hydration mechanisms depending on admixture variations, as well as of polymeric characteristics on concreting matters. It thus can be located in the centre of the circles illustrated in Figure 1.11, of which the intersection forms the knowledge that is required to understand all areas of SCC. The suggested rapid PCE performance test method (Chapter 5) and the concluding decision trees in Chapter 10 are simplified tools developed out of the

research results, in order to simplify the optimisation of the temperature robustness of SCC for practical engineers.

The results of this work are already directly incorporated into a European-African cooperation project, in which among other matters, considerations about optimised concrete mixtures for sub-equatorial countries are made and the extreme temperatures are a serious threat to the workability of fresh concrete. The result are mixture proportioning methods for self-compacting concrete based on locally available components such as cassava starch and bagasse ashes [330-334].

Similar concepts can be easily developed for any other region in the world based on the decision trees, suggested in Chapter 10. It is thus assumed that this work builds a small step towards a wider world-wide use of SCC as ready-mixed concrete.

Ongoing research at the BAM Federal Institute for Materials Research and Testing focuses on the influences of individual starch modifications on the rheology of cementitious pastes and concrete systems [285]. Another focus is put on the influence of the mixture composition of SCC on numerous hardened concrete properties. Both topics directly follow up the context of this work.

#### **10.5.5 Concluding remarks**

Based on the research experiences of the author with SCC from different European countries before this work was started, a major aim of this work was focusing on flowable concrete with validity for a wide range of rheological properties. The outcome of this work shows that a stereotypic analysis of SCC, only based on the assumption that it flows, is hardly possible. More emphasis needs to be put onto the distinction between SCC mixture compositions.

The same is valid for superplasticisers based on polycarboxylate ether. Solely the fact that the basic structure is that of polycarboxylate ether does not give sufficient distinction. More focused research on the characteristic specifications of PCEs and reviewing existing studies giving special considerations to the PCE properties can be expected to be a reasonable approach to further understand the interactions between PCEs and the early hydration of cementitious systems.

## Abbreviations and symbols

AFm	Alumina, ferric oxide mono-sulphate phase
AFt	Alumina, ferric oxide tri-sulphate phase
b <sub>PCE</sub>	Bulk PCE addition [% by mass]
c	Mass of cement [g]
C <sub>2</sub> S	Dicalcium silicate (Belite)
C <sub>3</sub> A	Tricalcium aluminate (Aluminate)
C <sub>3</sub> S	Tricalcium silicate (Alite)
C <sub>4</sub> AF	Tetracalcium alumina ferrite (Ferrite)
Ca(OH) <sub>2</sub>	Calcium hydroxide
Ca <sup>2+</sup>	Calcium ions
CaCO <sub>3</sub>	Calcium carbonate
C-A-H	Calcium aluminate hydrate
CaO	Calcium oxide
COM	Combination type SCC
C-S-H	Calcium silicate hydrates
d	Spacing between the planes in the atomic lattice [nm]
d	Particle diameter [mm]
d <sub>max</sub>	Maximum particle diameter [mm]
d <sub>min</sub>	Minimum particle diameter [mm]
d <sub>SF</sub>	Spread flow diameter of paste and mortar from the flow test [mm]
D	Diffusion coefficient [m <sup>2</sup> /s]
d <sub>0</sub> :	Lower opening diameter of the container used for the flow test [mm]
d <sub>1</sub> :	Largest slump flow or spread flow diameter [mm]
d <sub>2</sub> :	Diameter perpendicular to d <sub>1</sub> [mm]
DC	Decorated chain
DP	Average degree of polymerisation
d <sub>s</sub>	Shear plane distance [mm]
EO	Ethylene oxide
ESEM	Environmental scanning electron microscope
FA	Fly ash
FBS	Flexible backbone star
FBW	Flexible backbone worm
g	Apparent gravity [m/s <sup>2</sup> ]
GGBS	Ground granulated blast furnace slag
G-Yield	Relative value for the yield stress [A]
HEC	Hydroxyethyl cellulose
HPC	High performance concrete
HPMC	Hydroxypropymethyl cellulose
HRWRA	High range water reducing agent, used as synonym for SP in literature review sections and figures of other authors, where authors used HRWRA rather than SP
H-Viscosity	Relative value for the viscosity [Pa·s]
L	Flow length, LCPC-Box [m]
LS	Lignosulphonate
LSF	Limestone filler
m <sub>c</sub>	Initial mass of concrete placed onto the sieve [g]
MS	Microsilica
ML	Melamine based superplasticisers

$m_p$	Mass of powder [g]
$m_p$	Mass of the sieve receiver [g]
$m_{ps}$	Mass of sieve receiver plus passed material [g]
$m_w$	Mass of water [g]
N	Number of monomers in the backbone of a PCE
n	Flow behaviour index [-]
n	Integer for the diffraction order
N	Nano silica
$Na_2SO_4$	Sodium sulphate
NaCl	Sodium chloride
$n_{EO}$	Number of ethylene oxide units
$n_w$	Water demand according to the Puntke test [-]
OH <sup>-</sup>	Hydroxide ions
OMP	Organo mineral phase
P	Number of monomers in the side chain of a PCE
$P_{(d)}$	Cumulative finer fraction of particles and aggregates [%]
PC	Polycarboxylic superplasticisers
PCC	Polymer modified concrete
PCE HC	High charge density polycarboxylate ether
PCE LC	Low charge density polycarboxylate ether
PCE MC	Medium charge density polycarboxylate ether
PCE	Polycarboxylate ether
PEO	Polyethylene oxide
PMS	Polymelamine sulphonate
PNS	Polynaphtalene sulphonate
POW	Powder type SCC
PS	Polysaccharide
QF	Quartz filler
R	Half slump flow diameter [m]
RF	Relative humidity
SBS	Stretched backbone star
SBW	Stretched backbone worm
SCC	Self-compacting concrete
SCM	Self-compacting mortar
SCM	Supplementary cementitious materials
SEM	Scanning electron microscope
SF	Slump flow value or spread flow value of concrete [mm]
$SO_4^{2-}$	Sulphate ions
SP	Superplasticiser
$s_{PCE}$	Solid content of the PCE [%]
SR	Sieve segregation resistance [-]
SRA	Shrinkage reducing agent
SSA	Specific surface area [m <sup>2</sup> /g]
ST	Modified starch
ST1	Stabilising agent 1 based on modified potato starch
ST2	Stabilising agent 2 based on microbial polysaccharide
STA	Stabilising agent
T	Absolute temperature [K]
T	Ambient temperature [K]
t	Time [s]

$t_0$	Time-zero: transition of a setting system from plastic state into solid state [h]
$t_{500}$	Time for a concrete required to flow to a diameter of 500 mm during the slump flow test [s]
$t_{fin}$	Initial setting time [h]
$t_{ini}$	Final setting time [h]
$t_V$	V-funnel efflux time [s]
u	Unified atomic mass unit, equal to the unit dalton Da [-]
V	Cone volume [m <sup>3</sup> ]
VEA	Viscosity enhancing agent. Used as synonym for STA in literature review sections and figures of other authors, where authors used VMA rather than STA
VMA	Viscosity modifying agent. Used as synonym for STA in literature review sections and figures of other authors, where authors used VMA rather than STA
w/c	Water-cement ratio. Ratio of water to cement. If not explicitly stated, it is given in mass units.
w/cm	Water-cementitious materials ratio. The ratio of water to cementitious materials. If not explicitly stated, it is given in mass units.
w/p	Water-powder ratio. The ratio of the mass of water to the mass of cement and additions, typically the entire fraction of fines < 125 $\mu\text{m}$ . If not explicitly stated, it is given in mass units.
XRD	X-Ray Diffraction
XRF	X-Ray Fluorescence Method
$\Delta G_r$	Gibbs free energy [J]
$\Delta H_r$	Reaction enthalpy [J]
$\Delta S_r$	Reaction entropy [J/K]
$\dot{\gamma}$	Shear rate [1/s]
$\theta$	Angle between incident ray and scattering plane
$\lambda$	Wave length of the incident wave [nm]
$\rho$	Fresh concrete mass density [kg/m <sup>3</sup> ]
$\beta_P$	Water demand according to the method of Okamura
$\eta$ or $\eta_{pl}$	Plastic viscosity [Pa·s]
$\eta_{rel}$	Relative viscosity in a non fundamental unit [(Variable)·s]
$1/\eta$	Fluidity [(Pa·s) <sup>-1</sup> ]
$\Phi_{kz}$	Paste to aggregate ratio
$\kappa$	Flow consistency index [[Pa·s] <sup>n</sup> ]
$\rho_w$	Density of powder [g/mm <sup>3</sup> ]
$\rho_w$	Density of water [g/mm <sup>3</sup> ]
$\tau$	Shear stress [Pa]
$\tau_0$	Yield stress [Pa]
$\zeta$	Zeta potential [mV]



## Annex A – Rheometric results of SCC

Table A.1: Summary of G-Yield and H-Viscosity values of COM type SCC for all admixture combinations and time steps at 5 °C.

Mixture composition	PCE type	STA	Time after mixing	G-Yield	H-Viscosity
COM	LC	ST1	0	2011.2	8423.1
COM	LC	ST1	30	2295.8	12787.2
COM	LC	ST1	60	2759.9	17109.2
COM	LC	ST1	90	3765.8	12372.4
COM	LC	ST2	0	2831.7	8798.6
COM	LC	ST2	30	3487.4	21180.9
COM	LC	ST2	60	3309.3	23092.3
COM	LC	ST2	90	2961.6	22498.8
COM	MC	ST1	0	1582.8	6647.2
COM	MC	ST1	30	1522.6	10407.2
COM	MC	ST1	60	1978.9	12814.5
COM	MC	ST1	90	2847.2	11577.5
COM	MC	ST2	0	2039.7	6715.6
COM	MC	ST2	30	3044.7	11248.5
COM	MC	ST2	60	2655.8	12410.5
COM	MC	ST2	90	1877.2	14840.3
COM	HC	ST1	0	899.0	5463.7
COM	HC	ST1	30	1076.8	7960.8
COM	HC	ST1	60	1410.5	10735.6
COM	HC	ST1	90	1905.9	11333.7
COM	HC	ST2	0	2117.7	5688.7
COM	HC	ST2	30	2660.1	9801.8
COM	HC	ST2	60	2535.5	11261.6
COM	HC	ST2	90	2261.0	11585.2

Table A.2: Summary of G-Yield and H-Viscosity values of POW type SCC for all admixture combinations and time steps at 5 °C.

Mixture composition	PCE type	STA	Time after mixing	G-Yield	H-Viscosity
POW	LC	ST1	0	863	6709.6
POW	LC	ST1	30	663	9724.9
POW	LC	ST1	60	570	11743.5
POW	LC	ST1	90	536	12946.4
POW	LC	ST2	0	1113	7519.7
POW	LC	ST2	30	834	10755.4
POW	LC	ST2	60	979	10193.7
POW	LC	ST2	90	702	12200.9
POW	MC	ST1	0	1063	7277.9
POW	MC	ST1	30	991	9465.6
POW	MC	ST1	60	1021	10160.6
POW	MC	ST1	90	970	10976.0
POW	MC	ST2	0	1037	7861.9
POW	MC	ST2	30	776	9797.3
POW	MC	ST2	60	815	11002.9
POW	MC	ST2	90	869	11063.8
POW	HC	ST1	0	709	7958.6
POW	HC	ST1	30	537	11260.6
POW	HC	ST1	60	527	13411.7
POW	HC	ST1	90	771	13515.2
POW	HC	ST2	0	686	8396.5
POW	HC	ST2	30	711	10466.2
POW	HC	ST2	60	743	12178.1
POW	HC	ST2	90	834	12337.7

Table A.3: Summary of G-Yield and H-Viscosity values of COM type SCC for all admixture combinations and time steps at 20 °C.

Mixture composition	PCE type	STA	Time after mixing	G-Yield	H-Viscosity
COM	LC	ST1	0	884.9	7115.7
COM	LC	ST1	30	1156.8	8493.0
COM	LC	ST1	60	1194.1	10905.9
COM	LC	ST1	90	989.6	15004.8
COM	LC	ST2	0	813.4	7156.7
COM	LC	ST2	30	1543.6	11356.9
COM	LC	ST2	60	2585.2	10646.3
COM	LC	ST2	90	-	-
COM	MC	ST1	0	1041.9	7230.0
COM	MC	ST1	30	1301.7	10132.4
COM	MC	ST1	60	1609.9	11449.6
COM	MC	ST1	90	1570.4	12643.7
COM	MC	ST2	0	856.6	4046.1
COM	MC	ST2	30	936.1	6224.8
COM	MC	ST2	60	1073.6	7104.2
COM	MC	ST2	90	1083.1	7438.3
COM	HC	ST1	0	502.3	4995.3
COM	HC	ST1	30	898.2	7184.0
COM	HC	ST1	60	1319.7	8745.7
COM	HC	ST1	90	1698.9	9434.4
COM	HC	ST2	0	739.0	6534.6
COM	HC	ST2	30	1784.2	9014.2
COM	HC	ST2	60	3322.6	9223.0
COM	HC	ST2	90	-	-

Table A.4: Summary of G-Yield and H-Viscosity values of POW type SCC for all admixture combinations and time steps at 20 °C.

Mixture composition	PCE type	STA	Time after mixing	G-Yield	H-Viscosity
POW	LC	ST1	0	506.4	4106.0
POW	LC	ST1	30	589.1	6038.1
POW	LC	ST1	60	481.1	7864.1
POW	LC	ST1	90	417.1	8650.2
POW	LC	ST2	0	871.9	7162.6
POW	LC	ST2	30	857.3	12632.4
POW	LC	ST2	60	743.4	13905.2
POW	LC	ST2	90	410.3	16669.4
POW	MC	ST1	0	845.2	7656.5
POW	MC	ST1	30	946.5	10083.4
POW	MC	ST1	60	853.6	13189.8
POW	MC	ST1	90	928.4	14471.6
POW	MC	ST2	0	695.8	5969.5
POW	MC	ST2	30	702.6	9654.5
POW	MC	ST2	60	928.0	10210.6
POW	MC	ST2	90	790.0	11622.1
POW	HC	ST1	0	523.9	4904.9
POW	HC	ST1	30	1046.8	7145.6
POW	HC	ST1	60	1261.8	10422.3
POW	HC	ST1	90	2191.2	11131.9
POW	HC	ST2	0	750.0	9673.0
POW	HC	ST2	30	1855.1	14046.1
POW	HC	ST2	60	3478.9	18043.1
POW	HC	ST2	90	-	-

Table A.5: Summary of G-Yield and H-Viscosity values of POW type SCC for all admixture combinations and time steps at 30 °C.

Mixture composition	PCE type	STA	Time after mixing	G-Yield	H-Viscosity
COM	LC	ST1	0	1469.1	7100.9
COM	LC	ST1	30	1525.9	10580.9
COM	LC	ST1	60	1370.3	12494.5
COM	LC	ST1	90	1060.2	14133.6
COM	LC	ST2	0	1106.7	6723.7
COM	LC	ST2	30	1589.2	10046.9
COM	LC	ST2	60	2068.6	11206.9
COM	LC	ST2	90	2561.1	12373.5
COM	MC	ST1	0	1163.2	6812.1
COM	MC	ST1	30	1646.8	8783.9
COM	MC	ST1	60	1781.3	10325.3
COM	MC	ST1	90	1949.9	10181.5
COM	MC	ST2	0	1117.9	5827.5
COM	MC	ST2	30	1380.3	9155.1
COM	MC	ST2	60	2079.8	10760.2
COM	MC	ST2	90	2485.5	11513.0
COM	HC	ST1	0	570.5	7136.6
COM	HC	ST1	30	1298.7	9596.3
COM	HC	ST1	60	2299.9	11612.1
COM	HC	ST1	90	2643.6	12886.2
COM	HC	ST2	0	702.7	5448.3
COM	HC	ST2	30	1988.2	7581.5
COM	HC	ST2	60	2850.3	9891.6
COM	HC	ST2	90	4054.1	10453.3

Table A.6: Summary of G-Yield and H-Viscosity values of POW type SCC for all admixture combinations and time steps at 30 °C.

Mixture composition	PCE type	STA	Time after mixing	G-Yield	H-Viscosity
POW	LC	ST1	0	776.4	6935.6
POW	LC	ST1	30	840.7	11375.8
POW	LC	ST1	60	459.6	13561.2
POW	LC	ST1	90	483.2	14383.8
POW	LC	ST2	0	789.6	5366.4
POW	LC	ST2	30	840.4	7505.1
POW	LC	ST2	60	798.0	8805.5
POW	LC	ST2	90	520.2	10304.1
POW	MC	ST1	0	858.3	5275.5
POW	MC	ST1	30	1362.0	7281.7
POW	MC	ST1	60	1349.9	8904.4
POW	MC	ST1	90	1440.9	10348.7
POW	MC	ST2	0	835.8	4230.8
POW	MC	ST2	30	1092.2	7026.7
POW	MC	ST2	60	1527.8	7686.8
POW	MC	ST2	90	1517.9	8039.6
POW	HC	ST1	0	1073.1	6273.7
POW	HC	ST1	30	3745.1	10378.0
POW	HC	ST1	60	-	-
POW	HC	ST1	90	-	-
POW	HC	ST2	0	1481.3	6490.1
POW	HC	ST2	30	3995.9	10246.1
POW	HC	ST2	60	-	-
POW	HC	ST2	90	-	-

## Annex B – Compressive strength of SCC

Table B.1: Summary of 28-d compressive strength values of all COM mixes after casting at different temperature conditions.

	COM LC		COM MC		COM HC	
	ST1	ST2	ST1	ST2	ST1	ST2
5 °C	55.4	55.5	58.4	59	62.8	61.2
	53.1	56.0	59.2	58.3	62.7	57.7
	56.4	51.7	58.2	57.6	63.8	57.7
20 °C	62.5	62.4	62.0	65.9	64.6	60.3
	61.3	60.2	58.4	64.7	60.9	59.8
	60.7	59.3	58.2	64.8	59.3	62.4
30 °C	65.3	62.6	63.4	62.9	58.4	61.2
	61.7	63.1	61.4	65.1	61.9	56.5
	59.1	60.5	61.8	64.8	63.2	58.4

Table B.2: Summary of 28-d compressive strength values of all POW mixes after casting at different temperature conditions.

	POW LC		POW MC		POW HC	
	ST1	ST2	ST1	ST2	ST1	ST2
5 °C	59.9	55.4	61.8	59.9	62.6	64.3
	60.3	56.2	60.9	60.5	61	63.3
	60.6	57.6	61.2	58.8	63.5	64
20 °C	60.6	56.7	59.6	58.9	60.3	56.9
	59.8	58.1	60.8	59.5	59.8	54.5
	60.9	58	61.2	60.4	62.4	56.5
30 °C	61.8	59.4	61.6	61.6	53.2	57.4
	61.8	59.7	59.5	61.8	58.4	57.2
	61.5	59.3	59.3	62.8	52.1	57.3



## Annex C – Heat flow rates and Vicat setting times

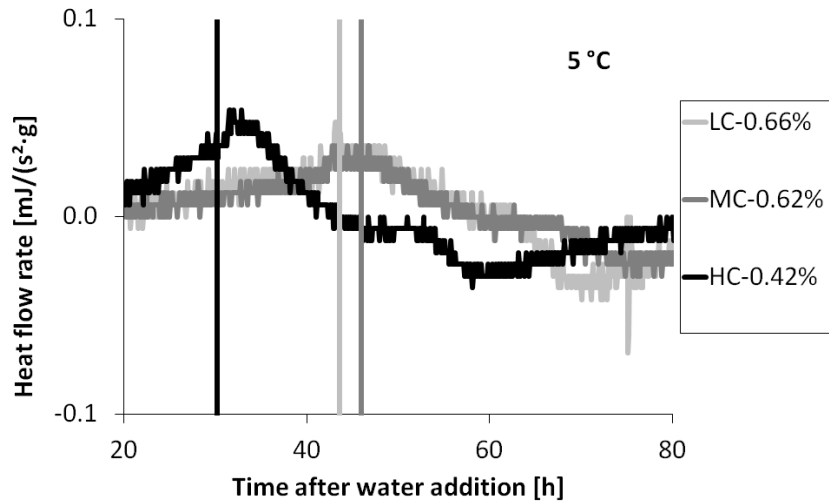


Figure C.1: Maxima of the derivatives of the heat flow curves vs. respective final setting times according to Vicat for PCE dosage for identical rheology at 5 °C.

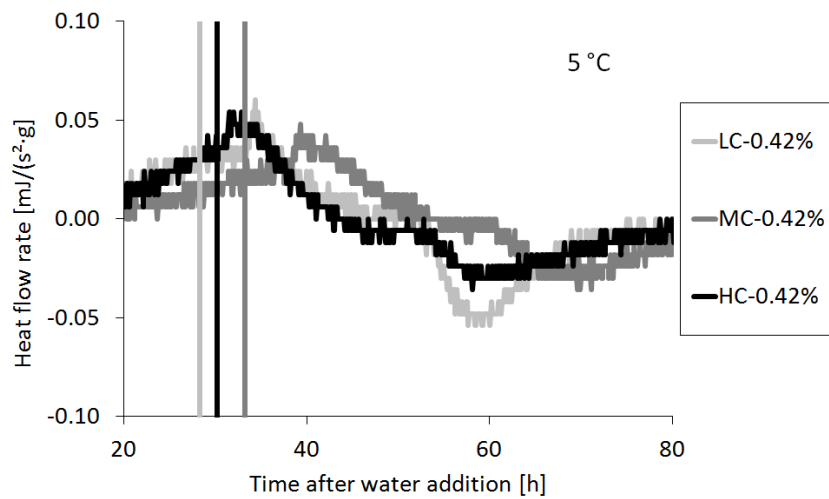


Figure C.2: Maxima of the derivatives of the heat flow curves vs. respective final setting times according to Vicat for PCE dosage for identical solid content at 5 °C.

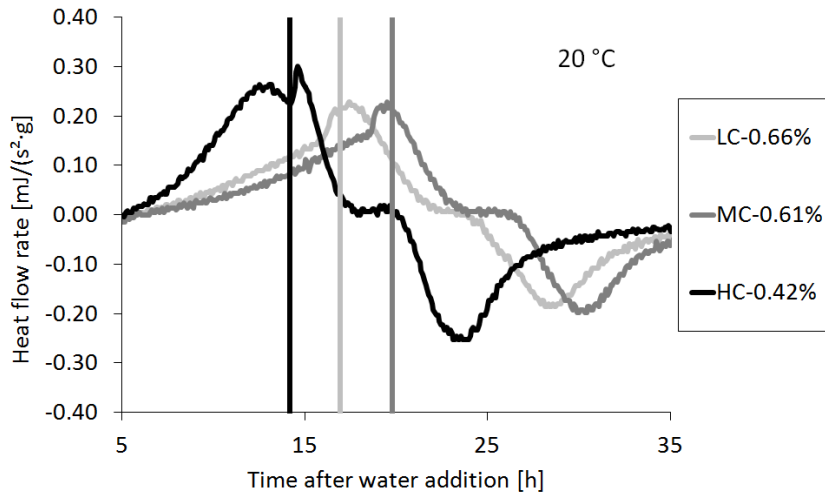


Figure C.3: Maxima of the derivatives of the heat flow curves vs. respective final setting times according to Vicat for PCE dosage for identical rheology at 20 °C.

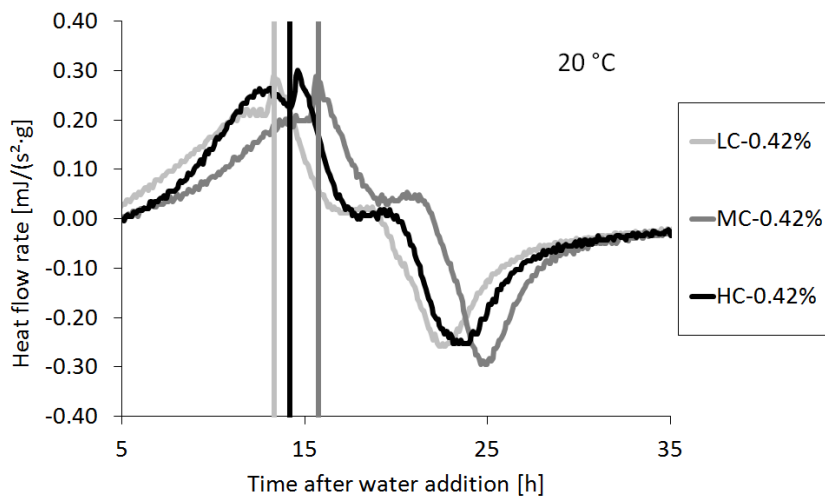


Figure C.4: Maxima of the derivatives of the heat flow curves vs. respective final setting times according to Vicat for PCE dosage for identical solid content at 20 °C.

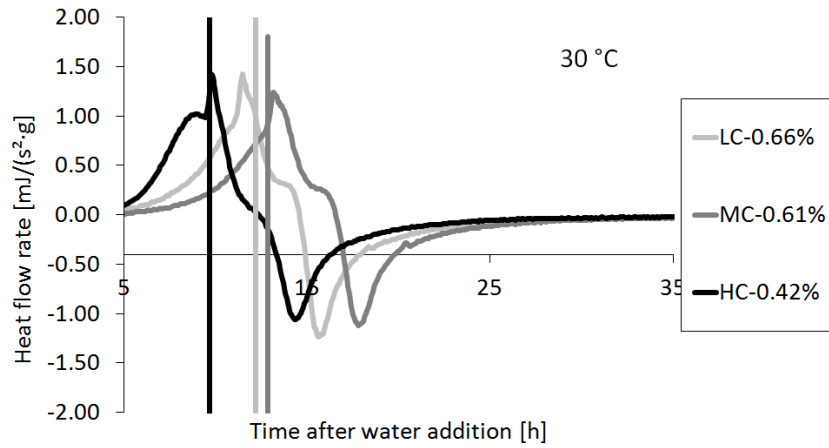


Figure C.5: Maxima of the derivatives of the heat flow curves vs. respective final setting times according to Vicat for PCE dosage for identical rheology at 20 °C.

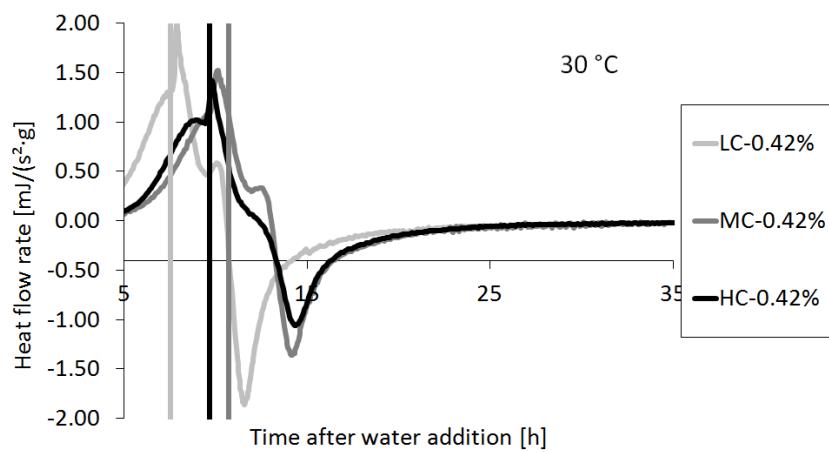


Figure C.6: Maxima of the derivatives of the heat flow curves vs. respective final setting times according to Vicat for PCE dosage for identical solid content at 30 °C.



## Annex D – XRD measurement intervals and patterns

Table D.1: Schedule of times after water addition for XRD measurement.

	no PCE	PCE HC-0.42%	PCE LC-0.66%	PCE LC-0.42%	Diffraction angles $2\theta$
Abbrev.	MPCn	MPCn	MPCn	OPCn	
n	Time of measurement after water addition				5° to 25°
1	0:10	0:17	0:15	0:09	
2	0:21	0:27	0:25	0:20	
3	0:32	0:38	0:35	0:30	
4	0:42	0:48	0:46	0:41	
5	0:52	0:58	0:56	0:51	
6	1:03	1:09	1:06	1:01	
7	1:13	1:19	1:17	1:12	
8	1:23	1:29	1:27	1:22	
9	1:34	1:40	1:37	1:32	
10	1:44	1:50	1:48	1:43	
11	1:54	2:00	1:58	1:53	
12	2:05	2:11	2:08	2:03	
13	3:01	3:11	3:08	2:59	5° to 45°
14	4:05	4:15	4:12	4:03	
15	5:09	5:19	5:16	5:07	
16	6:13	6:23	6:20	6:11	
17	7:44	7:27	7:25	7:16	
18	8:21	8:31	8:29	8:20	
19	9:25	9:35	9:33	9:24	
20	10:29	10:39	10:37	10:28	
21	11:33	11:43	11:41	11:32	
22	12:37	12:47	12:45	12:36	
23	14:41	14:51	14:49	14:40	
24	16:45	16:55	16:53	16:44	
25	18:49	18:59	18:57	18:48	
26	20:53	21:04	21:01	20:52	
27	22:58	23:08	23:06	22:57	
28	25:02	25:12	24:10	0:01	
29	27:06	27:36	27:14	3:05	
30	31:10	31:21	31:18	7:09	
31	35:15	35:25	35:23	11:14	
32	39:19	39:29	39:27	15:18	
33	43:23	43:34	43:32	19:23	
34	47:28	47:38	47:36	23:27	

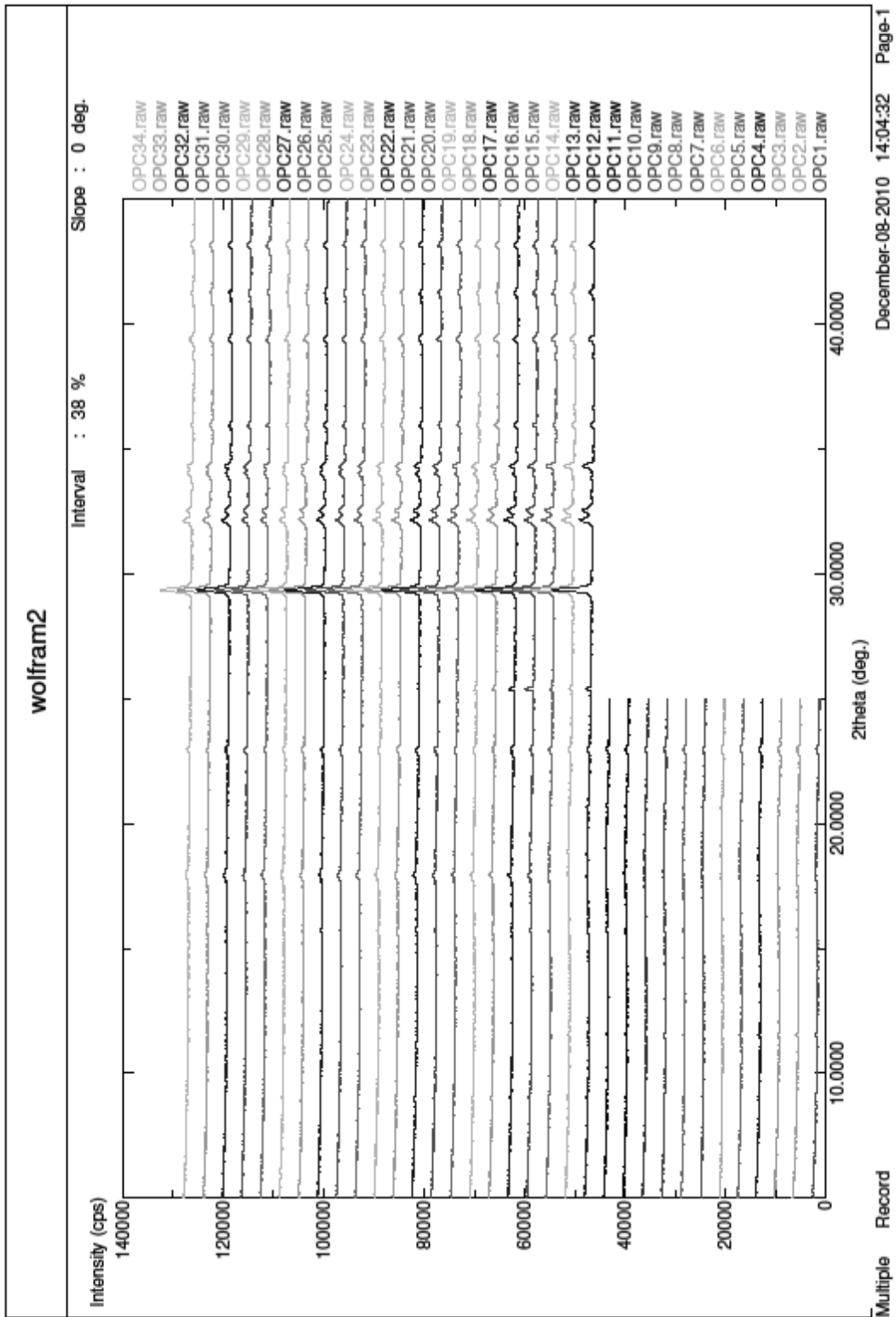


Figure D.1: XRD patterns for paste without SP.

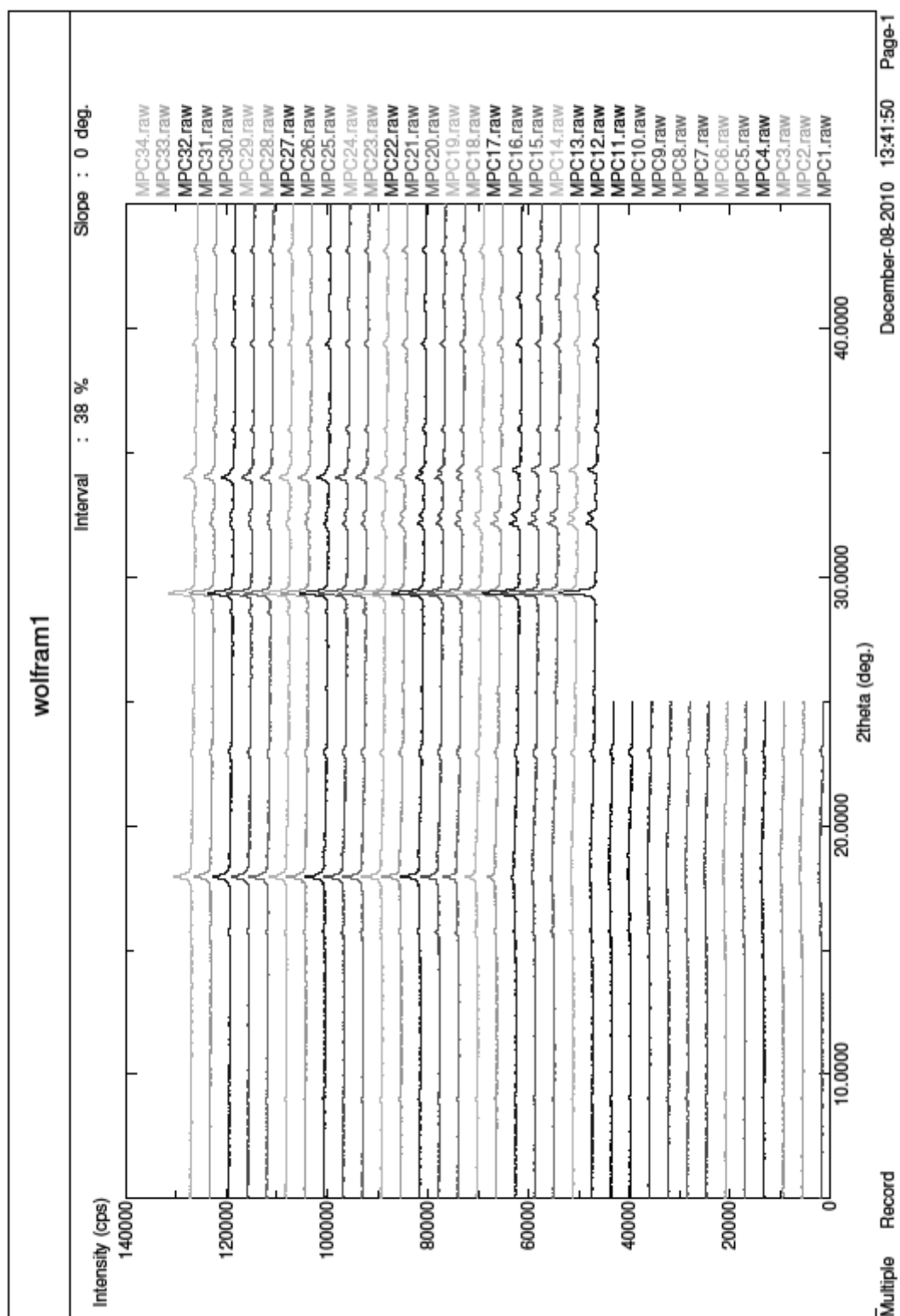


Figure D.2: XRD patterns for paste with 0.42% PCE HC.

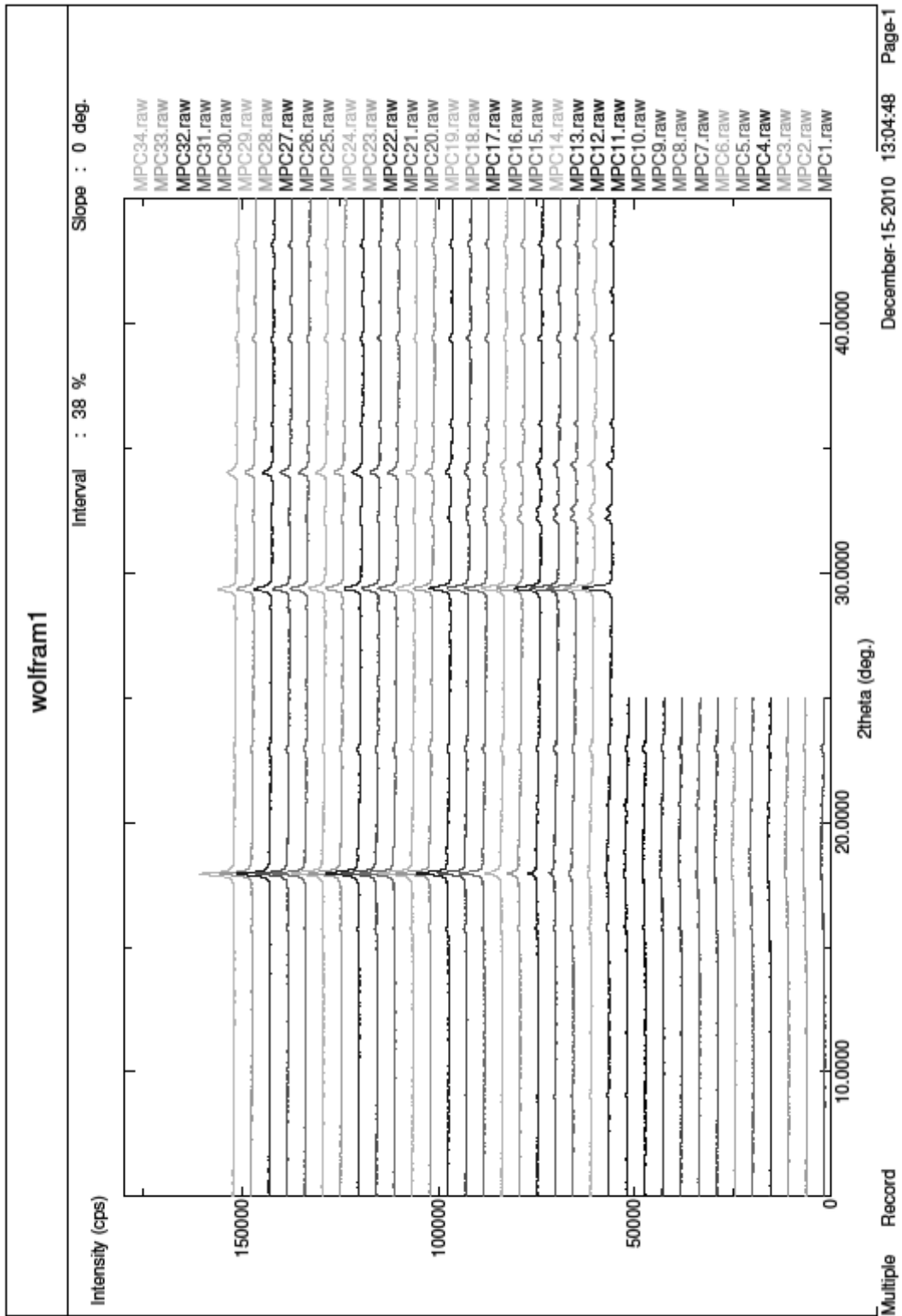


Figure D.3: XRD patterns for paste with 0.66% PCE LC.

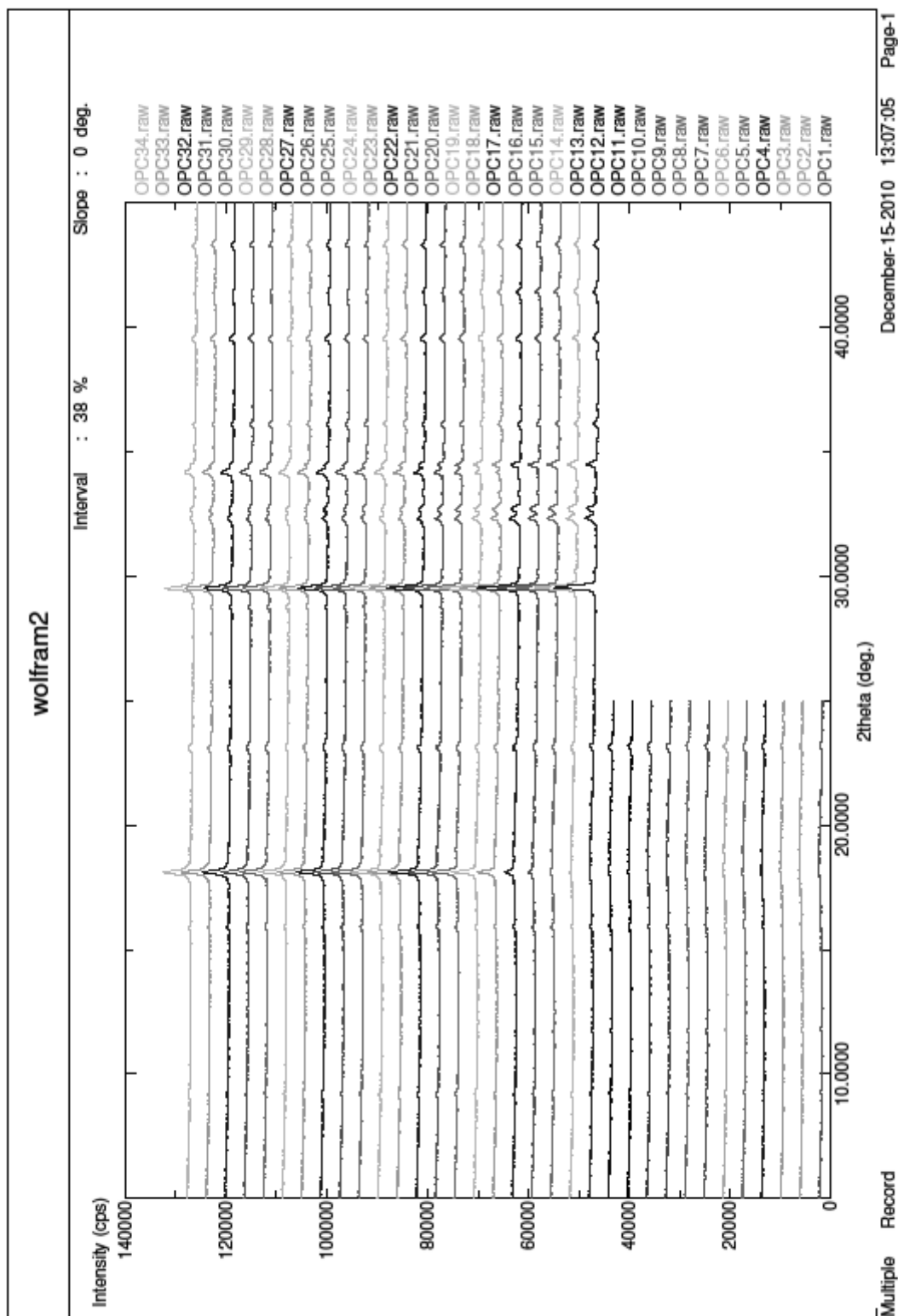


Figure D.4: XRD patterns for paste with 0.42% PCE LC.



## Annex E – Vicat setting times of COM and POW pastes

Table E.1: Initial and final setting times of COM and POW paste tests with low charge density PCE and ST1.

Temperature	Mixture modification	$t_{ini}$ as average out of three measurements	$t_{fin}$ as average out of three measurements
5 °C	COM - PCE LC	36.69	63.61
	COM - PCE LC - ST1	39.88	67.69
	COM - ST1	11.78	17.11
	COM	8.71	11.60
20 °C	COM - PCE LC	17.05	23.18
	COM - PCE LC - ST1	17.06	25.85
	COM - ST1	4.76	6.77
	COM	4.20	5.38
30 °C	COM - PCE LC	12.52	14.30
	COM - PCE LC - ST1	12.53	14.78
	COM - ST1	2.77	4.28
	COM	2.76	3.99
5 °C	POW - PCE LC	25.07	51.43
	POW - PCE LC - ST1	24.27	42.96
	POW - ST1	6.78	10.17
	POW	6.27	8.29
20 °C	POW - PCE LC	11.02	15.61
	POW - PCE LC - ST1	11.02	15.69
	POW - ST1	3.23	4.32
	POW	3.22	4.02
30 °C	POW - PCE LC	7.52	9.81
	POW - PCE LC - ST1	7.05	8.80
	POW - ST1	1.75	2.69
	POW	1.73	2.52

Table E.2: Initial and final setting times of COM and POW paste tests with low charge density PCE and ST2.

Temperature	Mixture modification	$t_{ini}$ as average out of three measurements	$t_{fin}$ as average out of three measurements
5 °C	COM - PCE LC	36.53	71.87
	COM - PCE LC - ST2	33.69	56.37
	COM - ST2	10.59	16.03
	COM	7.63	10.01
20 °C	COM - PCE LC	16.03	22.73
	COM - PCE LC - ST2	16.03	21.66
	COM - ST2	3.62	5.53
	COM	3.58	5.21
30 °C	COM - PCE LC	11.01	12.91
	COM - PCE LC - ST2	11.52	13.8
	COM - ST2	2.07	3.08
	COM	2.04	3.15
5 °C	POW - PCE LC	23.52	43.62
	POW - PCE LC - ST2	22.44	50.48
	POW - ST2	6.59	9.24
	POW	5.58	8.99
20 °C	POW - PCE LC	10.02	14.42
	POW - PCE LC - ST2	10.03	15.37
	POW - ST2	3.25	6.41
	POW	2.56	3.67
30 °C	POW - PCE LC	6.51	7.68
	POW - PCE LC - ST2	6.51	8.18
	POW - ST2	1.59	2.60
	POW	1.05	1.46

Table E.3: Initial and final setting times of COM and POW paste tests with medium charge density PCE and ST1.

Temperature	Mixture modification	$t_{ini}$ as average out of three measurements	$t_{fin}$ as average out of three measurements
5 °C	COM - PCE MC	31.57	45.74
	COM - PCE MC - ST1	36.05	55.34
	COM - ST1	11.35	17.76
	COM	9.19	15.27
20 °C	COM - PCE MC	18.04	23.60
	COM - PCE MC - ST1	18.55	25.39
	COM - ST1	4.56	5.82
	COM	3.73	4.71
30 °C	COM - PCE MC	13.02	15.55
	COM - PCE MC - ST1	13.52	16.37
	COM - ST1	2.70	3.72
	COM	2.18	3.10
5 °C	POW - PCE MC	20.56	41.83
	POW - PCE MC - ST1	23.53	41.93
	POW - ST1	7.73	12.41
	POW	7.69	12.05
20 °C	POW - PCE MC	11.40	15.13
	POW - PCE MC - ST1	12.03	15.67
	POW - ST1	2.75	4.01
	POW	3.19	4.62
30 °C	POW - PCE MC	8.51	10.18
	POW - PCE MC - ST1	8.52	10.19
	POW - ST1	1.75	2.58
	POW	1.75	2.67

Table E.4: Initial and final setting times of COM and POW paste tests with medium charge density PCE and ST2.

Temperature	Mixture modification	$t_{ini}$ as average out of three measurements	$t_{fin}$ as average out of three measurements
5 °C	COM - PCE MC	37.32	70.13
	COM - PCE MC - ST2	39.19	71.10
	COM - ST2	9.72	14.02
	COM	9.70	14.39
20 °C	COM - PCE MC	11.55	15.69
	COM - PCE MC - ST2	11.53	16.44
	COM - ST2	2.74	4.13
	COM	2.72	4.07
30 °C	COM - PCE MC	15.02	17.15
	COM - PCE MC - ST2	15.02	17.10
	COM - ST2	2.24	3.24
	COM	2.21	3.13
5 °C	POW - PCE MC	25.05	47.17
	POW - PCE MC - ST2	26.92	48.69
	POW - ST2	7.27	11.34
	POW	8.71	13.14
20 °C	POW - PCE MC	11.55	15.69
	POW - PCE MC - ST2	11.53	16.44
	POW - ST2	2.74	4.13
	POW	2.72	4.07
30 °C	POW - PCE MC	8.51	10.40
	POW - PCE MC - ST2	8.52	10.44
	POW - ST2	1.76	2.60
	POW	1.70	2.62

Table E.5: Initial and final setting times of COM and POW paste tests with high charge density PCE and ST1.

Temperature	Mixture modification	$t_{ini}$ as average out of three measurements	$t_{fin}$ as average out of three measurements
5 °C	COM - PCE HC	30.75	60.92
	COM - PCE HC - ST1	33.11	61.15
	COM - ST1	10.67	15.22
	COM	8.09	12.22
20 °C	COM - PCE HC	13.52	21.85
	COM - PCE HC - ST1	14.02	21.13
	COM - ST1	4.60	7.61
	COM	4.06	5.57
30 °C	COM - PCE HC	9.52	10.70
	COM - PCE HC - ST1	10.04	11.32
	COM - ST1	3.08	4.58
	COM	2.54	4.13
5 °C	POW - PCE HC	19.02	24.98
	POW - PCE HC - ST1	19.02	26.69
	POW - ST1	6.60	9.69
	POW	6.04	7.83
20 °C	POW - PCE HC	8.02	11.28
	POW - PCE HC - ST1	8.01	11.77
	POW - ST1	3.11	4.31
	POW	2.55	4.23
30 °C	POW - PCE HC	5.42	6.79
	POW - PCE HC - ST1	5.01	6.76
	POW - ST1	1.58	2.58
	POW	1.57	3.25

Table E.6: Initial and final setting times of COM and POW paste tests with high charge density PCE and ST2.

Temperature	Mixture modification	$t_{ini}$ as average out of three measurements	$t_{fin}$ as average out of three measurements
5 °C	COM - PCE HC	30.37	50.52
	COM - PCE HC - ST2	28.78	48.84
	COM - ST2	8.10	12.50
	COM	7.10	11.38
20 °C	COM - PCE HC	13.53	19.35
	COM - PCE HC - ST2	13.56	18.34
	COM - ST2	3.61	5.46
	COM	3.55	5.74
30 °C	COM - PCE HC	8.52	11.25
	COM - PCE HC - ST2	8.52	10.11
	COM - ST2	2.59	3.71
	COM	2.57	3.49
5 °C	POW - PCE HC	20.52	29.28
	POW - PCE HC - ST2	19.60	27.95
	POW - ST2	7.59	10.13
	POW	7.04	8.88
20 °C	POW - PCE HC	8.01	11.57
	POW - PCE HC - ST2	7.53	11.47
	POW - ST2	2.55	3.85
	POW	2.57	4.23
30 °C	POW - PCE HC	5.01	6.39
	POW - PCE HC - ST2	5.02	6.18
	POW - ST2	1.58	2.42
	POW	1.57	2.57

## References

- [1] H. Okamura and M. Ouchi, "Self-Compacting Concrete", *Journal of Advanced Concrete Technology*, vol. 1, pp. 5-15, 2003.
- [2] K. Ozawa, K. Maekawa, M. Kunishima, and H. Okamura, "Development of high performance concrete based on the durability design of concrete structures", *The second East-Asia and Pacific Conference on Structural Engineering and Construction*, 1989, pp. pp. 445-450.
- [3] H. Okamura and M. Ouchi, "Self-compacting concrete development, present use and future", *1st International RILEM Symposium on Self-Compacting Concrete*, Stockholm, Sweden, 1999, pp. 3-14.
- [4] S. Nagataki, "Present State of Superplasticizers in Japan", *International Symposium on Mineral and Chemical Admixtures in Concrete*, Toronto, Canada, 1998.
- [5] M. Hunger, "An integral design concept for ecological Self-Compacting Concrete." PhD thesis, Eindhoven, Netherlands: Eindhoven University of Technology, 2010, p. 240.
- [6] Y. Ohama, "Recent progress in concrete-polymer composites", *Advanced Cement Based Materials*, vol. 5, pp. 31-40, 1997.
- [7] M. Collepardi, "A very close precursor of self-compacting concrete " in *CANMET/ACI International Symposium on Sustainable Development and Concrete Technology (Supplementary Volume)*, San Francisco, USA, 2001.
- [8] G. De Schutter, "Towards the Concrete Factory of the Future with SCC", *5th North American Conference on the Design and Use of Self-Consolidating Concrete*, K. Wang, Ed. Chicago, USA, 2013.
- [9] J.C. Walraven, "Self Compacting Concrete: Properties, Development and Code Recommendations", *6th International RILEM Symposium on Self-Compacting Concrete and 4th North American Conference on the Design and Use of SCC*, Montreal, Canada, 2010, pp. 25-44.
- [10] M. Ouchi, "History of development and applications of self-compacting concrete in Japan " in *International Workshop on Self-Compacting Concrete*, Kochi, Japan, 1999, pp. 1-10.
- [11] JSCE, "Recommendation for Self-Compacting Concrete", 1999.
- [12] K. Takada, G.I. Pelova, and J.C. Walraven, "Self-Compacting Concrete Produced by Japanese Method with Dutch Materials", *12th European ready mixed concrete congress ERMCO 98*, Lisbon, Portugal, 1998, pp. 775-785.
- [13] K. P. Takada, G. I.; Walraven, J. C. , "Influence of mixing efficiency on the mixture proportion of general purpose self-compacting concrete", *International Symposium on High-Performance and Reactive Powder Concretes* Sherbrooke, Canada, 1998, pp. 19-39.
- [14] C.A.J. Winter, "Untersuchungen zur Verträglichkeit von Polycarboxylaten mit den Hydratationsverzögerern Citrat und Tartrat und zur Wirkung der Caseinfraktionen  $\alpha$ -,  $\beta$ - und  $\kappa$ - Casein im ternären Bindemittelsystem Portlandzement-Tonerdeschmelzzement-Synthetischer Anhydrit", *Lehrstuhl für Bauchemie der Technischen Universität München*. vol. PhD München: TU-München, 2007.

- [15] H. Uchikawa, D. Sawaki, and S. Hanehara, "Influence of kind and added timing of organic admixture on the composition, structure and property of fresh cement paste", *Cement and Concrete Research*, vol. 25, pp. 353-364, 1995.
- [16] H. Uchikawa, S. Hanehara, and D. Sawaki, "The role of steric repulsive force in the dispersion of cement particles in fresh paste prepared with organic admixture", *Cement and Concrete Research*, vol. 27, pp. 37-50, 1997.
- [17] S. Hanehara and K. Yamada, "Interaction between cement and chemical admixture from the point of cement hydration, absorption behaviour of admixture, and paste rheology", *Cement and Concrete Research*, vol. 29, pp. 1159-1165, 1999.
- [18] K. Yamada, T. Yanagisawa, and S. Hanehara, "Influence of temperature on the dispersibility of polycarboxylate type superplasticizer for highly fluid concrete", *1st International RILEM symposium on Self-Compacting Concrete*, Stockholm, Sweden, 1999, pp. 437-448.
- [19] A. Ohta, T. Sugiyama, and Y. Tanaka, "Fluidizing Mechanism and application of polycarboxylate-based superplasticizers", *5th CANMET/ACI International Conference on Superplasticizers and other chemical Admixtures in Concrete*, Rome, Italy, 1997, pp. 359-378.
- [20] R. Rivera-Villarreal, S. Akman, S. Nagataki, and R. Gagné, "Draft state-of-the-art report on admixtures in high-performance concrete-part 1", *Materials and Structures*, vol. 30, pp. 47-53, 1997.
- [21] C. Jolicoeur and M.-A. Simard, "Chemical admixture-cement interactions: Phenomenology and physico-chemical concepts", *Cement and Concrete Composites*, vol. 20, pp. 87-101, 1998.
- [22] Y.F. Houst, R.J. Flatt, P. Bowen, and H. Hofmann, "Influence of Superplasticizer Adsorption on the Rheology of Cement Paste", *International Symposium on: The Role of Admixtures in High Performance Concrete*, Monterrey, Mexico, 1999, pp. 387-402.
- [23] H. Yammamuro, T. Izumi, and T. Mizunuma, "Study of non-adsorptive viscosity agents applied to self-compacting concrete", *5th CANMET/ACI International Conference on Superplasticizers and other chemical Admixtures in Concrete*, Rome, Italy, 1997, pp. 427-444.
- [24] S. Rols, J. Ambroise, and J. Pera, "Effects of different viscosity agents on the properties of self-leveling concrete", *Cement and Concrete Research*, vol. 29, pp. 261-266, 1999.
- [25] K.H. Khayat, "Viscosity-enhancing admixtures for cement-based materials -- An overview", *Cement and Concrete Composites*, vol. 20, pp. 171-188, 1998.
- [26] M. Grauers, "Rational production and improved working environment through using self compacting concrete", Brite EuRam Contract No. BRPR-CT96-0366", 2000.
- [27] P. Bartos and J.C. Gibbs, "Measurement of properties of fresh self-compacting concrete - Final Report - European Union Growth Contract No. G6RD-CT-2001-00580", 2005.
- [28] bibm, CEMBUREAU, EFCA, EFNARC, and ERMCO, "The European Guidelines for Self-Compacting Concrete - Specification, Production and Use", <http://www.efnarc.org>.
- [29] S. Nagataki, "Keynote lecture: State of the art report on SCC in Japan", *SCC2010: Production and Placement of Self-Consolidating Concrete 2010 Montreal Canada*, 2010.

- [30] P. Gruebl, H. Weigler, and S. Karl, *Beton - Arten, Herstellung und Eigenschaften*, 2 ed. Munich, Germany: Ernst & Sohn, 2001.
- [31] DAfStb-Richtlinie, "Selbstverdichtender Beton (SVB-Richtlinie)", 2003.
- [32] M. Hunger and H.J.H. Brouwers, "Flow analysis of water-powder mixtures: Application to specific surface area and shape factor", *Cement and Concrete Composites*, vol. 31, pp. 39-59, 2009.
- [33] DAfStb-Richtlinie, "Selbstverdichtender Beton (SVB-Richtlinie) - Schlusssentwurf", 2012.
- [34] F. Cussigh, M. Sonebi, and G. De Schutter, "Project testing SCC-segregation test methods", *3rd International Symposium on Self-Compacting Concrete*, Reykjavik, Iceland, 2003, pp. 311-322.
- [35] N. Roussel, "The LCPC BOX: a cheap and simple technique for yield stress measurements of SCC", *Materials and Structures*, vol. 40, pp. 889-896, 2007.
- [36] R. Le Roy and N. Roussel, "The marsh cone as a viscometer: Theoretical analysis and practical limits", *Materials and Structures*, vol. 38, pp. 25-30, 2005.
- [37] V.H. Nguyen, S. Rémond, J.L. Gallias, J.P. Bigas, and P. Muller, "Flow of Herschel-Bulkley fluids through the Marsh cone", *Journal of Non-Newtonian Fluid Mechanics*, vol. 139, pp. 128-134, 2006.
- [38] N. Roussel and R. Le Roy, "The Marsh cone: a test or a rheological apparatus?", *Cement and Concrete Research*, vol. 35, pp. 823-830, 2005.
- [39] T. Shindoh and Y. Matsuoka, "Development of Combination-Type Self-Compacting Concrete and Evaluation Test Methods", *Journal of Advanced Concrete Technology*, vol. 1, pp. 26-36, 2003.
- [40] S. Kordts, "Herstellung und Steuerung der Verarbeitbarkeitseigenschaften selbstverdichtender Betone", *Fakultät VI – Bauingenieurwesen und angewandte Geowissenschaften*. vol. Dr.-Ing. Berlin: Technischen Universität Berlin, 2005, p. 191.
- [41] M. Collepardi and M. Valente, "Recent development in self-compacting concrete in Europe", *SCC'2005-China: 1st International Symposium on Design, Performance and Use of Self-Consolidating Concrete*, 2005, pp. 217-227.
- [42] N. Su and B. Miao, "A new method for the mix design of medium strength flowing concrete with low cement content", *Cement and Concrete Composites*, vol. 25, pp. 215-222, 2003.
- [43] F. Mueller and O.H. Wallevik, "Effect of Limestone Filler Addition in Eco-SCC", *6th International RILEM Symposium on Self-Compacting Concrete and 4th North American Conference on the Design and Use of SCC*. vol. 2, K. H. Khayat and D. Feys, Eds. Montreal, 2010, pp. 107-116.
- [44] P.L. Domone, "Self-compacting concrete: An analysis of 11 years of case studies", *Cement and Concrete Composites*, vol. 28, pp. 197-208, 2006.
- [45] O.H. Wallevik and J.E. Wallevik, "Rheology as a tool in concrete science: The use of rheographs and workability boxes", *Cement and Concrete Research*, vol. 41, pp. 1279-1288, 2011.
- [46] ERMCO, "Ready-Mixed Concrete Industry Statistics - Year 2010", 2011.

- [47] H.J.H. Brouwers and H.J. Radix, "Self-Compacting Concrete: Theoretical and experimental study", *Cement and Concrete Research*, vol. 35, pp. 2116-2136, 2005.
- [48] S. Nunes, H. Figueiras, P. Milheiro Oliveira, J. S. Coutinho, and J. Figueiras, "A methodology to assess robustness of SCC mixtures", *Cement and Concrete Research*, vol. 36, pp. 2115-2122, 2006.
- [49] R. Vogel, "Stabilität und Fließverhalten von Selbstverdichtendem Beton", *16th International Conference on Building Materials - ibausil*, Weimar, Germany, 2006, pp. 147-158.
- [50] D. Lowke, "Sedimentationsverhalten & Robustheit Selbstverdichtender Betone - Optimierung auf Basis der Modellierung interpartikulärer Wechselwirkungen", *DAfStb Doktorandensymposium 2010*, Kaiserslautern, Germany, 2010.
- [51] H.-C. Kühne and W. Schmidt, "Der Siebtrennversuch nach prEN 12350-11", *beton*, vol. 57, pp. 448-454, 2007.
- [52] M. Schneider, M. Romer, M. Tschudin, and H. Bolio, "Sustainable cement production - present and future", *Cement and Concrete Research*, vol. 41, pp. 642-650, 2011.
- [53] F. de Larrard and T. Sedran, "Mixture-proportioning of high-performance concrete", *Cement and Concrete Research*, vol. 32, pp. 1699-1704, 2002.
- [54] Z. Toutou and N. Roussel, "Multi Scale Experimental Study of Concrete Rheology: From Water Scale to Gravel Scale", *Materials and Structures*, vol. 39, pp. 189-199, 2006.
- [55] K.H. Khayat, N. Petrov, J. Assaad, R. Morin, and M. Thibault, "Performance of SCC Used in the Repair of Retaining Wall Elements " in *SCC 2005*, 2005, pp. 1003-1013.
- [56] O.H. Wallevik, S. Kubens, and F. Mueller, "Influence of cement-admixture interaction on the stability of production properties of SCC", *5th International RILEM Symposium on Self-Compacting Concrete*, Ghent, Belgium, 2007, pp. 211-216.
- [57] S. Kubens, "Interaction of cement and admixtures and its influence on rheological properties", *F.A. Finger Institut für Baustoffkunde*. vol. PhD Weimar, Germany: Bauhaus Universität Weimar, 2010.
- [58] M. Y. A. Mollah, W. J. Adams, R. Schennach, and D. L. Cocke, "A review of cement-superplasticizer interactions and their models", *Advances in Cement Research*, vol. 12, pp. 153-161, 2000.
- [59] K. Yamada, T. Takahashi, S. Hanehara, and M. Matsuhisa, "Effects of the chemical structure on the properties of polycarboxylate-type superplasticizer", *Cement and Concrete Research*, vol. 30, pp. 197-207, 2000.
- [60] K. Yamada, S. Ogawa, and S. Hanehara, "Controlling of the adsorption and dispersing force of polycarboxylate-type superplasticizer by sulfate ion concentration in aqueous phase", *Cement and Concrete Research*, vol. 31, pp. 375-383, 2001.
- [61] R.J. Flatt and Y.F. Houst, "A simplified view on chemical effects perturbing the action of superplasticizers", *Cement and Concrete Research*, vol. 31, pp. 1169-1176, 2001.
- [62] R. Flatt, "Towards a prediction of superplasticized concrete rheology", *Materials and Structures*, vol. 37, pp. 289-300, 2004.

- [63] J. Plank and B. Sachsenhauser, "Impact of Molecular Structure on Zeta Potential and Adsorbed Conformation of  $\alpha$ -Allyl- $\omega$ -Methoxypolyethylene Glycol - Maleic Anhydride Superplasticizers", *Journal of Advanced Concrete Technology*, vol. 4, pp. 233-239, 2006.
- [64] B. Lothenbach, F. Winnefeld, and R. Figi, "The influence of superplasticizers on the hydration of Portland cement", *12th International Congress on the Chemistry of Cement*, Montreal, Canada, 2007.
- [65] F. Winnefeld, S. Becker, J. Pakusch, and T. Gotz, "Effects of the molecular architecture of comb-shaped superplasticizers on their performance in cementitious systems", *Cement and Concrete Composites*, vol. 29, pp. 251-262, 2007.
- [66] I. Schober and R.J. Flatt, "Optimizing Polycarboxylate Polymers", *8th CANMET/ACI International Conference on Superplasticizers and other chemical Admixtures in Concrete*, Sorrento, Italy, 2006, pp. 169-184.
- [67] I. Schober and R.J. Flatt, "Optimierung von Polycarboxylat-Ether Polymeren", *16th International Conference on Building Materials - ibausil*, Weimar, Germany, 2006, pp. 93-100.
- [68] K. Yamada, "Basics of analytical methods used for the investigation of interaction mechanism between cements and superplasticizers", *Cement and Concrete Research*, vol. 41, pp. 793-798, 2011.
- [69] K. Yamada, "A Summary of Important Characteristics of Cement and Superplasticizers", *Ninth ACI International Conference on Superplasticizers and Other Chemical Admixtures in Concrete*, Seville, Spain, 2009, pp. 85-96.
- [70] J. Terpstra, "Stabilizing self-levelling concrete with polysaccharide additive", *SCC'2005-China: 1st International Symposium on Design, Performance and Use of Self-Consolidating Concrete*, 2005, pp. 207-213.
- [71] D. Hamada, T. Hamai, M. Shimoda, M. Shonaka, and H. Takahashi, "Development of New Superplasticizer Providing Ultimate Workability", *8th CANMET/ACI International Conference on Superplasticizers and other chemical Admixtures in Concrete*, Sorrento, Italy, 2006, pp. 31-50.
- [72] W. Brameshuber and S. Uebachs, "The influence of the temperature on the rheological properties of self-compacting concrete", *3rd International RILEM Symposium on Self-Compacting Concrete*, Reykjavik, Iceland, 2003, pp. 174-183.
- [73] V. Kossobokov, J.-L. Le Mouél, and V. Courtillot, "A statistically significant signature of multi-decadal solar activity changes in atmospheric temperatures at three European stations", *Journal of Atmospheric and Solar-Terrestrial Physics*, vol. 72, pp. 595-606, 2010.
- [74] K.H. Khayat, N. Petrov, R. Morin, M. Thibeault, and B. Bissonnette, "Comportement du béton autoplaçant fibré dans la réfection du passage inférieur du Viaduc Jarry-Querbes à Montréal", *8<sup>e</sup> Journées Scientifiques du (RF)<sup>2</sup>B*, Montreal, 2007, pp. 32-47.
- [75] D.A. Robinson, D.J. Leathers, M.A. Palecki, and K.F. Dewey, "Some observations on climate variability as seen in daily temperature structure", *Atmospheric Research*, vol. 37, pp. 119-131, 1995.
- [76] S.N. Seo, "An analysis of public adaptation to climate change using agricultural water schemes in South America", *Ecological Economics*, vol. 70, pp. 825-834, 2011.

- [77] N. Saigusa, S. Yamamoto, R. Hirata, Y. Ohtani, R. Ide, J. Asanuma, M. Gamo, T. Hirano, H. Kondo, Y. Kosugi, S.-G. Li, Y. Nakai, K. Takagi, M. Tani, and H. Wang, "Temporal and spatial variations in the seasonal patterns of CO<sub>2</sub> flux in boreal, temperate, and tropical forests in East Asia", *Agricultural and Forest Meteorology*, vol. 148, pp. 700-713, 2008.
- [78] SenStadtUm, "Digitaler Umweltatlas Berlin", Senatsverwaltung für Stadtentwicklung und Umweltschutz Berlin, 2001, p. [http://www.stadtentwicklung.berlin.de/umwelt/umweltatlas/da404\\_01.htm#Abb2](http://www.stadtentwicklung.berlin.de/umwelt/umweltatlas/da404_01.htm#Abb2).
- [79] K. Scrivener, "The Microstructure of Concrete", *Materials Science of Concrete*, pp. 127-161, 1989.
- [80] F.W. Locher, W. Richartz, and S. Sprung, "Erstarren von Zement. Teil I: Reaktion und Gefügeentwicklung", *Zement-Kalk-Gips International*, pp. 435-442, 1976.
- [81] W. Chen, "Hydration of slag cement - Theory, Modeling and Application", Enschede: University of Twente, 2006.
- [82] H.F.W. Taylor, "Hydration of Portland Cement", *Cement Chemistry, 2nd Edition*, T. Telford, Ed.: Thomas Telford Publishing, 1997, pp. 187-224.
- [83] E.M. Gartner, S. Sabio, and J.-P. Perez, "Equilibria in the System Calcium Hydroxide-Calcium Sulphate-Alkali Sulphate-Water at 5-30°C, and their Relevance to Portland Cement Hydration in the Presence of Superplasticizers", *11th International Congress on the Chemistry of Cement*, Durban, South Africa, 2003, pp. 635-644.
- [84] C. Jolicoeur, J. Sharmann, N. Otis, A. Lebel, M.A. Simard, and M. Pagè, "The Influence of Temperature on the Rheological properties of Superplasticized Cement Pastes", *5th CANMET/ACI International Conference on Superplasticizers and Other Chemical Admixtures in Concrete*, Rome, Italy, 1997, pp. 379-391.
- [85] J. Plank, G. Bassioni, Z. Dai, H. Keller, B. Sachsenhauser, and N. Zouaoui, "Neues zur Wechselwirkung zwischen Zementen und Polycarboxylat-Fließmitteln", *16th International Conference on Building Materials - ibausil*, Weimar, Germany, 2006, pp. 579-598.
- [86] F. Göller, S. Dikty, and D. Hamada, "The Relationship between Retention Stability and Chemical Structure of PCE", *Ninth ACI International Conference on Superplasticizers and Other Chemical Admixtures in Concrete*, Seville, Spain, 2009, pp. 249-260.
- [87] J. Plank and C. Hirsch, "Impact of zeta potential of early cement hydration phases on superplasticizer adsorption", *Cement and Concrete Research*, vol. 37, pp. 537-542, 2007.
- [88] VDZ, "Kompendium Zement und Beton", Duesseldorf 2002.
- [89] K.L. Scrivener and A. Nonat, "Hydration of cementitious materials, present and future", *Cement and Concrete Research*, vol. 41, pp. 651-665, 2011.
- [90] J.W. Bullard and R.J. Flatt, "New Insights Into the Effect of Calcium Hydroxide Precipitation on the Kinetics of Tricalcium Silicate Hydration", *Journal of the American Ceramic Society*, vol. 93, pp. 1894-1903, 2010.
- [91] J.W. Bullard, H.M. Jennings, R.A. Livingston, A. Nonat, G.W. Scherer, J.S. Schweitzer, K.L. Scrivener, and J. J. Thomas, "Mechanisms of cement hydration", *Cement and Concrete Research*, vol. 41, pp. 1208-1223, 2011.

- [92] J.G.M. de Jong, H.N. Stein, and J.M. Stevels, "Hydration of tricalcium silicate", *Journal of Applied Chemistry*, vol. 17, pp. 246-250, 1967.
- [93] H.N. Stein and J.M. Stevels, "Influence of silica on the hydration of  $3\text{CaO},\text{SiO}_2$ ", *Journal of Applied Chemistry*, vol. 14, pp. 338-346, 1964.
- [94] E.M. Gartner and H.M. Jennings, "Thermodynamics of Calcium Silicate Hydrates and Their Solutions", *Journal of the American Ceramic Society*, vol. 70, pp. 743-749, 1987.
- [95] F. Bellmann, D. Damidot, B. Moeser, and J. Skibsted, "Improved evidence for the existence of an intermediate phase during hydration of tricalcium silicate", *Cement and Concrete Research*, vol. 40, pp. 875-884, 2010.
- [96] F. Bellmann, T. Sowoidnich, and B. Möser, "Formation of an intermediate phase and influence of crystallographic defects on dissolution of C3S", *13th International Congress on the Chemistry of Cement*, Madrid, 2011.
- [97] H.M. Jennings and P.L. Pratt, "An experimental argument for the existence of a protective membrane surrounding portland cement during the induction period", *Cement and Concrete Research*, vol. 9, pp. 501-506, 1979.
- [98] S. Garrault-Gauffinet and A. Nonat, "Experimental investigation of calcium silicate hydrate (C-S-H) nucleation", *Journal of Crystal Growth*, vol. 200, pp. 565-574, 1999.
- [99] P. Juilland, E. Gallucci, R. Flatt, and K. Scrivener, "Dissolution theory applied to the induction period in alite hydration", *Cement and Concrete Research*, vol. 40, pp. 831-844, 2010.
- [100] E.M. Gartner, "Discussion of the paper "Dissolution theory applied to the induction period in alite hydration" by P. Juilland et al., *Cem. Concr. Res.* 40 (2010) 831-844", *Cement and Concrete Research*, vol. 41, pp. 560-562, 2011.
- [101] P. Juilland, E. Gallucci, R.J. Flatt, and K.L. Scrivener, "Reply to the discussion by E. Gartner of the paper 'Dissolution theory applied to the induction period in alite hydration'", *Cement and Concrete Research*, vol. 41, pp. 563-564, 2011.
- [102] J.M. Makar, J.J. Beaudoin, T. Sato, R. Alizadeh, and L. Raki, "Discussion of 'Dissolution theory applied to the induction period in alite hydration'", *Cement and Concrete Research*, vol. 41, pp. 565-567, 2011.
- [103] J.M. Makar and G.W. Chan, "End of the Induction Period in Ordinary Portland Cement as Examined by High-Resolution Scanning Electron Microscopy", *Journal of the American Ceramic Society*, vol. 91, pp. 1292-1299, 2008.
- [104] P. Juilland, E. Gallucci, R.J. Flatt, and K.L. Scrivener, "Reply to the discussion by J. Makar, J.J. Beaudoin, T. Sato, R. Alizadeh and L. Raki of 'Dissolution theory applied to the induction period in alite hydration'", *Cement and Concrete Research*, vol. 41, pp. 568-569, 2011.
- [105] S. Chatterji and J.W. Jeffery, "Studies of Early Stages of Paste Hydration of Different Types of Portland Cements", *Journal of the American Ceramic Society*, vol. 46, pp. 268-273, 1963.
- [106] H.E. Schwiete and E.M.G. Niël, "Formation of Ettringite Immediately After Gaging of a Portland Cement", *Journal of the American Ceramic Society*, vol. 48, pp. 12-14, 1965.
- [107] F.W. Locher, W. Richartz, and S. Sprung, "Erstarren von Zement Teil II: Einfluss des Calciumsulfatzusatzes", *Zement-Kalk-Gips International*, pp. 271-277, 1980.

- [108] F.W. Locher, W. Richartz, S. Sprung, and H.-M. Sylla, "Erstarren von Zement. Teil III: Einfluss der Klinkerherstellung", *Zement-Kalk-Gips International*, pp. 669-676, 1982.
- [109] F.W. Locher, W. Richartz, S. Sprung, and W. Rechenberg, "Erstarren von Zement. Teil IV: Einfluss der Lösungszusammensetzung", *Zement-Kalk-Gips International*, pp. 224-231, 1983.
- [110] M.C. Schlegel, "In-situ Untersuchungen an zementgebundenen Baustoffen mittels röntgenographischer Verfahren", Berlin, Germany: Humboldt University Berlin, 2013.
- [111] M.C. Schlegel, A. Sarfraz, U. Mueller, U. Panne, and F. Emmerling, "First Seconds in a Building's Life - An in-situ SyXRD Study on the ms-Scale", vol. 51, pp. 4993-4996, 2012.
- [112] H. Minard, S. Garrault, L. Regnaud, and A. Nonat, "Mechanisms and parameters controlling the tricalcium aluminate reactivity in the presence of gypsum", *Cement and Concrete Research*, vol. 37, pp. 1418-1426, 2007.
- [113] W. Lerch, "The Influence of Gypsum on the Hydration and properties of Portland Cement Pastes", American Society for Testing Materials, Philadelphia, USA 1946.
- [114] P.J. Sandberg, C. Portneuve, F. Serafin, J. Boomer, N. Loconte, V. Gupta, B. Dragovic, F. Doncaster, L. Alioto, and T. Vogt, "Effect of Admixture on Cement Hydration Kinetics by Synchrotron XRD and Isothermal Calorimetry", *12th International Congress on the chemistry of cement*, Montreal, Canada, 2007.
- [115] L. Wadsö, "Applications of an eight-channel isothermal conduction calorimeter for cement hydration studies", *CEMENT INTERNATIONAL*, pp. 94-101 2005.
- [116] P.L. Pratt and A. Ghose, "Electron microscope studies of Portland cement microstructures during setting and hardening", *Philosophical Transactions of the Royal Society of London*, London, United Kingdom, 1983, pp. 93-103.
- [117] J.A.N. Skalny and M.E. Tadros, "Retardation of Tricalcium Aluminate Hydration by Sulfates", *Journal of the American Ceramic Society*, vol. 60, pp. 174-175, 1977.
- [118] B. Lothenbach and F. Winnefeld, "Thermodynamic modelling of the hydration of Portland cement", *Cement and Concrete Research*, vol. 36, pp. 209-226, 2006.
- [119] B. Lothenbach, G. Le Saout, E. Gallucci, and K. Scrivener, "Influence of limestone on the hydration of Portland cements", *Cement and Concrete Research*, vol. 38, pp. 848-860, 2008.
- [120] M.M. Costoya Fernandez, "Effect of Particle Size on the Hydration Kinetics and Microstructural Development of Tricalcium Silicate", *Faculté Sciences et Techniques de l'Ingénieur, Laboratoire des Matériaux de Construction* Lausanne, Switzerland: École Polytechnique Fédérale de Lausanne, 2008.
- [121] F. Winnefeld and L. Holzer, "Monitoring early Cement Hydration by rheological Measurements", *11th International Congress on the Chemistry of Cement*, Durban, South Africa, 2003, pp. 330-340.
- [122] J. Weiss, "6.1 Experimental Determination of the 'Time-Zero'  $t_0$  (Maturity-Zero  $M_0$ )", *Early Age Cracking in Cementitious Systems - report of RILEM TC 181-EAS: Early age shrinkage induced stresses and cracking in cementitious systems*, A. Bentur, Ed.
- [123] W. Schmidt, P. Ramge, and H.-C. Kuehne, "Effect of the storage conditions of cement on the processing and hardening properties of concrete", *Concrete Plant + Precast Technology*, vol. 06, pp. 10-17, 2009.

- [124] W. Schmidt, H.J.H. Brouwers, H.-C. Kühne, and B. Meng, "Effects of Superplasticizer and Viscosity-Modifying Agent on Fresh Concrete Performance of SCC at Varied Ambient Temperatures", *Design, Production and Placement of Self-Consolidating Concrete - Proceedings of SCC2010, Montreal, Canada, September 26-29, 2010*, K.H. Khayat and D. Feys, Eds.: Springer, 2010, pp. 65-77.
- [125] W. Chen, "Hydration of Slag Cement - Theory, Modelling and Application.", PhD thesis, Enschede: University of Twente, 2007.
- [126] R. Ylmén, U. Jäglid, B.-M. Steenari, and I. Panas, "Early hydration and setting of Portland cement monitored by IR, SEM and Vicat techniques", *Cement and Concrete Research*, vol. 39, pp. 433-439, 2009.
- [127] S. Amziane, "Setting time determination of cementitious materials based on measurements of the hydraulic pressure variations", *Cement and Concrete Research*, vol. 36, pp. 295-304, 2006.
- [128] W. Schmidt, "Möglichkeiten zur Steuerung der Robustheit von selbstverdichtendem Beton gegenüber veränderlichen Umgebungstemperaturen", *DAfStb Doktorandensymposium 2010 - 51. Forschungskolloquium*, Kaiserslautern, Deutschland, 2010, pp. 527-538.
- [129] W. Schmidt and H.-C. Kühne, "Wechselwirkungen zwischen Zusatzmitteln und mineralischen Komponenten in selbstverdichtendem Beton beim Betonieren in unterschiedlichen Temperaturen", *Betonwerk international : BWI*, vol. 2, pp. 32-38, 2009.
- [130] W. Schmidt and H.-C. Kuehne, "Influence of the processing temperature on the properties of SCC in the presence of superplasticizer and other admixtures " *Concrete Plant + Precast Technology*, pp. 40-49, 2007.
- [131] W. Schmidt, H.-C. Kuehne, and B. Meng, "Temperature related effects on self-consolidating concrete due to interactions between superplasticizers, supplemental admixtures and additions", *9th ACI International Conference on Superplasticizers and Other Chemical Admixtures - Supplementary Papers*, Seville, Spain, 2009, pp. 135-147.
- [132] T.C. Powers, "Structure and Physical Properties of Hardened Portland Cement Paste", *Journal of the American Ceramic Society*, vol. 41, pp. 1-6, 1958.
- [133] S. Eppers, "Assessing the autogenous shrinkage cracking propensity of concrete by means of the restrained ring test", *Fakultät Bauingenieurwesen*. vol. PhD Dresden: Technischen Universität Dresden, 2010, p. 184.
- [134] P. Lura, "Autogenous Deformation and Internal Curing of Concrete", Delft, Netherlands: TU Delft, 2003.
- [135] G. Sant, P. Lura, and J. Weiss, "A discussion of analysis approaches for determining 'time-zero' from chemical shrinkage and autogenous strain measurements in cement paste", *International RILEM Conference on Volume Changes of Hardening Concrete: Testing and Mitigation*, Lyngby, Denmark, 2006, pp. 375-383.
- [136] P. Fontana, "Einfluss der Mischungszusammensetzung auf die frühen autogenen Verformungen der Bindemittelmatrix von Hochleistungsbetonen", *Fakultät Architektur, Bauingenieurwesen und Umweltwissenschaften* vol. PhD Braunschweig, Germany: Technische Universität Carolo-Wilhelmina zu Braunschweig, 2006.

- [137] A.B. Eberhardt and J.P. Kaufmann, "Schwindreduzierter Selbstverdichtender Beton", *16th International Conference on Building Materials - ibausil*, Weimar, Germany, 2006, pp. 117-124.
- [138] G. Sant, C.F. Ferraris, and J. Weiss, "Rheological properties of cement pastes: A discussion of structure formation and mechanical property development", *Cement and Concrete Research*, vol. 38, pp. 1286-1296, 2008.
- [139] M.R. Geiker, "Measurements of Chemical Shrinkage and a Systematic Evaluation of hydration Curves by means of the Dispersion Model", *Institute of Mineral Industry*. vol. Ph.D. Lyngby: Technical University of Denmark, 1983, pp. Knudsen, T.
- [140] J. Zhang, E.A. Weissinger, S. Peethamparan, and G.W. Scherer, "Early hydration and setting of oil well cement", *Cement and Concrete Research*, vol. 40, pp. 1023-1033, 2010.
- [141] H.A. Barnes, "The yield stress - a review or 'panta roi' - everything flows?", *Journal of Non-Newtonian Fluid Mechanics*, vol. 81, pp. 133-178, 1999.
- [142] E.C. Bingham, *Fluidity and Plasticity*, 1. ed. New York: Mcgraw-Hill Book Company, Inc., 1922.
- [143] E.C. Bingham, "Discussion on Plasticity", *Journal of the American Ceramic Society*, vol. 7, pp. 375-379, 1924.
- [144] E. Bingham and J. Robertson, "Eine Methode zur gleichzeitigen Messung von Plastizität und Elastizität", *Colloid & Polymer Science*, vol. 47, pp. 1-5, 1929.
- [145] W. Ostwald, "Ueber die Geschwindigkeitsfunktion der Viskosität disperser Systeme. I", *Colloid & Polymer Science*, vol. 36, pp. 99-117, 1925.
- [146] W. Ostwald, "Ueber die Geschwindigkeitsfunktion der Viskosität disperser Systeme. II", *Colloid & Polymer Science*, vol. 36, pp. 157-167, 1925.
- [147] W.H. Herschel and R. Bulkeley, "Konsistenzmessungen von Gummi-Benzollösungen", *Kolloid Zeitschrift*, vol. 39, pp. 291-300, 1926.
- [148] O. Wallevik, "Rheology – A New Dimension in Concrete Technology", *16th International Conference on Building Materials - ibausil*, Weimar, Germany, 2006, pp. 1417-1430.
- [149] G. Lemieux, S.-D. Hwang, and K.H. Khayat, "Effect of Plastic Viscosity and Static Stability on Uniformity of Self-Consolidating Concrete Elements", *6th International RILEM Symposium on Self-Compacting Concrete and 4th North American Conference on the Design and Use of SCC*. vol. 2, K.H. Khayat and D. Feys, Eds. Montreal, 2010, pp. 655-662.
- [150] W. Schmidt, H.-C. Kuehne, D. Rosignoli, and B. Meng, "Development and application of a novel ready-made compound including additions and admixtures for the easy production of SCC", *Concrete Plant + Precast Technology*, pp. 4-11, 2008.
- [151] J. Rickert and J. Herrmann, "Zemente mit mehreren Hauptbestandteilen - Wechselwirkungen mit PCE-Fließmitteln", *vdz Fachtagung "Betontechnik"* Düsseldorf: vdz, 2011.
- [152] W. Schmidt, "MICROCON - Report on Workpackage 6: Dry mixed binder compound for Self-compacting concrete - Approval Tests (confidential)", BAM Bundesanstalt für Materialforschung und -prüfung 2007.

- [153] P. Ramge and L. Lohaus, "Robustness by Mix Design – A New Approach for Mixture Proportioning of SCC", *Design, Production and Placement of Self-Consolidating Concrete*. vol. 1: Springer Netherlands, 2010, pp. 37-49.
- [154] P. Ramge, H.-C. Kuehne, and B. Meng, "MODINSYS - Modular systems for the protection and repair of concrete structures", *13th International Congress on Polymers in Concrete* Madeira Island, 2010.
- [155] N. Spiratos, M. Pagé, N.P. Mailvaganam, V.M. Malhotra, and C. Jolicoeur, *Superplasticizers for Concrete - Fundamentals, Technology, and Practice*. Ottawa, Canada: Supplementary Cementing Materials for Sustainable Development, 2003.
- [156] J. Plank, "Applications of biopolymers and other biotechnological products in building materials", *Applied Microbiology and Biotechnology*, vol. 66, pp. 1-9, 2004.
- [157] C. Giraudeau, J.-B. D'Espinose De Lacaillerie, Z. Souguir, A. Nonat, and R.J. Flatt, "Surface and Intercalation Chemistry of Polycarboxylate Copolymers in Cementitious Systems", *Journal of the American Ceramic Society*, vol. 92, pp. 2471-2488, 2009.
- [158] S.M. Lahallh, M. Absl-Halabi, and A.M. Ali, "Effect of polymerization conditions of sulfonated-melamine formaldehyde superplasticizers on concrete", *Cement and Concrete Research*, vol. 18, pp. 513-531, 1988.
- [159] M. Collepardi and M. Valente, "Recent Developments in Superplasticizers", *8th CANMET/ACI International Conference on Superplasticizers and other chemical Admixtures in Concrete*, Sorrento, Italy, 2006, pp. 1-14.
- [160] M.F. Magarotto R., Zeminian N., Albrecht G., Flakus S., "Polycarboxylate Superplasticizers to Ensure Workability Retention and Durability", *ICCC 13th International Congress on the Chemistry of Cement*, Madrid, Spain, 2011.
- [161] L. Zevnik, "Rheology of SCC mortar with different superplasticizer - Introduction to polyphosphonic superplasticizer", *21. Workshop und Kolloquium "Rheologische Messungen an Baustoffen"* Regensburg, Germany, 2012.
- [162] M. Bellotto, "On the origin of cement setting, and how to control the properties of the fresh and hardened material.", *International Congress on Materials & Structural Stability*, A. Diouri, Ed. Rabat, Morocco, 2013.
- [163] I. Odler, R. Schönfeld, and H. Dörr, "On the combined effect of water soluble lignosulfonates and carbonates on portland cement and clinker pastes - II. Mode of action and structure of the hydration products", *Cement and Concrete Research*, vol. 8, pp. 525-538, 1978.
- [164] G. Spanka, H. Grube, and G. Thielen, "Wirkungsmechanismen verflüssigender Betonzusatzmittel", *beton*, pp. 802-808, 1995.
- [165] K. Yamada and S. Hanehara, "Working Mechanism of Polycarboxylate Superplasticizer Considering the Chemical Structure and Cement Characteristics", *11th International Congress on the Chemistry of Cement*, Durban, South Africa, 2003, pp. 538-549.
- [166] J. Plank, B. Sachsenhauser, and J. de Reese, "Experimental determination of the thermodynamic parameters affecting the adsorption behaviour and dispersion effectiveness of PCE superplasticizers", *Cement and Concrete Research*, vol. 40, pp. 699-709, 2010.

- [167] M. Daimon and D.M. Roy, "Rheological properties of cement mixes: I. Methods, preliminary experiments, and adsorption studies", *Cement and Concrete Research*, vol. 8, pp. 753-764, 1978.
- [168] J. Plank, Z. Dai, N. Zouaoui, and D. Vlad, "Intercalation of Polycarboxylate Superplasticizers into C<sub>3</sub>A Hydrate Phases", *8th CANMET/ACI International Conference on Superplasticizers and other chemical Admixtures in Concrete*, Sorrento, Italy, 2006, pp. 201-214.
- [169] J. Plank, H. Keller, and B. Yu, "Conditions Determining the Formation of Organo-Mineral Phases in Concrete", *Ninth ACI International Conference on Superplasticizers and Other Chemical Admixtures in Concrete - Supplementary Papers*, Seville, Spain, 2009, pp. 235-257.
- [170] S. Ng and J. Plank, "Formation of Organo-Mineral Phases Incorporating PCE Superplasticizers During Early Hydration of Calcium Aluminate Cement", *ICCC 13th International Congress on the Chemistry of Cement*, Madrid, Spain, 2011.
- [171] J. Plank and B. Sachsenhauser, "Experimental Determination of the Thermodynamic Parameters Affecting the Adsorption Behavior and Dispersion Effectiveness of PCE-Superplasticizers", *Ninth ACI International Conference on Superplasticizers and Other Chemical Admixtures in Concrete - Supplementary Papers*, Seville, Spain, 2009, pp. 87-103.
- [172] J. Björnström and S. Chandra, "Effect of superplasticizers on the rheological properties of cements", *Materials and Structures*, vol. 36, pp. 685-692, 2003.
- [173] M. Daimon and D.M. Roy, "Rheological properties of cement mixes: II. Zeta potential and preliminary viscosity studies", *Cement and Concrete Research*, vol. 9, pp. 103-109, 1979.
- [174] P.F.G. Banfill, "A discussion of the papers "rheological properties of cement mixes" by M. Daimon and D.M. Roy", *Cement and Concrete Research*, vol. 9, pp. 795-796, 1979.
- [175] G. Li, T.-H.A., and P.C. Aïtcin, "Improving Cement-Superplasticizer Compatibility by Using Soluble Alkalis as a Chemical Additive in Concrete", *11th International Congress on the Chemistry of Cement*, Durban, South Africa, 2003, pp. 655-666.
- [176] K. Yoshioka, E.-I. Tazawa, K. Kawai, and T. Enohata, "Adsorption characteristics of superplasticizers on cement component minerals", *Cement and Concrete Research*, vol. 32, pp. 1507-1513, 2002.
- [177] L. Nachbaur, P.-C. Nkinamubanzi, A. Nonat, and J.-C. Mutin, "Electrokinetic Properties which Control the Coagulation of Silicate Cement Suspensions during Early Age Hydration", *Journal of Colloid and Interface Science*, vol. 202, pp. 261-268, 1998.
- [178] H. Viallis-Terrisse, A. Nonat, and J.-C. Petit, "Zeta-Potential Study of Calcium Silicate Hydrates Interacting with Alkaline Cations", *Journal of Colloid and Interface Science*, vol. 244, pp. 58-65, 2001.
- [179] E. Sakai, K. Yamada, and A. Ohta, "Molecular Structure and Dispersion-Adsorption Mechanisms of Comb-Type Superplasticizers Used in Japan", *Journal of Advanced Concrete Technology*, vol. 1, pp. 16-25, 2003.
- [180] J. Plank and C. Winter, "Competitive adsorption between superplasticizer and retarder molecules on mineral binder surface", *Cement and Concrete Research*, vol. 38, pp. 599-605, 2008.

- [181] C. Roessler, B. Moeser, and J. Stark, "Influence of Superplasticizers on C<sub>3</sub>A Hydration and Ettringite Growth in Cement Paste", *12th International Congress on the Chemistry of Cement*, Montreal, Canada, 2007.
- [182] C. Roessler and T. Sowoidnich, "Influence of Superplasticizer on Long term Variation in C<sub>3</sub>A Hydration and Formation of AFm Phases - Effects on Durability", *ICCC 13th International Congress on the Chemistry of Cement*, Madrid, Spain, 2011.
- [183] C. Roessler, A. Eberhardt, H. Kucerová, and B. Moeser, "Influence of Hydration on the Fluidity of Normal Portland Cement Pastes", *12th International Congress on the Chemistry of Cement*, Montreal, Canada, 2007.
- [184] C. Roessler, "Hydratation von C<sub>3</sub>S und Portlandzement in Gegenwart von Fließmitteln", *16th International Conference on Building Materials - ibausil*, Weimar, Germany, 2006, pp. 569-578.
- [185] J. Plank, D. Zhimin, H. Keller, F. v. Hössle, and W. Seidl, "Fundamental mechanisms for polycarboxylate intercalation into C<sub>3</sub>A hydrate phases and the role of sulfate present in cement", *Cement and Concrete Research*, vol. 40, pp. 45-57, 2010.
- [186] J. Plank, Z. Dai, and N. Zouaoui, "Novel hybrid materials obtained by intercalation of organic comb polymers into Ca-Al-LDH", *Journal of Physics and Chemistry of Solids*, vol. 69, pp. 1048-1051, 2006.
- [187] N. Zouaoui, M. Lesti, R. Sieber, and J. Plank, "Zur Wechselwirkung zwischen PCE-Fließmitteln und Mikrosilika", *Jahrestagung der Fachgruppe Bauchemie*, Siegen, 2007, pp. 313-320.
- [188] J. Plank, A. Habbaba, and R. Sieber, "Wechselwirkung von Polycarboxylat-basierten Fließmitteln mit Hüttensandmehlen", *Internationale Baustofftagung - IBAUSIL, 2009*, Weimar, 2009.
- [189] J. Herrmann and J. Rickert, "Wechselwirkungen zwischen Hüttensand bzw. Kalkstein als Zementhauptbestandteil und Fließmitteln auf der Basis von Polycarboxylatether", *DAfStb Doktorandensymposium 2010*, Kaiserslautern, 2010, pp. 613-623.
- [190] C.M. Kok and A. Rudin, "Relationship between the Hydrodynamic Radius and the Radius of Gyration of a Polymer in Solution", *Die Makromolekulare Chemie, Rapid Communications*, vol. 2, pp. 655-659, 1981.
- [191] B.B. Weiner, "What Is Particle Size?", Holtville, USA 2010.
- [192] H. Uchikawa and S. Hanehara, "Effect of electrostatic and steric repulsive force of organic admixture on the dispersion of cement particles in fresh cement paste", *10th International Congress on the Chemistry of Cement*, Gothenburg, Sweden, 1997.
- [193] H. Keller and J. Plank, "Zusammenhang zwischen Intercalation und Wirkung von Polycarboxylat-Fließmittel bei früher und später Zugabe", *Jahrestagung der Fachgruppe Bauchemie*, Siegen, 2007, pp. 69-77.
- [194] C. Gay and E. Raphael, "Comb-like polymers inside nanoscale pores", *Advances in Colloid and Interface Science*, vol. 94, pp. 229-236, 2001.
- [195] K. Pistol, C. Prinz, F. Weise, P. Klobes, and P. Ramge, "Strukturveränderungen in Selbstverdichtendem Beton (SVB) infolge Hochtemperaturbeanspruchung " in *XV. Workshop über die Charakterisierung von feinteiligen und porösen Festkörpern*, Bad Soden 2011.

- [196] K. Pistol, "Strukturorientierte Analyse des thermomechanischen Verhaltens von selbstverdichtendem Beton - Internal Report " BAM Federal Institute for Materials Research and Testing, Berlin, Germany 2010.
- [197] K. Vasilic, H.-C. Kuehne, B. Meng, and N. Roussel, "Modelling of fresh SCC flow through reinforced sections", 52. *DAfStb-Forschungskolloquium*, Berlin, Germany, 2011.
- [198] H.F.W. Taylor, "Modification of the Bogue calculation", *Advances in Cement Research*, vol. 2, pp. 73-77, 1989.
- [199] J. Terpstra, "Stabilizing low-viscous self-compacting concrete " in *2nd North American Conference on the Design and Use of Self-Consolidating Concrete (SCC) and 4th International RILEM Symposium on Self-Compacting Concrete*, Chicago, 2005, pp. 47-53.
- [200] H. Simonides and J. Terpstra, "Use of innovative starch ethers for paving blocks and other concrete products", *Concrete Plant + Precast Technology*, pp. 38-45, 2007.
- [201] A. Phyfferoen, H. Monty, B. Skaggs, N. Sakata, S. Yanai, and M. Yoshizaki, "Evaluation of the biopolymer, Diutan gum, for use in self-compacting concrete", *First North American Conference on the Design and Use of Self-Consolidating Concrete*, 2002, pp. 141-146.
- [202] M. Sonebi, "Rheological characterization of cement-based materials pastes containing Diutan Gum and limestone powder", *12th International Congress on the Chemistry of Cement*, Montreal, Canada, 2007.
- [203] M. Sonebi, "Rheological properties of grouts with viscosity modifying agents as diutan gum and welan gum incorporating pulverised fly ash", *Cement and Concrete Research*, vol. 36, pp. 1609-1618, 2006.
- [204] W. Schmidt, H.J.H. Brouwers, H.-C. Kuehne, and B. Meng, "Influence of Environmental Temperatures on the Performance of Polymeric Stabilising Agent in Fresh Cementitious Materials", *Key Engineering Materials*, vol. 466, pp. 97-104, 2011.
- [205] H. Okamura and K. Ozawa, "Mix Design for self-compacting concrete", *Concrete Library of JSCE*, pp. 107-120, 1995.
- [206] S. Kordts and H. Grube, "Steuerung der Verarbeitbarkeitseigenschaften von selbstverdichtendem Beton als Transportbeton.", *beton*, vol. 52, pp. 217-223, 2002.
- [207] *Selbstverdichtender Beton*. Düsseldorf, Germany: Verlag Bau + Technik, 2004.
- [208] D. Niekamp, "Untersuchungen zur Beurteilung des Verarbeitungsbereiches von selbstverdichtenden Betonen", Diploma Thesis, Berlin, Germany: Technische Fachhochschule zu Berlin, 2006, p. 187.
- [209] H. Kuosa, W. Schmidt, and P. Dessy, "Interim Report to the FP6 Project MICROCON - WP3: Mix design", 2006.
- [210] H. Kuosa, M. Sarkkinen, W. Schmidt, P. Dessy, H. Miller, I.H.B. Miller, V. Vimmr, and T. Vimmr, "Interim Report to the FP6 Project MICROCON - WP2: Base Product Analysis", 2006.
- [211] J.E. Funk and D.R. Dinger, *Predictive Process Control of Crowded Particulate Suspensions - Applied to Ceramic Manufacturing*. Boston, USA: Kluwer Academic Publishers., 1994.

- [212] A.H.M. Andreasen, "Ueber die Beziehung zwischen Kornabstufung und Zwischenraum in Produkten aus losen Körnern (mit einigen Experimenten)", *Kolloid-Zeitschrift*, vol. 50, pp. 217-228, 1930.
- [213] S.A.A.M. Fennis, "Design of Ecological Concrete by Particle Packing Optimization." PhD thesis, Delft, Netherlands: Technische Universiteit Delft, 2011.
- [214] G. Hüsken, "A Multifunctional Design Approach for Sustainable Concrete - With Application to Concrete Mass Products." PhD thesis, Eindhoven, Netherlands: Technische Universiteit Eindhoven, 2010.
- [215] N. Roussel, C. Stefani, and R. Leroy, "From mini-cone test to Abrams cone test: measurement of cement-based materials yield stress using slump tests", *Cement and Concrete Research*, vol. 35, pp. 817-822, 2005.
- [216] T.L.H. Nguyen, N. Roussel, and P. Coussot, "Correlation between L-box test and rheological parameters of a homogeneous yield stress fluid", *Cement and Concrete Research*, vol. 36, pp. 1789-1796, 2006.
- [217] C. Ferraris, "Concrete Rheology: What is it and why do we need it?", *SCC'2005-China: 1st International Symposium on Design, Performance and Use of Self-Consolidating Concrete*, 2005, pp. 229-236.
- [218] E.P. Koehler and D.W. Fowler, "Summary of Concrete Workability Test Methods", International Center for Aggregates Research, Austin, Texas 2003.
- [219] "ConTec Rheometer-4SCC - Operating manual", O.H. Wallevik, Ed.
- [220] R.J. Flatt, D. Larosa, and N. Roussel, "Linking yield stress measurements: Spread test versus Viskomat", *Cement and Concrete Research*, vol. 36, pp. 99-109, 2006.
- [221] L. Frunz, D. Lootens, R. J. Flatt, F. Wombacher, and U. Velten, "Smart Polycarboxylate Design for SCC in Precast Applications", *Design, Production and Placement of Self-Consolidating Concrete*. vol. 1: Springer Netherlands, 2010, pp. 53-63.
- [222] R. Vogel, "Eine Messzelle für Spezialmörtel", Vogel-Labor, Weimar 2007.
- [223] R. Vogel, "A measuring cell for special mortars", *Concrete Plant + Precast Technology*, pp. 124-126, 2008.
- [224] C. Ancey, "Solving the Couette inverse problem using a wavelet-vaguelette decomposition", *Journal of Rheology*, vol. 49, pp. 441-460, 2005.
- [225] A. Gavrus, E. Massoni, and L. Chenot, "Constitutive parameter identification using a Computer-Aided Rheology approach", *International Conference on Numerical Methods in Industrial Forming Processes*, Ithaca, 1995, pp. 563-568.
- [226] G. Heirman, R. Hendrickx, L. Vandewalle, D. Van Gemert, D. Feys, G. De Schutter, B. Desmet, and J. Vantomme, "Integration approach of the Couette inverse problem of powder type self-compacting concrete in a wide-gap concentric cylinder rheometer: Part II. Influence of mineral additions and chemical admixtures on the shear thickening flow behaviour", *Cement and Concrete Research*, vol. 39, pp. 171-181, 2009.
- [227] R. Vogel, "A stability criterion for self-compacting concrete (SCC)", *Concrete Plant + Precast Technology*, pp. 42-49, 2005.

- [228] K. Vasilic, W. Schmidt, H.-C. Kühne, and B. Meng, "Experimental and numerical studies on calibration of a rotational rheometer for cementitious materials", *17. Internationale Baustofftagung - ibausil*, Weimar, 2009, pp. 1.1135-1.1140.
- [229] G. Heirman, L. Vandewalle, D. Van Gemert, and O. Wallevik, "Integration approach of the Couette inverse problem of powder type self-compacting concrete in a wide-gap concentric cylinder rheometer", *Journal of Non-Newtonian Fluid Mechanics*, vol. In Press, Corrected Proof.
- [230] R. Vogel, "Eine Messzelle für Fluide und Spezialmörtel - Einsatzgebiete und Messergebnisse " in *16. Kolloquium und Workshop "Rheologische Messungen an mineralischen Baustoffen"* Regensburg, 2007.
- [231] C.F. McKenna, "Hardness of Plasters and Cements, and a Simple Chronographic Apparatus for Recording Set", *Journal of Industrial and Engineering Chemistry*, vol. 4, pp. 110-114, 1912.
- [232] S. Eppers, "Autogene Schwindrissneigung richtig messen", *vdz Fachtagung "Betontechnik"* Düsseldorf, 2011.
- [233] W. Puntke, "Wasseranspruch von feinen Kornhaufwerken", *beton*, vol. 2002, pp. 242-248, 2002.
- [234] I. Marquardt, "Determination of the composition of self-compacting concretes on the basis of the water requirements of the constituent materials - presentation of a new mix concept", *Betonwerk + Fertigteiltechnik*, pp. 22 – 30, 2002.
- [235] A.F. Hollemann and E. Wiberg, *Lehrbuch der Anorganischen Chemie. 101. Auflage. Von Nils Wiberg. Walter de Gruyter, Berlin/New York, 1995. 2033 S., geb. 158.00 DM. ISBN 3-11-012641-9* vol. 101. Berlin/New York: Walter de Gruyter, 1995.
- [236] M. Heunisch, M. Hoepfner, R. Pierson, F. Dehn, and M. Orgass, "Selbstverdichtender Beton (SVB) im Straßentunnelbau", Bergisch Gladbach, August 2008 2008.
- [237] J. Roncero, R. Gettu, E. Vazquez, and J.M. Torrents, "Effect of superplasticizer content and temperature on the fluidity and setting on cement pastes", *International Symposium on: The Role of Admixtures in High Performance Concrete*, Monterrey, Mexico, 1999, pp. 343-356.
- [238] ASTM C 939-87, "Standard test method for flow of grout for preplaced-aggregate concrete (flow cone method)", ASTM, 1991.
- [239] W. Brameshuber, S. Uebachs, and F. Spoerel, "Selbstverdichtender Beton - Temperatureinflüsse und Schalungsdruck bei Frischbeton, Verformungseigenschaften bei Festbeton", *Forschungskolloquium des Deutschen Beton- und Bautechnikvereins*, Darmstadt, 2004, pp. 214-219.
- [240] H.G. Svavarsson and O.H. Wallevik, *Geothermal well cementing: the effect of temperature and time on workability loss* vol. 12. Reykjavik, Iceland, 2004.
- [241] J.-Y. Petit, K.H. Khayat, and E. Wirquin, "Coupled effect of time and temperature on variations of yield value of highly flowable mortar", *Cement and Concrete Research*, vol. 36, pp. 832-841, 2006.
- [242] J.-Y. Petit, E. Wirquin, and B. Duthoit, "Influence of temperature on yield value of highly flowable micromortars made with sulfonate-based superplasticizers", *Cement and Concrete Research*, vol. 35, pp. 256-266, 2005.

- [243] J.-Y. Petit, E. Wirquin, Y. Vanhove, and K. Khayat, "Yield stress and viscosity equations for mortars and self-consolidating concrete", *Cement and Concrete Research*, vol. 37, pp. 655-670, 2007.
- [244] J.Y. Petit, "Effet de la temperature, des superplastifiants et des ajouts sur les variations rheologiques des micromortiers et betons auto-compactants", *Faculté de génie, Département génie civil, Université de Sherbrooke and Faculté des sciences appliquées, Filière génie civil, Université d'Artois*. vol. PhD Sherbrooke, Canada: Université de Sherbrooke and Université d'Artois, 2005.
- [245] J.-Y. Petit, E. Wirquin, and K.H. Khayat, "Effect of temperature on the rheology of flowable mortars", *Cement and Concrete Composites*, vol. 32, pp. 43-53, 2010.
- [246] V. Fernandez-Altable and I. Casanova, "Influence of mixing sequence and superplasticiser dosage on the rheological response of cement pastes at different temperatures", *Cement and Concrete Research*, vol. 36, pp. 1222-1230, 2006.
- [247] M. Nehdi and S. Al Martini, "Estimating time and temperature dependent yield stress of cement paste using oscillatory rheology and genetic algorithms", *Cement and Concrete Research*, vol. 39, pp. 1007-1016, 2009.
- [248] W. Schmidt, H.-C. Kuehne, and B. Meng, "Performance and interactions of admixtures for SCC exposed to different climatic conditions", *Concrete under Severe Conditions: Environment & Loading*, Tours, France, 2007, pp. 979-986.
- [249] H.-C. Kuehne, W. Schmidt, and B. Meng, "The influence of temperature on self-compacting concrete in presence of superplasticizer and additional admixtures", *5th International RILEM Symposium on Self-Compacting Concrete*, Ghent, Belgium, 2007, pp. 405-410.
- [250] W. Schmidt and H.-C. Kühne, "Einfluss der Verarbeitungstemperatur auf die Eigenschaften von SVB bei Verwendung von Fließmittel und weiteren Zusatzmitteln", *Betonwerk + Fertigteil-Technik*, pp. 40-49, 2007.
- [251] L. Lohaus and H. Hoeveling, "Robustimprovement für Selbstverdichtenden Beton (SVB)", *15th International Konferenz on Building Materials - ibausil*, Weimar, Germany, 2003, pp. 177-187.
- [252] J. Assaad and K.H. Khayat, "Effect of casting rate and concrete temperature on formwork pressure of self-consolidating concrete", *Materials and Structures*, vol. 39, pp. 333-341, 2006.
- [253] J. Golaszewski and G. Cygan, "Einfluss der Temperatur auf die Verarbeitbarkeit selbstverdichtender Betonmischungen", *BWI - Betonwerk International*, pp. 40 -46, 2009.
- [254] S. Weisheit, D. Waldmann, and M. Greger, "Influence of Environmental Conditions on the Rheological Properties of SCC", *6th International RILEM Symposium on Self-Compacting Concrete and 4th North American Conference on the Design and Use of SCC*, 2010, pp. 453-460.
- [255] S. Al-Martini and M. Nehdi, "Rheology of Superplasticized Cement Paste and Concrete Subjected to High Temperature and Prolonged Mixing Time", *6th International RILEM Symposium on Self-Compacting Concrete and 4th North American Conference on the Design and Use of SCC*, Montreal, Canada, 2010, pp. 461-469.

- [256] N. Ghafoori and H. Diawara, "Influence of temperature on fresh performance of self-consolidating concrete", *Construction and Building Materials*, vol. 24, pp. 946-955, 2010.
- [257] F. Winnefeld, A. Zingg, L. Holzer, J. Pakusch, and S. Becker, "Ettringite-Superplasticizer Interaction and its Impact on the Ettringite Distribution in Cement Suspensions", *Ninth ACI International Conference on Superplasticizers and Other Chemical Admixtures and Tenth ACI International Conference on Recent Advances in Concrete Technology and Sustainability Issues*, Seville, Spain, 2009, pp. 420.1-420-17.
- [258] I. Schober and U. Mäder, "Selecting the optimum HRWR for SCC", *2nd North American Conference on the Design and Use of Self-Consolidating Concrete (SCC) and 4th International RILEM Symposium on Self-Compacting Concrete*, Chicago, 2005, pp. 39-45.
- [259] S. Hanehara and K. Yamada, "Rheology and early age properties of cement systems", *Cement and Concrete Research*, vol. 38, pp. 175-195, 2008.
- [260] H. Fujita, K. Haga, M. Shibata, and M. Mihara, "Concentration and Molecular Weight of Superplasticizer Contained in Pore Solution Extracted from Hardened Cement Pastes", *Journal of Advanced Concrete Technology*, vol. 6, pp. 389-395, 2008.
- [261] J. Pourchez, A. Peschard, P. Grosseau, R. Guyonnet, B. Guilhot, and F. Vallee, "HPMC and HEMC influence on cement hydration", *Cement and Concrete Research*, vol. 36, pp. 288-294, 2006.
- [262] T. Izumi, S. Dikty, and H. Yamamuro, "Properties of New Polysaccharide as a Thickener for Concrete", *8th CANMET/ACI International Conference on Superplasticizers and other chemical Admixtures in Concrete*, Sorrento, Italy, 2006, pp. 105-116.
- [263] J. Pourchez, A. Govin, P. Grosseau, R. Guyonnet, B. Guilhot, and B. Ruot, "Alkaline stability of cellulose ethers and impact of their degradation products on cement hydration", *Cement and Concrete Research*, vol. 36, pp. 1252-1256, 2006.
- [264] A. Zingg, F. Winnefeld, L. Holzer, J. Pakusch, S. Becker, R. Figi, and L. Gauckler, "Interaction of polycarboxylate-based superplasticizers with cements containing different C3A amounts", *Cement and Concrete Composites*, vol. 31, pp. 153-162, 2009.
- [265] J.J.M. Swinkels, "Composition and Properties of Commercial Native Starches", *Starch - Stärke*, vol. 37, pp. 1-5, 1985.
- [266] C. Brumaud, R. Baumann, M. Schmitz, and N. Roussel, "Influence Of High Molar Mass Polymers On The Rheological Behavior Of Fresh Cement Pastes", *ICCC 13th International Congress on the Chemistry of Cement*, Madrid, Spain, 2011.
- [267] B. Fugmann and A. Lützen, "Cellulose (RD-03-00833)", *Thieme RÖMPP Online*: Copyright © 2012 Georg Thieme Verlag, 2012.
- [268] H. Bessaies, R. Baumann, and N. Roussel, "Consequences of competitive adsorption between polymers on the rheological behaviour of cement pastes", *Fifth North American Conference on the Design and Use of Self-Consolidating Concrete*, Chicago, Illinois, 2013.
- [269] J. Hot and N. Roussel, "How adsorbing polymers decrease the macroscopic viscosity of concentrated cement pastes?", *Fifth North American Conference on the Design and Use of Self-Consolidating Concrete*, Chicago, USA, 2013.

- [270] M. Palacios, R. Flatt, F. Puertas, and A. Sanchez-Herencia, "Compatibility between Polycarboxylate and Viscosity-Modifying Admixtures in Cement Pastes", *10th International Conference on Superplasticizers and Other Admixtures in Concrete*, Prague, Czech Republic, 2012, pp. 29-40.
- [271] J.N. BeMiller and K.C. Huber, "Starch", *Ullmann's Encyclopedia of Industrial Chemistry*: Wiley-VCH Verlag GmbH & Co. KGaA, 2000.
- [272] A. Lützen and V. Lander, "Amylose (RD-01-02289)", *Thieme RÖMPP Online*: Copyright © 2012 Georg Thieme Verlag, 2012.
- [273] W. Burchard, "Light Scattering from Polysaccharides", *Polysaccharides - Structural diversity and functional versatility, second edition*, 2 ed, S. Dumitriu, Ed.: Marcel Dekker, New York, 2005, 2005, pp. 189-237.
- [274] A. Bechthold and J. Seibel, "Stärke (RD-19-03654)", *Thieme RÖMPP Online*: Copyright © 2012 Georg Thieme Verlag, 2012.
- [275] V. Lander, "Amylopektin (RD-16-03559)", *Thieme RÖMPP Online*: Copyright © 2012 Georg Thieme Verlag, 2012.
- [276] R. Coleman, Y. Patel, and N. Harding, "Identification and organization of genes for diutan polysaccharide synthesis from *Sphingomonas* sp. ATCC 53159", *Journal of Industrial Microbiology & Biotechnology*, vol. 35, pp. 263-274, 2008.
- [277] K.S. Kang and W.H. McNeely, "Polysaccharide and bacterial fermentation process for its preparation", *US Patent Publication (Source: DOCDB)*, International: C12D 13/04 ed USA: KELCO CO 1973, p. 14.
- [278] F. Freitas, V.D. Alves, and M.A.M. Reis, "Advances in bacterial exopolysaccharides: from production to biotechnological applications", *Trends in Biotechnology*, vol. 29, pp. 388-398, 2011.
- [279] M. Sonebi and D. McKendry, "Effect of Mix Proportions on Rheological and Hardened Properties of Composite Cement Pastes", *The Open Construction and Building Technology Journal*, pp. 15-23, 2008.
- [280] K.H. Khayat and A. Ghezal, "Effect of viscosity-modifying admixture-superplasticizer combination on flow properties of scc equivalent mortar", *3rd International RILEM Symposium on Self-Compacting Concrete*, Reykjavik, Iceland, 2003, pp. 369-385.
- [281] V. Rajayogan, M. Santhanam, and B. S. Sarma, "Evaluation of hydroxy propyl starch as a viscosity-modifying agent for self compacting concrete", *3rd International RILEM Symposium on Self-Compacting Concrete*, Reykjavik, Iceland, 2003, pp. 386-394.
- [282] J.N. Israelachvili, *Intermolecular and Surface Forces*, 3 ed. Burlington: Academic Press, 2011.
- [283] A. Phyfferoen and C.B. Skaggs, "Optimizing the use of welan gum in cementitious and gypsum-based systems", *ConChem - International Exhibition & Conference*, Duesseldorf, Germany, 1997, pp. 193-202.
- [284] A. Izaguirre, J. Lanás, and J. I. Álvarez, "Behaviour of a starch as a viscosity modifier for aerial lime-based mortars", *Carbohydrate Polymers*, vol. 80, pp. 222-228, 2010.
- [285] W. Schmidt, "Einfluss der Polymerstruktur von Stabilisierern auf die Rheologie von selbst-verdichtendem Beton und Mörtel " in *20. Workshop und Kolloquium Rheologische Messungen an Baustoffen*, Regensburg, Germany, 2011.

- [286] *Handbook of Chemistry and Physics*, 65 ed.: CRC Press, 1984.
- [287] W. Schmidt, J. Brouwers, H.-C. Kühne, and B. Meng, "Effects of Superplasticizer and Viscosity-Modifying Agent on Fresh Concrete Performance of SCC at Varied Ambient Temperatures", *Design, Production and Placement of Self-Consolidating Concrete*. vol. 1: Springer Netherlands, 2010, pp. 65-77.
- [288] W. Schmidt, "Influence of the processing temperature and combined admixtures on the properties of Self-Compacting Concrete", *7th International PhD Symposium in Civil Engineering*, Stuttgart, 2008, pp. 75-84.
- [289] S. Pourchet, C. Comparet, L. Nicoleau, and A. Nonat, "Influence of PC superplasticizers on tricalcium silicate hydration", *12th International Congress on the Chemistry of Cement*, Montreal, Canada, 2007.
- [290] A. Zingg, "Cement-superplasticizer interaction - link between macroscopic phenomena and microstructural data of the early cement hydration by Anatol Zingg". vol. Doctor of Natural Science Zuerich: ETH Zuerich, 2008, p. 150.
- [291] U. Mueller, B. Meng, W. Österle, and A. Gardei, "Characterization of Granulated Blast Furnace Slag by Means of the Combined Application of the FIB/TEM Technique", *16th International Conference on Building Materials - ibausil*, Weimar, Germany, 2006, pp. 198-196.
- [292] Y. Luan, T. Ishida, T. Nawa, and T. Sagawa, "Enhanced model and simulation of hydration process of blast furnace slag in blended cement", *Journal of Advanced Concrete Technology*, vol. 10, pp. 1-13, 2012.
- [293] D.P. Bentz and C.F. Ferraris, "Rheology and setting of high volume fly ash mixtures", *Cement and Concrete Composites*, vol. 32, pp. 265-270, 2010.
- [294] B. Craeye, G. De Schutter, B. Desmet, J. Vantomme, G. Heirman, L. Vandewalle, Ö. Cizer, S. Aggoun, and E.H. Kadri, "Effect of mineral filler type on autogenous shrinkage of self-compacting concrete", *Cement and Concrete Research*, vol. 40, pp. 908-913, 2010.
- [295] K.W.B.W. Langan, M.A. Ward,, "Effect of silica fume and fly ash on heat of hydration of Portland cement", *Cement and Concrete Research*, vol. 32, pp. 1045-1051, 2002.
- [296] J. Zelić, D. Rušić, D. Veža, and R. Krstulović, "The role of silicafume in the kinetics and mechanisms during the early stage of cement hydration", *Cement and Concrete Research*, vol. 30, pp. 1655-1662, 2000.
- [297] O.S.B. Al-Amoudi, M. Maslehuddin, M. Shameem, and M. Ibrahim, "Shrinkage of plain and silicafume cement concrete under hot weather", *Cement and Concrete Research*, vol. 29, pp. 690-699, 2006.
- [298] T. Østnor, K. De Weerd, H. Justnes, and Ø. Bjøntegaard, "Reactivity and Microstructure of Ternary Cement Pastes", *ICCC 13th International Congress on the Chemistry of Cement*, Madrid, Spain, 2011.
- [299] D. Damidot, B. Lothenbach, D. Herfort, and F.P. Glasser, "Thermodynamics and cement science", *Cement and Concrete Research*, vol. 41, pp. 679-695, 2011.
- [300] K. De Weerd and H. Justnes, "The effect of limestone powder additions on strength and microstructure of fly ash blended cements", *ICCC 13th International Congress on the Chemistry of Cement*, Madrid, Spain, 2011.

- [301] V.S. Ramachandran, "Thermal analyses of cement components hydrated in the presence of calcium carbonate", *Thermochimica Acta*, vol. 127, pp. 385-394, 1988.
- [302] J. Stark and B. Gathemann, "Hochleistungscompound – Optimierte Bindemittel für selbstverdichtenden Beton", *48th BetonTage*, 2004, pp. 14-16.
- [303] J. Pera, S. Husson, and B. Guilhot, "Influence of finely ground limestone on cement hydration", *Cement and Concrete Composites*, vol. 21, pp. 99-105, 1999.
- [304] G. Ye, X. Liu, G. De Schutter, A.M. Poppe, and L. Taerwe, "Influence of limestone powder used as filler in SCC on hydration and microstructure of cement pastes", *Cement and Concrete Composites*, vol. 29, pp. 94-102, 2007.
- [305] N. Voglis, G. Kakali, E. Chaniotakis, and S. Tsvilis, "Portland-limestone cements. Their properties and hydration compared to those of other composite cements", *Cement and Concrete Composites*, vol. 27, pp. 191-196, 2005.
- [306] T. Vuk, V. Tinta, R. Gabrovsek, and V. Kaucic, "The effects of limestone addition, clinker type and fineness on properties of Portland cement", *Cement and Concrete Research*, vol. 31, pp. 135-139, 2001.
- [307] C. Hesse, M. Degenkolb, P. Gäberlein, F. Götz-Neunhoeffler, M. Kutschera, J. Neubauer, and V. Schwarz, "In-situ XRD-Untersuchungen zur Hydratation von Zementpasten bei verschiedenen Temperaturen und Wasser-Zement-Werten", *Jahrestagung der Fachgruppe Bauchemie*, Siegen, 2007, pp. 213-220.
- [308] V. Baroghel-Bouny, P. Mounanga, A. Khelidj, A. Loukili, and N. Rafai, "Autogenous deformations of cement pastes: Part II. W/C effects, micro-macro correlations, and threshold values", *Cement and Concrete Research*, vol. 36, pp. 123-136, 2006.
- [309] M. Heikal, M. S. Morsy, and I. Aiad, "Effect of treatment temperature on the early hydration characteristics of superplasticized silica fume blended cement pastes", *Cement and Concrete Research*, vol. 35, pp. 680-687, 2005.
- [310] D. Sohn and D.L. Johnson, "Hardening process of cement-based materials monitored by the instrumented penetration test: Part 1: Neat cement paste and mortar", *Cement and Concrete Research*, vol. 32, pp. 557-563, 2002.
- [311] F. Ridi, L. Dei, E. Fratini, S.-H. Chen, and P. Baglioni, "Hydration Kinetics of Tri-calcium Silicate in the Presence of Superplasticizers", *Journal of Physical Chemistry B*, vol. 107, pp. 1056-1061, 2003.
- [312] E. Fratini, F. Ridi, S.-H. Chen, and P. Baglioni, "Hydration water and microstructure in calcium silicate and aluminate hydrates", *Journal of Physics: Condensed Matter*, vol. 18, pp. 2467-2483, 2006.
- [313] T. Ke-feng and J. Nichols, "Performances of concrete under elevated curing temperature", *Journal of Wuhan University of Technology--Materials Science Edition*, vol. 19, pp. 65-67, 2004.
- [314] A. Zingg, L. Holzer, A. Kaech, F. Winnefeld, J. Pakusch, S. Becker, and L. Gauckler, "The microstructure of dispersed and non-dispersed fresh cement pastes - New insight by cryo-microscopy", *Cement and Concrete Research*, vol. 38, pp. 522-529, 2008.
- [315] J. Minet, N. Lequeux, and P. Boch, "A New Approach for the Organic-Inorganic C-S-H", *11th International Congress on the Chemistry of Cement*, Durban, South Africa, 2003, pp. 629-634.

- [316] S. Pourchet, C. Comparet, A. Nonat, and P. Maitresse, "Influence of Three Types of Superplasticizers on Tricalciumaluminate Hydration in Presence of Gypsum", *8th CANMET/ACI International Conference on Superplasticizers and other chemical Admixtures in Concrete*, Sorrento, Italy, 2006, pp. 151-168.
- [317] J. Rieger, J. Thieme, and C. Schmidt, "Study of Precipitation Reactions by X-ray Microscopy: CaCO<sub>3</sub> Precipitation and the Effect of Polycarboxylates", *Langmuir*, vol. 16, pp. 8300-8305, 2000.
- [318] F. Winnefeld, A. Zingg, L. Holzer, R. Figi, J. Pakusch, and S. Becker, "Interaction of Polycarboxylate-based Superplasticizers and Cements: Influence of Polymer Structure and C3A-content of Cement", *12th International Congress on the Chemistry of Cement*, Montreal, Canada, 2007.
- [319] T. Sowoidnich and C. Rößler, "The Influence of Superplasticizers on the Dissolution of C<sub>3</sub>S", *Ninth ACI International Conference on Superplasticizers and Other Chemical Admixtures in Concrete*, Seville, Spain, 2009, pp. 335-346.
- [320] W. Michaelis, "Ueber den Portland-Cement", *Journal für Praktische Chemie*, vol. 100, pp. 257-303, 1867.
- [321] L. Nachbaur, J.C. Mutin, A. Nonat, and L. Choplin, "Dynamic mode rheology of cement and tricalcium silicate pastes from mixing to setting", *Cement and Concrete Research*, vol. 31, pp. 183-192, 2001.
- [322] H. Sleiman, A. Perrot, and S. Amziane, "A new look at the measurement of cementitious paste setting by Vicat test", *Cement and Concrete Research*, vol. 40, pp. 681-686, 2010.
- [323] A. Zingg, L. Holzer, F. Winnefeld, B. Münch, J. Pakusch, P. Uribe-Arocha, S. Becker, A. Käch, and L. Gauckler, "Einfluss von Fließmitteln auf die Nukleation von Hydratphasen und auf die Partikelstruktur frischer Zementpasten", *Jahrestagung der Fachgruppe Bauchemie*, Siegen, 2007, pp. 55-62.
- [324] A. Peschard, A. Govin, P. Grosseau, B. Guilhot, and R. Guyonnet, "Effect of polysaccharides on the hydration of cement paste at early ages", *Cement and Concrete Research*, vol. 34, pp. 2153-2158, 2004.
- [325] D.A. Silva and P.J.M. Monteiro, "The influence of polymers on the hydration of portland cement phases analyzed by soft X-ray transmission microscopy", *Cement and Concrete Research*, vol. 36, pp. 1501-1507, 2006.
- [326] A. Leemann and F. Winnefeld, "The effect of viscosity modifying agents on mortar and concrete", *Cement and Concrete Composites*, vol. 29, pp. 341-349, 2007.
- [327] W. Schmidt, H.J.H. Brouwers, H.-C. Kuehne, and B. Meng, "Influence of Temperature on Stabilizing Agents in Presence of Superplasticizers", *Tenth International Conference on Superplasticizers and Other Chemical Admixtures in Concrete*, Prague, Czech Republic, 2012.
- [328] J. Seibel, "Dextrine (RD-04-00906)", *Thieme RÖMPP Online*: Copyright © 2013 Georg Thieme Verlag, 2013.
- [329] W. Schmidt, H.J.H. Brouwers, H.-C. Kuehne, and B. Meng, "Influence of ambient temperature conditions on the effect of stabilising polymers in cementitious building materials", *13th International Congress on Polymers in Concrete- ICPIC 2010 Madeira*, Portugal, 2010, pp. 241-249.

- [330] W. Schmidt, "Challenges of the African Environmental Conditions for Concrete Mixture Composition", *Workshop Cement and Concrete for Africa*, Berlin, Germany, 2011, pp. 37-49.
- [331] W. Schmidt, H.C. Kühne, H.C. Uzoegbo, and N.S. Msinjili, "Building practice and Concrete Infrastructure Development in Eastern and Southern Africa", *Concrete Plant International*, vol. 2011, pp. 32-37, 2011.
- [332] W. Schmidt, N.S. Msinjili, H.-C. Kuehne, M.V.A. Florea, G.S. Kumaran, and P. Nibasumba, "Robustness improvement of fresh concrete and mortar performance for challenging casting environments with focus on sub-Saharan Africa", *3rd International Conference on Concrete Repair, Rehabilitation and Retrofitting*, Cape Town, South Africa, 2012.
- [333] W. Schmidt, A. Radlińska, C. Nmai, A. Buregyeya, W.L. Lai, and S. Kou, "Why does Africa need African concrete? An observation of concrete in Europe, America, and Asia – and conclusions for Africa", *International Conference on Advances in Cement and Concrete Technology in Africa*, Johannesburg, South Africa, 2013, pp. 1139-1148.
- [334] W. Schmidt, N.S. Msinjili, and H.-C. Kühne, "Rheological Optimisation for Flowable Mixture Compositions Specified for African Boundary Conditions", *International Conference on Advances in Cement and Concrete Technology in Africa*, Johannesburg, South Africa, 2013, pp. 359-366.



## Publications by the author

### Journals (peer reviewed)

W. Schmidt, H.J.H. Brouwers, H.-C. Kuehne, and B. Meng, “Influence of Environmental Temperatures on the Performance of Polymeric Stabilising Agent in Fresh Cementitious Materials“, *Key Engineering Materials*, vol. 466, pp. 97-104, 2011.

W. Schmidt, N.N.M. Hirya, D. Bjegovic, H.C. Uzoegbo, and S.G. Kumaran, “Cement technology in sub-Saharan Africa—Practical and scientific experiences“, *American Ceramic Society Bulletin* vol. 91, p. 82, 2012.

W. Schmidt, H.J.H. Brouwers, H.-C. Kühne, and B. Meng, “Optimierung der Robustheit von selbstverdichtendem Beton - Robustness optimisation of self-compacting concrete regarding temperature effects“, *Beton- und Stahlbetonbau*, vol. 108, pp. 13-21, 2013.

W. Schmidt, H.J.H. Brouwers, H.-C. Kühne, and B. Meng, “The working mechanism of starch and diutan gum in cementitious and limestone dispersions in presence of polycarboxylate ether superplasticizers“, *Applied Rheology*, vol. 23, pp. 52903-1 – 52903 – 12, 2013.

W. Schmidt, H.J.H. Brouwers, H.-C. Kühne, and B. Meng, “Influences of the superplasticizer modification and the mixture composition on the performance of self-compacting concrete at varying ambient temperatures“, *Cement and Concrete Composites*, 2014.

W. Schmidt, H.J.H. Brouwers, H.-C. Kuehne, and B. Meng, “Effects of the Characteristics of High range Water Reducing Agents and the Water to Powder Ratio on Rheological and Setting Behavior of Self-Consolidating Concrete“, *Adv. in Civil Engineering Materials*, vol. 3, 2014.

M. Sonebi, W. Schmidt, J. Khatib, “Influence of the type of viscosity-modifying admixtures and metakaolin on the rheology of grouts“, *Chemistry and Materials Res.*, vol. 5, pp. 106-111, 2013.

W. Schmidt, M. Sonebi, H.J.H. Brouwers, H.-C. Kühne, B. Meng, “Rheology Modifying Admixtures: The Key to Innovation in Concrete Technology – A General Overview and Implications for Africa, *Chemistry and Materials Res.*, vol. 5, pp. 115-120, 2013.

W. Schmidt, Ch. Lehmann, H.J.H. Brouwers, H.-C. Kühne, and B. Meng, “Influence of the PCE charge density on the early hydration of cement“, in progress.

W. Schmidt, H.J.H. Brouwers, H.-C. Kühne, and B. Meng, “A rapid method to qualitatively distinguish PCEs by their adsorption properties“, in progress.

W. Schmidt, H.J.H. Brouwers, H.-C. Kühne, and B. Meng, “Influence of stabilising agents on the rheology of self-compacting concrete at varying ambient temperatures“, in progress.

W. Schmidt, J. Stroh, H.J.H. Brouwers, F. Emmerling, and B. Meng, “Influence of stabilising agents on the hydration of cement“, in progress.

### Conference papers

W. Schmidt, H.-C. Kuehne, and B. Meng, “Performance and interactions of admixtures for SCC exposed to different climatic conditions“, *Concrete under Severe Conditions: Environment & Loading*, Tours, France, 2007, pp. 979-986.

H.-C. Kühne, W. Schmidt, and B. Meng, “The influence of temperature on self-compacting concrete in presence of superplasticizer and additional admixtures“, *5th International RILEM Symposium on Self-Compacting Concrete*, Ghent, Belgium, 2007, pp. 405-410.

H. C. Kühne and W. Schmidt, “Spezifische Einflüsse der Mischtechnik auf Beton“, *Fachseminar - Moderne Betone wirksam Mischen Berlin*, Germany, 2007.

- W. Schmidt, "Influence of the processing temperature and combined admixtures on the properties of Self-Compacting Concrete", 7th International PhD Symposium in Civil Engineering, Stuttgart, 2008, pp. 75-84.
- K. Vasilic, W. Schmidt, H.-C. Kühne, and B. Meng, "Experimental and numerical studies on calibration of a rotational rheometer for cementitious materials", 17. Internationale Baustofftagung - ibausil, Weimar, 2009, pp. 1.1135-1.1140.
- W. Schmidt, H.-C. Kuehne, and B. Meng, "Temperature related effects on self-consolidating concrete due to interactions between superplasticizers, supplemental admixtures and additions", 9th ACI International Conference on Superplasticizers and Other Chemical Admixtures - Supplementary Papers, Seville, Spain, 2009, pp. 135-147.
- W. Schmidt, "Verbesserung der Verarbeitungseigenschaften fließfähiger Betone bei veränderlichen Temperaturen", 19. Workshop und Kolloquium Rheologische Messungen an Baustoffen, Regensburg, Germany, 2010.
- W. Schmidt, H.J.H. Brouwers, H.-C. Kuehne, and B. Meng, "Influence of ambient temperature conditions on the effect of stabilising polymers in cementitious building materials", 13th Int. Congress on Polymers in Concrete- ICPIC 2010 Madeira, Portugal, 2010, pp. 241-249.
- W. Schmidt, "Möglichkeiten zur Steuerung der Robustheit von selbstverdichtendem Beton gegenüber veränderlichen Umgebungstemperaturen", DAFStb Doktorandensymposium 2010 - 51. Forschungskolloquium, Kaiserslautern, Deutschland, 2010, pp. 527-538.
- W. Schmidt, H.J.H. Brouwers, H.-C. Kuehne, and B. Meng, "Correlation between setting, heat evolution, and deformations of cementitious binder systems depending on type and amount of superplasticizer", 13th International Congress on the Chemistry of Cement, Madrid, Spain, 2011.
- N.S. Msinjili, W. Schmidt, and H.-C. Kühne, "The SPIN project", Workshop cement and concrete for Africa (Proceedings), Berlin, Germany, 2011, pp. 5-9.
- W. Schmidt, "Challenges of the African Environmental Conditions for Concrete Mixture Composition", Workshop Cement and Concrete for Africa, Berlin, Germany, 2011, pp. 37-49.
- M.V.A. Marinescu, W. Schmidt, N.S. Msinjili, H.C. Uzoegbo, I. Stipanovic Oslakovic, G.S. Kumaran, H.J.H. Brouwers, H.-C. Kühne, and A. Rogge, "Recent developments and perspectives regarding the standardisation and quality surveillance of cement in the east, central and south african region", 13th ICC - International congress on the chemistry of cement (Proceedings), Madrid, Spain, 2011.
- W. Schmidt, "Einfluss der Polymerstruktur von Stabilisierern auf die Rheologie von selbstverdichtendem Beton und Mörtel " in 20. Workshop und Kolloquium Rheologische Messungen an Baustoffen, Regensburg, Germany, 2011.
- W. Schmidt, "Spearhead network for innovative, clean and safe cement & concrete technologies (SPIN)", Joint Stakeholders Conference of the ACP-EU EDULINK and Science & Technology Programmes, Brussels, Belgium, 2011.
- M. Meinel, W. Schmidt, H.-C. Kühne, and B. Meng, "Betonpflastersteine mit erweiterten Leistungsmerkmalen", 52. DAFStb-Forschungskolloquium, Berlin, Deutschland, 2011, pp. 194-203.
- B. Meng, W. Schmidt, and H.-C. Kühne, "Aktuelle Forschungsansätze zur Rheologie von Frischbeton", 52. DAFStb-Forschungskolloquium, Berlin, Deutschland, 2011, pp. 33-39.
- N.S. Msinjili, W. Schmidt, and H.-C. Kühne, "Cement and concrete development in Africa: the role of the SPIN project", 52. DAFStb-Forschungskolloquium., Berlin, Deutschland, 2011, pp. 339-344.

W. Schmidt, H.-C. Kühne, and B. Meng, “Zum Einfluss des Mischungsentwurfs und des Fließmittels auf temperaturbedingte Veränderungen der Rheologie von SVB“, 52. DAfStb-Forschungskolloquium, Berlin, Germany, 2011, pp. 40-49.

A.A. Akindahunsi, H.C. Uzoegbo, S.E. Iyuke, and W. Schmidt, “Technological Advances in the Potential Uses of Cassava Starch in Concrete“, The 6th International Conference of the Africa Materials Research Society, Victoria Falls, Zimbabwe, 2011.

W. Schmidt, A.A. Akindahunsi, N.S. Msinjili, H.-C. Kühne, and H.C. Uzoegbo, “Technologische und wirtschaftliche Lösungsansätze für rheologisch optimierte Betone für subsaharische afrikanische Länder“, 21. Workshop und Kolloquium "Rheologische Messungen an Baustoffen", Regensburg, 2012.

W. Schmidt, “The African-European SPIN Expert Network – Objectives and Experiences“, DAAD Seminar zur Antragstellung im ACP-EU Kooperationsprogramm, Bonn, Germany 2012.

M. Barthel, H.-C. Kühne, and W. Schmidt, “Concrete Solutions for the Mitigation of the Urban Heat Island Effect“, fib Symposium: Concrete Structures for Sustainable Community Stockholm, Schweden, 2012.

W. Schmidt, N.S. Msinjili, H.-C. Kuehne, M.V.A. Florea, G.S. Kumaran, and P. Nibasumba, “Robustness improvement of fresh concrete and mortar performance for challenging casting environments with focus on sub-Saharan Africa“, 3rd International Conference on Concrete Repair, Rehabilitation and Retrofitting, Cape Town, South Africa, 2012.

N.S. Msinjili, W. Schmidt, G. Gluth, M.V.A. Florea, G.S. Kumaran, A.A. Akindahunsi, H.-C. Uzoegbo, and I.S. Oslakovic, “Concrete knowledge improvement in sub-Saharan Africa“, 3rd International conference on concrete repair, rehabilitation and retrofitting III, Cape Town, South Africa, 2012, pp. 1459-1465.

W. Schmidt, “Self-Compacting Concrete – A Solution to Improve the Fresh Concrete and Mortar Performance for the Challenging Casting Environments of Sub-Saharan Africa“, SPIN Workshop at the University of the Witwatersrand, Johannesburg, South Africa, 2012.

W. Schmidt, “The African-European SPIN Network – Linking Experts to Foster Innovation in Cement and Concrete“, SPIN Workshop at the University of the Witwatersrand, Johannesburg, South Africa, 2012.

W. Schmidt, “Robustness Improvement of Fresh Concrete and Mortar Performance for Challenging Casting Environments with Focus on Sub-Saharan Africa“, SPIN Workshop at the University of the Witwatersrand, Johannesburg, South Africa, 2012.

M. Barthel, W. Schmidt, and H.-C. Kühne, "Betontechnologische Ansätze zur Vermeidung innerstädtischer Hitzeinseln“, 18. Ibausil - Internationale Baustofftagung, Weimar, Germany, 2012, pp. 2-0042 - 2-0050.

W. Schmidt, H.J.H. Brouwers, H.-C. Kühne, and B. Meng, “Zum Einfluss der Menge und Modifikation des Fließmittels auf das Erstarren, die Wärmeentwicklung und die frühen Verformungen von Bindemittelleimen“, 18. Ibausil - Internationale Baustofftagung, Weimar, Germany, 2012, pp. 2-0392 - 2-0399.

W. Schmidt, H.J.H. Brouwers, C. Lehmann, H.-C. Kuehne, and B. Meng, “Effect of PCE type on Setting, Hydration, And Early Deformations of Cement Paste“, Tenth International Conference on Superplasticizers and Other Chemical Admixtures in Concrete - Supplementary Papers, Prague, Czech Republic, 2012, pp. 229-239.

A.A. Akindahunsi, W. Schmidt, H.C. Uzoegbo, and S.E. Iyuke, “The Influence of Starches on some Properties of Concrete“, International Conference on Advances in Cement and Concrete Technology in Africa, Johannesburg, South Africa, 2013, pp. 637-646.

- M. Barthel, W. Schmidt, and H.-C. Kühne, "Concrete Pavers for the Mitigation of the Urban Heat Island Effect", International Conference on Advances in Cement and Concrete Technology in Africa, Johannesburg, South Africa, 2013, pp. 953-960.
- G.S. Kumaran, N.S. Msinjili, W. Schmidt, M.V.A. Florea, and P. Nibasumba, "A Study on Sustainable Energy for Cement Industries in Rwanda", Intl. Conference on Advances in Cement and Concrete Technology in Africa, Johannesburg, South Africa, 2013, pp. 1169-1176.
- P. Ränge, W. Schmidt, and H.-C. Kühne, "Effect of the storage of cement on early properties of cementitious systems", International Conference on Advances in Cement and Concrete Technology in Africa, Johannesburg, South Africa, 2013, pp. 339-348.
- W. Schmidt, N.S. Msinjili, and H.-C. Kühne, "Rheological Optimisation for Flowable Mixture Compositions Specified for African Boundary Conditions", Int. Conference on Advances in Cement and Concrete Technology in Africa, Johannesburg, South Africa, 2013, pp. 359-366.
- W. Schmidt, A. Radlińska, C. Nmai, A. Buregyeya, W.L.Lai, and S. Kou, "Why does Africa need African concrete? An observation of concrete in Europe, America, and Asia – and conclusions for Africa", International Conference on Advances in Cement and Concrete Technology in Africa, Johannesburg, South Africa, 2013, pp. 1139-1148.
- W. Schmidt, H.C. Uzoegbo, N.S. Msinjili, H.-C. Kühne, and A. Rogge, "Experiences in an African-European-Cooperation Project: Strengthening Research Capacity in Cement and Concrete in Africa", International Conference on Advances in Cement and Concrete Technology in Africa, Johannesburg, South Africa, 2013, pp. 1177-1184.
- W. Schmidt, "Eine einfache experimentelle Methode zur qualitativen Bewertung des Einflusses beliebiger Polycarboxylatether-Fließmittel auf die Rheologie" in 22. Workshop und Kolloquium Rheologische Messungen an Baustoffen, Regensburg, Germany, 2013.
- W. Schmidt, H.J.H. Brouwers, H.-C. Kühne, and B. Meng, "Casting process improvement by optimization of mixture composition and high range water reducing agent modification", Fifth North American Conference on the Design and Use of Self-Consolidating Concrete, Chicago, Illinois, USA, 2013.
- W. Schmidt, H.J.H. Brouwers, H.-C. Kühne, and B. Meng, "A Simple Test Method to Assess the Influence of PCEs on The Rheology of Flowable Cementitious Systems", 7th International RILEM Symposium on Self-Compacting Concrete in Conjunction with the 1st International RILEM Conference on Rheology and Processing of Construction Materials - Supplementary Papers, N. Roussel, Ed. Paris, France, 2013.
- W. Schmidt, N.S. Msinjili, and H.-C. Kühne, "Rheological Optimisation for Flowable Concrete for Sub-Saharan Environmental Conditions", 7th International RILEM Symposium on Self-Compacting Concrete in Conjunction with the 1st International RILEM Conference on Rheology and Processing of Construction Materials - Supplementary Papers, N. Roussel, Ed. Paris, France, 2013.
- W. Schmidt, "Peculiarities of African Cement and Concrete Markets - Challenges and Opportunities", Global Issues in Concrete Construction - Markets, Perspectives, Technologies, Johannesburg, South Africa, 2013.
- W. Schmidt, H.J.H. Brouwers, H.-C. Kühne, and B. Meng, "Interactions between polycarboxylate ether superplasticizers and different polysaccharides and influences on the early hydration of cement", 1st International Conference on the Chemistry of Construction Materials, Germany, 2013, pp. 49-53.
- W. Schmidt, "Controlling Rheology – The Key to Individual Concrete Performance Specifications", European Coating Conference on Facade coatings and plasters, Düsseldorf, Germany, 29-30 October, 2013, pp. 93-103.

M. Barthel, W. Schmidt, and H.-C. Kühne, "Mitigation of the Urban Heat Island Effect by self-cooling Concrete Pavers", International Congress on Materials & Structural Stability CMSS-2013, Rabat, Morocco, 2013.

W. Schmidt, M. Sonebi, H.J.H. Brouwers, H.-C. Kühne, and B. Meng, "Rheology Modifying Admixtures: The Key to Innovation in Concrete Technology – A General Overview and Implications for Africa", International Congress on Materials & Structural Stability CMSS-2013, Rabat, Morocco, 2013.

W. Schmidt, H.C. Uzoegbo, N. Bella, G. Rongai, H.-C. Kühne, and T. Diergardt, "Cement Testing in Africa – Conclusions from the First Africa-Wide Proficiency Testing Scheme", International Congress on Materials & Structural Stability CMSS-2013, Rabat, Morocco, 2013.

M. Sonebi, W. Schmidt, and J. Khatib, "Influence of the type of viscosity-modifying admixtures and metakaolin on the rheology of grouts", International Congress on Materials & Structural Stability CMSS-2013, Rabat, Morocco, 2013.

### Professional journals

H.-C. Kühne and W. Schmidt, "Der Siebtrennversuch nach prEN 12350-11", beton, vol. 57, pp. 448-454, 2007.

W. Schmidt and H.-C. Kuehne, "Influence of the processing temperature on the properties of SCC in the presence of superplasticizer and other admixtures " Concrete Plant + Precast Technology, pp. 40-49, 2007.

W. Schmidt, H.-C. Kuehne, D. Rosignoli, and B. Meng, "Development and application of a novel ready-made compound including additions and admixtures for the easy production of SCC", Concrete Plant + Precast Technology, pp. 4-11, 2008.

W. Schmidt and H.-C. Kuehne, "Interactions between admixtures and mineral components in Self-Compacting Concrete cast at different temperatures", Concrete Plant International, pp. 32-39, 2009.

W. Schmidt, P. Ramge, and H.-C. Kuehne, "Effect of the storage conditions of cement on the processing and hardening properties of concrete", Concrete Plant + Precast Technology, vol. 06, pp. 10-17, 2009.

W. Schmidt, H.-C. Kühne, H.C. Uzoegbo, and N.S. Msinjili, "Building practice and Concrete Infrastructure Development in Eastern and Southern Africa", Concrete Plant International, vol. 2011, pp. 32-37, 2011.

H.C. Uzoegbo, D. Bjegovic, W. Schmidt, and W. Kitobo, "SCM Potential in Africa", World Cement, 2012.

W. Schmidt, D. Wend, H.-C. Kühne, and B. Meng, "The influence of superplasticiser modifications on early hydration processes", Concrete Plant International, vol. 4, pp. 64-69, 2012.

W. Schmidt, "Start of round-robin test for cement testing in Africa / Start für Ringversuch zur Zementprüfung in Afrika", BFT international : concrete plant + precast technology, vol. 08, pp. 54-55, 2012.

W. Schmidt and G. Gluth, "Knowledge transfer and quality assurance - key factors for the future prospects of building with cement in Africa / Wissenstransfer und Qualitätssicherung - Schlüsselfaktoren für die Zukunftsperspektiven der Bauweise mit Zement in Afrika", ZKG International, vol. 65, pp. 34-38, 2012.

W. Schmidt, H.-C. Kühne, and N.S. Msinjili, "Optimising the rheology of concrete for sub-Saharan African boundary conditions," *Concrete Plant + Precast Technology*, vol. 78, pp. 60-65, 2012.

W. Schmidt, H.C. Uzoegbo, K. Wunderlich, and G. Rongai, "A first pan-African proficiency testing scheme," BFT-International, 2013.

### **Book chapters**

W. Schmidt, H.J.H. Brouwers, H.-C. Kühne, and B. Meng, "Effects of Superplasticizer and Viscosity-Modifying Agent on Fresh Concrete Performance of SCC at Varied Ambient Temperatures", *Design, Production and Placement of Self-Consolidating Concrete - Proceedings of SCC2010*, Montreal, Canada, September 26-29, 2010, K.H. Khayat and D. Feys, Eds.: Springer, 2010, pp. 65-77.

W. Schmidt, H.J.H. Brouwers, H.-C. Kuehne, and B. Meng, "Influence of Temperature on Stabilizing Agents in Presence of Superplasticizers", *Tenth International Conference on Superplasticizers and Other Chemical Admixtures in Concrete*, Prague, Czech Republic, 2012, pp. 365-377.

### **Books**

W. Schmidt and N.S. Msinjili, "Proceedings of the Workshop on Cement and Concrete for Africa", W. Schmidt and N.S. Msinjili, Eds. Berlin: BAM, 2011, p. 81.

H.C. Uzoegbo and W. Schmidt, "Advances in Cement and Concrete Technology in Africa", H.C. Uzoegbo and W. Schmidt, Eds. Berlin: BAM, 2013, p. 1218.

W. Schmidt and H.C. Uzoegbo, "Global Issues in Concrete Construction – Markets, Perspectives, Technologies" South Africa", W. Schmidt and H.C. Uzoegbo, Eds. Berlin: BAM, 2013, p. 67.

### **Publications with excerpts from this Thesis**

Parts of this Thesis were incorporated into the following peer-reviewed publications:

W. Schmidt, H.J.H. Brouwers, H.-C. Kühne, and B. Meng, "Optimierung der Robustheit von selbstverdichtendem Beton - Robustness optimisation of self-compacting concrete regarding temperature effects", *Beton- und Stahlbetonbau*, vol. 108, pp. 13-21, 2013.

W. Schmidt, H.J.H. Brouwers, H.-C. Kühne, and B. Meng, "Influences of superplasticizer modification and mixture composition on the performance of self-compacting concrete at varied ambient temperatures", (accepted for publication)", *Cement and Concrete Composites*, 2014.

W. Schmidt, H.J.H. Brouwers, H.-C. Kühne, and B. Meng, "The working mechanism of starch and diutan gum in cementitious and limestone dispersions in presence of polycarboxylate ether superplasticizers", *Applied Rheology*, Vol. 23, No. 5, pp. 52903-1-52903-12, 2013

W. Schmidt, H.J.H. Brouwers, H.-C. Kuehne, and B. Meng, "Influence of Temperature on Stabilizing Agents in Presence of Superplasticizers", *Tenth International Conference on Superplasticizers and Other Chemical Admixtures in Concrete*, Prague, Czech Republic, 2012, pp. 365-377.

W. Schmidt, H.J.H. Brouwers, H.-C. Kuehne, and B. Meng, "Effects of the Characteristics of High range Water Reducing Agents and the Water to Powder Ratio on Rheological and Setting Behavior of Self-Consolidating Concrete", (accepted for publication)*Advances in Civil Engineering Materials*, Vol. 3, No. 2, 2014.

## Summary

Self-compacting concrete is not well established today in the field of ready-mixed concrete. One of the reasons is the lack of robustness against changes in the ambient temperatures. The major distinction items of self-compacting concrete from conventional concrete are the powder composition and the extensive use of admixtures and polycarboxylate ether superplasticisers in particular. This Thesis aims to better understand effects of these items, by investigating the influence of the mixture composition as well as the charge density of the superplasticiser on the rheology and the early hydration period of self-compacting concrete. Furthermore, influences of stabilising admixtures are discussed.

It is shown that depending upon the environmental temperature different mixture compositions can behave less robust than others and that the choice of the superplasticiser has a prominent influence on the temperature related workability and its retention. Stabilising agents have significantly less influence on temperature induced rheology changes, but they can also amplify or counteract particular temperature induced effects.

The influences of the mixture composition, superplasticisers, and stabilising agents on the early hydration period until the final setting are also studied and discussed in this Thesis. It is shown that the charge density of a superplasticiser has a strong influence on the retardation of the hydration reactions. This can be mainly linked to the amount of total polymers required to reduce the yield stress effectively. Furthermore, the influence of stabilising agents is observed and interactions between superplasticisers and stabilising agents are discussed.

The Thesis finally gathers the findings of the experimental research in decision paths which give recommendations for SCC mixture compositions tailored for individual temperature cases or for highest robustness for a wide range of temperatures.

## Curriculum Vitae

Wolfram Schmidt was born in Cologne on the 7<sup>th</sup> October 1974. After grammar school and military service, he studied Civil Engineering at the RWTH Aachen. After receiving his intermediate diploma, he majored in structural engineering. He received his Masters degree (Dipl.-Ing.) in 2005 for the thesis “Concepts for highly compressible concrete for pressure shaped components“ under supervision of Prof. Dr.-Ing. Brameshuber at the Institute of Building Materials Research (Institut für Bauforschung) at the RWTH Aachen. After a short period as research assistant at the company Alpha Ceramics in Aachen he went to the BAM Federal Institute for Materials Research and Testing in Berlin as responsible project co-worker for the European research project MICROCON. After the project he has been employed as researcher in the department “Safety of Structures”. His research focus is admixtures, rheology, and high performance concrete. He successfully attracted funds for the collaborative European research projects UNACON, SeCCoPa, and SPIN and he has been co-founder of an Africa-wide inter laboratory testing scheme for cement testing and he is co-initiator of the conference series ACCTA. He has been active member of the RILEM committee “Mechanical Properties of Self-Compacting Concrete” and the fib task group “Flowable Concrete”. In 2008 he started his PhD research for this Thesis under the supervision of prof.dr.ir. H.J.H. Brouwers and Prof. and Dir’in Dr. rer. nat. Brigit Meng.

Self-compacting concrete is not well established today in the field of ready-mixed concrete. One of the reasons is the lack of robustness against changes in the ambient temperatures. The major distinction items of self-compacting concrete from conventional concrete are the powder composition and the extensive use of admixtures and polycarboxylate ether superplasticisers in particular. This Thesis aims to better understand effects of these items, by investigating the influence of the mixture composition and the charge density of the superplasticiser on the rheology and the early hydration of self-compacting concrete. Furthermore, influences of stabilising admixtures and interactions with superplasticiser are discussed. The focus is put on temperature effects on the rheology and the early hydration of self-compacting concrete.

It is shown that depending upon the environmental temperature different mixture compositions can behave less robust than others and that the choice of the superplasticiser has a prominent influence on the temperature related workability and its retention. Stabilising agents have significantly less influence on temperature induced rheology changes, but they can amplify or counteract particular temperature induced effects.

The influences of the mixture composition, superplasticisers, and stabilising agents on the early hydration period until the final setting are also studied and discussed in this Thesis. It is shown that the charge density of a superplasticiser has a strong influence on the retardation of the hydration reactions. This can be mainly linked to the amount of total polymers required to reduce the yield stress effectively. Furthermore, the influence of stabilising agents is observed and interactions between superplasticisers and stabilising agents are discussed.

The findings of the experimental research are discussed and the conclusions are brought together in decision paths which give recommendations for the mixture compositions of self-compacting concrete tailored for individual temperature cases or for highest robustness for a wide range of temperatures.

F

A

C

B

W

H

E

H

U

/ Department of the Built Environment